



Novel metabolic regulations exerted by LKB1 signaling in polarized cells: impact on tissue ontogeny

Anca Gabriela Iordache Radu

► To cite this version:

Anca Gabriela Iordache Radu. Novel metabolic regulations exerted by LKB1 signaling in polarized cells: impact on tissue ontogeny. Subcellular Processes [q-bio.SC]. Université Grenoble Alpes, 2018. English. NNT : 2018GREAV011 . tel-01977028

HAL Id: tel-01977028

<https://theses.hal.science/tel-01977028>

Submitted on 10 Jan 2019

HAL is a multi-disciplinary open access archive for the deposit and dissemination of scientific research documents, whether they are published or not. The documents may come from teaching and research institutions in France or abroad, or from public or private research centers.

L'archive ouverte pluridisciplinaire **HAL**, est destinée au dépôt et à la diffusion de documents scientifiques de niveau recherche, publiés ou non, émanant des établissements d'enseignement et de recherche français ou étrangers, des laboratoires publics ou privés.

THÈSE

Pour obtenir le grade de

DOCTEUR DE LA COMMUNAUTÉ UNIVERSITÉ GRENOBLE ALPES

Spécialité : **Biologie Cellulaire**

Arrêté ministériel : 25 mai 2016

Présentée par

« **Anca Gabriela RADU** »

Thèse dirigée par **Chantal THIBERT**,

Préparée au sein de l'équipe **Pathologie Moléculaire des
Cancers et Biomarqueurs**, dirigée par PR. Pierre HAINAUT à
l'**Institut pour l'Avancée des Biosciences** dans l'**École
Doctorale Chimie et Sciences du Vivant**

Nouvelles régulations métaboliques exercées par la signalisation LKB1 dans les cellules polarisées: conséquences pour l'ontogénie tissulaire.

Thèse soutenue publiquement le « **18 mai 2018** »,
devant le jury composé de :

M, Francois, BOUCHER

PR, Université Grenoble Alpes, TIMC-IMAG, CNRS, Grenoble/La
Tronche, France (Président du jury)

Mme, Sylvie, DUFOUR

DR2, INSERM, Institut Mondor de Recherche Biomédicale, INSER U955,
Creteil, France (Rapporteur)

M, Roberto, MAYOR

PR, University College London, London, United Kingdom (Rapporteur)

M, Pierre, ROUX

DR2, INSERM, Centre de Recherche en Biologie Cellulaire de
Montpellier, CNRS, CRBM/UMR 5237, Montpellier, France (Examineur)

M, Julien, COURCHET

CR1, INSERM, Institut NeuroMyoGene UCBL CNRS UMR5310/ INSERM
U1217, Lyon, France (Examineur)

M, Marc, BILLAUD

DR1, CNRS, Centre de Recherche en Cancerologie de Lyon, UMR 5286,
Lyon, France (Examineur)

Mme, Chantal, THIBERT

CR1, CNRS, Institut pour l'Avancée des Biosciences, UGA, INSERM
U1209, CNRS UMR 5309, Grenoble, France (Directrice de thèse)



THESIS

To obtain the degree of

DOCTOR FROM UNIVERSITY OF GRENOBLE ALPES

Specialty: Cellular Biology

Ministerial order: May 25, 2016

Presented by

« **Anca Gabriela RADU** »

PhD thesis supervised by **Chantal THIBERT**

Prepared in the laboratory **Tumor molecular pathology and Biomarkers**, headed by PR. Pierre HAINAUT in the Institute for Advanced Biosciences at « **École Doctorale Chimie et Sciences du Vivant** »

Novel metabolic regulations exerted by LKB1 signaling in polarized cells: impact on tissue ontogeny.

Defended in public « **May 18, 2018** »,

In front of the jury composed of:

Mr, Francois, BOUCHER

PR, University Grenoble Alpes, TIMC-IMAG, CNRS, Grenoble/La Tronche, France (President of the jury)

Mrs, Sylvie, DUFOUR

DR2, INSERM, Institut Mondor de Recherche Biomédicale, INSER U955, Creteil, France (Reviewer)

Mr, Roberto, MAYOR

PR, University College London, London, UK (Reviewer)

Mr, Pierre, ROUX

DR2, INSERM, Centre de Recherche en Biologie Cellulaire de Montpellier, CNRS, CRBM/UMR 5237, Montpellier, France (Examiner)

Mr, Julien, COURCHET

CR1, INSERM, Institut NeuroMyoGene UCBL CNRS UMR5310/ INSERM U1217, Lyon, France (Examiner)

Mr, Marc, BILLAUD

DR1, CNRS, Centre de Recherche en Cancerologie de Lyon, UMR 5286, Lyon, France (Examiner)

Mrs, Chantal, THIBERT

CR1, CNRS, Institute for Advanced Biosciences, UGA, INSERM U1209, CNRS UMR 5309, Grenoble/ La Tronche, France (Supervisor)



*"Sfânta munca e aceea
ce răsplata-n ea-și găsește.
De-nțelegi tu asta, cheia
fericirii tale-o ții."*

Alexandru Vlahuță

Acknowledgements

As a very well-known proverb says, "All good things must come to an end". For me, this means that my period as a PhD student is over and that I will start a new phase in my life. During these years of my thesis I was surrounded all the time by wonderful peoples that guided me and wanted to see me succeed and from which I learned a lot of things, both on a personal and a professional level. Therefore, I would like to thank all these people that have been part of my life and hopefully will continue to be part of it.

First, I would like to thank the members of the jury, namely: **Francois Boucher, Sylvie Dufour, Roberto Mayor, Pierre Roux, Julien Curchet and Marc Billaud**, for accepting to participate and to evaluate my PhD work and for the interesting discussion that we had during my PhD defense.

Sylvie Dufour and Roberto Mayor thank you also for your thorough review of my PhD manuscript, for your valuable advices and for your appreciations.

Thanks to the people that made possible my PhD

In 2014 I started my PhD in the laboratory "Polarity, development and cancer", headed by Dr. **Marc Billaud** and in 2016 I continued my PhD in the laboratory "Tumor molecular pathology and biomarkers", headed by Pr. **Pierre Hainaut**.

Marc, I would like to thank you for your support during all my PhD. Even after you moved to Lyon, you regularly came to Grenoble to discuss about our projects. Thank you for all the interesting scientific discussions that we had, for all your advices and all the opportunities you have given me.

Pierre, thank you for believing in me and for welcoming me in your team. Thank you for your degree of involvement, for your kindness, your scientific advices, for the interesting discussions that we had and for always being there for me.

A special mention goes to my supervisor, **Chantal Thibert**. My thesis has been a wonderful experience. Thank you, Chantal, for all the things that I learned from you, for helping me grow and become autonomous, for your trust, support and for all the time you dedicated for me.

I also thank the members of our team:

Sakina Torch, thank you for always being there for me, for your kindness, support and advices. I am very grateful that I met you during my second year of licence and that you gave me the opportunity to do an internship in the lab. You were the first person that inspired me to continue in a research career.

Thank you **Anthony Lucas** for all your help with the mice, for the immunohistochemistry and immunofluorescence that you have done and for all our funny discussions during the coffee break. Thanks also to **Patrick Vernet, Sophie Michallet and Cyrielle Colomb** for their help with the mice.

Thank you **Renaud Blervaque** for all your help with the PCR assays, for your support and for always knowing to listen and to be there for others.

Thank you **Marie Mevel** for your kindness, your hard work and dedication. I am sure that you will do a great thesis and you will have a bright future.

Thank you, **Nicolas Reynoird**, for all your help and advice on both personal and professional levels. Thank you also for all the good moments that we spent at Le Synesthète, L'Absolu or Dr.D, and that

you and others organized. You are an amazing person and I am sure that you will soon become a great team leader.

Thank you, **Sandrine Blanchet** for all your energy, your positive attitude, your encouragement when I needed it most, for all the things that you did for the lab and for your strength, which inspired me.

Nathanael Lemonnier, thank you for your help with my presentation and for all the good discussions we had each time we met. You are an amazing person and your ambition, kindness and friendship have inspired me.

Thanks also to my bureau colleges: **Hind Hafsi**, **Alexandre Casanova**, **Gael Roth** and **Valentina Lukinovic** for all the funny moments and crazy laughs, for always listening and encouraging me. You are all great friends and I appreciate you a lot.

Thanks to students that I supervised during my PhD: **Nina Tcaciuc**, **Melissa Bouzar**, **Tanguy Lorin** and **Maud Schweitzer** for your help and involvement.

Thanks also to other members of the team: **Amelie Fauconnet**, **Cécile Caron**, **Benedicte Elena**, **Emilie Montellier** and **Anne McLeer** for their support.

Thanks to the members of the former team:

Thanks to **Maya Ghawitian**, **Maïlys Le Borgne**, **Chloé Prunier** and **Anne Martinez** for all the things that I learned from you, for your energy and for all the good moments that we had in the lab.

Thank you **Laurance Lafanechère** for being there for me and to **Jean Viallet** and **Jacques Thélou** for your help.

Thanks to our local collaborators

Thank you **Mylène Pezet**, **Jacques Mazzega** and **Alexeï Grichine** for your help and assistance with microscopy and cell sorting.

Thank you **Florence Fauvelle** from Grenoble Institute of Neurosciences for HRMAS technique and to **Karin Pernet-Gallay**, **Julie Delaroche** and **Anne Bertrand** for electronic microscopy.

Thanks to **Uwe Schlattner lab** for their help with metabolic analysis.

Thanks to our national and international collaborators:

Thanks to **Lionel Larue** from Institut Curie, Orsay; **Nadège Bondurand** and **Véronique Pingault** from Hopital H. Mondor pour la Recherche Biomédicale, Créteil; **Sylvie Dufour** from Institut Mondor de Recherche Biomédicale, Créteil; **Nicolas Tricaud** from Institute of Neurosciences, Montpellier; **Christine Perret** from Institut Cochin, Paris; **Vincent Mirouse** from Institut GReD, Clermont Ferrand; **Sophie Creuzet** from Paris-Saclay Institute of Neuroscience and **Raquel Almeida** and **Bruno Pereira** from Institute of Molecular Pathology and Immunology, Portugal.

Thanks to the IAB administrative staff

Dalenda Benmedjahed, je suis très contente de t'avoir connue. Tu es une personne merveilleuse qui pense beaucoup aux autres. Merci beaucoup pour tous les moments d'encouragement et pour tous les petites gâteaux/fleurs que tu m'as donné, ainsi que pour le cadeau de fin de thèse.

Johanna Mumber, félicitations pour ton petit ! Je ne m'attendais pas de se voir à la clinique. Merci beaucoup pour tous les efforts faits pour moi. Merci aussi à **Grégory Charles-Bernard**, **Melania Colella**, **Eleonore Italiano** and **Roseline Licata** pour leur aide.

Je remercie aussi aux autres membres de l'équipe administrative **Natacha Herlem, Corinne Martinez, Michail Gidopoulos, Alexandre Babin** et **Norbert Masciave** pour tout ce qu'ils ont fait pour moi.

Thanks to the member of team "Cell adhesion dynamics and differentiation", headed by Corinne Albiges Rizo.

Especially thanks to **Eva Faurobert** for accepting to be part of my PhD committee, to **Olivier Destaing** for our discussions and good moments, **Sanela Mrkonjic** for her friendship. Sanela, as I already told you, if you want you can become a psychotherapist because you are a great listener and you give great advices. I would also like to thank **Adele Kerjouan, Alexander Kyumurkov (Sacho)** and **Kate Miroshnikova** for their energy and happiness.

Thanks to my friends and to the members of IAB PhD committee:

Lauralie Peronne, I am very glad that you came to Grenoble. A real friendship was born between us and I thank you for all the extraordinary moments that we had at IAB but also outside IAB, around Grenoble, in Marseille and US. I hope our friendship lasts forever!

Nejma Belaadi, thank you for the nice moments that we spent in US and for all your encouragements before my PhD defense.

To **Sivan Koskas, Anne-Sophie Hatat, Jonathan Lavaud, Adele Kerjouan, Alexis Gonon, Laure Laforgue, Mathieu Dangin, Afsaneh Goudarzi** and **NaghmeH Hoghoughi** thank you all for your friendship and smiles.

Special thanks to my family

My dear husband, you are the person I love most and without you I would have never arrived here. You have been a real support for me during all these 15 years that we spent together and I dedicate my PhD to you. Thank you for all the time that you spent in the car, in front of IAB, waiting for me because I finished late and for all the weekends when you accompanied me at the lab. Especially thank you for always believing in me and letting me think that I can do everything and that I am the best. Te iubesc!

Mami și tati vă iubesc mult. Vă mulțumesc enorm că ați avut întotdeauna încredere în mine, că m-ați încurajat să fiu cea mai bună și că întotdeauna v-ați dorit tot ce este mai bun pentru mine. Știu că ați făcut multe eforturi și uite că acum am reușit să vă răsplătesc și să vă fac mândri de mine devenind Doctor. Sper că de acum înainte să vă aduc și mai multe împliniri.

Mihai îți mulțumesc pentru tot ajutorul pe care mi l-ai dat pentru teză și în general pentru școală. Mă bucur mult că suntem în același oraș și că am putut să ne vedem și să ne sfătuim ori de câte ori simțeam nevoia. Îți mulțumesc pentru momentele frumoase pe care le-am petrecut împreună.

Mamaie (Gabi) chiar dacă nu mai ești printre noi, îți mulțumesc pentru că ai existat în viața mea, că am împărțit aceeași casă și cameră și că datorită ție nu am fost niciodată singură. Te iubesc și o să te port în inimă întotdeauna. **Mamaie (Natalia)** și **Ion** știu că vă bucurați pentru mine și vă mulțumesc că deși suntem departe vă gândiți mereu la noi și noi la voi.

Table of Contents

<i>Preface</i>	3
<i>Introduction</i>	5
I. ENERGY METABOLISM.....	6
1. Definition of energy metabolism and historical context.....	6
2. Energy metabolic reprogramming.....	8
3. Amino acids acting as metabolic regulators.....	10
II. NEURAL CREST CELLS.....	19
1. Neural crest cells formation.....	19
2. NCC subpopulations and their derivatives.....	22
3. Neural crest cell defects.....	31
III. METABOLIC REGULATORS: LKB1 and p53.....	38
III.A. THE MASTER KINASE LKB1.....	38
III.A.1. LKB1 structure, localization and regulation.....	39
III.A.2. LKB1 signaling: focus on AMPK/mTOR pathway.....	44
III.A.3. Cellular regulations by LKB1/AMPK signaling.....	50
III.A.4. Role of LKB1 in development.....	54
III.A.5. Association of LKB1 mutations with human pathologies.....	56
III.B. THE MASTER REGULATOR p53.....	58
III.B.1. Structure and activation of the p53 protein.....	58
III.B.2. p53 biological functions.....	62
III.B.3. Role of p53 in development.....	67
III.B.4. Role of p53 in neural crest cell formation.....	69
IV. LYSOSOMES: a signaling hub to maintain cell metabolism and homeostasis.....	73
1. Lysosomes: multifunctional organelles required for recycling and clearance.....	73
2. Lysosomes as a signaling hub to control nutrient homeostasis.....	76
3. Lysosomal roles in normal and pathological processes.....	79
<i>PhD context & objectives</i>	86
<i>Results</i>	87
I. Project 1: LKB1 in cranial neural crest cells.....	88
1. LKB1 signaling is essential for cranial neural crest cells development.	88

2. Regulation of LKB1 by acetyl transferase GCN5.....	109
II. Project 2: LKB1 metabolic and signaling regulations during NCC commitment.....	120
1. The tumor suppressor LKB1 controls NCC fate through pyruvate-alanine transamination.....	120
2. LKB1 regulates NCC differentiation by limiting p53 signaling and controlling lysosomal activity.....	164
III. Project 3 Energy metabolic regulations of Lkb1 signaling in other polarized cells.	181
1. Lkb1-metabolic regulations in Sertoli cells are essential for testis homeostasis and germ cells maturation.....	182
2. Characterization of MEX-3A-associated metabolic profile.....	191
<i>Conclusions</i>	195
<i>General discussions & Prospects</i>	198
I. LKB1 contributions to neural crest cells and underlying mechanisms.....	199
1. LKB1 in neural crest cells lineage.....	199
2. LKB1 & Neurocristopathies.....	200
Is LKB1 involved in NCC defects associated with lysosomal storage disorders?	202
3. Regulation of Schwann Cell Precursors by LKB1?	203
II. LKB1 contributions to intercellular communication and tissue homeostasis	204
III. Metabolic regulations exerted by LKB1	205
1. Feedback loops between aminotransferases and the mTOR pathway.	205
2. How LKB1 signaling regulates aminotransferases activity?	206
IV. Wider implication for LKB1 in human metabolic diseases and cancers?	208
1. Is LKB1 involved in neurocristopathies associated with metabolic syndromes?	208
2. Does LKB1 contribute to regulate peripheral neuropathies through the control of alanine levels?.....	209
3. How metabolic regulations exerted by LKB1 contribute to its tumor suppressor activity?.....	211
<i>Bibliography</i>	214

Preface

Energy metabolism represents all chemical reactions generating adenosine triphosphate, a molecule providing the energy required for most metabolic and cell processes that are essential to sustain life. Main pathways contributing to energy metabolism are glycolysis, citric acid cycle and oxidative phosphorylation. Recent “omics” explorations allowing collective characterization and quantification of chemical reactions, emphasized that metabolic pathways control cell fate and tissue homeostasis. In particular, mapping of energy metabolic signalings that are activated in early stem cells has begun to shed light on the respective contribution of glycolysis versus oxidative phosphorylation in the maintenance of pluripotency and cell fate commitment. Moreover, energy metabolism controls the balance between proliferation and quiescence by regulating metabolic enzymes called transaminases and consequently amino acid levels.

Amino acids are critical build up units required for proteinogenesis. Besides, amino acids act as metabolic regulators of several enzymes and/or metabolic fluxes either locally in the cell they were biosynthesized or through paracrine action. Amino acids also regulate signaling pathways such as the mammalian target of rapamycin mTOR which coordinates nutrient availability to cell growth through the regulation of most anabolic and catabolic processes. Interestingly, mTOR activation specifically takes place at the lysosomal surface and amino acids are known for years to regulate lysosomal proteolysis. Such regulations could be critical to limit premature aging and promote individuals healthspan and longevity. However, the role of metabolic remodeling and in particular amino acids contribution in cell fate during development remains poorly understood. Therefore, my **PhD project aimed at characterizing the underlying mechanisms that coordinately regulate energy metabolism and cell fate.** In the lab where I did my PhD, one model generated to study this coordinated regulation was based on neural crest stem cells.

Neural Crest Cells (NCC) are multipotent cells delaminating from the neural tube and migrating along stereotypical routes to colonize embryonic territories. In their target organs, NCC give rise to a broad range of derivatives including neurons and glial cells of the peripheral nerves and enteric nervous system, most of the head skeleton and melanocytes. Disruption of neural crest formation is causative of human diseases called neurocristopathies or ribosomopathies, which combine various symptoms derived from neural crest dysfunction such as skin pigmentation defects, craniofacial malformations, enteric defects and exceptionally peripheral neuropathies. NCC fate and stemness maintenance are controlled by transcriptional

and epigenetic inputs driven by numerous transcription factors and chromatin remodelers. However, the metabolic processes underlying NCC development remain poorly understood.

Uncovering connections between metabolic responses and cell signaling pathways has recently encounter an impressive increase. One important signaling pathway regulating energy metabolism is controlled by the tumor suppressor Liver Kinase B1 (LKB1) mainly through its downstream substrate 5' Adenosine MonoPhosphate (AMP)-activated protein kinase (AMPK) and subsequent inhibition of mTOR. The tumor suppressor p53 signaling pathway is also intimately connected to energy metabolism especially upon cellular stress. Furthermore, p53 dosage has been shown to be crucial for neural crest cells development.

During my PhD, I demonstrated that LKB1 is essential for the formation of several NCC-derived structures in vertebrates such as the face, pigmented cells, the enteric nervous system and peripheral nerves. I have uncovered that metabolic regulations exerted by LKB1 during NCC fate act through the regulation of amino acid levels and subsequent mTOR limitation. In particular, we identified that LKB1 controls pyruvate-alanine cycling during glial differentiation. Interestingly, this metabolic regulation is also conserved in Sertoli cells that share similar metabolic functions with glial cells. Moreover, we identified signaling crosstalk between LKB1 and p53 pathways. These signaling could converge especially through lysosome homeostasis thereby potentially impacting cellular aging. Altogether, our findings suggest that deregulations of LKB1 signaling could be involved in a broader range of human pathologies than suspected so far.

As energy metabolism has been the guideline of my PhD project, the bibliographic chapters of the introduction of this manuscript open with a short and general presentation of how the energy metabolic network impacts cell functions during development and diseases and how it is regulated, with a focus on transaminases and amino acids. Next, I briefly describe neural crest cell development and human disorders associated with defects of neural crest formation. The third chapter concerns some knowledge about signaling pathways of the two metabolic regulators LKB1 and p53, as well as their roles during development. The last chapter is about the importance of LKB1/AMPK and mTOR signaling in connection with lysosomal homeostasis, p53 hyperactivation, aberrant lysosome formation and premature aging.

Then, for the results chapter, a brief paragraph addresses the main questions asked during my PhD followed by three chapters describing my experimental contributions. These results sections include three articles (one published, one submitted and one in preparation) and three additional projects in progress.

A general discussion expands our results in a broader context and proposes some perspectives to my PhD work.

Introduction

I. ENERGY METABOLISM

1. Definition of energy metabolism and historical context

Intermediary metabolism regroups all the life-sustaining chemical transformations that take place within cells and tissues. These chemical reactions are usually divided in two categories: catabolic reactions that are required to recycle molecules and refurnish the pool of energy and anabolic reactions necessary for biosynthesis of molecules and which consume energy. Over a century ago, Theodor Schwann, a German physiologist who defined the cell as the basic unit of animal structures and discovered Schwann cells in the peripheral nervous system, also coined the term metabolism which comes from the Greek *metabole* (to change) (Schwann and Schleyden, 1847).

Until the mid-20th century, many research groups in University science and medical departments were working on enzymes and metabolic pathways. But this research field was overtaken by the revolutions in genomics and cell biology as well as the idea that metabolism was more like a housekeeping process. Recently, there was a strong renewed interest in energy metabolism based (i) on our understanding that cell needs and functions are intimately associated to their metabolic activities and (ii) on the development of new technologies to measure metabolic processes *in vivo* in particular with new tools allowing the integration of data at the “omics” scale. This recrudescence of research on metabolism has enabled the recent awareness that energy metabolism is finely tuned during development and deregulations of these processes are responsible of multiple diseases (Metallo and Vander Heiden, 2013).

Energy metabolism is the process of generating energy (adenosine triphosphate: ATP) from nutrients. It comprises a set of interconnected pathways that function in the presence or absence of oxygen. Anaerobic metabolism, also called glycolysis, converts one glucose into 2 pyruvates and produces 2 ATP (Figure 1). The reverse process is called gluconeogenesis. Pyruvate can be transformed into lactate and possibly exported or transported to the mitochondria where it is converted into Acetyl CoA by the citric acid cycle (TCA, also called Krebs cycle) while producing 2 ATP per glucose (Figure 1). Finally, aerobic metabolism, the mitochondrial oxidative phosphorylation (OXPHOS), also produces ATP and this is the most efficient system. *In fine*, combining glycolysis, TCA and OXPHOS produces up to 38 ATP molecules from one glucose molecule (Figure 1).

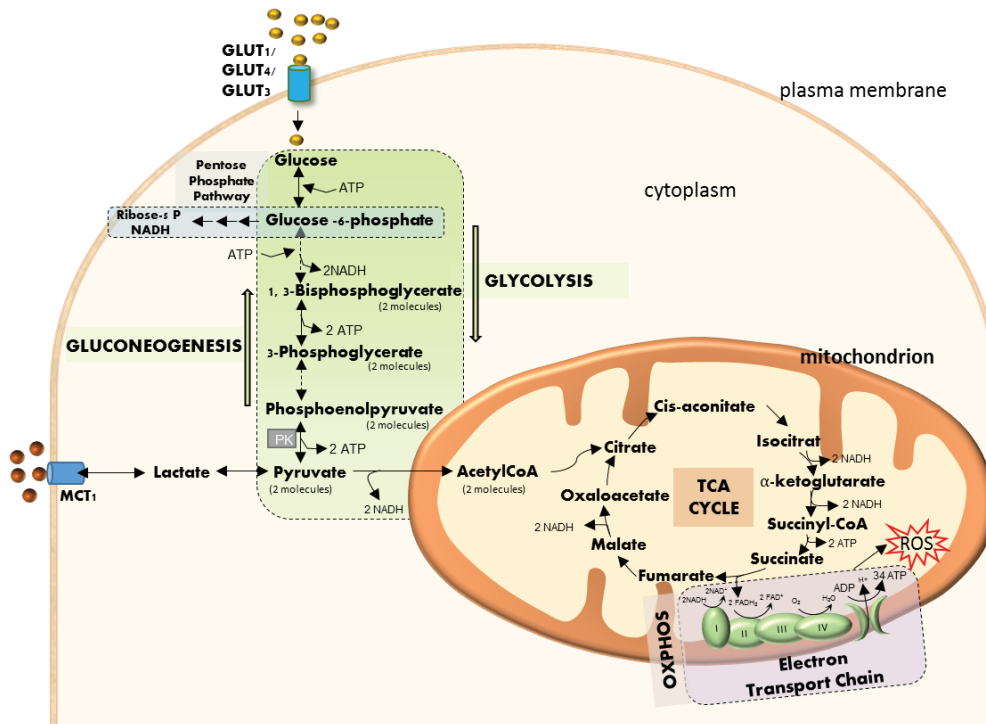


Figure 1: Energy metabolism

Glycolysis: one molecule of glucose forms 2 molecules of pyruvate. This mechanism is cytoplasmic and generates 2 molecules of ATP and 2 NADH. **Gluconeogenesis** is the generation of glucose from pyruvate. **Krebs cycle or TCA (tricarboxylic acid cycle)** is happening inside the mitochondria. Pyruvate enters into the mitochondria and forms AcetylCoA and NADH. 2 molecules of Acetyl CoA (per glucose molecule) are oxidized to CO₂, releasing different chemical energy during the process such as: 2 ATP, 6 NADH, 2 FADH₂. **Oxidative phosphorylation (OXPHOS)** is also a mitochondrial process performed by the electron transport chain. It uses the NADH and FADH₂ produced by TCA cycle and generates up to 34 ATP molecules. ROS, Reactive Oxygen Species.

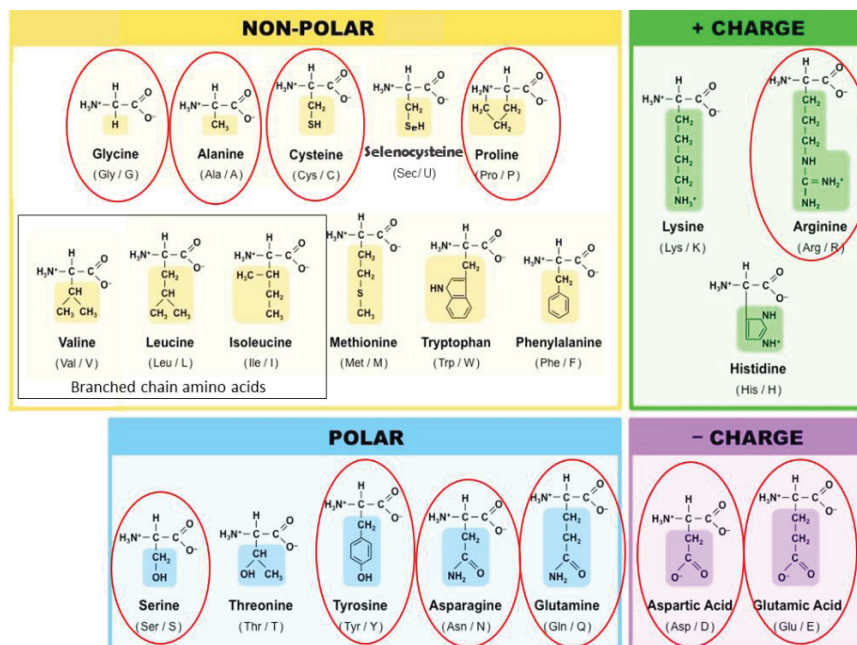


Figure 2: Amino acids

There are twenty-one amino acids grouped according to their side chains. In **yellow** are amino acids with non polar uncharged side chains, in **blue** are amino acids with polar uncharged side chains, in **green** are amino acids with electrically positive charged side chains and in **purple** with electrically negative charged side chains. There are eleven non-essential amino acids (synthesized by the body), **encircled in red**. The others are essential amino acids (obtained from nutrition), except for selenocysteine which is a rare, non-standard amino acid (modified from <http://ib.bioninja.com.au/standard-level/topic-2-molecular-biology/24-proteins/amino-acids.html>).

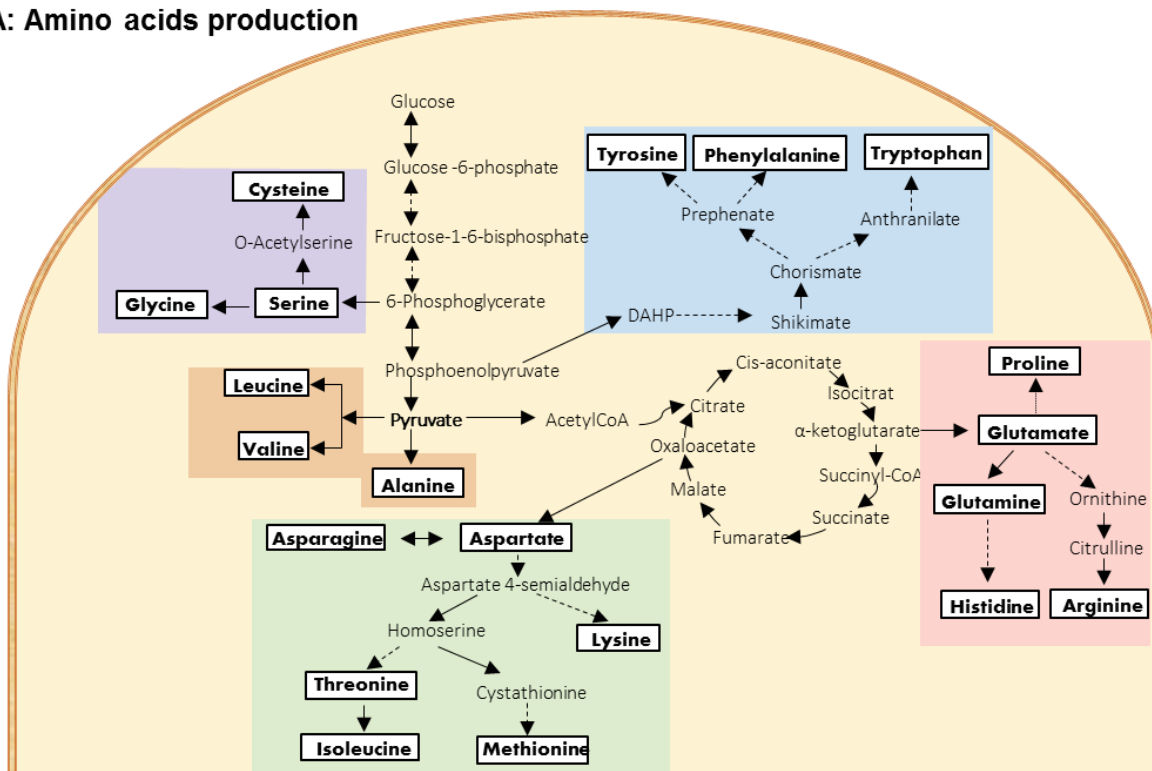
2. Energy metabolic reprogramming

Energy metabolism of the cells is very plastic and it is adjusted multiple times and by different manners during normal development. For example, during the first two days of mouse embryonic development, embryos can do more oxidative phosphorylation than glycolysis. When the blastocyst is formed, the oxygen consumption increases even more. But after blastocyst formation, cells undergo a metabolic switch leading to a large increase in their glycolytic capacities (Leese, 2012, 2015). Therefore, embryonic stem cells (ESC), which are pluripotent cells derived from the inner cell mass of blastocyst, are producing energy to maintain their rapid proliferation and self-renewal mostly by glycolysis (Varum et al., 2011). The metabolic balance between oxidative phosphorylation and glycolysis is therefore critical for the self-renewal status of the cells (Chandel et al., 2016) but also for their differentiation as blocking glycolysis induced myogenic differentiation whereas inhibiting oxidative phosphorylation impaired muscle stem cells differentiation (Bracha et al., 2010; Chung et al., 2007). Thus, mapping the metabolic pathways that are activated in early stem cells has begun to shed light on the respective contribution of glycolysis versus oxidative phosphorylation in the maintenance of pluripotency and cell fate commitment (Ochocki and Simon, 2013).

Deregulations of energy metabolism are associated to numerous human pathologies such as developmental diseases, metabolic disorders (e. g. diabetes) and cancers. In particular, Otto Warburg suggested in 1926 that energy metabolism is a key regulator of tumor formation (Koppenol et al., 2011). He showed that cancer cells switched from oxidative phosphorylation to glycolysis, even in presence of oxygen (Warburg, 1956). Since, energy metabolic reprogramming has been suggested as a key hallmark of cancer progression (Hanahan and Weinberg, 2011; Ward and Thompson, 2012). It has been shown in many different situations that cancer cells adapted their energy metabolism to the tumor microenvironment in order to fulfill the bioenergetic and biosynthetic needs for rapid cell proliferation (Biswas, 2015).

Therefore, there are striking similarities in metabolic reprogramming contributing to development or tumorigenesis. Abundant work described how metabolic adjustments modulate the supply of precursor metabolites for building blocks of the cells such as nucleotides, lipids and amino acids depending on cell needs. Likewise, external stimuli and/or signaling pathways involved in these metabolic adaptations are more and more documented. In particular, the mTOR signaling pathway, composed of mTORC1 and mTORC2 complexes, is a major regulator of cell growth as it governs most anabolic and catabolic processes depending on nutrients availability from the environment (see chapter III.A.1.2.1) (Laplante and Sabatini, 2012; Sabatini, 2017). Interestingly, intermediary metabolites also modify metabolic fluxes through regulation of metabolic pathways. This is the case for amino acids, the basic structural units of proteins, now known to control non-proteinogenic processes (mTOR activity

A: Amino acids production



B: Amino acids catabolism

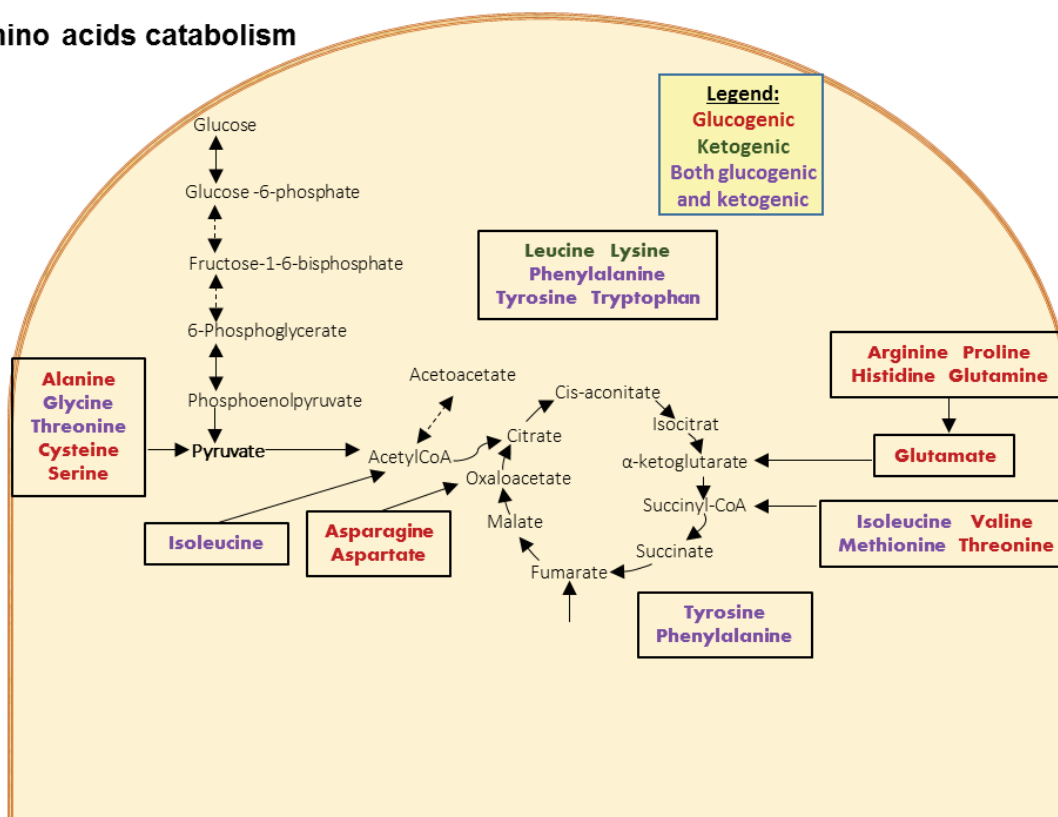


Figure 3: Amino acid metabolism

- Metabolic pathways essential for amino acid synthesis.
- Amino acids degradation. Glucogenic amino acids are the amino acids whose degradation form metabolic intermediates give rise to glucose via gluconeogenesis. Amino acids which are forming ketone bodies such as acetoacetate and are not involved in gluconeogenesis are named ketogenic. All amino acids are glucogenic, except leucine and lysine which are only ketogenic.

being one such example) involved in various cell fate such as self-renewal, differentiation and growth (Ito and Suda, 2014; Meijer, 2003; Ryall et al., 2015).

3. Amino acids acting as metabolic regulators

There are 21 amino acids mainly classified depending on their electric charge or the presence of a hydrophobic chain. Apart from selenocysteine, 9 amino acids are obtained from nutrition and represent essential amino acids whereas the 11 others are synthesized by the body and are therefore called non-essential amino acids (Figure 2). Many enzymes are required for amino acid biogenesis and catabolism. Several non-essential amino acids such as serine, alanine, aspartate and glutamate are synthesized from metabolites that derive from glycolysis or mitochondrial citric acid cycle (Figure 3A). Others are generated by direct or indirect biochemical reactions from another amino acid. Among enzymes required for amino acid biosynthesis, transaminases, also known as aminotransferases, are the enzymes catalyzing a transamination reaction between an amino acid and an α -keto acid and a very recently growing literature supports their essential contribution to cell behavior (Table 1).

The first paragraph below describes the capacity of amino acids to monitor intrinsic energy metabolism. The second one is focused on amino acids as paracrine factors to regulate metabolism of neighboring cells, or even of distant organs via their transport through the bloodstream. Finally, in the last paragraph I present the role of amino acids in development and tumorigenesis. The following paragraphs briefly illustrate these 3 roles for amino acids based on specific and not exhaustive examples, with a special focus on transaminases.

3.1 Amino acids regulate intrinsic metabolism

As previously mentioned, amino acids are not only essential for protein synthesis but also for metabolic regulations either by modulating levels of metabolites and thus controlling metabolic fluxes or through their direct interaction with proteins such as metabolic enzymes or signaling proteins thereby modifying their activities.

Amino acids catabolism is essential to produce metabolites involved in several metabolic processes such as gluconeogenesis, TCA cycle as well as folate and methionine cycles (Figure 3B). Amino acids also regulate these processes indirectly by controlling different cytosolic/mitochondrial shuttles like the malate/aspartate one, which is important for mitochondrial NADH formation and therefore for mitochondrial respiration and ATP production (Lanoue et al., 1974; Lu et al., 2008; Meijer and Van Dam, 1974; Stein and Imai, 2012). Furthermore, amino acids dependent shuttles control other mechanisms such as lactate oxidation and pyruvate transport (Kane, 2014; Stein and Imai, 2012) (Figure 4). Moreover, in some cases amino acids act as compensatory mechanism. For example, alanine is essential for hepatic glucose production when the pyruvate transporter from cytosol to mitochondria is

Enzymes	Genes	Subcellular locations	Catalytic activity	Functions
Branched-chain aminotransferase (BCAT)	BCAT1	Cytoplasm Mitochondrion	L-leucine + 2-oxoglutarate <-> glutamate + 4-methyl-2-oxopentanoate	Catalyze the first reaction in the catabolism of essential branched chain amino acids leucine, isoleucine, and valine.
	BCAT2 isoform A	Mitochondrion	L-isoleucine + 2-oxoglutarate <-> (S)-3-methyl-2-oxopentanoate + L-glutamate	
	BCAT2 isoform B	Cytoplasm	L-valine + 2-oxoglutarate <-> 3-methyl-2-oxobutanoate + L-glutamate	
Phosphoserine Aminotransferase (PSAT)	PSAT1	Cytoplasm	3-phospho-L-serine + 2- α Ketoglutarate <-> 3-phosphopyruvate + L-glutamate	- Regulates the methyl donor S-adenosylmethionine
Aspartate Aminotransferase ASAT	GOT1	Cytoplasm Nucleoplasm	L-aspartate + 2-oxoglutarate <-> oxoglutarate + L-glutamate	<u>Controls:</u> <ul style="list-style-type: none"> - Levels of glutamate. Acts as a scavenger of glutamate in brain neuroprotection. - Hepatic glucose synthesis during development - Adipocyte glyceroneogenesis
	GOT2	Mitochondrion Cell membrane		<ul style="list-style-type: none"> - Regulates metabolite exchanges between mitochondria and cytosol - Facilitates cellular uptake of long-chain free fatty acids.
Glutamine Fructose-6-Phosphate Transaminase (GFAT)	GFPT1	Nucleus Nucleoli	L-glutamine + D-fructose 6-phosphate <-> L-glutamate + D-glucosamine 6-phosphate	<ul style="list-style-type: none"> - Controls the flux of glucose into the hexosamine pathway. - Regulates N- and O-linked glycosylation of proteins.
	GFPT2	Vesicles		
Alanine Aminotransferase (ALAT)	Glutamic-Pyruvic Transaminase 1 (GPT1)	Cytoplasm	pyruvate + L-glutamate <-> L-alanine + 2-oxoglutarate	Regulates: <ul style="list-style-type: none"> - cellular nitrogen metabolism - liver gluconeogenesis
	GPT2	Mitochondrion		
Alanine-Glyoxylate Aminotransferase (AGXT ou AGT) ou Serine-Pyruvate Aminotransferase (SPT)	AGXT1	- Predominantly localized in peroxisome - Mitochondrion	glycine + pyruvate <-> glycoylate + alanine	Metabolize dimethylarginine which inhibits nitric-oxide synthase (the mechanism by which kidney regulates blood pressure).
	AGXT2	Mitochondrion	L-serine + pyruvate <-> 3-hydroxypyruvate + L-alanine	

Table 1: Aminotransferases and their activities.

Aminotransferases or transaminases are enzymes able to transfer nitrogenous groups between an amino acid and an α -keto acid. This list of aminotransferases is not exhaustive, there are 101 enzymes presented on ExPASy database. Data obtained from GeneCards Human Gene database.

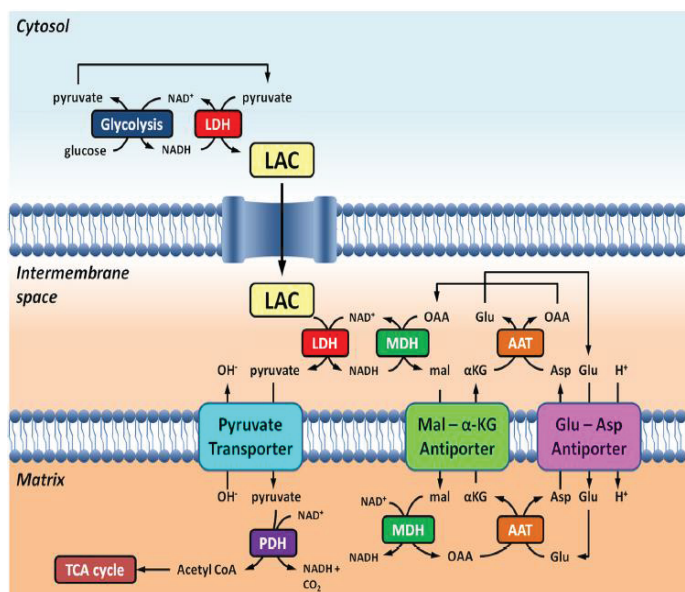


Figure 4: Lactate oxidation and malate-aspartate shuttle

Lactate (LAC) is transported to mitochondria where it is oxidized to pyruvate by lactate dehydrogenase (LDH). Amino acids such as glutamate (Glu) and aspartate (Asp) regulate NAD^+ regeneration via different cycles such as malate (Mal) - aspartate cycles. MDH, malate dehydrogenase; AAT aspartate-aminotransferase; PDH, pyruvate dehydrogenase; α KG, alpha-ketoglutarate; OAA, oxaloacetate (Kane, 2014).

deficient. Indeed, in this situation alanine is preferentially generated from cytosolic pyruvate via Alanine aminotransferase1 (ALAT1) and translocates into mitochondria. There, ALAT2, the mitochondrial transaminase, retransforms alanine into pyruvate which then supplies the TCA cycle (McCommis et al., 2015).

Another metabolic regulation exerted by amino acids is through the control of metabolic enzymes such as Pyruvate Kinases. These kinases catalyze the last reaction of glycolysis and therefore control pyruvate levels. It has been shown that alanine and ATP are allosteric inhibitors of two isoforms of the pyruvate kinases (PK) family (PKM2 and PKL) whereas they are not affecting PKM1 isoform (Ibsen and Marles, 1976; Llorente et al., 1970; van Veelen et al., 1977). Inhibition of pyruvate kinases is thereby essential to control the balance between glycolysis and the reverse metabolic pathway that is gluconeogenesis.

Amino acids also directly regulate mTOR pathway which controls cell metabolism such as amino acid biosynthesis, glucose homeostasis and lipid metabolism (Kim and Chen, 2004; Um et al., 2004). Recently it has been shown that mTOR signaling is activated at the lysosomal surface in a dependent manner of several amino acid concentrations such as leucine, glutamine and arginine (see also Chapter IV.2).

Altogether these data underline the role of amino acids as metabolic regulators by controlling metabolic fluxes, metabolic enzyme activities and the signaling mTOR pathway.

3.2 Paracrine and systemic activities of amino acids

Besides their capacity to regulate intrinsic metabolism, amino acids also act through a paracrine activity as signal molecules in cell-cell communication to regulate tissue homeostasis and organ functions. Furthermore, metabolites and in particular amino acids are secreted and enter the bloodstream thus having also systemic activities.

One example to illustrate this metabolic communication between cells is the glutamate-glutamine cycle that takes place in the nervous system between neurons and their adjacent glial cells. Glial cell metabolism is important for neuronal survival as glial cells uptake the glutamate secreted by neurons to convert it into glutamine to sustain neurotransmission. This mechanism requires ATP because glutamate transport into glial cells as well as its transformation into glutamine are ATP dependent processes (Figure 5 A). Therefore, to produce energy, glial cells uptake glucose and synthesize ATP but also lactate which is secreted to fuel neuronal mitochondria for TCA cycle. Hence, neurons are doing oxidative phosphorylation whereas glial cells are glycolytic. Lactate regulates also the expression of genes involved in synaptic plasticity (Magistretti and Allaman, 2015). In *Drosophila*, glial cells not only secrete lactate to fuel neuronal mitochondria but also alanine (Trevisiol and Nave, 2015; Volkenhoff et al., 2015).

Similarly to glial cells, Sertoli cells are also glycolytic cells which produce alanine and lactate from pyruvate and export them to germ cells by specific monocarboxylate transporters (MCTs) (Figure 5 B). This supply has an antiapoptotic effect on germ cells and is essential for their maturation (Oliveira and Alves, 2015; Rato et al., 2012).

Another example of metabolic communication with epithelial cells is the dialogue between Paneth cells and intestinal epithelial stem cells. Paneth cells are glycolytic cells that provide lactate to intestinal stem cells to sustain their enhanced mitochondrial oxidative phosphorylation (OXPHOS). Increased OXPHOS promotes mitochondrial reactive oxygen species (ROS) production which activates p38 MAP kinase, a regulator of intestinal stem cells function (Figure 2B) (Rodríguez-Colman et al., 2017).

Furthermore, paracrine regulation of energy metabolism through amino acids is also observed in tumor cells. Indeed, cancer cell metabolism is regulated by the tumor microenvironment, notably by the stromal cells (Figure 5 B). It has been shown recently that stroma-associated pancreatic stellate cells increase the OXPHOS of pancreatic ductal adenocarcinoma through the secretion of non-essential amino acids such as alanine (Sousa et al., 2016).

Moreover, amino acids have systemic activities. It has been suggested more than 45 years ago that alanine and lactate are synthesized by different tissues and released in plasma.

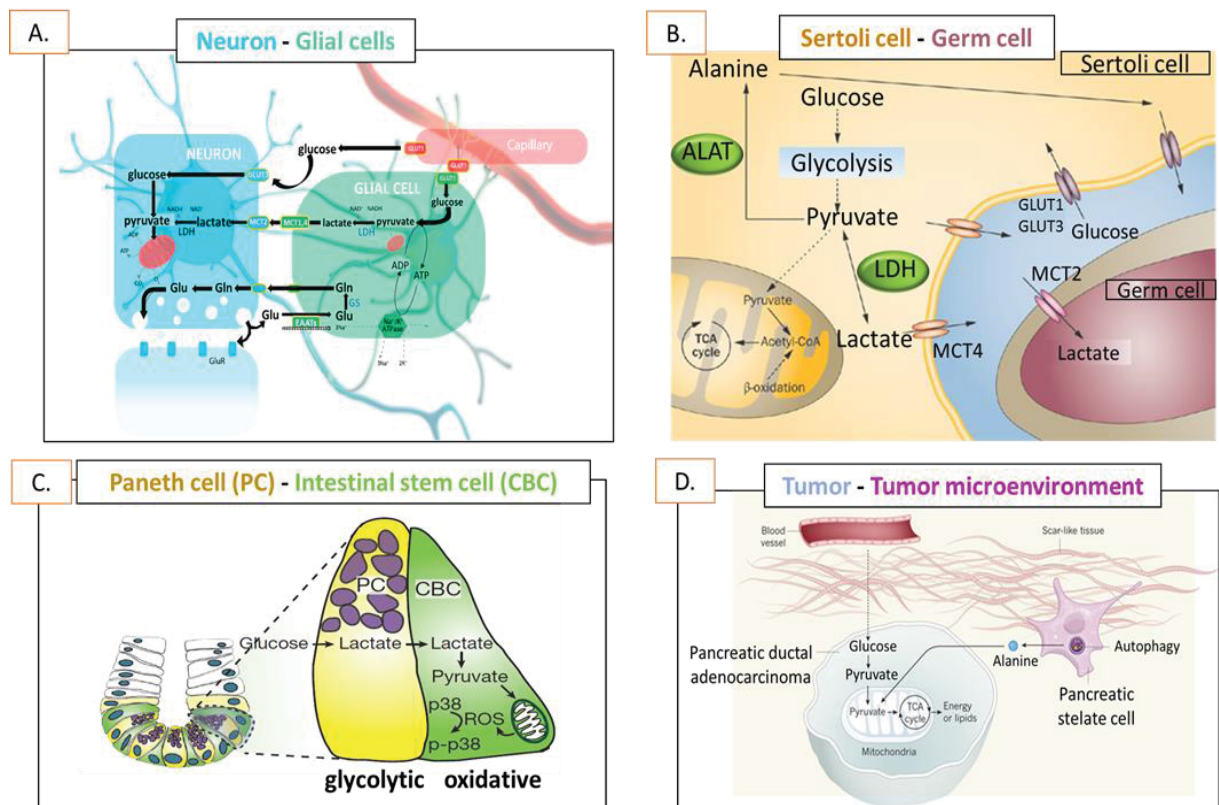


Figure 5: Metabolite shuttles between cells

- Glial cells regulate neuronal mitochondrial respiration and ATP production via lactate shuttle. Glial cells are also involved in recycling of synaptic glutamate through glutamate-glutamine cycling (Magistertti and Allaman, 2015).
 - Sertoli cells as glial cells are more glycolytic cells and regulate germ cell mitochondrial respiration and ATP production via lactate or alanine shuttles through MCT (Rato et al., 2012).
 - Paneth cells control Intestinal stem cell function through lactate shuttle which increases mitochondrial respiration, ROS production and p38 activity in intestinal stem cells (CBC) (Adapted from Rodriguez-Colman *et al.*, 2017).
 - Tumor microenvironment regulates tumor cell energy and lipid production through amino acids and most notably alanine shuttle (Adapted from Kamphorst and Gottlieb, 2016).
- GLUT, glucose transporter; LDH, lactate dehydrogenase; MCT, monocarboxylate transporters; GS, glutamine synthetase; GLS, glutaminase; EAAT, excitatory amino acid transporters; ALAT, alanine aminotransferase. p-p38, phospho-p38, ROS, reactive oxygen species.

For example, alanine and lactate are released by muscle cells into the blood circulation and subsequently enter into the liver where they sustain gluconeogenesis and promote urea cycle (Figure 6A) (Felig, 1973; Felig et al., 1970). Consoli et al. suggested that muscle is the major source of plasma alanine and lactate in the fasting state in humans (Consoli et al., 1990).

Recently, scientists emphasized that lactate is much more abundant than glucose in circulating blood. Systemic lactate is a primary source of carbon for TCA cycle in all tissues except brain and muscle in fasted or fed mice as well as in tumors (Figure 6B) (Faubert et al., 2017; Hensley et al., 2016; Hui et al., 2017).

Collectively, these data demonstrate that the behavior of a cell and its energy metabolism depends in part on amino acids levels either intrinsically or locally available from the microenvironment. These regulations play an important role during both development and tumorigenesis.

3.3. Amino acids as regulators of cell fate

During the past years, it has been shown that metabolic pathways control cell fate and self-renewal partly through epigenetic reprogramming (Ryall et al., 2015). In particular, amino acid metabolism (synthesis and catabolism, Figure 3 A and B) regulates metabolic pathways and thereby modulates epigenetic changes necessary for stem cell properties (Table 2) (Kilberg et al., 2016; Shyh-Chang et al., 2013).

For example, threonine and glycine catabolism are essential for self-renewal and differentiation of embryonic stem cells by regulating methionine cycle. Methionine is transformed into S-Adenosyl Methionine (SAM), which is a methyl donor for numerous reactions (Locasale, 2013). Threonine and glycine degradation are essential for SAM activation and trimethylation of lysine 4 on histone 3 (H3K4). H3K4 trimethylation is associated with open chromatin and has been shown to be crucial for maintaining the pluripotency and proliferation of embryonic stem cells (Shyh-Chang et al., 2013; Wang et al., 2016, 2009).

Amino acid metabolism is not only a regulator of prenatal stem cells development but also of their postnatal development, including adult stem cell commitment (Table 2). One example is glutamine catabolism which is crucial for hematopoietic stem cell specification. The differentiation of hematopoietic stem cell into erythroid rather than myeloid lineage needs glutamine utilization for nucleotide biosynthesis. Thus, glutamine synthetase which transforms glutamate into glutamine is highly expressed during erythropoiesis (Oburoglu et al., 2014). So far, it is hard to point out a specific mechanism because amino acids involved in cell commitment seems to be stem cell type specific.

Interestingly, proliferating cells generate aspartate and alanine via transaminases, by using glutamine-derived nitrogen whereas in quiescent cells, transaminase expression and glutamine consumption are decreased leading to reduced levels of aspartate and alanine production (Figure 7 and Table 2).

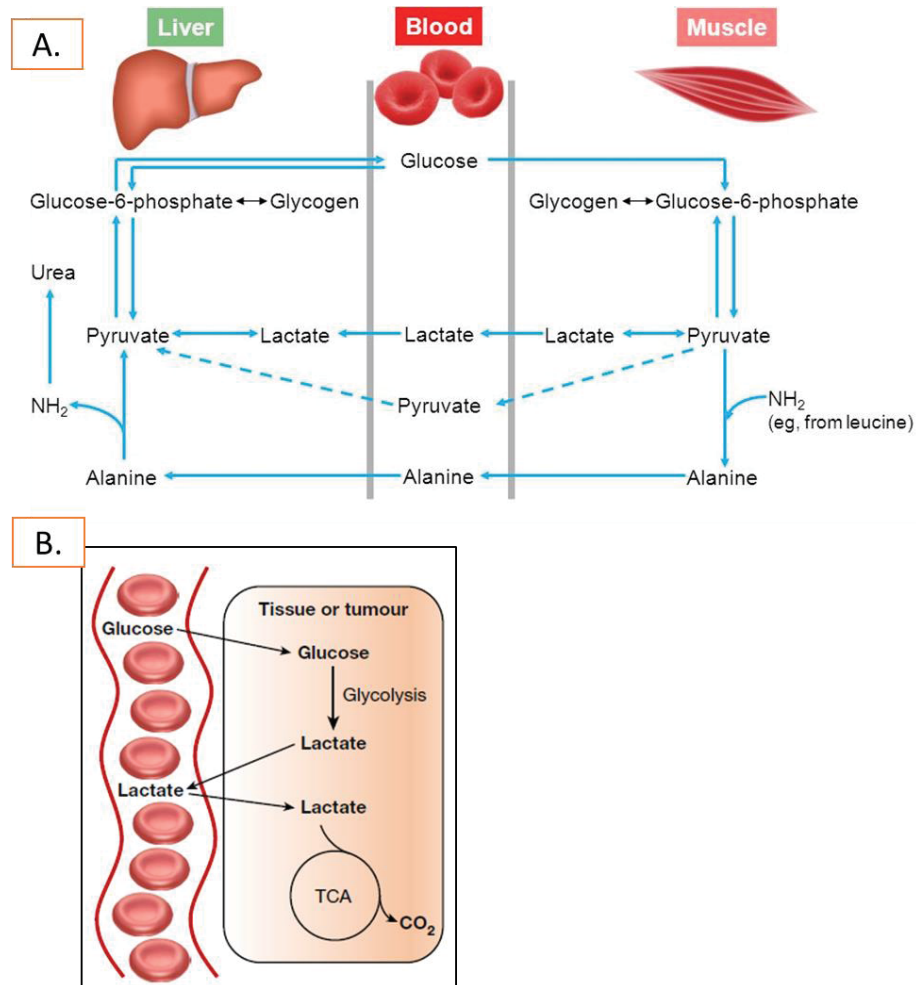


Figure 6: Systemic activity of amino acids

A. Glucose-alanine cycle (Cahill cycle) and glucose –lactate cycle (Cori cycle) between liver and muscle are important for hepatic gluconeogenesis and urea cycle (Berg JM et al., 2002). NH_2 ; amino functional group.
B. Circulating lactate as major TCA substrate in tissues and tumors (Adapted from Sheng Hui et al., 2017).

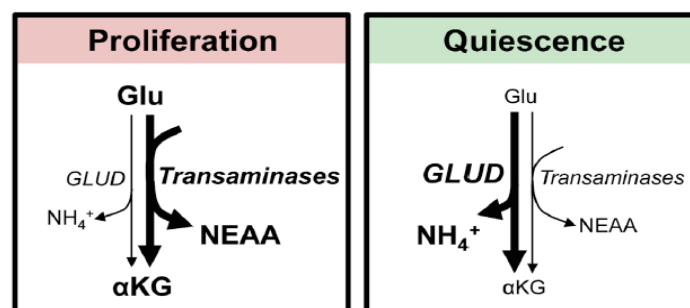


Figure 7: Amino acids metabolism coordinates the balance between proliferation and quiescence.

Glutamate metabolism is different in proliferated cells compared to quiescent cells. Proliferative cells are characterized by increased transaminase expression, increased NEAA synthesis and low GLUD expression. In opposition, GLUD is induced in quiescent cells and transaminases and NEAA expression are decreased. Glu, glutamate; GLUD, glutamate dehydrogenase; NEAA, non-essential amino acids; αKG , α Ketoglutarate. (Coloff et al., 2016).

These differences partly result of mTOR activity which increases transaminases expression and decreases glutamate deshydrogenase expression, favoring non-essential amino acids production (Coloff et al., 2016).

As cancer cells are highly proliferative, it is possible to limit their growth by regulating amino acid levels (Lorincz and Kuttner, 1965; Lorincz et al., 1969). Coloff et al. showed that most highly proliferative tumors depend on glutamine anaplerosis and generate non-essential amino acids such as alanine, serine and aspartate via transaminases (Coloff et al., 2016). Several other studies also suggest that alanine is accumulating in cancer cells, its concentration being directly proportional with tumor malignancy (Table 2) (Cornel et al., 1993; Tessem et al., 2008; Ziegler et al., 2001).

Strikingly, alanine is also accumulated in human Hereditary Sensory and Autonomic Neuropathy type 1 (HSAN1) and metabolic syndromes associated with peripheral neuropathies (Hla and Dannenberg, 2012). In these pathologies alanine is responsible for deoxysphinganine formation, a neurotoxic sphingolipid (see Table 2 and Discussion Figure 2).

Thus, amino acids are acting as signaling components to regulate stem cell renewal and differentiation as well as to increase proliferation and tumor growth. They also control neuronal survival through deoxysphingolipids formation. Therefore, knowing how the levels of non-essential amino acids are regulated and how they act in cells represent a first step for prevention of developmental diseases or cancer therapy. Moreover it could allow novel approaches to reverse pathological phenotypes associated with deoxysphingolipids.



As a general conclusion to this first chapter, metabolism exploration is recently experiencing a renewed interest. First, because there are striking similarities between the metabolic shifts observed in normal development and those characterized in tumors. Second, amino acids regulate intrinsic energy metabolism and control energy metabolism of neighboring cells or distant organs due to their paracrine and/or systemic activities as signal molecules during cell-cell communication. Third, through all their actions as signal molecules, amino acids regulate stem cell development, cell fate and tumorigenesis. However, metabolic reprogramming during development remains poorly identified and there is still a lot to explore concerning the drivers and regulators. Particularly the role of metabolic remodeling in neural crest cells (NCC) is poorly understood. Thus, during my PhD, I studied metabolic regulations during NCC fate. Therefore, in the next Chapter, I will describe the NCC formation and differentiation and I will present some human pathologies due to NCC defects.

	Cell types	Amino acids metabolism	Metabolic enzymes expression	Cell functions regulated by amino acids	Signaling pathways regulated by amino acids	Reference
Normal	Embryonic stem cells	<u>Humans</u> Methionine catabolism	+++ Methionine adenosyltransferase	Pluripotency and proliferation	Epigenetic processes	Shiraki, N. et al., 2014 (Cell Metabolism)
		<u>Mice</u> Proline catabolism	+++ Proline oxidase			Comes et al., 2014 (Stem Cell Reports)
		Threonine And Glycine catabolism	+++ Threonine dehydrogenase +++ Glycine decarboxylase			Wang et al., 2009, Shyh-Chang et al., 2013. (Both Science)
	Mesenchymal stem cells	<u>Humans</u> Arginine catabolism Alanine, glutamate and glycine synthesis	Not reported	Proliferation and differentiation	Not reported	Choi et al., 2007 (Korean J. Chem. Eng.); Higuera G.A. et al., 2012 (Tissue engineering).
Cancer	Hematopoietic stem cells	<u>Humans & Mice</u> Glutamine catabolism	+++ Glutamine synthetase	Specification and commitment	Nucleotide biosynthesis	Oburoglu et al., 2014 (Cell stem cell)
	Epithelial cell line (MCF10A)	<u>Humans</u> Alanine, serine and aspartate synthesis	+++ Glutamate-dependent transaminases --- Glutamate deshydrogenase	Proliferation	Not reported	Coloff et al., 2016 (Cell Metabolism)
	Pancreatic cancer cells	<u>Humans</u> Serine synthesis	+++ Phosphoserine aminotransferase1	Tumor growth	Epigenetic processes	Kottakis et al., 2016 (Nature)
	Breast tumors	<u>Humans</u> Alanine, serine and aspartate synthesis	+++ Aspartate aminotransferase 1 (ASAT1) +++ Alanine aminotransferase 2 (ALAT2) +++ Phosphoserine aminotransferase 1 (PSAT1) --- Glutamate deshydrogenase (GDH)	Proliferation	Not reported	Coloff et al., 2016 (Cell Metabolism)
Peripheral neuropathies	Prostate cancer cells	<u>Humans</u> Alanine synthesis	Not reported	Tumor growth	Not reported	M Tessem et al., 2008 (Magn Reson Med)
	Lung cancer cells	<u>Humans</u> Alanine synthesis	+++ Alanine aminotransferase	Tumor growth	Not reported	G.Beuster et al., 2011 (Journal of Biological Chemistry)
	Hereditary sensory and autonomic neuropathy type 1	<u>Humans & mice</u> Alanine catabolism	Mutated serine palmitoyltransferase	Neuronal survival in peripheral nervous system	Deoxysphinganine formation (neurotoxic)	Garofalo et al., 2011 (The Journal of Clinical Investigation)
	Metabolic syndromes like diabetes	<u>Humans & mice</u> Alanine catabolism	Mutated serine palmitoyltransferase	Neuronal survival in peripheral nervous system	Deoxysphinganine formation (neurotoxic)	Hla and Dannenberg, 2012 (Cell Metabolism) Othman A et al., 2015 (BMJ Open Diabetes Research and Care)

Table 2: Representative examples of amino acids as signaling molecules for cell proliferation, differentiation and survival

II. NEURAL CREST CELLS

1. Neural crest cells formation

Neural crest cells (NCC) are embryonic multipotent cells specific to vertebrates, discovered by Wilhelm His in chick embryos in 1868 (Hall, 2008). NCC originate during early embryogenesis from the neural plate border (Figure 8 A). NCC delaminate through an epithelial to mesenchymal transition from the dorsal part of the neural tube (Figure 8 C) (Duband et al., 1995). Then NCC migrate throughout the embryo to reach their target organs where they differentiate into multiple cell types (Figure 8 D, E) (Acloque et al., 2009; Simões-Costa and Bronner, 2015). There are five NCC subpopulations depending on their localization along the anterior-posterior axis (Burns et al., 2000; Douarin and Kalcheim, 1999; Dupin and Sommer, 2012; Lumb et al., 2017):

- Cranial NCC arise anterior to somite 5 and give rise to melanocytes and head structures such as bone, cartilage and tendons.
- Cardiac NCC arise from somites 1 to 3 and give rise to melanocytes, vascular smooth muscles lining of the outflow tract and contribute to the aortic-pulmonary septum.
- Vagal NCC arise between somites 1-7 and form melanocytes as well as neurons and glia of the enteric nervous system.
- Trunk NCC arise posterior to somite 4 and differentiate into neurons of the sensory and sympathetic systems as well as into Schwann cells and melanocytes.
- Sacral NCC arise posterior to somite 28 and generate melanocytes, enteric neurons and glial cells.

Thus, not all NCC give rise to all derivatives since they have fate restriction depending on their anterior-posterior position along the neural tube. Melanocytes represent an exception since they are generated by all NCC subpopulations (Cichorek et al., 2013; Gilbert, 2000). Another exception concerns Schwann Cell Precursors (SCP) generated by cranial, vagal and truncal NCC subpopulations (see paragraph 2.3). During embryogenesis SCP differentiate into immature Schwann cells which constitute the first step of the Schwann cell lineage. Very recently it has been shown that SCP persist through adulthood and conserve the multipotency and high plasticity of NCC, being therefore able to generate several cell types during both embryogenesis and adulthood (Gargiulo and Mesones-Arroyo, 2017) (see paragraph 2.3).

In the past 150 years, studies of NCC were mostly based on various animal models (mouse, chick, quail-chick chimeras, frog, zebrafish) in order to understand NCC origin and destination, induction and specification, polarized migration, stem cell properties and functions upon differentiation into specific cell types (Theveneau and Mayor, 2012; Barriga et al., 2018; Dupin and Le Douarin, 2014; Milet and Monsoro-Burq, 2012).

Based on quail-chick chimeras, Le Douarin lab identified NCC contribution to head, heart and

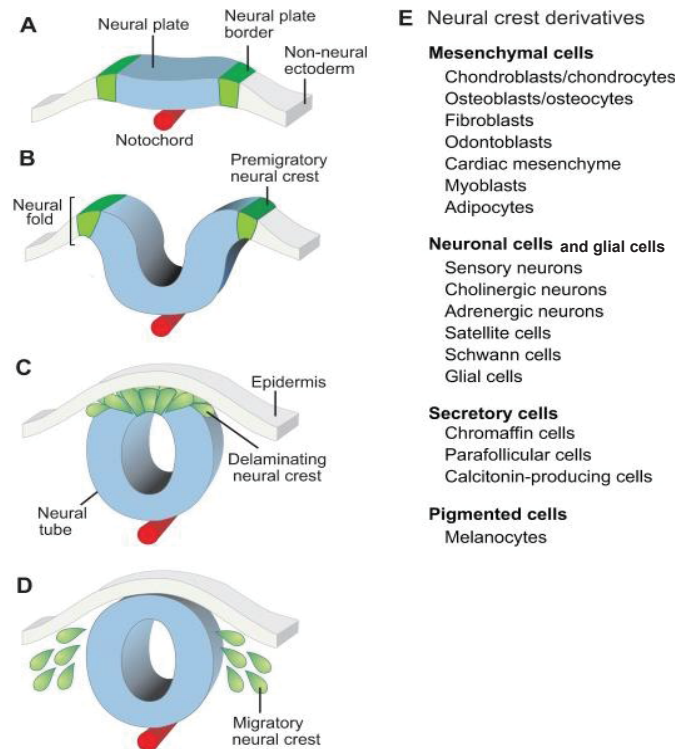


Figure 8: Neural crest formation and derivatives.

A. During neurulation, neuroectoderm forms the neural plate. Junctional tissue between neural plate and ectoderm corresponds to the neural plate border. B. During the process of neural tube closure, neural plate borders are specified into neural crest. C. After neural tube formation, neural crest cells undergo an epithelial-to-mesenchymal transition and delaminate from the neural tube. D. Neural crest cells then migrate towards their target organs where they differentiate into several derivatives. E. Non exhaustive list of neural crest derivatives (Simões-Costa and Bronner, 2015).

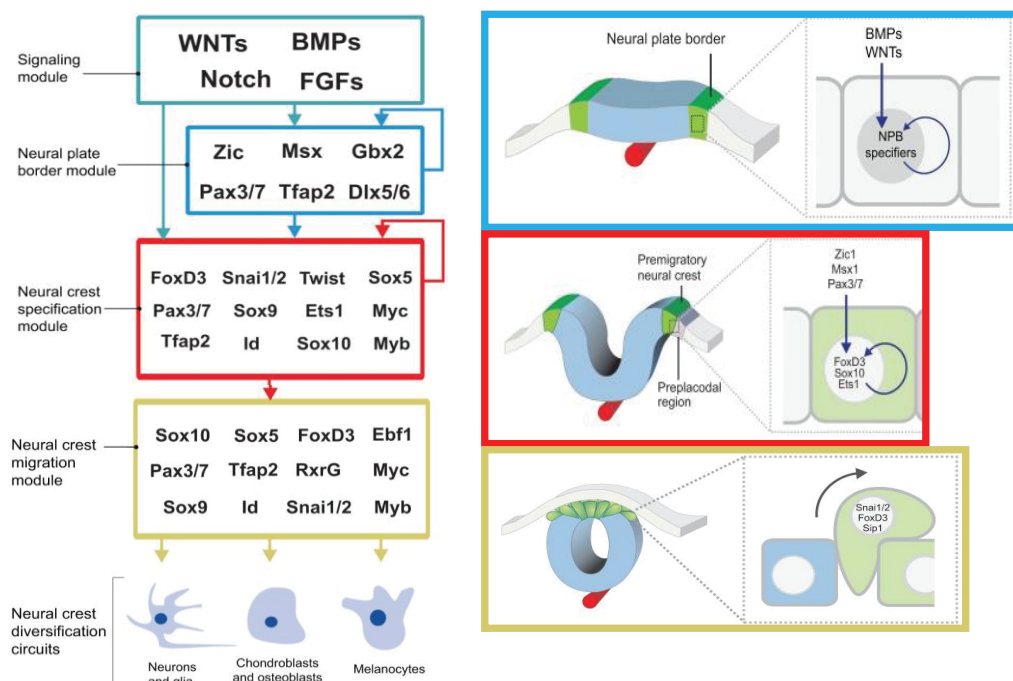


Figure 9: Molecular mechanisms which control neural crest ontogeny

Description of the gene regulatory network which controls neural plate border formation, neural crest specification and neural crest cells migration. Each gene module can auto-regulate itself and positively regulate the next gene module (Adapted from Simões-Costa and Bronner, 2015).

other organs (Le Douarin et al., 2004).

Single cell tracing of migratory NCC in mice has been obtained using the so-called Confetti model. This inducible multicolor Cre-reporter allowed to characterize the multipotency of trunk NCC *in vivo* (Baggiolini et al., 2015; Zurkirchen and Sommer, 2017) and to analyze facial vertebrate shaping (Kaucka et al., 2016). It has been demonstrated that while original NCC are totipotent, when they divide, they become tripotent and then bipotent progenitors before being committed to a specific cell type (Le Douarin et al., 2004). Besides, Bronner lab and others have shown that progressive development of neural crest is regulated by a neural crest gene regulatory network. This network is composed of a multisteps cascade of genes activation (Simões-Costa and Bronner, 2015). The first step corresponds to inductive signals such as *Wnt*, *Bone Morphogenetic Protein (BMP)*, *Notch* and *Fibroblast Growth Factor (FGF)*, which induce the formation of neural plate border. Then a second set of genes are activated such as *Paired box (Pax)*, *Zinc finger (Zic)* and *Homeobox (Msx)* genes. These neural plate border genes in a third step up-regulate expression of neural crest specifier genes such as *Sox10*, *Forkhead box gene D3 (FoxD3)* and *Snail family transcriptional repressor 2 (Snai2)*. Finally, these specifier genes activate in a fourth step downstream pathways essential for NCC migration (partly through cadherins expression and thereby their epithelial-to-mesenchymal transition) (Dady and Duband, 2017; Duband et al., 2015) as well as for NCC differentiation and selfrenewal capacity (Simões-Costa and Bronner, 2015) (Figure 9). NCC migration is also regulated by cell-cell interaction and guidance cues (Kulesa et al., 2010; Scarpa and Mayor, 2016). For example, NCC and placode cells, which are embryonic ectodermal cells that contribute to sensory organs, undergo a chase-and-run mechanism essential for their collective cell migration (Theveneau et al., 2013).

Although the cascade of molecular and cellular events that specify neural crest territories, orchestrate NCC delamination and guide their polarized migration throughout the embryo has been extensively explored, the contribution of metabolic regulations to NCC formation has received less attention to date. To our knowledge the only study that analyzed the metabolism in NCC was done by Monsoro-Burq lab. They revealed that during NCC specification *pfkfb4* (6-phosphofructo-2-kinase/fructose-2,6-bisphosphatase 4) which encodes a glycolytic enzyme, is upregulated and controls NCC migration, in *Xenopus laevis*, through the regulation of both AKT signaling and glycolysis (Figueiredo et al., 2017). Moreover, inactivation of PFKFB4 in *Xenopus laevis* leads to craniofacial malformations (Figueiredo et al., 2017).

In the next paragraphs, I will further detail the origin, fate and functions of cranial, trunk and vagal NCC, the three NCC subpopulations that I studied during my PhD.

2. NCC subpopulations and their derivatives

2.1. Cranial neural crest cells

Cranial NCC originate from different parts of the brain and differentiate into many cell types like melanocytes, cells of cranial nerve sensory ganglia, facial bones and cartilage, inner ear, cranial vault, parafollicular and Schwann cells (Trainor, 2005). Cranial NCC represent the only NCC subpopulation that can differentiate into skeletal tissues. Before 19th century, it has been thought that all the skeletal structures originate exclusively from mesoderm (Knight and Schilling, 2013). Later, tracing of cranial NCC showed that these cells directly participate to the formation of head skeleton as they give rise to premaxilla, maxilla, mandible, to a part of temporal bones, the incus and the malleus of middle ear, hyoid bone, thymus as well as cartilages such as thyroid and epiglottis (Dupin and Le Douarin, 2014; Lumsden et al., 1991; Santagati and Rijli, 2003; Schilling and Kimmel, 1994).

Many other experimental studies on mouse, zebrafish and amphibian confirmed the involvement of cranial NCC in craniofacial morphogenesis and showed how cranial NCC positional identity is regulated by homeodomain transcription factors (Hox and Otx2) and environmental signals such as BMP (bone morphogenetic proteins from the TGF β family), FGF (Fibroblast growth factor) and Shh (Sonic hedgehog) (Bhatt et al., 2013; Borchers et al., 2001; Creuzet et al., 2005; Donoghue et al., 2008; Minoux and Rijli, 2010; Nissen et al., 2003). Moreover, Mayor lab has recently underlined the importance of cell micro-environment for cranial NCC migration. They showed that the stiffening of the head mesoderm during early developmental stages of *Xenopus laevis* induces cranial NCC epithelial-to-mesenchymal transition as well as their collective migration (Barriga et al., 2018).

In conclusion, cranial NCC are multipotent stem cells essential for head formation. These cells are key for human face diversity regarding the shape, size and individual features. Thus, defects in cranial NCC development, migration and specification are responsible for many craniofacial malformations that I will present in more details in Chapter II.3.

2.2 Trunk, vagal and sacral neural crest cells

The trunk, vagal and sacral NCC generate sensory neurons and glial cells that are forming the peripheral nervous system (PNS) and melanocytes. PNS comprises nerves and ganglia localized outside the brain and spinal cord. Peripheral nerves are primary structures of PNS and contain axons of sensory and motor neurons, glial cells as well as blood vessels and connective tissues necessary for nutrients supply (Figure 11). The enteric nervous system (ENS) also belongs to PNS. ENS, one of the main autonomic nervous system (also named the second brain), innervates the gastrointestinal tract and governs digestive motricity (Furness and Stebbing, 2018).

2.2.1 Trunk NCC & peripheral nerves development

The specification of trunk NCC depends on the pathways they are following. Trunk NCC which migrate dorsolaterally differentiate into melanocytes. Trunk NCC that migrate ventrolaterally form sensory neurons of dorsal root ganglia. NCC that migrate more ventrally generate several cell types such as Schwann cells and sympathetic ganglia (Gilbert, 2000). Although trunk NCC are a major source of Schwann cells, other NCC such as cranial NCC also give rise to Schwann cells (Bronner and Le Douarin, 2012; Dupin and Sommer, 2012). Trunk NCC participate also to ENS formation, however their participation is very minor in comparison with vagal and sacral NCC (Heanue and Pachnis, 2007; Lake and Heuckeroth, 2013).

Trunk NCC fate is controlled by the path they are following during their migration but also depends on the time course of embryo development. As my PhD subject focused on Schwann cells, I will further detail the time course of Schwann cells-derived neural crest development.

The glial cell specification process is defined by two transitional steps. Firstly, NCC differentiate into Schwann Cell Precursors (SCP) and secondly SCP differentiate into immature Schwann cells. This second step is associated with an up-regulation of glial markers: Glial Fibrillary Acidic Protein (GFAP) and S100 calcium-binding protein β (S100 β) and a down-regulation of N-cadherin (Figure 10) (Balakrishnan et al., 2016; Jessen and Mirsky, 2005; Woodhoo and Sommer, 2008). In mice, SCP are specified at embryonic day 12 or 13 (E12/E13) and they differentiate at E15/16 into immature Schwann cells which persist until birth (Figure 10). Thus, Schwann cell maturation and myelination occurs after birth.

When the embryonic nerves are formed, they are exclusively composed of axon bundles and SCP derived from NCC. They do not have extracellular matrix, connective tissue and blood vessels (Woodhoo and Sommer, 2008). These neural crest-derived cells migrate along nerves through embryo tissues to reach distant target organs. Once NCC reach the developing nerves, they are specified into SCP (Adameyko et al., 2009). After E14, when SCP are already formed and the axons present in peripheral nerves are developing the first synaptic connections with their target tissues, the nerve enriched its composition with more cell types: endothelial cells and pericytes that surround the blood vessels and endoneurial fibroblasts (Jessen and Mirsky, 2005; Joseph et al., 2004; Woodhoo and Sommer, 2008). At this period of time there is also development of perineurial cells which are forming a protective sheath around the nerves. Inside the nerves, axons are grouped together and are surrounded by SCP (Figure 10). The interaction between these two cell types is essential for reciprocal regulation:

- first, SCP regulate neuronal survival. They are not required for motor and sensory neurons development or for guidance of axons at their target tissues. Instead they are necessary

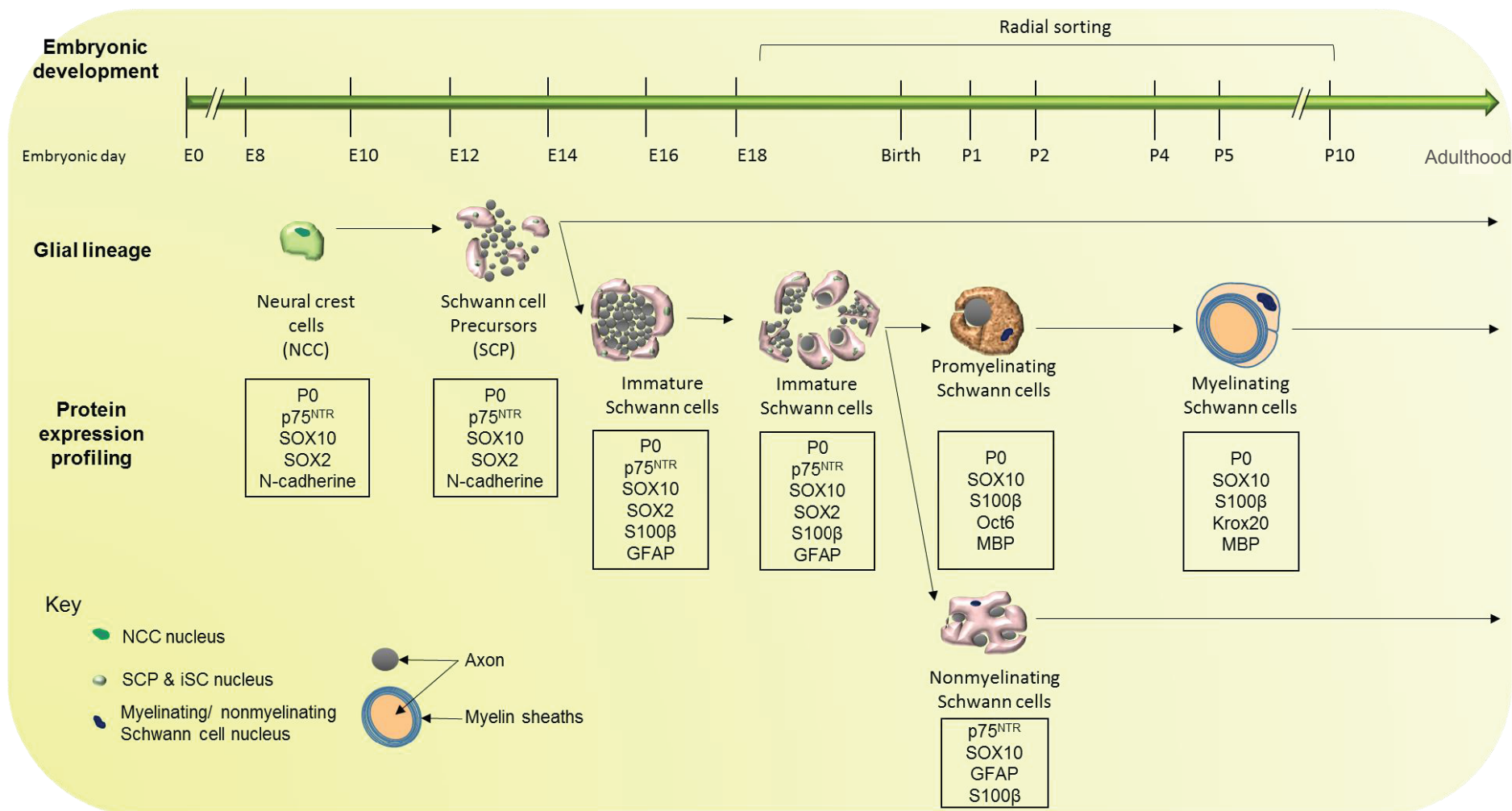


Figure 10: Time course of Schwann cell lineage & protein expression profiling

Neural crest cells committed to form Schwann cell precursors (SCP) are present in peripheral nerves at embryonic day 8.5 (E8.5). These cells differentiate into SCP at E12.5 and into immature Schwann cells (iSC) around E15.5. Only after birth immature Schwann cells mature into myelinating or nonmyelinating Schwann cells. The radial sorting starts before birth and finishes 10 days after birth (P10).

for neuronal maintenance because after axons reach their target organs, SCP loss triggers a massive neurodegeneration (Woodhoo and Sommer, 2008).

- second, neurons are also essential for SCP survival. The axon-derived factor neuregulin1 (NRG1) regulates SCP survival and induces a direct migration of these cells (Jessen and Mirsky, 2005; Woodhoo and Sommer, 2008).
- finally, the direct contact between axons and Schwann cells is important for the differentiation of SCP into immature Schwann cells (Adameyko and Lallemand, 2010; Adameyko et al., 2009; Joseph et al., 2004; Woodhoo and Sommer, 2008). NRG1 is able and sufficient to promote Schwann cells maturation, beside its capacity to regulate SCP survival and direct migration.

As mentioned, SCP are multipotent precursors. Indeed, they differentiate into immature Schwann cells as well as into fibroblasts (see paragraph 2.3, Figure 14). These two cell fates depend on the interaction of SCP with axons. SCP which are not in contact with axons are giving rise to endoneurial fibroblasts. However, when SCP interact with axons, they integrate axonal signals (such as NRG1 and Notch which inhibit their capacity to generate endoneurial fibroblasts) and differentiate into immature Schwann cells (Joseph et al., 2004; Woodhoo and Sommer, 2008). Thus, fibroblasts, in addition to Schwann cells and neurons, are neural crest derivatives, whereas other cells found in nerves (perineurial cells, pericytes and endothelial cells) are not.

Before birth, immature Schwann cells change their morphology and develop long cytoplasmic extensions that promote axon defasciculation. Axons with a large diameter ($>1\mu\text{m}$) undergo radial sorting and are surrounded by one immature Schwann cell destined to become a myelinating Schwann cell (Figure 10). In this case, the axon-Schwann cell interaction is one to one. Axons with smaller diameter are intended to remain un-myelinated and are in contact with an immature Schwann cell committed to become non-myelinating Schwann cell. In this case, the axon-Schwann cell relationship is several neurons for one non-myelinating Schwann cell. Thus, the radial sorting is an embryonic process that happens before Schwann cell maturation into myelinating and non-myelinating cells and continues until 10 days after birth (P10) (Figure 10) (Balakrishnan et al., 2016; Feltri et al., 2016; Woodhoo and Sommer, 2008). Moreover, the temporal molecular expression profile of each cell type in the Schwann cell lineage was characterized in different studies although these observations remain controversial. Therefore, in Figure 10 I mentioned only proteins that were common to several studies and/or that I used during my PhD for stem and glial lineage characterization (Figure 10) (Balakrishnan et al., 2016; Blake and Ziman, 2014; Jessen and Mirsky, 2005). The post-natal peripheral nerve organization is represented in Figure 11.

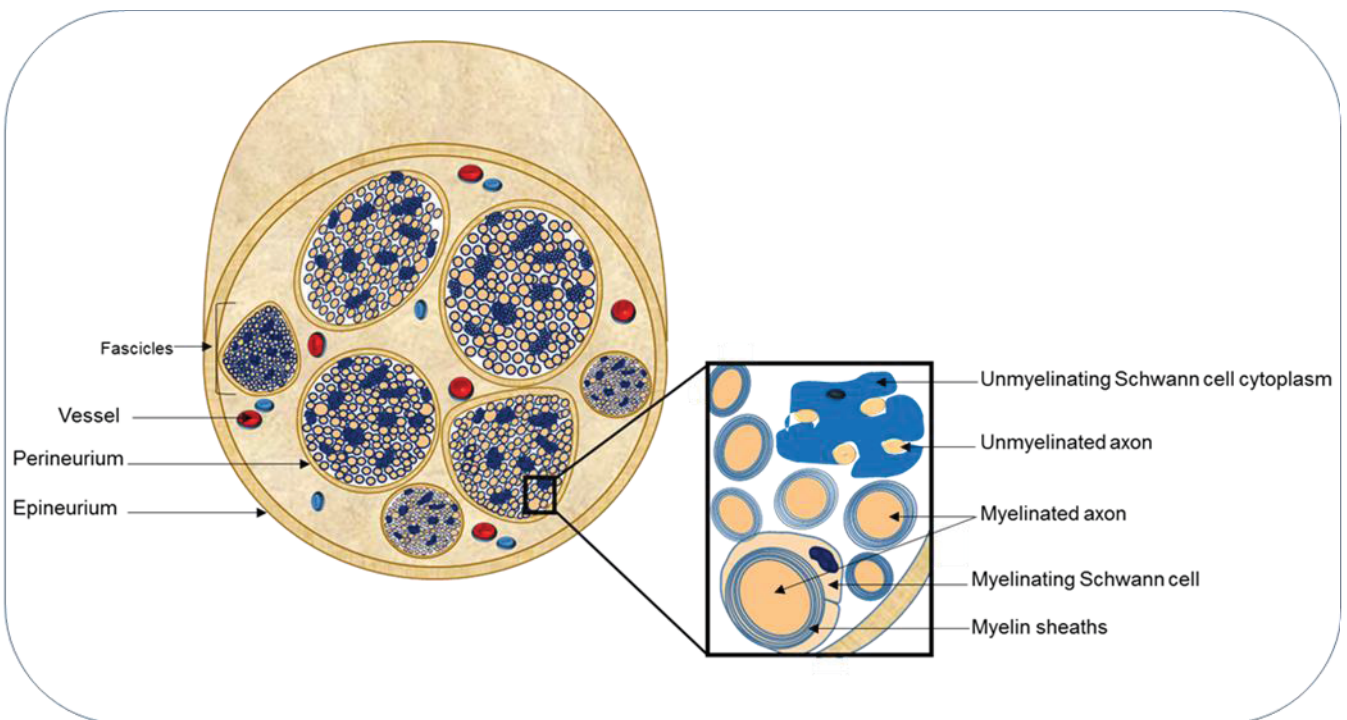


Figure 11: Peripheral nerve organization

Epineurium, a layer of fibrous connective tissue, is surrounding the nerve. In the nerve, axons are bundled into fascicles, surrounded by perineurium. The fascicles are composed of axons of motor and sensory neurons, myelinating and non myelinating Schwann cells. Within the nerves there are also fibroblasts, endothelial cells and pericytes. The ratio of myelinating Schwann cells to neurons is 1 to 1 whereas unmyelinating Schwann cells surround several axons of small diameter.

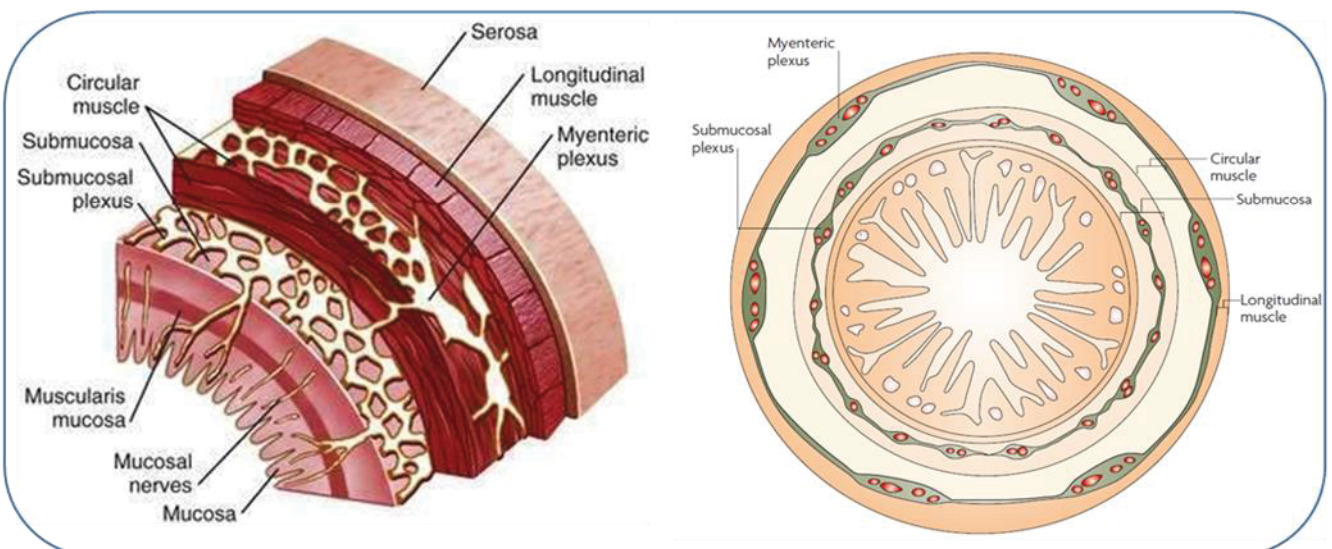


Figure 12: Enteric nervous system organization

Left image: schematic representation of the different layers composing the small intestine (Rodger A. Liddle, 2015). **Right image:** schematic representation of a transverse section of small intestine (Heanue and Pachnis, 2007). Enteric neurons and glial cells are organized in two circular plexi forming myenteric and submucosal ganglia. Myenteric plexus is a continuous network located from esophagus to anal sphincter, between the circular muscle and longitudinal muscle and is composed of parasympathetic and sympathetic fibers. Submucosal plexus contains only parasympathetic fibers derived from myenteric plexus and is localized, as its name suggests in the submucosa.

Thus, trunk NCC are differentiating into several cell types, including Schwann cells. Over the recent years, lots of studies analyzed Schwann cells development from their specification to myelination and characterized the molecular profiles of each stage of their glial lineage.

2.2.2. Vagal and sacral NCC & Enteric nervous system

Vagal NCC specification also depends on the pathways they are following. Vagal NCC that migrate to the pharyngeal arches and the heart take the dorsolateral pathway, while the cells that take the ventral pathway are forming the enteric nervous system (ENS). Vagal NCC are the most abundant source of ENS precursors and are colonizing the rostral part of the gut and secondly the more caudal part of the gut (Anderson et al., 2013; Le Douarin and Teillet, 1973; Pomeranz et al., 1991). Sacral NCC form neuronal and glial populations of ENS but their contribution is less important than vagal NCC (Burns and Le Douarin, 1998; Kapur, 1999). Indeed, these cells are mostly present in the distal part of the colon and rectum where they form up to 17% of enteric neurons (Burns and Le Douarin, 1998).

In human, the ENS is composed of 200-600 million neurons and glial cells which are grouped into many small ganglia distributed in 2 plexuses: the myenteric and submucosal plexuses (Figure 12) (Furness and Stebbing, 2018; Furness et al., 2014).

Contrary to the peripheral nerves, ENS is fully formed during embryonic development. At E9-E9.5 in mice (4 weeks in humans), pre-enteric-derived NCC colonize the foregut and migrate rostro-caudally (Figure 13) (Heanue and Pachnis, 2007; Lake and Heuckeroth, 2013). At the same time they migrate, they proliferate and start to differentiate. Indeed, they differentiate at E10 into neurons and later, at E11.5, into glial cells (the earliest enteric glial marker discovered so far is brain fatty acid-binding protein, BFABP) (Figure 13) (Lake and Heuckeroth, 2013). Thus, in ENS development, unlike in other nervous systems like the central nervous system, glial cells and neurons proliferate at the same time they differentiate (Heanue and Pachnis, 2007). The ENS is composed of sensory and motor neurons, interneurons and glial cells. At E13.5 (7 weeks in humans) NCC migration and contribution to myenteric plexus is complete and the pre-enteric-derived NCC undergo inward radial migration in the mucosa to form submucosal plexuses (Figure 13) (Lake and Heuckeroth, 2013).

Finally, sacral NCC colonize the gut in significant numbers only 4 days after vagal NCC had completed their migration along the entire length of the gut. These cells, as vagal NCC, contribute to the formation of both myenteric and submucosal plexuses (Burns and Le Douarin, 1998; Burns et al., 2000).

Enteric NCC survival, proliferation, migration and differentiation are controlled, among other signaling, by glial-derived neurotrophic factor (Gdnf) / Ret receptor (Sasselli et al., 2012). Gdnf is expressed in the gut mesenchyme and interacts with Ret and co-receptor Gdnf family

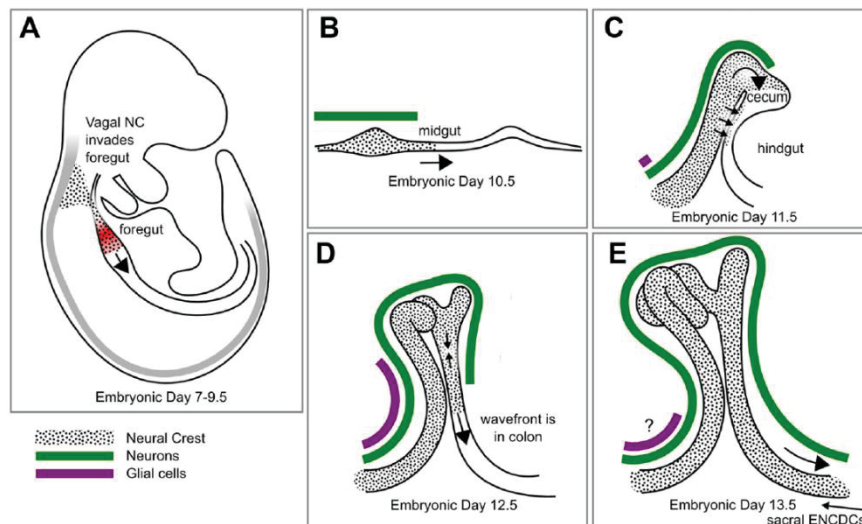


Figure 13: Mouse enteric nervous system development

Enteric nervous system is formed during embryogenesis. The myenteric plexus is formed before the submucosal plexus. Vagal neural crest cells are present into the foregut at embryonic days 7-9.5 and are forming the myenteric plexus. These cells migrate and differentiate in neurons at around E10 –E10.5 and in glial cells at E12-E12.5. At E13.5 they finish their migration and sacral neural crest cells are undergoing an inward migration in order to form the submucosal plexus (Lake and Heuckeroth, 2013).

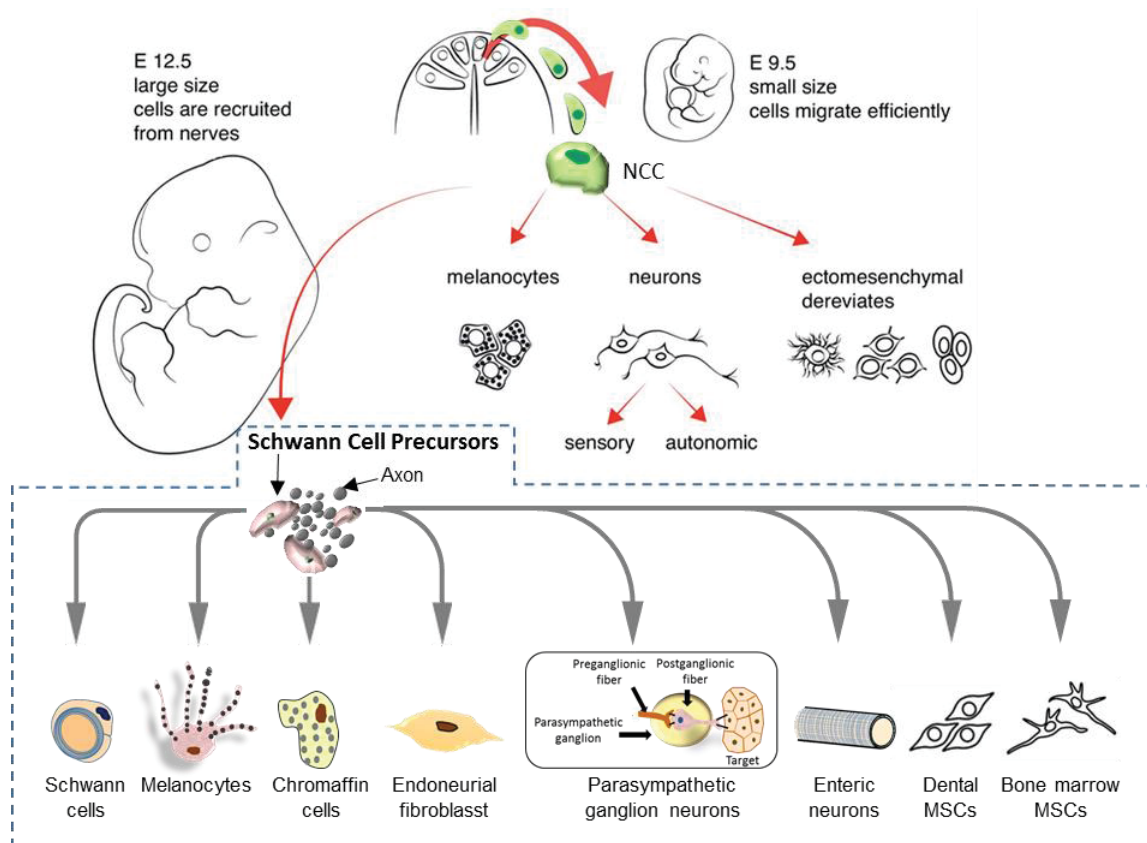


Figure 14: Multipotency of Schwann cell precursors

Neural crest cells (NCC) are multipotent cells which migrate and differentiate into many cell types such as melanocytes, neurons, ectomesenchymal derivatives and Schwann cell precursors (SCP). SCP are conserving the multipotency of NCC and therefore are giving rise to several cell types. By contrast to NCC, SCP do not have migratory properties, they are transported throughout the embryo by the nerves (Modified from Petersen and Adameyko, 2017).

receptor $\alpha 1$ (GFR $\alpha 1$) which are present at the surface of migrating enteric NCC. This pathway promotes cell differentiation required for the formation of ENS during normal development (McKeown et al., 2017; Taraviras et al., 1999). On the contrary, Endothelin 3- endothelin B receptor (EDNRB) signaling blocks the differentiation of enteric NCC and increases the proliferation and maintenance of undifferentiated progenitors which are important for gut colonization during development (Bondurand et al., 2003, 2006; Sasselli et al., 2012). Endothelin 3 –EDNRB signaling regulates ENS ontogeny also through its interaction with other pathways like Gdnf/Ret (Sasselli et al., 2012), $\beta 1$ integrin pathway (Gazquez et al., 2016) or with Sox10 (Stanchina et al., 2006) which controls the expression of *Itgb1*, encoding for $\beta 1$ integrin (Watanabe et al., 2013).

Similarly to cranial NCC, enteric NCC undergo a collective migration regulated by complement anaphylatoxin C3a (Broders-Bondon et al., 2012, 2016). Complement is known for its role in immune system, as well as its chemotactic properties (Carmona-Fontaine et al., 2011). Enteric NCC express both the receptor C3aR and C3a. Secreted C3a by enteric NCC has a paracrine effect: it interacts with C3aR at the surface of neighbor enteric NCC and regulates their collective migration. Hence, C3a/C3aR co-attraction modulates gut colonization. Moreover, it has been proposed that this process is linked to N-cadherin signaling (Broders-Bondon et al., 2016).

To conclude, both vagal and sacral NCC participate to enteric nervous system formation by following specific migration pathways.

2.3 Schwann Cell Precursors

2.3.1 Embryonic Schwann Cell Precursors

As previously described, SCP derive from truncal and cranial NCC and give rise to immature Schwann cells at embryonic stages E15.5 (Jessen and Mirsky, 2005). Strikingly, it has been discovered that they also give rise to many other cell types and thereby constitute an amazing new population of embryonic and adult stem cells.

It has been first identified that SCP along nerves are also a source of melanocytes (Figure 14). The direct contact of SCP with axons, and more precisely the NRG1 signal delivered by axons, blocks the melanocytic fate and promotes immature Schwann cell development. However, expression of insulin-like growth factor (IGF) and platelet-derived growth factor (PDGF) by immature Schwann cells in absence of NRG1 signal, induces melanocytic differentiation of SCP in nerves (Adameyko et al., 2009, 2012).

This capacity of SCP to form melanocytes is evolutionary conserved: not only mammals develop nerve-derived melanocytes but also birds and bony fishes (Petersen and Adameyko, 2017).

Neurons also derived from SCP. Indeed, SCP migrate along developing preganglionic nerves and differentiate into both Schwann cells and parasympathetic neurons (Dyachuk et al., 2014; Espinosa-Medina et al., 2014).

It has long been known that SCP originate from truncal and cranial cells. Recently, it was shown that vagal NCC from somites 1 and 2 are also forming SCP which give rise to enteric neurons of the foregut. More precisely, the stomach and half of the esophageal nervous system originate from SCP which are migrating along vagus nerves (Espinosa-Medina et al., 2017). Interestingly, the involvement of vagus nerves into the formation of ENS was suggested in 1910 but it has been overlooked since then (Kuntz, 1910).

Finally, SCP multipotency passes far beyond their ability to differentiate into melanocytes, glial cells and neurons, as recently reviewed (Petersen and Adameyko, 2017).

Indeed, SCP generate (Figure 14):

- endoneurial fibroblasts during embryo development as mentioned previously (Joseph et al., 2004)
- bone marrow mesenchymal stem cells which specify hematopoietic stem cell niche functions (Isern et al., 2014)
- dental mesenchymal stem cells in the murine incisor (Kaukua et al., 2014).
- chromaffin cells in the medulla of the adrenal glands in mammals (Furlan et al., 2017).

Thus, during development, embryonic SCP conserve the multipotency profile of NCC. They travel along nerves and give rise to numerous cell types.

2.3.2 Adult Schwann Cell Precursors

In the last few years, it has been shown that SCP multipotency is not restricted to development. Indeed, SCP migrating across nerves also give rise to several cell types during adulthood (Petersen and Adameyko, 2017):

- adult SCP from nerves represent a cellular origin of melanocytes (Adameyko et al., 2009).
- adult SCP also differentiate into dental mesenchymal stem cells in mice incisor and promote the formation of odontoblasts and pulp cells (Kaukua et al., 2014).
- SCP invade the submucosal region of the small intestine alongside the extrinsic nerves and differentiate into neurons in the postnatal period, therefore promoting postnatal expansion of ENS (Uesaka et al., 2015).
- Sox2 positive Schwann cells, including SCP, are also important for regeneration of dermis after injury (Johnston et al., 2013). Moreover, during mouse digit tip regeneration, SCP migrate into the injured zone and induce mesenchymal cell proliferation and regeneration through paracrine secretion of oncostatin M and platelet-derived growth factor AA (PDGF) (Johnston et al., 2016).

- Finally, SCP are also essential to repair nerve injury. They differentiate into specific Schwann cells dedicated for nerve repair and form the Bungner band; these cells are necessary to direct axons inside the wounded region (Jessen and Mirsky, 2005; Jessen et al., 2015a, 2015b).

To conclude, in the last three years many studies underlined the existence of SCP into the nerves and their contribution to numerous cell types such as neurons, Schwann cells, mesenchymal stem cells and melanocytes during embryogenesis and adulthood (Figure 14). All these findings completely changed the vision about neural crest cells and peripheral nerves. We now know that peripheral nerves are structures which contain multipotent cells. Therefore, peripheral nerves could represent a niche for adult stem cells. Exploring the molecular mechanisms underlying SCP selfrenewal and differentiation is a topic of growing interest as SCP multipotency could lead to several potential clinical applications.

3. Neural crest cell defects

Neural crest cells (NCC) defects lead to complex human pathologies named neurocristopathies by R. Bolande in 1974. Perturbations in NCC ontogeny are also observed in other diseases called ribosomopathies, which are human pathologies due to defects in ribosomal biogenesis (Figure 15). These pathologies can result from germline mutations (e.g. CHARGE syndrome and Diamond blackfan anemia), from inappropriate micro-environment (e.g. Fetal alcohol syndrome), from age-related defects associating in particular somatic mutations (5q deletion syndrome).

3.1 Neurocristopathies

Neurocristopathies arise from NCC defects at different developmental stages, such as their formation, delamination, migration, differentiation and survival (Ross and Zarbalis, 2014; Trainor, 2014). These disorders include common human birth defects combining several defaults such as colon aganglionosis, craniofacial malformations (cleft lip/palate, sensorineural deafness, smelling defects), heart malformations, skin/hair pigmentation defects and for some patients, demyelination (Trainor, 2013) (Table 3). Some examples of these human pathologies are listed below.

Hirschsprung's disease (HSCR) is characterized by the lack of ENS in the distal colon (Butler Tjaden and Trainor, 2013; Ross and Zarbalis, 2014). In 80% of HSCR patients the aganglionosis is limited to rectum and sigmoid colon and in 20% of cases the aganglionosis is found also proximally to the sigmoid colon. Only 3 to 8 % of patients have a total colonic aganglionosis (Amiel and Lyonnet, 2001; Butler Tjaden and Trainor, 2013; Parisi, 1993). Several genes, which are known to be involved in NCC proliferation, migration, differentiation and survival, such as *SOX10*, *RET*, *GDNF* and *EDNRB* have been identified to regulate the

etiology of HSCR (Table 3) (Butler Tjaden and Trainor, 2013; Gazquez et al., 2016; Lecerf et al., 2014).

Waardenburg syndrome (WS) is divided in four types (Arias, 1971; Zaman et al., 2015):

- Types I (WS1) and II (WS2) are characterized by abnormal pigmentation and sensorineural deafness due to a partial or total loss of melanocytes (Arias, 1971; Etchevers et al., 2006; Ross and Zarbalis, 2014).
- Type III (WS3) includes all of the WS1 and 2 features in association with musculoskeletal abnormalities of the upper limbs (Table 3) (Alford and Sutton, 2011).
- Type IV (WS4) also named Waardenburg-Shah syndrome combines Waardenburg symptoms and Hirshprung disease (Inoue et al., 2004; Trainor, 2013). A subtype of WS4 is PCWH which includes a **P**eripheral demyelinating neuropathy, **C**entral dysmyelinating leukodystrophy, **W**aardenburg syndrome and **H**irschsprung disease (Inoue et al., 2004; Trainor, 2013).

Thus, PCWH patients have a deficiency of melanocytes, enteric neurons, Schwann cells and oligodendrocytes (Table 3).

CHARGE syndrome is characterized by different clinical features (Table 3) related to craniofacial malformations, heart defects, blindness, deafness and balance disorders (Harris et al., 1997; Issekutz et al., 2005; Pauli et al., 2017). Approximately 80% of CHARGE syndrome patients present heterozygous mutations in *CHD7* gene (Aramaki et al., 2006; Lalani et al., 2006; Sanlaville et al., 2006; Vissers et al., 2004). *CHD7* is a chromatin remodeling enzyme which uses the ATP produced by ATP hydrolysis to alter nucleosome structure in order to create DNA access (Eberharter and Becker, 2004; Narlikar et al., 2002; Sif, 2004). It controls nucleoplasmic and nucleolar genes transcription. Therefore, *CHD7* inactivation decreases the formation of 45S pre-rRNA, being therefore involved in CHARGE syndrome (Zentner et al., 2010).

Di George syndrome also known as velocardiofacial syndrome is due to chromosome 22q11.2 deletion (Van Nostrand and Attardi, 2014) which corresponds to over 35 genes (McDonald-McGinn and Sullivan, 2011). Due to this large number of genes involved, the phenotype is extremely variable even within families. The major phenotypic features are heart anomalies, palatal anomalies, immune deficiency and learning difficulties (Table 3) (McDonald-McGinn and Sullivan, 2011).

Even if numerous studies characterized the underlying molecular mechanisms responsible for these pathologies, there is so far no treatment or cure for these diseases. In order to foster our knowledge and prevention of these disorders, several mouse models reliably mimicking human neurocristopathies were generated and are presented in Table 4.

Disease	Incidence	Commonly causative genes	Clinical features	Treatment	References
Hirschsprung (HSCR) (OMIM 142623)	1/5000	<i>RET, GDNF, GFRA1, NRTN, EDNRB, ET3, ZFXH1B, PHOX2b, SOX10, and SHH</i>	Vomiting, anemia, chronic constipation and distension due to colon aganglionosis. 10% of HSCR can develop enterocolitis, fever and septicemia. Risk to develop medullary thyroid carcinoma	Surgical restriction of the aganglionic bowel.	▪ Butler Tjaden and Trainor, 2013 ▪ Vackavikova et al., 2012; ▪ Skába et al., 2006
Waardenburg I (OMIM 193500) and III (OMIM 148820)	1/40000	<i>PAX3</i>	Congenital sensorineural deafness, heterochromia iridis, skin and hair hypopigmentation, dystopia canthorum	No treatment	▪ Waardenburg, 1951; ▪ Tassabehji, 1992; ▪ Song et al., 2015;
Waardenburg Shah (WS4) (OMIM 277580)	1/500000	<i>SOX10, EDN3, EDNTB</i>	Abnormal pigmentation of the skin, heterochromia iridis, sensorineural deafness, aganglionic megacolon, chronic constipation, enterocolitis, intestinal pseudo-obstruction, inability to feed orally from the first few days of life	Surgical restriction of the aganglionic bowel. No treatment for Waardenburg syndrome symptoms.	▪ Inoue et al., 2014 ▪ Mahmoudi et al., 2013 ▪ Etchevers et al., 2006
PCWH (OMIM 609136)	1/1000000	<i>SOX10</i>	Sensorineural hearing loss, small cochlea, heterochromia iridis, anosmia, olfactory bulb agenesis, decreased submucosal and myenteric ganglia, intestinal pseudo-obstruction, genitourinary defects, hypopigmented skin and hair, central nervous system defects and peripheral nervous system anomalies such as demyelinating peripheral neuropathy and distal muscle weakness due to neuropathy. In some cases the patients risk to have heart arrhythmia	Coordinated multidisciplinary care for all the symptoms. Surgical restriction of the aganglionic bowel.	▪ Inoue et al., 2014 ▪ Trainor, 2013
Di George syndrome (OMIM 188400)	1/4000	22q deletion: e.g. <i>TBX1, DGCR8</i>	Facial defects, heart defects, thymic aplasia, cleft palate, feeding problems, hearing loss, hypocalcemia, immune deficiency, learning difficulties, renal anomalies, dental issues, ophthalmic anomaly. Some symptoms overlap with CHARGE syndrome	Involve many health care specialties. Blood transfusion, thymus transplantation, cardiac surgery.	▪ Van Nostrand and Attardi, 2014; ▪ McDonald-McGinn and Sullivan, 2011
CHARGE syndrome (OMIM 214800)	1/10000	<i>CHD7</i>	Retarded growth and development, facial paralysis, feeding problems, hearing loss, coloboma, genital hypoplasia, heart defects, airways problems like choanal atresia, immune deficiency, hypocalcemia, gastroesophageal reflux, chronic constipation	Involve many health care specialties. For airway problems may be necessary a tracheostomy, severe gastroesophageal reflux requires Nissen fundoplication and G tube insertion, severe hearing defects requires cardiac surgery etc.	▪ Pauli et al., 2017 ▪ Lalani et al., 2012 ▪ Bergman et al., 2011

Table 3: Description of some human neurocristopathies

All the data were also obtained from OMIM data base.

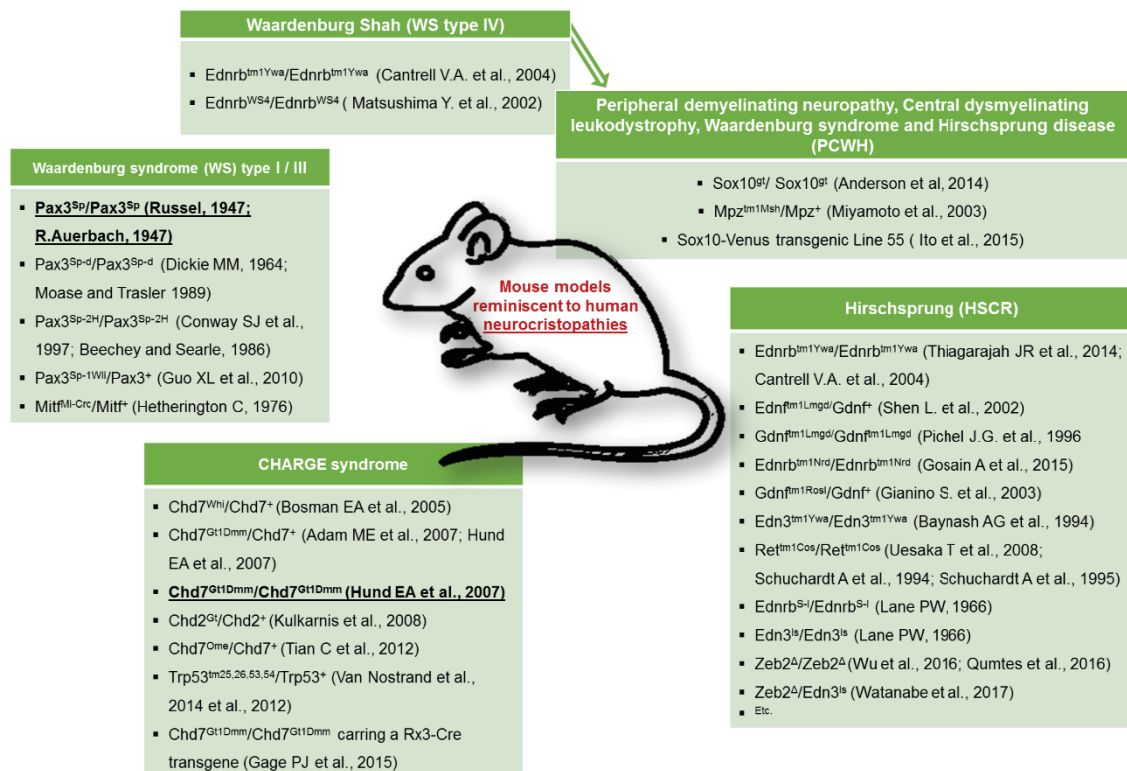


Table 4: Mouse models reminiscent to human neurocristopathies

Here are listed only some examples of murine models reminiscent to human neurocristopathies but there are many other models with neural crest cells defects. Di George syndrome mouse models were not included in this list because of their large number. In bold and underlined are the mouse models that have been used in studies presented in Table 8 (Introduction, Chapter III.B.4) to be mated to *p53* null mice to study if *p53* loss rescues the phenotype.

3.2 Ribosomopathies

Ribosomes represent a complex molecular system, containing proteins and RNA, essential for protein translation (Figure 16). They are important for polypeptide chain formation by promoting the interaction between amino acids in the order specified by messenger RNA. Ribosomes contain two components: the small 40S ribosomal subunit and the large 60S. The 40S subunit is composed of 18S rRNA and 32 Ribosomal Protein Small subunit (RPS). The 60S subunit contains 5S, 5.8S and 28S rRNA and 47 Ribosomal Protein Large subunit (RPL). The 40S and 60S subunits are then exported into the cytoplasm, where they assemble with mRNA to form the 80S ribosome critical for amino acids assembly (van Riggelen et al., 2010; Rodnina and Wintermeyer, 2009).

In this introduction, I focused on two of these pathologies among others presented in Table 5:

Treacher-Collins Syndrome is an autosomal dominant disease characterized by craniofacial malformations due to deficit of cranial NCC development (Trainor et al., 2009). It is hard to classify this syndrome as a neurocristopathy or ribosomopathy because it is caused by ribosomal biogenesis defects but it affects only neural crest cell derivatives (Figure 15).

In this manuscript, I have chosen to present it as a ribosomopathy. It is caused by *Tcof1* mutations. *Tcof1* encodes a nucleolar protein named Treacle which is essential for ribosomal RNA transcription and thereby for ribosomal biogenesis (Ross and Zarbalis, 2014; Trainor et al., 2009). When its expression is lost, many cranial neural cells die by apoptosis thereby leading to craniofacial malformations. TCS patients undergo speech therapy, hearing, orthodontic and ophthalmologic aid as well as multiple reconstructive craniofacial surgeries, which are rarely fully corrective.

Diamond black anemia (DBA) is another hereditary ribosomopathy characterized by craniofacial malformations as well as anemia (Narla and Ebert, 2010; Ross and Zarbalis, 2014). This inherited pathology is associated to mutations in different genes encoding ribosomal proteins of the large ribosome subunit (RPL15, RPL26, RPL35, RPL35a, RPLP2, RPS14) or the small ribosome subunit (RPS19) (Ross and Zarbalis, 2014). These mutations reduce the number of mature ribosomes which impact the quantity of erythroid progenitors in the bone marrow and of immature red blood cells hence leading to severe anemia. Mutations in ribosomal proteins also cause, as in TCS, deficiency of cranial NCC and thereby craniofacial defects (Narla and Ebert, 2010; Ross and Zarbalis, 2014).

In order to better understand the molecular mechanisms underlying these pathologies, a broad list of mouse models was generated (Table 6). They harbor phenotypes reminiscent of human ribosomopathies therefore allowing to explore therapeutic strategies.

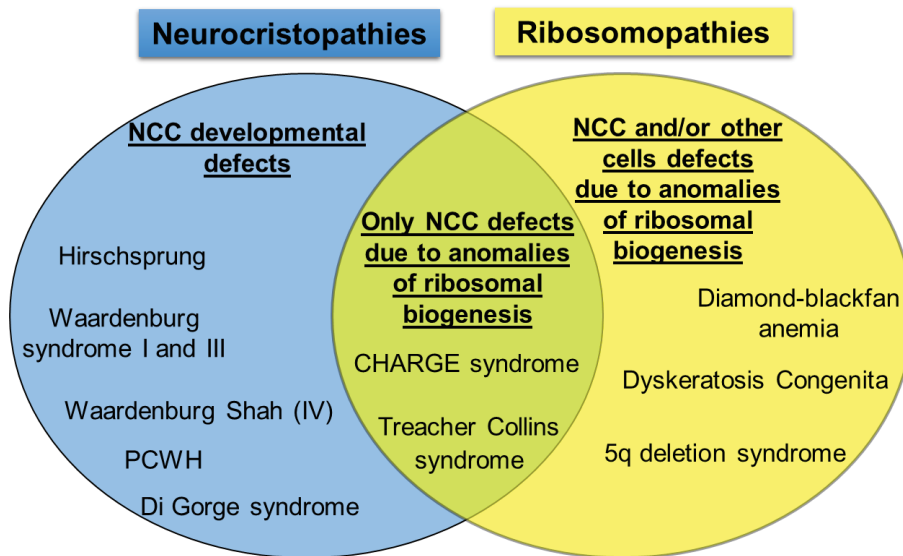


Figure 15: Examples of neurocristopathies and ribosomopathies

In **blue** are examples of neurocristopathies which are only due to Neural Crest Cells (NCC) defects. In **yellow** are examples of ribosomopathies due to ribosomal biogenesis that have several defects, among which NCC defects (except for 5q deletion syndrome). In **green** are pathologies which can be classified in both categories because they are due to both NCC defects (without other cell type defects) and ribosomal biogenesis defects.

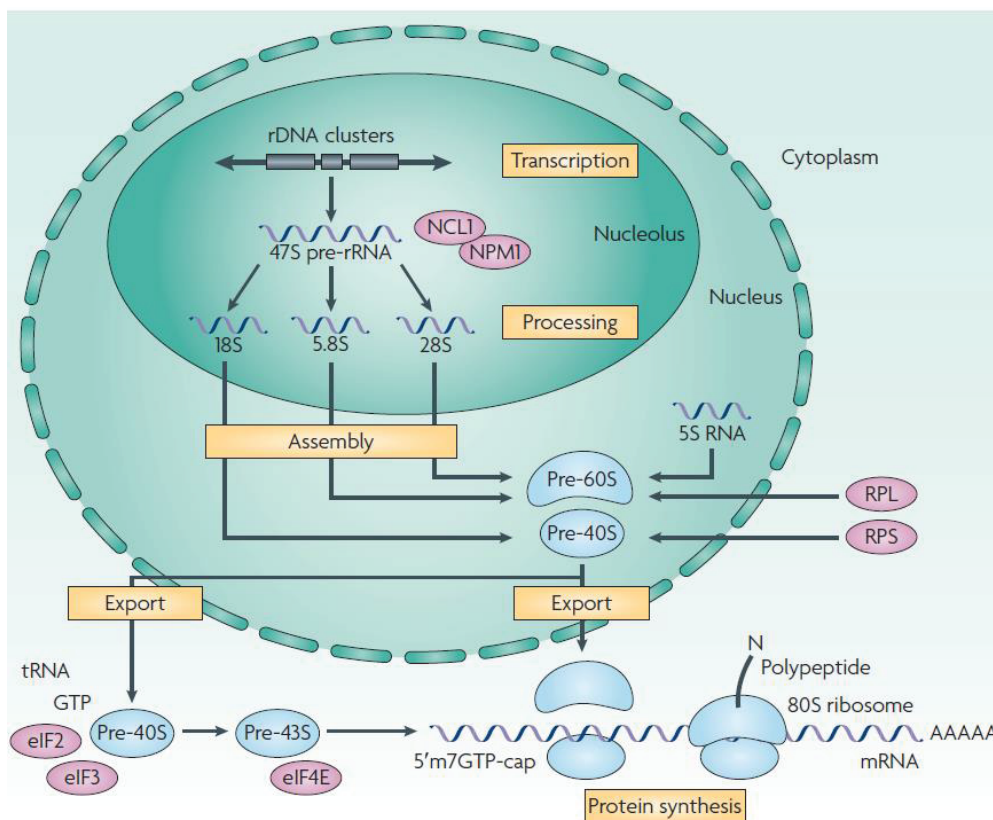


Figure 16: Ribosomal biogenesis

Ribosomal synthesis requires 47S ribosomal RNA formation which is cleaved in 18S, 5.6S and 28S rRNA. The 40S small ribosomal subunit is composed of 18S rRNA and ribosomal proteins RPS. The 60S large ribosomal subunit is composed of one 5.8S rRNA and one 28S rRNA as well as ribosomal proteins RPL. Ribosomal subunits 40S and 60S are exported into the cytoplasm where they assemble with mRNA and form the 80S ribosome necessary for protein synthesis (Van Riggelen et al., 2010).



In conclusion, neural crest cells represent a fascinating stem cell population, migrating far from their tissue of origin and giving rise to numerous differentiated cell types. Neural crest cells are therefore sometimes considered as the 4th embryonic germ layer besides ectoderm, mesoderm and endoderm. Recent identification of Schwann Cell Precursors contributions to developmental and adult processes stir up interest about this subpopulation of cells. Defects in NCC development lead to severe pathologies, named neurocristopathies and ribosomopathies. Their main treatment so far is surgery but is often variable and rarely entirely corrective. In some cases, surgery is not even possible. Recent prevention using antioxidant treatment as well as better understanding of Schwann Cell Precursors open new avenues for cellular therapeutic approaches (see Discussion). Surprisingly, not much is known about energy metabolism in NCC.

Disease	Incidence	Commonly causative genes	Clinical features	Cancer risk	Treatment	References
Treacher Collins syndrome (OMIM 154500)	1/50000	<i>TCOF1</i> , <i>POLR1C</i> , <i>POLR1D</i>	Craniofacial abnormalities, cleft palate, coloboma, ear anomalies, Intestine pseudo-obstruction (1 patient), cardiac defects (1 patient)	Non reported	Reconstructive surgery, speech therapy, hearing aid	<ul style="list-style-type: none"> Trainor et al., 2009; Sakai and Tranor, 2009; Jones et al., 2008; Ross and Zarbalis, 2014
Diamond-blackfan anemia (OMIM 105650)	1/100000	<i>RPL5</i> , <i>RPL11</i> , <i>RPL35A</i> , <i>RPS7</i> , <i>RPS10</i> , <i>RPS17</i> , <i>RPS19</i> , <i>RPS24</i> , <i>RPS26</i>	Cranio-facial anomalies, Cleft palate, Anemia, cardiac defects, urogenital malformations	Osteosarcoma, myelogenous leukemia (AML), myelodysplastic syndrome (MDS)	Reconstructive surgery, corticosteroids, leucine supplementation, blood transfusion, bone marrow transplantation	<ul style="list-style-type: none"> Van Nostrand and Attardi, 2014; Ross and Zarbalis, 2014; Bursac et al., 2014
Dyskeratosis Congenita (OMIM 127550)	1/1000000	Mutation in DKC associated genes: <i>DKC1</i> , <i>TERT</i> , <i>TINF2</i> , <i>RTEL1</i>	Cytopenias, skin hyperpigmentation, nail dystrophy, oral leukoplakia, increased risk of impair bone marrow function, pulmonary fibrosis	AML, MDS, head and neck tumors	Coordinated multidisciplinary care for all the symptoms, cure bone marrow failure, survey and treat cancer that may be caused by this disease	<ul style="list-style-type: none"> Van Nostrand and Attardi, 2014; Bursac et al., 2014
5q deletion syndrome (OMIM 153550)	1/140000	<i>RSP14</i> , <i>MIR145</i> , <i>MIR146A</i>	Macrocytic anemia, enhanced platelet number, reduced neutrophil number	10% patients develop AML 14% patients with MDS	Syngenic bone marrow transplantation	<ul style="list-style-type: none"> Van Nostrand and Attardi, 2014; Bursac et al., 2014

Table 5: Description of some human ribosomopathies

All the data were also obtained from OMIM data base.


<p>Treacher Collins syndrome (TCS)</p> <ul style="list-style-type: none"> ▪ <i>Tcof1^{tm1Mid}/Tcof1⁺</i> (Dixon J et al., 2000) ▪ <u><i>Tcof1^{tm1Mid}/Tcof1⁺</i> on a mixed DBA x C57BL/6 genetic background (Dixon J. et al., 2006)</u> 	
<p>Dyskeratosis Congenita (DKC)</p> <ul style="list-style-type: none"> ▪ <i>Dkc1^{tm1.1Pjma}/Y</i> (Gu BW et al., 2011) ▪ <i>Dkc1^{tm1Ppp}/Dkc1⁺</i> (Ruggero D et al., 2003) ▪ <i>Dkc1^{tm1Ppp}/Y</i> (Ruggero D et al., 2003) ▪ <i>Tinf2^{tm2.2Tcl}/Tinf2⁺</i> (Frescas D and de Lange T, 2014) ▪ <i>Trp53^{Δ31}/Trp53^{Δ31}</i> (Simeonova I et al., 2013) ▪ <i>Pot1b^{tm1.1Schg}/Pot1b^{tm1.1Schg}</i> (He H et al., 2009) ▪ <u><i>Terc^{tm1Rdp}/Terc^{tm1Rdp}</i> (He H et al., 2009)</u> 	 <p>Mouse models reminiscent to human ribosomopathies</p>
<p>Diamond-blackfan anemia (DBA)</p> <ul style="list-style-type: none"> ▪ <i>Flvcr1^{tm1.1Jlab}/Flvcr1^{tm1.1Jlab}</i> (Keel S.B et al., 2008) ▪ <i>Flvcr1^{tm1.1Jlab}/Flvcr1^{tm1.1Jlab}</i> carrying Mx1-Cre transgene (Keel S.B et al., 2008) ▪ <i>Rpsa^{tm1Ells}/Rpsa⁺</i> (Han J et al., 2008) ▪ <u><i>Rps19^{Dsk3}/Rps19⁺</i> (Mc Gowan et al, 2008)</u> ▪ <u><i>Rps7^{Zuma}/Rps7⁺</i> (Watkins-Chow et al., 2013)</u> ▪ <i>Rps7^{Montu}/Rps7⁺</i> (Watkins-Chow et al., 2013) 	
<p>5q-syndrome</p> <ul style="list-style-type: none"> ▪ <u><i>Cd74^{tm1Anjm}/Cd74⁺</i> and <i>Nid67^{tm1Anjm}/Nid67⁺</i> carrying Lmo2-Cre transgene (<i>Rps14^{+/+}</i>) (Barlow et al., 2010)</u> 	

Table 6: Mouse models reminiscent to human ribosomopathies

In bold and underlined are the mouse models that have been used in studies presented in Table 8 (Introduction, Chapter III.B.4) to be mated to *p53* null mice in order to assess if *p53* loss rescues the phenotype.

III. METABOLIC REGULATORS: LKB1 AND p53

Signal transduction that dictates cell fate depending on the cell environment participates to metabolism reprogramming. Furthermore, metabolically sensitive posttranslational modifications of signaling proteins (such as phosphorylation or acetylation) provide a feedback mechanism to control signaling pathways. The relationship between cell signaling and metabolism is thus bidirectional (Ward and Thompson, 2012).

Several signaling pathways are known to regulate energy metabolism: the growth factor pathway through PI3K-Akt and mTOR signaling, the receptor tyrosine kinase pathway through Ras/MEK/ERK and Myc, etc... Among them, the LKB1/AMPK pathway is able to sense ATP levels and in a context of low ATP versus high AMP, it consequently regulates energy metabolism. Several data from the literature suggest that the master kinase LKB1 could be a regulator of neural crest cells (NCC) ontogeny. First, LKB1 is essential in early embryonic development since *Lkb1* knockout mice are embryonic lethal. *Lkb1* null mice exhibit, among other defects, an absence of the first branchial arch which is mainly composed of NCC and therefore suggest an agenesis of NCC. Second, germline mutations of *LKB1* in human are responsible for the Peutz-Jeghers syndrome, an autosomal dominant disease characterized, among other symptoms, by defects in melanocytes which are NCC derivatives. Third, LKB1 is essential to establish and maintain cell polarity, an important process for NCC migration and differentiation. Finally, LKB1 is also a well-known metabolic regulator. As mentioned previously, the potential contribution of metabolic regulations during NCC formation remains largely unexplored. These data prompted the lab in which I did my PhD to explore LKB1 functions during neural crest formation as a good candidate to control NCC fate potentially through both the regulation of cell polarity and energy metabolism. Therefore, the first part of this chapter will describe some characteristics of the LKB1 signaling pathway.

Another pathway which regulates different aspects of cell metabolism is p53 signaling. Furthermore, p53 dosage is crucial for NCC formation as aberrant p53 signaling is associated with neural crest defects both in patients and animal models. Therefore, the second part of this chapter will describe p53 signaling, how it regulates energy metabolism and how p53 deregulations are involved in neural crest defects.

III.A. THE MASTER KINASE LKB1

Over the last decade, researchers have shown that LKB1 is a newly regulator of metabolism and is considered as a novel uncovered link between metabolism and growth control (Shackelford and Shaw, 2009). The master kinase LKB1 is a serine/threonine kinase encoded by the *LKB1* gene, also known as *STK11*, which regulates lipid, carbohydrate, and energy metabolism mostly through mechanisms dependent of 5'-adenosine monophosphate

(AMP)-activated protein kinase (AMPK) (Hardie and Alessi, 2013; Srivastava et al., 2012) but in some cases also independently of AMPK (Jeppesen et al., 2013).

I will start this Chapter by giving some general information about LKB1 structure, expression, localization and regulation. After that I will describe some functions of the LKB1 signaling pathway. As metabolism was the guideline of my PhD work, I will focus on metabolic functions of LKB1. I will next describe how LKB1 signaling contributes to cell polarity and embryonic development. Of note, the bibliographic data showed here will not exhaustively present the massive knowledge available about LKB1 signaling.

III.A.1. LKB1 structure, localization and regulation.

1.1 Structure and expression of LKB1 isoforms

The human *LKB1* gene, localized on chromosome 19p13.3, was discovered by Junichi Nezu of Chugai Pharmaceuticals, in 1996, in a screen used to find new kinases (Zhao and Xu, 2014). Three isoforms for LKB1, mostly generated by alternative splicing, have been described so far: LKB1 full-length, LKB1 Short isoform (S) and LKB1 deleted of the N-terminal domain (Δ N-LKB1) (Figure 17).

Human LKB1 full-length is composed of 433 amino acids (436 amino acids in mice) and has a molecular weight of 50kDa. It comprises a catalytic domain (amino acids 49 to 309) and a nuclear localization site (NLS, amino acids 38-43) (Figure 17). This isoform is ubiquitously expressed with a wide pattern of expression in embryonic and adult tissues. During mouse and human development, LKB1 is ubiquitously expressed at the early stages of embryogenesis and with time its expression becomes restricted in specific tissues, being more pronounced in lungs, stomach, small intestine, colon, kidney, pancreas and seminiferous tubules of testes (Table 7). Later in embryonic development, prominent expression of *Lkb1* was observed in central nervous system and in peripheral nervous system, in both glial cells and neurons (Luukko et al., 1999; Rowan et al., 2000). In adult tissues LKB1 expression is widespread but is predominant in epithelia, glial cells, seminiferous tubules of the testis and myocytes from skeletal muscle (Table 7) (Conde et al., 2007; Sanchez-Cespedes, 2007).

LKB1S (48kDa, 404 amino acids) differs from full length isoform in its C-terminal domain (Figure 17). The expression pattern of LKB1S is more restricted than LKB1 full-length since LKB1S is specific to spermatids, the haploid male germ cells, in testis. *Lkb1S* inactivation in mice causes male infertility (Kong et al., 2017; Towler et al., 2008).

C. Perret lab in collaboration with our team uncovered the existence of another isoform of LKB1 called Δ N-LKB1 (Figure 17) (Dahmani et al., 2015). This isoform of 42kDa is mainly expressed in heart and skeletal muscle. This protein is exclusively cytoplasmic and is catalytic inactive. However, it is capable to enhance AMPK metabolic activity because it has a dominant

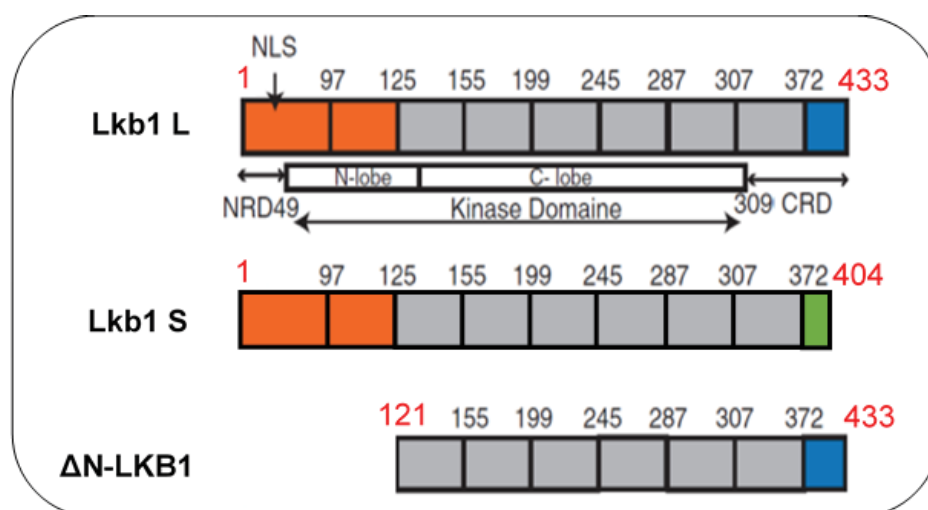


Figure 17: Structure of human LKB1 isoforms

Example of three different isoforms of LKB1 protein generated by alternative splicing. Human full-length LKB1 form (LKB1 L) has 433 amino acids. Human short LKB1 form (LKB1 S) has only 404 amino acids and amino acids from 372-404 are not the same as in LKB1 L isoform. Human ΔN-LKB1 isoform has only 312 amino acids. It is characterized by a N-terminal truncation of Lkb1 and is catalytic inactive due to the absence of a part of its catalytic domain. NLS, nuclear localization signal; CRD, C-terminal regulated domain (Modified from Dahmani et al., 2015).

LKB1 protein localization			
ADULT		EMBRYO	
HIGH	MODERATE	HIGH	MODERATE
Cerebral cortex (neurons and glial)	Breast	Small intestine	Colon
Ovary (follicles and corpus luteum)	Colon	Stomach	Heart
Salivary glands (serous acini)	Small intestine		Lung
Skeletal muscle	Endometrium (glandular epithelium)		Pancreas
Testis	Heart		Kidney
	Kidney		Esophagus
	Thyroid		Testis

Table 7: LKB1 localization in adult and embryonic normal tissues
(Modified from Sanchez-Cespedes, 2007)

positive effect on LKB1 full-length-induced AMPK activity (Thibert et al., 2015). Moreover, it has also pro-oncogenic properties which may explain why in some sporadic cancers LKB1 is inactivated and in others its expression is increased (Dahmani et al., 2015).

1.2 LKB1 subcellular localization and activation.

LKB1 is localized both in the cytoplasm and nucleus as well as to the plasma membrane. In the nucleus, LKB1 is present in a heterotrimeric complex with the mouse protein 25 (MO25 α) and the pseudokinase STE20 related kinase adaptor (STRAD α) (Figure 18). MO25 connects LKB1 and the C-terminal part of STRAD α thereby stabilizing the interaction between LKB1 and STRAD α . This association is essential for LKB1 translocation from nucleus to cytoplasm and for its kinase activity (Boudeau et al., 2003a, 2003b).

LKB1 phosphorylation on serine 428 could also be important for both its cytoplasmic translocation and its kinase activity (Xie et al., 2008) although being controversial (Denison et al., 2009; Hou et al., 2008). The C-terminal part of LKB1 contains a prenylation site (cysteine 433) necessary for the localization of LKB1 to the plasma membrane (Houde et al., 2014).

LKB1 acetylation on lysine 48 regulates also its subcellular localization (Lan et al., 2008). Indeed, NAD⁺-dependent sirtuin 1 (Sirt1) deacetylates LKB1 on lysine 48 promoting its translocation into the cytoplasm. LKB1 deacetylation increases its phosphorylation on serine 428 and threonine 336 thereby changing its subcellular localization and its kinase activity quantified by AMPK activation (Lan et al., 2008).

Finally, LKB1 is also transported to the lysosome membrane where it activates AMPK (Zhang et al., 2014) (see Chapter IV.2).

1.3 Regulation of LKB1 activity by post translational modifications

Several post translational modifications have been described for LKB1. These modifications include ubiquitination which leads to LKB1 degradation by the proteasome (Gaude et al., 2012; Nony et al., 2003) and prenylation, phosphorylation and acetylation which regulate LKB1 activity, subcellular localization and interaction with other proteins (Figure 19). Below, I will focus on LKB1 phosphorylation and acetylation.

1.3.1 Phosphorylation

Phosphorylation is a post translational modification of a protein characterized by the addition of phosphate groups being able to alter the structural conformation of the protein and to modify its function. This post translational modification is regulated by phosphatases and kinases. LKB1 is phosphorylated by different upstream kinases such as Ataxia-telangiectasia mutated kinase (ATM), Proline-directed kinase, Protein kinase B (AKT) and Protein kinase A

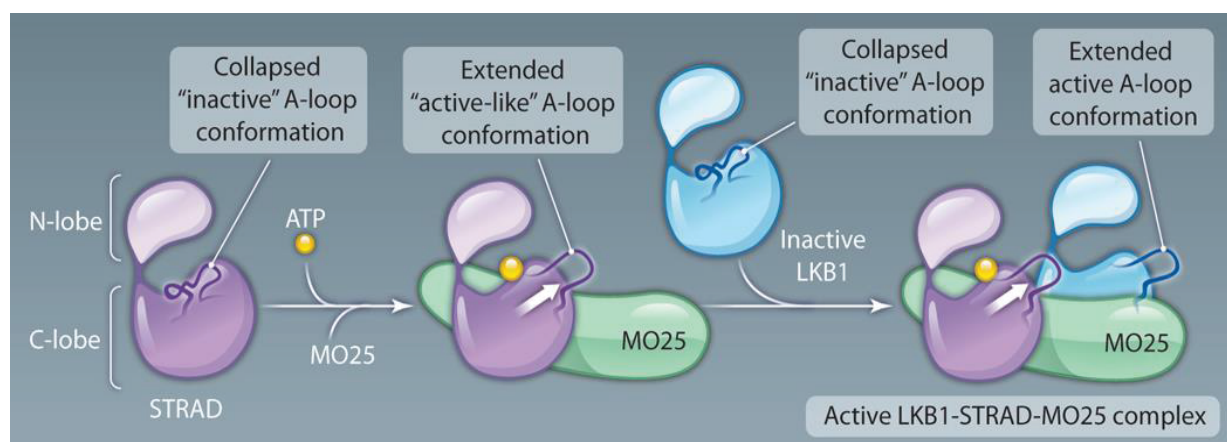


Figure 18: The active heterotrimeric complex LKB1-STRAD-MO25

STRAD in association with ATP and MO25, adopt an active like conformation similar to active protein kinases. This change of conformation promotes STRAD interaction with LKB1 as a pseudosubstrate and subsequently leads to LKB1-conformational changing from an inactive kinase conformation to an active one. MO25 stabilizes LKB1 activation by binding to its A-loop and promotes an extended active A-loop conformation of LKB1 (Rajakulendran and Sicheri, 2010).

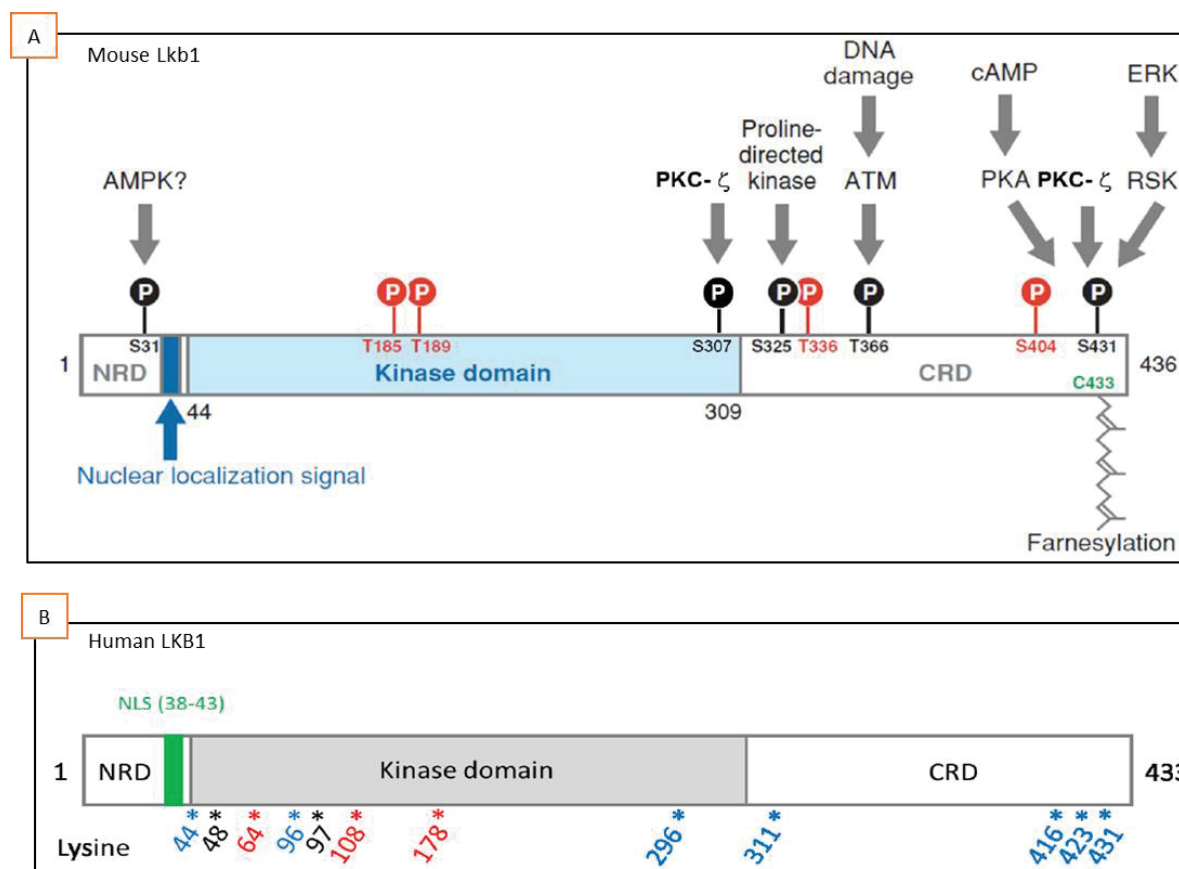


Figure 19: LKB1 post-translational modifications

A. Mouse Lkb1 phosphorylation and prenylation. In red are represented the autophosphorylation residues, in black are the amino acids phosphorylated by others kinases and in green is represented the prenylation site. Amino acids T366, S404, S431 and C433 in mice correspond to T363, T402, S428 and C430 in humans. S, Serine; T, Threonine; C, Cysteine; AMPK, AMP-activated protein kinase; PKC-γ, Protein kinase C gamma; ATM, Ataxia-telangiectasia mutated kinase; PKA, Protein kinase A; ERK, Extracellular signal-regulated kinases; RSK, Ribosomal S6 kinase. (Adapted from Alessi et al., 2006). **B.** Human LKB1 acetylation sites identified by Ido's team (Lan et al., 2008) (represented here in blue), by our team – unpublished data (in red), and common to both studies (in black) (Ghawittian, 2015).

(PKA) (Figure 19A). The most studied phosphorylation sites in human LKB1 are serines 31, 325, 428 and threonine 363 (Alessi et al., 2006a; Baas et al., 2004a; Sapkota et al., 2002a, 2002b). LKB1 also autophosphorylates on several sites: threonine 185 and 189, serine 404 and also threonine 336 which is the major site of autophosphorylation.

Phosphorylation of LKB1 at all these sites is not involved in regulating its kinase activity or its subcellular localization (Boudeau et al., 2003a; Sapkota et al., 2002) except serine 428 which has a controversial role regarding LKB1 localization that I presented previously (cf. paragraph 1.2). Instead, some of these sites are essential for the tumor suppressor function of LKB1 (Alessi et al., 2006a). For example, the replacement of serine 431 by an alanine (to prevent phosphorylation) or threonine 336 with glutamate (to mimic phosphorylation) inhibits the capacity of LKB1 to limit cell growth (Alessi et al., 2006a). However, not all the phosphorylation sites regulate LKB1 tumor suppressor capacity because sites as serine 31, serine 325 or threonine 366 have no effect on cell growth (Alessi et al., 2006; Boudeau et al., 2003a; Sapkota et al., 2002).

1.3.2 Acetylation

Acetylation is a post translational modification of a protein involving the addition of an acetyl group obtained from the metabolite acetyl-CoA. This post translational modification is regulated by the combined functions of deacetylases and acetyltransferases, themselves modulated by energy metabolism (Wellen and Thompson, 2012). For example, Sirtuin deacetylases are regulated by metabolic status of the cell because these enzymes are dependent on coenzyme NAD⁺ which is involved in redox reactions and plays important roles in energy metabolism. Protein acetylation is also regulated by metabolism because it depends on Acetyl-CoA availability which is a key node in metabolism.

Our team and Y. Ido lab have shown by mass spectrometry that LKB1 is acetylated on different lysines (Figure 19 B) (Lan et al., 2008). The acetylation of lysine 97 regulates LKB1 activity and function during oxidative stress (Calamaras et al., 2012) and, as already mentioned, LKB1 acetylation on lysine 48 controls its subcellular localization. We identified the acetyltransferase GCN5 as one of the enzymes which acetylates LKB1 on lysine 48 (cf Results Project 1.2).

GCN5 was the first histone acetyltransferase described which regulates transcriptional activity of proteins (Brownell and Allis, 1995). Since, it has been shown that GCN5 also acetylates non-histone proteins. GCN5 is composed of three important domains:

→ a bromodomain in the C terminal part, important for anchoring to its substrates (Owen et al., 2000). But this domain is not the only region that is responsible for GCN5 binding to its substrates (Carré et al., 2005).

→ an acetyltransferase central domain which contains the catalytic activity of GCN5.

→ a p300/CBP Associated Factor (PCAF) homology domain. This domain is unique to animals

(Smith et al., 1998) and allows the interaction of GCN5 with p300 and CBP.

GCN5 acetyltransferase regulates several cellular processes such as energy metabolism. One example is the acetylation of the transcription factor peroxisome proliferator-activated receptor-gamma coactivator-1 alpha (PGC1 α) which induces its translocation from the promoter regions of its target genes encoding gluconeogenic enzymes to nuclear foci. Thus, GCN5 regulates glucose metabolism through transcriptional repression of PGC1 α (Lerin et al., 2006). Moreover, these GCN5 metabolic activities are controlled by the Sirtuin deacetylase 6 (Sirt6). Indeed, Sirt6 directly deacetylates GCN5 on lysine 549 which promotes its phosphorylation on serine 307 and threonine 735 and therefore triggers its activation. Activated GCN5 acetylates PGC1 α and limits gluconeogenesis (Dominy et al., 2012).

III.A.2. LKB1 signaling: focus on AMPK/mTOR pathway

LKB1 is a master kinase which phosphorylates 14 kinase substrates that are members of the AMPK family. Through the regulation of its downstream kinases, LKB1 contributes to several cellular processes such as cell polarity and energy metabolism (Figure 20) (Gan and Li, 2014; Shackelford and Shaw, 2009; Shaw, 2009a). Among the 14 kinases, some of them control cell polarity, like Synapses of the Amphid Defective kinases (SAD), Microtubule Affinity Regulating Kinases (MARK/Par-1) and Sucrose-Non-fermenting protein-Related Kinase (SNRK/NUAK) (Figure 20) (Barnes et al., 2007; Shaw, 2009a; Shelly et al., 2007). NUAK regulates neurons maturation through mitochondria immobilization (Courchet et al., 2013) and is also expressed during early chick development being important for vertebrate head formation (Bekri et al., 2014). Other kinases like AMPK and Salt-Inducible Kinases (SIK) control cell growth and metabolism (Figure 20) (Patel et al., 2014; Shaw, 2009b).

During my PhD, as my objective was to analyze the energy metabolism, I focused on LKB1-AMPK pathway, AMPK being an energy sensor that activates catabolic processes and inhibits anabolic ones. Therefore, in this manuscript I will present data mostly about the AMPK substrate which is, so far, the only LKB1 substrate sensing the cellular energy status.

2.1 AMPK activation

AMPK is a serine/threonine kinase which consists of three subunits: a catalytic subunit (AMPK α) and two regulatory subunits (AMPK β and AMPK γ) (Figure 21). Each subunit is represented by several isoforms: α 1, α 2, β 1, β 2, γ 1, γ 2, γ 3 (Viollet et al., 2009).

2.1.1. AMPK phosphorylation

AMPK α is the catalytic subunit. It contains, in its N terminal part, the kinase domain (Figure 21) (Crute et al., 1998) and the threonine 172 site which can be phosphorylated by several kinases: LKB1, CaMKK β (Ca²⁺/calmodulin-dependent protein kinase kinase β) and

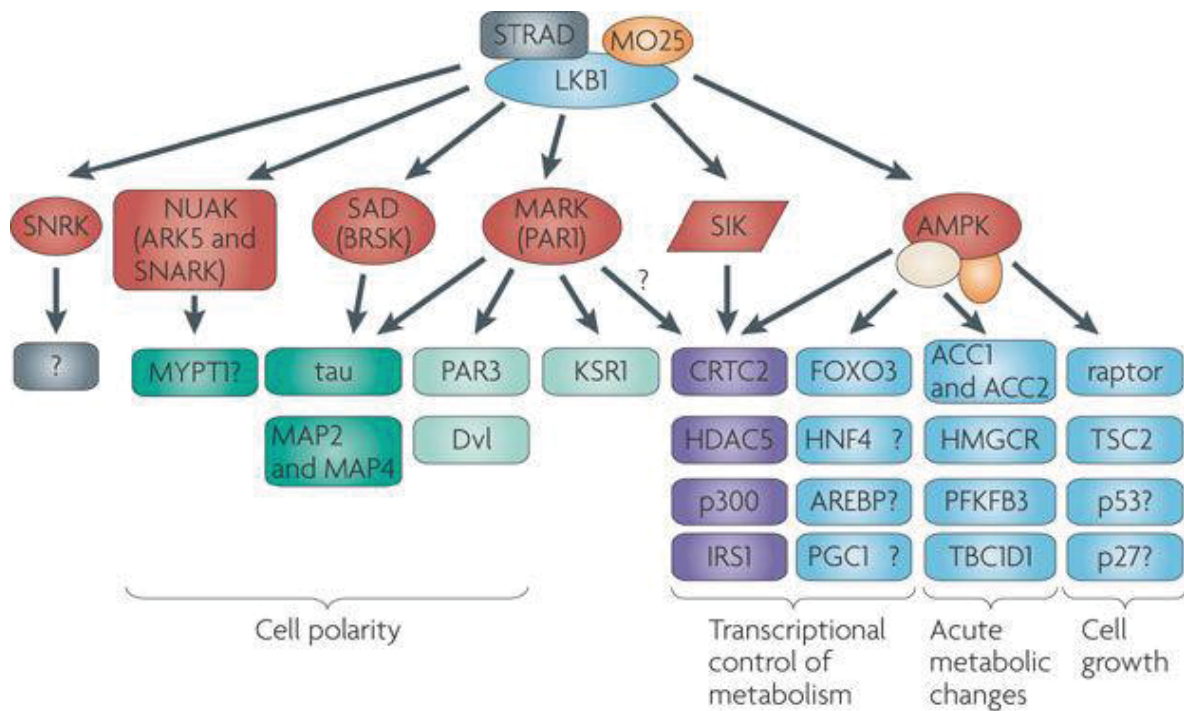


Figure 20: LKB1 phosphorylates the 14 members of the AMPK-related kinase family

LKB1 is a master kinase which regulates 14 kinase substrates which in turn phosphorylate other proteins, being therefore implicated in many cellular processes such as cell polarity, energy metabolism, cell proliferation, differentiation, etc. (Shackelford and Shaw, 2009).

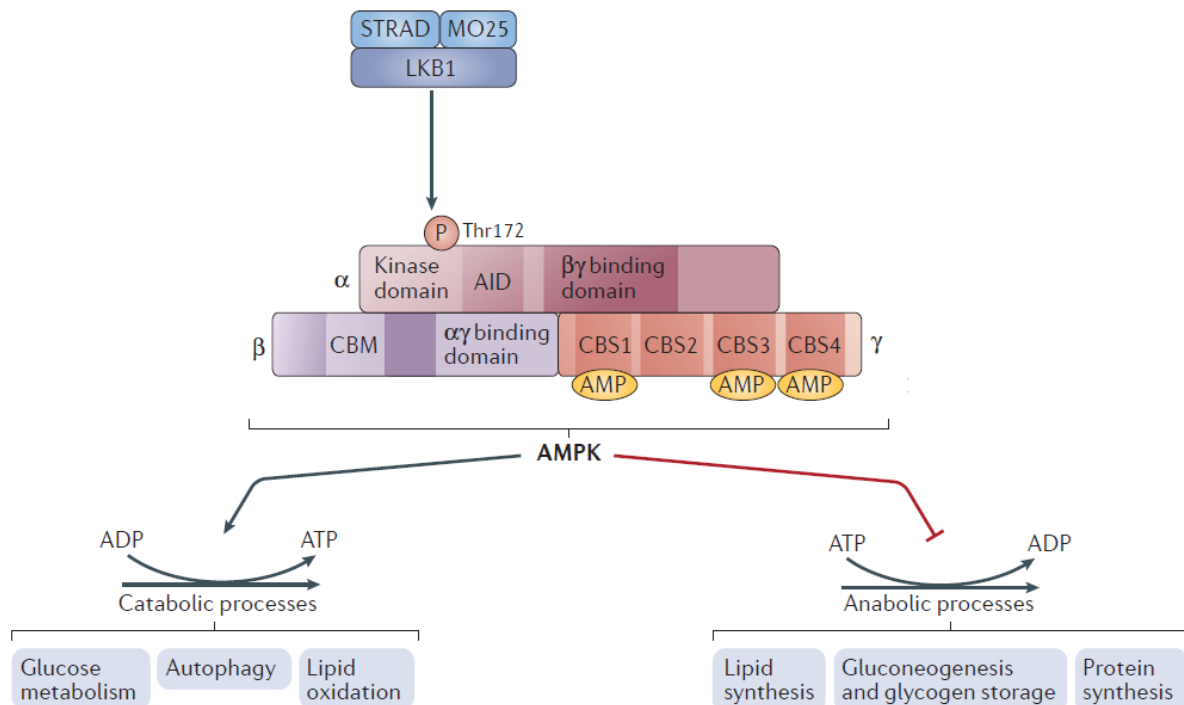


Figure 21: AMPK structure and regulation by LKB1

AMPK is a heterotrimeric complex composed of α , β and γ subunits. α - subunit contains Thr172 which is phosphorylated by LKB1. Activated AMPK increases catabolic processes (ATP production) and decreases anabolic processes (ATP consumption). AID, auto-inhibitory domain; CBM, carbohydrate-binding module; CBS, cystathionine- β -synthase (Adapted from Herzing and Shaw, 2017).

TAK1 (Transforming growth factor beta-activated kinase 1) (Hawley et al., 2005; Momcilovic et al., 2006; Shaw et al., 2004; Tamás et al., 2006) The master kinase LKB1 is the major activator of AMPK in many cell types that we and others used as cellular models such as mouse embryonic fibroblast cells (MEF), human embryonic cells (HEK-293), mouse glial cells (S16 and glial differentiated JoMa1), mouse Sertoli cells (TM4) and kidney monkey cells (COS7). Indeed, LKB1 inactivation in these cell lines leads to a nearly complete loss of AMPK phosphorylation on threonine 172, in response to different stimuli (Hawley et al., 2003; Tanwar et al., 2012a; Woods et al., 2003); our studies –cf Results. Projects 1.2, 2.1 and 3.1).

2.1.2. AMPK regulation

AMPK is an energy sensor activated by AMP and ADP (less than AMP) and inhibited by ATP (Hardie et al., 2012) The sensitivity to AMP/ATP or ADP/ATP ratio is due to its γ subunit (Figure 21). This subunit contains four tandem sequence repeats named cystathionine β synthase (CBS). These domains allow AMPK to reversibly bind AMP or ATP and the binding choice depends on their concentration (Xiao et al., 2007). In other words, if AMP is at high concentration, it competes with ATP to bind to AMPK γ subunit. Even if mammalian AMPK have four CBS domains only CBS 1, 3 and 4 can reversibly bind AMP or ATP (Figure 21). In normal conditions, AMPK is inactive because the ATP concentration is high and one molecule of ATP binds each CBS domain. In stress conditions, ATP is depleted and therefore the concentration of AMP is higher and can replace ATP from CBS motifs. First, AMP replaces ATP from CBS3 and protects the threonine 172 site to be dephosphorylated. This replacement increased AMPK activity 100 times. Secondly, if the energetic stress is even higher, the ATP from CBS1 is also replaced by AMP which activates AMPK by an allosteric regulation (Xiao et al., 2007). This second replacement increases AMPK activity 10 times more than the first activation. Thus, in stress conditions, AMP activates AMPK by two complementary mechanisms: by protecting threonine 172 from dephosphorylation and by an allosteric activation. To restore normal ATP levels, AMPK inhibits anabolic processes which consume energy, such as triglyceride and protein synthesis and induces catabolic processes which produce energy, like fatty acid oxidation or mitochondrial biogenesis (Ruderman et al., 2013).

Beside upstream kinases and AMP/ATP ratio, there are others regulators of AMPK activity (Figure 22). Among these regulators, we can find hormones (adiponectine, leptin, IL-6), natural compounds (rooibos, resveratrol, α -lipoic acid, berberine, AICAR) and pharmacological drugs which are indirect (biguanides, thiazolidinediones) or direct (A-769662, PT1) activators (Coughlan et al., 2014; Fogarty and Hardie, 2010). Indirect drugs activate AMPK by increasing the cellular AMP/ATP ratio. Drugs activating directly AMPK act as AMP, preventing threonine 172 dephosphorylation and causing AMPK allosteric activation.

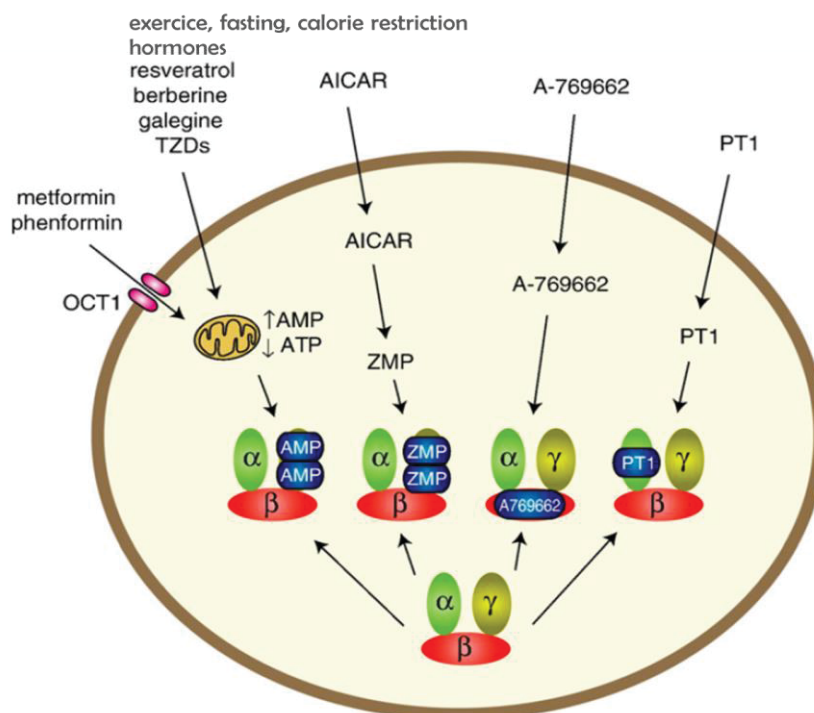


Figure 22: Natural or Pharmacological regulators of AMPK activity

Drugs such as resveratrol, berberine and biguanids are able to block mitochondrial ATP synthesis and thus to increase AMP: ATP ratio which leads to AMPK activation. AICAR is a metabolic drug which is up-taken by the cells and transformed in ZMP which mimics AMP and which binds to γ -subunit and activates AMPK. A-769662 has also the ability to mimic AMP and to activate AMPK but through another subunit, the β -subunit. PT1 increases AMPK activity through its interaction with AMPK α -subunit and inhibition of autoinhibitory domain (Adapted from Foaarty and Hardie, 2009).

AICAR (5-Aminolimidazole-4-Carboxamide Ribonucleotide) was the first AMPK-activator molecule discovered *in vivo* and *in cellulo* (Corton et al., 1995; Sullivan et al., 1994). AICAR is a natural intermediate in purine nucleotide synthesis and thus a precursor of several purine monophosphates including ZMP, IMP and AMP (Figure 22) (Mikanagi, 2012). AICAR mode of action is actually ambiguous since it has been shown to act:

- directly on AMPK as an AMP analogue: AICAR is taken up into cells through the adenosine transporter and is metabolized by adenosine kinase in ZMP. ZMP synthesis from extracellular AICAR is faster than its subsequent metabolism. As a consequence, ZMP accumulates and mimics the effects of AMP by binding AMPK CBS domains. Hence, ZMP activates AMPK (Figure 22) either by triggering an increase of threonine 172 phosphorylation or by allosteric regulation (Corton et al., 1995; Henin et al., 1996).

- indirectly on AMPK through replenishing the pools of AMP. During the purine nucleotide pathway, AICAR is transformed into inosine 5'-monophosphate (IMP), a precursor of AMP.

- independently of AMPK through ZMP which interacts with other AMP-regulated enzymes such as fructose-1,6-bisphosphatase (Vincent et al., 1991) or glycogen phosphorylase (Longnus et al., 2003)(Longnus et al., 2013) and inhibits or respectively

activates them, blocking gluconeogenesis. One well established AMPK-independent function of AICAR is its ability to induce astroglial differentiation of neural stem cells (Zang et al., 2008).

Altogether, these data demonstrated that AMPK is an LKB1 substrate as well as an energy sensor controlled by AMP/ATP ratio and other different regulators like AICAR.

2.2 mTOR downstream pathway and functions

LKB1/AMPK have many downstream targets (Figure 23) being involved in several cellular processes like cell growth, autophagy, metabolism and polarity. Below I focused only on serine/threonine kinase mTOR, the most studied downstream target of this pathway.

mTOR is present in two complexes: mTORC1, which is a major growth regulator and mTORC2 which promotes cellular survival (Figure 24). AMPK blocks mTOR activation by two mechanisms:

1. it directly phosphorylates Tuberous Sclerosis Complex 2 (TSC2) at serine 1387 (in human) and therefore stimulates the GTPase activating protein (GAP) activity of TSC1/TSC2 complex in order to transform Rheb^{GTP} in Rheb^{GDP}. Rheb is a G protein which activates mTORC1 only when it is bound to GTP (Inoki et al., 2003; Shaw, 2009a).

2. it also directly phosphorylates Raptor, a subunit of mTORC1 complex, at two conserved sites: serines 722 and 792 and therefore induces binding of Raptor with the scaffolding 14-3-3 protein which leads to mTORC1 inhibition (Gwinn et al., 2008; Shaw, 2009a).

mTOR activation promotes protein biosynthesis, lipid anabolism and nucleotides production, all these processes being important for **cell growth and proliferation** (Wullschleger et al., 2006). The main mTOR downstream targets that promote expression of factors involved in cell growth and proliferation are:

- S6 protein kinase1 (S6K1) (Figure 24) which activates S6 ribosomal protein (S6RP) and translational initiation factor eIF4B (Guertin and Sabatini, 2007).

- eIF4E-binding protein (4E-BP1) (Figure 24) which inhibits the activation of translation initiation factor eIF4E (Holz et al., 2005).

In addition to the control of cell proliferation by TORC1 complex, LKB1/AMPK/mTOR pathway has other cellular functions such as:

- regulating actin **cytoskeleton dynamic** (Jacinto et al., 2004). TORC2 activates Rho1 GTPase which activates Protein Kinase C (PKC) and in turn signals to the actin cytoskeleton via a Mitogen-Activated Protein (MAP) kinase pathway (Figure 24) (Wullschleger et al., 2006).

- monitoring **autophagy** in mammalian cells (Lum et al., 2005) (Figure 24).

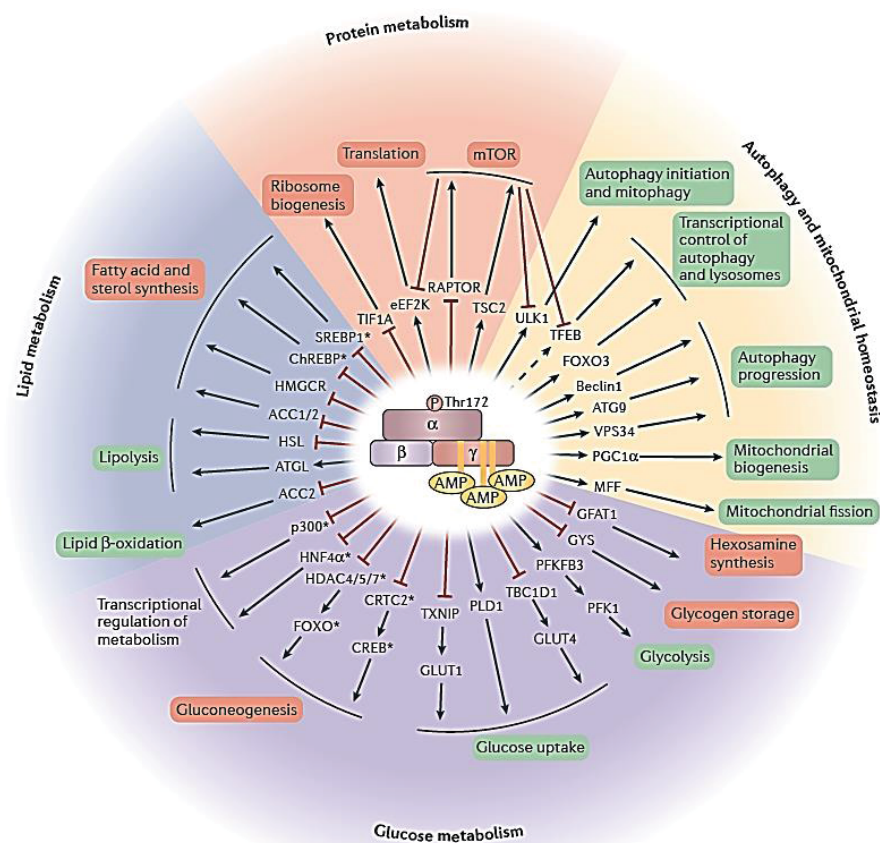


Figure 23: AMPK downstream targets and their involvement in different cellular processes.

In red are the inhibited biological processes and in green are the activated ones. Protein activation is denoted by \rightarrow and protein inhibition is denoted by \dashv . Transcriptional regulators are symbolized by * (Herzig and Shaw, 2017).

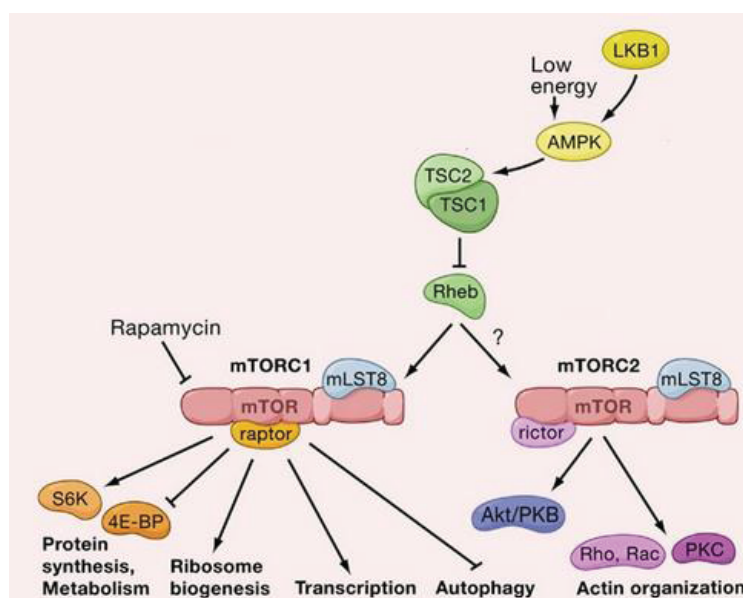


Figure 24: mTOR pathway and complexes

mTORC1 complex controls several cellular processes such as ribosomal biogenesis, transcription and metabolism and thus regulates cell growth. mTORC2 complex regulates AKT (Protein kinase B) and Rho pathway being therefore involved in cell survival and proliferation. Modified from <http://slideplayer.it/slide/10665517/>

- controlling cell **metabolism** such as amino acid biosynthesis, glucose homeostasis and fatty acids metabolism (Kim and Chen, 2004; Um et al., 2004).



To conclude, LKB1/AMPK signaling regulates numerous downstream targets, one of them being mTOR. In particular through this regulation, this signaling pathway controls several cellular processes such as energy metabolism. LKB1/AMPK also regulates cell growth, migration, polarity and autophagy through other downstream substrates than mTOR not described in this manuscript.

III.A.3. Cellular regulations by LKB1/AMPK signaling

3.1 LKB1 is a major metabolic regulator

LKB1 is a key regulator of energy homeostasis and it controls the lipid and glucose metabolism in several tissues such as liver, adipose tissue and skeletal muscles.

3.1.1 Regulation of lipid metabolism

LKB1 regulates lipids and cholesterol synthesis through AMPK activation which phosphorylates and inhibits Acetyl-CoA carboxylase (ACC), glycerol phosphate acyl-transferase (GPAT) and 3-hydroxy-3-methyl glutamyl (HMG)-CoA reductase (Figure 23) (Carlson and Kim, 1973; Hardie and Alessi, 2013; Hardie et al., 2012). There are two ACC isoforms. ACC1 is expressed in lipogenic tissues like liver and adipose tissues and is involved in fatty acid synthesis (Davies et al., 1992) ACC2 is expressed in oxidative tissues like heart and muscles and is involved in fatty acid oxidation (Merrill et al., 1997). Both isoforms are directly phosphorylated and inhibited by AMPK. GPAT is involved in triglyceride and phospholipid synthesis and HMG-CoA reductase (HMGR) is localized at the membrane of endoplasmic reticulum and regulates cholesterol synthesis. AMPK negatively regulates HMGR through its direct phosphorylation but also by regulating its gene expression via degradation of Forkhead transcription factor 1a (FoxO1a) (Fisslthaler and Fleming, 2009).

3.1.2. Regulation of glucose metabolism

LKB1 regulates glucose uptake and gluconeogenesis by increasing Peroxisome proliferator-activated receptor gamma coactivator 1-alpha (PGC1 α) levels through AMPK activation (Foretz et al., 2010; Shaw et al., 2005). AMPK directly interacts and phosphorylates PGC1 α (Jäger et al., 2007). This phosphorylation represents a priming signal for the subsequent PGC1 α deacetylation by Sirtuin 1. Hence AMPK, in opposition with GCN5 presented in paragraph 1.3.2, regulates glucose metabolism through PGC1 α activation (Cantó and Auwerx, 2009; Jeninga et al., 2010).

However, AMPK is not the only substrate of LKB1 which regulates gluconeogenesis.

For example, Salt-inducible kinase (SIK2) is also able to phosphorylate CREB regulated transcription coactivator 2 (CRTC2). This phosphorylation stimulates CRTC2 cytosolic translocation and inhibits transcriptional activation of its hepatic gluconeogenic target genes (Patel et al., 2014).

3.1.3. Regulation of mitochondria dynamic

Another important mechanism regulated by LKB1/AMPK is mitochondrial biogenesis (O'Neill et al., 2011; Winder et al., 2000). In hematopoietic stem cells (HSC), *Lkb1* inactivation decreases mitochondrial biogenesis and energy production by downregulating PGC1 α levels (Figure 23) (Gan et al., 2010; Gurumurthy et al., 2010; Nakada et al., 2010; Saito and Nakada, 2014). PGC1 α is a transcription coactivator which not only regulates glucose metabolism, as seen above, but it also enhances the expression of some mitochondrial genes (Lin et al., 2005). Thus, LKB1/AMPK pathway regulates mitochondria biogenesis. This pathway controls also mitochondria degradation by autophagy, named mitophagy (Egan et al., 2011; Hardie et al., 2012; Kim and Lemasters, 2011) as well as their mobility (Courchet et al., 2013) and fragmentation (Toyama et al., 2016).

Moreover, mitochondria defects are associated with increased oxidative damage which controls the production of reactive oxygen species (ROS) (see Chapter IV.3.2). In addition, several researchers have observed that LKB1 is also a regulator of ROS levels. It controls the activity and expression of antioxidant proteins such as superoxide dismutase 2 (SOD2) and catalase and thereby protects the genome integrity (Gurumurthy et al., 2010; Xu et al., 2015). AMPK is also capable to increase antioxidants production through activation of Forkhead box O (FoxO) transcription factor (Chiacchiera and Simone, 2010).

LKB1/AMPK pathway connects the energy metabolism to ROS production. Upon energy stress like glucose starvation, activated AMPK induces metabolic reprogramming and subsequently controls redox balance and ROS production (Zhao et al., 2017).

Thus, LKB1 is a metabolic regulator which, by activating AMPK and other substrates, controls both glycolysis and oxidative phosphorylation (OXPHOS) as well as ROS formation. It is also involved in protein metabolism mainly by controlling mTOR pathway, in lipid metabolism, autophagy and mitochondrial functions (biogenesis, degradation, dynamic and fission).

3.2 LKB1 establishes and maintains cell polarity

Another process controlled by LKB1 is cell polarity which represents the asymmetric distribution of molecules inside cells. Regulation of cell polarity is evolutionary conserved (Figure 25). The role of LKB1 in cell polarity was discovered for the first time in *C. elegans*. The *Lkb1* ortholog *Par4*, controls the first asymmetric division of cells during early

embryogenesis, which leads to the formation of the anterior-posterior axis during embryogenesis (Figure 25) (Kemphues et al., 1988; Watts et al., 2000). In mammalian cells, LKB1 controls cell polarity of several cell types (Figure 25). For example, Lkb1 expression induces axon formation in hippocampal neurons (Shelly et al., 2007) and in neurons of developing cerebral cortex (Barnes et al., 2007). Lkb1 also establishes and maintains polarity in various cells including pancreatic acinar cells (Hezel et al., 2008), intestinal epithelial cells (Baas et al., 2004a; Shorning et al., 2009), Sertoli cells (Tanwar et al., 2012) and hepatocytes (Fu et al., 2011). However, the molecular mechanisms by which LKB1 controls cell polarity are tissue specific (Hezel and Bardeesy, 2008).

Interestingly the capacity of LKB1 to regulate cell polarity in mammalian cells is due to its cytoplasmic functions (Baas et al., 2004a, 2004b; Sebbagh et al., 2009). Our team has shown that the C-terminal region of LKB1 is essential to control cell polarity of both intestinal epithelial cells and migrating astrocytes via the AMPK pathway (Forcet et al., 2005). Our team also showed that Lkb1-AMPK pathway regulates cranial NCC polarized migration through the sequential activation of the Rho/Rock kinases, phosphorylation of Myosin Regulatory Light Chain (MRLC) and actin dynamic (cf Results Project1.1; (Creuzet et al., 2016)). These results are in line with the literature. It is known that AMPK activates Rock kinase which phosphorylates MRLC through MLC kinase (Figure 26) (Miranda et al., 2010). Moreover, the expression of MRLC phosphomimetic mutant in *Drosophila* embryos rescued the polarity defects observed after inactivation of *ampk* or *lkb1* (Lee et al., 2007). Another AMPK downstream effector important for cell polarity is cytoplasmic linker protein-170 (CLIP-170) (Figure 26). CLIP-170 is a plus-end tracking protein (+TIP). AMPK phosphorylates directly CLIP-170 on serine 311. Hence, it promotes microtubules dynamic and polymerization which is crucial for cell polarity (Nakano and Takashima, 2012).

AMPK is not the only kinase which mediates LKB1 functions in regulating cell polarity. NUAK1 is also able to enhance MRLC phosphorylation by inhibiting MLC phosphatase (Lee et al., 2007). There are also MAPK, BRSK and SAD-A and B kinases which are mainly associated with epithelial and neuronal polarity (Figures 25, 26) (Barnes et al., 2007; Courchet et al., 2013; Hurov and Piwnicka-Worms, 2007; Jansen et al., 2009; Kojima et al., 2007).

Thus, LKB1 controls both energy metabolism and polarity. However the link between these two processes is not very well characterized. Recently it has been shown that cells submitted to a contractile force stimulate the translocation of LKB1 to the plasma membrane and the LKB1-dependent recruitment of AMPK to E-cadherin cell-cell junctions. Here, AMPK regulates the actomyosin dynamic and therefore cell polarity. This function is dependent on glucose uptake and ATP production (Bays et al., 2017).

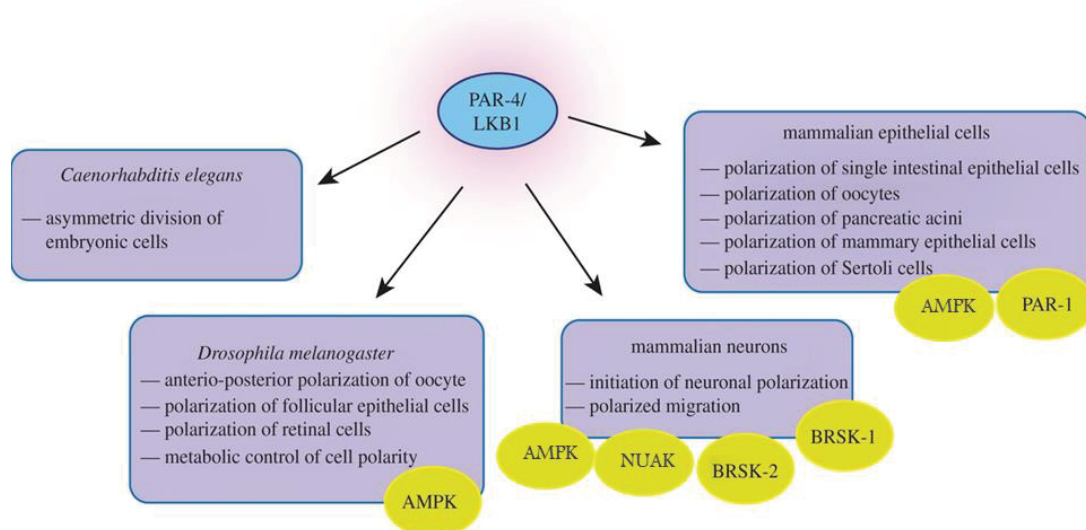


Figure 25: Evolutionary conservation in LKB1 role as a regulator of cell polarity

Examples of LKB1 functions in regulation of cell polarity. In green are some examples of kinases involved in these processes. Of note is that the list of enzymes is not exhaustive. Modified from Partanen et al., 2013.

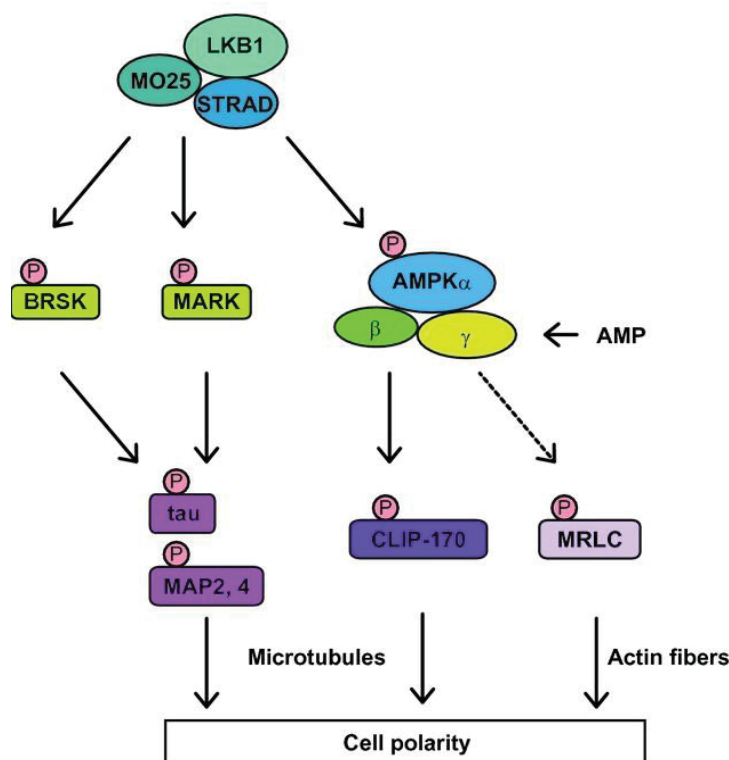


Figure 26: Molecular mechanisms underlying regulation of cell polarity by LKB1

LKB1 phosphorylates kinases like AMPK, MARK and BRSK which directly activate proteins involved in microtubules dynamic such as cytoplasmic linker protein-170 (CLIP-170), Tubulin-associated unit (Tau), Microtubule-Associated Proteins (MAP) 2 and 4. AMPK is also able to control actin dynamic through indirect (dotted line) phosphorylation of Myosin Regulatory Light Chain (MRLC) (Nakano and Takashima, 2012).



To conclude, LKB1 has different biological functions including cellular metabolism and polarity control. This metabolic regulator is involved in gluconeogenesis, fatty acid synthesis and oxidation as well as in mitochondrial biogenesis and energy metabolism, mostly by phosphorylating and activating AMPK. It also controls the polarity of cells and their polarized migration in physiological conditions such as neuronal migration and cranial NCC migration or in pathological conditions like cancer cell metastasis.

III.A.4. Role of LKB1 in development

4.1 Role of Lkb1 in embryogenesis

Lkb1 full inactivation (*Lkb1*^{-/-}) in mice is embryonic lethal at embryonic day 11 (E11) (Figure 27) (Jishage et al., 2002; Ylikorkala et al., 2001). *Lkb1*^{-/-} embryos developed normally up to E8. At E8.5-E9.5 *Lkb1*-inactivated mice presented defects in angiogenesis due to elevated levels of VEGF (Vascular endothelial growth factor) and anomalies in head formation. Embryos exhibited defects also in neural tube closure and an absence of the first branchial arch which is derived from neural crest cells and form head structures at late stages (Ylikorkala et al., 2001). This is a phenotype compatible with a dysgenesis of cranial neural crest cells.

The extra embryonic tissues of *Lkb1*^{-/-} embryos, such as yolk sac and placenta, presented also anomalies (Ylikorkala et al., 2001). Therefore, to test if embryonic defects were due to *Lkb1* absence and not to extra embryonic tissue deformations, *Lkb1* was specifically inactivated in epiblast by using the *Mox2*-Cre driver (Londesborough et al., 2008). These mice mimic the embryonic lethal phenotype of full *Lkb1* inactivation, thereby demonstrating the direct role of *Lkb1* in embryonic tissue formation.

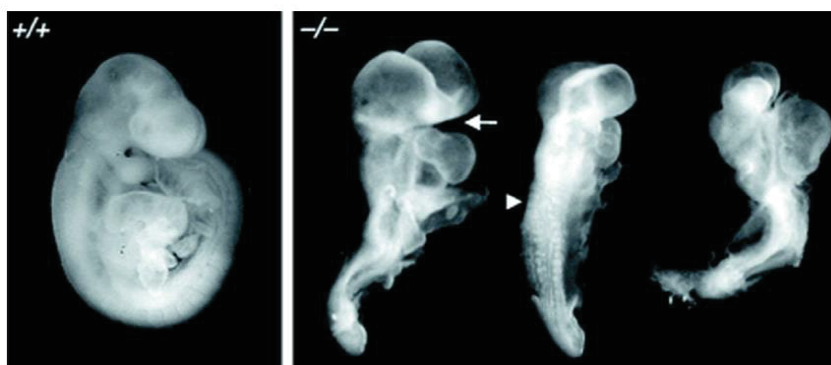


Figure 27: Lkb1 involvement in embryonic development

Left panel: Light microscopy of normal, wild type mouse embryo (+/+) at embryonic day 9.25.
Right panel: *Lkb1* knockout mouse embryos showing unfold embryos with open neural folds and a missing branchial arch (Ylikorkala et al., 2001)

LKB1 regulates the differentiation of human embryonic stem cells (hESC) (Lai et al., 2012). These pluripotent cells differentiate in all cell types of human body. *LKB1* inactivation in hESC inhibited their differentiation (decreased differentiation markers like Nestin, Runx1, GAT, Sox17) and increased the pluripotency marker genes (for example Oct4 and Nanog). LKB1 controls p21/WAF1 transcription in hESC, as in somatic cells. Thus, in absence of LKB1 p21/WAF1 is downregulated and therefore there is an increased proliferation correlated with a decreased differentiation of these cells.

Other studies have analyzed LKB1 roles during the development and maintenance of specific tissues such as liver, nervous system and skeletal muscles, using different transgenic murine models (Ollila and Mäkelä, 2011). In the next paragraph, I will present only the role of LKB1 in the nervous system since this is a part of my PhD program.

4.2 Role of Lkb1 in nervous system

4.2.1. Lkb1 is essential for neuronal development

Barnes and his colleagues deleted *Lkb1* specifically in cerebral cortex of developing mice, by using Emx::Cre driver (Emx is a protein marker for pyramidal neurons of the cerebral cortex). They observed an absence of axon formation in neurons of studied mice and proposed that Lkb1 is activating BR serine/threonine kinase (BRSK) in neurons which phosphorylates Mitogen-activated proteins (MAP) and affects the cytoskeleton dynamics allowing axon specification (Barnes et al., 2007). In the same year Shelly M. and her coworkers also observed that Lkb1 is essential for neuronal differentiation (Shelly et al., 2007). Absence of Lkb1 in the spinal cord, hypothalamus and in the endocrine pancreas (Rip2-Cre driver) induced hind-limb paralysis in 7 weeks old mice. The neurons and axons were developed normally. Instead, with age, the lack of Lkb1 promotes demyelination and axon degeneration in spinal cord (Sun et al., 2011). Thus, Lkb1 is essential for both axon formation and maintenance.

Milbrand team also showed that Lkb1 is essential for axonal maintenance through Schwann cell communication. They deleted *Lkb1* specifically in Schwann cells of adult mice by using PLP-Cre^{ERT} driver (PLP is a myelin proteolipid protein) and observed a massive axonal loss. The most affected axons were the unmyelinated sensory ones. Thereby, the axonal degeneration was not due to demyelination but to metabolic changes in Schwann cells. Lkb1-deficient Schwann cells exhibited mitochondrial dysfunction with increased mitochondrial reactive oxygen species (ROS) production and increased lactate levels (Beirowski et al., 2014). These metabolic changes affected neuronal survival.

All these data demonstrate that LKB1 is essential for neurons formation and function as well as for the metabolic dialogue between Schwann cells and neurons which is essential for neuronal survival.

4.2.2. Lkb1 is essential for glial cells development

Shen *et al.* also deleted *Lkb1* specifically in Schwann cells but this time the inactivation was done in developing mice, by using 2'-3' cyclic nucleotide 3' phosphodiesterase *CNP::Cre* driver, *CNP* being a myelin-associated enzyme (Shen et al., 2014). With this mouse model the researchers showed that *Lkb1* is essential for Schwann cell maturation. *Lkb1* is asymmetrically localized in the cytoplasm of Schwann cells, at the interface between these cells and neurons. *Lkb1* phosphorylation on Serine 431 by Protein Kinase A (PKA) attracts Par3, a mediator of cell polarity, in the same compartment and activates the initiation of myelination.

In the same time, Dasgupta lab showed that *Lkb1* controls Schwann cells differentiation by another mechanism, via its metabolic regulation capacity. Cellular differentiation is a process which demands a lot of energy and therefore is associated with a metabolic shift from glycolysis to oxidative phosphorylation. *Lkb1* loss in Schwann cells decreased oxidative phosphorylation, including the synthesis of citrate which is a Krebs cycle substrate and consequently decreased myelin lipid levels (Pooya et al., 2014).

Altogether, these data highlighted that *Lkb1* regulates Schwann cell mitochondrial metabolism and controls their differentiation. Still, the underlying molecular mechanisms are not very clear.

III.A.5. Association of LKB1 mutations with human pathologies

LKB1 was for the first time linked to human disease when germline mutations in one allele of *LKB1* were found to be responsible for the Peutz-Jeghers syndrome (PJS; Hemminki et al., 1998; Jenne et al., 1998; Mehenni et al., 1998).

PJS is a human autosomal dominant disease characterized by the presence of hamartomatous gastrointestinal polyps, melanin spots on the lips, buccal mucosa, fingers and toes (Figure 28A) and a high predisposition to develop malignant tumors in various organs (Figure 28B) (McGarrity et al., 2000). The incidence of PJS is estimated to be 1 in 120,000 births (Lindor and Greene, 1998).

It has been shown that approximately 80% of individuals with PJS have an *LKB1* pathogenic variant, suggesting that *LKB1* is the major gene responsible for this pathology (Volikos et al., 2006). *Lkb1* monoallelic inactivation in mice (*Lkb1*^{+/-}) was sufficient for the development of hamartomatous gastrointestinal polyps similar to PJS patient polyps (Bardeesy et al., 2002; Jishage et al., 2002; Miyoshi et al., 2002; Rossi et al., 2002). These mice developed later gastrointestinal carcinoma due to loss of heterozygosity of *Lkb1*. Genetic analyses confirmed that loss of *Lkb1* wildtype allele is responsible for predisposition of PJS

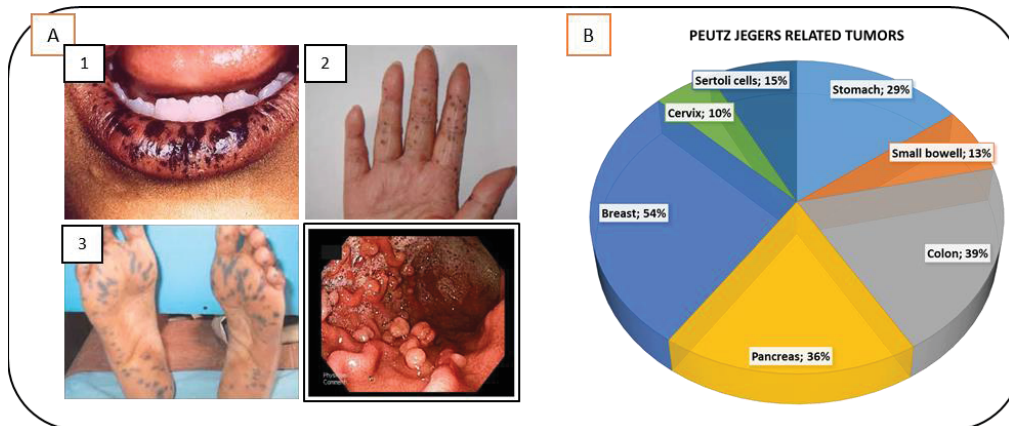


Figure 28: Clinical characteristics of Peutz-Jeghers Syndrome

- A. PJS patients have hyperpigmented macules on their 1. lips (<http://www.intelligentdental.com/wp-content/uploads/2012/06/untitled.png>), 2. fingers (adapted from <https://f6publishing.blob.core.windows.net/4e2f5565-51a9-4a87-b909-5975b513af54/WJG-14-7397-g001.jpg>) 3. toes (http://www.ijdv.com/articles/2008/74/2/images/ijdv_2008_74_2_154_39705_2.jpg) and hamartomatous polyps in the gastrointestinal tract (<https://img.medscapestatic.com/pi/meds/ckb/71/10371tn.jpg>).
- B. PJS patients have also a high risk to develop different malignant tumors. (Janse et al., 2009; Sanchez-Cespedes, 2007; Brandao and Lage, 2015 and <http://slideplayer.com/slide/10890820/39/images/12/Cancer+risk+in+P-J+syndrome.jpg>).

patients to develop cancer (BANNO et al., 2013; Wang et al., 1999). Additional somatic mutations in other genes such as *p53* accelerate the polyposis observed in PJS mouse.

LKB1 somatic mutations have also been described in patients with sporadic cancers and are associated with:

- 30% of non-small cell lung cancers (Sanchez-Cespedes et al., 2002). Moreover, it has been observed that *LKB1* regulates lung cancer initiation, differentiation and metastasis (Ji et al., 2007).
- 20% of cervical cancers (Wingo et al., 2009).
- 27% of intraductal papillary mucinous neoplasms (Sahin et al., 2003).
- 10% of cutaneous melanomas (Liu et al., 2012).



In conclusion, as seen in this chapter, the tumor suppressor *LKB1* is a metabolic regulator involved in embryonic development and cell fate. It is a master kinase which has 14 substrates members of AMPK-family, being therefore able to regulate a multitude of cellular outcomes. However, mutations of *LKB1* are associated so far only with tumor formation: germline mutations are responsible for the human Peutz-Jeghers syndrome whereas somatic mutations are associated with sporadic tumors. Owing to all the cellular processes regulated by *LKB1* signaling, we could expect a broader implication of *LKB1* in human diseases. To this regard, *LKB1* has been proposed as a genetic risk factor for multiple sclerosis (Boullerne et al., 2015). However so far there are not many studies supporting this hypothesis.

III.B. THE MASTER REGULATOR p53

p53 is a tumor suppressor gene discovered in 1979 which regulates energy metabolism. It is one of the keystones in tumorigenesis (Levine and Oren, 2009), being mutated or repressed in more than half of cancers (Figure 29) (Brady and Attardi, 2010). Its tumor suppressor role was confirmed by the fact that *p53* null mice display a totally penetrant cancer phenotype (Kenzelmann Broz and Attardi, 2010). Inheritance of mutant *p53* allele predisposes humans to the Li-Fraumeni cancer syndrome (Olivier et al., 2010).

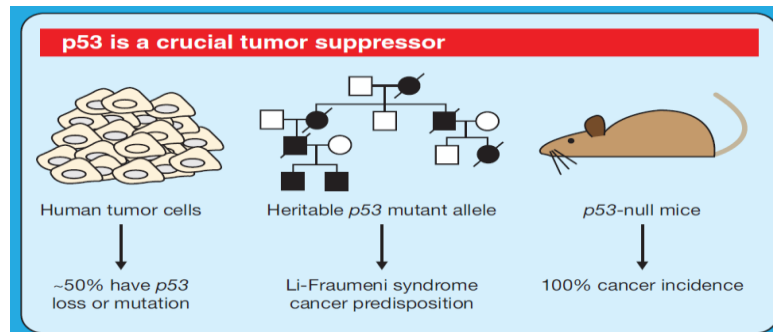


Figure 29: p53 has an essential function in tumor suppression
(Brady and Attardi, 2010)

p53 prevents cancer development by multiple manners, however its exact contributions to embryonic development are less clear. In this manuscript I will focus mainly on *p53* functions during embryogenesis.

During my PhD, I initiated the characterization of the link between *p53* and LKB1 signalings and its importance in pathologies due to neural crest cells (NCC) defects.

Therefore, the guideline of this chapter is the known connections between *p53* & energy metabolism and *p53* & NCC development. The bibliographic data that I will further present regarding *p53* are not exhaustive. After a brief description of *p53* structure and activation by cellular stresses, I will succinctly report an overview of some mechanistic regulations exerted by *p53* in various cellular responses such as cell cycle arrest, metabolic reprogramming, autophagy and differentiation. I will then describe how *p53* contributes to embryo development and neural crest cells in particular and how *p53* deregulations are associated with neurocristopathies and ribosomopathies.

III.B.1. Structure and activation of the p53 protein

p53 is a transcription factor composed of 393 amino-acids organized in several domains (Figure 30) as indicated below from the N-terminal to the C-terminal part of the protein (Hainaut and Hollstein, 2000; Joerger and Fersht, 2010):

- two transactivation domains (TAD): TAD1 (residues 1-42) and TAD2 (43-73)
- a prolin-rich region (61-94)
- a DNA-binding domain (102-292)

- a flexible linker region (300-318)
- a tetramerization domain (326-355) which contains a regulatory domain.
- a basic domain (363-393)

p53 is localized in both cytoplasm and nucleus, since it contains :

- two nuclear export signals (NES), one located within the C-terminal oligomerization domain and the other within the N-terminal TDA1 domain (Stommel et al., 1999; Zhang and Xiong, 2001a, 2001b) (Figure 30).
- three nuclear localization signals (NLS), one located just before the oligomerization domain (316-325) and two minor NLS which reside in basic domain (Shaulsky et al., 1990) (Figure 30).

p53 has a short half-life, around 30 minutes in most cells and tissues, therefore, its basal level is low and often undetectable (Stommel and Wahl, 2004; 2005; Hainaut and Wiman, 2005). This low level of p53 is regulated by several E3 ubiquitin ligases (Figure 31) including Mdm2 (Haupt et al., 1997; Kubbutat et al., 1997), COP1 (Dornan et al., 2004), Pirh2 (Leng et al., 2003; Sheng et al., 2008) and ARF-BP1. All these regulators control p53 ubiquitination and consequently p53 degradation via 26S proteasome. Interestingly, p53 activates the expression level of genes encoding the E3 ubiquitin ligases thereby establishing a negative feedback loop (Figure 31) (Brooks and Gu, 2006; Hollstein and Hainaut, 2010; Hainaut and Wiman, 2005). In the following paragraph, I focused on Mdm2 as it is the most studied p53 regulator and it is essential during embryogenesis.

1.1 Regulation of p53 by ubiquitination

Mdm2 in mammals (Hdm2 in human) is an E3-ubiquitin ligase that covalently binds one or several ubiquitin proteins on lysine residues. It regulates p53 via two key mechanisms:

(i) first it interacts with p53 TAD thereby blocking p53-dependent transcription (Chen et al., 1993; Minsky and Oren, 2004; Momand et al., 1992; Nag et al., 2013).

(ii) second, it promotes p53 degradation by ubiquitination-mediated proteolysis (Haupt et al., 1997; Kubbutat et al., 1997; Wade et al., 2010) (Figure 32). Mdm2 mono- or poly-ubiquitinates p53 and this is essential for p53 function: mono-ubiquitination leads to p53 nuclear export and mitochondrial translocation (Marchenko and Moll, 2007; Marchenko et al., 2010) while poly-ubiquitination induces its degradation (Figure 32) (Li et al., 2003). The balance between these two types of ubiquitination depends on Mdm2 levels: increased Mdm2 levels promote p53 poly-ubiquitination as low Mdm2 levels mediate mono-ubiquitination (Li et al., 2003). However, other studies suggest that the interaction of Mdm2 with different proteins such as p300, Gankyrin, Kap1 and Sival regulates Mdm2 to perform poly-ubiquitination (Du et al., 2009; Grossman et al., 2003; Higashitsuji et al., 2005; Jain and Barton, 2010; Sui et al., 2004; Wang et al., 2005).

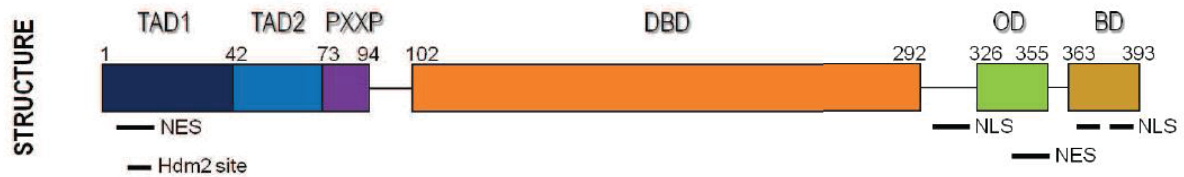


Figure 30: p53 protein structure

P53 contains in its N-terminal region two transactivation domains (TAD1 and TAD2) and a proline-rich region (PXXP). In the central region there is a DNA-binding domain (DBD) and in the C-terminal region an oligomerization domain (OD) and a basic domain (BD). Nuclear Export Signal (NES), Nuclear Localization Signal (NLS) and Hdm2 binding site are represented by a black line (Hind Hafs, PhD manuscript, 2012).

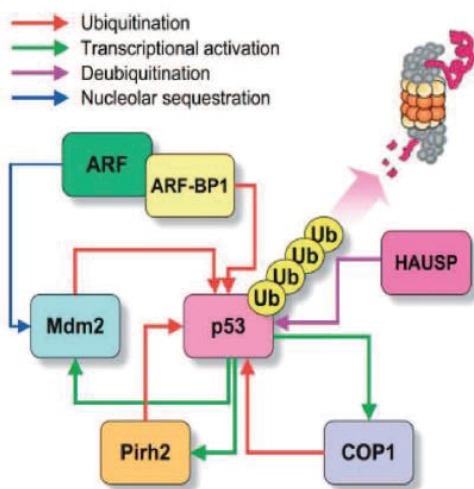


Figure 31: p53 regulatory network

p53 half-life is controlled by several E3 ubiquitin ligases. There are different negative feedback loops, including Mdm2, Pirh2, COP1 which regulate p53 ubiquitination and are regulated by p53 at the transcriptional level (Hollstein and Hainaut, 2010)

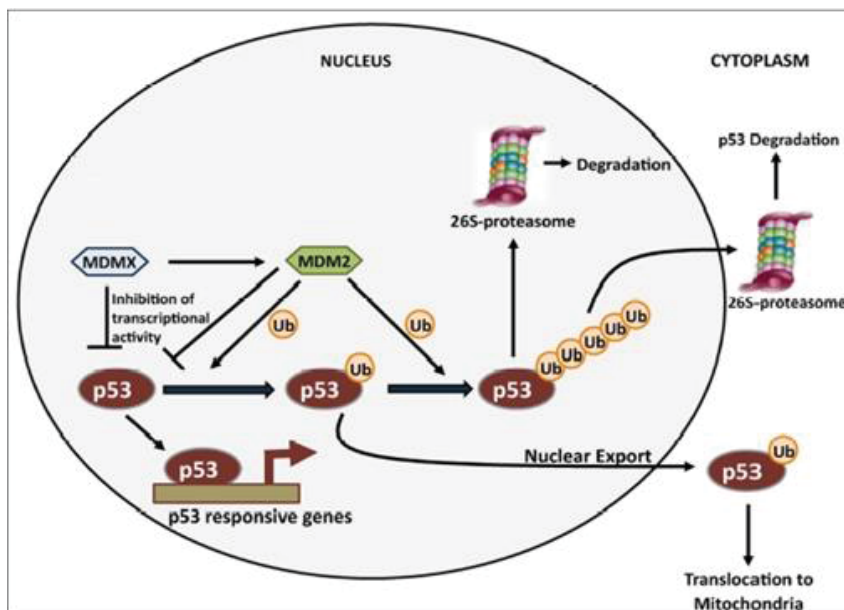


Figure 32: p53 ubiquitination by Mdm2 and Mdm4 (Mdmx)

Proteasomes of both nucleus and cytoplasmic compartments are able to degrade polyubiquitinated p53 but with a preference for nuclear p53 turnover as p53, Mdm2 and Mdm4 (Mdmx) colocalize in nucleus. Mdm2 in presence or not of Mdm4 (Mdmx) poly-ubiquitinates p53 which is degraded by proteasome. Mdm2 also mono-ubiquitinates p53 which promotes its nuclear export and its translocation to mitochondria. Mdm4 (Mdmx) is also able to bind p53 and renders the p53 transcriptionally inactive (Jain and Barton, 2010).

Mdm4, also known as Mdmx, is another regulator of p53 stability, but not directly since it is not an E3 ubiquitin ligase (Figure 32) (Stad et al., 2001). Mdm4 forms a heteromeric complex with Mdm2, stabilizes Mdm2 and promotes Mdm2-mediated degradation of p53 (Gu et al., 2002). Similarly to Mdm2, it also binds to p53 and inhibits its transcriptional activity. Mdm4 can also be recruited to p53 target gene promoters where it binds to p53 TAD and thereby blocks the ability of p53 to interact with the transcriptional machinery (Jain and Barton, 2010).

1.2 p53 stabilization and activation upon stress

Many cellular stresses are responsible for p53 stabilization and activation (Bálint and Vousden, 2001). They include DNA-damaging agents triggering “bulky” DNA lesions (such as ultraviolet (UV), cisplatin) or DNA strand breaks (infrared, reactive oxygen species (ROS) such as H₂O₂), inhibiting topoisomerase (e.g. etoposide) or RNA pol II. Other stresses involving non-DNA-damaging agents can also activate p53. Proteasome inhibition, hypoxia, antioxidants, heat/cold shocks, some viral infections or oncogene expression are some examples among others.

Various post translational modifications regulate p53 stability and function such as ubiquitination, phosphorylation, acetylation and methylation.

Ubiquitination, as previously described, is associated to p53 degradation and mitochondrial trafficking. In response to many stress signals, p53 is accumulated partly via Mdm2 and Mdm4 inhibition. Upon DNA damage, Mdm2 mediates its own ubiquitination as well as ubiquitination of its partner Mdm4 leading to their inhibition (Kawai et al., 2003; Pan and Chen, 2003; Stommel and Wahl, 2004). Other stress signals can induce different post translational modifications of both Mdm2 and p53 which perturb the Mdm2-p53 interaction and thereby stabilize p53. Ribosomal stress also inhibits Mdm2 and Mdm4 and promotes p53 activation. It has been shown that several mutated ribosomal proteins such as RPL5, RPL11 and RPL23 (for ribosome proteins functions see chapter II.3.2) interact with the acidic domain of Mdm2 and blocks the ubiquitination of p53 (Gilkes et al., 2006).

Phosphorylation, methylation and acetylation of p53 are mostly associated to its accumulation and activation (Bode and Dong, 2004; Chuikov et al., 2004; Gu and Roeder, 1997; Ito et al., 2002; Lake and Bedford, 2007). For example, ionizing radiations activate DNA-dependent protein kinase (DNA-PK) (Morozov et al., 1994) or ataxia telangiectasia mutated (ATM) (Morgan and Kastan, 1997) which phosphorylate p53 on serine 15. This serine is localized in the Mdm2-binding domain, therefore its phosphorylation disrupts Mdm2-p53 binding and stabilizes p53. UV exposure activates Chk1 and Chk2 which phosphorylate p53 on Serine 20 and therefore also perturbs MDM2-p53 binding (Chehab et al., 2000). Genotoxic factors such as UV and ionizing radiations promote ROS formation thereby triggering oxidative

DNA damage. ROS levels also regulate p53 stability by inducing its phosphorylation on serine 15 through activation of several kinases like p38 α MAPK (Bragado et al., 2007), ATM (Kurz and Lees-Miller, 2004) and ERK (Persons et al., 2000) and as described above this phosphorylation affects Mdm2-p53 binding thus inducing p53 accumulation and activation.

III.B.2. p53 biological functions

p53 is known to possess several biological functions, the most characterized one being its transcription factor capacity. Thus, p53 acts principally as an activator or repressor of genes expression, being therefore able to dictate several cellular outcomes such as cell cycle arrest, autophagy, energy metabolism and cellular differentiation (Brown et al., 2009; Loughery and Meek, 2013). In addition to its transcription-dependent functions, p53 has also cytoplasmic, independent transcription functions such as apoptosis activation and autophagy inhibition (Green and Kroemer, 2009). Further I will briefly describe only some p53 biological functions which, as I will present later (Chapter III.B 3), are essential for embryonic development.

2.1 Cell-cycle arrest

p53, also known as the guardian of the genome, is capable of detecting anomalies in cell growth and in regulating genes expression mediating cell cycle arrest, in order to help the cell repair before division. p53 regulates many genes involved in this cellular process, but here I present only two cell cycle regulator-genes known to be involved also in neural crest development (see Chapter III.B.4).

The first p53 target gene identified was p21 which encodes for cyclin-dependent kinase inhibitor 1 responsible for G1 cell cycle arrest (el-Deiry et al., 1992; El-Deiry, 2016; Harper et al., 1993). Several studies have shown that p53 capacity to upregulate p21 expression and thereby to block cell cycle is essential for its tumor suppressor activity (Lozano, 2010). Interestingly, nuclear Lkb1 is also modulating p21 expression and consequently the cell cycle arrest via physical interaction with p53 (Zeng and Berger, 2006) and its downstream kinases either AMPK (Bungard et al., 2010) or NUAK2 (Hou et al., 2011) on the promoter regions of p21. However the direct phosphorylation of NUAK and AMPK by p53 remains controversial.

CyclinG1 (*Ccng1*) is another p53 target gene that causes cell-cycle arrest (Okamoto and Beach, 1994; Zauberman et al., 1995) and inhibits cell growth (Zhao et al., 2003). Upon DNA damage or other cellular stresses, cyclinG1 promotes G2/M arrest (Kimura et al., 2001). Bungard et al. have shown that the nuclear complex Lkb1, AMPK, p53 is also essential for *cyclinG* transcription (Bungard et al., 2010).

2.2 Metabolism

As presented in the first chapter, cellular metabolism is a fundamental process involved in embryonic development. The most recent characterized ability of p53 is its capacity to

mediate metabolic changes in cells. Depending on the type of stress, p53 modulates the metabolism via different mechanisms (Berkers et al., 2013; Kruiswijk et al., 2015):

- it interacts with AMPK and mTOR
- it regulates mitochondrial mass and activity
- it controls lipid metabolism

As energy metabolism has been the guideline of my PhD project, I focused on the interaction of p53 with AMPK/mTOR pathway as well as its involvement in glycolysis and oxidative phosphorylation. Indeed, p53 controls glycolysis and oxidative phosphorylation by activating or inhibiting different regulators of these two processes.

❖ **Crosstalk with AMPK/mTOR signaling pathway**

Upon genotoxic stress, p53 inhibits mTORC1 in order to limit cell proliferation, growth and energy consumption. This inhibition relies on (Figure 33):

- transcriptional upregulation by p53 of Sestrins, a family of highly conserved stress-responsive proteins that protect cells from oxidative stress (Budanov and Karin, 2008a, 2008b). Sestrins activate AMPK (Budanov et al., 2010; Budanov and Karin, 2008) to inhibit mTOR (Feng et al., 2005).
- transcriptional upregulation of mTOR inhibitors such as AMPK β , TSC2 among others (Feng et al., 2007). Of note, *LKB1* expression is also controlled by p53 (Pappas et al., 2017).

This capacity of p53 to regulate AMPK activity or expression and thereby to inhibit mTOR pathway was also observed in nongenotoxic conditions (Drakos et al., 2009).

❖ **p53 regulates aerobic glycolysis**

p53 regulates glucose flux to pyruvate by either down- or up-regulating gene expression of glycolytic effectors that intervene at various steps of the glycolysis (Figure 34).

p53 downregulates the expression of :

- * glucose transporters responsible for glucose uptake into cells (Kawauchi et al., 2008; Schwartzberg-Bar-Yoseph et al., 2004; Zhang et al., 2013a).
- * Hexokinase2 (HK2), the enzyme which catalyzes the first step of glycolysis, through p53-inducible miR-34a (Kim et al., 2013a).
- * TIGAR (TP53 induced glycolysis regulatory phosphatase), which limits Phosphofructokinase 1 (PFK1) activity (Bensaad et al., 2006, 2009).

However, p53 also has the capacity to enhance the expression of some glycolytic enzymes such as Phosphoglycerate mutase (PGAM) in cardiocytes (Ruiz-Lozano et al., 1999) and HK2

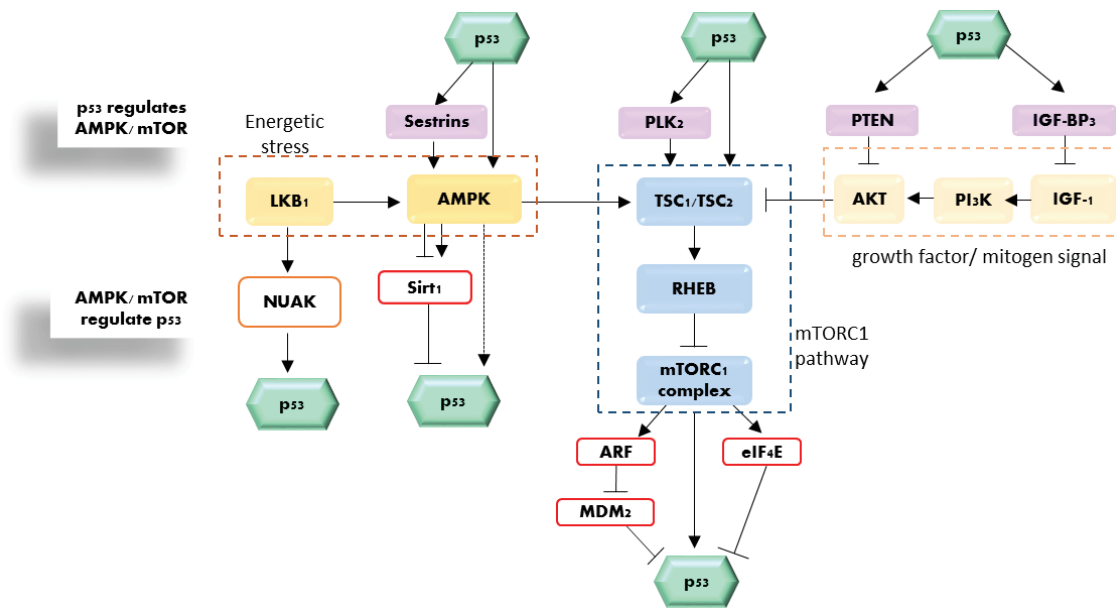


Figure 33: Regulatory feedback loops between p53, AMPK and mTOR pathways

p53 regulates AMPK and mTORC1 through many downstream targets. AMPK and mTORC1 are also able to activate or inhibit p53 via different factors (indirectly) (Modified from Berkers et al., 2013).

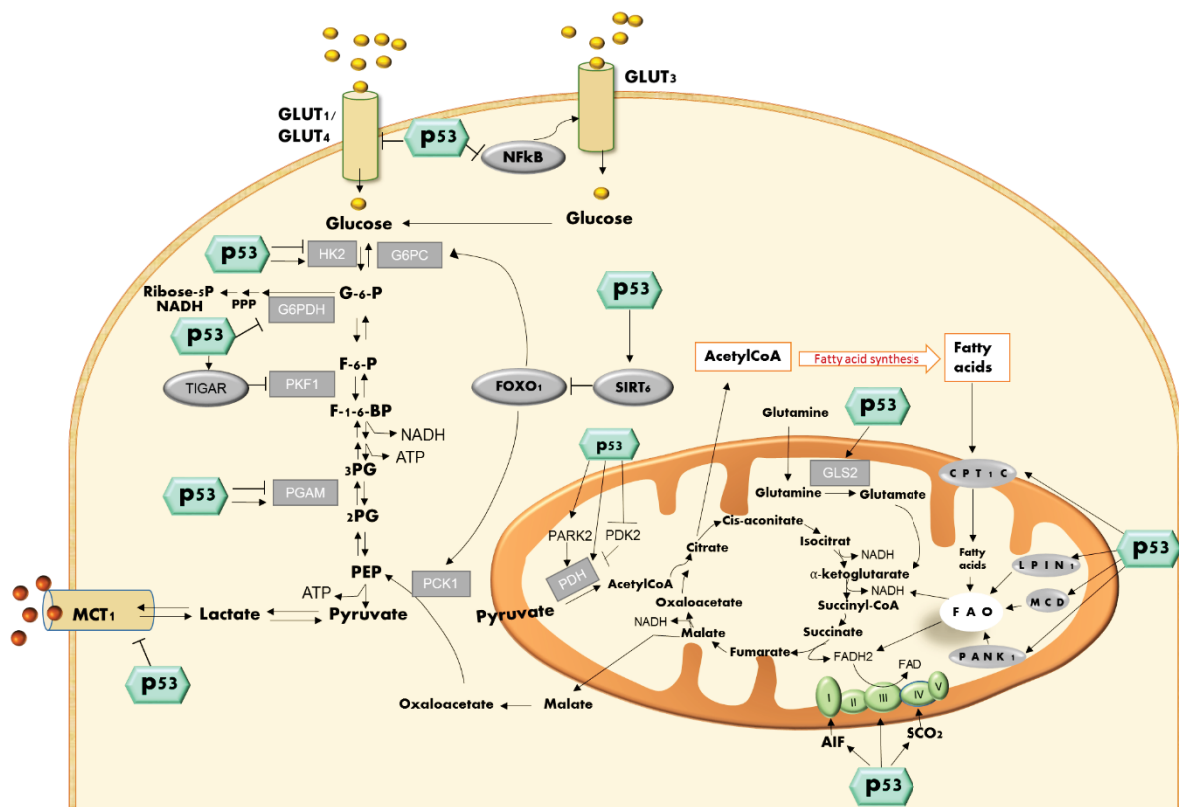


Figure 34: p53 controls energy metabolism

p53 controls aerobic glycolysis by regulating several enzymes like: HK2, Hexokinase 2; PKF1, Phosphofructo kinase 1; TIGAR, p53-induced glycolysis and apoptosis regulator; PGAM, phosphoglycerate mutase. It also regulates gluconeogenesis through inhibition of G6PC, Glucose-6-phosphatase and PCK1, Phosphoenolpyruvate carboxykinase 1 via activation of Sirt6; Sirtuin 6. The mitochondrial respiration is positively regulated by p53 through the activation of PDH, pyruvate dehydrogenase; GLS2, Phosphate-activated glutaminase and electron transport chain complexes in the mitochondria. The fatty acid oxidation (FAO) which takes place into the mitochondria is also induced by p53.

(Cheung et al., 2012; Ruiz-Lozano et al., 1999; Mathupala et al., 1997). So far, this dual role of p53 in glycolysis is not well documented. Several studies suggest that the glycolytic regulation by p53 is tissue and context specific (Maddocks and Vousden, 2011; Vousden and Ryan, 2009).

❖ **p53 regulates mitochondrial and TCA activities**

p53 protects mitochondrial integrity, increases mitochondrial mass (Kitamura et al., 2011; Lebedeva et al., 2009; Wang et al., 2014) and enhances oxidative phosphorylation (OXPHOS).

Firstly, to increase OXPHOS, p53 regulates the activity of protein complexes of the mitochondrial electron transport chain (Figure 34) by directly upregulating the expression of apoptosis inducing factor (AIF) and synthesis of cytochrome C oxidase 2 (SCO2) which are important for the function of complexes I and IV respectively (Matoba et al., 2006; Stambolsky et al., 2006).

Secondly, p53 increases the TCA flux (Figure 34) by:

- positively regulating pyruvate dehydrogenase (PDH) levels through inhibition of PDH kinase 2 (PDK2) (Contractor T and Harris, 2012) or through activation of Parkinson Protein 2 (PARK2) (Zhang et al., 2011).
- positively regulating α -ketoglutarate (α KG) levels via the mitochondrial enzyme Glutaminase 2 (GLS2) which catalyzes the conversion of glutamine into glutamate that is catabolized into α KG and ammonia (Hu et al., 2010; Suzuki et al., 2010).

To conclude, p53 is involved in several aspects of energy metabolism, including downregulation of glycolysis and upregulation of mitochondrial respiration, as well as the control of AMPK/mTOR pathway essential for cell growth and the regulation of ATP pool inside the cells by activating catabolic reactions and inhibiting anabolic ones.

2.3 Autophagy

p53 regulates metabolism also by controlling autophagy, a cytoplasmic catabolic process (see Chapter IV.1.3). Depending on its subcellular localization, p53 has opposite effects on autophagy: cytoplasmic p53 turns autophagy off (Morselli et al., 2008; Tasdemir et al., 2008) whereas nuclear p53 turns autophagy on by positively regulating autophagy gene expressions such as Damage-Regulated Autophagy Modulator (DRAM) (Balaburski et al., 2010; Crighton et al., 2006; Levine and Abrams, 2008; Tasdemir et al., 2008).

As both nuclear p53 and inhibition of cytoplasmic p53 can induce autophagy, how does the cell “decide” between autophagy induction by cytoplasmic p53 inhibition or by nuclear p53? The answer to this question could depend of the type of cellular stress. Autophagy is induced in response to various stress stimuli such as starvation, endoplasmic reticulum (ER) stress,

DNA damage and oxidative stress (Figure 35) (Kuma et al., 2004; Shimizu et al., 2004; Yu et al., 2004).

ER stress induces autophagy by promoting cytoplasmic translocation of p53 and its subsequent degradation by Mdm2 ubiquitination-mediated proteolysis (Fabbro and Henderson, 2003; Pluquet et al., 2005; Qu et al., 2004; Tasdemir et al., 2008). This cytoplasmic localization of p53 induced by ER stress is regulated by posttranslational modifications in the nuclear localization signal (NLS) such as phosphorylation of serines 315 and 376 (Pluquet et al., 2005; Qu et al., 2004).

On the other hand, other stimuli such as DNA damage and oxidative stress stabilize and activate p53 and enhance its nuclear functions, regulating positively the autophagy in a transcriptional dependent and independent manner (Figure 35) (Feng et al., 2005; Levine and Abrams, 2008; Zeng and Kinsella, 2007).

It is known that autophagy is essential for physiological processes such as preimplantation development, cell differentiation during adipogenesis, lymphogenesis and erythropoiesis (Mizushima and Levine, 2010) and Schwann cell maturation because it properly reduces the cytoplasm of Schwann cells during myelination in the peripheral nervous system (Jang et al., 2016). Instead little is known about p53-dependent induction of autophagy during these processes. Thus, the capacity of p53 to modulate autophagy in a context-dependent

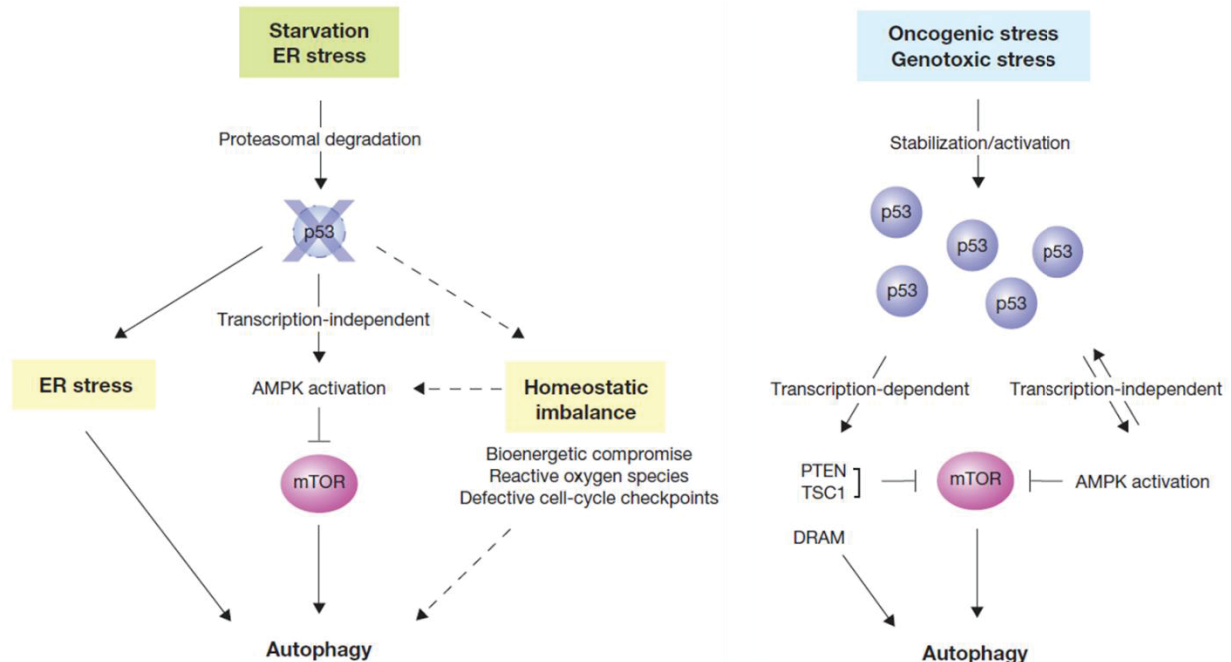


Figure 35: p53 dual role in autophagy regulation

Left panel: Inhibition of p53 upon starvation or ER stress leads to autophagy activation. p53 absence promotes ER stress-induced autophagy. p53 loss leads to homeostatic imbalance (for example reactive oxygen species generation) which triggers autophagy. Dotted lines represent a speculative pathway by which p53 depletion may also result in autophagy. **Right panel:** Positive regulation of autophagy by p53 upon oncogenic stress. p53 induces autophagy through both transcription dependent or independent functions (Levine and Abrams, 2008).

manner might be essential to drive the rapid cellular changes necessary for proper differentiation and development.

To conclude, the link between p53 and autophagy is complex given that p53 is able to activate or suppress autophagy depending on the type of stress and its subcellular localization.

2.4 Cell differentiation

Another physiological process regulated by p53 is cell differentiation. Again, p53 has a dual role, inhibiting or promoting differentiation, depending on cell type and the specific differentiation program (Molchadsky et al., 2008).

For example, it has been shown that p53 accumulation and activation blocks muscle differentiation by directly binding to myogenin promoter and suppressing its transcription (Yang et al., 2015) and inhibits osteoblast differentiation by downregulating Runx2 and Osterix gene expression, two transcription factors essential for the mesenchymal stem cells commitment into osteoprogenitor lineage (Lengner et al., 2006; Wang et al., 2006; Zambetti et al., 2006). Later, Molchadsky et al. confirmed this inhibitory role of p53 but he also showed that p53 is able to positively regulate both myogenic and osteogenic differentiation of skeletal muscle cells (Molchadsky et al., 2008).

Thus, p53 is a metabolic regulator having a dual function regarding cell fate and it has been suggested that p53 acts as a “guardian of differentiation”.

III.B.3 Role of p53 in development

Although most research on p53 focused on its tumor suppressor activity, several studies underlined the importance of p53 during development (Almog and Rotter, 1997; Brady

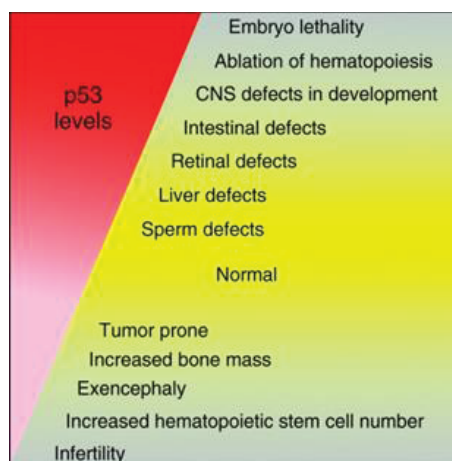


Figure 36: Both p53 accumulation and depletion are responsible for lethal phenotypes (Lozano, 2010)

and Attardi, 2010; Hainaut and Hollstein, 2000; Lozano, 2010). These studies suggest that p53 levels are important during embryogenesis since both loss or stabilization of p53 are responsible for developmental defects (Figure 36).

About 8-16% mouse embryos (mostly females) which are not expressing p53 exhibit defects in neural tube closure with an overgrowth of neural tissue in the midbrain region, an affection known as exencephaly (Sah et al., 1995). In parallel with exencephaly, affected mice also exhibit craniofacial malformations like ocular defects and anomalies in upper incisor tooth formation

(Armstrong et al., 1995). However, the capacity of p53 to regulate mammalian embryogenesis remains controversial because the majority of p53-null mice embryos are

developing normally and their only phenotype is a high risk to form tumors (Donehower et al., 1992; Sah et al., 1995). Absence of developmental defects can be due to the presence of two others p53 family members, p63 and p73 which have a similar structure to p53, are also expressed during early embryogenesis and are likely to have a compensatory effect for the loss of p53 (Stiewe, 2007). Even if they are expressed in early embryos, these two proteins are more involved in central nervous system development. p63 nullizygosity is perinatal lethal with defects in epithelium stratification, limb and craniofacial development and skeletal defects (Mills et al., 1999; Yang et al., 1999). p73 nullizygosity is lethal postnatally. The mice die several weeks after birth and until then they have a complex phenotype: reduced size, hippocampal dysgenesis, hydrocephalus, chronic infections, inflammation and pheromone sensing defects that impede breeding (Yang et al., 2000).

Recently, several labs have shown that combined loss of p53/p63, p53/p73 or p63/p73 have the same developmental defects than those described in single knockout embryos (Lee et al., 2004; Nemajerova et al., 2009, 2016; Van Nostrand et al., 2017). These results suggest that p53 family members have different roles during mammalian embryonic development.

In order to better analyze the possible compensatory pathways, Attardi lab generated p53, p63, p73 triple knockout mice (TKO). These TKO embryos are viable and showed no dramatic developmental defects compared with single knockout embryos (Van Nostrand et al., 2017). Instead, Wang et al., developed a TKO mouse model using CRISPR/Cas9 and observed that it promotes early defects in embryo development, starting at E7.5, due to an absence of mesendodermal differentiation from pluripotent embryonic stem cells. According to their model, these three protein members of p53 family have an important and redundant role during early embryo development (Okuda et al., 2017; Wang et al., 2017). L. Attardi suggested that the discrepancy between the two studies may relate to variations in genetic background of the mice or to a different time course of compensatory pathways upregulation due to the two different genetic technics used for *p53*, *p63* and *p73* inactivation.

As mentioned previously, not only *p53* inactivation induces embryonic defects but also p53 stabilization and activation during development lead to embryonic lethality. When p53 is accumulated and activated in murine models, due to Mdm2 or Mdm4 inactivation, mice die at E3.5 or E7.5 respectively and this phenotype is fully rescued upon p53 loss (Chavez-Reyes et al., 2003; Jones et al., 1995; Migliorini et al., 2002; Montes de Oca Luna et al., 1995; Parant et al., 2001). In normal conditions p53 half-life is very short: 30 minutes in undifferentiated ESC and only 10 minutes in more differentiated cells (Wang et al., 2011).

Thus, p53 dosage and activity are particularly important for embryonic and tissue development.

Furthermore, several studies emphasized that p53 is essential during NCC ontogeny and defective p53 signaling is associated with neurocristopathies and ribosomopathies.

III.B.4. Role of p53 in neural crest cell formation

It is known that NCC proliferation is essential to fine-tune epithelium-mesenchymal transition (EMT)-driven delamination from neural tube. p53 regulates cranial NCC proliferation by controlling p21 and CyclinG1 expression (Rinon et al., 2011).

By using a chick embryo model, it has been shown that p53 is expressed in neural plate and later in cranial NCC progenitors and its expression decreases when cells undergo an EMT (Figure 37A). p53 downregulation is necessary to prevent cell cycle arrest and to induce EMT gene expression (Snail2, Ets1, Mycn, Sox9, Pax7) (Figure 37B). Thus, Rinon et al. have shown that p53 coordinates cranial NCC growth and EMT/delamination during neural tube closure (Figure 37C).

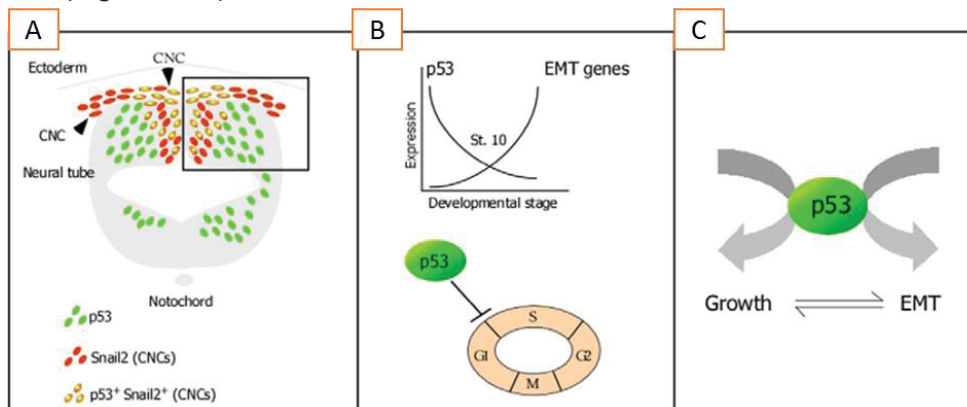


Figure 37: p53 regulates cranial neural crest cell migration

A: Schematic representation of a transverse section of 9-10 somite chick neural tube showing the expression of p53 (green cells) and SNAIL (cranial NCC (CNC) marker, red cells); p53⁺SNAIL⁺ CNC cells are yellow.

B: p53 expression decreased in CNCs undergoing EMT/delamination. p53 regulates cell cycle genes and proliferation. **C:** p53 coordinates CNC growth and EMT processes during neural tube closure (Rinon et al., 2011).

In line with this study, in Mdm4 knockout mice, p53 accumulation promoted cell cycle arrest which leads to embryonic lethality at E7.5 (Chavez-Reyes et al., 2003).

Mdm2 is preferentially expressed in neural folds and at E8-9 it is expressed in migratory NCC in head region, in migratory NCC in the tail region and in the first three branchial arches. At E9.5 Mdm2 becomes ubiquitously expressed (Daujat et al., 2001; Jain and Barton, 2010). Thus, at early stages Mdm2 expression may be essential for NCC migration. Mdm2 deletion, as Mdm4, may lead to an accumulation of p53 in NCC that could block their migration.

Hence, it has been shown that p53 accumulation and activation are responsible for disorders due to NCC defects like Treacher Collins syndrome and CHARGE syndrome (Table 8), among others neurocristopathies and ribosomopathies.

Co-expression of one p53 allele with mutations in both TAD1 and 2 (mutant p53^{25, 26, 53, 54}) along with a wild-type p53 allele in mice leads to a phenotype of CHARGE syndrome. Mutation of residues 25 and 26 in TAD1 of p53 protein blocked the interaction of p53 with

Mdm2 and thereby stabilized mutant p53. This mutant interacts, stabilizes and activates wild type p53 thereby triggering the CHARGE syndrome (Van Nostrand et al., 2014a).

Wild type p53 is accumulated in CHARGE syndrome also as a consequence of *Chd7* mutations (Van Nostrand and Attardi, 2014). It has been suggested that *Chd7* regulates p53 directly by binding to p53 promoter region and inhibiting its transcription. *Chd7* also regulates p53 indirectly by inducing p53 post translational modifications or via ribosomal biogenesis defects which perturb Mdm2-p53 interaction and promote p53 stabilization (Van Nostrand et al., 2014). *p53* inactivation in *Chd7*-deficient mice rescued their embryonic phenotype (Table 8) (Van Nostrand and Attardi, 2014).

By using a Treacher Collins syndrome (TCS) mice model (*Tcof1*^{+/-}) it has been shown that p53 is stabilized and activated in neuroepithelium and in premigratory cranial NCC and promotes craniofacial malformations (Jones et al., 2008). This accumulation of p53 increases CyclinG1 expression and promotes cell cycle arrest of cranial NCC progenitors (Jones et al., 2008). These observations support results from Rinon et al. presented above (Rinon et al., 2011).

Treacle, the protein encoded by *Tcof1* is important for DNA damage repair. Treacle is ubiquitously expressed in all stages of embryo development but its expression is increased in neuroepithelium and pre-migratory cranial NCC at E8.5-E10.5. This period of time and cellular localization also correlates with an increase in ROS levels (Sakai and Trainor, 2016). Thus, when Treacle is mutated or inactivated in TCS syndrome, the neuroepithelium and cranial NCC have high levels of ROS and DNA damage which activate p53 and promote apoptosis (Sakai et al., 2016). This apoptotic elimination of cranial NCC is the cause of TCS craniofacial malformations.

Limiting ROS formation and consequently oxidative DNA damage via treatment with antioxidants such as N-acetyl cysteine (NAC) decreases p53 activation and rescues craniofacial malformations (Sakai et al., 2016). Strikingly, p53 inactivation in *Tcof1*^{+/-} mice rescues the phenotype (Table 8) (Sakai and Trainor, 2016; Bursac et al., 2014; Van Nostrand and Attardi, 2014).

p53 mutants are also able to promote p53 accumulation and activation and lead to ribosomopathies. Homozygous expression in mice of p53^{Δ31} mutant, which does not have a functional negative regulatory domain localized in the C-terminal region and thus leads to increased p53 activity, triggers a phenotype similar to the ribosomopathy Dyskeratosis congenita (Simeonova et al., 2013).

Collectively, these data suggest an important role of p53 responses in the pathogenesis of ribosomo/neurocristopathies.

Neurocristopathies / Ribosomopathies	p53 accumulation in human patient samples	Mutated genes causing NCC defects	Genetic p53 alteration	Rescue time course	References
Treacher Collins syndrome (TCS)	Not reported	Tcof1 ^{+tm1Mid}	p53 ^{+/-} → 50% rescued for TCS phenotype p53 ^{-/-} → 100% rescued for TCS phenotype	E10.5 (hypoplasia of sensory neurons) E17.5 (cranioskeleton defects) Adult (6 months)	<ul style="list-style-type: none"> Sakai et al., 2016 Jones et al., 2008
Diamond Blackfan anemia	✓	Rps19 ^{+Dsk3} Rps7 ^{+Zma}	p53 ^{+/-} (p53 ^{+tm1TyJ}) → Partially ameliorates the phenotype of Rps19 ^{+Dsk3} mice p53 ^{-/-} (p53 ^{tm1TyJ/tm1TyJ}) → 100% reversed the phenotype of Rps19 ^{+Dsk3} mice p53 ^{+/-} (p53 ^{+tm1TyJ}) → 50% postnatal offspring viability → 47% rescued embryonic belly spot → 100% rescued for others embryonic defects of Rps7 ^{+Zma}	Adult (for Rps19 ^{Dsk3} /Rps ⁺) E10.5 –E12.5 (for Rps7 ^{+Zma})	<ul style="list-style-type: none"> Duff et al., 2011 McGowan et al., 2008 Daniola et al., 2008 Watkins-Chow et al., 2013
5q-syndrome	✓	5q- deletion: several genes affected including Cd74 ^{+tm1Aqjm} , Nid67 ^{+tm1Aqjm} and Rps14 ^{+/-} (Lmo2-Cre transgene)	p53 ^{+/-} (p53 ^{+tm1Bld}) → intermediate phenotype p53 ^{-/-} (p53 ^{tm1Bld/tm1Bld}) → 100% rescued phenotype	Adult	<ul style="list-style-type: none"> Barlow et al., 2010
Dyskeratosis Congenita	✓	Terc ^{tm1Rdp/tm1Rdp}	p53 ^{+/-} (p53 ^{+tm1TyJ}) → does not rescue the phenotype p53 ^{-/-} (p53 ^{tm1TyJ/tm1TyJ}) → phenotype partially rescued	Adult	<ul style="list-style-type: none"> Fok et al., 2017 He et al., 2009 Chin et al., 1999
CHARGE syndrome	✓	Chd7 ^{Gt1Dmm/Gt1Dmm}	p53 ^{+/-} (p53 ^{+tm1TyJ}) → phenotype partially rescued	E10.5	<ul style="list-style-type: none"> Hurd et al., 2007
Waardenburg I / III	✓	Pax3 ^{SpSp}	p53 ^{+/-} (p53 ^{+tm1TyJ}) → 42% embryo rescued for neural tube defects p53 ^{-/-} (p53 ^{tm1TyJ/tm1TyJ}) → 100% embryo rescued for neural tube defects	E8.5 (NTD) E10.5 (OFT defects)	<ul style="list-style-type: none"> Wang et al., 2017 Wang et al., 2011 Morgan et al., 2008 Pani et al., 2002
Di George syndrome	Not reported	Tbx1 ^{+tm1Bld}	p53 ^{+/-} (p53 ^{+tm1TyJ}) → 100% embryo rescued for Di George syndrome	E10.5	<ul style="list-style-type: none"> Caprio and Baldini, 2014 Lindsay et al., 2001

Table 8: Rescue of the neurocristo/ribosomopathy phenotype by p53 inactivation.

Genetic engineered mouse models with alteration of genes causatives of neural crest cells (NCC) defects were bred with mouse models of p53 inactivation. p53^{tm1TyJ} allele: neomycin cassette replacing exons2-6 (Jacks et al., 1994). p53^{tmBrd} allele: pol II-neomycin cassette inserted in exon 5 with small deletions in exons 4 and 5 (Donehower et al., 1992). NTD, neural tube closure defects; OFT, heart ventricular out flow tract.



To conclude, NCC are particularly sensitive to p53 dosage. The ability of p53 to initiate cell cycle arrest at specific developmental stages regulates NCC development. Disruption of this process can promote craniofacial defects and lead to human developmental pathologies such as neurocristopathies and ribosomopathies or can even lead to embryonic lethality. As we have seen in Chapter II.3, surgery ameliorates the symptoms of these developmental diseases but is often variable and rarely entirely corrective and in some cases the surgery is not even possible. Therefore, limiting downstream effectors of p53 signaling and/or limiting oxidative stress with antioxidants (such as NAC or vitamin C delivered as prenatal dietary supplements) may be successfully used for therapeutic prevention of these pathologies.

IV. LYSOSOMES: a signaling hub to maintain cell metabolism and homeostasis

In the previous chapter, we have seen that both metabolic regulators p53 and LKB1 are able to control AMPK and mTOR pathways. In the past years, it has been shown that lysosomes are not only important for macromolecules degradation, recycling and material storage but are also essential for the regulation of AMPK and mTOR signaling pathways and therefore are involved in several cellular processes. In this chapter I will describe the processes underlying lysosomal biogenesis. I will then detail the cellular functions attributed to lysosomes and I will focus on their capacity to regulate signaling pathways. Further, I will present how the microenvironment can affect lysosomal homeostasis and what are the consequences of lysosomal dysfunctions.

1. Lysosomes: multifunctional organelles required for recycling and clearance

1.1 Historical context

Lysosomes were discovered in 1955 from rat liver fraction studies. At first, C. de Duve lab observed that an enzyme, acid phosphatase, is enclosed within a special type of cytoplasmic granules upon starvation stress. Next, they searched for liver enzymes that, like acid phosphatase, were concentrated in these granules and they found five other liver enzymes: glucuronidase, cathepsin D, ribonuclease, deoxyribonuclease and urate oxidase. The presence, in the same membrane-limited pockets, of five acid hydrolases which have different substrates strongly suggested that these organelles are involved in intracellular digestion (de Duve, 2005; de Duve et al., 1955). This discovery led de Duve to name these structures lysosomes, derived from the greek for “digestive body”.

Nowadays, we know that lysosomes contain more than 50 acid hydrolases that can degrade proteins, lipids, polysaccharides, RNA and DNA.

1.2 Lysosome biogenesis

One important biological function for lysosomes is the degradation of material taken up from outside the cell by endocytosis. Endocytosis is not only crucial for lysosome function but also during lysosome formation. Material from outside the cell is taken up in clathrin-coated endocytic vesicles which fuse with early endosomes, the primary sorting station in the endocytic pathway. The early endosomes gradually mature into late endosomes, which are the precursors to lysosomes. During their formation, lysosomes will be progressively charged with hydrolases as these enzymes are transported into clathrin-coated vesicles from *trans*

Golgi to the lysosome. One of the important modifications during endosome maturation is the pH acidification to 5.5 which is made possible due to the presence of vacuolar H⁺-ATPase at the membrane of the lysosome. Indeed, this protein will pump the protons inside the lysosome thus acidifying the lysosome lumen. Such an acidification is essential for hydrolases activity (Cooper, 2000).

1.3 Classical lysosomal functions

These acidic vesicles are involved in several cellular processes such as:

- Macroautophagy, in this manuscript referred to as autophagy (digestion of misfolded or long-live proteins, organelles and other material inside the cell) (Figure 38) (Hubert et al., 2016). Autophagy can be defined as a two-steps process with:
 1. an induction step where an autophagosome is formed around the cytoplasmic components that have to be degraded (on-rate process).
 2. a turnover step corresponding to the formation of the autolysosome after the fusion between the autophagosomes and lysosomes which are vesicles containing hydrolytic enzymes (off-rate process). During this second step, the cargo of autophagosome are degraded by lysosomal hydrolases (Baehrecke, 2005).
- Heterophagy (digestion of materials from outside the cell such as bacteria). Lysosomes are able to fuse with phagocytic vesicles, which ingest outside macromolecules or parasites, and form secondary lysosomes degrading macromolecules.
- Autolysis (complete break-down of died cells). Lysosomes promote autolysis by releasing digestive enzymes into the cytoplasm of cells.
- Exocytosis (release of enzymes and metabolites outside of the cell). Lysosomes promote exocytosis via the proteins present at their surface, necessary for lysosome movement and fusion with the plasma membrane.

All these lysosomal functions are important for recycling the products of biochemical reactions but lysosomes are also involved in others cellular functions such as (Saftig and Klumperman, 2009):

- plasma membrane repair, a calcium dependent process (Idone et al., 2008).
- cholesterol homeostasis via the lipidic transporter Niemann-Pick C1 protein (NPC1) localized at their membrane surface (Chang et al., 2006).
- Major Histocompatibility Complex (MHC) class II – dependent antigen presentation (van Niel et al., 2006; Shin et al., 2006).
- other physiological processes such as cell migration (e.g. neural crest cells via Ca²⁺ storage), morphogenesis (e.g. limb development), synaptic plasticity and cell maturation (e.g. Schwann cells) that I will detail later, in paragraph IV.3.1.

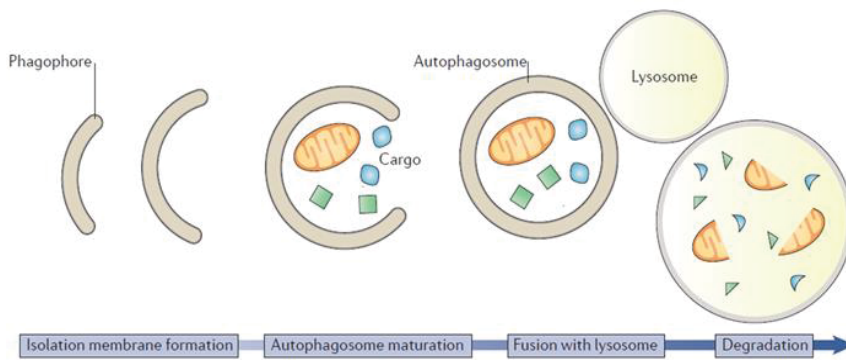


Figure 38: Cellular mechanisms of autophagy

The first step of autophagy is the phagophore formation, an isolated membrane which matures and forms autophagosome that contains the cargo for degradation. Autophagosome interacts with lysosome which contains the enzymes necessary for the degradation of autophagosome cargo. (Modified from Herzig and Shaw, 2017)

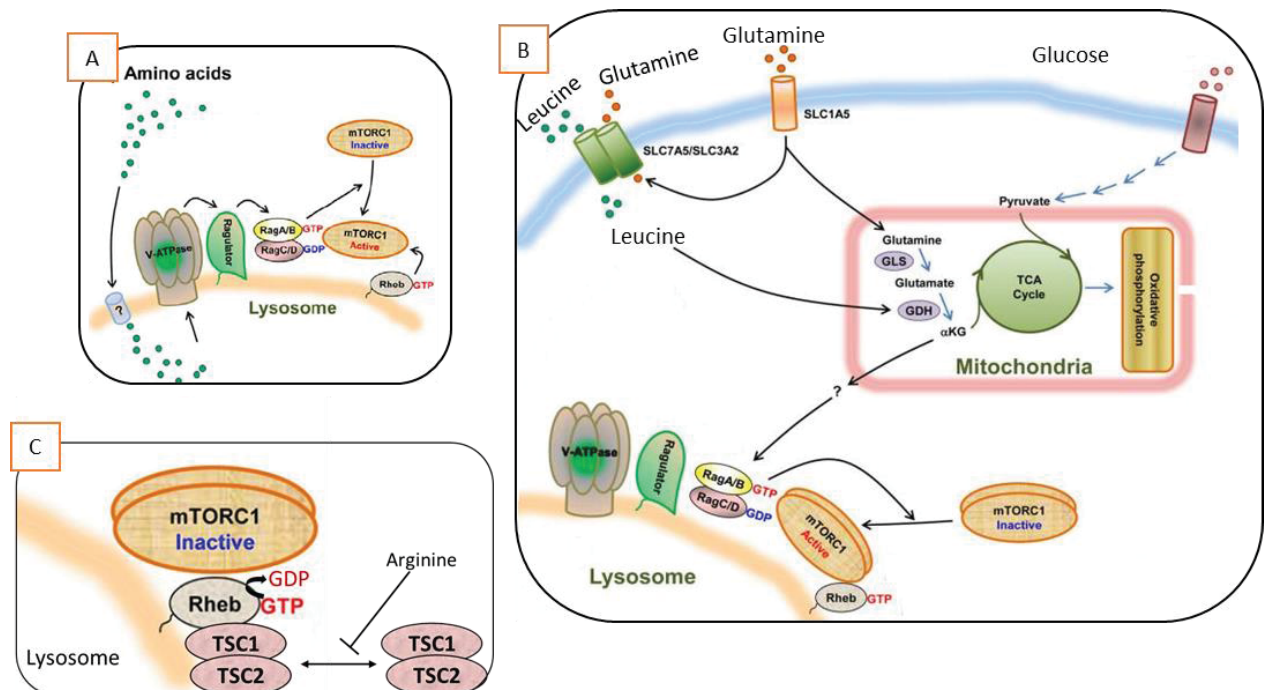


Figure 39: mTORC1 activation at the lysosomal surface

A. mTORC1 recruitment to lysosome membrane through v-ATPase/ Ragulator/ RagGTPase activation in an amino acid dependent manner. **B.** Leucine in presence of glutamine is responsible for RagGTPase activation and mTORC1 translocation at lysosomal surface. **C.** mTORC1 activation at lysosomal membrane in an amino acid dependent manner. TSC1/TSC2 are negative regulators of Rheb which is an mTORC1 activator (Adapted from Kim et al., 2013).

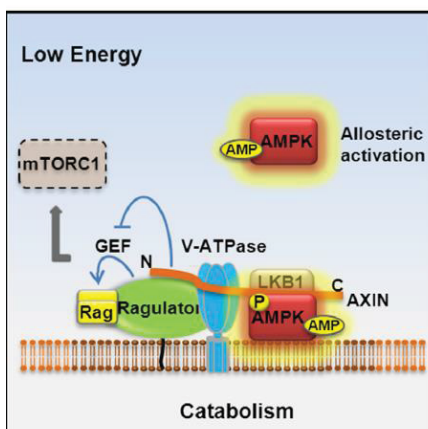


Figure 40: AMPK activation at the lysosomal surface

Upon starvation, AMPK is recruited to the lysosomal membrane via Axin. Axin recruits also LKB1 which phosphorylates AMPK on threonine 172. AMPK activation, as mTORC1, depends on v-ATPase and Ragulator activities. When AMPK is activated, mTORC1 is detached from lysosome and is inactivated (Zhang et al., 2014).

2. Lysosomes as a signaling hub to control nutrient homeostasis

Recently it was shown that lysosomes serve as a platform to activate signaling pathways such as mTOR and AMPK in an amino acid dependent manner, being therefore involved in the regulation of nutrient and energy homeostasis. Thus, in the following paragraphs, I will describe the mechanisms needed for mTOR and AMPK recruitment and activation at lysosomal surfaces and the crosstalk between p53 signaling and mTOR activation at this subcellular location.

2.1 mTOR pathway at the lysosomal surface

Recruitment of mTORC1 at the lysosome

mTORC1 binds to lysosomal membrane via a small G protein named RagGTPase (Figure 39A). RagGTPase is a heterodimer (RagA or B with RagC or D) that interacts with Ragulator, a hetero-pentameric complex anchored within the lysosomal membrane (Figure 39A) (Bar-Peled et al., 2012). Thus, Ragulator recruits RagGTPase to lysosomal membrane but it can also activate RagGTPase by acting as a guanine nucleotide exchange factor for RagA or B (Figure 39A) (Kim et al., 2013b). Concomitantly, the active form of RagGTPase binds to p62/SQSTM1 which associates with Raptor, a subunit of mTORC1 complex, and therefore indirectly recruits mTORC1 to lysosomes (Bitto et al., 2014; Nicastro et al., 2017).

The guanine nucleotide exchange factor activity of Ragulator is controlled by vacuolar H⁺-ATPase (v-ATPase) which can be activated by amino acids present into the lumen of the lysosomes (Figure 39A) (Bar-Peled et al., 2012). Therefore, amino acids are also important regulators of mTORC1 localization to lysosomes. They can regulate the activity and conformation of RagGTPase and subsequently the translocation of mTORC1 to the lysosome surface (Bar-Peled et al., 2012; Demetriades et al., 2014; Sancak et al., 2010). α -Ketoglutarate (α KG) is an intermediate of the Krebs cycle and a by-product of many amino acid transaminations. This metabolite is also essential for mTORC1 lysosomal translocation because it stimulates RagGTPase activity by promoting GTP loading on RagA or B (Figure 39B). α KG production is regulated by leucine. This essential amino acid directly binds to GDH (glutamate dehydrogenase) which catalyzes the formation of α KG from glutamate (Figure 39A). However, leucine alone is not sufficient to activate mTORC1. It has been shown that intracellular glutamine is necessary for stimulation of mTORC1 by leucine (Figure 39B) (Durán et al., 2012).

Thus, mTORC1 localization to lysosomal membrane is controlled by RagGTPase and Raptor and regulated by amino acids such as leucine and glutamine. This specific localization of mTORC1 at the surface of lysosomes is essential for its activation.

Activation of mTORC1 at the lysosome

This specific lysosomal membrane localization brings mTORC1 near its regulator called Ras homologue enriched in brain (Rheb), a cell-membrane protein localized to lysosome and other endomembranes (Figure 39A and B). It is known that Rheb is crucial for mTORC1 activity but little is known about the underlying mechanism. What is known so far, based on *in vivo* and *in vitro* studies, is that the direct interaction between Rheb and mTORC1 is sufficient to promote mTOR kinase activity (Avruch et al., 2009a, 2009b; Sato et al., 2009).

TSC1 and TSC2 are negative regulators of Rheb. When TSC interacts with Rheb, it promotes the conversion of active Rheb^{GTP} to inactive Rheb^{GDP}, delocalizing it from lysosomes (Figure 39C). This delocalization consequently inactivates mTORC1.

It is also known that amino acids or growth factors maintain Rheb at the lysosome and therefore regulate mTORC1 activity (Carroll and Dunlop, 2017). For example, arginine acts as a specific inhibitor of TSC2 recruitment to lysosomes (Figure 39C) (Carroll et al., 2015). Another example is with MiCRoSpherule protein-1 (MCRS1) which avoids the Rheb-TSC2 interaction, in an amino acid dependent manner, maintaining Rheb at the lysosomal surface and connecting Rheb to mTORC1 (Fawal et al., 2015).

Altogether, these data point out a novel function of lysosomes in the regulation of mTOR activity and underline the importance of amino acids and growth factors for lysosomal localization and activation of the mTOR pathway.

Interestingly, lysosomes are also involved in recruitment and activation of AMPK, a physiological antagonist of mTOR.

2.2 Recruitment and activation of AMPK at the lysosomal surface

AMPK is localized in cytoplasm or nucleus, depending on the stimuli that the cells received such as energy stress, cell density etc. Recently, it has been shown that AMPK, under energy stress, is also localized and activated at lysosomes. One protein responsible for AMPK lysosomal localization and activation is Axin (Zhang et al., 2018). In 2013, Zhang Y.L *et al.* have observed that Axin controls AMPK activity by regulating AMPK phosphorylation on threonine (Thr) 172 by LKB1 (Zhang et al., 2013b). Indeed, Axin physically binds to both LKB1 and AMPK and stimulates the interaction between these two kinases (Figure 40). Axin/LKB1/AMPK complex formation is regulated by AMP and energy stress as follows:

Upon energy stress such as glucose deprivation, the N-terminal region of Axin interacts with LAMTOR1, a subunit of the Ragulator complex while the C-terminal region of Axin interacts with LKB1 and triggers its translocation to the lysosome (Figure 40) (Zhang et al., 2014, 2018). Ragulator, and more precisely LAMTOR1, is localized on the late-endosome which will form the lysosome. Therefore, the formation of the complex between LAMTOR1 and Axin/LKB1/AMPK occurs on late endosomes. When the maturation of the late endosome

is damaged, it strongly impairs AMPK activation. Thus, lysosomes are important for AMPK activation upon energy stress. Moreover, upon glucose starvation, the v-ATPase changes its conformation, being capable of interacting with Axin but losing its capacity to activate GEF function of Ragulator (Figure 40). Thus, this new conformation promotes Axin/LKB1 translocation to the lysosome and AMPK activation and delocalizes mTORC1 from the lysosomal membrane (Figure 40) (Zhang et al., 2014). This suggest that depending on stimuli, v-ATPase and Ragulator control the lysosomal translocation of either Axin/LKB1/AMPK or mTORC1 complexes.

Metformin (N,N-dimethylbiguanide), the most widely used treatment for type 2 diabetes, is using this Axin/LKB1/v-ATPase/Ragulator lysosomal pathway to increase AMPK activity and to inhibit mTOR (Howell et al., 2017; Zhang et al., 2016).

To conclude, lysosomes are crucial for both mTOR and AMPK activation. mTOR is anchored at lysosomal membrane through RagGTPase, v-ATPase and Ragulator. Its presence at the lysosomal surface allows its interaction with the activator Rheb. Both localization and activation of mTOR are amino acid dependent. AMPK, under energetic stress, is also translocated at the lysosome surface via Axin interaction with Ragulator and v-ATPase. This interaction is also important for LKB1 localization to the lysosomal membrane where it phosphorylates AMPK at threonine172. However, this interaction delocalizes mTORC1 from the lysosome. Thus, the activation of AMPK and mTORC1 at the lysosomal surface is mutually exclusive.

Interestingly, the other tumor suppressor protein p53, previously described in this manuscript, also plays an important role during mTOR/AMPK activation at lysosome's surface.

2.3 p53 signaling and mTOR/AMPK activation at lysosomes surface

It has been shown by Xuetao Cao lab that p53 can also translocate to lysosomal membranes (Li et al., 2007). In general, p53 phosphorylation on serine15 is associated with its stabilization and with the activation of its nuclear function. However, in Nan Li et al. study, the phosphorylation of p53 on serine15 is essential for its lysosomal translocation.

Lysosome-localized adaptor protein (LAPF) is the protein which recruits phosphorylated p53 on Serine15 to the lysosome (Li et al., 2007). Upon apoptotic stimuli such as TNF α and ionizing irradiations, LAPF physically interacts with TAD domains of p53. This interaction is dependent on p53 phosphorylation on serine15. p53 phosphorylation on other serine positions such as 6, 9, 20, 33, 37 or 46 did not promote any interaction between p53 and LAPF and did not recruit p53 at the lysosomes (Li et al., 2007).

At the lysosome, p53 promotes lysosomal membrane permeabilization which involves leakage of luminal lysosomal hydrolases into the cytoplasm and will induce apoptosis. For the moment, nothing is known about a possible regulation of mTORC1 by LAPF or by lysosomal phosphorylated p53 on Serine15 in vertebrates. However, it has been shown in the yeast *Saccharomyces cerevisiae* that the LAPF-like protein named Pib2, present at the lysosomes, promotes the lysosomal membrane permeabilization and subsequently cell death through mTORC1 regulation, upon ER stress (Kim and Cunningham, 2015).

Thus, cytosolic p53 triggers apoptosis in a transcription-independent manner, through its translocation to lysosomes thanks to LAPF while nuclear p53 regulates mTORC1 and AMPK lysosomal localization and activation through its transcriptional activity (Chapter III.B-2.2). For the moment, nothing is known about p53 lysosomal role regarding mTORC1/AMPK localization and activation.



Altogether, these studies have shown that lysosomes are acidic vesicles involved in many cellular processes, the most recently discovered one being adjustment to nutrient conditions through mTOR/AMPK lysosomal translocation and activity. Lysosomal localization and activation of these pathways depend on the presence of several amino acids such as leucine, arginine and glutamine. Interestingly, both LKB1 and p53 translocate at lysosome surface where they regulate different processes: LKB1 activates AMPK and subsequent cell adaptation to energetic stress while p53 induces lysosomal membrane permeabilization and apoptosis.

Thus, lysosomes are signaling hub that can integrate and relay external and nutritional information. In the next paragraph, I will describe the impact of lysosomes on physiological processes.

3. Lysosomal roles in normal and pathological processes

3.1 Lysosomal functions during development and adult maintenance

It is known that calcium (Ca^{2+}) is a cell migration-regulator because increased Ca^{2+} levels modulate cytoskeleton dynamics and promote cell contraction and adhesion (Praitis et al., 2013; Sumoza-Toledo et al., 2011). Lysosomes are acidic organelles capable of modulating intracellular Ca^{2+} levels. They uptake Ca^{2+} from cytosol via $\text{Ca}^{2+}/\text{H}^{+}$ exchangers (CAX) channels (Melchionda et al., 2016) and are able to release it via other calcic channels such as TRMPL1 (Lloyd-Evans, 2016; Patel and Cai, 2015).

It has been proposed that lysosomes regulate embryonic development (Tsukamoto et al., 2013). In particular, it was shown that lysosomes are important for early developmental processes such as frog neural crest cell migration through calcic level regulation (Lloyd-Evans, 2016; Melchionda et al, 2016). Morpholino-mediated knockdown of CAX expression, in frog, increased cytosolic Ca^{2+} amount and blocked neural crest cell migration (Lloyd-Evans, 2016; Melchionda et al, 2016).

The capacity of Ca^{2+} to enhance cell attachment was also observed in cardiac NCC (Heidenreich et al., 2008). Thus, lysosomes are essential regulators of neural crest cell migration through Ca^{2+} level modulation.

Lysosomes control also more tardive developmental processes than NCC migration such as morphogenesis. It is known that the majority of organ-development is regulated by a well-defined zone of programmed cell death. Zuzarte-Luis et al., have shown that lysosomal cathepsins such as cathepsin D and B are crucial for mice and chick limb development because it regulates embryonic programmed cell death through Bone Morphogenetic Protein (BMP) pathway (Zuzarte-Luis et al., 2006). Thus, lysosomes have a sculpturing function during limb morphogenesis and are responsible for the difference in webbed digits between chick and duck.

Lysosomes are also able to sustain adult physiological processes such as plasma membrane repair, defense from parasites, energy pool maintenance, synaptic plasticity and cell maturation. Cells such as melanocytes, astrocytes or hematopoietic cells, harbor specialized secretory lysosomes. They contain, in addition to hydrolases, proteins necessary for secretion and, at their surfaces, proteins necessary for lysosome movement and fusion with the plasma membrane. These secretory lysosomes are called lysosome-related organelles and are important for plasma membrane repair and defense from parasites (Andrews et al., 2002; Divangahi et al., 2009a, 2009b; Reddy et al., 2001). Moreover, it has been shown in astrocytes that extracellular glutamate induces partial exocytosis of lysosomes which contain abundant ATP. The release of ATP from astrocytes is required for Ca^{2+} wave propagation among astrocytes and for feedback modulation of synaptic functions (Li et al., 2008; Zhang et al., 2007). Synaptic plasticity is regulated through lysosomal function of degradation which decreases the number of dendritic spines, essential for long-term memory and cognition (Goo et al., 2017; Kononenko, 2017). Lysosomes can also control Schwann cell maturation because, due to their degradation capacity, they properly reduce Schwann cell cytoplasm during myelination in the peripheral nervous system (Jang et al., 2016).

Thus, lysosomes are essential for many physiological processes and therefore defects in lysosomal functions are generating a large panel of human pathologies.

As both LKB1 and p53 are regulators of reactive oxygen species production and as oxidative stress is responsible for some neurocristopathies (Chapter II.3), I have chosen to further detail the effect of oxidative stress on lysosomal homeostasis. I will then describe how defective lysosomes impact cell homeostasis and in particular how they trigger senescence, age-related diseases and other human pathologies called lysosomal storage disorders.

3.2 Oxidative stress and lysosome homeostasis

3.2.1. Reactive oxygen species production

Reactive oxygen species (ROS) are chemical molecules containing oxygen such as hydrogen peroxide (H_2O_2), superoxide (O_2^-) and hydroxyl radical ($\cdot OH$). They are produced by several organelles: mitochondria, peroxisomes, endoplasmic reticulum, plasma membrane through the oxidative metabolism (Muller F., 2000; Han D. *et al.*, 2001).

In the cell, there are several non-enzymatic and enzymatic antioxidants like superoxide dismutase 1 and 2 (SOD1, SOD2) and catalase which are capable to detoxify ROS and to prevent oxidative stress (Figure 41) (Zhao *et al.*, 2017).

In normal conditions ROS production by mitochondria through incomplete one-electron reduction of oxygen represent 1-2% of the total rate of oxygen consumption (Zhao *et al.*, 2017). However, if mitochondria are damaged higher levels of ROS are formed and antioxidants are not anymore able to prevent oxidative stress (Figure 41) (Chance *et al.*, 1979; Gorrini *et al.*, 2013; Panieri and Santoro, 2016; Zhao *et al.*, 2017).

Cells adjust differently depending on ROS levels. For example, moderate ROS levels are able to promote tumor growth and malignant progression by inactivating the protein tyrosine phosphatases and therefore regulating kinases pathways involved in tumor progression such as phosphoinositide 3-kinase (PI3K) and tyrosine kinase receptor (TKR) signaling (Locasale and Cantley, 2011). While, high ROS levels promote DNA damage and affects genome integrity, leading to cell senescence and death (Figure 41) (Gorrini *et al.*, 2013).

3.2.2. ROS & lysosomal membrane permeability

Mitochondrial dysfunction increases ROS production which affects the lysosomal membrane integrity via lipid peroxidation and causes lysosomal alkalinization (Demers-Lamarche *et al.*, 2016; Kurz *et al.*, 2008; Pivtoraiko *et al.*, 2009). Under oxidative stress, H_2O_2 is able to translocate from cytoplasm into lysosome where it interacts with ferric ions and produces ferrous ions and hydroxyl radicals (Figure 42) (Fenton reaction). Hydroxyl radicals induce lysosomal membrane peroxidation which leads to membrane rupture (Pivtoraiko *et al.*, 2008). Thus, oxidative stress causes dysfunction in lysosomes.

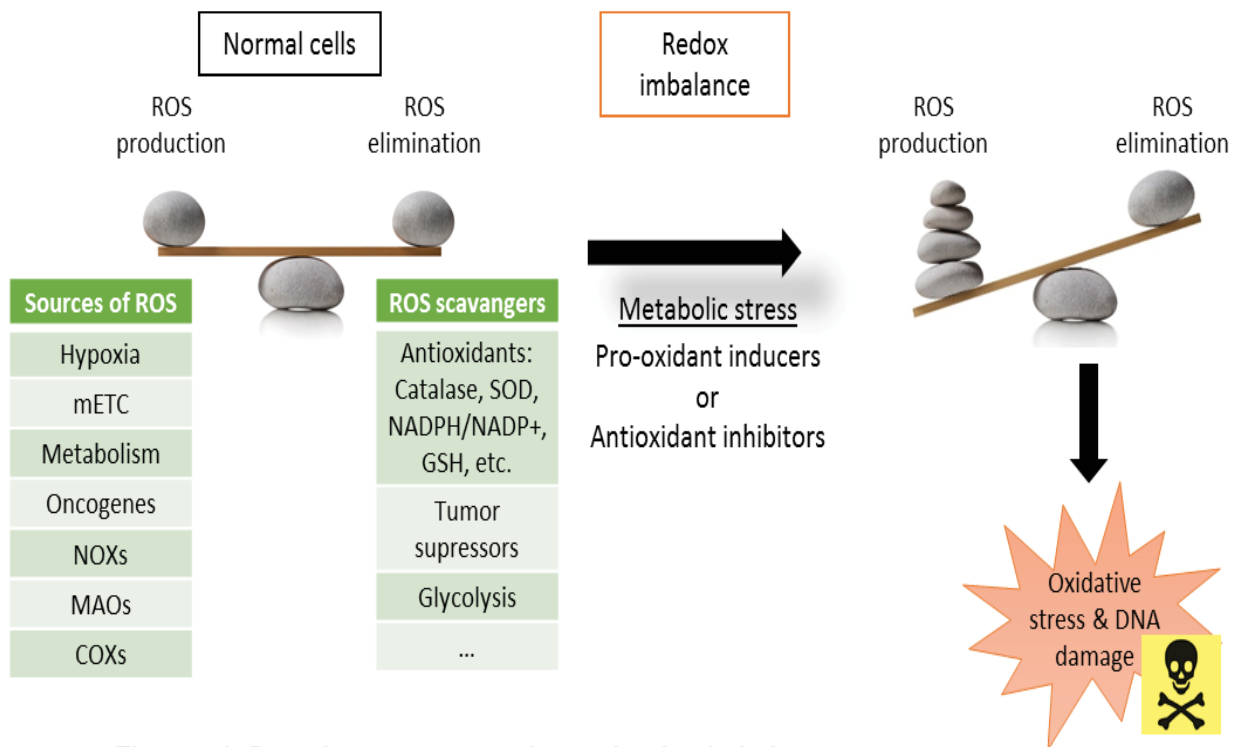


Figure 41: Reactive oxygen species and redox imbalance outcome

In normal cells there is a balance between reactive oxygen species (ROS) production and elimination. A metabolic stress is able to imbalance this mechanism and if the ROS production is very high it promotes DNA damage and cell death. mETC, mitochondria electron transport chain; NADPH, nicotinamide adenine dinucleotide phosphate; NOXs, NADPH oxidase family of enzymes; MAOs, mitochondrial MonoAmine Oxidase; COXs, cyclooxygenase; SOD, Superoxide dismutase; GSH, glutathione.

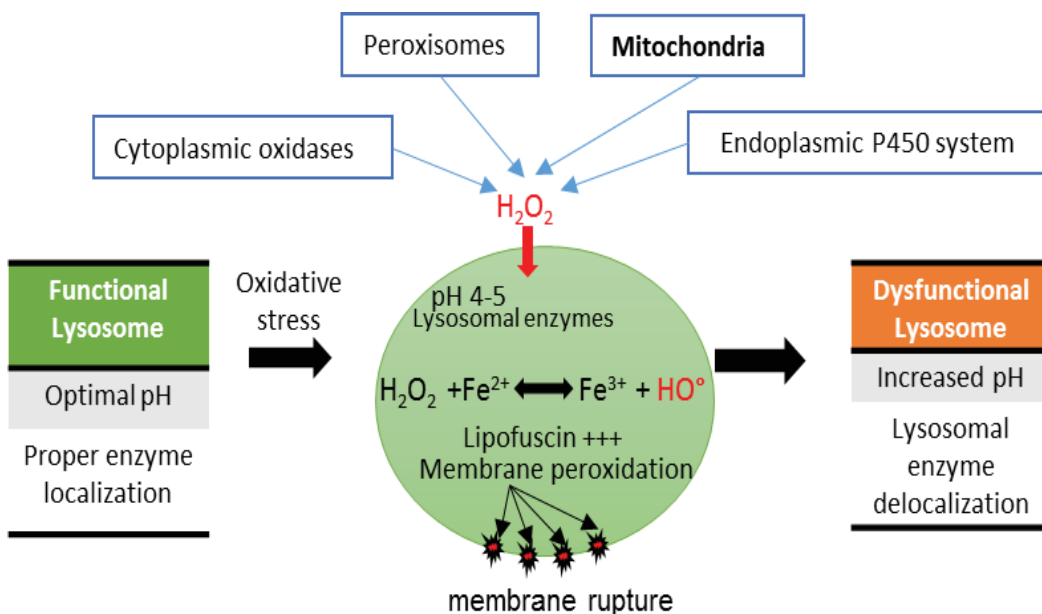


Figure 42: Oxidative stress-induced lipofuscin formation within lysosomes

(Adapted from Terman and Brunk, 1998; Brunk et al., 1992)

The lysosomal leakage is directly proportional with the intralysosomal iron concentration (Kurz et al., 2008) and with the increased lysosomal pH due to proton leakage (Porter et al., 2013). There is heterogeneity regarding lysosomal resistance to oxidative stress between cell types but also within cells. Scientists suggested that these differences between lysosomes depend on several parameters (Chen, 2002; Nilsson et al., 1997):

- antioxidant properties of cells to eliminate H₂O₂ before it reaches lysosomes.
- iron concentration inside the lysosomes.
- lysosomal lumen pH.

Iron accumulation (mostly in mitochondria and lysosomes) which subsequently increases the sensitivity to oxidative stress (Kurz et al., 2008) and lysosomal alkalinization (Guha et al., 2014) was found in many diseases associated with protein accumulation such as Alzheimer's disease and acute myeloid leukemia. Interestingly, Mitchell lab suggested that increasing cAMP concentration decreases the lysosomal pH and reduces the protein buildup in these pathologies (Coffey et al., 2014).

To conclude, oxidative stress due most generally to mitochondrial malfunction causes lysosomal membrane permeabilization which perturbs the pH gradient and induces lysosomal enzyme delocalization inside the cytoplasm where they can affect other organelles such as mitochondrial permeability directly or indirectly via phospholipases.

3.3 Characteristics of defective lysosomes (lipofuscin granules)

Oxidative stress is responsible for lysosomal peroxidation which leads to accumulation of lipofuscin into the lysosomes (only 1% of lipofuscin is found free into the cytoplasm) (Armstrong et al., 2010; Carmona-Gutierrez et al., 2016; Höhn et al., 2010a; Terman and Brunk, 1998). Lipofuscin is an aging pigment (Ames et al., 1993) discovered a long time ago, in 1842, by Hannover. Even if it was identified 175 years ago the exact cellular function of this material is still not well understood.

Lipofuscin is an electron dense, autofluorescent material detected by a range of excitation wavelengths including ultraviolet (330-380nm), blue (450-480nm) and green (510-560nm) light (Tohma et al., 2011). 30-70% of its composition is represented by oxidized proteins, 20-50% by lipids (Höhn et al., 2010b; Jung et al., 2007; Porter et al., 2013; Terman and Brunk, 1998), low amounts of saccharides (Benavides et al., 2002) and 2% by metals, including Fe, Cu, Zn, Al, Mn and Ca (Jolly et al., 1995). Lysosomal proteolysis decreases with age and since proteins represent a high percentage in lipofuscin composition, decreased intralysosomal degradation can cause lipofuscin accumulation (Skoczyńska et al., 2017). Lipofuscin is accumulated with age in lysosomes of postmitotic cells such as neurons, glial cells, cardiac myocytes, muscle fibers, Sertoli cells and retinal pigment epithelial cells (Terman and Brunk, 1998). However, inhibition of lysosomal proteases and lipases (Marzabadi et al.,

1991) or the presence of high amount of active iron into lysosomes (which increases oxidative stress and peroxidation processes as seen above) leads to increase rate of lipofuscin accumulation in an age independent manner (Terman and Brunk, 1998). Therefore, antioxidants such as Vitamin E, glutathion or ions chelators are protecting cells from lipofuscin accumulation while prooxidants have the opposite effect and significantly increase lipofuscin formation (Terman and Brunk, 1998). Lipofuscin is also able to stimulate its own production by increasing prooxidant molecules expression (Hohn et al., 2010) and by inhibiting oxidized protein degradation through proteasome inhibition (Hohn et al., 2011; Sitte et al., 2000; Powell et al., 2005).

3.4 Lysosome functions in human pathologies

3.4.1 Age-related diseases

Lipofuscin granules are generally associated with aging and with age –related diseases such as neurodegenerative diseases like Alzheimer, Parkinson, and Huntington diseases (Brunk and Terman, 2002). High levels of lipofuscin and lysosomal enzymes are observed in amyloid deposits in Alzheimer's patients (Skoczyńska et al., 2017). Lipofuscin accumulation was also observed in premature aging syndromes (Brunk and Terman, 2002).

Lipofuscin is frequently observed in association with senescence, an irreversible mechanism that arrests cell cycle (Georgakopoulou et al., 2012). Senescent cells are associated with four biological processes: carcinogenesis (Shay and Roninson, 2004), tumor suppression (Collado and Serrano, 2010), age-related disorders and tissue repair (Rodier and Campisi, 2011). Considering the results I have obtained during my PhD linking LKB1 and p53 to lipofuscin granules formation (Results. Project 2.2), I will further focus on cellular senescence and aging.

Among the most compelling evidences that senescence promotes age-related disorders are the phenotypes of mice with hyperactivated p53. In particular, heterozygous mice harboring one p53 allele deleted in the first six exons of the *p53* gene (Tyner et al., 2002) or transgenic mice expressing the $\Delta 40p53$ or $\Delta Np53$ isoforms (Maier et al., 2004; Rufini et al., 2013) exhibit an important resistance to develop spontaneous tumors. However these mice have a reduced lifespan characterized by accumulation of senescent cells in different tissues and a complex phenotype, including loss of fertility, with a "Sertoli cell only" phenotype in most of the seminiferous tubules, loss of subcutaneous fat, osteoporosis, sarcopenia and reduced hair growth (Maier et al., 2004; Tyner et al., 2002).

As presented in Chapter III.B.1.2, oxidative stress activates p53. Activated p53 induces a specific transcriptional response that regulates cellular senescence and aging (Gambino et

al., 2013). p53-mediated senescent cells are associated with the formation and accumulation of lipofuscin and premature aging (Georgakopoulou et al., 2012).

In conclusion, lysosomes are important organelles which prevent premature aging by controlling signaling pathways, lipofuscin formation and cell senescence.

3.4.2 Lysosomal storage disorders

Defects in lysosomal glycan, lipid or protein degradation or defects in lysosomal transporters or trafficking are responsible for lysosomal storage disorders. These human diseases constitute a group of metabolic developmental disorders characterized by accumulation of non-degraded material in the lysosomes (Ballabio and Gieselmann, 2009; Greiner-Tollersrud and Berg, 2013; Onyenwoke and Brenman, 2015; Schultz et al., 2011). There are more than 50 types of lysosomal storage disorders and many are associated to neurodegeneration. This neural death can be due to neuron mitochondrial defects or to glial cell dysfunctions which lead to demyelination (Folkerth, 1999; Onyenwoke and Brenman, 2015; Rama Rao and Kielian, 2016; Saher and Stumpf, 2015). As discussed above, lysosomes also regulate synaptic plasticity and therefore long-term memory and cognition, cognitive defects representing the first sign of lysosomal storage disorders in patients (Goo et al., 2017).



To sum up, lysosomes are not only important for degradation processes but have many other cellular functions during embryonic development and adult physiological processes, such as cell migration, differentiation, cell protection and repair, nutrient and energy homeostasis. Therefore, lysosomal defects due to oxidative stress are responsible for various human pathologies as lysosomal storage disorders and neurodegenerative diseases. Momently, there is no cure for lysosomal storage disorders or lipofuscin accumulation. Treatments such as bone marrow transplantation and enzyme replacement therapy have partially decreased lysosomal storage disorders and Parkinson's disease symptoms and improved lysosomal enzyme activity (Clarke and Iwanochko, 2005; McNeill et al., 2014). Interestingly, treatments decreasing oxidative stress such as iron chelators, vitamin E and glutathione treatments, delay lipofuscin production and accumulation in murine models (Brunk and Terman, 2002; Skoczyńska et al., 2017).

PhD context & objectives

As highlighted in the introduction, uncovering connections between metabolic responses and cell signaling pathways has recently encounter an impressive increase. One important signaling pathway regulating energy metabolism is controlled by the tumor suppressor LKB1. Before studies underlining LKB1 role in metabolic regulations through AMPK pathway, functions of Lkb1/AMPK pathway were predominantly explored in cell polarity in *Caenorhabditis elegans* (J.L. Watts et al., 2000) and *Drosophila melanogaster* (Martina and St Johnston, 2003). These studies established that LKB1 signaling is a major regulator of cell polarity through in particular the establishment and maintenance of cell junctions. Data from the literature prompted us to better characterize if LKB1 coordinately regulates cell metabolism and polarity partly through the control of its downstream kinase AMPK and the negative regulation of the mTOR pathway.

In particular, it is now well established that cell polarity is essential for neural crest cells (NCC) development, including their migration and differentiation. However, the metabolic processes underlying NCC development remain poorly understood. Therefore, during my PhD, I explored the contribution of LKB1 in the control of polarity and energy metabolism in NCC.

Along this line, in a first PhD project, I participated to the exploration of LKB1 involvement during cranial NCC polarized migration and vertebrate head development. I also contributed to the characterization of LKB1 post-translational modification by acetylation, and how acetylated LKB1 could regulates cranial NCC ontogeny.

In a second PhD project which was also my main project, I investigated the metabolic regulations exerted by LKB1 during NCC fate and assessed if LKB1 controls NCC differentiation by limiting oxidative stress and p53 activation while favoring lysosomal activity, possibly in order to prevent premature aging.

Finally, during my third PhD project, I analyzed energy metabolism in other models of cell polarity that are Sertoli cells and epithelial colorectal adenocarcinoma cells to better understand how LKB1 signaling coordinately regulates cell polarity and metabolism.

Results

I. Project 1: LKB1 in cranial neural crest cells

Multipotent neural crest cells (NCC) originate from the dorsolateral folds of the neural tube and constitute a population of highly motile embryonic cells. These cells give rise to a broad range of derivatives including pigmented cells, most of the head skeleton, peripheral nerves and the enteric nervous system that allows the motricity of the digestive tract (Simões-Costa and Bronner, 2015).

The tumor suppressor gene *LKB1* encodes a serine/threonine kinase that acts as a pivotal regulator of energy metabolism via the activation of AMPK, a sensor of the cellular energy status (Force et al., 2007; Hezel et al., 2008). *LKB1* is a tumor suppressor gene and germline mutations of *LKB1* are responsible for the human Peutz-Jeghers syndrome, an autosomal dominant disease characterized by the presence of mucosal gastrointestinal polyps and an increased risk to develop malignant tumors (see Introduction, Chapter III.A.5). Peutz-Jeghers syndrome also associates hyperpigmented macules of the skin, suggestive of defective melanocytes homeostasis and *LKB1* role in the biology of melanocytes has been established (Liu et al., 2012). Homozygous disruption of *Lkb1* in mice is embryonic lethal and causes defects in the neural tube closure, an absence of the first branchial arch (mostly composed of NCC) and facial reduction (Ylikorkala et al., 2001).

Altogether, these data were convincing arguments hinting at a role of the *LKB1* protein kinase in the development of the neural crest lineage.

1. *LKB1* signaling is essential for cranial neural crest cells development.

Article Nb1: Creuzet et al., Dev. Biol. 418:283-296, 2016

1.1 Results summary

To address the contribution of *Lkb1* during cranial NCC development, our team generated a mouse model with a temporal disruption of *Lkb1* specifically in NCC just after their delamination from the neural tube, at embryonic day 8.5 (E8.5). Conditional inactivation of *Lkb1* was achieved by breeding *Lkb1*^{Flox} mice (Bardeesy et al., 2002) with mice expressing the recombinase Cre under the human tissue plasminogen activator (Ht-PA) promoter using the Ht-PA::Cre transgene established by S. Dufour (Institut pour la Recherche Biomédicale, Créteil) (Pietri et al., 2003).

The lab also took advantage of the tractable system provided by the avian embryo. To inhibit chick *Lkb1* expression specifically in cranial NCC, we used the RNA interference

approach combined with a triple electrode system enabling a bilateral electroporation of the cephalic neural folds with double-stranded RNA molecules before the emigration of cranial NCC out of the neural tube (at 4–5 somites stages).

Combining studies on mouse and chick models of *Lkb1* inactivation, our team has shown that *Lkb1* is required for the development of cephalic NCC in vertebrates. *Lkb1* regulates the delamination of pre-migratory NCC from the neural primordium as well as their polarization and survival. In the absence of this kinase, the embryos are affected by severe craniofacial and brain defects. These *Lkb1*-mediated effects on the development of cephalic NCC involve the sequential activation of the AMPK, the Rho-dependent kinase (ROCK) and the actin-based motor protein myosin II. *Lkb1* mutant mice died around one day after birth due to cranial facial malformations that prevent the newborn pups to suckle milk from their mother.

The work was published in 2016 in *Developmental Biology* (Creuzet et al., 2016). Experiments performed on chick embryos were mainly done by Jean Viallet, Maya Ghawitian and Jacques Thélou from M. Billaud lab in collaboration with Sophie Creuzet lab (Neurosciences Institut, Paris-Saclay). Phenotypic characterization of the mouse model was mainly done by S. Torch and C. Thibert in M. Billaud lab. During my PhD, I contributed to the revisions required for the publication of our article at *Developmental Biology* on both mouse and chick models. Our work has been selected to illustrate the cover of the journal issue.



1.2 Results

Developmental Biology 418 (2016) 283–296



Contents lists available at ScienceDirect

Developmental Biology

journal homepage: www.elsevier.com/locate/developmentalbiology

Original research article

LKB1 signaling in cephalic neural crest cells is essential for vertebrate head development



Sophie E. Creuzet^{a,*}, Jean P. Viallet^{b,c,1}, Maya Ghawitian^{b,c}, Sakina Torch^{b,c}, Jacques Thélou^{b,c,2}, Moussab Alrajeh^a, Anca G. Radu^{b,c}, Daniel Bouvard^{b,c}, Floriane Costagliola^{b,c}, Mailys Le Borgne^{b,c}, Karine Buchet-Poyau^{b,c,3}, Nicolas Aznar^{b,c,4}, Sylvie Buschlen^a, Hiroshi Hosoya^d, Chantal Thibert^{b,c,**}, Marc Billaud^{b,c,5,**}

^a Institut de Neurobiologie, Laboratoire Neurobiologie et Développement, CNRS-UPR3294, Avenue de la Terrasses, F-91198 Gif-sur-Yvette, France^b University Grenoble Alpes, IAB, F-38000 Grenoble, France^c INSERM, IAB, F-38000 Grenoble, France^d Department of Biological Science, Hiroshima University, Higashi-Hiroshima 739-8526, Japan

ARTICLE INFO

Article history:

Received 24 February 2016

Received in revised form

19 July 2016

Accepted 6 August 2016

Available online 12 August 2016

Keywords:

Cephalic neural crest cells

Head development

Cell polarity

Lkb1

AMPK

Actin dynamic

ABSTRACT

Head development in vertebrates proceeds through a series of elaborate patterning mechanisms and cell-cell interactions involving cephalic neural crest cells (CNCC). These cells undergo extensive migration along stereotypical paths after their separation from the dorsal margins of the neural tube and they give rise to most of the craniofacial skeleton. Here, we report that the silencing of the *LKB1* tumor suppressor affects the delamination of pre-migratory CNCC from the neural primordium as well as their polarization and survival, thus resulting in severe facial and brain defects. We further show that *LKB1*-mediated effects on the development of CNCC involve the sequential activation of the AMP-activated protein kinase (AMPK), the Rho-dependent kinase (ROCK) and the actin-based motor protein myosin II. Collectively, these results establish that the complex morphogenetic processes governing head formation critically depends on the activation of the *LKB1* signaling network in CNCC.

© 2016 Elsevier Inc. All rights reserved.

1. Introduction

The neural crest is a transient embryonic structure that arises at the dorsal lips of the folding neural tube (Le Douarin and Kalchauer, 1999). Cephalic neural crest cells (CNCC) constitute a population of invasive multipotent cells that originate from mid- and

hindbrain levels and give rise to a large part of the head skeleton as well as to musculo-connective derivatives (Minoux and Rijli, 2010). These embryological observations coupled with paleontological arguments suggested the emergence of the neural crest as an evolutionarily novelty – one that was key to the development of the “new head” that epitomizes vertebrates (Gans and Northcutt, 1983; Manzanares and Nieto, 2003). Once specified, CNCC undergo an epithelium to mesenchymal transition (EMT), delaminate from the neuroepithelium and migrate into three main streams that colonize the nasofrontal bud, the branchial arches and the heart (Théveneau and Mayor, 2012). Although the persistent directionality and polarized morphology of migrating CNCC have been recognized for more than four decades, it is only recently that a series of studies have conclusively shown that CNCC migrate collectively rather than individually (Théveneau and Mayor, 2012). Furthermore, homotypic contact inhibition of locomotion (CIL), a phenomenon by which cells change their direction of migration after contact with another cell of the same type confines the extension of cell protrusions to the free edge, thereby reinforcing their ability to respond to chemoattractants (Théveneau et al., 2010). Yet, our knowledge of the signaling networks that govern

* Corresponding author.

** Corresponding authors at: Institut de Neurobiologie, Laboratoire Neurobiologie et Développement, CNRS-UPR3294, Avenue de la Terrasses, F-91198 Gif-sur-Yvette, France; INSERM, IAB, F-38000 Grenoble, France.

E-mail addresses: Sophie.Creuzet@inaf.cnrs-gif.fr (S.E. Creuzet), chantal.thibert@univ-grenoble-alpes.fr (C. Thibert), Marc.Billaud@ujf-grenoble.fr (M. Billaud).

¹ The two first authors have equally contributed to this work.² Current address: University of Grenoble 1-Joseph Fourier/CNRS/TIMC-IMAG UMR 5525 (Equipe SyNaBi), Grenoble, France.³ Current address: Hospices Civils de Lyon, Pôle Information Médicale Evaluation Recherche, Lyon F-69003, France.⁴ Current address: Department of Medicine, University of California San Diego, 9500 Gilman Drive 0651, La Jolla, CA 92093-0726, USA.⁵ Current address: Univ Lyon, Université Claude Bernard Lyon 1, INSERM 1052, CNRS 5286, centre de Recherche en Cancérologie de Lyon, Lyon 69008 France.<http://dx.doi.org/10.1016/j.ydbio.2016.08.006>

0012-1606/© 2016 Elsevier Inc. All rights reserved.

the migratory properties of neural crest cells (NCC) is still limited.

Inactivating germ line mutations of the human *LKB1* tumor suppressor gene (also named *STK11*) are responsible of the Peutz-Jeghers syndrome, an autosomal-dominant disorder characterized by pigmented macules of the lips, multiple gastrointestinal polyps and an increased risk of various cancers (Hemminki et al., 1998). *LKB1* is a serine/threonine kinase that regulates cell polarization and acts as a metabolic sensor by phosphorylating and activating the AMP-activated protein kinase (AMPK), a heterotrimer composed of a catalytic (AMPK α) subunit and two regulatory (AMPK β and AMPK γ) subunits (Alessi et al., 2006; Shackelford and Shaw, 2009; Hezel and Bardeesy, 2008). In addition, *LKB1* phosphorylates 12 additional AMPK-related kinases that are involved in distinct biological processes including the regulation of hepatic gluconeogenesis as well as the polarization and axon branching of cortical neurons (Alessi et al., 2006; Shackelford and Shaw, 2009; Hezel and Bardeesy, 2008). *LKB1* associates with the pseudokinase STRAD (STRAD α or STRAD β) and the scaffolding molecule MO25 to form the *LKB1* holoenzyme complex (Alessi et al., 2006; Shackelford and Shaw, 2009; Hezel and Bardeesy, 2008). Homozygous disruption of *Lkb1* in mice causes a defect in neural tube closure and an absence of the first branchial arch (Ylikorkala et al., 2001; Bardeesy et al., 2002), a phenotype compatible with, at least in part, a dysgenesis of CNCC. These data suggest that the *LKB1* pathway may be involved in the ontogenesis of CNCC.

To gain insight into this question, we used the tractable system provided by the avian embryo. With this model, we found that the *Lkb1* signaling pathway controls both the polarized migration and the survival of CNCC. As a consequence of *Lkb1* inactivation, expression of morphogens that pattern the prosencephalic region was abrogated in the anterior neuroepithelium and inhibited forebrain development. Consistent with these observations, we found that genetic ablation of *Lkb1* in mouse neural crest cells at the time of their emigration from the neural primordium also led to severe craniofacial defects. Finally, delineation of the *Lkb1* pathway active in CNCC revealed that the signal converges on myosin II via AMPK and ROCK kinases. Collectively, our results establish that the *Lkb1* network orchestrates several aspects of CNCC development that are crucially required during cephalogenesis.

2. Results

2.1. Chick *Lkb1* gene is expressed in delaminating and migrating neural crest cells

For the purpose of this study, we cloned and sequenced the chicken homolog of *Lkb1* cDNA. Sequence analysis revealed that the human and chicken *LKB1* proteins are 90% identical at the amino acid level, and all of the phosphorylation sites and post-translational motifs in human *LKB1* are conserved in the chick *Lkb1* homolog. To determine *Lkb1* gene expression patterns at neurula stages, we performed a series of *in situ* hybridization analyses. The *Lkb1* transcript was detected at 6 somites stage (ss) when the neural folds elevate before the neural tube closure. The accumulation of *Lkb1* transcripts intensified at later stages and was detected throughout the neural primordium before the egress of CNCC from the neural tube (Fig. 1A–C). From this stage on, *Lkb1* expression was detected in the migrating CNCC, which progressed along the cephalic vesicles and populated the naso-frontal and maxillo-mandibular regions, as well as the more caudal branchial arches (Fig. 1D–G).

2.2. *Lkb1* expression in CNCC is crucial for head development

To inhibit *Lkb1* expression in CNCC, we used the RNA interference (RNAi) approach combined with a triple electrode system enabling a bilateral electroporation of the cephalic neural folds with double-stranded RNA (dsRNA) molecules before the emigration of CNCC out of the neural tube (at 4–5 ss ie HH8) (Creuzet, 2009; Garcez et al., 2014; Aguiar et al., 2014). Several studies based on electroporation of long dsRNA to silence gene expression in chicken embryos have successfully been performed and validated (Pekarik et al., 2003; Creuzet, 2009). Using rhodamine-dextran to label transfected cells, we verified that this electroporation procedure selectively transfected the rostral dorsal region of the neural folds and consequently targeted the delaminating NCC (Fig. 2A and B), although non-NCC can also be electroporated. To assess to what extent *Lkb1* gene expression is affected after CNCC electroporation of dsRNA specifically targeting chick *Lkb1*, we performed quantitative PCR on dissected faces of electroporated embryos. After dsRNA electroporation, *Lkb1* gene expression in the head of HH14 (20–21 ss) embryos was significantly reduced (Fig. 2C). Upon *Lkb1* knockdown, we observed that the craniofacial region was clearly underdeveloped 90 h (E5 stage ie HH27) post-electroporation (Fig. 2D and E). Fifty-six dsRNA electroporated embryos were analyzed in 12 independent experiments and the craniofacial defects observed were highly reproducible. Micrographs of scanning electron microscopy of embryos at E5 revealed that the silencing of *Lkb1* in CNCC compromised the development of nasofrontal and maxillo-mandibular processes, which appeared distorted and eventually failed to fuse together (Fig. 2F and G). To visualize the effects of the loss of *Lkb1* on the formation and the migration of CNCC, we labeled embryos with the monoclonal antibody HNK1 that recognizes a glycolipid epitope expressed on chicken pre-migratory and migratory NCC (Vincent et al., 1983). As shown in Fig. 2I, a marked reduction of the CNCC population that colonizes the nasofrontal region was observed at 25–30ss following *Lkb1* knockdown (Fig. 2H and I). To address further the role of *Lkb1* in head skeletogenesis, we used Alcian blue and Alizarin red to stain cartilage and ossified bone, respectively. At E11 (HH37), the chondrogenic differentiation of the nasal septum and capsule and Meckel's cartilages of *Lkb1*-deprived embryos were reduced and calcification as seen by alizarin red staining, a proxy for osteogenic differentiation, was absent (Fig. 2J and K). Finally, to ascertain that the phenotypic effects observed were specific to the silencing of *Lkb1*, we co-electroporated dsRNA-*Lkb1* together with a vector expressing the human *Lkb1* insensitive to the dsRNA targeting its chicken homolog. Using this strategy, we observed that the craniofacial development was rescued with the human *LKB1* wild type, whereas the kinase-dead *LKB1* failed to restore cephalic development (Fig. 2L and M; Supp Fig. 1A–C). Cumulatively, these results indicate that *Lkb1* activity is required for the development of CNCC.

Brain and craniofacial development is coordinated (Aoto and Trainor, 2015) and neural tube closure defects were indeed observed either after the ablation of CNCC in birds (Creuzet et al., 2004; Creuzet, 2009) or *Lkb1* null-mutation in mice (Ylikorkala et al., 2001). Yet the phenotypes resulting from *Lkb1* dsRNA electroporation at 4–5 ss to target NCC did not perturb neural tube closure. We reasoned that *Lkb1* silencing in NCC at 4–5ss may occur too late to affect this process. To investigate if we could reproduce the anencephalic phenotype by earlier silencing of *Lkb1* during development by electroporating a broader area in the neural plate, we bilaterally transfected *Lkb1*-dsRNA at 1ss at the neural plate border (Supp Fig. 1D and E). When performed in early neurula, the inhibition of *Lkb1* generated consistent neural tube defects and resulted in anencephalic embryos. These observations indicated that the spatio-temporal silencing of *Lkb1* expression

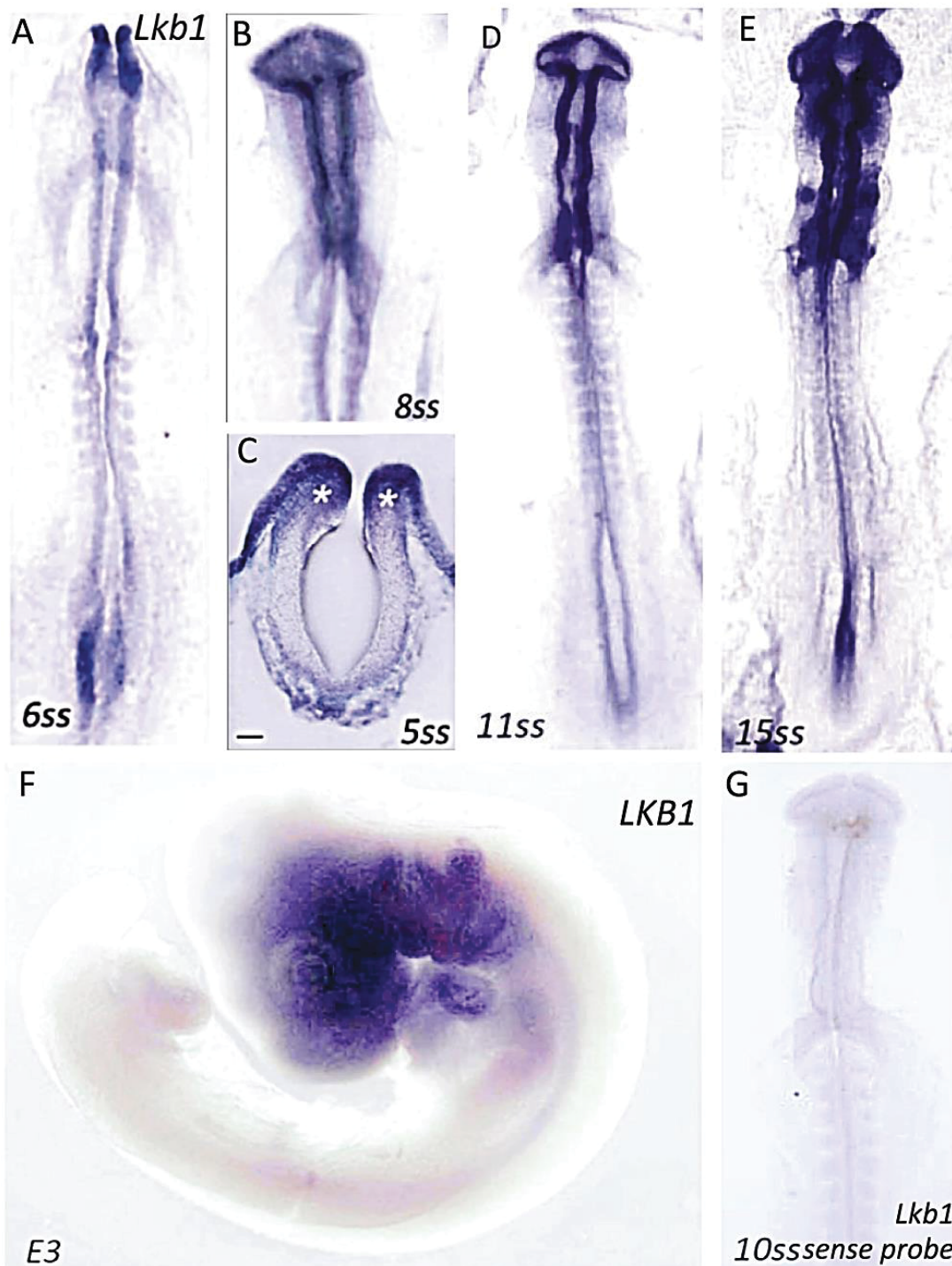
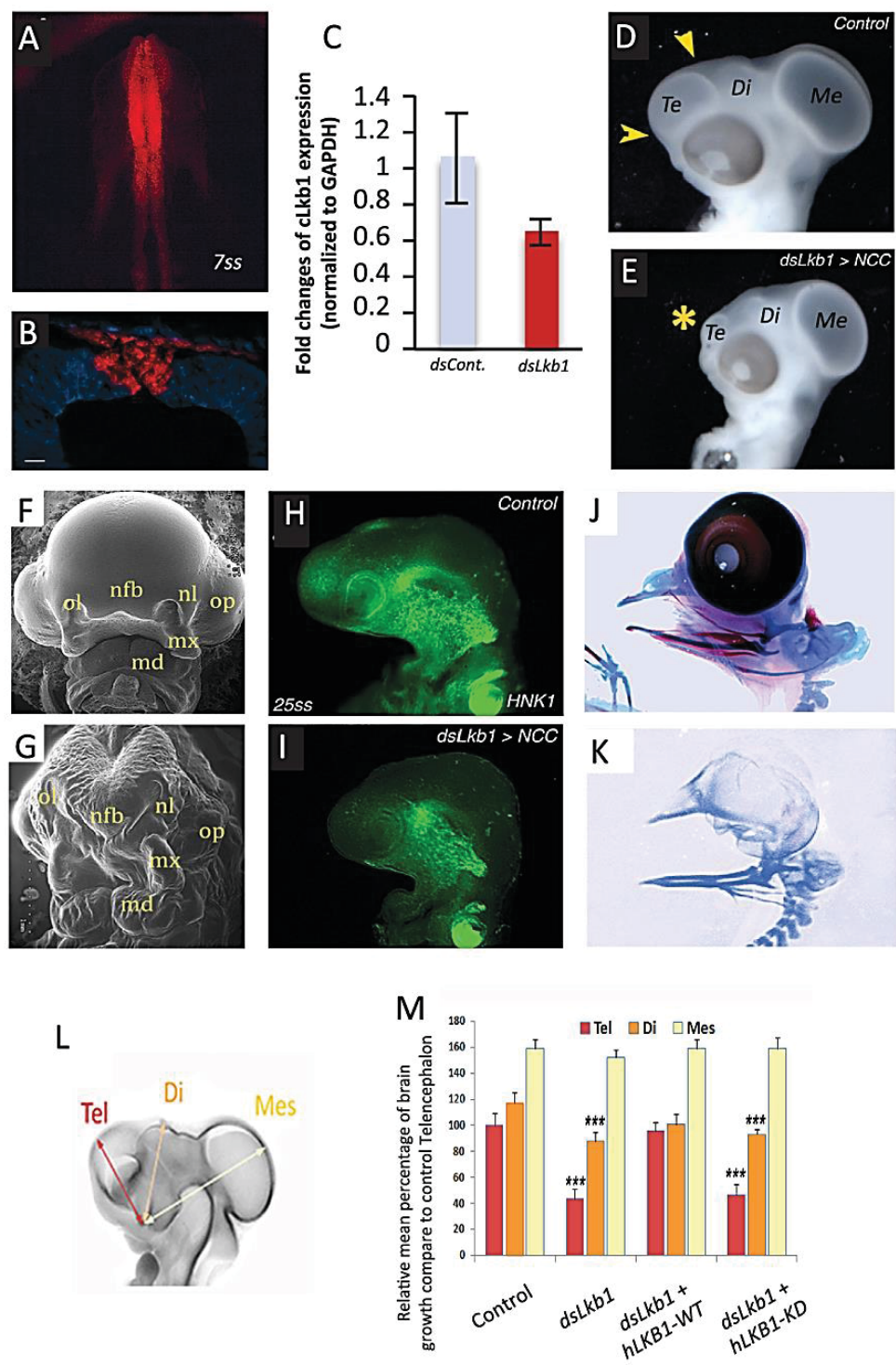


Fig. 1. *Lkb1* gene expression pattern in chick embryos. Detection of *Lkb1* transcripts in the cranial neural crest of 6ss chick embryo (A) and in the migrating CNCC at 8ss stage (B). On section, note the high level of transcript accumulation in CNCC (C, stars). *Lkb1* expression is maintained in delaminating and migrating CNCC at 11ss (D), and gains in intensity at 15ss (E). From 20ss on, *Lkb1* expression is sustained in the maxillo-mandibular and the nasofrontal CNCC as well as in BA2 and BA3 and to a lesser extent in BA4–6 as shown at E3 (F). Absence of signal after *in situ* hybridization with *Lkb1* sense probe (ISH Control) (G).



elicited the spectrum of dysmorphology recorded in *Lkb1* null-mice.

2.3. *Lkb1*-deficient mice in NCC-derivatives display severe craniofacial abnormalities

To explore whether the phenotypic effects observed in avians could be confirmed in another experimental model, we deleted *Lkb1* (Bardeesy et al., 2002) with a transgene containing the human tissue plasminogen activator (*Ht-PA*) promoter that drives the expression of the Cre recombinase (Fig. 3A). The *Ht-PA::Cre* transgene targets NCC after their delamination from the neural tube (from embryonic day 8.5) and is expressed in all NCC-derivatives (Pietri et al., 2003). Homozygous mutant neonates were unable to feed normally and died during the first day after birth. These animals showed a reduced stature and craniofacial abnormalities including a shortened nose and a micrognathia (Fig. 3B). Staining with Alizarin red and Alcian blue to respectively mark ossified bones and cartilages provided evidence that the skull was smaller in mice deleted for *Lkb1* (Fig. 3C). Surface measurements of bones of the cranial base (Fig. 3D) showed that CNCC-derived bones were greatly reduced in the absence of *Lkb1*, such as the premaxillae, maxillae, vomer, palatine, sphenoid alae, squamous temporal, presphenoid and basisphenoid thus leading to a large cleft of the secondary palate (McBratney-Owen et al., 2008; Richtsmeier and Flaherty, 2013) (Fig. 3E). On the contrary, mesodermal-derived occipital bones such as the basioccipital bone were unaffected by the absence of *Lkb1* (Fig. 3E). Interestingly, although mandibles of the jaw of the *Lkb1*-deficient mice were clearly shorter, they presented a distinct mandibular hyperplasia especially at the alveolar part of the mandible (Fig. 3C and Fig. 3F). Moreover, some bones of the skull vault were also affected in the absence of *Lkb1*, such as the frontal bone in particular and as a consequence, the anterior fontanel was wide open (Fig. 3C, G). We also observed that even if bone surface was not reduced as for example for the nasal bone, bone porosity was increased and many bones of the skull displayed osteopenia in the absence of *Lkb1*. Altogether, these findings confirm that upon *Lkb1* inactivation specifically in NCC, the skeletogenic properties of mouse CNCC are severely affected. Dysmorphic phenotype of *Lkb1* mutant mouse is strongly reminiscent to that of chick embryos with *Lkb1* inactivation in CNCC thus supporting a conserved role for *Lkb1* during vertebrate head formation.

2.4. *Lkb1* silencing impacts CNCC delamination, survival and directional migration

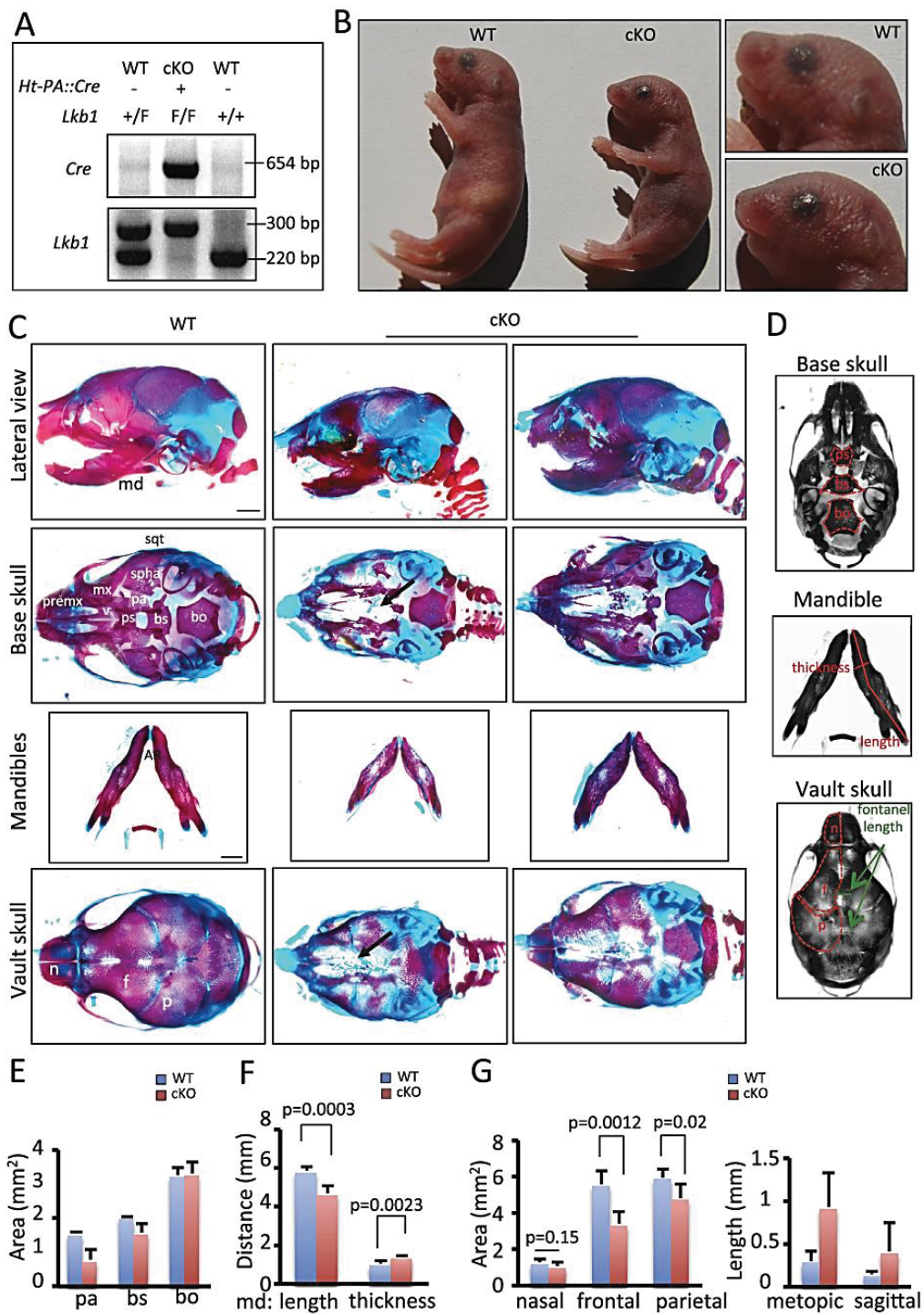
To determine how *Lkb1* silencing specifically affects the developmental capacity of CNCC, we focused on the earliest stage at which *Lkb1* silencing altered the behavior of these cells. As early as 8 h after *Lkb1*-dsRNA transfection, HNK1 labeling revealed a striking reduction in the population of CNCC that have emigrated from the neural tube (Fig. 4A and B). To further examine the

consequences of *Lkb1* silencing on CNCC development, we studied the expression pattern of both the transcription factors AP2 and the homophilic adhesion molecule N-cadherin on neural tube sections at 10 ss. AP2 α and AP2 β are expressed in premigratory and migratory CNCC and the former is required to maintain the specification of CNCC (Luo et al., 2003; de Crozé et al., 2011). N-cadherin is located at the apicolateral junctions of the neuroepithelium and expression of this adherens junction protein is downregulated in the neural folds prior to the emigration of CNCC, thereby contributing to the delamination of these cells from the neural primordium (Dady et al., 2012; Nakagawa and Takeichi, 1998). As shown in Fig. 4 (Fig. 4C and D), labeling with the anti-AP2 antibody showed that *Lkb1* depletion led to a marked reduction of the CNCC population migrating underneath the surface ectoderm. Concomitantly, the expression of N-cadherin in the dorsal neural folds was sustained upon *Lkb1* silencing (Fig. 4E–H). To further analyze pre-migratory and migratory NCC, we performed immunofluorescence detection of Sox9 and Sox10 proteins on 10 somite stages chick embryos (HH10) after either *Control*- or *dsLkb1*-electroporation. Sox9 is expressed in pre-migratory NCC whereas Sox10 expression identifies delaminating NCC (Cheung and Briscoe, 2003; for a review see Simoes-Costa and Bronner, 2015). Upon *Lkb1* knockdown, both Sox9 and Sox10 expression in NCC territory was reduced compared to control embryos (Fig. 4I–L). Collectively, these data indicate that *Lkb1* is required for the delamination process.

Since *Lkb1* is a regulator of cell polarity, we further examined whether the loss of this molecule impacted on the directional migration of CNCC. The reorientation of the Golgi apparatus together with the centrosome is known to occur during cell polarization (Pouthas et al., 2008). Moreover, *Lkb1* controls the morphology and the asymmetric distribution of the Golgi at the base of the dendrites of hippocampal neurons, thereby governing polarized dendritogenesis (Huang et al., 2014). Using an antibody labeling the Golgi matrix protein GM130 and considering the dorso-ventral direction of CNCC migration, we found that the Golgi complex was consistently located behind the nucleus, at the rear of the cells with respect to the front edge of the migrating CNCC. In this study, we analyzed a population of NCC located very close to the dorsal part of the neural tube right after their delamination. Cells in this area are most exclusively NCC as shown by AP2 labeling (Fig. 4C and D). Strikingly, *Lkb1* silencing resulted in a randomized positioning of the Golgi (Fig. 4I and J). Further quantification of this effect confirmed that the polarized positioning of the Golgi was significantly disrupted upon *Lkb1* knockdown (Fig. 4K and L). Altogether, these results indicate that *Lkb1* acts on the recruitment of CNCC from the neural primordium, promotes their delamination and, once these cells have detached from the neural tube, controls their front-rear polarity.

The defects of CNCC polarization led us to explore the viability of *Lkb1*-deprived CNCC. Using LysoTracker to stain apoptotic cells (Sugishita et al., 2004), we found that CNCC egress from the neural tube is rarely accompanied by cell death events, which are

Fig. 2. *Lkb1* expression in CNC is crucial for head development. (A, B) Delivery of dsRNA targeting chick *Lkb1* into NCC was performed by electroporation of 4–5ss (HH8) chick embryo using a triple electrodes procedure, which selectively targeted the delaminating NCC. Electroporation of delaminated and migrated CNCC was visualized through the coelectroporation with rhodamine-dextran as shown on the dorsal view (A) and on section (B) of 7ss (HH9) embryo. (C) Reduction of chick *Lkb1* expression was validated by quantitative PCR on RNA extracted from the dissected face of HH14 embryos. (D, E) Morphology of E5 (HH27) control (D) and *Lkb1*-dsRNA-treated (E) embryos; animals subjected to *Lkb1* silencing in CNC exhibit forebrain hypoplasia (star in E) when compared to control (arrowheads; D). (F, G) Scanning electron-micrograph of E5 control (F) and *Lkb1*-deprived (G) specimen. (H, I) The population of migrating CNCC visualized by HNK1 labeling at 30ss (HH18 or E3), is hypoplastic in knocked-down *Lkb1* embryos compared to control (H, I). (J, K) *Lkb1* inactivation alters the maxillo-facial development. Whole-mount preparation of control (J) and experimental (K) skeletons at E11: Alcian blue staining shows reduced formation and Alizarin red staining reveals the absence of osteogenic differentiation after inactivation of *Lkb1* expression. (L) Brain growth measurements were performed on 6 half-cut E5 embryos per each condition. Tel: optic stalk-dorsal telencephalon; Di: optic stalk-epiphysis; Mes: optic stalk-optic tectum. (M) When compared to control, *Lkb1* silencing leads to microcephaly; rescue experiments with exogenously expressed human LKB1 restored brain growth, while electroporation of a kinase-dead form of LKB1 (LKB1-KD) did not rescue forebrain defects. p values from Student's t-test comparing telencephalon and diencephalon measures to control condition are respectively: $p=2.95 \times 10^{-6}$ and 3.07×10^{-4} for *dsLkb1* condition, and $p=7.42 \times 10^{-6}$ and 4.66×10^{-4} for *dsLkb1* + hLKB1-KD condition. Values between *dsLkb1* + hLKB1 and control conditions were not statistically different ($p=0.59$ and 0.0582 for telencephalon and diencephalon respectively). ol: olfactory placode; op, optic vesicle; md, mandibular bud; mx, maxillary process; nl, nasolateral bud; nlb, nasofrontal bud. Scale bars, 20 μ m.



mostly restrained to the anterior mesencephalic region (Supplementary Fig. 2A). In stage-matched experimental embryos, *Lkb1* silencing at 5ss triggered expansion of cell death at the expense of the entire pre-otic neural folds at 7ss, and simultaneously affected the diencephalic, mesencephalic, and anterior rhombencephalic CNCC. Using co-labeling with Lysotraker and HNK1, we observed on chick embryo sections at cephalic level that cell death occurs mainly in CNCC (Supp Fig. 2B). Quantification of the percentage of dying NCC clearly illustrates the drastic increase of NCC death upon *Lkb1* knockdown (Supplementary Fig. 2C). CNCC are known to potentiate *Fgf8* expression in the anterior neural ridge (ANR) (Creuzet et al., 2004), considered as the prosencephalic-organizing center (Hoch et al., 2009). Reciprocally, *Fgf8* exerts a trophic and chemotactic effect on CNCC (Creuzet et al., 2004, 2006; Creuzet, 2009; Kubota and Ito, 2000). Concomitant to the increase CNCC death in *Lkb1*-dsRNA-treated neurula, *Fgf8* expression visualized by *in situ* hybridization was strongly reduced in the ANR (Supplementary Fig. 2D). Change in *Fgf8* expression upon *Lkb1* silencing was confirmed by qRT-PCR (Supplementary Fig. 2E). Furthermore, expression of three additional genes coding for morphogenetic molecules (Sonic hedgehog (Shh), *Wnt1* and *Wnt8b*) whose activity in the brain is associated with the migration of CNCC (Creuzet et al., 2006) was also perturbed. Quantification of these results showed that *Lkb1* silencing significantly affected the expression of *Fgf8*, *Wnt1*, *Wnt8b* and *Shh* (Supplementary Fig. 2E), a condition reminiscent of what has been previously described when CNCC are ablated (Creuzet et al., 2004, 2006).

2.5. AMPK transduces LKB1 morphogenetic signal in CNCC

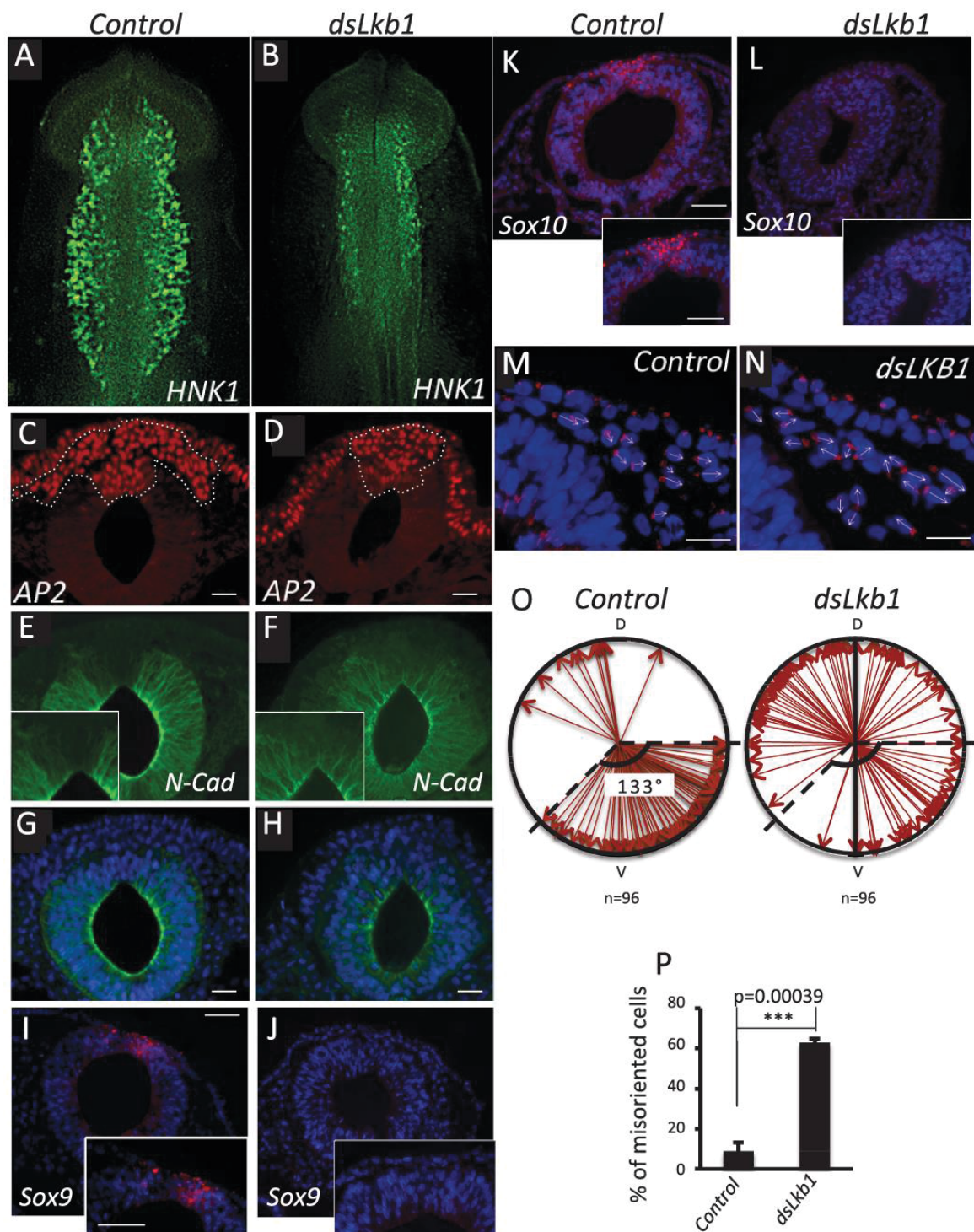
LKB1 is a master kinase that phosphorylates and activates AMPK and 12 related members of the AMPK family. Although each of these AMPK kinases, either singly or in combination, may relay the LKB1 signal in CNCC, previous studies provided evidence that AMPK regulates the assembly of tight junctions, the dynamics of actin cytoskeleton and participates in the mechanisms of hepatocyte and neuronal polarization (Zhang et al., 2006; Fu et al., 2010; Miranda et al., 2010; Amato et al., 2011; Williams et al., 2011). These findings prompted us to explore the role of AMPK in CNCC ontogeny. To this end, we cloned the cDNAs coding for the two chicken catalytic AMPK α -subunits, termed $\alpha1$ and $\alpha2$. *In situ* hybridization revealed that AMPK $\alpha1$ and $\alpha2$ have an overlapping pattern of expression during neurulation with a strong labeling of the rostral neural folds at 5ss stage (Supplementary Fig. 3). *dsRNAs* targeting $\alpha1$ and $\alpha2$ in CNCC were then electroporated either alone or in combination. No phenotype was observed upon silencing of each AMPK α subunit but the combination of both *dsRNAs* led to a marked disorganization of the cephalic region with an extensive lack of facial structures (Fig. 5A and B). These results demonstrate that AMPK exerts a crucial role during head morphogenesis in chicken and suggest that this kinase transduces the *Lkb1* signal in CNCC. To examine this question, we assessed whether electroporation of two distinct constitutively active forms of AMPK (AMPK $\alpha2$ -CA; AMPK $\gamma1$ -CA) (Woods et al., 2000; Hamilton et al., 2001) in CNCC was able to rescue the *LKB1*-*dsRNA* phenotype. As

shown in Fig. 5, expression of each AMPK-CA fully restores normal cephalogenesis in *Lkb1*-silenced embryos (Fig. 5C–G). Furthermore, expression AMPK $\gamma1$ -CA in *Lkb1* knockdown interfered with CNCC apoptosis (Fig. 5H–J) and rescued *Fgf8* expression in the ANR (Fig. 4K–M), along with other morphogens (Supplementary Fig. 2E). Overall, these findings indicate that the *Lkb1*-AMPK signaling pathway regulate molecular morphogenetic processes that govern head formation.

2.6. ROCK and MRLC are polarity effectors of the LKB1-AMPK pathway in CNCC

LKB1 is known to control cell polarity through the activation of the actin molecular motor myosin II (Lee et al., 2007; Rodriguez-Fraticelli et al., 2012). The activity of myosin II and the stability of myosin II filaments are upregulated by phosphorylation of the Myosin II Regulatory Light Chain (MRLC) at two sites corresponding to Thr-18/Ser-19 in humans (Banko et al., 2011). In *Drosophila*, expression of a phosphomimetic mutant form of MRLC rescues cell polarity defects generated by the deletion of either *Lkb1* or AMPK genes (Lee et al., 2007). Furthermore, AMPK has been found to regulate MRLC phosphorylation through its opposing effect on the phosphatase PP1CB-PPP1R12C complex and the p21-activated protein kinase 2 (PAK2) (Banko et al., 2011). These results prompted us to investigate the role of MRLC in CNCC development. Embryos subjected to *Lkb1* silencing were co-electroporated with vectors encoding mutant forms of MRLC in which both Thr-18 and Ser-19 were replaced by phosphomimetic aspartate (MRLC-DD) (Fumoto et al., 2003). Expression of MRLC-DD resulted in a complete restoration of brain development and facial morphogenesis in *Lkb1* knockdown embryos (Fig. 6A–C). Since MRLC is not a direct AMPK substrate (Bultot et al., 2009), we focused our attention on the Rho-associated protein kinase (ROCK). This kinase is implicated in CNCC delamination (Groysman et al., 2008; Berndt et al., 2008; Clay and Halloran, 2013), regulates the phosphorylation of MRLC and has been proposed as an AMPK effector (Bultot et al., 2009). In a first approach, we inhibited ROCK pharmacologically with the Y-27632 compound (Uehata et al., 1997). Microinjection of this molecule into the neural tube at 5ss led to a reduction of facial and cephalic structures that virtually reproduced the *Lkb1* loss of function phenotype (Fig. 6D). In a second approach, co-electroporation of *Lkb1*-*dsRNA* together with a constitutively active form of the ROCK1 isoform restored the cephalic development of *Lkb1*-depleted embryos whereas a ROCK1 kinase-dead mutant failed to rescue the cephalic phenotype (Fig. 6E, F and I). Finally, to determine the epistatic position of ROCK within the *Lkb1*-AMPK-myosin II pathway, we carried out a series of rescue experiments. We first observed that the cephalic defect obtained upon *dsRNA* targeting AMPK $\alpha1$ and AMPK $\alpha2$ was rescued when the constitutively active form of ROCK1 was co-electroporated (Fig. 6I). Expression of the constitutively active form of AMPK (AMPK $\gamma1$ -CA) did not restore proper cephalic development in embryos treated with Y-27632, whereas MRLC-DD was largely able to correct the shortening of the prosencephalic region induced by this compound (Fig. 6G, H and J). Thus, taken together these data place ROCK activity downstream of AMPK and

Fig. 3. Craniofacial abnormalities in *Lkb1*-deficient mice in NCC-derivatives. (A) Genotyping of *Lkb1*^{+/+} Ht-PA::Cre⁺, *Lkb1*^{+/+} Ht-PA::Cre⁺ and *Lkb1*^{-/-} Ht-PA::Cre⁺ mice by PCR. (B) Images of a *Lkb1*-deficient newborn mouse (right, cKO) and a wild-type (WT) littermate (left). All of the 12 *Lkb1*-inactivated animals studied (out of a total of 51 newborns) had a reduced stature and died at P1. (C) Head skeleton of two *Lkb1*-deficient mice and a wild-type littermate stained with Alizarin red and Alcian blue at P0 showing both ossification and cartilage defects respectively. Bones that are particularly reduced are labeled on the lateral view (md: mandible) or on the vault skull (n: nasal; f: frontal; p: parietal) and base skull (premx: premaxillae; mx: maxillae; v: vomer; ps: presphenoid; bs: basisphenoid; pa: palatine; spha: sphenoid alae; sqt: squamous temporal). *Lkb1*-inactivation mostly triggers ossification defects of NCC-derived facial bones and other bones of the skull such as the basioccipital (bo) bone were not affected by *Lkb1* absence. Vault and base skull bones surface reduction lead to wide open fontanel and cleft palate respectively (arrows). Mandible dissections allowed visualization of *Lkb1*-inactivation associated defects in alveolar rim (AR) formation in particular. Scale bars, 1 mm. (D) Bone surfaces and linear distances were measured for 6 WT and 4 cKO animals as illustrated. (E) Mean of bone surfaces of the vault skull (left) and length of fontanels at metopic (between frontal bones) and sagittal (between parietal bones) areas (right). (F) Mean of bone surfaces of the base skull. (G) Average of mandible (md) length and thickness.



upstream of myosin II in the *Lkb1* signaling cascade operating in CNCC (Fig. 6K).

3. Discussion

By combining experimental approaches in chick and mouse, we have established for the first time that the LKB1 network controls the fate of CNCC by acting at different stages of their development. LKB1 directs forebrain formation *via* its cumulated effects on the delamination of pre-migratory CNCC, on their directional migration and their survival. As a consequence of *Lkb1* silencing, the morphogenesis of cranial skeleton structures that derive from CNCC is severely impaired. Consistent with this observation, expression of several diffusible molecules that are required for the patterning of the prosencephalic region and play a key role in the vertebrate head ontogenesis, such as *Fgf8*, *Wnt1* and *Wnt8*, is abrogated in the anterior neuroepithelium. Finally, we show that the developmental signal transduced downstream of LKB1 in CNCC involves the sequential triggering of AMPK, ROCK and myosin-II.

Disruption of *Lkb1* before the onset of CNCC emigration from the neural tube results in CNCC hypoplasia as attested by the marked diminution of the cell population expressing the markers *HNK1*, *AP2* and *Sox10*. Furthermore, upon *Lkb1* depletion, a persistent expression of N-cadherin at 10ss was observed in the neuroepithelium. These findings are consistent with a defect in the inductive molecular events that contribute to the delamination process. The switch of cadherin expression, from type I cadherin (N-cadherin) associated with stable intercellular contacts to type II cadherins with weaker adhesiveness (Cadherin-6/7/11) is assumed to prevent the mixing between NCC and non NCC in pre-migratory NC territory and to favor NCC delamination (Théveneau and Mayor, 2012; Kerosuo and Bronner-Fraser, 2012). Although the *Lkb1* pathway participates in the molecular mechanisms controlling delamination, we also observed that a substantial proportion of CNCC egressed from the neural tube even in the absence of *Lkb1*. Thus, alternative pathways may supersede the lack of *Lkb1* and could involve the web of transcription factors including *Ets1*, *Id2*, *Lsox5* and *p53*, known to control CNCC delamination (Théveneau and Mayor, 2012).

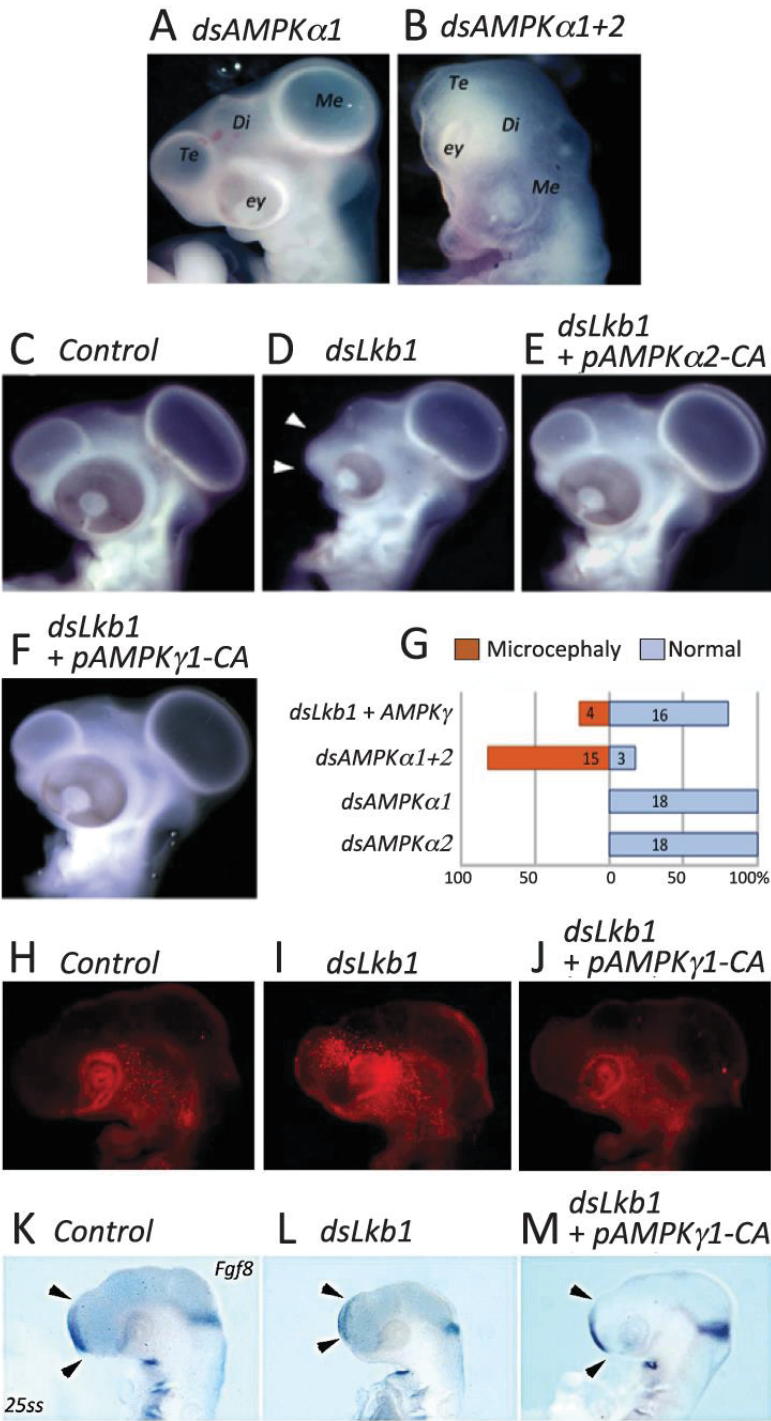
Using the direction of the Golgi-nucleus axis as a marker of cell polarity, we found that the *Lkb1*-AMPK pathway controls CNCC polarity. We also recorded a marked apoptosis of these cells upon *Lkb1* silencing, an observation consistent with the cell death observed in various physiological settings when *Lkb1* is ablated (Shaw et al., 2003; Gurumurthy et al., 2010). We posit that by ensuring the directional guidance of CNCC, the *Lkb1* polarizing signal promotes the survival of CNCC that become exposed during their long-range migration to the chemotactic and trophic effects of *Fgf8* (Creuzet et al., 2004). Reciprocally, it is anticipated that the *Lkb1* pathway regulates the prosencephalic development *via* its effect on the directional migration and survival of CNCC that interact with the ANR and controls the territory of *Fgf8* expression as already demonstrated in a different experimental setting (Creuzet et al., 2006; Creuzet, 2009). Although this remains speculative, the demonstration that the genetic ablation of *Lkb1* in mice after the

delamination of CNCC results in severe craniofacial abnormalities provides evidence that the contribution of *Lkb1* in both the directional migration and the survival of CNCC are critical for head morphogenesis. Interestingly, cell death upon *Lkb1* knockdown was not only observed in CNCC but also in cells of surrounding tissues such as ectodermal cells and neuroblasts from the neural tube (data not shown). These data support emerging findings highlighting the importance of cell communication between NCC and other tissues during embryogenesis as recently illustrated for the coordinated development of the brain and the face (Aguiar et al., 2014; Aoto and Trainor, 2015; for a review see Richtsmeier and Flaherty, 2013).

We show here that AMPK relays the signal downstream of *Lkb1* in CNCC. AMPK is activated by metabolic stresses that decrease the ATP:AMP intracellular ratio (Shackelford and Shaw, 2009). It is known that low-oxygen tension that triggers AMPK activation characterizes the permissive microenvironment of migrating CNCC (Etchevers, 2003). Accordingly, the hypoxia-inducible factor 1 α (HIF1 α) is expressed in the cephalic mesenchyme, and CNCC do not colonize branchial arches in *HIF1 α* -null mouse embryos (Compernelle et al., 2003). Thus, the *Lkb1*-AMPK signaling node may sense environmental cues and convert this information into morphogenetic outputs. Although, our study establishes a role for AMPK downstream of *Lkb1* in CNCC, we cannot rule out the contribution of other AMPK-related kinases, such as NUA1 and NUA2 whose double inactivation in mice leads to exencephaly and facial clefting (Ohmura et al., 2012).

We also report in this study that *Lkb1* regulates the actomyosin II dynamics in CNCC through the activation of ROCK and the subsequent phosphorylation of MRLC. These data are in agreement with previous reports that uncovered a role for RhoA and ROCK downstream of LKB1 in actin filament assembly and in actomyosin II contractility (Rodríguez-Fraticelli et al., 2012; Xu et al., 2010). It is also established that the *Caenorhabditis elegans* orthologue of *Lkb1* controls cell polarization and cytokinesis during the early stage of the worm embryonic development *via* its effect on anillin and non-muscle myosin (Chartier et al., 2011). In addition, the Rho-ROCK signaling is required for the apical detachment of truncal neural crest cells (Clay and Halloran, 2013) and for the survival of neural crest cells that form the craniofacial region (Phillips et al., 2012). Here, we show that LKB1 controls actomyosin II in CNCC through an AMPK-dependent activation of ROCK. Yet, it remains to be determined how ROCK is activated *via* LKB1 in CNCC and what is the respective contribution of ROCK1 and ROCK2 isoforms (Riento and Ridley, 2003) downstream of LKB1. As already shown in epithelial cells, it is possible that *Lkb1* induces the exchange of GDP for GTP on Rho GTPases *via* the Dbp1 RhoGEF (Xu et al., 2010). Our rescue experiments indicate that AMPK exerts a specific action upstream of ROCK and may thus directly modulate the activity or localization of Rho exchange factors expressed in CNCC (Fort and Théveneau, 2014). If AMPK is known to regulate MRLC phosphorylation through its opposing effect on the phosphatase PPP1R12C and the kinase PAK2 (Banko et al., 2011), our data establish that ROCK acts downstream of AMPK and controls MRLC phosphorylation, possibly through the activation of the MLC kinase or through the inhibition of the myosin phosphatase (Zagorska et al., 2010).

Fig. 4. *Lkb1* silencing impacts CNCC delamination, survival and directional migration. (A, B) HNK1 labeling at 7ss shows the emigration of CNCC from the neural primordium in control (A) and *Lkb1*-depleted (B) embryos. (C, D) Migration of AP2 expressing CNCC at 10ss. *Lkb1* silencing prevents CNCC delamination and migration (D). (E–H) N-cadherin expression is repressed at the dorsal part of the neural tube in control embryos (E, G) whereas its expression is maintained upon *Lkb1* silencing (F, H). Expression of both premigratory marker *Sox9* and delaminating marker *Sox10* is reduced upon *Lkb1* knockdown (J, L) compared to WT embryos (I, K). The directional migration of the CNCC is altered in *Lkb1* knocked-down embryos (m–p). The Golgi matrix protein GM130 is accumulated opposite to the front edge of migrating CNCC in controls (M), whereas *Lkb1* silencing resulted in a randomized positioning (N). Centered distribution of individual cell polarity given by the “GM130-nucleus” axis (arrow) in controls and *shRNA* transfected embryos, respective to the dorso-ventral axis of the neural tube (O). Graphic representation of the percentage of misoriented cells (P). Student's *t*-test statistical analyses to compare the percentage of misoriented cells between controls and *dsLkb1* treated embryos were performed on 3 different embryos per condition (at least 3 different sections per embryos were used to analyze a total of 96 cells for both controls and *dsLkb1* treated embryos). Scale bars, C–D, G–H: 40 μ m; I–L: 50 μ m; M–N: 10 μ m.



In conclusion, our study shows that the formation of the head in vertebrates critically depends on the activation of the LKB1 network in CNCC. Bi-allelic deletion of the *STRADα* gene, encoding the pseudokinase of the LKB1-activating complex, is responsible for an inherited disease called polyhydramnios, megalencephaly, and symptomatic epilepsy (PMSE) (Puffenberger et al., 2007). All PMSE patients present craniofacial abnormalities, a genetic trait evoking a defect in CNCC development. Thus, our findings raise the idea that a decrease of LKB1 signaling in CNCC owing to the loss of *STRADα* is the causative origin of the dysmorphic traits of PMSE patients and further suggest that perturbations of this pathway might be implicated in the etiology of other human neural crest disorders.

4. Methods

Chick embryos were used as a model throughout this study and were operated according to techniques previously described (Creuzet, 2009).

4.1. Constructs

Chick *Lkb1*, *AMPKα1*, and *α2* sequences were amplified from E8.5 embryo cDNA using primers: *Lkb1* (For-ctcgatgaaggaactaattcaggatg; Rev-ggatcctgctccggctcactg), *AMPKα1* (For-gcagtgagatcctgaatcgac; Rev-tagagaataacccctgctcc) and *AMPKα2* (For-tcggcaccctcggcaagtc; Rev-agggtgggcacatgctcatc) designed based on GenBank sequences NM_001045833.1, NM_001039603.1 and NM_001039605.1 respectively and cloned to pGEM[®]-T Easy vector (Promega) according to the manufacturer's instructions. These plasmids encoding chick *Lkb1*, *AMPKα1* and *AMPKα2* target genes were used for the synthesis of both double-strand RNA (dsRNAs) by *in vitro* transcription and probes for *in situ* hybridization as previously described (Creuzet, 2009).

4.2. Gene silencing in avian embryos

Delivery of RNAi molecules was achieved by *in ovo* electroporation at 4–5 somites stage (4–5 ss equivalent to HH8 ie about 29 h of embryonic development) using a triple electrode system (Creuzet et al., 2002). Nucleic acid solution (1 μg/μl of dsRNA; 5 μg/μl of plasmidic DNA) was blown in the neural groove at 4–5ss and bilaterally electroporated to the NCC by iterative pulses (5 × 27 V square pulses, T830 BTX, Genetronics, CA). Co-electroporation with rhodamine-dextran enables the targeted CNCC to be visualized. Solutions of non-annealed sense and anti-sense RNA strands were used for control series and transfected according to the same paradigm. For Fig. S1D and E, electroporations were performed at 1ss to target the neural plate border. For the characterization of each phenotype the brain growth was evaluated on 6 embryos. The heads of the embryo were cut in half along the sagittal plane and we measured the distance between: the optic stalk and the dorsal telencephalon (Tel); the optic stalk and the epiphysis (Di); the optic stalk and the mesencephalon (Mes). Values are given as the relative mean percentage of brain growth compare to control Telencephalon and standard error of the mean (SEM) (Creuzet, 2009). The unpaired Student's *t*-test was used to

generate *p*-values for selected pairwise comparisons and *p* < 0.05 was considered significant.

4.3. Quantitative real-time PCR analysis of gene expression

Frontal part of the heads of 14HH stage embryos was dissected from posterior diencephalon to rhombomeres 2–3. Total RNA was then extracted using RNeasy Plus Mini kit (Macherey-Nagel). Two micrograms of total RNA were transcribed with oligo-dT primers using MMLV reverse transcriptase (Promega). To assess chick *Lkb1* gene expression, quantifications were performed by qPCR on a pool of 7 control or 7 *dsLkb1*-treated embryos. For morphogens analysis, quantifications were performed on 4 controls, 3 *dsLkb1*-treated and 4 rescued embryos. Primers were as followed: *Gapdh* (For-gaggaaggtcgctggtggtatcg; Rev-ggtaggacaagcagtgaggacg), *Lkb1* (For-agataaggcagcacaattggtt; Rev-gctaggaggtatggcacc), *Fgf8* (For-gtaccagggctgtacatg; Rev-cggtgaagggttagttgag), *Wnt1* (For-aaatgggactgggtgtct; Rev-cctcgagggtcatctacgg), *Wnt3a* (For-gagatcatgcccagctag; Rev-gcggattccctgtagcttt), *Wnt8b* (For-gaactcagcctggagatt; Rev-tctcagggcatccacaac) and *Shh* (For-gctgcaaggacaagctgaa; Rev-ggacgacattccgtacttg) primers were customized to be specific for each mRNA species and synthesized by Invitrogen. Quantitative PCR reactions were performed using LightCycler[®] carousel-based system (Roche).

Each biological sample was subjected to the assay in triplicates per gene. Ct values were obtained by using Promega software (v.2.0.4). Fold changes were calculated using either absolute quantification (*Lkb1* gene expression) or the relative quantification ($\Delta\Delta Ct$). Fold changes were normalized on *GAPDH* gene activity.

Statistical analyses were performed with the GraphPad Prism5.0 software assuming a confidence interval of 95%. Data collected for all the independent observations were compared using the non-parametric significance test of Mann–Whitney U.

4.4. Rescue experiments

To investigate the functionality of *Lkb1* pathway in CNCC cells, we challenged rescue of *Lkb1* hypomorphic phenotypes by co-electroporating *Lkb1*-dsRNA with the following constructs: p-AMPKγ1, p-AMPKα2 (gifts from Benoît Viollet), p-Un-phospho-MLC, p-Pseudo-phospho-MLC (Fumoto et al., 2003), p-Rock-KD, p-Rock-CA (gifts from Pierre Roux).

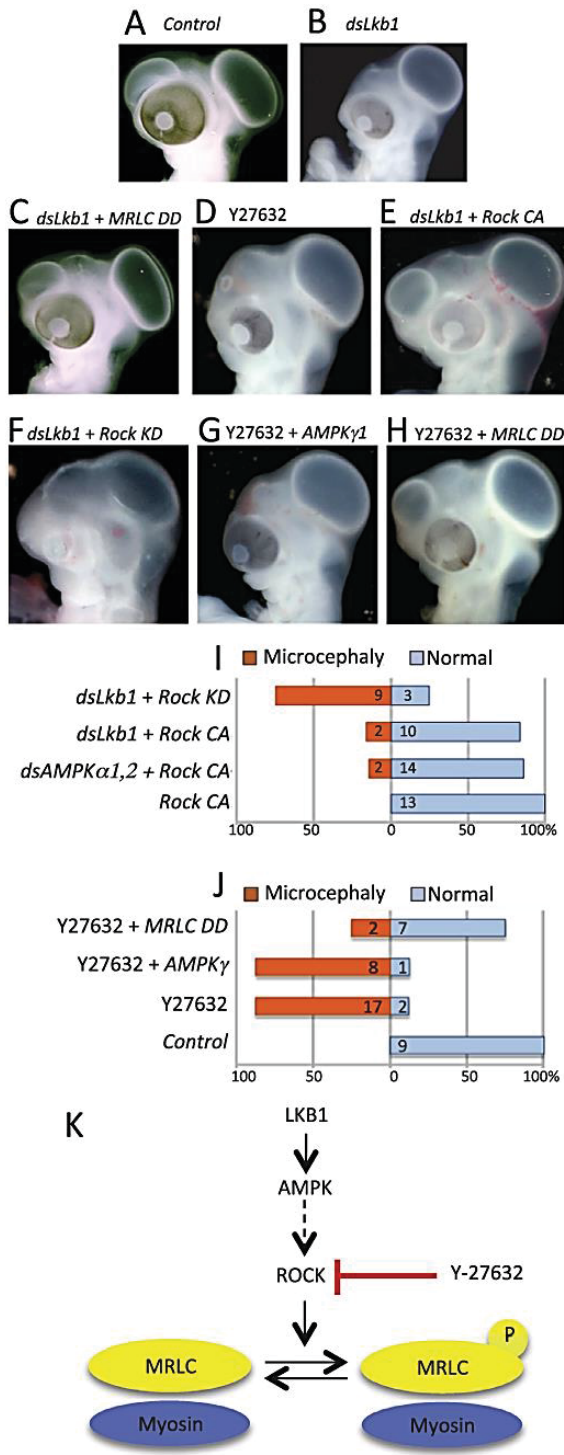
4.5. Pharmacological treatment

A solution of Rock inhibitor Y27632 (50 μM in PBS) (Calbiochem) was blown in the cephalic neural groove of 3–5ss embryos *in ovo*. Control embryos were injected with PBS only. As for nucleotide injection, the solutions were contrasted with rhodamine-dextran to visualize the injection site.

4.6. Embryo processing

Control and experimental embryos were collected at 7ss, 10ss and 25ss (i.e. 8 or 24 h post-transfection) and subjected to whole-mount immunofluorescence or immunostaining on section with HNK1 (Santa-Cruz Biotechnology), AP2 (3B5, DSHB), N-Cad (6B3; DSHB), Sox9 or Sox10 (a kind gift from JL Duband) and GM130 (BD

Fig. 5. AMPK transduces LKB1 morphogenetic signal in CNCC. Cephalic phenotype of chicken embryos at E4 stage subjected to AMPKα1 catalytic subunit silencing (A), or both AMPKα1 and α2 catalytic subunits silencing (B) were compared to Control (C) and *Lkb1* silencing (D). D–F: Restored cephalic development of *dsRNA Lkb1* embryos (D) expressing constitutively active forms of AMPK (AMPK-CA). Embryos coelectroporated with dsRNA *Lkb1* and either AMPKα2-CA (E) or AMPKγ1-CA (F). Quantification of microcephalic versus normal embryos following AMPKα1 and/or α2 silencing, and AMPKγ1-CA rescue of *Lkb1* knockdown (G). Values in the bars of the graph indicate the number of analyzed embryos per each condition. H–J: Expression of AMPK-CA rescues CNCC apoptosis induced by *dsLkb1*. Apoptotic cells are identified with lysotracker staining in Control (H), *Lkb1*-dsRNA-treated (I), *Lkb1*-dsRNA and AMPKγ1-CA co-electroporated embryos (J). K–M: expression of a constitutively active form of AMPK restores *Fgf8* expression in the ANR. *Fgf8* expression in controls (K), *Lkb1*-dsRNA-treated (L), *Lkb1*-dsRNA and AMPKγ1-CA co-electroporated (M) embryos. Di, diencephalon; ey, eye; Me, mesencephalon; Te, telencephalon.



Biosciences) monoclonal antibodies. *In situ* hybridizations with *Lkb1*, *Fgf8*, *AMPK α 1*, and *AMPK α 2* probes were performed as described previously (Creuzet et al., 2002). Cell death detection with Lysotracker was performed as described in Sugishita et al. (2004).

4.7. Scanning electron microscopy

Embryos were dissected in PBS and fixed in formaldehyde 4% overnight at 4 °C, briefly washed in PBS, and then transferred in 7% sucrose solution in PBS for 48 h at 4 °C for cryo-protection. Specimens were then mounted onto aluminum stubs and photographed using a HITACHI S-3000N.

4.8. Mice conditional mutant

Floxed *Lkb1* mice were obtained from RA. DePinho (Boston, USA) and *Ht-PA::Cre* mice from S. Dufour (Paris, France). Heterozygous (*Lkb1*^{+/-}) and homozygous (*Lkb1*^{+/F}) mice were crossed with *Lkb1*^{+/-};*Ht-PA::Cre*⁰ mice to generate *Lkb1* homozygous conditional knockout in neural crest-derived tissues (referred to as cKO in the text) and wild-type littermate animals. Mice were genotyped by PCR using DNA extracted from tails with *Cre* primers (*For*-cctggaaaatgcttctgtcgtttgccc; *Rev*-gagttgatagctggctggggagatg) and *Lkb1* primers (*Lkb1*-55-tctaacaatgcgctcatcgtcctcgcc; *Lkb1*-36-gggcttcacactgggtgccagcctgt and *Lkb1*-39-gagatgggtaccaggagttggggct). Mice were maintained under standard housing conditions and maintained on a mixed genetic background. All animal experimental procedures were conducted according to the standard operating procedures of the laboratory animal facility and were approved by the Animal Ethics Committee of Grenoble (Permit number 276_ IAB-U823-CT-03). *Lkb1*-inactivated newborn died one day after birth. cKO and wild type littermate pups were thus sacrificed by decapitation the day of birth at P0. Mice population was amplified by crossing heterozygous animals with wild-type animals to avoid generating unnecessary cKO animals.

4.9. Cartilage and bone staining

For whole-mount skeletal analysis, newborn mice heads were skinned, fixed overnight in pure ethanol and stained with Alcian Blue and Alizarin Red for 48 h. After staining, samples were incubated in 20% glycerol in a 1% KOH solution to remove soft tissue. To improve transparency, specimens were cleared in 50% glycerol in a 0.5% KOH solution at 37 °C for 2 days, which was then replaced with 80% glycerol solution for completion of the reaction. Surface and linear bone measurements from skulls were performed on 6 WT animals and 4 *Lkb1*-inactivated animals. Statistical analyses were performed using paired Student *t*-tests when the variances were following a uniform distribution (*F*-test *p* > 0.05) or unpaired *t*-test when the variances were not comparable (*F*-test *p* < 0.05).

Fig. 6. ROCK and MRLC are polarity effectors of the LKB1-AMPK pathway in CNCC. (A, C): Cephalic development in control (A) or *Lkb1*-silenced (B) embryos at E4. Electroporation of MRLC-DD rescues *dsLkb1*-induced microcephaly (C). (D) Microcephaly resulting from treatment with a ROCK inhibitor, Y-27632. (E) *Lkb1* silencing when combined to a constitutively active form of ROCK (ROCK-CA) results in rescued phenotype, (F) while in combination with a kinase-dead mutant (ROCK-KD), it leads to microcephaly. (G) In Y-27632-treated embryos, the constitutively active form of AMPK- γ 1 fails to rescue the Y-27632-induced microcephaly, (H) while expression of MRLC-DD restores the cephalic development of *dsRNA Lkb1* electroporated embryos. (I, J) Quantification of microcephalic versus normal embryos in experiments (I) exploring the effects of ROCK, (J) of ROCK inhibitor Y-27632 and the respective roles of AMPK γ 1-CA and MRLC-DD. Values in the bars of the graph indicate the number of analyzed embryos per condition. (K) Schematic diagram of the Lkb1/AMPK signaling pathway involved in CNCC development.

Acknowledgments

This work benefited from the facilities and expertise of the Imagif Cell Biology Unit of the Gif campus (www.imagif.cnrs.fr; supported by the Conseil Général de l'Essonne). We thank Anaïs Carpentier for excellent technical assistance with Scanning Electron Microscopy. We thank Nabeel Bardeesy for sharing with us the *Lkb1* floxed mouse, Benoît Viollet and Pierre Roux for the kind gifts of reagents and Geneviève Chevallier for her help with mice breeding. We thank Christine Perret, Eva Faurobert, Jean-Pierre Rouault, Nicolas Chartier and Kiran Padmanabhan for the critical reading of the manuscript. The works performed in SC and MB labs were supported by the CNRS. This work also benefited from the support of the project PolarCrest of the French National Research Agency (ANR).

Appendix A. Supplementary material

Supplementary data associated with this article can be found in the online version at <http://dx.doi.org/10.1016/j.ydbio.2016.08.006>.

References

- Aguiar, D.P., Sghari, S., Creuzet, S.E., 2014. The facial neural crest controls fore- and midbrain patterning by regulating *Foxg1* expression through *Smad1* activity. *Development* 141, 2492–2505.
- Alessi, D.R., Sakamoto, K., Bayascas, J.R., 2006. LKB1-dependent signaling pathways. *Annu. Rev. Biochem.* 75, 137–163.
- Amato, S., Liu, X., Zheng, B., Cantley, L., Rakic, P., Man, H.Y., 2011. AMP-activated protein kinase regulates neuronal polarization by interfering with PI3-kinase localization. *Science* 332, 247–251.
- Aoto, K., Trainor, P.A., 2015. Co-ordinated brain and craniofacial development depend upon Patched1/XIAP regulation of cell survival. *Hum. MO Genet.* 24, 698–713.
- Banko, M.R., Allen, J.J., Schaffer, B.E., Wilker, E.W., Thou, P., White, J.L., Villen, J., Wang, B., Kim, S.R., Sakamoto, K., Gygi, S.P., Cantley, L.C., Yaffe, M.B., Shokat, K., Brunet, A., 2011. Chemical genetic screen for AMPKα2 substrates uncovers a network of proteins involved in mitosis. *Mol. Cell.* 44, 878–892.
- Bardeesy, N., Sinha, M., Hezel, A.F., Signoretti, S., Hathaway, N.A., Sharpless, N.E., Loda, M., Carrasco, D.R., DePinho, R.A., 2002. Loss of the *Lkb1* tumour suppressor provokes intestinal polyposis but resistance to transformation. *Nature* 419, 162–167.
- Berndt, J.D., Clay, M.R., Langenberg, T., Halloran, M.C., 2008. Rho-kinase and myosin II affect dynamic neural crest cell behaviors during epithelial to mesenchymal transition in vivo. *Dev. Biol.* 324, 236–244.
- Bultot, L., Horman, S., Neumann, D., Walsh, M.P., Hue, L., Rider, M.H., 2009. Myosin light chains are not a physiological substrate of AMPK in the control of cell structure changes. *FEBS Lett.* 583, 25–28.
- Chartier, N.T., Salazar Ospina, D.P., Benkemoun, L., Mayer, M., Grill, S.W., Maddox, A. S., Labbé, J.C., 2011. PAR-4/LKB1 mobilizes nonmuscle myosin through anillin to regulate *C.elegans* embryonic polarization and cytokinesis. *Curr. Biol.* 21, 259–269.
- Cheung, M., Briscoe, J., 2003. Neural crest development is regulated by the transcription factor *Sox9*. *Development* 130, 5681–5693.
- Clay, M.R., Halloran, M.C., 2013. Rho activation is apically restricted by *Ahrap1* in neural crest cells and drives epithelial-to-mesenchymal transition. *Development* 140, 3198–3209.
- Compennolle, V., Brusselmans, K., Franco, D., Moorman, A., Dewerchin, M., Collen, D., Carmeliet, P., 2003. Cardiac bifida, defective heart development and abnormal neural crest migration in embryos lacking hypoxia-inducible factor-1α. *Cardiovasc. Res.* 60, 569–579.
- Creuzet, S., Couly, G., Vincent, C., Le Douarin, N.M., 2002. Negative effect of Hox gene expression on the development of the neural crest-derived facial skeleton. *Development* 129, 4301–4313.
- Creuzet, S., Schuler, B., Couly, G., Le Douarin, N.M., 2004. Reciprocal relationships between Fgf8 and neural crest cells in facial and forebrain development. *Proc. Natl. Acad. Sci. USA* 101, 4843–4847.
- Creuzet, S.E., Martinez, S., Le Douarin, N.M., 2006. The cephalic neural crest exerts a critical effect on forebrain and midbrain development. *Proc. Natl. Acad. Sci. USA* 103, 14033–14038.
- Creuzet, S.E., 2009. Regulation of pre-otic brain development by the cephalic neural crest. *Proc. Natl. Acad. Sci. USA* 106, 15774–15779.
- Dady, A., Blavet, C., Duband, J.L., 2012. Timing and kinetics of E- to N-cadherin switch during neurulation in the avian embryo. *Dev. Dyn.* 241, 1333–1349.
- de Crozé, N., Maczowiak, F., Monsoro-Burq, A.H., 2011. Repetitive AP2a activity controls sequential steps in the neural crest gene regulatory network. *Proc. Natl. Acad. Sci. USA* 108, 155–160.
- Etchevers, H.C., 2003. Early expression of hypoxia-inducible factor 1α in the chicken embryo. *Gene Expr. Patterns* 3, 49–52.
- Fort, P., Thévenau, E., 2014. Pleiotropic Rho pathways are essential for all stages of Neural Crest development. *Small GTPases* 5, e27975.
- Fu, D., Wakabayashi, Y., Ido, Y., Lippincott-Schwartz, J., Arias, I.-M., 2010. Regulation of bile canalicular network formation and maintenance by AMP-activated protein kinase and LKB1. *J. Cell. Sci.* 123, 3294–3302.
- Fumoto, K., Uchimura, T., Iwasaki, T., Ueda, K., Hosoya, H., 2003. Phosphorylation of myosin II regulatory light chain is necessary for migration of HeLa cells but not for localization of myosin II at the leading edge. *Biochem. J.* 370, 551–556.
- Gans, C., Northcutt, R.G., 1983. Neural crest and the origin of vertebrates: a new head. *Science* 220, 268–273.
- Garcez, R.C., Le Douarin, N.M., Creuzet, S.E., 2014. Combinatorial activity of Six1-2-4 genes in cephalic neural crest cells controls craniofacial and brain development. *Cell Mol. Life Sci.* 71, 2149–2164.
- Groisman, M., Shoval, I., Kalchauer, C., 2008. A negative modulatory role for rho and rho-associated kinase signaling in delamination of neural crest cells. *Neural Dev.* 27, 1749–1804-3.
- Gurumurthy, S., Xie, S.Z., Alagesan, B., Kim, J., Yusuf, R.Z., Saez, B., Tzatsos, A., Ozsolak, F., Milos, P., Ferrari, F., Park, P.J., Shirihai, O.S., Scadden, D.T., Bardeesy, N., 2010. The LKB1 metabolic sensor maintains haematopoietic stem cell survival. *Nature* 468, 659–664.
- Hamilton, S.R., Stapleton, D., O'Donnell, J.B., Kung, J.T., Dalal, S.R., Kemp, B.E., Witters, L.A., 2001. An activating mutation in the gamma1 subunit of the AMP-activated protein kinase. *FEBS Lett.* 500, 163–168.
- Hemminki, A., Markie, D., Tomlinson, I., Azizienyte, E., Roth, S., Loukola, A., Bignell, G., Warren, W., Aminoff, M., Höglund, P., Järvinen, H., Kristo, P., Pelin, K., Rindapää, M., Salovaara, R., Toro, T., Bodmer, W., Olschwang, S., Olsen, A.S., Stratton, M.R., de la Chapelle, A., Aaltonen, L.-A., 1998. A serine/threonine kinase gene defective in Peutz-Jeghers syndrome. *Nature* 391, 184–187.
- Hezel, A.F., Bardeesy, N., 2008. LKB1: linking cell structure and tumor suppression. *Oncogene* 27, 6908–6919.
- Hoch, R.V., Rubenstein, J.L., Pleasure, S., 2009. Genes and signaling events that establish regional patterning of the mammalian forebrain. *Semin. Cell Dev. Biol.* 20, 378–386.
- Huang, W., She, L., Chang, X.Y., Yang, R.R., Wang, L., Ji, H.B., Jiao, J.W., Poo, M.M., 2014. Protein kinase LKB1 regulates polarized dendrite formation of adult hippocampal newborn neurons. *Proc. Natl. Acad. Sci. USA* 111, 469–474.
- Kerosuo, L., Bronner-Fraser, M., 2012. What is bad in cancer is good in the embryo: importance of EMT in neural crest development. *Semin. Cell. Dev. Biol.* 23, 320–332.
- Kubota, Y., Ito, K., 2000. Chemotactic migration of mesenchymal neural crest cells in the mouse. *Dev. Dyn.* 217, 170–179.
- Le Douarin, N., Kalchauer, C., 1999. The neural crest. 2nd edn (Cambridge University Press).
- Lee, J.H., Koh, H., Kim, M., Kim, Y., Lee, S.Y., Kares, R.E., Lee, S.H., Shong, K., Kim, J.M., Chung, K., 2007. Energy-dependent Regulation of Cell structure by AMP-activated protein kinase. *Nature* 447, pp. 1017–1020.
- Luo, T., Lee, Y.H., Saint-Jeanet, J.P., Sargent, T.D., 2003. Induction of neural crest in *Xenopus* By Transcription factor AP2. *Proc. Natl. Acad. Sci. USA* 100, 532–537.
- Manzanares, M., Nieto, M.A., 2003. A celebration of the new head and an evaluation of the new mouth. *Neuron* 37, 895–898.
- McBratney-Owen, B., Iseki, S., Bamforth, S.D., Olsen, B.R., Morris-Kay, G.M., 2008. Development and tissue origins of the mammalian Cranial Base. *Dev. Biol.* 322, 121–132.
- Minoux, M., Rijli, F.M., 2010. Molecular mechanisms of cranial neural crest cell migration and patterning in craniofacial development. *Development* 137, 2605–2621.
- Miranda, L., Carpentier, S., Platek, A., Hussain, N., Gueuning, M.A., Vertomme, D., Ozkan, Y., Sid, B., Hue, L., Courtoy, P.J., Rider, M.H., Horman, S., 2010. AMP-activated protein kinase induces actin cytoskeleton reorganization in epithelial cells. *Biochem. Biophys. Res. Commun.* 396, 656–661.
- Nakagawa, S., Takeichi, M., 1998. Neural crest emigration from the neural tube depends on regulated cadherin expression. *Development* 125, 2963–2971.
- Ohmura, T., Shioi, G., Hirano, M., Aizawa, S., 2012. Neural tube defects by NUA1 and NUA2 double mutation. *Dev. Dyn.* 241, 1350–1364.
- Pekarik, V., Bourikas, D., Miglino, N., Joset, P., Preiswerk, S., Stoeckli, E.T., 2003. Screening for gene function in chicken embryo using RNAi and electroporation. *Nat. Biotechnol.* 21, 93–96.
- Pietri, T., Eder, O., Blanche, M., Thierry, J.P., Dufour, S., 2003. The human tissue plasminogen activator-Cre mouse: a new tool for targeting specifically neural crest cells and their derivatives in vivo. *Dev. Biol.* 259, 176–187.
- Phillips, H.M., Papoutsis, T., Soenen, H., Ybot-Gonzales, P., Henderson, D.J., Chaudry, B., 2012. Neural crest cell survival is dependent on Rho kinase and is required for development of the mild face in mouse embryos. *PLoS One* 7, e37685.
- Pouthis, F., Girard, P., Lecaudey, V., Ly, T.B., Gilmour, D., Boulon, C., Pepperkok, R., Reynaud, E.G., 2008. In migrating cells, the Golgi complex and the position of the centrosome depend on geometrical constraints of the substratum. *J. Cell. Sci.* 121, 2406–2414.
- Puffenberger, E.G., Strauss, K.A., Ramsey, K.E., Craig, D.W., Stephan, D.A., Robinson, D.L., Hendrickson, C.L., Gottlieb, S., Ramsay, D.A., Siu, V.M., Heuer, G.G., Crino, P. B., Morton, D.H., 2007. Polyhydramnios, megalencephaly and symptomatic epilepsy caused by a homozygous 7-kilobase deletion in *LYK5*. *Brain* 130, 1929–1941.
- Richtsmeier, J.T., Faherty, K., 2013. Hand in glove: brain and skull in development

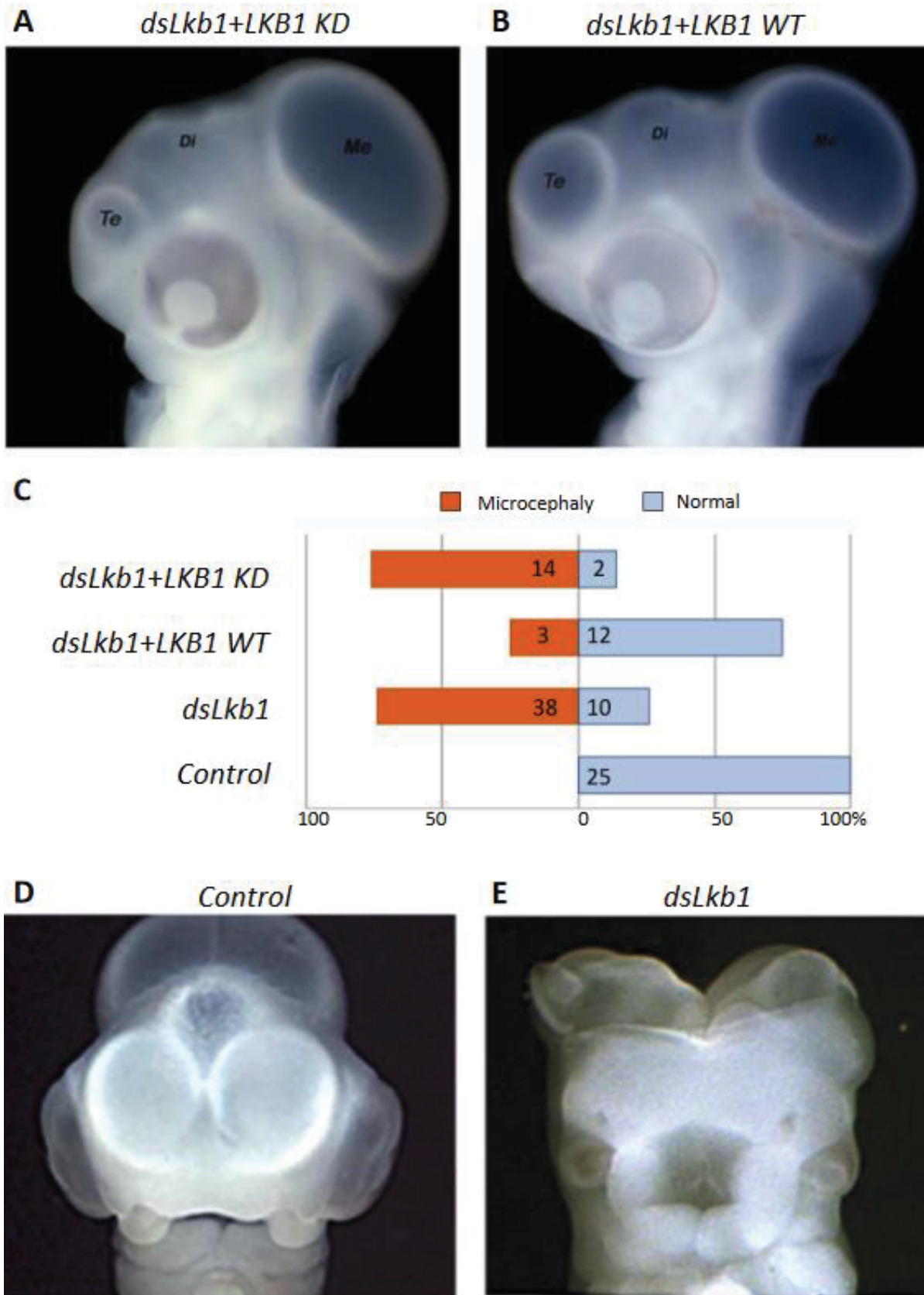
- and dysmorphogenesis. *Acta Neuropathol.* 125, 469–489.
- Riento, K., Ridley, A.J., 2003. Rocks: multifunctional kinases in cell behaviour. *Nat. Rev. Mol. Cell Biol.* 6, 446–56.
- Rodriguez-Fraticelli, A.E., Auzan, M., Alonso, A.M., Bornens, M., Martin-Belmonte, F., 2012. Cell confinement controls centrosome positioning and lumen initiation during epithelial morphogenesis. *J. Cell. Biol.* 198, 1011–1023.
- Shackelford, D.B., Shaw, R.J., 2009. The LKB1-AMPK pathway: metabolism and growth control in tumour suppression. *Nat. Rev. Cancer* 9, 563–575.
- Shaw, R.J., Kosmatka, M., Bardeesy, N., Hurley, R.L., Witters, L.A., DePinho, R.A., Cantley, L.C., 2003. The tumor suppressor LKB1 kinase Directly activates AMP-activated kinase and regulates apoptosis in response to energy stress. *Proc. Natl. Acad. Sci. USA* 101, 3329–3335.
- Simoës-Costa, M., Bronner, M.E., 2015. Establishing neural crest identity: a gene regulatory recipe. *Development* 142, 242–257.
- Sugishita, Y., Watanabe, M., Fisher, S.A., 2004. Role of myocardial hypoxia in the remodeling of the embryonic avian cardiac outflow tract. *Dev. Biol.* 267, 294–308.
- Théveneau E., Mayor R., 2012. Neural crest delamination and migration: from epithelium-to-mesenchyme transition to collective cell migration. *Dev Biol.* 366, pp. 34–54.
- Théveneau, E., Marchant, L., Kuriyama, S., Gull, M., Moepps, B., Parsons, M., Mayor, R., 2010. Collective chemotaxis requires contact-dependent cell polarity. *Dev. Cell* 19, 39–53.
- Uehata, M., Ishizaki, T., Satoh, H., Ono, T., Kawahara, T., Morishita, T., Tamakawa, H., Yamagami, K., Inui, J., Maekawa, M., Narumiya, S., 1997. Calcium sensitization of smooth muscle mediated by a Rho-associated protein kinase in hypertension. *Nature* 389, 990–994.
- Vincent, M., Duband, J.L., Thiery, J.P., 1983. A cell surface determinant expressed early on migrating avian neural crest cells. *Dev. Brain Res.* 9, 235–238.
- Williams, T., Courchet, J., Viollet, B., Brenman, J.E., Polleux, F., 2011. AMP-activated protein kinase (AMPK) activity is not required for neuronal development but regulates axogenesis during metabolic stress. *Proc. Natl. Acad. Sci. USA* 108, 5849–5854.
- Woods, A., Azzout-Marniche, D., Foretz, M., Stein, S.C., Lemarchand, P., Ferré, P., Foufelle, F., Carling, D., 2000. Characterization of the role of AMP-activated protein kinase in the regulation of glucose-activated Gene Expression using constitutively active and dominant negative forms of the kinase. *Mol. Cell Biol.* 20, 6704–6711.
- Xu, X., Omelchenko, T., Hall, A., 2010. LKB1 tumor suppressor protein regulates actin filament assembly through Rho and its exchange Factor Dbl independently of kinase activity. *BMC Cell. Biol.* 12, 11–77.
- Ylikorkala, A., Rossi, D.J., Korsisaari, N., Luukko, K., Alitalo, K., Henkemeyer, M., Mäkelä, T.P., 2001. Vascular abnormalities and deregulation of VEGF in Lkb1-deficient mice. *Science* 293, 1323–1326.
- Zagorska, A., Deak, M., Campbell, D.G., Banerjee, S., Hirano, M., Aizawa, S., Prescott, A.R., Alessi, D.R., 2010. New roles for the LKB1-NUAK pathway in controlling myosin phosphatase complexes and cell adhesion. *Sci. Signal.*, 5.
- Zhang, L., Li, J., Young, L.H., Caplan, M.J., 2006. AMP-activated protein kinase regulates the assembly of epithelial tight junctions. *Proc. Natl. Acad. Sci. USA* 103, 17272–17277.

Supplementary material **S1 Fig. Cephalic defects in *Lkb1*-deprived embryos.** (A, B) Cotransfection of *Lkb1*-dsRNA with a vector producing hLKB1. The human LKB1-KD cannot rescue cephalic development (A), while a vector producing human wild-type LKB1 does so (B). (C) Quantification of microcephalic *versus* normal phenotypes in control, *Lkb1*-dsRNA series, and after the co-transfection of *Lkb1*-dsRNA with either *hLKB1*-WT or *hLKB1*-KD. Values in the bars of the graph indicate the number of analyzed embryos per each condition. (D-E) When performed in early neurula (1ss), inhibition of *Lkb1* generates consistent neural tube defects and results in anencephalic embryos (E).

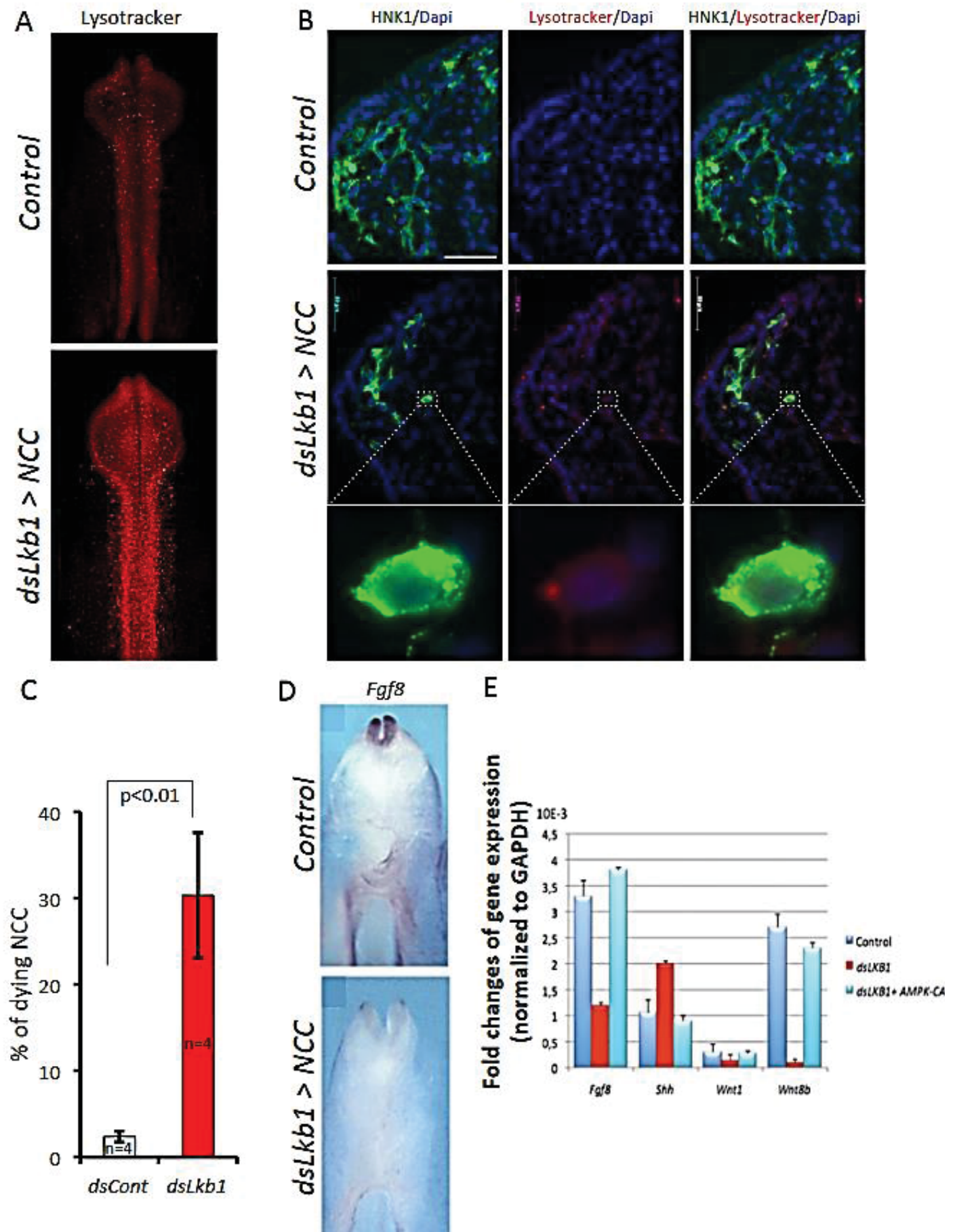
Supplementary material **S2 Fig. *Lkb1* silencing impacts CNCC survival, and morphogen expression.** (A) When compared to control embryos electroporated with scramble dsRNA, Lysotracker staining of 7ss embryos electroporated with dsLkb1 reveals expanded cell death. (B) HNK1 immunofluorescence with lysotracker revealed that NCC display increased cell death in the absence of *Lkb1*. (C) Quantification of the average percentage of dying NCC (HNK1 and lysotracker positive cells) in control or dsLkb1 conditions. Increased cell death in NCC in the absence of *Lkb1* was statistically significant as evaluated by a Student *t*-test. (D) *Fgf8*, which is strongly expressed in ANR, is down-regulated by *Lkb1*-silencing in CNCC. (E) Quantification of gene expression by qRT-PCR showed that *Lkb1* silencing significantly affected the mRNA levels of *Fgf8* ($Fgf8\Delta=60\%$), *Wnt1* ($Wnt1\Delta=40\%$), and *Wnt8b* ($Wnt8b\Delta=90\%$). By contrast, *Shh* expression was up-regulated (1.5 fold). The number of embryos used for qRT-PCR analyses was $n=4$ in control condition, $n=3$ in *dsLkb1* and $n=4$ in *dsLkb1*+AMPK-CA. Statistical analyses were performed using Mann-Whitney *U* test.

Supplementary material **S3 Fig. Gene expression pattern of *AMPK α 1* and *AMPK α 2* in chick embryos.** Accumulation of *AMPK α 1* (A-C) and *AMPK α 2* (D-F) transcripts at 5ss (A, D), 10ss (B, E), 12–13ss (C, F). At neurula stages, at which electroporation experiments are performed, *AMPK α 1* and *AMPK α 2* are expressed in the diencephalic and mesencephalic neural crest cells (5ss; A, D). The expression of these two genes is maintained in migratory neural crest cells once they have started to migrate, according to a similar pattern at 10ss (B,E) and 12–13 ss (C-F). (G) Absence of signal after *in situ* hybridization with *AMPK* sense probes (ISH Control).

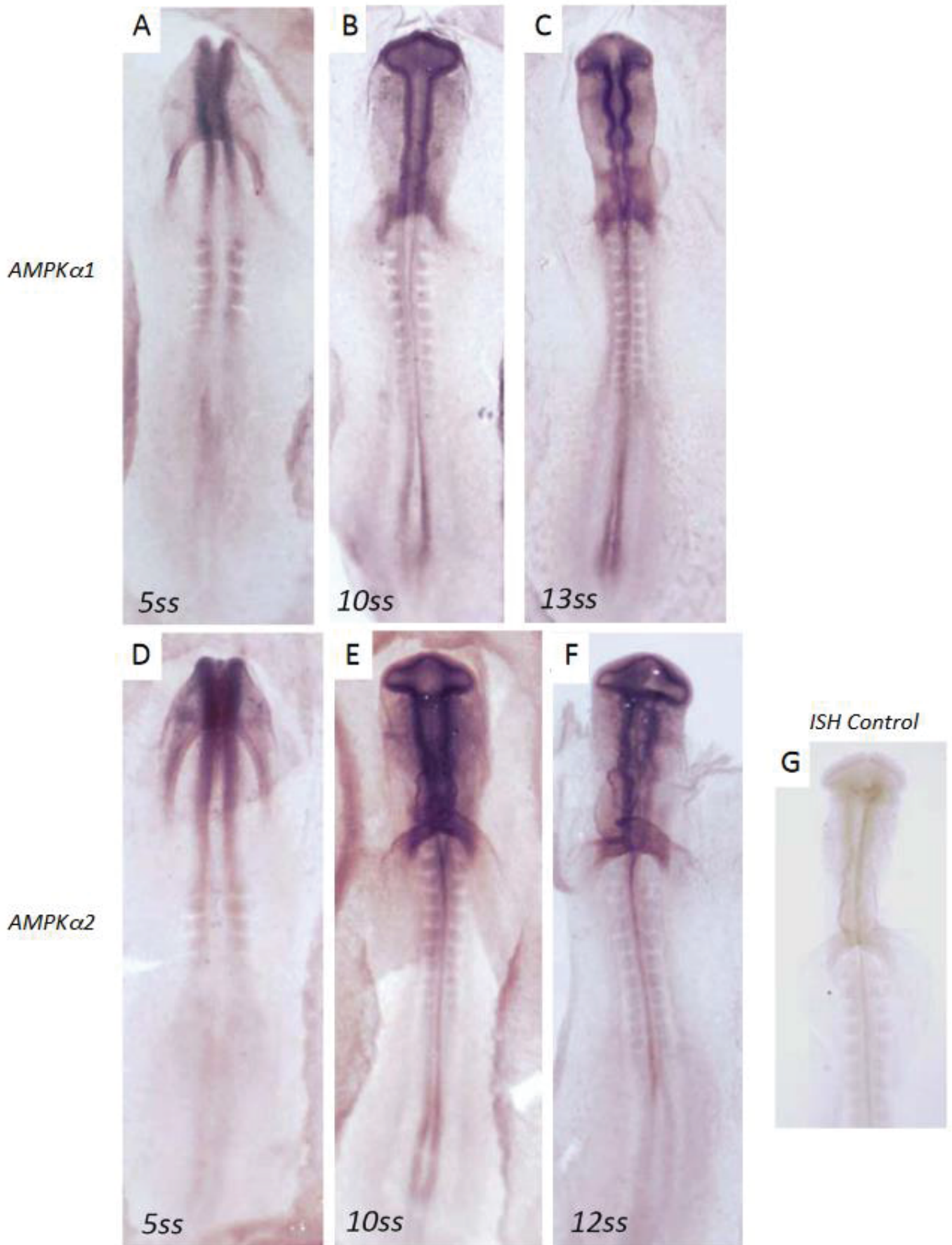
Creuzet Sup Figure 1



Creuzet Sup Figure 2



Creuzet Sup Figure 3



1.3 Conclusions

In this study, we characterized the role of Lkb1 in cranial NCC delamination, polarized migration and survival. *Lkb1* silencing by RNA interference in chick cranial NCC or genetic ablation of *Lkb1* in mouse NCC just after their delamination led to craniofacial malformations. These defects included severe reduction of the telencephalic vesicle and of the development of naso-frontal and maxillo-mandibular structures.

Upon *Lkb1* loss, the expression of Sox9, marker of pre-migratory NCC, and Sox10, marker of delaminating NCC, were decreased compared to control embryos. Furthermore, using the Golgi-nucleus axis as a marker of cell polarity, we demonstrated that *Lkb1* loss resulted in a randomized positioning of chick migrating cranial NCC. We also explored viability of cranial NCC and found an expansion of cell death upon *Lkb1* silencing. We have shown that Lkb1 controls cranial NCC formation through AMPK pathway by sequential activation of ROCK kinase and the actin molecular motor Myosin II.

Altogether, these data point out that Lkb1 pathway orchestrates several steps of cranial NCC development that are essential for cephalogenesis. Therefore, this study is of particular interest in order to better understand the molecular mechanisms responsible for craniofacial abnormalities which represent one-third of all congenital birth defects (Dixon et al., 2006).

2. Regulation of LKB1 by acetyl transferase GCN5.

Results not published which are part of an article in preparation

(Ghawitian, Radu, et al., in preparation).

2.1 Scientific context

After underlining the role of Lkb1 signaling in cranial NCC fate and vertebrate head development, I also contributed to the investigation of the molecular mechanisms underlying LKB1 regulation by upstream factors. This project was initiated by Maya Ghawitian, a former PhD student in Marc Billaud lab.

As mentioned in the introduction of this manuscript, LKB1 undergoes post-translational modifications such as phosphorylation, prenylation, ubiquitination and acetylation (see Chapter III.A.1.3). Regarding acetylation, data from the literature described several acetylated residues of LKB1 (Lan et al., 2008); Figure 19 B intro). In particular, lysine 48 (K48) deacetylation by the class III histone deacetylase Sirt1 regulates LKB1 subcellular localization and its catalytic activity (Lan et al., 2008). Along this line, our team also identified by mass spectrometry that five lysine residues of LKB1 are acetylated (lysines 48, 64, 97, 108 and 178, see Introduction Figure 19 B). Exploration of upstream acetyltransferases involved in LKB1 acetylation demonstrated that among 4 different enzymes, the acetyltransferase GCN5 was the major enzyme capable of acetylating LKB1 (N. Aznar, M. Billaud, unpublished data).

GCN5 is crucial during embryogenesis. GCN5 null mice are embryonic lethal early during development, just after the beginning of gastrulation (Xu et al., 2000). Mice expressing GCN5 harboring mutations inactivating its catalytic domain (GCN5^{HAT}) also lead to embryonic lethality but later on, at mid-gestation (Bu et al., 2007). GCN5^{HAT} mutants exhibit neural tube closure defects limited to cranial region and reduced telencephalon formation. This suggests that GCN5 regulates early embryonic development via both acetyltransferase dependent and independent functions.

The malformations observed upon GCN5 loss or when GCN5 catalytic activity is abrogated are similar with those observed after cranial NCC agenesis (Creuzet et al., 2005; Kurihara et al., 1994) thereby suggesting that GCN5 is essential for cranial NCC development. Interestingly, GCN5 mutant phenotype is evocative of the defects we described upon *Lkb1* inactivation in cranial NCC (Creuzet et al., 2016).

To characterize the potential contribution of GCN5 upstream LKB1 signaling in NCC during vertebrate head formation, our team firstly explored the regulation of LKB1 by GCN5 *in vitro*. Secondly, we assessed how LKB1 acetylation and GCN5 contribute to neural crest formation *in vivo*.

2.2 Results

Nicolas Aznar and Maya Ghawitian, former PhD students in Marc Billaud lab, identified by mass spectrometry five acetylated lysine residues on LKB1, one of them being lysine 48 (K48). They validated by western blot on cell extracts that LKB1 can indeed be acetylated (Fig.1A) and that GCN5 is the major acetyltransferase responsible for LKB1 acetylation (Fig.1B). One of our collaborators, Vincent Mirouse (Genetic, Reproduction, Development (GReD), Clermont-Ferrand), has developed an antibody which recognizes specifically the acetylated form of LKB1 on K48. Validation of this home-made antibody was performed by comparing acetylation levels of LKB1 wildtype or a non-acetylatable mutant (K48R) (Fig.1C).

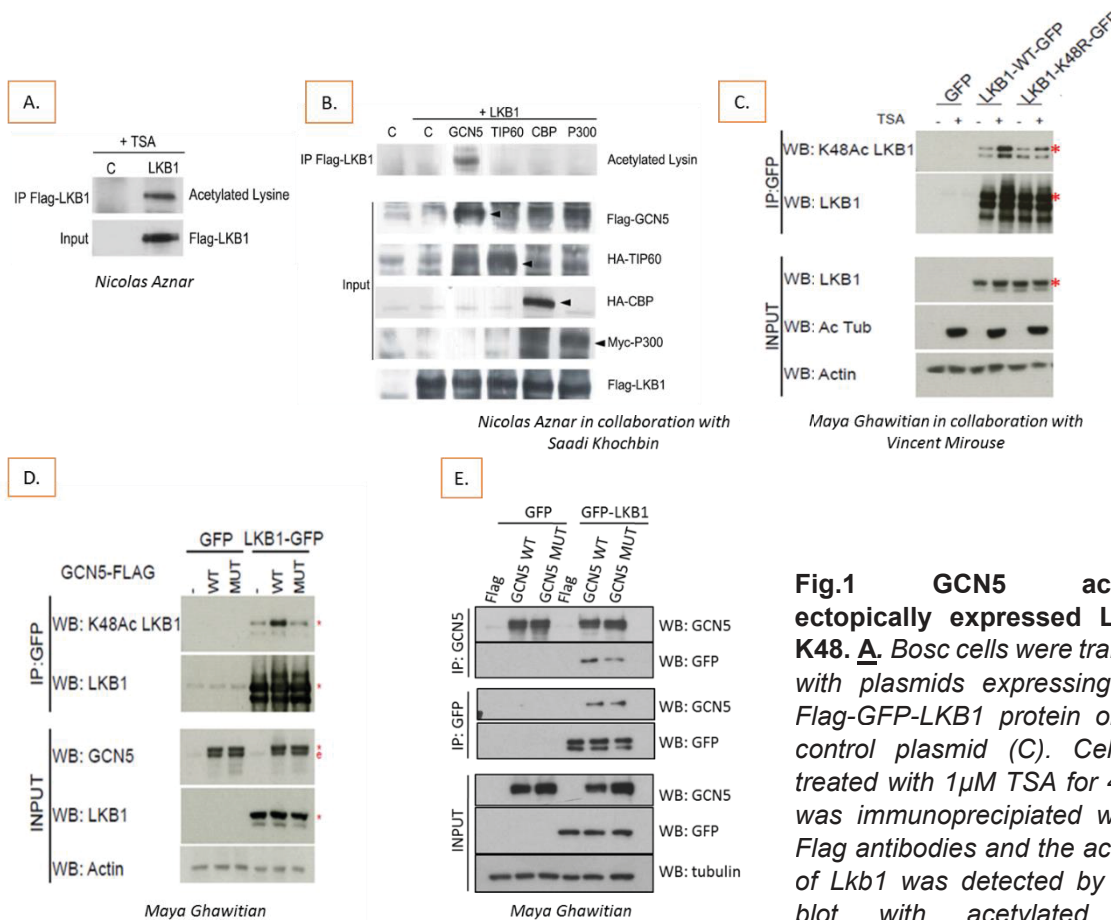


Fig.1 GCN5 acetylates ectopically expressed LKB1 at K48. **A.** Bosc cells were transfected with plasmids expressing a WT-Flag-GFP-LKB1 protein or with a control plasmid (C). Cells were treated with 1μM TSA for 4h. Lkb1 was immunoprecipitated with anti-Flag antibodies and the acetylation of Lkb1 was detected by western blot with acetylated lysines antibody.

B. Bosc cells were co-transfected with plasmids expressing Flag-GCN5, HA-TP60, HA-CBP, Myc-P300 and plasmids expressing WT-Flag-GFP-LKB1 or control plasmid. Immunoprecipitation of Lkb1 and acetylated Lkb1 were done as previously described. **C.** Bosc cells were transfected with plasmids expressing WT-Flag-GFP-LKB1 or K48R-GFP-LKB1 or plasmid control (only pe-GFP) and treated with 1μM TSA for 4h. Lkb1 was immunoprecipitated with anti-GFP antibody and acetylated LKB1 K48 was analyzed by Western Blot with the home made antibody (V. Mirouse). **D.** Bosc cells were co-transfected with plasmids expressing WT-Flag-GFP-LKB1 or with peGFP and with plasmids expressing WT-Flag GCN5 or MUT-flag GCN5. MUT= GCN5 mutant in its catalytic domain (Y621A/F622A). Immunoprecipitation of Lkb1 and acetylated Lkb1 K48 were done as previously described. **E.** Bosc cells were transfected as presented in D. and Lkb1 was immunoprecipitated with anti-GFP antibody and GCN5 was immunoprecipitated with anti-GCN5 antibody.

Next, our lab showed using overexpressed proteins that LKB1 is acetylated at K48 by GCN5 (Fig.1D) and that both proteins are in the same complex (Fig.1E).

During my PhD, I confirmed these results on endogenous immunoprecipitated LKB1 from HEK293T BOSC cells treated with Trichostatin A (TSA), a selective inhibitor of histone deacetylases class I and II, to stabilize acetylated proteins. Indeed, I identified by Western Blot that endogenous LKB1 is acetylated at K48 and that TSA treatment increased LKB1 acetylation at K48, suggesting that the signal observed is specific to an acetylated form of LKB1 (Fig.2A). I have also shown that endogenous LKB1 and GCN5 interact together. The specificity of this interaction was confirmed by decreased GCN5 signal after immunoprecipitation of LKB1 in *GCN5* silencing conditions (Fig.2B). Moreover, the physical interaction between GCN5 and LKB1 was not impacted when the acetylation status of lysine 48 was modified. Indeed, LKB1 mutants such as LKB1 K48R and LKB1 K48Q (acetyl mimetic mutant) still interact with GCN5 as wild type LKB1 (Fig.2C). Overall the interaction between LKB1 and GCN5 does not rely on acetyltransferase activity of GCN5 since *GCN5^{HAT}* mutant still interacts with LKB1 (Fig.1D, E).

Altogether, these results emphasize that endogenous LKB1 is acetylated at K48 and that LKB1 is physically interacting with GCN5.

Further, I analyzed the distribution of acetylated LKB1 at K48. LKB1 is expressed in both cytoplasm and nucleus and depending of cell types, it is almost exclusively nuclear or more cytoplasmic. In HEK293T BOSC cells, endogenous LKB1 is both nuclear and cytoplasmic with a clear accumulation in the nucleus. In these cells, I analyzed if endogenous GCN5 regulates LKB1 subcellular localization. Interestingly, I observed that upon *GCN5* knockdown, LKB1 was exclusively localized in the nucleus (Fig.2D). Instead, overexpressing LKB1 and GCN5 in Hela cells triggered cytoplasmic accumulation of LKB1 compare to overexpressed LKB1 alone which is mainly nuclear (Fig2E). However, GCN5 controls LKB1 cellular localization independently of its capacity to acetylate LKB1 since GCN5 mutant impaired for its acetyl transferase activity still triggers LKB1 relocalization from nucleus to cytoplasm (Fig.2E).

I next assessed the localization of acetylated LKB1. Lan *et al.* have shown that LKB1 K48 acetylation is nuclear and that deacetylation of K48 by Sirtuin1 increases the cytoplasmic translocation of LKB1 from nucleus (Lan et al., 2008). In line with their results, I observed by immunofluorescence that K48 acetylated form of LKB1 is exclusively nuclear (Fig.2E right panels). I confirmed this result by cellular fractionation (validation shown left in Fig2F) followed by immunoprecipitation of endogenous LKB1 and western blot analyses of acetylated LKB1 K48. As seen in Figure 2F (right panels) acetylated LKB1 at K48 is exclusively nuclear.

Since acetylated K48 is nuclear and GCN5 is the acetyltransferase responsible for this acetylation I studied in which cellular compartment is taking place the physical interaction

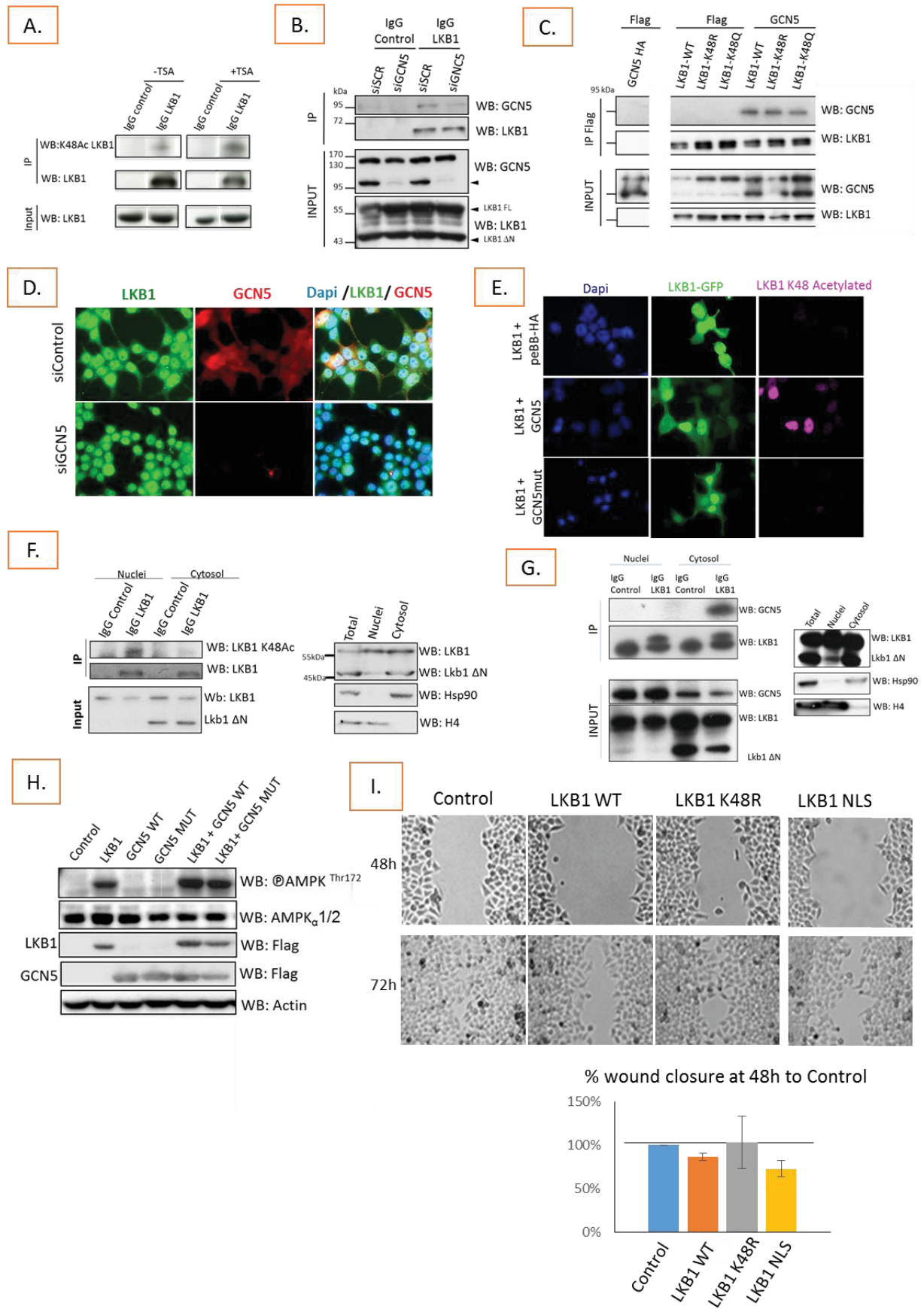


Fig.2 GCN5 acetylates LKB1 at K48 and regulates Lkb1 cellular functions.

A. Bosc cells were treated with TSA 1 μ M for 4h and Lkb1 was immunoprecipitated with anti-LKB1 antibody. Mouse IgG were used as control immunoprecipitation. Acetylated Lkb1 K48 was analyzed by western blot with anti-acetylated LKB1 K48 antibody. **B.** Bosc cells were transfected with siRNA targeting GCN5 mRNA (siGCN5) for 48h. Non-targeting siRNA were used as control. LKB1 was immunoprecipitated as in A. Lkb1 interaction with GCN5 was analyzed by western blot with anti-GCN5 antibody. **C.** Bosc cells were co-transfected with plasmids expressing WT-Flag-GFP-LKB1, K48-Flag-LKB1 or K48Q-Flag-LKB1 proteins and with plasmids expressing WT-HA-GCN5 or control plasmid (pSG5-Flag). LKB1 immunoprecipitation and interaction with GCN5 were done as in B. **D.** Bosc cells were transfected with siRNA as in B and immunofluorescence was used to detect Lkb1 (green) and GCN5 (red). Nuclei were labeled with Dapi (blue). **E.** Hela cells were co-transfected with plasmids expressing WT-Flag-GFP-LKB1 protein and plasmids expressing GCN5 wildtype (WT) or mutant in its catalytic domain Y621A/F622A (GCN5mut) or control (peBB-HA). Acetylated LKB1 K48 (in magenta) was detected by immunofluorescence with anti-acetylated LKB1 K48 antibody. Lkb1-GFP (in green) was visualized with an epifluorescent microscope. Nuclei were labeled with Dapi (blue). **F.** Cellular fractionation was performed on Bosc cells to separate cytoplasmic and nuclear fractions. LKB1 was immunoprecipitated in both fractions with anti-LKB1 antibody. Acetylated-LKB1-K48 was analyzed by western blot (left panel). Cellular fractionation was also verified (right panel) by western blot using anti-Hsp90 antibody for the detection of cytoplasmic fractions and anti-H4 antibody for nuclear fractions. LKB1 was detected with anti-LKB1 antibody from Santa Cruz (Ley37DG6) which recognize the C terminal part of LKB1 and therefore it detects also the LKB1 Δ N isoform. **G.** The cellular fractionation and LKB1 immunoprecipitation were done as described above. LKB1 interaction with GCN5 was analyzed in both fractions by western blot with anti-GCN5 antibody. **H.** Hela cells were transfected with plasmids expressing WT Flag-GFP- LKB1 proteins and/or WT-Flag GCN5 or MUT-Flag-GCN5 proteins for 48h. AMPK phosphorylation was analyzed by western blot. **I.** The migration of Hela cells was analyzed by wound healing assay using ibidi. Cells were transfected with plasmids expressing WT-Flag-LKB1 or K48R-Flag-K48R or NLS-Flag-LKB1 for 48h. Representative pictures of the size of the wound 48h and 72h after wounding are shown. The percentage of closure for each wound was evaluated from microscopy images at 48h after wounding relative to Control from 2 independent experiments.

between Lkb1 and GCN5. It is known that GCN5, as LKB1, can be present in both nucleus and cytoplasm (Maralice Conacci-Sorrell et al., 2010). As observed in figure 2G, I have shown that Lkb1 can interact with GCN5 in the cytoplasm. Instead, I did not detect any nuclear interaction. However, it is difficult to conclude that this interaction is only cytoplasmic because it is known that GCN5 in nucleus is part of large complexes, the best characterized one being the SAGA (Spt-Ada-GCN5 acetyltransferase) complex which has a size of 1.8-2 MDa (K.K. Lee et al., 2011; Weake and Workman, 2012). Therefore, it is possible that during LKB1 immunoprecipitation, nuclear GCN5 complexes were lost at centrifugation steps. Thus, other analyses have to be done in order to conclude in which compartment the two proteins interact.

As GCN5 is important for LKB1 translocation into the cytoplasm and as LKB1 kinase activity correlates with its cytoplasmic localization, I analyzed the role of GCN5 regarding LKB1 catalytic activity. AMPK is the most studied substrate of LKB1 (see Introduction Chapter III.A.2). Therefore, I analyzed AMPK phosphorylation at threonine 172 in presence or not of GCN5. As expected overexpressed LKB1 led to AMPK phosphorylation on threonine 172 (Fig. 2H). Preliminary results have shown that GCN5 transfection, in presence of overexpressed LKB1, led to increased AMPK phosphorylation compared to overexpression of LKB1 alone (Fig. 2H). This augmentation is not dependent of GCN5 acetyltransferase activity because GCN5 mutant in its catalytic subunit did not significantly decrease AMPK phosphorylation

(Fig.2H). These data suggest that GCN5 regulates LKB1 catalytic activity independently of its acetyltransferase activity. Further studies have to be done to confirm these results.

GCN5 acetyltransferase activity is essential for neural tube closure and contributes to head formation especially telencephalon morphogenesis. We next assessed whether LKB1 acetylation by GCN5 could regulate neural crest cell fate. I therefore analyzed if acetylated LKB1 K48 regulates cell migration. To do so, I used LKB1 null Hela cells transfected with empty vector, wild type LKB1 (LKB1 WT), non-acetylatable mutant of LKB1 (LKB1 K48R) or LKB1 harboring mutations in its nuclear localization sequence (LKB1 NLS) and which is therefore cytoplasmic only. As shown in figure 2I, LKB1 WT limited Hela cells migration due to its known tumor suppressor activity. LKB1 NLS also impaired cellular migration thereby suggesting that limitation of cell migration by LKB1 does not require its nuclear localization (Fig 2I). Interestingly, the non-acetylatable form of LKB1 (LKB1 K48R) failed to limit cellular migration. These preliminary results suggest that the acetylated form of LKB1 on K48 is essential to control cellular migration and that this LKB1 function is cytoplasmic. However, more experiments need to be done to confirm these findings.

In order to analyze the role of GCN5 during development and more precisely in cranial NCC, Marc Billaud team first studied GCN5 expression during embryogenesis by whole mount *in situ* hybridization in chick embryos. They cloned and sequenced chicken homologue of GCN5 cDNA and observed that 89% of the chicken GCN5 amino-acid sequence was conserved with the human long isoform of GCN5. Second they synthesized labeled probes that recognize GCN5 mRNA (antisens probes). After whole mount *in situ* hybridization, GCN5 mRNA were detected at 4 somites stage in the neural folds, just before neural tube closure. At 7 somites stage GCN5 mRNA accumulated in neural folds but also started to localize in migrating NCC. At 11 somites stages GCN5 transcripts continued to be observed in migrating cranial NCC.

Next, the team silenced GCN5 specifically in chick cranial NCC and observed that GCN5 absence leads to dramatic craniofacial malformations including reduction of the telencephalic vesicle and of the development of naso-frontal and maxilla-mandibular structures (Fig.2J).

Collectively, our results suggested that Lkb1 is a downstream target of GCN5. We also demonstrated that GCN5 is essential for vertebrate head formation and that GCN5 loss mimics the phenotype associated with *Lkb1* inactivation I previously described (Project 1.1, Creuzet et al., 2016). These results strongly suggest a crosstalk between Lkb1 and GCN5.

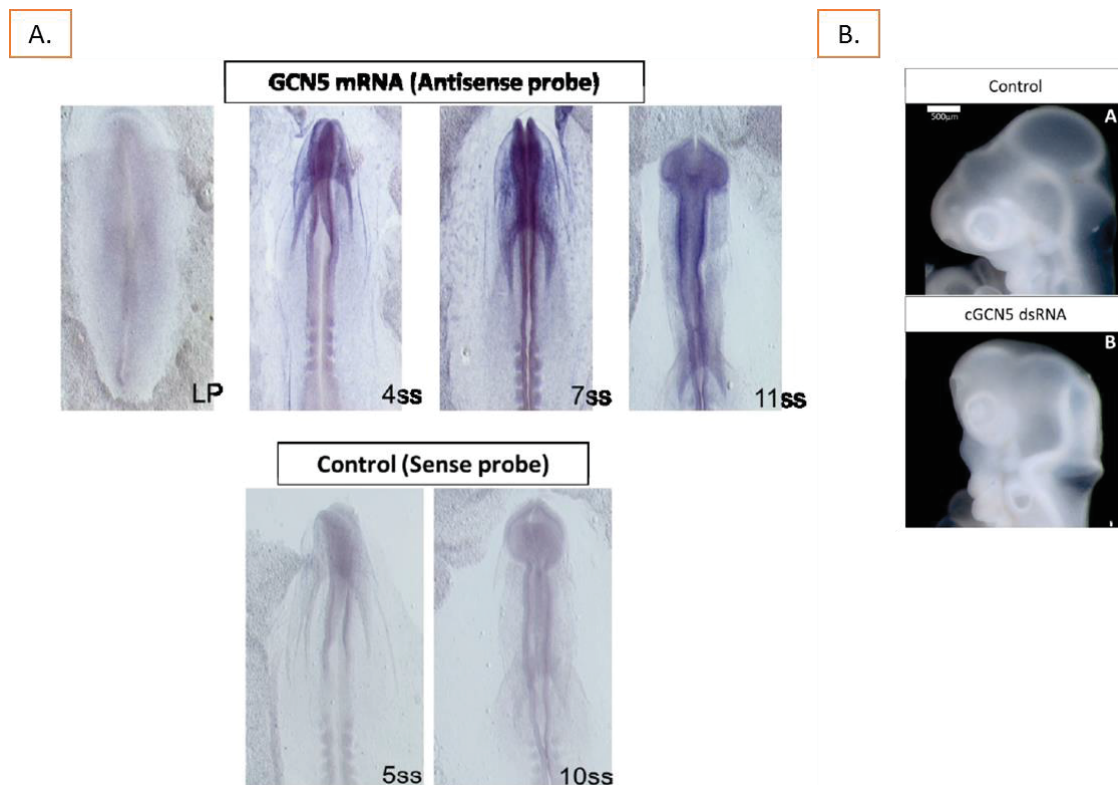


Fig.3 GCN5 expression in cranial NCC is essential for vertebrate head formation.

A. Whole-mount in situ hybridization of chick embryos at different somite stages (ss) with the GCN5 antisense probe and control sense probe (experiments performed by Jacques Thélou) **B.** Chicken embryos at 4 somite stage. A-control embryo. B-representative embryo subjected to GCN5 silencing via electroporation with cGCN5 dsRNA (experiments performed by Jean Viallet).

2.3 Conclusions

This study allowed us to identify the acetyltransferase GCN5 as a novel upstream regulator of LKB1. During this project, I showed that endogenous LKB1 and GCN5 are in the same complex, that GCN5 acetylates LKB1 on lysine 48 and that this acetylated form of LKB1 is nuclear.

I also observed that GCN5 controls LKB1 subcellular localization and consequently LKB1 catalytic activity independently of its acetyltransferase activity.

Interestingly, it has been shown that GCN5 has developmental functions that depend of its acetyltransferase activity but also that are independent of its catalytic activity. For example, homozygous point mutations in GCN5 catalytic domain (GCN5^{Hat/Hat}) lead to embryonic lethality due to neural tube closure defects and exencephaly, demonstrating that the acetyl transferase activity is essential for neural tube closure and correct head patterning (Bu et al., 2007). However, these mice survive longer than GCN5 knockout mice (Xu W et al., 2000), suggesting that GCN5 exerts other developmental regulations independently of its acetyltransferase activity.

The role of GCN5 in early embryonic development and neural tube closure was also described in humans. Human amniotic fluid and blood cells were isolated from pregnant women, in the second trimester, with normal fetuses or with fetuses displaying craniofacial abnormalities due to neural tube defects such as myelomeningocele and anencephaly (Tsurubuchi et al., 2013). In fetuses with myelomeningocele, GCN5 expression was decreased along with decreased histone H3 acetylation (in particular H3K9 and H3K18) (Tsurubuchi et al., 2013). This suggest that GCN5 and histone H3 acetylation are crucial for neural tube closure in human early development.

In our study, we have shown that GCN5 is expressed in cranial NCC and that GCN5 silencing in cranial NCC mimics the phenotype observed upon *Lkb1* inactivation. We previously identified that *Lkb1* regulates cranial NCC migration among several NCC behavior, through actin dynamic thereby controlling vertebrate head formation (Creuzet et al., 2016). In the present study, I have shown that the acetylation of LKB1 on K48 is important for the control of cell migration. This result suggests that GCN5 may have the capacity to control vertebrate head formation through LKB1 acetylation on K48. In order to test this hypothesis, further studies require to be performed. **First**, studying the impact of LKB1 acetylation in neural crest stem cells is primordial. To do so, *Lkb1* could be silenced in the neural crest stem cell line (JoMa1.3 cells, see next project) cultivated as progenitors and LKB1 re-expression will be performed by retroviral infection. Viral vectors were constructed to allow the re-expression of human LKB1 (insensitive to murine *Lkb1* siRNA) either wildtype or non-acetylatable mutant (collaboration C. Thibert and L. Attardi). Using classical protocols, cell survival, proliferation and migration in transwell containing a TGF β gradient of concentration (Murphy et al., 2011) could then be assessed. **Second**, to evaluate *in vivo* contribution of *Lkb1* acetylation, chick embryos at 4 somite stage could be co-electroporated with double stranded RNA targeting chick GCN5 and plasmids allowing expression of LKB1 wildtype or the non-acetylatable K48 mutant (LKB1 K48R) or acetylmimetic mutant (LKB1 K48Q). Analyzing if a correct cephalic morphology is differentially rescued depending on LKB1 form will be performed as previously (Creuzet et al., 2016).

Thus, several studies could be done in order to emphasize the role of LKB1 K48 acetylation by GCN5 in neural crest ontogeny and complete this study before submission.

2.4 Materials and methods

Cell line and cell culture

Bosc cells (human kidney epithelial cells) and Hela cells (human epithelial cervix adenocarcinoma cells) were obtained from American Tissue Culture Collection. Both were cultured in DMEM (Ref. 41966-029, ThermoFisher Scientific) with 10% of heat-inactivated fetal bovine serum, supplemented with 1% of penicillin/ streptomycin, at 37°C in 5% CO₂.

During some experiments cells were treated for 4h before lysis with 1µM TSA (Trichostatin A) (Sigma-Aldrich) at 37°C.

Short interfering RNAs (siRNA) against the human GCN5 gene and the Non-targeting control siRNA were purchased from Fermentas /Thermo Scientific, Germany (SMARTpool ON-TARGET plus KAT2A (GCN5) human siRNA (ref. L-009722-02-0005) and ON-TARGET plus Non-targeting Pool (ref. D -001810-10-05)). siRNAs were transfected into Bosc cells by using RNAi Max reagent (Invitrogen/Life technologies) according the manufacturer's protocol. Experiments were realized 48h post-transfection.

pSG5-LKB1 wild type vector was previously described (Nony et al., 2003). The human Flag-LKB1 fused N-terminally to eGFP was described by Forcet et al., 2005. The non-acetyltable mutant of LKB1, K48R (a single point mutation of lysine 48 to arginine) or the acetyl mimetic mutant K48Q (a single point mutation of lysine 48 to glutamine) were obtained by Maya Ghawitian (Maya Ghawitian, 2015, PhD). The peB-flag and peBB-flag-GCN5 wild type vectors were obtained from E. Burstein, UT Southwestern medical center, Dallas, Texas. The GCN5 mutant in its catalytic domain (Y621A/F622A) was obtained by Maya Ghawitian.

The different vectors were transfected into Bosc or Hela cells using JetPRIME transfectant (Ozyme/Polyplus) according to the manufacture's protocol. Experiments were realize 48h post-transfections.

Immunoprecipitation

Bosc cells were seeded in 8 dishes of 10cm of diameter at 2x10⁶ cells/plate for endogenous protein immunoprecipitation or in 2 dishes per condition for overexpressed protein immunoprecipitation. Cells were lysed with NP-40 lysis buffer containing 20 mM Tris-HCl pH 7.5, 150 mM NaCl, 2 mM EDTA and 1% NP-40, supplemented with 1% proteases inhibitors (protease inhibitor cocktail /ref. P8340, SIGMA) and 10% PMSF (Phenylmethanesulfonyl fluoride/ref. P7626, SIGMA). After lysis and protein quantification, 1mg of lysates (for endogenous proteins) or 500µg of lysate (for overexpressed proteins) were completed to 1ml with lysis buffer. They were incubated for 1h at 4°C on a wheel with protein A -coupled sepharose beads (Dutscher). After 1 mins of centrifugation at 4°C and 8000 rpm, beads were

eliminated and lysates were incubated for 2h at 4°C with 4 µg of LKB1-K48 acetylated antibody developed by Vincent Mirouse team or with 4 µg of anti-Lkb1 antibody from Santa Cruz (Ley37DG-6) or with 1 µg of anti-Flag antibody from Sigma (clone M2). Further the lysates were incubated with protein A -coupled sepharose beads for 1h. The beads were then recovered by centrifugation, washed 4 times with the lysis buffer and boiled in 50uL of 2X Laemmli buffer, 5 mins at 95°C. Finally, they were analyzed by western blot.

Western blot analysis

Antibodies	Species	Dilutions	References
Lkb1	Mouse	1/1000	Santa Cruz, Ley37DG-6
Lkb1 K48 Acetylated	Rabbit	1/500	Vincent Mirouse team
©AMPK^{Thr172}	Rabbit	1/1000	Cell Signaling
AMPK	Rabbit	1/1000	Santa Cruz Biotechnology
GCN5 L2 (C26A10)	Rabbit	1/1000	Cell Signaling
HSP90	Mouse	1/1000	Stressgen
H4	Mouse	1/2000	Stressgen
Flag	Mouse	1/1000	Clone M2 Sigma
Actin	Mouse	1/5000	MAB1501 Millipore

Table1. Primary antibodies used for western blot

room temperature. Immunoreactive proteins were detected with Amersham ECL chemiluminescence reagents (GE Healthcare) according to the manufacturer's instructions.

Cell Fractionation

For cellular fractionation, Bosc cells were seeded in 2 dishes of 10 cm of diameter at 2×10^6 cells/dish. Cells were harvested and centrifuged for 4 minutes at 1200rpm. Cells pellet was incubated with 400µL lysis buffer containing 10mM Tris-HCl, ph 7.5 and 2 mM EDTA and 1% of protease inhibitors, for 1h in ice and vortexed every 15 minutes. Then, the lysate was passed 6 times in 26g syringes.

300µl of lysate was loaded on the top of a sucrose gradient formed by a 60% sucrose solution (500µl) and 10% sucrose solution (500µl). This solution contains 20mM Tris-HCl, ph 7.5, 0.5 mM EDTA, 100mM NaCl and the respective sucrose quantity.

Lysates were then centrifuged on a *Sorval* RC M120ex ultracentrifuge using a *RP55s-164* rotor at 16800rpm (35087g) during 30min at 4°C. Fractions were then collected and analyzed by Western Blot.

Immunofluorescence

Cells were plated at 10^5 cells/ well in a 6-well plate with 4 coverslips (12mm of diameter) per well. After 24h, cells were transfected with different vectors as previously presented. After 48h, cells were fixed in 4% paraformaldehyde, for 10 minutes. Then, cells were permeabilized with 0.5% Triton X-100, 0,3% BSA for 5minutes and blocked 1h in PBS-BSA3%. Cells were incubated for 1h45 with antibody anti Lkb1 N19 (Santa Cruz, sc-8185, lotJ1212) at 1/100 and anti GCN5L2 (C26A10) (Cell Signaling 3305S, lot4) at 1/100. Donkey anti-Rabbit Cy3 (1/1000) and anti goatAlexa488 (1/1000) secondary antibodies used were from Jackson ImmunoResearch. Cells were mounted in Moviol/Dapi.

Cell Migration, wound healing assay

Hela cells were transfected with different vectors expressing WT-Flag-LKB1 or K48R-Flag-LKB1 or K48Q-Flag-LKB1 for 48h. After that cells were re-suspended and seeded at the 1×10^4 cells/well (total volume 50 μ l/well) in both ibidis wells (ibidis Culture-Insert with 2 wells, 80201). The ibidi was used on a 12 well plate with 1 ibidi per well of 12 wells plate. The outer area was filled with 500 μ l of cell medium. The plate was incubated at 37°C and 5% CO₂. After 24h, the ibidi was gently removed with sterile tools and the well was filled with 500 μ l medium (total 1ml/well). The images were taken at 0h, 24h, 48h and 72h after wounding.

II. Project 2: LKB1 metabolic and signaling regulations during NCC commitment.

As described in Project 1, we recently uncovered that Lkb1 governs several aspects of cranial NCC development that are crucial during vertebrate head formation (Creuzet et al., 2016). In addition to this first project, I also investigated the role of Lkb1 in truncal, vagal and sacral NCC which give rise to various derivatives including melanocytes, glial and neural cells in the peripheral nerves and in the enteric nervous system (Introduction Chapter II.2).

Based on a second mouse model of *Lkb1* conditional inactivation in NCC, as well as an *in vitro* model of NCC differentiation, we identified that LKB1 signaling is essential during NCC lineage and exert crucial metabolic regulations.

1. The tumor suppressor LKB1 controls NCC fate through pyruvate-alanine transamination.

Article Nb2: Submitted, Radu, Torch *et al.*

1.1 Scientific context and results summary

To address the contribution of the Lkb1-dependent control of energy metabolism during the formation and the maintenance of NCC, our team generated another mouse model with temporal disruption of *Lkb1* later in NCC development ("late" inactivation) compared to the model used in the first project ("early" inactivation). This model consists in *Lkb1*^{Flox} mice bred with Tyr::Cre transgenic mice established by L. Larue lab (Curie Institute, Orsay) thus allowing the recombinase Cre expression under the Tyrosinase (Tyr) promoter in NCC from E10.5 i.e. after their migration to target tissues (Delmas et al., 2003).

We reported that *Lkb1* mutant mice die between 2 to 6 weeks after birth and exhibit coat depigmentation, intestinal pseudo-obstruction and a severe peripheral neuropathy. Using this mouse model, we established that LKB1 controls the development of Schwann cells in the peripheral nerves and the post-natal maintenance of ganglion cells of the enteric nervous system. Metabolomic profiling of peripheral nerves highlighted that *Lkb1* loss triggers increased alanine and glutamate levels.

To better understand the metabolic defects in the absence of Lkb1, I used a neural crest stem cells line that can be committed, *in vitro*, into the early steps of glial lineage. Using this cell line, I confirmed that Lkb1 is key for glial differentiation. Mechanistically, *Lkb1* loss led to increased alanine and glutamate levels as observed *in vivo*. Interestingly, inhibition of the alanine amino-transaminase responsible of pyruvate and glutamate conversion into alanine (transamination reaction) rescued glial differentiation of *Lkb1*-silenced NCC, in a mTOR-dependent manner. Furthermore, glutamate synthase inhibition, the enzyme which converts

glutamate into glutamine, phenocopied *Lkb1* loss as it impaired glial differentiation in a mTOR-dependent manner.

One hypothesis explaining impaired glial differentiation upon *Lkb1* loss was that NCC lineage is blocked early in glial commitment due to a lack of energy. Interestingly, AICAR (5-aminoimidazole-4-carboxamide), a known agonist of AMPK but only in the presence of LKB1, has been described with AMPK-independent functions (Guigas et al., 2007). Furthermore, AICAR is an AMP precursor (see Introduction, Chapter III.A.2.1.2) which was shown to replenish IMP/AMP pools upon glutamate synthase inhibition (Tardito et al., 2015) and to induce astroglial differentiation (Zang et al., 2008). We demonstrated *in vitro* that AICAR rescued glial differentiation of *Lkb1*-deficient NCC and *in vivo* treatment of *Lkb1*-deficient mice with AICAR prevented the peripheral nerve and ENS phenotypes (Radu et al., submitted).

Altogether, these findings highlighted the novel and crucial role of *Lkb1* during neural crest cell fate and uncovered a link between *Lkb1*-mediated pyruvate-alanine cycling and glial differentiation. These results provide new insights to understand the metabolic regulations exerted by *Lkb1* during development and tumorigenesis.

1.2 Results

LKB1 controls cell fate of the neural crest lineage through pyruvate-alanine transamination

Anca G Radu^{1§}, Sakina Torch^{1§}, Florence Fauvelle², Karin Pernet-Gallay³, Renaud Blervaque¹, Anthony Lucas¹, Véronique Delmas⁴, Uwe Schlattner⁵, Laurence Lafanechère¹, Pierre Hainaut¹, Nicolas Tricaud⁶, Véronique Pingault⁷, Nadège Bondurand⁷, Nabeel Bardeesy⁸, Lionel Larue⁴, Chantal Thibert^{1*}, Marc Billaud^{1, 9*}

1. Institute for Advanced Biosciences, INSERM U1209, CNRS UMR5309, Université Grenoble Alpes, 38000 Grenoble, France
2. Grenoble MRI Facility IRMAGE, INSERM/CEA U817 Univ Grenoble Alpes, Grenoble Neurosciences Institut Grenoble, F-38700, France; Armed Forces Biomedical Research Institute
3. INSERM U836, F-38700 Grenoble, France; Univ. Grenoble Alpes, GIN, F-38700 Grenoble, France
4. Institut Curie, Normal and Pathological Development of Melanocytes, CNRS UMR3347; INSERM U1021; Equipe Labellisée–Ligue Nationale Contre le Cancer, Orsay, France
5. Laboratory of Fundamental and Applied Bioenergetics, Univ Grenoble Alpes, 38185 Grenoble, France; Inserm, U1055, 38041 Grenoble, France
6. INSERM U1051, Institut des Neurosciences de Montpellier (INM), Université de Montpellier, Montpellier, France.
7. INSERM, U1163, Institut Imagine, France
8. Cancer Center, Massachusetts General Hospital, 185 Cambridge Street, Boston, MA 02114, USA; Center for Regenerative Medicine, Massachusetts General Hospital, 185 Cambridge Street, Boston, MA 02114, USA; Department of Medicine, Harvard Medical School, Boston, MA 02114, USA.
9. “Clinical and experimental model of lymphomagenesis” Univ Lyon, Université Claude Bernard Lyon1, INSERM 1052, CNRS 5286, Centre Léon Bérard, Centre de recherche en cancérologie de Lyon, France.

§ Contribute equally to this work

* co-senior authors and co-corresponding authors: to whom correspondence should be sent: marc.billaud@lyon.unicancer.fr, chantal.thibert@univ-grenoble-alpes.fr

Abstract

The metabolic processes underlying the setting up of the neural crest lineage, which generates an embryonic population of multipotent migratory cells, remain poorly understood. Here, we report that mice with conditional ablation of the metabolic sensor *Lkb1* in a subpopulation of neural crest stem cells exhibited hindlimb paralysis, intestinal pseudo-obstruction and coat depigmentation suggestive of human neural crest disorders. Part of the phenotype originated from an impaired differentiation of Schwann cells and from a post-natal degeneration of the enteric nervous ganglia. Metabolomics profiling revealed an accumulation of glutamate and alanine in *Lkb1*-deficient peripheral nerves and, mechanistically, inhibition of alanine transaminases or treatment with the metabolic modulator AICAR restored glial differentiation in an mTOR-dependent manner. Remarkably, administration of AICAR to *Lkb1* mutant mice prevented Schwann cell and enteric defects. These data uncover a link between pyruvate-alanine cycling and glial commitment, and further suggest that disruption of the *Lkb1* signaling contributes to the pathogenesis of neural crest diseases.

Key words: neural crest cells; LKB1/AMPK; glial lineage; pyruvate-alanine transamination.

Introduction

Neural crest cells (NCC) are highly invasive stem cells that originate from the dorsolateral folds of the neural tube and delaminate from the neuroepithelium through an epithelial-mesenchymal transition (Le Douarin and Kalcheim 1999). NCC migrate along stereotypical paths and give rise to a broad array of derivatives including most of the craniofacial skeleton, neuroendocrine tissues and pigment cells. Furthermore, the peripheral nervous system, comprising sensory neurons and Schwann cells (SC)

of the parasympathetic and sympathetic nervous systems, as well as neurons and glial cells that constitute the enteric nervous system (ENS), arise from NCC. Defects in human neural crest development are the cause of a constellation of disorders called neurocristopathies. The most common clinical phenotypes include cranio-facial abnormalities, hearing loss, absence of pigmentation, cardiac defects and enteric ganglia agenesis (Mayor and Theveneau 2013). Although the cascade of molecular events that specify neural crest territories, orchestrate NCC delamination and guide their polarized migration throughout the embryo has been extensively explored, the contribution of metabolic regulation to NCC formation and differentiation has received less attention. In this regard, morphogenesis requires adjustment of the metabolism of embryonic cells to cope with alterations in nutrient availability and tissue oxygenation specific to their microenvironment (Simon and Keith 2008). The mapping of the metabolic pathways that are activated in early stem cells has begun to shed light on the respective contribution of glycolysis versus oxidative phosphorylation in the maintenance of pluripotency and cell fate commitment (Ochocki and Simon 2013). However, the role of metabolic remodeling in later developmental stages, including the formation of neural crest derivatives, remains poorly understood.

The tumor suppressor *LKB1* (also named *STK11*) encodes a serine/threonine kinase that has been evolutionarily conserved from invertebrates to mammals (Baas et al. 2004; Hardie and Alessi 2013). Germline mutations of *LKB1* are responsible for the Peutz-Jeghers syndrome, a dominantly inherited cancer disorder and somatic mutations of this gene have been associated with various cancers including lung and cervical tumors (Shorring and Clarke 2016). The binding of *LKB1* to the pseudokinase STRAD (STRAD α or STRAD β) and the scaffolding molecule MO25 allosterically controls *LKB1* catalytic activity and promotes its nuclear export (Baas et al. 2003). *LKB1* acts as a key regulator of energy metabolism through the activation of the AMP-activated protein

kinase (AMPK), a sensor that adapts energy supply to the nutrient demands of cells facing situations of metabolic stress (Shackelford 2013). AMPK phosphorylates a large array of substrates to achieve metabolic adaptations. In particular, AMPK phosphorylates the acetyl CoA carboxylase (ACC) to inhibit fatty acid synthesis (Davies et al. 1990; Merrill et al. 1997) as well as two regulators of mammalian target of rapamycin complex 1 (mTORC1), RAPTOR and TSC2, to inhibit the mTOR pathway (Gwinn et al. 2008; Inoki et al. 2003). In addition to AMPK, *LKB1* also phosphorylates 12 AMPK-related kinases that regulate cell polarization, axon branching of cortical neurons and hepatic neoglucogenesis (Alessi et al. 2006; Hezel and Bardeesy 2008; Shackelford and Shaw 2009; Shorring and Clarke 2011).

We recently showed that *Lkb1* governs several aspects of cephalic NCC development that are crucial during vertebrate head formation (Creuzet et al. 2016). To better understand the contribution of *Lkb1* to the formation of neural crest derivatives, we disrupted this gene in a subset of vagal and truncal mouse NCC using the *tyrosinase* Cre (Tyr::Cre) transgene. We report here that *Lkb1*-deficient mice exhibit coat depigmentation as well as progressive hindlimb paralysis originating from a blockade of SC differentiation and intestinal pseudo-obstruction arising from a degeneration of the ENS. Using a neural crest cell line, we demonstrate that *Lkb1* is key to establish the glial lineage. Although *Lkb1* loss induces mitochondrial dysfunction, we show that mitochondrial respiration is dispensable for glial differentiation. Metabolomics profiling of peripheral nerves demonstrates that *Lkb1* loss leads to alanine and glutamate accumulation. By mechanistic analyses, we identify that *Lkb1* knockdown triggers a preferential transformation of pyruvate into alanine by the alanine aminotransferase (ALAT) and inhibition of this enzyme rescues glial differentiation of *Lkb1*-null NCC in an mTOR-dependent manner. AICAR, an analogue of AMP, normalizes mTOR signaling, promotes glial differentiation *in vitro* and prevents hindlimb defects and ENS degeneration *in vivo*. Altogether, our results provide evidence that *Lkb1*

signaling contributes to the setting up of several different neural crest-derived cell populations that belong to the melanocytic, enteric and Schwann cell lineages. These data also highlighted that *Lkb1* signaling controls glial lineage by repressing a non-essential amino acids biosynthetic program coupled to pyruvate-alanine transamination.

Results

***Lkb1* deletion results in a complex neural crest phenotype**

To explore *Lkb1* functions in neural crest derivative cells in vivo, *Lkb1* conditional mutant mice (*Lkb1*^{F/F}) (Bardeesy et al. 2002) were interbred to the *Tyr::Cre* deleter (Delmas et al. 2003; Puig et al. 2009) and the R26R reporter (Soriano 1999) strains (Figure S1A). The tyrosinase promoter is active from embryonic day E10.5 in subsets of NCC, thereby allowing the targeting of migrating melanoblasts (Delmas et al. 2003) as well as NCC-derived cells of the ENS (Puig et al. 2009)(Delmas et al. 2003; Puig et al. 2009)(Delmas et al. 2003) (Figure 1A). *Lkb1*^{+F};*R26RF*/*F*;*Tyr::Cre*[°] offspring females were then interbred with *Lkb1*^{+F};*R26RF*/*F* or *Lkb1*^{F/F};*R26RF*/*F* males to generate *Lkb1*^{F/F};*R26RF*/*F*;*Tyr::Cre* mutants and wild-type control littermates in a mixed genetic background mostly C57BL6/J (Figure S1B). Since the *Tyr::Cre* transgene is localized on the X-chromosome, to avoid a bias due to X chromosome inactivation, our study is solely based on the analysis of males. Heterozygous *Lkb1*^{+F};*Tyr::Cre*[°] male mice were fully healthy and fertile (data not shown). Homozygous *Lkb1*-deficient mice (*Lkb1*^{F/F};*Tyr::Cre*[°] referred here as cKO) were born at the expected Mendelian ratio (Figure S1C) but showed either an almost complete lack of coat color pigmentation or white spotting (Figure 1B and Figure S1D). Since a previous report demonstrated that *Lkb1* function is required for the proper development of melanocytes, we did not focus our study on the physiological mechanisms underlying the depigmented phenotype. Most of the cKO mice failed to thrive and died within a few weeks after birth

(Figure 1C). cKO mice exhibited a reduced weight gain (Figure 1D) and a distended abdomen (Figure S1E). Necropsy revealed an intestinal pseudo-obstruction with abnormal dilation of the small intestine and/or colon, atrophy of the cecum and at more advanced stage, a reduction of the stomach accompanied by hypertrophy of the cecum (Figure 1E). The mutant mice also displayed significantly reduced mobility due to progressive hindlimb paralysis (Figure S1F). When lifted by their tail, 21 days old (P21) cKO mice reflexively contracted their limbs, sometimes unilaterally, but more often bilaterally whereas control littermates extended their legs when challenged to the same test (Figure 1F). Gait tests were also performed by footprint analysis at P21 (Figure S1G). The stride distance was significantly reduced in cKO mice, while the sway distance was unaffected, resulting in a shorter gait in the absence of *Lkb1*. At the macroscopic level, the sciatic nerves of cKO mice appeared thinner and more translucent than in control littermates and lacked the characteristic banded pattern of myelin (Figure 1G).

Thus, conditional deletion of *Lkb1* in truncal and vagal NCC results in a complex phenotype consisting of coat depigmentation, intestinal pseudo-obstruction and a peripheral neuropathy.

***Lkb1* loss causes ENS degeneration**

To explore the mechanisms leading to the intestinal pseudo-obstruction in cKO mice, we first analyzed by immunohistochemistry the expression pattern of *Lkb1* in mouse intestine and colon. We observed that *Lkb1* is expressed in myenteric and submucosal plexuses both in the intestine and in the colon of 21 days old mice (P21; Figure 1H, left panels), and corresponds to enteric ganglia reflected by colocalization with the neural marker *Tuj1* (Figure S2A). As expected, less or no *Lkb1* was detected in the ganglia of cKO mice, although the retention of staining in a few ganglia indicated that *Lkb1* deletion is mosaic. Analysis of intestinal expression of β -galactosidase as a reporter of Cre-mediated *Lkb1* deletion revealed a staining in cells that were

identified as neural and glial enteric using antibodies recognizing the RNA-binding protein HuC/D and GFAP respectively (Figure S2B). A similar *Lkb1* expression pattern was observed in human intestine and colon specimens (Figure S2C). Altogether, these results indicate that *Lkb1* is expressed in the ENS cells of human and mouse tissues and that *Lkb1* inactivation in our mouse model occurred in neural and glial enteric cells.

To determine whether the ENS was affected in cKO mice, we used several complementary approaches. First, we studied by whole-mount staining the development of enteric neurons using the neural marker Tuj1 at embryonic day 15.5 (E15.5, not shown) and at birth (P0; Figure 1I). Four different areas of the digestive tract were analyzed: proximal and distal intestine and proximal and distal colon (PI, DI, PC and DC, respectively). No overt sign of alteration of the ENS network was observed at E15.5 or P0 suggesting that *Lkb1* inactivation starting from E10.5, when Cre is produced by enteric NCC precursors, neither altered NCC migration nor their differentiation into neurons. Second, we used AcetylCholine Esterase (AChE) activity in whole-mount to visualize the ENS at P21. In wild-type intestine and colon, ganglia developed correctly and the neuronal network that connects the nervous plexuses was clearly visible (Figure 1J). In contrast, in *Lkb1*-deficient mice the staining was either strongly reduced or undetectable in several regions of the intestine. The affected areas were variable in length and involved either the proximal or distal parts of the intestine or colon, with the distal regions being most commonly affected. Hematoxylin-eosin staining indicated that the *tunica muscularis* and enterocyte epithelium had normal morphology. However, we frequently observed damaged intestinal villi in the distal intestine, probably due to fecal accumulation in the digestive tract (Figure S2D). Taking advantage of the R26R allele, we visualized β -galactosidase expression as a reporter of Cre expression on whole-mount intestine of P21 animals (Figure S2E). In these conditions, the enteric network was stained in wild-

type animals whereas the ENS of cKO animals showed a drastic decrease of labeling.

The results were corroborated by neural (Tuj1) and glial (GFAP) staining on intestine and colon sections of P21 mice, which revealed that *Lkb1*-deficiency resulted in a strong reduction of both neural and glial cells labeled by Tuj1 and GFAP respectively along the intestine and colon (Figure 1K). The individual analysis of cKO mice showed that all mutants had at least one area of the digestive tract with hypoganglionosis. The most frequently hypoganglionic area was the distal intestine while the proximal colon did not appear to be affected (Figure S2F). To quantify these anomalies, we counted the number of enteric neurons per length of tunica muscularis (Figure 1L). In cKO animals, the number of Tuj1-positive neurons was 2-fold lower in the distal intestine and 1.6-fold lower in the distal colon as compared to WT controls. Thus, the lack of *Lkb1* leads to an ENS hypoganglionosis.

We next sought to evaluate if the defects observed at P21 were also present at earlier stages. As shown in Figure S2G (left panels), *Lkb1* loss was observed in 6 days old cKO animals (P6). At this time point, compared to WT mice, cKO animals exhibited clearly diminished numbers of Tuj1 and GFAP-positive ganglia in the distal intestine and colon and reduced staining of the remaining ganglia that were smaller in size and displayed punctiform morphology (Figure S2G right panels). These results indicated that *Lkb1* deficiency is associated with a progressive postnatal degeneration.

To determine whether the progressive loss of enteric neurons observed in *Lkb1*-deficient mice after birth at P6 and P21 was due to an increase in neuronal death, we used TUNEL assays and cleaved caspase-3 immunostaining. No apoptosis was detected in enteric ganglia of cKO animals at all stages analyzed (Figure S2H and not shown).

By immunohistochemistry we observed that phospho-AMPK staining was specifically decreased in the remaining enteric ganglia of cKO mice compared to control littermates, whereas no changes were seen in smooth muscle cell layers or enterocytes (Figure S2I). Consistently,

phosphorylation of the S6 ribosomal protein (S6RP), a substrate of the p70S6 kinase acting downstream of mTORC1, was enhanced in the enteric ganglia of intestine and colon regions of cKO mice (Figure 1M). Collectively, our results provide evidence that Lkb1 function is key for the postnatal maintenance of the ENS.

The peripheral neuropathy arises from a blockade of Schwann cell differentiation

To explore the role of Lkb1 in peripheral nerves, we first analyzed Lkb1 expression by immunofluorescence on longitudinal sections of sciatic nerves at P6 and P21. We observed a relatively homogeneous staining in wild-type animals (Figure 2A). Lkb1 staining was confirmed by immunohistochemistry using a second antibody specific for Lkb1 (Nakada et al. 2013) (Figure S3A). In cKO mice, Lkb1 staining was clearly reduced on sections of sciatic nerves (Figures 2A and S3A). However, the loss of *Lkb1* was not homogeneous as *Lkb1* expression was still detected in some areas. To confirm *Lkb1* loss of function, we evaluated the phosphorylation status of the LKB1 substrate AMPK. By immunohistochemistry on longitudinal sections of sciatic nerves we observed that AMPK phosphorylation at the LKB1 target residue, AMPK α ^{Thr172}, was markedly decreased in absence of *Lkb1* (Figure S3B). Consistent with our previous observations in the enteric nervous system, phospho-S6RP labeling was enhanced in the sciatic nerves (Figure 2B). These data confirm that inactivation of *Lkb1* in sciatic nerves results in the dysregulation of AMPK-mTORC1 signaling.

Although expression of the Cre recombinase driven by the tyrosinase promoter has been previously observed in peripheral nerves (Delmas et al. 2003), its precise pattern of expression was unknown. Thus, in order to discriminate whether Lkb1 was inactivated in peripheral sensory axons, in SC or in both cell types, we first exploited reporter Tyr::Cre;Z/EG mice which allow labeling of neural crest-derived cells expressing the Cre recombinase with enhanced green fluorescent protein (EGFP) (Colombo et al.

2010). Immunofluorescence on embryonic sections allowed the detection of glial cells, labeled with an antibody recognizing the intermediate filament protein GFAP that were also positives for EGFP (Figure S3C) whereas neuron-specific β -tubulin staining recognized by the Tuj1 antibody was never co-localized with EGFP (Figure S3D). We also took advantage of the presence of the R26R reporter in the Tyr::Cre;Lkb1 mice to stain semi-thin sections of sciatic nerves from wild-type animals with X-Gal. These studies revealed cytoplasmic staining in SC but not in the axons (Figure S3E). Finally, we analyzed sections of the dorsal root ganglia, which contain neuronal cell bodies and glial cells with Salmon Gal, another substrate of the β -galactosidase allowing a more sensitive detection of the enzymatic activity. We detected a sustained β -galactosidase activity in the dorsal root ganglia of either WT or cKO animals (Figure S3F). Immunofluorescence analyses of β -galactosidase expression in dorsal root ganglia revealed a clear co-localization with glial GFAP-positive cells but not with neuronal Tuj1-positive cells (Figure S3G). Altogether, these results indicate that *Lkb1* inactivation was restricted to SC and did not occur in sensory neurons. We next examined the ultrastructure of sciatic nerves at P21 by transmission electron microscopy. The sciatic nerves of control animals were composed of myelinated sensory and motor axons of medium to large diameters as well as clusters of small-diameter unmyelinated sensory axons shown on Figures 2Ca-c. The number of myelinated axons in cKO animals was reduced and degeneration of axons and myelinating SC was observed (Figures S3H and 2Cd,e respectively). Large clusters of unsorted axons were also identified (Figures 2Cf and S3H). Non-myelinating SC of cKO mice did not enwrap axons individually as in wild-type animals (Figures 2Cc,f) but wrapped axons in bulk. Several axons achieved an appropriate 1:1 relationship with SC but others showed aberrant sorting or remained unsorted (Figure 2Cg,h). To quantify axon myelination defects in cKO animals, we measured the g-ratio: the ratio of the axonal diameter to the myelinated fiber diameter. We found an increased g-ratio in mutant mice (Figure

2Ci) indicating hypomyelination of axons in cKO animals. Altogether, these results indicated that *Lkb1* is involved in the sorting of axons by Schwann cells, the myelination process and the maintenance of myelinated axons.

As axon sorting and SC myelination in the mouse begins shortly after birth, we assessed neural and glial cell differentiation in the sciatic nerves of cKO mice at P6 and P21. Tuj1 neuron-specific staining was strongly reduced in cKO animals compared to wild-type at both ages (Figures 2D, left panels and S3I). By contrast, the staining of SC visualized with the GFAP antibody was not reduced at P6 and P21, although the subcellular localization of GFAP was disrupted at P21 (Figures 2D, right panels, insets and S3J), thus suggesting that SC polarity was disrupted. Next, we examined the distribution of E-cadherin, a cell adhesion protein concentrated in subdomains corresponding to Schmidt-Lanterman incisures and paranodal loops adjacent to nodes of Ranvier in myelinating Schwann cells (Tricaud et al. 2005). In dissociated nerve fibers of cKO animals, E-cadherin staining was diffuse and the typical localization of E-cadherin was lost suggesting that SC polarity is disorganized in absence of *Lkb1* (Figure 2E), an observation consistent with a recent report (Shen et al., 2014).

While studying transverse and longitudinal sections of cKO sciatic nerves, we observed an increased number of Schwann nuclei at P6 and at P21 (Figure S3K). To assess the nature of these supernumerary cells, we labeled immature/promyelinating SC with Sox2 immunostaining (Bremer et al. 2011) and observed that cKO mice exhibited a marked increase in Sox2 staining at P6 compared to WT, and this was also evident to a lower extent at P21 (Figure 2F). We confirmed these data using an antibody that recognizes Krox20, a transcription factor that is a pivotal regulator of SC myelination, to visualize myelinating SC differentiation (Figure S3L). At P6 no Krox20 nuclei were detected in cKO animals, thus suggesting a delay in myelinating SC differentiation in the absence of *Lkb1*.

Altogether, these results suggest that in the absence of *Lkb1*, SC failed to differentiate, thus resulting in the accumulation of SC precursors localized in the nerve.

***Lkb1* controls glial fate specification**

To examine the consequences of *Lkb1* inactivation on NCC fate, at the early steps of glial commitment of the Schwann cell lineage, we utilized the JoMa1.3 mouse neural crest stem cell line, which can either be maintained in a progenitor state or differentiated into glial cells among other NCC derivatives (Figure 3A) (Maurer et al., 2007). Cells are kept in the progenitor state through the inducible expression of the c-myc^{ER} oncogene which exerts its transcription factor activity upon treatment of cells with 4-OHT (Figure S4A). In glial differentiation medium (without 4-OHT and supplemented with Heregulin and Forskolin), JoMa1.3 cells underwent morphological changes, acquiring a spindle shape (Figures S4B and S4C). The induction of glial differentiation was confirmed by positive staining for the glial markers GFAP and S100, and loss of expression of the progenitor marker p75^{NTR} (Figure 3B and S4D). We then established and validated a protocol to efficiently down-regulate *Lkb1* expression by transfecting *Lkb1* siRNA either in progenitor cells or during NCC-derived glial differentiation. siRNA-mediated knockdown of *Lkb1* triggered a reduction of AMPK phosphorylation and an activation of the mTOR pathway in JoMa1.3 cells (Figures S4E-H) as observed *in vivo*. *Lkb1* knockdown strongly impacted cell morphology during glial differentiation as visualized with the formation of stress actin fibers labeled with phalloidin (Figure S4I). Accordingly, glial differentiation was impaired as assessed by the reduced expression of glial specific markers S100 or GFAP (Figure 3C). RT-qPCR revealed that *Lkb1* knockdown resulted in an increase of p75^{NTR} expression and a loss of *GFAP*, further confirming that cells were maintained as progenitors and showed impaired glial differentiation (Figure 3D; data not shown).

***Lkb1* ablation impairs mitochondrial activity**

Owing to the crucial role of *Lkb1* and AMPK in controlling mitochondrial activity (Beirowski et al. 2014; Gurumurthy et al. 2010; Nakada et al. 2013; Pooya et al. 2014; Toyama et al. 2016), we tested whether glial differentiation blockade upon *Lkb1* inactivation was associated with mitochondrial defects. Using Mitotracker, a vital stain that accumulates in active mitochondria, and flow cytometry analyses we observed a significant increase of the mitochondrial mass upon *Lkb1* knockdown in JoMa1.3 cells (Figure 3E). Mitotracker analyses by confocal microscopy revealed a marked reorganization of the mitochondria network that acquired a large circular morphology upon *Lkb1* silencing (Figure 3F). Cellular distribution of mitochondria in isolated sciatic nerve fibers is altered and appeared more dispersed in myelinated fibers of cKO mice compared to WT littermates (Figure 3G). Electron microscopy showed dilated mitochondrial cristae in the absence of *Lkb1* (Figure 3H). Next, we assessed the respiratory capacities of *Lkb1*-deficient glial JoMa1.3 cells with the Seahorse metabolic analyzer and found a significant diminution of oxygen consumption during basal, maximal and spare respiration. In addition, ATP production was significantly reduced (Figures 3I and S4J). Taken together, these results confirm that *Lkb1* regulates the distribution and the activity of mitochondria during glial differentiation (Beirowski et al. 2014; Pooya et al. 2014).

Several reports have shown that *Lkb1* and AMPK inactivation trigger a metabolic shift towards aerobic glycolysis (Faubert et al. 2014; Kishton et al. 2016; Kottakis et al. 2016; Shackelford 2013). Thus, our data demonstrated that *Lkb1* has critical functions in the control of energy metabolism during glial differentiation, acting in particular to maintain mitochondria structure and activity.

Rewiring of metabolism in *Lkb1*-deficient nerves

The mitochondrial effect of *Lkb1* ablation in our systems prompted us to characterize the metabolome of sciatic nerves. For that purpose, we performed high-resolution magic angle spinning

(HRMAS) proton NMR spectroscopy on sciatic nerves, a technique that does not require prior solubilization of the samples. With the original application of this technique to structurally preserved nerves, we were able to record variations in both polar metabolite and lipid levels in *Lkb1* cKO sciatic nerves compared to WT (Figure 4A). The broad resonances (L) arise from lipids and macromolecules, mainly methyl (L1) and methylene groups (L2 to L6) along fatty acids chains while sharp peaks arise from small molecules, i.e. metabolites (Figures 4A and B). We could detect and assign 17 metabolites (Figure 4C), and the main spectral contributions were due to total creatine (8), phospholipid intermediates (9, 10, 11, 12), taurine (14) and myo-inositol (15). Peaks corresponding to aliphatic chains of lipids and macromolecules were all down-regulated (Figure 4D). The multivariate statistical model showed a very good separation between the two mouse genotypes (Figure 4E), mainly due to downregulation of all acyl chain groups (L4 to L6). These analyses also showed that the most discriminant changes in metabolite levels between WT and cKO groups concerned β -D-glucose (17), glutamate (6) and alanine (2) (Figure 4C). Quantification of these metabolites confirmed the statistically significant decrease of β -D-glucose and increase of glutamate and alanine levels in sciatic nerves of cKO animals (Figure 4F). Altogether, these results indicate that *Lkb1* loss rewires sciatic nerves metabolism (Figure 4G).

Pyruvate-alanine transamination dictates glial differentiation.

To further characterize how *Lkb1* loss triggers alanine and glutamate deregulation, we took advantage of the *in vitro* JoMa1.3 NCC model. We first evaluated alanine levels in JoMa1.3 cells committed to glial differentiation upon *Lkb1* knockdown. As observed on sciatic nerves, alanine concentration was increased in the absence of *Lkb1* (Figure 5A). In addition, we confirmed the accumulation of alanine in *Lkb1*-null Mouse Embryonic Fibroblasts (Figure S5A). Conversely,

alanine was not increased in JoMa1.3 progenitor cells upon *Lkb1* knockdown (Figure S5B).

Our results support a mechanistic link between *Lkb1* function and pyruvate-alanine transamination via the alanine transferase (ALAT, Figure 5B upper panel), either cytoplasmic (ALAT1) or mitochondrial (ALAT2). We thus blocked ALAT enzymatic activity using the inhibitor Chloro-alanine (Figure 5B lower panel) (Beuster et al. 2011) and observed normalized alanine levels upon *Lkb1* knockdown, demonstrating that the Chloro-alanine is indeed an inhibitor of ALAT in glial JoMa1.3 cells (Figure S5C). We also measured lactate levels and observed that *Lkb1* knockdown resulted in a decrease of lactate concentration whereas Chloro-alanine treatment led to an increase of lactate level (Figure S5D). These data indicate that *Lkb1* knockdown results in an enhanced conversion of the pyruvate into alanine instead of lactate. To further test if the preferential transformation of pyruvate into alanine could also be associated with deregulation in glycolysis *per se*, we measured the medium acidification resulting from lactate and proton production via glycolysis using the Seahorse analyzer in the presence or not of Chloro-alanine. We first observed that basal glycolysis and glycolytic capacity, based on extracellular acidification rate (ECAR) measurement, were slightly reduced while the glycolytic reserve was diminished in the absence of *Lkb1* (Figure S5E). However, upon ALAT inhibition with Chloro-alanine treatment, the extracellular pH of cells with or without *Lkb1* was similar, thus demonstrating that glycolysis was not affected (Figure 5C). These data strongly support the hypothesis that the pyruvate is preferentially transformed into alanine upon *Lkb1* knockdown independently of glycolytic rate.

Metabolomic profiling of sciatic nerves also identified an increase of glutamate level. Glutamate is required for the transamination of pyruvate (see Figures 4G and 5B). We thus determined glutamate levels in JoMa1.3 cells in conditions of glial differentiation. *Lkb1* knockdown during glial differentiation led to glutamate accumulation but only when ALAT is

inhibited, most probably because glutamate is readily transformed into alanine by ALAT (Figure 5D).

Analyses of the expression of a set of genes coding for metabolic enzymes during glial differentiation revealed that progenitor cells exhibited an increased expression of the genes coding for the Lactate Dehydrogenase A (*LDHA*) and the Pyruvate Kinase M2 (*PKM2*) whereas glial cells had enriched expression of the Lactate Dehydrogenase B (Figure S5F). *LDHA* and *PKM2* are often associated with cell proliferation (Wang et al., 2014) and their enriched expression in progenitor cells therefore fits with the neural crest stem phenotype of JoMa1.3 cells. However, *Lkb1* knockdown did not drastically change the expression levels of these metabolic genes (Figure S5G). With a low threshold (over -0.5 or 0.5), we nevertheless observed that *GPT2* expression, which encodes the mitochondrial form of ALAT, was enriched in glial cells upon *Lkb1* knockdown, thereby suggesting that alanine accumulation observed in the absence of *Lkb1* could result, at least partly, from an elevated expression of *GPT2*. We also assessed by RT-qPCR the expression of *GLUL*, which encodes Glutamine Synthetase (GS), and observed that *GLUL* expression was high in progenitor cells (Figure S5F). Of note, JoMa1.3 progenitor cells are maintained in a proliferative status by inducible *c-Myc^{ER}* expression and *c-Myc* is known to trans-activate the expression of *GLUL* (Tardito et al. 2015). Thus, progenitor cells artificially express high levels of GS compared to glial cells as confirmed by western blotting (Figure S5H). Western blot analyses confirmed that the level of GS protein is not affected by the absence of *Lkb1* in glial cells (Figure S5I), thereby indicating that GS regulation did not occur neither at transcriptional nor at translational levels.

To examine the impact of alanine and glutamate levels during differentiation of NCC-derived glial cells, we used the ALAT inhibitor Chloro-alanine, since we found that this compound normalized alanine and glutamate concentrations. In these conditions, Chloro-alanine treatment of *Lkb1*-knockdown cells led to a drastic reduction of actin stress fibers formation (Figure 5E). Furthermore, incubation with

the ALAT inhibitor rescued expression of the glial marker S100 (Figure 5F).

We next evaluated the mitochondrial respiration under Chloro-alanine treatment and observed that the impaired oxygen consumption due to *Lkb1* silencing was not prevented (Figures 5G). Conversely, we observed a significant decrease of mTOR activation (Figure 5H), suggesting that this kinase acts downstream of the signaling pathway involving *Lkb1* and pyruvate-alanine cycling.

Normalizing NEAA levels or mTOR activity rescues glial differentiation

As glutamate conversion into glutamine is known to be essential during glial differentiation (Saitoh and Araki 2010), we reasoned that GS inhibition should phenocopy *Lkb1* silencing in JoMa1.3 differentiation in glial cells. These cells were treated with Methionine Sulfoximine (MSO; Figure 6A), a specific non-reversible inhibitor of GS (Ghoddoussi et al. 2010). MSO treatment triggered glutamate (Figure 6B) as well as alanine (Figure 6C) accumulation in a dose dependent manner. Moreover, incubation of JoMa1.3 cells cultivated in glial differentiation conditions with MSO induced stress fibers formation in a dose dependent manner (Figure 6D) and impaired S100 expression in NCC-derived glial cells (Figure 6E).

We also observed that GS inhibition by MSO led to mTOR activation (Figure 6F). Interestingly, although MSO treatment promoted a reorganization of the mitochondrial network that was similar to the one observed upon *Lkb1* knockdown (Figure S5J), the mitochondrial respiration was not decreased but rather increased (Figure S5K). Furthermore, glycolysis was not affected by MSO treatment (Figure S5L). These results therefore establish that GS inhibition blocked glial differentiation and phenocopied *Lkb1* silencing.

Interestingly, it has been reported that treatment of cells with AICAR (5-aminoimidazole-4-carboxamide ribonucleotide), the purine precursor for inosine monophosphate (IMP), favored astroglial differentiation (Zang et al. 2008) while AICAR was depleted in glioblastoma cells following GS inhibition

(Tardito et al. 2015). AICAR is phosphorylated by adenosine kinase inside the cells and is converted to purine nucleotides, among them ZMP and AMP, two allosteric activators of AMPK (Rattan et al. 2005). Although AICAR has been described as an AMPK agonist in the presence of *Lkb1*, there is increasing evidence that this molecule exerts AMPK-independent metabolic effects (Liu et al. 2014; Vincent et al. 2015). Given that GS inhibition phenocopies *Lkb1* inactivation, it prompted us to test whether AICAR rescued glial differentiation upon *Lkb1* knockdown. AICAR treatment decreased actin stress fibers formation (Figure S6A) and rescued S100 expression (Figure 6G). Similarly, this compound reduced stress fiber formation (Figure S6B) and rescued S100 expression of MSO-treated cells (Figure 6H). Interestingly, glutamate levels were decreased after AICAR addition to *Lkb1*-silenced cells (Figure S6C) or MSO-treated cells (Figure S6D) whereas AICAR had no effect on alanine levels (Figure S6E). AICAR treatment affected neither mitochondrial respiration (Figure S6F) nor glycolysis (Figure S6G) but significantly diminished mTOR activation without restoring AMPK phosphorylation (Figure 6I). These findings indicate that AICAR compensated for *Lkb1* loss by acting downstream of GS and upstream of mTOR.

Our data hinted at a mechanistic link between the sensing of alanine-glutamate levels and mTOR activity. To address this question, we treated *Lkb1* knockdown JoMa1.3 cells with the mTOR inhibitor Torin1. We first showed that Torin1 normalized mTOR activation in JoMa1.3 cells silenced for *Lkb1* (Figure S6H). Then, immunofluorescence staining with the glial marker S100 revealed that Torin1 treatment rescued glial differentiation of *Lkb1* knockdown cells (Figure 6J). Altogether, these data provide evidence that *Lkb1* controls glial cell differentiation through the regulation of alanine and glutamate levels upstream of the mTOR pathway.

AICAR treatment prevents peripheral nerves and ENS defects.

We next explored the *in vivo* effects of AICAR on *Lkb1* cKO mice. *Lkb1*-deficient mice were treated by

intraperitoneal injections of AICAR (0.5 mg/g of body weight) every two days from P10 to P21. We first observed that weight loss of cKO animals was reduced upon AICAR treatment (Figure 7A). Furthermore, at P21, mutant mice treated with AICAR displayed increased mobility and ameliorated leg reflex extension when lifted by their tail compared to mutant mice treated with vehicle (Figure 7B). In addition, P21 mutant mice treated with AICAR showed less intestinal dilation (Figure 7C). Inhibition of the mTOR signaling was restored upon AICAR treatment both in sciatic nerves (Figure 7D) and in the enteric nervous system (Figure 7E). We did not detect any undesirable side effects induced by AICAR on both wild-type and cKO animals. Strikingly, neuronal and glial enteric cells were maintained in mutant mice with AICAR (Figure 7F). These results show that AICAR treatment prevented, at least partly, expression of the neurocristopathy phenotype of cKO mice.

Discussion

Multipotent NCC face a limiting supply of oxygen and nutrients during both their journey through the embryonic landscape and the distant colonization of anatomical structures. The metabolic adaptation of NCC to these microenvironmental conditions is thought to constrain their migration as well as their proliferation, differentiation and survival once they reach their final destination. In agreement with this notion, we show here that *Lkb1* is essential for NCC fate commitment and controls a metabolic program in NCC that is key for glial differentiation and survival of ganglion cells of the ENS.

Our work reveals that the NCC-specific ablation of *Lkb1* results in a progressive peripheral neuropathy stemming from an impaired differentiation of SC. These results are consistent with recent studies demonstrating the role of *Lkb1* in SC-axon maintenance and myelination (Beirowski et al. 2014; Pooya et al. 2014; Shen et al. 2014). Through the combination of *in vivo*, metabolomic and pharmacological approaches, we find that *Lkb1* deletion leads to an intracellular accumulation of

glutamate and alanine. Inhibition of pyruvate-alanine transamination restores glial differentiation of *Lkb1*-deficient NCC. Consistently, increase of the glutamate level through inhibition of GS led to an accumulation of pyruvate-alanine transamination, thereby blocking glial differentiation and phenocopying *Lkb1* inactivation. It has been recently reported that rapidly proliferating mammary epithelial cells utilize transaminases to link NEAA synthesis to the production of α -ketoglutarate and tricarboxylic acid anaplerosis (Coloff et al. 2016). Conversely, activation of glutamate dehydrogenase that decouples carbon and nitrogen utilization promotes cell quiescence (Coloff et al. 2016). These findings fit with our observation since the unrestrained activation of the pyruvate-alanine cycling is incompatible with the transition of *Lkb1*-deficient NCC to quiescence and subsequent glial differentiation. Interestingly, *Lkb1* loss has also been associated with an increased expression of phosphoserine amino transferase, an enzyme participating to the serine-glycine one carbon network whose aberrant activation supports the malignant transformation of *Lkb1*-mutant pancreatic cells (Kottakis et al. 2016). These data point to *Lkb1* acting as a key component of a metabolic checkpoint that controls a switch between cell proliferation and differentiation through transaminases-dependent NEAA synthesis. They also suggest that the *Lkb1* pathway may act in the glutamate-glutamine cycle that participates directly in the glial-neuron metabolic dialogue.

The mitochondria topology is altered in cKO myelinated fibers and although mitochondrial mass is increased, both respiration and ATP production are severely reduced in *Lkb1*-deficient Joma1.3 cells. Surprisingly, the restoration of glial differentiation via ALAT inhibition is independent of the rescue of mitochondrial metabolic defects. However, myelination and axon sorting could not be studied with the Joma1.3 model, and an active mitochondrial oxidative metabolism is probably needed for the final step of NCC differentiation into mature myelinating SC ((Pooya et al. 2014). We also report that mTORC1 hyperactivation is connected to the

elevated level of alanine and downregulation of mTOR restored glial differentiation of *Lkb1*-deficient NCC. In accordance with our data, mTORC1 is known to drive the early steps of SC differentiation, and an adequate dosage of mTOR activity is required for the peripheral nervous system myelination (Norrmén et al. 2014; Preitschopf et al. 2014; Sherman et al. 2012; Beirowski et al. 2017). Although leucine and arginine are major activators of mTORC1 (Meijer et al. 2015), additional amino acids are suspected to be involved in this process (Bar-Peled and Sabatini 2014; Hara et al. 1998), and it will be relevant to investigate how alanine sensing is tied to the mTOR signaling machinery. We further find that treatment of *Lkb1*-silenced NCC with the cell-permeable nucleoside AICAR normalizes mTOR signaling without restoring AMPK phosphorylation and promotes glial differentiation. This result is unexpected since AICAR is known to exert most of its biological effects through AMPK, although it has become progressively evident that this metabolite has additional cellular targets (Daignan-Fornier and Pinson 2012). The rescue of hindlimb paralysis and of ENS degeneration obtained with AICAR indicates that this compound or molecules upregulating its intracellular level (Asby et al. 2015) may represent a viable therapeutic intervention to target the metabolic defects induced by *LKB1* inactivation.

Our work unveils a critical function of *Lkb1* in the post-natal maintenance of myenteric and submucous plexi. If our data clearly establish a role for *Lkb1* in cell survival of the ENS, we cannot exclude that *Lkb1* activity is required at earlier stage of vagal NCC migration, since NCC invade the rostral foregut at E8.5-E9 and the tyrosinase promoter is turned on at E10.5. TUNEL assays and immunostaining of active caspase 3 do not show an increase of apoptosis in the ENS of cKO mice. A similar unconventional death of postmigratory enteric neurons has been described in mice with a conditional ablation of each subunit of the GDNF receptor, *GFR α 1* and *RET* (Uesaka et al. 2007, 2008). Interestingly, SC precursors (SCP) that display NCC stem-like properties and depend on GDNF signalling populate the gut through extrinsic

nerves to contribute to the post-natal integrity of the ENS (Green et al. 2017; Uesaka et al. 2015). It is thus plausible that the post-natal degeneration of the ENS occurring in cKO mice reflects an attrition of this pool of cells. Since SCP give rise to melanocytes (Adameyko et al. 2009), the coat depigmentation observed in *Lkb1* cKO mice may also result from the compromised competence of SCP to generate pigmented cells.

Collectively, this study and our precedent report (Creuzet et al., 2016) identify the *LKB1* pathway as a central orchestrator of neural crest development and highlight the pivotal role of energy metabolism in the formation of NCC derivatives. These results should also extend our understanding of the metabolic etiology of human neurocristopathies.

Methods

Animals and genotyping

Floxed *Lkb1* mice were obtained from RA. DePinho (Boston, USA) and R26R mice were provided by P. Soriano (New York, USA). Characterizations of *Lkb1* Floxed (Bardeesy et al. 2002), *Tyr::Cre* (Delmas et al. 2003; Puig et al. 2009) and *R26R* (Soriano 1999) mice have been reported previously. Since *Tyr::Cre* transgene is located on the chromosome X, the study was restricted to male animals. Heterozygous (*Lkb1*^{+/-}) and homozygous (*Lkb1*^{F/F}) males were crossed with *Lkb1*^{+/-} *Tyr::Cre*^o females to generate *Lkb1* homozygous conditional knockout in neural crest-derived tissues (referred to as cKO in the text) and wild-type littermate animals (WT: *Lkb1*^{+/-}, *Lkb1*^{F/F} and *Lkb1*^{+/-}; *Tyr::Cre* male mice). Embryos and mice were genotyped by multiplex PCR using DNA extracted from tails with primers indicated in Table 3 and PCR conditions in original references cited previously. For timed pregnancies, mice were bred and the time of plug identification was counted as day 0.5. Mice were maintained under standard housing conditions at the animal facility PHTA of Grenoble, and maintained on a mixed genetic background. *Tyr::Cre*^o; *Z/EG*^o mice were described previously (Colombo et al. 2010; Novak et al. 2000). All animal experimental procedures were conducted according to the standard operating procedures of the lab

animal facility and were approved by the Animal Ethics Committee of Grenoble (Permit number 261_IAB-U823-CT-01).

Human samples

Normal Human intestine and colon tissue samples were obtained from biopsies of patients with peritoneal intestinal carcinosis. All samples collected were taken at distance from the bulk of the tumor, stored and used with the informed consent from the patients.

Neural crest cell culture conditions, siRNA transfection, metabolic drug treatments

Mouse immortalized neural crest cells (JoMa1.3) were cultured as described previously (Maurer et al. 2007). Differentiation of these cells into glial cells was achieved by adding Heregulin (50 ng/mL; Peprotech, 120-02) and Forskolin 5 μ M (Sigma) to the JoMa1.3 culture medium during 6 days.

Short interfering RNAs (siRNA) against the mouse *Lkb1* gene and the Non-targeting control siRNA were purchased from Dharmacon (ON-TARGET plus mouse Stk11 SMART pool and ON-TARGET plus Non-targeting Pool, Dharmacon). siRNAs were transfected (11 nM) into JoMa1.3 cells by using JetPrime (Ozyme) according the manufacturer's protocol. For non-differentiated JoMa1.3, experiments were realized 72h post-transfection. For differentiated JoMa1.3, two cycles of 96h of *Lkb1* knockdown were realized, as described in Figure S4E.

During the 6 days of cell differentiation and the second cycle of *Lkb1* inactivation, cells were preincubated, or not, at 37°C in NCC medium every two days from D4 to D9 with different metabolic inhibitors: 100 μ M β -Chloro-L-alanine (Chloro-ala, ALAT inhibitor, Sigma), 2 mM MSO (Glutamine Synthetase irreversible inhibitor) and 50 μ M AICAR (a metabolic regulator and AMPK agonist).

Electron microscopy

For electron microscopy, mice were anesthetized with Ketamine/Xylazine, perfused with 2% paraformaldehyde and 0.2% glutaraldehyde in phosphate buffer saline (0.1M, pH7.4) and dissected sciatic nerves were fixed with 2% paraformaldehyde

and 2.5% glutaraldehyde in phosphate buffer saline (0.1M, pH7.4) for 1h at room temperature, post fixed in 1% osmium tetroxide in cacodylate buffer (0.1M, pH7.2) for 1h at 4°C. After washing, tissues were stained in 0.5% uranyl acetate (pH4) for 1h at 4°C, then dehydrated through graded alcohols and embedded in Epon. Semi-thin sections (500 nm) were stained with toluidine blue before being observed with an optical microscope. Ultrathin sections (50 nm) were analyzed with a transmission electron microscope (JEOL 1200EX; Grenoble-Institute of Neurosciences, France) at 80 kV and images were acquired using a digital camera (Veleta, Olympus). Morphometric measurements were done with item software (Sof Imaging System, Olympus). The same protocol was applied for electron microscopy on JoMa1.3 cells.

Teased fibers preparation and staining

Sciatic nerves were isolated from wild-type or cKO mice, teased on glass-slides, fixed for 30 minutes in 4% paraformaldehyde and subsequently washed in PBS (Tricaud et al. 2005). After teasing, the nerves were dried overnight at room temperature and stored at -20°C. For E-cadherin immunostaining, the teased fibers were permeabilized in cold acetone for 10 minutes, washed with PBS, incubated 1h at room temperature in blocking solution (10% goat serum and 0.3% Triton X-100 in PBS) and then incubated with primary antibodies in blocking solution overnight at 4°C. Samples were washed in PBS and incubated for 1h at room temperature with secondary antibodies. Finally, samples were washed in PBS incubated in Hoechst to stain nuclei and mounted in Mowiol. Images were acquired using a Zeiss biphoton confocal microscope LSM510.

To label mitochondria, teased fibers were incubated with MitoTracker® Red CMX-ROS (Invitrogen) 30 minutes at 37°C (500 nM), washed in PBS, fixed 10 minutes in 4% paraformaldehyde, incubated in Hoechst 10 minutes and mounted in Mowiol. Images were acquired using a Zeiss biphoton confocal microscope LSM510.

Seahorse analyses

The extracellular acidification rate (ECAR) and O₂ consumption rate (OCR) were analyzed by using the Seahorse XF-Analyzer (Seahorse Bioscience) and 3×10⁴ cells were seeded in 96-well Seahorse plates in DMEM with 10% FCS 16 h before assay. Cells were equilibrated with DMEM lacking bicarbonate at 37°C for 1 h in a custom incubator without CO₂. OCR and ECAR were measured at baseline and following addition of reagents for indicated times. For the mitochondrial respiration, the spare respiratory capacity was calculated by subtracting the maximal respiration values by the basal respiration values. For both respiration and glycolysis, quantifications were performed by calculating for each category the mean and standard deviation from the values obtained from several independent experiments.

Biochemical dosages

Metabolites were quantified from 10⁷ JoMa1.3 cells using Alanine assay kit (Biovision, K652-100), Glutamate assay kit (Biovision, K629-100), Lactate assay kit (Biovision, K2092-100) and Citrate assay kit (Biovision, K655-100) according to the manufacturer's protocols.

AICAR treatment of mice

WT and cKO mice were treated with AICAR (0.5 mg/g bw) or vehicle by i.p. injection (100 µl/mouse) every two or three days from P10 to P21. Mice received 5 injections and were sacrificed at P21 and analyzed as described previously.

Graphical representations and Statistical analyses

All cell culture experiments were realized at least by three independent experiments and for one experiment, each condition was performed in triplicate. *In vivo* analyses were conducted with at least three animals per condition. The exact number of experiments is indicated in the figures or in the legends. Values are given as mean with standard deviation. Normality of the data was checked with the F-Test. The unpaired Student's *t*-test was used to generate p-values for selected pairwise comparisons and *p* < 0.05 was considered significant.

Nerve metabolomic profiling by HRMAS

NMR

Sciatic nerves from 16 WT mice and 13 cKO animals were rapidly dissected at p21, cleaned of surrounding fat and connective tissues and immediately frozen in liquid nitrogen. Left and right nerves of each animal were inserted in a disposable insert for HRMAS NMR spectroscopy in a -20°C cooling chamber.

Sample preparation for HRMAS NMR

7 µL of D₂O containing trimethylsilylpropionate (TSP, 1 mM) as chemical shift internal standard (0 ppm) was added to the sample in the disposable insert, which was sealed and inserted in a 80 µL zirconium rotor.

¹H HRMAS NMR acquisition

¹H-NMR spectra were acquired with a Bruker Avance III 500 spectrometer (BrukerBiospin, Wissembourg, France) (CEA-Grenoble and IRMaGE facility). Samples were spun at 4000 Hz and temperature maintained at 4°C for all experiments. 1D spectra were acquired with a Carr-Purcell-Meiboom-Gill (CPMG) pulse sequence synchronized with the spinning rate (inter-pulse delay 250 µs, total spin echo time 30 ms). The acquisition of one ¹H-NMR spectrum consisted of 512 scans lasted 32 min. Residual water signal was presaturated during the 1.5 s relaxation delay time.

Spectra pre-processing

All pre-processing steps were performed using the TOPSPIN 3.1 Bruker software (Bruker Biospin, Karlsruhe, Germany). Spectra were aligned to TSP signal at zero ppm and phase corrected. A five-order polynomial was systematically applied for baseline correction.

All spectra from 4.678 to 0.60 ppm were divided into intervals or buckets equal to 10⁻³ ppm using the AMIX software (Bruker). Each bucket was normalized to total spectrum amplitude. Since this procedure can mask minor peak variations when very intense peaks are present in the spectra, e.g. lipid peaks (fig 4A, L2 peak), we also performed bucketing on a reduced spectral region starting from 1.825 ppm (fig 4A into brackets). Resonance assignment was performed as previously described (for metabolites: Govindaraju et

al. 2000; Fauvelle et al. 2012; for lipids: Behar et al. 1994; Zietkowski et al. 2010).

Multivariate statistical Analysis

Buckets were then imported into SIMCA V13 software (UmetricsAB, Umea, Sweden) for multivariate statistical analysis. Buckets were mean centered, scaled to unit variance (i.e., weighted by 1/standard deviation for a given variable) and submitted to a principal component analysis (PCA) to ensure good homogeneity of data and possibly to exclude outliers. For this aim, data were visualized by score plots, where each point represents a NMR spectrum and thus a sample. Supervised analyzes like orthogonal partial least square discriminatory analyses (OPLS-DA) were thus performed, using the group belonging (control or exposed) as Y matrix. The number of components was determined using the cross-validation procedure that produces R²Y and Q² factors (> 0.5). Moreover, the reliability of our OPLS-DA model was assessed by a CV-ANOVA test. The results were visualized by plotting the score of individuals relative to two first components of the model. In order to highlight metabolites that are the most discriminating between controls and exposed, S-line were examined. This plot allows the visualization in a single graph, which mimics a NMR spectrum, the covariance (peak intensity) and correlation (peak color) between cKO and WT animals. Moreover, the signs of peaks in S-line give indications about the direction of change of metabolites increased (positive peaks) or decreased (negative peaks) relative to WT.

Acknowledgments

We are grateful to E. Fontaine for helpful comments about the results. We thank S. Michallet, B. Seffrin and P. Vernet from the animal facility of the Institute for Advanced Biosciences and F. Blanquet and C. Colomb from the animal facility PHTA of Grenoble. We are grateful for D. Bouvard for discussions and for giving us the R26R mice and the help of G. Chevallier with mouse breeding and genotyping. We thank V. Blanc-Marquis for her technical help. S. Michallet was very helpful with excellent technical

assistance. C. Caron helped us with human sample studies. J. Delaroche and A. Bertrand from the electron microscopy facility of the Neuroscience Institute of Grenoble performed semi-thin sections, staining and electronic microscopy experiments and analyses. We thank N. Gadot and the ANIPATH facility, University Lyon1 Laennec, for tissue sections. This work was founded by "l'Institut National du Cancer" (Programme recherche translationnelle en cancérologie) and "la Ligue régionale contre le cancer" (comité de l'Isère).

References

- Adameyko I, Lallemand F, Aquino JB, Pereira JA, Topilko P, Müller T, Fritz N, Beljajeva A, Mochii M, Liste I, et al. 2009. Schwann Cell Precursors from Nerve Innervation Are a Cellular Origin of Melanocytes in Skin. *Cell* **139**: 366–379.
- Alessi DR, Sakamoto K, Bayascas JR. 2006. LKB1-dependent signaling pathways. *Annu Rev Biochem* **75**: 137–163.
- Asby DJ, Cuda F, Beyaert M, Houghton FD, Cagampang FR, Tavassoli A. 2015. AMPK Activation via Modulation of De Novo Purine Biosynthesis with an Inhibitor of ATIC Homodimerization. *Chem Biol* **22**: 838–848.
- Baas AF, Boudeau J, Sapkota GP, Smit L, Medema R, Morrice NA, Alessi DR, Clevers HC. 2003. Activation of the tumour suppressor kinase LKB1 by the STE20-like pseudokinase STRAD. *EMBO J* **22**: 3062–3072.
- Baas AF, Kuipers J, van der Wel NN, Battle E, Koerten HK, Peters PJ, Clevers HC. 2004. Complete polarization of single intestinal epithelial cells upon activation of LKB1 by STRAD. *Cell* **116**: 457–466.
- Bardeesy N, Sinha M, Hezel AF, Signoretti S, Hathaway NA, Sharpless NE, Loda M, Carrasco DR, DePinho RA. 2002. Loss of the Lkb1 tumour suppressor provokes intestinal polyposis but resistance to transformation. *Nature* **419**: 162–167.
- Barlow A, de Graaff E, Pachnis V. 2003. Enteric nervous system progenitors are coordinately controlled by the G protein-coupled receptor EDNRB and the receptor tyrosine kinase RET. *Neuron* **40**: 905–916.
- Bar-Peled L, Sabatini DM. 2014. Regulation of mTORC1 by amino acids. *Trends Cell Biol* **24**: 400–406.
- Behar O, Ovadia H, Polakiewicz RD, Rosen H. 1994. Lipopolysaccharide induces proenkephalin gene expression in rat lymph nodes and adrenal glands. *Endocrinology* **134**: 475–481.
- Beirowski B, Babetto E, Golden JP, Chen Y-J, Yang K, Gross RW, Patti GJ, Milbrandt J. 2014. Metabolic regulator LKB1 is crucial for Schwann cell-mediated axon maintenance. *Nat Neurosci* **17**: 1351–1361.
- Beirowski B, Wong KM, Babetto E, Milbrandt J. 2017. mTORC1 promotes proliferation of immature Schwann cells and myelin growth of differentiated Schwann cells. *Proc Natl Acad Sci U S A* **114**: E4261–E4270.
- Beuster G, Zarse K, Kaleta C, Thierbach R, Kiehnopf M, Steinberg P, Schuster S, Ristow M. 2011. Inhibition of Alanine Aminotransferase in Silico

- and in Vivo Promotes Mitochondrial Metabolism to Impair Malignant Growth. *J Biol Chem* **286**: 22323–22330.
- Bremer M, Fröb F, Kichko T, Reeh P, Tamm ER, Suter U, Wegner M. 2011. Sox10 is required for Schwann-cell homeostasis and myelin maintenance in the adult peripheral nerve. *Glia* **59**: 1022–1032.
- Chalazonitis A, Tang AA, Shang Y, Pham TD, Hsieh I, Setlik W, Gershon MD, Huang EJ. 2011. Homeodomain interacting protein kinase 2 regulates postnatal development of enteric dopaminergic neurons and glia via BMP signaling. *J Neurosci Off J Soc Neurosci* **31**: 13746–13757.
- Coloff JL, Murphy JP, Braun CR, Harris IS, Shelton LM, Kami K, Gygi SP, Selfors LM, Brugge JS. 2016. Differential Glutamate Metabolism in Proliferating and Quiescent Mammary Epithelial Cells. *Cell Metab* **23**: 867–880.
- Colombo S, Kumasaka M, Lobe C, Larue L. 2010. Genomic localization of the Z/EG transgene in the mouse genome. *Genes N Y N* **2000** **48**: 96–100.
- Creuzet SE, Viallet JP, Ghawitlan M, Torch S, Thélou J, Alrajeh M, Radu AG, Bouvard D, Costagliola F, Borgne ML, et al. 2016. LKB1 signaling in cephalic neural crest cells is essential for vertebrate head development. *Dev Biol* **418**: 283–296.
- Daignan-Fornier B, Pinson B. 2012. 5-Aminoimidazole-4-carboxamide-1-beta-D-ribofuranosyl 5'-Monophosphate (AICAR), a Highly Conserved Purine Intermediate with Multiple Effects. *Metabolites* **2**: 292–302.
- Davies SP, Sim AT, Hardie DG. 1990. Location and function of three sites phosphorylated on rat acetyl-CoA carboxylase by the AMP-activated protein kinase. *Eur J Biochem* **187**: 183–190.
- Delmas V, Martinozzi S, Bourgeois Y, Holzenberger M, Larue L. 2003. Cre-mediated recombination in the skin melanocyte lineage. *Genes N Y N* **2000** **36**: 73–80.
- Enomoto H, Araki T, Jackman A, Heuckeroth RO, Snider WD, Johnson EM, Milbrandt J. 1998. GFR alpha1-deficient mice have deficits in the enteric nervous system and kidneys. *Neuron* **21**: 317–324.
- Faubert B, Vincent EE, Griss T, Samborska B, Izreig S, Svensson RU, Mamer OA, Avizonis D, Shackelford DB, Shaw RJ, et al. 2014. Loss of the tumor suppressor LKB1 promotes metabolic reprogramming of cancer cells via HIF-1α. *Proc Natl Acad Sci U S A* **111**: 2554–2559.
- Fauvel F, Carpentier P, Dorandeu F, Foquin A, Testyler G. 2012. Prediction of neuroprotective treatment efficiency using a HRMAS NMR-based statistical model of refractory status epilepticus on mouse: a metabolomic approach supported by histology. *J Proteome Res* **11**: 3782–3795.
- Ghoddoussi F, Galloway MP, Jambekar A, Bame M, Needleman R, Brusilow WSA. 2010. Methionine sulfoximine, an inhibitor of glutamine synthetase, lowers brain glutamine and glutamate in a mouse model of ALS. *J Neurol Sci* **290**: 41–47.
- Govindaraju V, Young K, Maudsley AA. 2000. Proton NMR chemical shifts and coupling constants for brain metabolites. *NMR Biomed* **13**: 129–153.
- Green SA, Uy BR, Bronner ME. 2017. Ancient evolutionary origin of vertebrate enteric neurons from trunk-derived neural crest. *Nature* **544**: 88–91.
- Gurumurthy S, Xie SZ, Alagesan B, Kim J, Yusuf RZ, Saez B, Tzatsos A, Ozsolak F, Milos P, Ferrari F, et al. 2010. The Lkb1 metabolic sensor maintains haematopoietic stem cell survival. *Nature* **468**: 659–663.
- Gwinn DM, Shackelford DB, Egan DF, Mihaylova MM, Mery A, Vasquez DS, Turk BE, Shaw RJ. 2008. AMPK phosphorylation of raptor mediates a metabolic checkpoint. *Mol Cell* **30**: 214–226.
- Hara K, Yonezawa K, Weng QP, Kozlowski MT, Belham C, Avruch J. 1998. Amino acid sufficiency and mTOR regulate p70 S6 kinase and eIF-4E BP1 through a common effector mechanism. *J Biol Chem* **273**: 14484–14494.
- Hardie DG, Alessi DR. 2013. LKB1 and AMPK and the cancer-metabolism link - ten years after. *BMC Biol* **11**: 36.
- Hezel AF, Bardeesy N. 2008. LKB1; linking cell structure and tumor suppression. *Oncogene* **27**: 6908–6919.
- Inoki K, Zhu T, Guan K-L. 2003. TSC2 mediates cellular energy response to control cell growth and survival. *Cell* **115**: 577–590.
- Kishton RJ, Barnes CE, Nichols AG, Cohen S, Gerriets VA, Siska PJ, Macintyre AN, Goraksha-Hicks P, de Cubas AA, Liu T, et al. 2016. AMPK Is Essential to Balance Glycolysis and Mitochondrial Metabolism to Control T-ALL Cell Stress and Survival. *Cell Metab* **23**: 649–662.
- Kottakis F, Nicolay BN, Roumane A, Karnik R, Gu H, Nagle JM, Boukhali M, Hayward MC, Li YY, Chen T, et al. 2016. LKB1 loss links serine metabolism to DNA methylation and tumorigenesis. *Nature* **539**: 390–395.
- Le Douarin N, Kalcheim C. 1999. *The neural crest*. 2nd ed. Cambridge University Press, Cambridge, UK; New York, NY, USA.
- Liu X, Chhipa RR, Pooya S, Wortman M, Yachyshin S, Chow LML, Kumar A, Zhou X, Sun Y, Quinn B, et al. 2014. Discrete mechanisms of mTOR and cell cycle regulation by AMPK agonists independent of AMPK. *Proc Natl Acad Sci U S A* **111**: E435–444.
- Maurer J, Fuchs S, Jäger R, Kurz B, Sommer L, Schorle H. 2007. Establishment and controlled differentiation of neural crest stem cell lines using conditional transgenesis. *Differ Res Biol Divers* **75**: 580–591.
- Mayor R, Theveneau E. 2013. The neural crest. *Dev Camb Engl* **140**: 2247–2251.
- Meijer AJ, Lorin S, Blommaert EF, Codogno P. 2015. Regulation of autophagy by amino acids and MTOR-dependent signal transduction. *Amino Acids* **47**: 2037–2063.
- Merrill GF, Kurth EJ, Hardie DG, Winder WW. 1997. AICA riboside increases AMP-activated protein kinase, fatty acid oxidation, and glucose uptake in rat muscle. *Am J Physiol* **273**: E1107–1112.
- Nakada Y, Stewart TG, Peña CG, Zhang S, Zhao N, Bardeesy N, Sharpless NE, Wong K-K, Hayes DN, Castrillon DH. 2013. The LKB1 tumor suppressor as a biomarker in mouse and human tissues. *PLoS One* **8**: e73449.
- Nony P, Gaude H, Rossel M, Fournier L, Rouault J-P, Billaud M. 2003. Stability of the Peutz-Jeghers syndrome kinase LKB1 requires its binding to the molecular chaperones Hsp90/Cdc37. *Oncogene* **22**: 9165–9175.
- Normén C, Figlia G, Lebrun-Julien F, Pereira JA, Trötzmüller M, Köfeler HC, Rantanen V, Wessig C, van Deijk A-LF, Smit AB, et al. 2014. mTORC1 controls PNS myelination along the mTORC1-RXRγ-SREBP-lipid biosynthesis axis in Schwann cells. *Cell Rep* **9**: 646–660.
- Novak A, Guo C, Yang W, Nagy A, Lobe CG. 2000. Z/EG, a double reporter mouse line that expresses enhanced green fluorescent protein upon Cre-mediated excision. *Genes N Y N* **2000** **28**: 147–155.
- Ochocki JD, Simon MC. 2013. Nutrient-sensing pathways and metabolic regulation in stem cells. *J Cell Biol* **203**: 23–33.
- Pingault V, Ente D, Dastot-Le Moal F, Goossens M, Marlin S, Bondurand N. 2010. Review and update of

- mutations causing Waardenburg syndrome. *Hum Mutat* **31**: 391–406.
- Pooya S, Liu X, Kumar VBS, Anderson J, Imai F, Zhang W, Ciralo G, Ratner N, Setchell KDR, Yoshida Y, et al. 2014. The tumour suppressor LKB1 regulates myelination through mitochondrial metabolism. *Nat Commun* **5**: 4993.
- Preitschopf A, Li K, Schörghofer D, Kinslechner K, Schütz B, Thi Thanh Pham H, Rosner M, Joo GJ, Röhl C, Weichhart T, et al. 2014. mTORC1 is essential for early steps during Schwann cell differentiation of amniotic fluid stem cells and regulates lipogenic gene expression. *PLoS One* **9**: e107004.
- Puig I, Yajima I, Bonaventure J, Delmas V, Larue L. 2009. The tyrosinase promoter is active in a subset of vagal neural crest cells during early development in mice. *Pigment Cell Melanoma Res* **22**: 331–334.
- Rattan R, Giri S, Singh AK, Singh I. 2005. 5-Aminoimidazole-4-carboxamide-1-beta-D-ribofuranoside inhibits cancer cell proliferation in vitro and in vivo via AMP-activated protein kinase. *J Biol Chem* **280**: 39582–39593.
- Saitoh F, Araki T. 2010. Proteasomal degradation of glutamine synthetase regulates schwann cell differentiation. *J Neurosci Off J Soc Neurosci* **30**: 1204–1212.
- Shackelford DB. 2013. Unravelling the connection between metabolism and tumorigenesis through studies of the liver kinase B1 tumour suppressor. *J Carcinog* **12**: 16.
- Shackelford DB, Shaw RJ. 2009. The LKB1-AMPK pathway: metabolism and growth control in tumour suppression. *Nat Rev Cancer* **9**: 563–575.
- Shen Y-AA, Chen Y, Dao DQ, Mayoral SR, Wu L, Meijer D, Ullian EM, Chan JR, Lu QR. 2014. Phosphorylation of LKB1/Par-4 establishes Schwann cell polarity to initiate and control myelin extent. *Nat Commun* **5**: 4991.
- Sherman DL, Krots M, Wu L-MN, Grove M, Nave K-A, Gangloff Y-G, Brophy PJ. 2012. Arrest of Myelination and Reduced Axon Growth When Schwann Cells Lack mTOR. *J Neurosci* **32**: 1817–1825.
- Shorning BY, Clarke AR. 2016. Energy sensing and cancer: LKB1 function and lessons learnt from Peutz-Jeghers syndrome. *Semin Cell Dev Biol* **52**: 21–29.
- Shorning BY, Clarke AR. 2011. LKB1 loss of function studied in vivo. *FEBS Lett* **585**: 958–966.
- Simon MC, Keith B. 2008. The role of oxygen availability in embryonic development and stem cell function. *Nat Rev Mol Cell Biol* **9**: 285–296.
- Soriano P. 1999. Generalized lacZ expression with the ROSA26 Cre reporter strain. *Nat Genet* **21**: 70–71.
- Tardito S, Oudin A, Ahmed SU, Fack F, Keunen O, Zheng L, Miletic H, Sakariassen PØ, Weinstock A, Wagner A, et al. 2015. Glutamine synthetase activity fuels nucleotide biosynthesis and supports growth of glutamine-restricted glioblastoma. *Nat Cell Biol* **17**: 1556–1568.
- Toyama EQ, Herzig S, Courchet J, Lewis TL, Losón OC, Hellberg K, Young NP, Chen H, Polleux F, Chan DC, et al. 2016. Metabolism. AMP-activated protein kinase mediates mitochondrial fission in response to energy stress. *Science* **351**: 275–281.
- Tricaud N, Perrin-Tricaud C, Brusés JL, Rutishauser U. 2005. Adherens junctions in myelinating Schwann cells stabilize Schmidt-Lanterman incisures via recruitment of p120 catenin to E-cadherin. *J Neurosci Off J Soc Neurosci* **25**: 3259–3269.
- Uesaka T, Jain S, Yonemura S, Uchiyama Y, Milbrandt J, Enomoto H. 2007. Conditional ablation of GFRalpha1 in postmigratory enteric neurons triggers unconventional neuronal death in the colon and causes a Hirschsprung's disease phenotype. *Dev Camb Engl* **134**: 2171–2181.
- Uesaka T, Nagashimada M, Enomoto H. 2015. Neuronal Differentiation in Schwann Cell Lineage Underlies Postnatal Neurogenesis in the Enteric Nervous System. *J Neurosci* **35**: 9879–9888.
- Uesaka T, Nagashimada M, Yonemura S, Enomoto H. 2008. Diminished Ret expression compromises neuronal survival in the colon and causes intestinal aganglionosis in mice. *J Clin Invest* **118**: 1890–1898.
- Vincent EE, Coelho PP, Blagih J, Griss T, Viollet B, Jones RG. 2015. Differential effects of AMPK agonists on cell growth and metabolism. *Oncogene* **34**: 3627–3639.
- Zang Y, Yu L-F, Pang T, Fang L-P, Feng X, Wen T-Q, Nan F-J, Feng L-Y, Li J. 2008. AICAR induces astroglial differentiation of neural stem cells via activating the JAK/STAT3 pathway independently of AMP-activated protein kinase. *J Biol Chem* **283**: 6201–6208.
- Zietkowski D, Davidson RL, Eykyn TR, De Silva SS, Desouza NM, Payne GS. 2010. Detection of cancer in cervical tissue biopsies using mobile lipid resonances measured with diffusion-weighted (1)H magnetic resonance spectroscopy. *NMR Biomed* **23**: 382–390.

PROJECT 2. LKB1 METABOLIC & SIGNALING REGULATION IN NCC

Genotyping PCR	Primer sequences	Band size
<i>Cre</i>	Cre5: 5'-CCTGGAAAATGCTTCTGTCCGTTTGCC-3'	654 bp Cre allele
	Cre3: 5'-GAGTTGATAGCTGGCTGGTGGGAGATG-3'	
<i>Lkb1</i>	Lkb1-55: 5'-TCTAACAATGCGCTCATCGTCATCCTCGGC-3'	220 bp WT allele
	Lkb1-36: 5'-GGGCTTCCACCTGGTGCCAGCCTGT-3'	300 bp Flox allele
	Lkb1-39: 5'-GAGATGGGTACCAGGAGTTGGGGCT-3'	
<i>R26R</i>	R26RGT1: 5'-AAAGTCGCTCTGAGTTGTTAT-3'	500 bp WT allele
	R26RGT2: 5'-GCGAAGAGTTTGTCTCAACC-3'	250 bp Flox allele
	R26RGT3: 5'-GGAGCGGGAGAAATGGATATG-3'	
qPCR	Primer sequences	Band size
<i>AUP1</i>	mAUP1-F: 5'-tgcgctccgtgtacaacagc-3'	95 bp
	mAUP1-R: 5'-tttgctcgcttcatgtgttct-3'	
<i>RELA</i>	mRELA-F: 5'-cgggatggctactatgagg-3'	96 bp
	mRELA-R: 5'-ctccaggtctcgcttctt-3'	
<i>cMyc</i>	mcMyc-F: 5'-gcctagaattggcagaaatga-3'	130 bp
	mcMyc-R: 5'-aactgagaagaatcctattcagcac-3'	
<i>Lkb1</i>	mLkb1-F: 5'-CTCCGAGGGATGTTGGAGTA-3'	119 bp
	mLkb1-R: 5'-GCTTGGTGGGATAGGTACGA-3'	
<i>Sox10</i>	mSox10-F: 5'-AGATCCAGTTCGTGTCAATAA-3'	136 bp
	mSox10-R: 5'-GCGAGAAGAAGGCTAGGTG-3'	
<i>p75^{NTR}</i>	mp75-F: 5'-ATGGATCACAAGGTCTACCCC-3'	190 bp
	mp75-R: 5'-GGAGCAATAGACAGGAATGAGG-3'	
<i>GFAP</i>	mGFAP-F: 5'-cgccacctacaggaaattg-3'	76 bp
	mGFAP-R: 5'-ctggaggttgagaaagtctgt-3'	
<i>S100B</i>	mS100B-F: 5'-tgaaggagcttatcaacaacga-3'	79 bp
	mS100B-R: 5'-tccatcactttgtccaccac-3'	
<i>Gpt1</i>	mGPT1-F: 5'-GGTGCTAACTCTGGATAC-3'	143 bp
	mGPT1-R: 5'-TGGCACGGATAACCTCAG-3'	
<i>Gpt2</i>	mGPT2-F: 5'-atgtgaaggctgtggagtaagg-3'	60 bp
	mGPT2-R: 5'-ctgcagtgtgggactataggg-3'	
<i>LdhA</i>	mLDHA-F: 5'-ggcactgacgcagacaag-3'	73 bp
	mLDHA-R: 5'-tgatcacctcgtaggcactg-3'	
<i>LdhB</i>	mLDHB-F: 5'-acaagtgggtatggcatgtg-3'	72 bp
	mLDHB-R: 5'-acatccaccagggcaagtt-3'	
<i>Pkm1</i>	mPKM1-F: 5'-cgcatgcagcacctgata-3'	61 bp
	mPKM1-R: 5'-caaacagcagacggtgga-3'	
<i>Pkm2</i>	mPKM2-F: 5'-aagggggactaccctctgg-3'	91 bp
	mPKM2-R: 5'-cctcgaatagctgcaagtgg-3'	
<i>GluL</i>	mGluL-F: 5'-ctcgctctcctgacctgttc-3'	94 bp
	mGluL-R: 5'-ttcaagtgggaacttgctga-3'	

Table 2- Antibodies used throughout the study.

Table 1- Primers used for genotyping and qPCR

PROJECT 2. LKB1 METABOLIC & SIGNALING REGULATION IN NCC

Technic	Primary antibody	Producing specie	Dilution	References
IHC	LKB1 D60C5 IHC formulated	Rabbit, polyclonal	1/200	Cell Signaling
	Sox2	Rabbit, polyclonal	1/1000	Chemicon Int.
	phospho-AMPK (Thr 172)	Rabbit, polyclonal	1/100	Cell Signaling
	phospho-S6RP (Ser 235/236)	Rabbit, polyclonal	1/200	Cell Signaling
IF	LKB1 SAB4502888	Rabbit, polyclonal	1/100	Sigma
	Tuj1	Mouse, monoclonal	1/1000	Covance
	GFAP	Rabbit, polyclonal	1/200	Pierce Biotechnology
	HuC/D (16A11)	Mouse, monoclonal	1/100	Molecular probes Invitrogen
	Krox20	Mouse, monoclonal	1/100	Abcam
	βgalactosidase	Chicken, polyclonal	1/500	Abcam
	E-Cadherin	Mouse, monoclonal	1/500	BD Transduction
	Active Caspase3	Rabbit, polyclonal	1/100	Cell Signaling
	S100	Rabbit, Polyclonal	1/1000	Dako
	Tubulin YL1/2 from hybridoma	Monoclonal, Rat	1/2	Homemade (gift from L. Lafanechère)
WB	LKB1 Ley37DG6	Mouse monoclonal	1/1000	Santa Cruz
	Actin	Mouse monoclonal	1/1000	Millipore
	phospho-AMPK α 1/2 (Thr 172) (40H9)	Rabbit, monoclonal	1/1000	Cell Signaling
	Total AMPK α 1/2 (H-300)	Rabbit, polyclonal	1/1000	Santa Cruz Biotechnology
	phospho-S6RP (Ser 235/236) (D57.2.2E)	Rabbit, monoclonal	1/1000	Cell Signaling
	Total S6RP (5G10)	Rabbit, monoclonal	1/1000	Cell Signaling
	c-Myc (9E10)	Mouse, monoclonal	1/1000	Roche Diagnostics
	H4	Mouse, monoclonal	1/1000	Abcam
	HSP90 (AC88)	Mouse, monoclonal	1/2000	Stressgen
	GS	Rabbit, polyclonal	1/2000	Abcam

Figure Legends

Figure 1. *Lkb1* is crucial for neural crest cells lineage and enteric maintenance.

(A) Schematic representation of the conditional ablation of *Lkb1* specifically in neural crest cells (NCC) with the *Tyr::Cre* driver after they migrated to their target organs. NCC derivatives targeted for *Lkb1* inactivation with this model are represented on the right and below with indications about their origin, their normal timing of differentiation and the stage of genetic ablation. (B) Representative picture of a male animal with homozygous *Lkb1* ablation (*Lkb1* cKO) which typically displays coat color hypopigmentation. (C) Kaplan-Meier graph comparing the survival of *Lkb1*-knockout (cKO), heterozygous (Htz) and wild-type (WT) male littermates. The number of animals is indicated above the curves. (D) *Lkb1* cKO mice rapidly loosed weight compare to WT littermates (weight curves for cKO indexed to WT). (E) cKO mice develop a progressive intestinal pseudo-obstruction as shown at postnatal day 21 (P21) (middle panel) by empty colon (Co) and atrophy of the cecum (Ce) and at adulthood (lower panel) with atrophy of the stomach (St, dotted arrow), dilation of the small intestine (Int, arrow head), hypertrophy of the cecum (arrow) and colon constriction (empty arrow) compare to WT (upper panel) (n≥8 mice per group). (F) Loss of hind limb extension reflex in *Lkb1* cKO P21 mice compared to control animal (WT) manifested by hind limb clenching when lifted by the tail. (G) Appearance of sciatic nerves from control and *Lkb1* cKO mice at P21 showing myelination defects in the mutant. (H) Staining with *Lkb1* Cell Signaling D60C5 antibody of myenteric ganglia in P21 mice in WT (arrows) and cKO animals. (I) Whole-mount Tuj1 labeling at birth (P0) on digestive tract from WT or *Lkb1* cKO animals. No obvious difference in proximal and distal intestine (PI, DI) and proximal and distal colon (PC, DC) was observed in cKO animals compare to WT. (J) Whole-mount Acetylcholinesterase (AChE) staining of enteric nervous system at P21 showed marked loss of enteric ganglia. (K) Neural (Tuj1) and glial (GFAP) staining on roll sections of intestine and colon (WT

n=5; cKO n=8). (L) Histograms indicating the average number of Dapi⁺Tuj1⁺ cells per mm in the distal intestine (DI) and distal colon (DC). cKO animals with unaffected neuronal density (Unaf.), hypoganglionosis (Hypog.) or hyperplasia (Hyperp.) are plotted separately. Increased density of Tuj1-positive cells due to ganglia hyperplasia was observed in distal colon of 2/8 cKO analyzed. (M) Increased phospho-S6RP staining was observed in cKO animals both in intestine and colon. Myenteric ganglia are surrounded by dotted lines. The graphs below represent the percentage of highly phospho-S6RP stained ganglia in the distal intestine and distal colon.

Figure 2. Defective myelination of sciatic nerves in *Lkb1* cKO mice correlates with defects in maturation of Schwann cells

(A) Longitudinal sections of sciatic nerves of WT and *Lkb1* cKO mice at P6 and P21 immunostained with *Lkb1* antibodies. (B) Increased phospho-S6RP staining was observed in cKO animals in transverse sections of sciatic nerves (n=5 WT, n=4 cKO). (C) Electron microscopy of sciatic nerves of P21 WT (a-c) and *Lkb1* cKO mice (d-h). Transverse sections of WT nerves show normally myelinated nerve fibers (a,b) and regular unmyelinated axons in Remak bundles (c) whereas sections of cKO nerves show disorganization of the tissue (d) with neurodegenerative figures (e), aberrantly unsegregated axons of small to large diameter (f) and axonal sorting defects (g, h). (i) Scatter plot of *g* ratio values with linear regressions in sciatic nerves of WT (blue, n=410 axons, 2 animals) and cKO (red, n=473 axons, 3 animals). Scale bars represent 10 μm (Ja and d), 5 μm (Jb), 2 μm (Je, g, h) and 1 μm (Jc and f). (D) Tuj1 and GFAP immunostaining on transverse sections of P21 sciatic nerves. Insets show higher magnification of images with neural loss (Tuj1) and glial marker mislocalization (GFAP) in cKO animals (WT n=5, cKO n=3). (E) E-cadherin (E-cad) staining on isolated nerve fibers from sciatic nerve of P21 mice showing aberrant E-cad localization. (F) Immature Schwann cell marker Sox2

immunostaining on cross-sections of WT and cKO animals was increased in the absence of *Lkb1* (see quantification at P6).

Figure 3. *Lkb1* knockdown impairs NCC-derived glial differentiation.

(A) Schematic representation of the Schwann cell lineage depicting first steps involved in glial commitment and later steps in Schwann cell differentiation. (B) Transformed mouse NCC JoMa1.3 cells were maintained either as progenitors or differentiated into glial cells (first steps of the lineage) as validated by staining against glial markers GFAP (left panels, n=3) or S100 (right panels, n=3). (C) Transfected JoMa1.3 cells during glial commitment with *Lkb1*-targeting siRNA (siLKB1) showed decrease of glial markers compared to non-targeting control siRNA (scramble, siScr); GFAP n=3; S100 n=4. (D) RT-qPCR showing expression of *Sox10* and *p75^{NTR}* genes in glial JoMa1.3 cells upon *Lkb1* silencing. Data are expressed as relative expression in control cells compare to siLkb1 cells (siCont./siLkb1, n=4). Expression level of endogenous mouse *Lkb1* in JoMa1.3 cells is also shown (n=4). (E) Mitochondrial mass was quantified by FACS analyses with Mitotracker Green staining (n=3). (F) Mitochondrial topology of glial JoMa1.3 cells stained with Mitotracker Red was analyzed by confocal microscopy (n=3). (G) Mitotracker staining on isolated myelinated nerve fibers of wildtype (WT) or *Lkb1*-deficient mice (cKO). (H) Representative electron microscopy images of mitochondria from control (siCont.) and *Lkb1* knockdown (siLkb1) glial JoMa1.3 cells showing increased cristae width in the absence of *Lkb1*. Quantification was performed on 429 and 336 cristae from mitochondria of control and *Lkb1*-silenced cells respectively. (I) A representative trace showing change in oxygen consumption rates (OCR) during a mitochondrial stress assessed by Seahorse analyses on control (siCont.) and *Lkb1*-silenced (siLkb1) glial JoMa1.3 cells (n=12; quantification is shown in S4J).

Figure 4. *Lkb1* loss in sciatic nerves triggers a metabolic reprogramming.

(A) ¹H HRMAS NMR spectrum of the two sciatic nerves of a cKO mouse. Insets showing lipids and macromolecules peaks. (B) Zoom on small metabolites from A (blue bracket). Loadings of the predictive component of the multivariate statistical model built with spectral buckets of WT and cKO mouse spectra for identification of up (positive) and down (negative) regulated metabolites in cKO mice. The loading plots are colored according to variable importance to the projection and some assignments are indicated. Glucose, glutamate, alanine and lipid peaks have the highest correlation value. (C, D) List of small metabolites (C) and lipids (D) with identical (=), up (+) and down (-) regulation in cKO mice. For lipids, the underlined groups are assigned based on neighbor groups since lipids are a very complex mixture. (E) Score scatter plot of the multivariate statistical model relative to the predictive and orthogonal components. The model is robust with R²Y=0.95 and Q²=0.82. WT n=16, cKO n=13 mice. (F) Mean relative amplitude of glucose (d=4.65 ppm), alanine (d=1.48 ppm) and glutamate (d=2.35 ppm) peaks in each mouse group, relative to TSP 0 ppm. (G) Schematic representation of metabolic pathways illustrating the defects observed by metabolomics profiling on sciatic nerves upon *Lkb1* ablation. αKG: α-ketoglutarate; OAA: oxaloacetate; ALAT: alanine aminotransferase; ASAT: aspartate aminotransferase; GLS: Glutaminase; GS: glutamine synthetase; LDHA: lactate dehydrogenase A; LDHB: lactate dehydrogenase B; PC: pyruvate carboxylase; PKM2: pyruvate kinase M2; PSAT: phosphoserine aminotransferase.

Figure 5. *Increased levels of the alanine and glutamate are associated with impaired glial differentiation.*

(A) Intracellular alanine concentration of control (siCont.) or *Lkb1* knockdown (siLkb1) glial JoMa1.3 cells (n=3). (B) Schematic representation of metabolic reprogramming triggered by *Lkb1* silencing (siLkb1, up) or by ALAT inhibition with Chloro-alanine inhibitor (Cl-ala, down). (C) Representative curves (left) of pH medium acidification (ECAR) of JoMa1.3 cells control (siCont.) or with *Lkb1* knockdown

(siLkb1) upon ALAT inhibition (+Cl-ala). Percent change (right) in medium acidification (ECAR %) of *siLkb1* JoMa1.3 cells relative to control cells (n=2). (D) Intracellular glutamate concentration of control (siCont.) or *Lkb1* knockdown (siLkb1) glial JoMa1.3 cells expressed as the percentage relative to control cells (siCont.) (n=7 for siCont. and siLkb1 and n=4 with Cl-ala treatment). (E) Actin reorganization was assessed by phalloidin staining of control (Cont.) or *Lkb1*-silenced (siLkb1) cells treated or not with Cl-ala. Nuclei were counterstained with Dapi (n=4). (F) Glial differentiation assessed by S100 immunostaining of JoMa1.3 cells upon Cl-ala treatment. Representative images (left) and quantification (right) of the percentage of S100-positives cells (n=3). (G) Representative curves showing change in oxygen consumption (OCR, left) and quantification of % OCR relative to control cells (siCont. with the control condition of treatment) (n=4). (H) ALAT inhibition by Cl-ala normalized the mTOR pathway activity. Representative western blots are shown on the left. Right: quantification of phosphorylated S6RP protein relative to total S6RP protein (n=2).

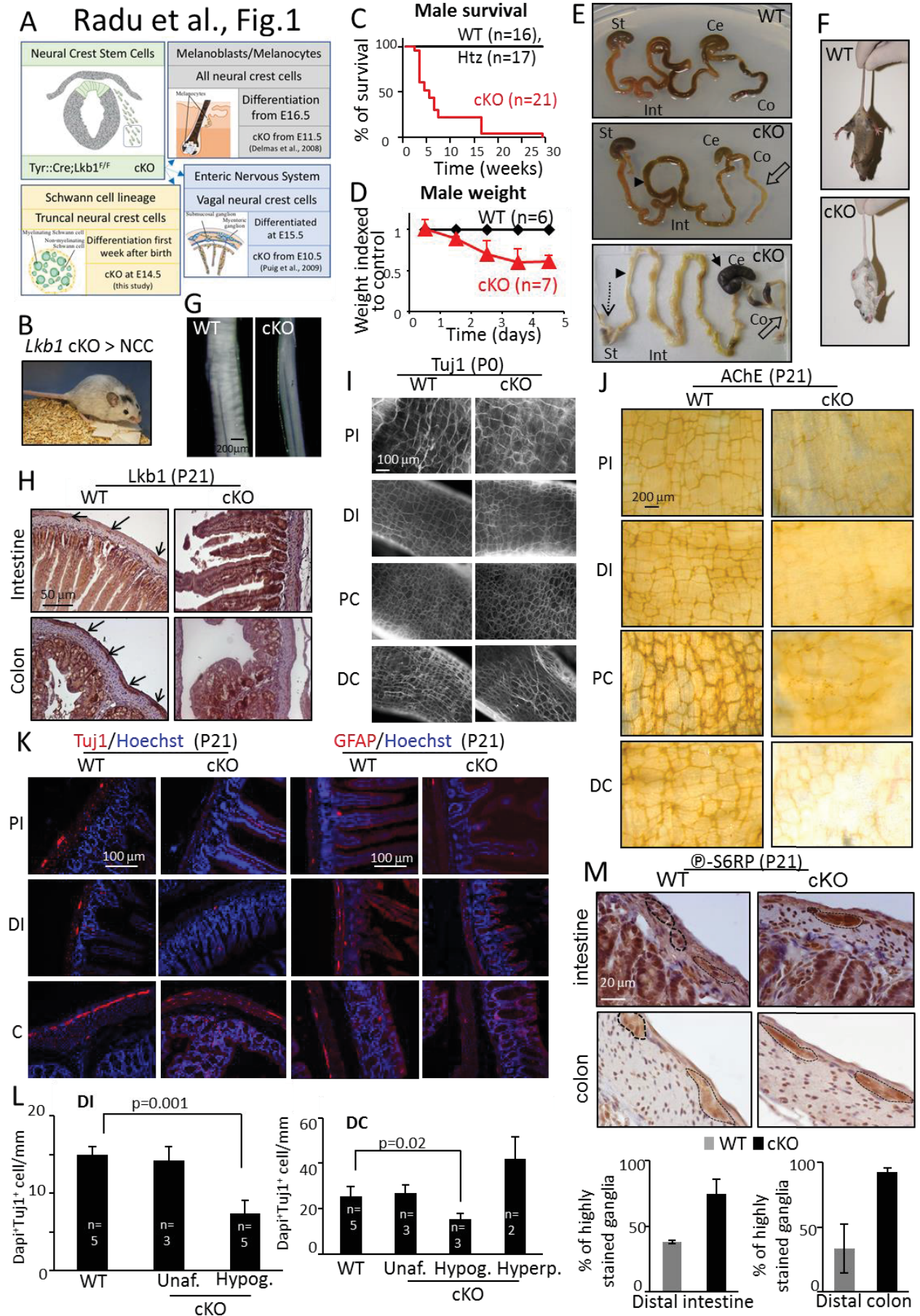
Figure 6. Normalizing alanine and glutamate levels or mTOR activity rescues glial differentiation.

(A) Schematic representation of glutamine synthetase (GS) inhibition by Methionine Sulfoximine (MSO). (B) Glutamate concentration upon dose-dependent MSO treatment of glial JoMa1.3 cells compare to non-treated cells (Cont.) (n=4). (C) Alanine concentration of MSO-treated glial JoMa1.3 cells (n=2). (D) Cytoskeleton organization was assessed by phalloidin staining of control (Cont.) or MSO-treated cells. Nuclei were counterstained with Dapi (n=4). (E) Glial differentiation assessed by S100 immunostaining of JoMa1.3 cells upon MSO treatment (n=3). (F) Western blot (left) of glial cells after MSO treatment showing the relative level of phosphorylated S6RP with quantitative analysis (right) (n=4). (G) Impaired glial differentiation visualized with the S100 glial marker due to *Lkb1* knockdown was rescued by AICAR treatment. Graph on the right side shows the percentage of S100-positives cells (n=3). (H) AICAR addition also

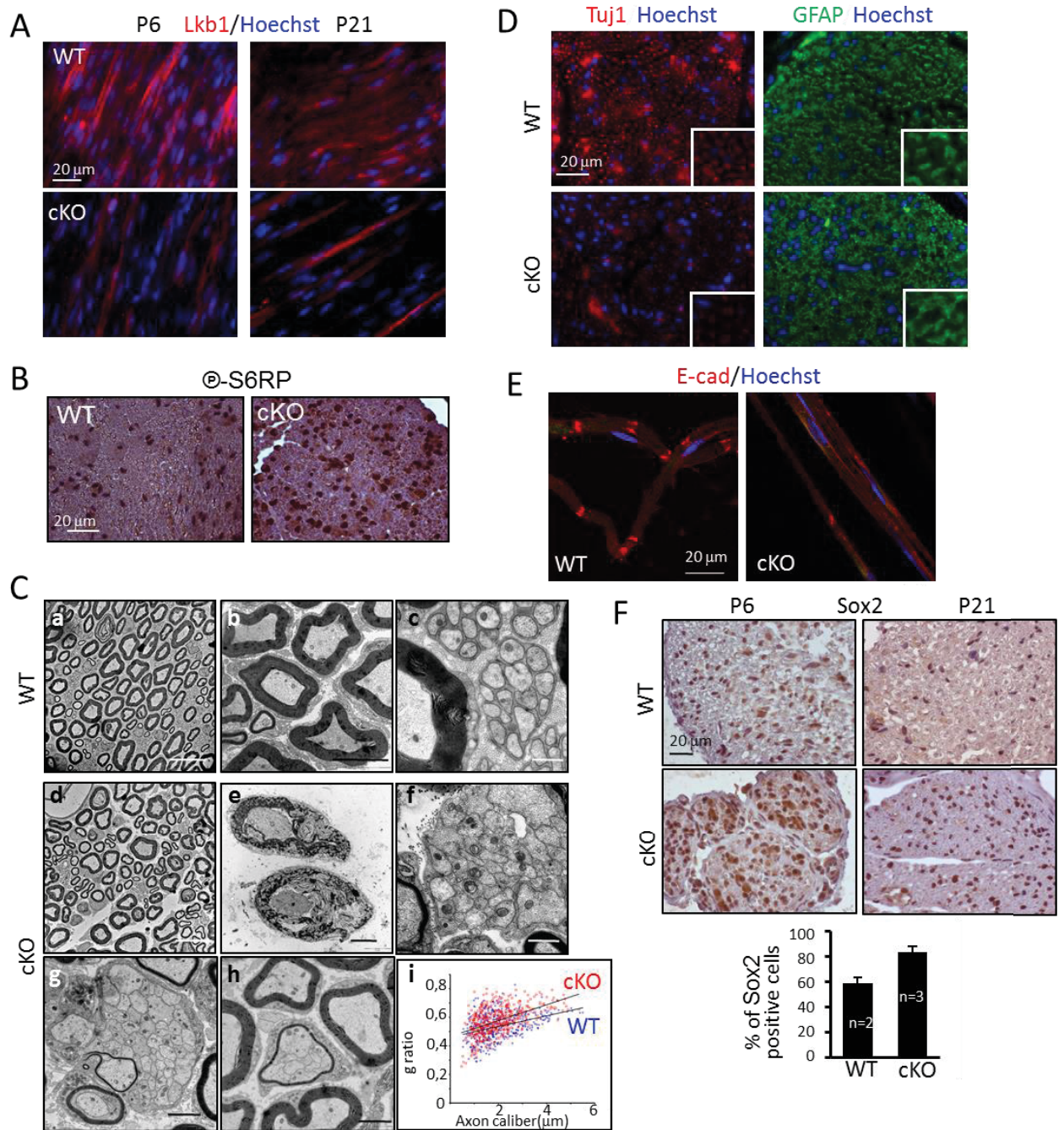
rescued glial differentiation of MSO-treated cells (n=2). (I) Western blot showing that AICAR treatment normalizes mTOR activity with quantification (right; n=2). (J) mTOR inhibition by Torin1 rescues glial differentiation as shown by representative images (left) and evaluation of the percentage of S100-positives cells (right, n=2).

Figure 7. AICAR treatment of *Lkb1*-deficient mice prevents the peripheral neuropathy and the enteric nervous system degeneration.

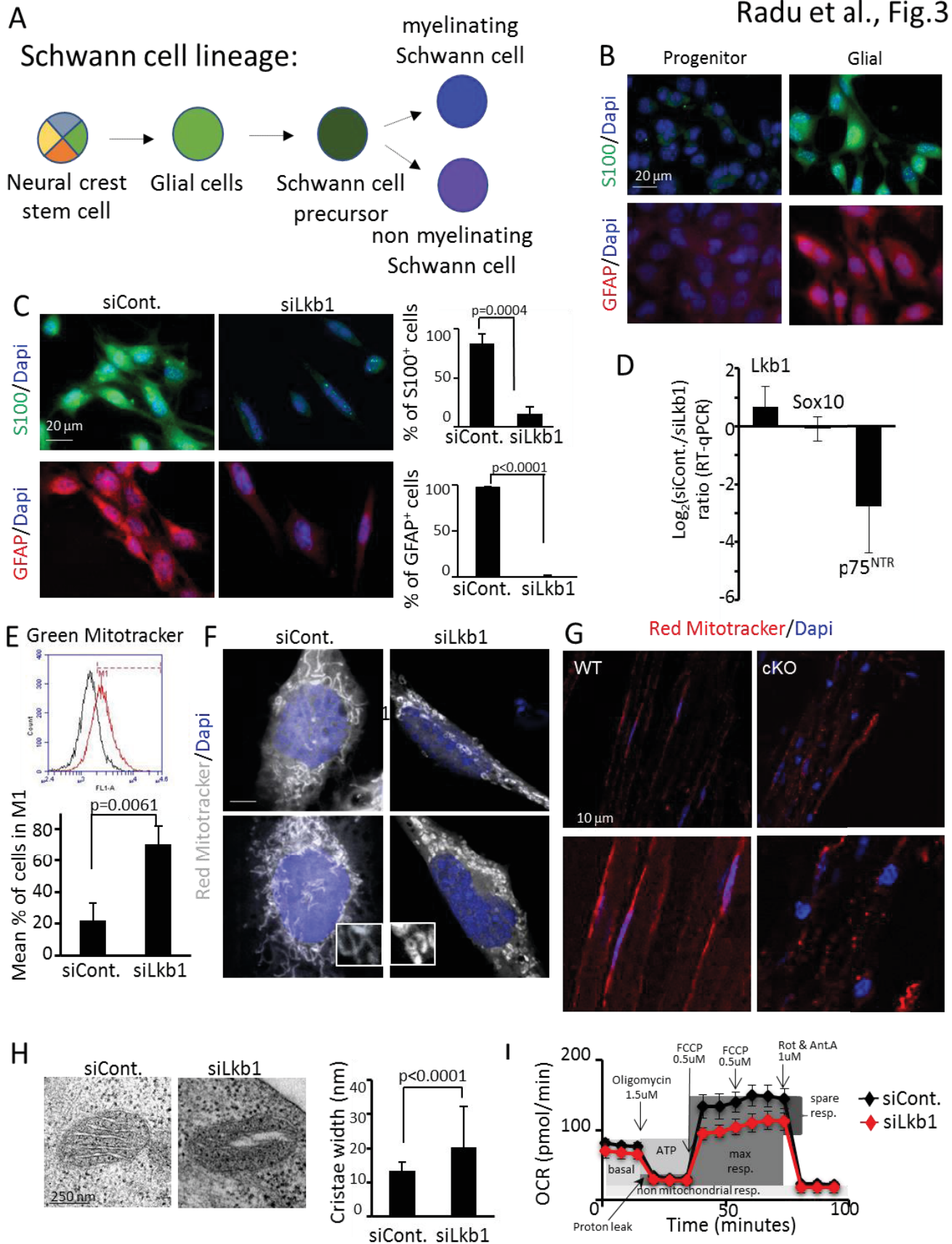
(A, B, C) Injection of *Lkb1*-deficient animals by i.p. from P10 to P18 with the AMP analogue AICAR partly rescued weight loss (A), improved hind limb extension reflex (B) and prevented intestinal dilation (C). (D, E) AICAR treatment of cKO mice rescued mTOR inhibition compare to vehicle-treated cKO animals both in sciatic nerves (D) and enteric nervous system (E). Myenteric ganglia are surrounded by dotted lines. Graph in E represents the percentage of phospho-S6RP stained ganglia in the distal intestine (DI). (F) The integrity of the intestinal villi and the number of enteric neurons (red) and glial cells (green) are rescued in AICAR-treated mice. Representative pictures from two different animals are shown (upper and lower pictures). n=5 mice per condition.



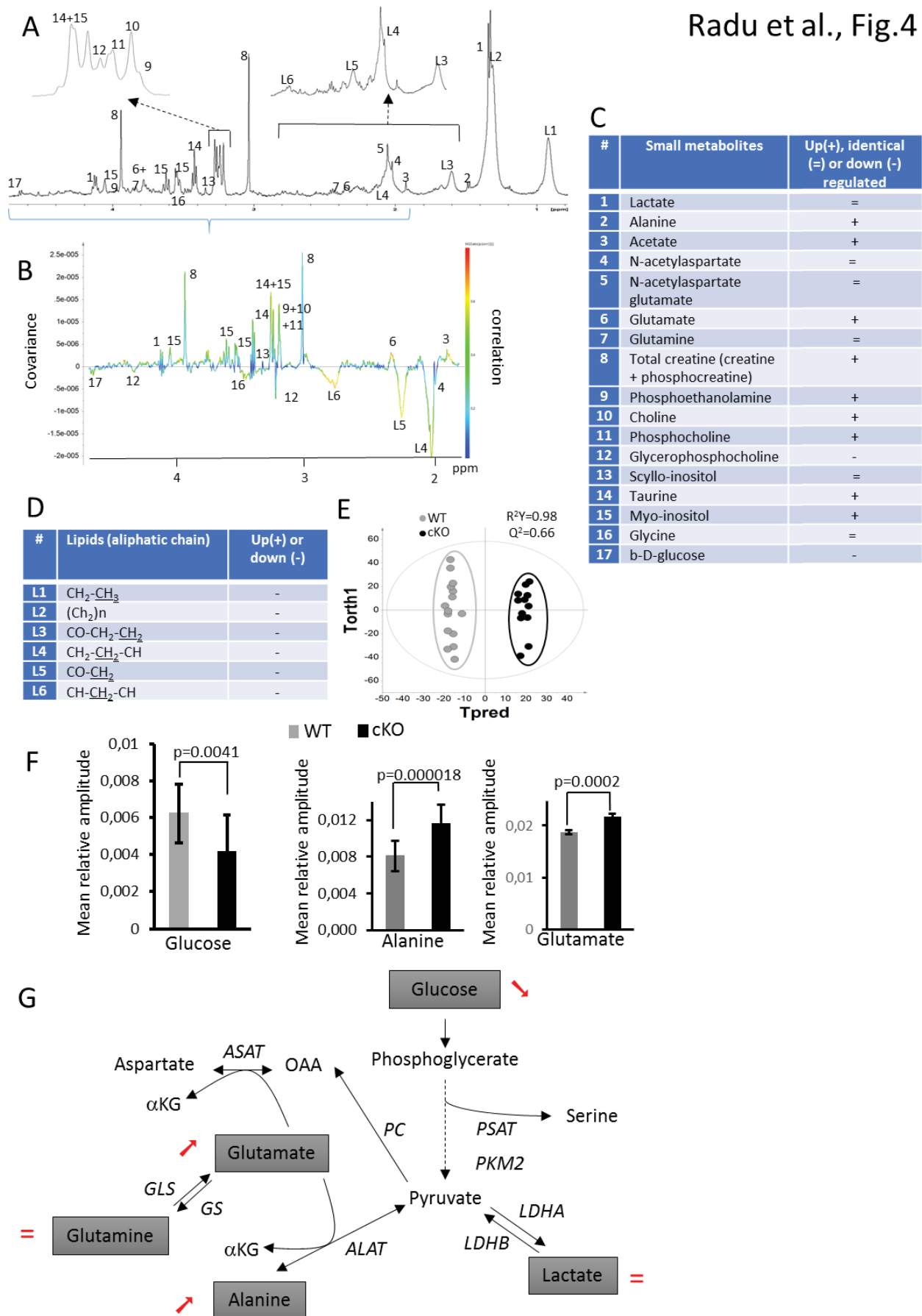
Radu et al., Fig.2



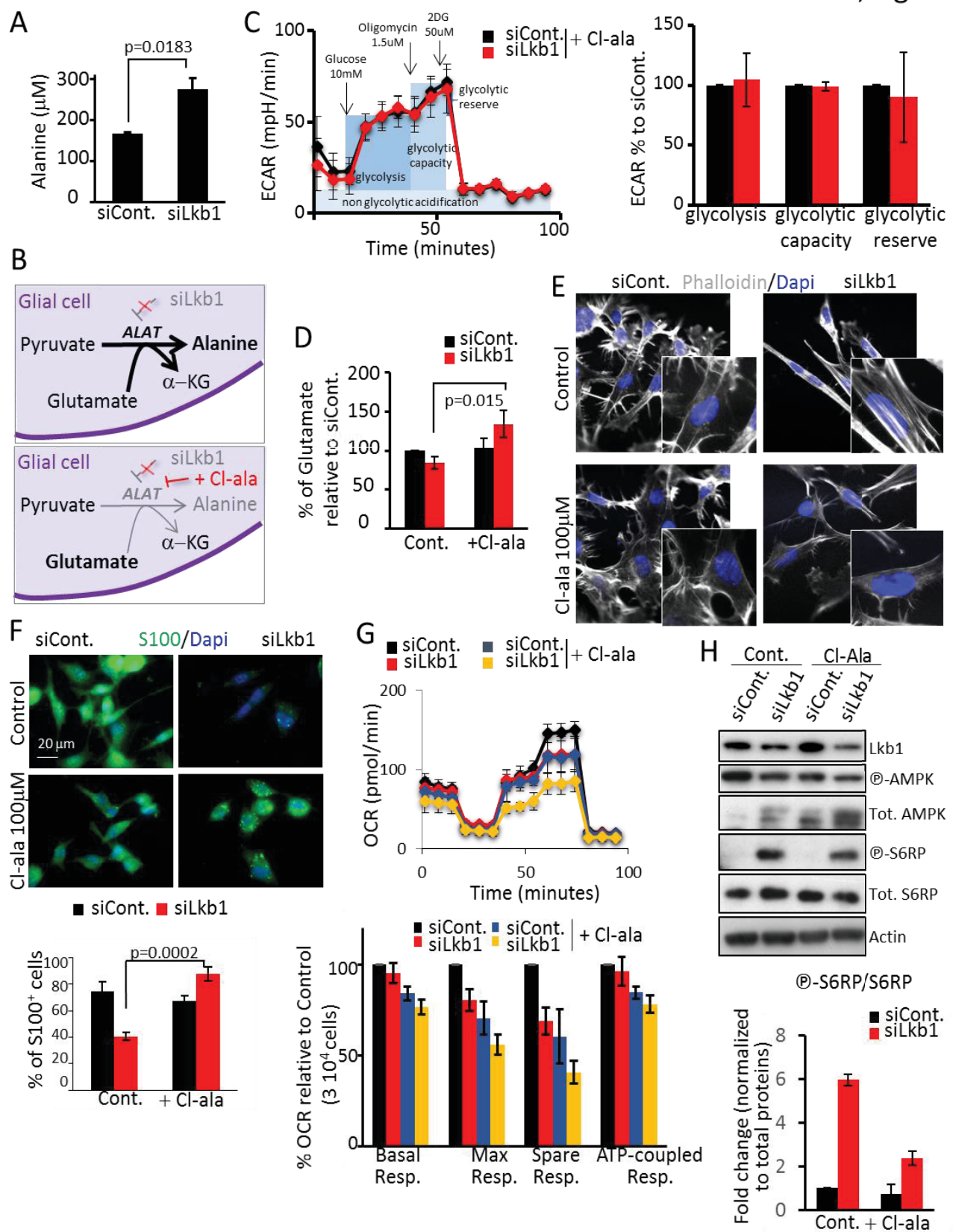
Radu et al., Fig.3



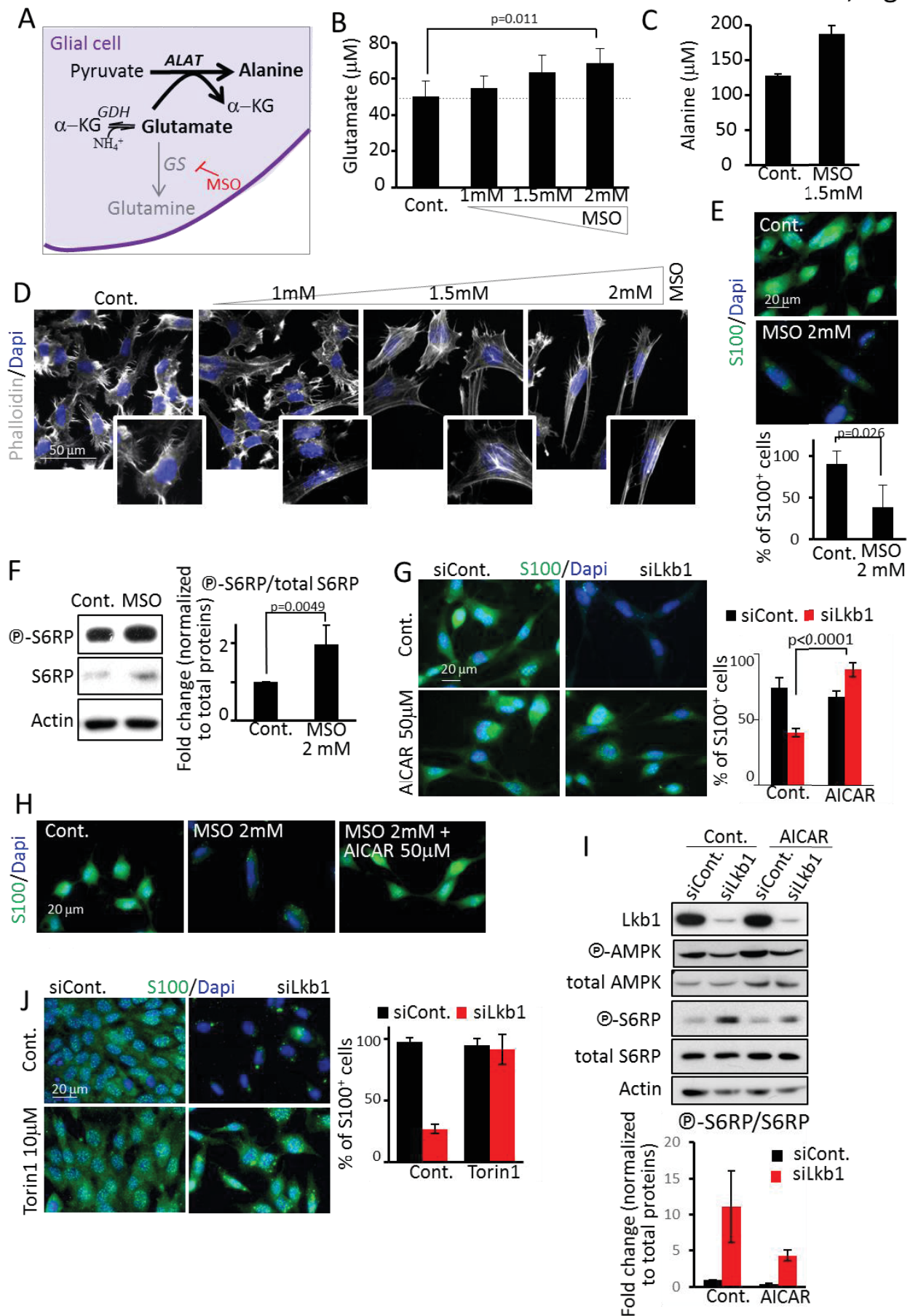
Radu et al., Fig.4



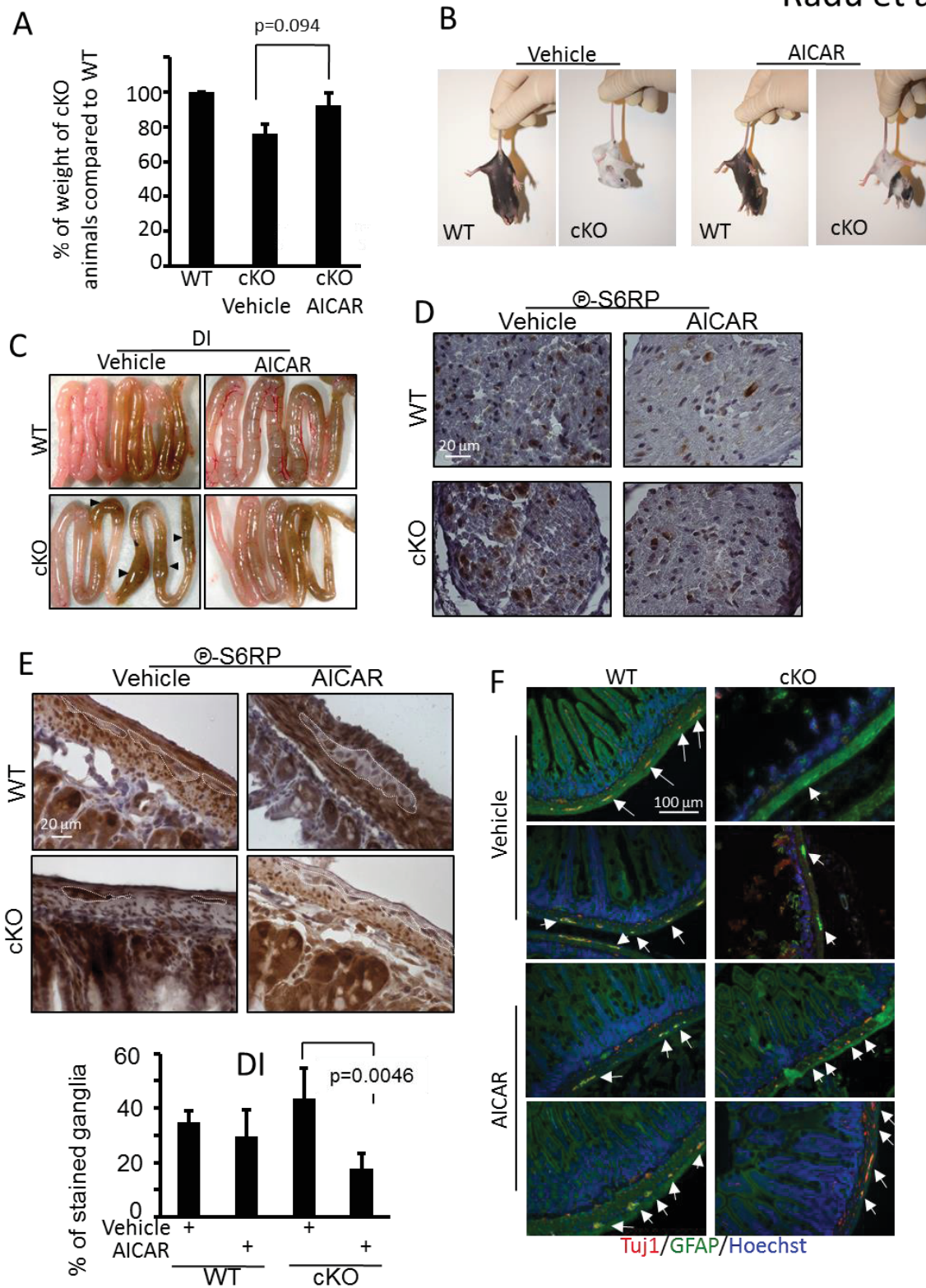
Radu et al., Fig. 5



Radu et al., Fig. 6



Radu et al., Fig.7



SUPPLEMENTAL DATA

Supplemental Figure legends

Figure S1. *Conditional ablation of Lkb1 in neural crest cells causes hypopigmentation, hind limb paralysis and intestinal pseudo-obstruction.* Related to Figure1.

(A) Schematic representation of mice interbred: mice harboring wild-type *Lkb1* allele flanked by loxP sequences, transgenic mice with *Tyr::Cre* transgene and R26R reporter mice. (B) Genotyping of heterozygous *Lkb1* floxed mice (*Lkb1*^{+/F}), WT (*Lkb1*^{+/+}) or homozygous (*Lkb1*^{F/F}) with (tg) or without (+) the transgene *Tyr::Cre*. Positions of the different alleles are indicated. (C) Breeding tables. (D) Variable hypopigmentation of *Lkb1* cKO mice. (E) *Lkb1*-ablated mice exhibit distended bowel (dotted line). (F) *Lkb1*-deficient mice display motor defects illustrated by the stiffness and outward position of the hind limb (arrows). (G) Footprints of wild-type and cKO mice at P21. Chinese ink was placed on the hindpaws of mice and representative footprint patterns are shown (WT: n=7; cKO: n=9). The walking direction is indicated by the arrows. Inset: higher magnification of a footprint showing tip-toe walking of cKO mice indicative of postural abnormalities. Histogram represent differences in left and right stride length but not in sway length.

Figure S2. *Lkb1 inactivation in neural crest derived enteric cells triggers degeneration.* Related to Figure1.

(A) *Lkb1* immunostaining on Swiss-roll sections of wild-type mice intestine and colon. *Lkb1* expression in myenteric and submucosal ganglia colocalized with the neural marker Tuj1. *Lkb1* immunostaining of cKO mice shows a strong reduction both on intestine and colon Swiss-roll sections (n=6 mice/group). (B) Confocal analysis of β Galactosidase-labeled cells (β Gal) of an intestinal myenteric ganglion (left) or an isolated glial cell (right) showing co-staining with neural (HuC/D) or glial (GFAP) markers. (C) *LKB1*

staining by IHC with Cell Signaling D60C5 antibody (left panels) of human tunica muscularis. Human ganglia in intestine and colon biopsies are surrounded by dotted lines. *LKB1* immunofluorescent staining with Sigma *LKB1* antibody on sections of human intestine or colon biopsy showing *LKB1* expression in enteric ganglia cells (right panels). (D) Hematoxylin-Eosin staining of intestine and colon cross-sections of wild-type and cKO P21 mice showing shortened villi in distal intestine (DI). At least 4 animals were analyzed per condition. (E) Whole-mount X-Gal staining of P21 distal intestine (DI) reveals the labelled cells organized in a network in WT animals and dramatically reduced in number in cKO mice typical of hypoganglionosis. (F) Table showing for each cKO animal used to quantify the number of enteric neurons per mm which area of the digestive tract has reduced number of positive Tuj1⁺Dapi⁺ cells. (G) *Lkb1* staining with Cell Signaling D60C5 antibody on P6 transverse sections of intestine and colon of WT and cKO animals (left panels) showing *Lkb1*-stained ganglia in WT (black arrows) but not in cKO animals. Tuj1 and GFAP staining were also performed (right panels). Ganglia were nicely stained (white arrows) in WT animals whereas in *Lkb1*-deficient animals, ganglia were fewer, smaller and the intensity of staining was reduced (n=3). (H) TUNEL staining on roll sections of WT and cKO distal intestine (DI) of P21 mice showing no staining in enteric ganglia although apoptotic cell death was detected at the apex of intestinal villi as described in the literature (white arrow). (I) IHC for phospho-AMPK α 1/2 in ENS of intestine and colon showing decreased in phospho-AMPK staining in cKO animals. Myenteric ganglia are surrounded by dotted lines. Scale bars: 10 μ m (B), 20 μ m (C left, E, I), 100 μ m (C right, D, G left, G right, H) and 200 μ m (A).

Figure S3. *Defective myelination of sciatic nerves in Lkb1 cKO mice correlates with defects in maturation of Schwann cells.* Related to Figure2.

(A) Lkb1 immunostaining with Cell Signaling D60C5 antibody on transverse section of sciatic nerves of P21 WT and cKO animals. (B) IHC for phospho-AMPK α 1/2 on longitudinal sections of sciatic nerves showing decreased in phospho-AMPK staining in cKO animals. (C) Transverse section at the forelimb level of a E14.5 Tyr::Cre^{+/o};Z/EG^{+/o} subjected to immunofluorescence against GFP (green) and counter stained with DAPI (blue) (left picture). Several images of the same embryo section are shown on the right panels from proximal (up) and distal (down) parts of the forelimb. They illustrate colocalization of the glial marker GFAP (red) and GFP staining (green) labelling Cre expressing cells. (D) Sections of the same embryo showed no colocalization between immunofluorescence staining with the neuronal marker Tuj1 (red) and GFP (green). (E) Sciatic nerves of WT P21 mice were stained with X-Gal and semithin sections were performed. X-Gal blue coloration was observed only at the periphery of the sections due to weak X-Gal diffusion in solid tissues. Insets show X-Gal staining restricted to Schwann cells. Toluidine blue staining of one section allows the visualization of the tissue organization. (F) Salmon Gal staining was performed on cross sections of spinal cords of E18.5 embryos. (G) Dorsal root ganglia were studied on transverse sections of spinal cord from WT E18.5 embryo. Immunofluorescence targeting the reporter β -galactosidase (β Gal) shows its colocalization with neurons (Tuj1 positive cells) or glial GFAP-positive cells. (H) Toluidine blue-stained semithin cross-sections of sciatic nerves of WT and *Lkb1* cKO mice at P21 (n=4). The graph represents the mean number of myelinated axons per 1000 μ m². (I) Transverse sections of sciatic nerves from wild-type and cKO P6 mice were stained with Tuj1 neural marker. (J) Longitudinal sections of sciatic nerves from wild-type and cKO P6 mice were stained with GFAP glial marker. (K) Number of nuclei per field on transverse sections of sciatic nerves of P6 and P21 WT or *Lkb1* cKO mice. (L) Krox20 immunostaining (red) reveals myelinating Schwann cells at P6 in longitudinal sections of sciatic nerves. Scale bars represent 20

μ m (A, B, E, H, I, J, L), 50 μ m (C right, D), 100 μ m (G), 200 μ m (F) and 500 μ m (C left).

Figure S4. *Lkb1 is crucial for mitochondrial respiration during in vitro NCC-derived glial differentiation.* Related to Figure 3.

(A) Although inducible *c-Myc* expression is not significantly different in glial cells (G) compare to progenitors (P) (left qPCR results, n=3), *c-Myc*^{ER} protein translocates into the nucleus (western blot, right panels) and its further activation maintains the progenitor status of NCC *in vitro*. Histone 4 (H4) and the chaperone protein HSP90 are used to validate the fractionation and are associated with nuclear and cytoplasmic fractions respectively. (B) Cultivating NCC in specific medium for glial differentiation triggers cell morphology changes as assessed by phase contrast. (C) The morphologic reorganization during glial differentiation was also visualized by staining of cytoskeleton components with phalloidin for actin filaments (left pictures) and tubulin antibody for the microtubules (middle pictures) (n=3). (D) Progenitor cells express more of the stem cell marker *p75^{NTR}* whereas cells committed to glial differentiation express more of the glial marker *GFAP* as assessed by RT-qPCR (n=5). (E) Experimental protocol performed in order to knockdown *Lkb1* expression during glial differentiation and performed treatment as mentioned throughout the study. (F) Western blot to validate *Lkb1* knockdown at the protein level. Phosphorylation of AMPK and S6RP (as an indicator of mTOR activity) are also shown compare to total protein level. Actin was used as a loading control. (G) The relative *Lkb1* protein level observed by western blot has been quantified in progenitors (P) and glial (G) cells (n=4). (H) Fold changes have been quantified for phospho-AMPK to total AMPK protein (left graph, n=4) or phospho-S6RP to total S6RP protein (right graph) (n=4 in glial cells (G); n=3 in progenitors (P)). (I) *Lkb1* knockdown during glial differentiation triggers the occurrence of actin stress fibers as visualized by phalloidin staining (n=6). (J) Quantification of mitochondrial respiration (OCR) assessed with the metabolic analyzer

Seahorse (n=12). Scale bars represent 10 μ m (I right), 50 μ m (I left) and 100 μ m (B, C).

Figure S5. *Normalizing NEAA levels.* Related to Figures 5 and 6.

(A) Intracellular alanine concentration of control (Rescue *Lkb1* WT) or *Lkb1* knockout (*Lkb1*^{-/-}) MEF cells (n=3). (B) Intracellular alanine level of control (siCont.) or *Lkb1* knockdown (siLkb1) progenitor JoMa1.3 cells expressed as the percentage relative to control cells (siCont.) (n=5). (C) Percentage of intracellular alanine relative to control cells (siCont.) in glial JoMa1.3 cells upon *Lkb1* knockdown and ALAT inhibition with Chloro-alanine (Cl-ala) (n=2). (D) Intracellular lactate level of control (siCont.) or *Lkb1* knockdown (siLkb1) glial JoMa1.3 cells with Cl-ala treatment expressed as the percentage relative to control cells (siCont.). P: progenitors; G: glial cells (n=3). (E) Glycolytic activity of one representative experiment evaluated by pH extracellular acidification of glial JoMa1.3 cells either control (siCont.) or upon *Lkb1* knockdown (siLkb1) (n=4). Right graph: Seahorse quantification of medium acidification (ECAR; n=4). (F) Expression of some metabolic genes assessed by RT-qPCR on progenitor and glial cells. *GPT1*, 2: Glutamic pyruvate transaminase (encoding ALAT1, 2); *LDHA*, B: Lactate dehydrogenase A, B; *PKM1*, 2: Pyruvate kinase M1, 2; *GLUL*: Glutamate ammonia Ligase (encoding GS). *LDHB* expression is enriched in glial cells whereas *PKM2* and *GLUL* expression is enriched in progenitor cells (n=5). (G) Expression of the same metabolic genes as in (F) in glial JoMa1.3 cells either control (siCont) or silenced for *Lkb1* (siLkb1). Only *GPT2* expression is slightly enriched in siLkb1-treated cells (n=4). (H) Glutamine synthetase (GS) protein levels illustrated from a representative experiment (upper panels). Quantification of GS quantity normalized to actin is shown on the graph (n=4). (I) GS levels upon *Lkb1* silencing (western blot, left; quantification graph, right, n=3). (J) Mitochondrial topology of MSO-treated JoMa1.3 cells stained with Mitotracker Red analyzed by confocal microscopy (n=3). Scale bar represent 10 μ m. (K) Representative curves (top graph) of

oxygen consumption (OCR) of glial JoMa1.3 cells control (Cont.) or treated with the GS inhibitor Methionine Sulfoximine (MSO). Percent change (bottom graph) in OCR of MSO-treated cells relative to control cells (n=4). (L) Representative curves (top graph) of medium acidification (ECAR) of JoMa1.3 cells control (Cont.) or MSO-treated (MSO). Percent change (bottom graph) in medium acidification of MSO-treated cells relative to control cells (n=4).

Figure S6. *Glial differentiation in Lkb1-silenced cells is rescued by normalizing NEAA levels or the mTOR pathway.* Related to Figures 6.

(A) Confocal imaging illustrating cytoskeleton reorganization assessed by phalloidin staining of control (siCont.) or *Lkb1* knockdown (siLkb1) cells with or without AICAR treatment. Nuclei were counterstained with Dapi (n=4). Scale bars: 50 μ m; 10 μ m for the inset pictures. (B) Phalloidin staining of glial JoMa1.3 control or MSO-treated cells in the presence or absence of AICAR treatment (n=3). Scale bar: 20 μ m. (C) Percentage of intracellular glutamate relative to control cells (siCont.) in glial JoMa1.3 cells treated with MSO in the presence (+) or absence (-) of AICAR (n=4). (D) Same as in (C) with MSO-treated glial JoMa1.3 cells (+) in the presence (+) or absence (-) of AICAR (n=2). (E) Percentage of intracellular alanine relative to control cells (siCont.) in glial JoMa1.3 cells upon *Lkb1* knockdown and AICAR treatment (n=3). (F) Quantification of oxygen consumption (OCR) in control or siLkb1 JoMa1.3 cells with or without AICAR treatment (n=5). (G) Representative curves showing medium acidification (ECAR) in control or siLkb1 JoMa1.3 cells with or without AICAR treatment (n=4). (H) Torin1 is a potent mTOR inhibitor in JoMa1.3 glial cells as illustrated by a representative western blot (n=2).

Supplemental Methods

Histology, Immunohistochemistry and immunofluorescence staining

P21 intestines and colons of mice were collected, rinsed in cold PBS, and then fixed in 4 % PFA

overnight at 4°C. Swiss-rolls were performed before fixation when necessary. Tissue samples were dehydrated, embedded in paraffin and sectioned into 4-8 µm-thick transverse sections. Sciatic nerves samples were dehydrated, embedded in paraffin and sectioned by Anipath (Lyon, France). Tyr::Cre^{+/+};Z/EG^{+/+} E14.5 embryo were fixed in PFA 4% for 1h30 at 4°C washed in PBS, incubated in 30% sucrose for 4 hours, embedded in 30% sucrose- 50% OCT and sectioned at 7 µm.

Sections for histology were stained with Harris Hematoxylin and Eosin (Sigma-Aldrich) according to the supplier's protocol.

For immunohistochemistry, sections were deparaffinized and rehydrated, rinsed in PBS and boiled for 20 minutes at 95°C in a decloacking chamber (Biocare Medical) in 10 mM Sodium citrate antigen retrieval buffer (pH 6). Sections were then treated with 1% H₂O₂ for 20 minutes. After 1 hour incubation in a blocking buffer (PBS-3% BSA-10% Goat preimmune serum for polyclonal antibodies or ABC MOM kit from Vector laboratories for monoclonal antibodies according to the supplier's protocol), sections were incubated overnight at 4°C with the primary antibody (see Table 3 for dilutions and antibodies references). Secondary antibodies used for immunohistochemistry were anti Mouse- and anti Rabbit-Biotin conjugated (Vector laboratories). For phospho-AMPK, tissues were blocked with horse serum and ImmPRESS anti-Rabbit-HRP conjugated secondary antibodies were used to amplify the staining, according to the supplier's protocol (Clinisciences). DAB peroxidase substrate kit was used for detection of the antibodies (Vectors laboratories). Sections were then counterstained with Harris Hematoxylin (Sigma-Aldrich), dehydrated and mounted in Merckoglas (Merck).

For immunofluorescence, sections and cells were treated with standard protocols using primary antibodies as described in Table 3. Secondary antibodies used were from Jackson ImmunoResearch (Donkey anti-Mouse Alexa-488, Donkey anti-Mouse Cya3, Donkey anti-Rabbit Alexa-

488, Donkey anti-Rabbit Cya3, Donkey anti-Rabbit Cya2 and Goat anti-Chicken A488). For tissue sections, nuclei were stained with Hoechst 33342 (10 µg/ml, Invitrogen). For JoMa1.3 cells, nuclei were stained with Dapi. Sections and cells were mounted in mowiol. Actin cytoskeleton was stained with phalloidin conjugated to TRITC (1/400, Sigma).

TUNEL staining was performed according to the supplier's protocol (Roche). Analyses and acquisitions were performed using a Zeiss AxioImager Z1 microscope equipped with an AxioCam MRm camera, a Zeiss AxioImager M2 microscope, equipped with a Hamamatsu Orca R2 camera or for confocal microscopy a Zeiss AxioObserver Z1 multiparameter microscope LSM710 NLO – LIVE7 – Confocor3.

Whole-mount Tuj1 immunostaining of enteric nervous system

The enteric neural network was visualized according to the protocol previously described (Barlow et al. 2003; Pingault et al. 2010). Briefly, embryonic (E15.5) and postnatal intestines (P0) were fixed for 2 hours in 4% paraformaldehyde at 4°C. After washing twice in PBT (phosphate buffer saline-0.1% Triton X-100), tissues were incubated overnight with the neural marker Tuj1 (mouse, Covance, 1:1000), diluted in PBT containing 1% BSA and 0.15% Glycine (PBG). After extensive washings, tissues were then incubated overnight with anti-mouse Cya3-conjugated secondary antibody (1/500; Jackson ImmunoResearch). After washing three times in PBG, tissues were counterstained with the nuclei dye Hoechst 33342, mounted in Mowiol and analyzed with a Zeiss AxioImager M2 microscope, equipped with a Hamamatsu Orca R2 camera.

Whole-mount Acetylcholinesterase (AChE) activity staining

Acetylcholinesterase activity was visualized histochemically according to previously described protocols (Chalazonitis et al. 2011; Enomoto et al. 1998). Briefly, after gut dissection of P21 animals and removal of mesenteric attachments, tissues were post fixed with 4% PFA for 1-2 hours at 4°C, and transferred to saturated sodium sulfate overnight at

4°C. Gut samples were then incubated in coloration buffer (0.2 mM ethopropazine HCl, 4 mM acetylthiocholine iodide, 10 mM glycine, 2 mM cupric sulfate and 65 mM sodium acetate, pH5.5) for 2-4 hours. Acetylcholinesterase staining was developed by incubation in sodium sulfide for 1.5 min (1.25%, pH6).

Whole-mount X-Gal Staining

Whole mount detection of β -galactosidase activity was performed on P21 stages. Dissected guts were fixed on ice for 2 hours in phosphate buffer saline containing 0.2% glutaraldehyde. Guts were stained overnight at 37°C in 5-Bromo-4-chloro-3-indolyl- β -D-galactopyranoside (X-Gal) solution, containing 1 mg/ml X-Gal, 5 mM potassium ferricyanide, 5 mM potassium ferrocyanide, 2 mM $MgCl_2$, 0.01% sodium deoxycholate, and 0.02% nonidet P-40 (NP-40) in phosphate buffer saline. After staining, guts were washed in phosphate buffer saline containing 2 mM $MgCl_2$, 0.01% sodium deoxycholate and 0.02% NP-40, postfixed in 4% paraformaldehyde and examined under a stereomicroscope.

DRG Salmon gal staining and Immunofluorescence

Spinal cords from L1 to L6 lumbar vertebrae level were dissected from freshly collected E18.5 male embryos and fixed in 1% PFA/0.2% Glutaraldehyde in Phosphate buffer pH7.4 for 10 minutes. Tissues were rinsed 3 times with PBS and then prestained overnight at 37°C in a pre-stain solution without substrate (200mM ferricyanide potassium, 200mM ferrocyanide potassium, 4mM $MgCl_2$, 0.04% NP40, in PBS) to reduce endogenous β -galactosidase activity. Staining was performed for 30 minutes at 37°C, in a stain solution with 2mM $MgCl_2$, 0.04% NP40, Salmon Gal 1mg/ml, NBT (4-nitro blue tetrazolium chloride) 0.33mg/ml in PBS. Spinal cords were then rinsed and postfixed in PFA 4% in PBS, transferred to 20% sucrose cryoprotective solution overnight and OCT-mounted for cryosections and treated for immunofluorescence with standard protocols (See Table 2 for antibodies description).

Tails were collected at the time of dissection for genotyping of the embryos.

For β galactosidase immunodetection we used a chicken polyclonal antibody against β galactosidase (Abcam) followed by a goat anti chicken IgY secondary antibody conjugated to CyTM2 (Abcam). Neuronal cells were identified using the monoclonal antibody against neuronal class III tubulin (Tuj1, Covance) and glial cells using the rabbit polyclonal anti GFAP (Thermofisher).

Foot printing measurement

Walking pattern was documented in both WT and LKB1 cKO mice at P21 by dipping foot pads of the hind feet into black Chinese ink and allowing the animal to walk on paper strips. Parameters of footprints were evaluated by measuring left and right stride length and sway length (distance between the two feet).

Western blot analysis.

Western blot analysis was performed as described previously (Nony et al. 2003). Briefly, JoMa1.3 cells were lysed in classical lysis buffer (Hepes 50 mM, NaCl 150 mM, EDTA 5 mM, 1% NP40) and 20 μ g of protein extracts were separated in SDS-10% polyacrylamide gels and transferred to PVDF Immobilon-P membranes (Millipore). After blocking, membranes were incubated overnight with different antibodies as described above and in Table 4 in blocking solution at 4°C and with horseradish peroxidase-conjugated anti-rabbit or anti-mouse immunoglobulin G (Biorad) for 1 h at room temperature. Immunoreactive proteins were detected with Amersham ECL chemiluminescence reagents (GE Healthcare) according to the manufacturer's instructions. Quantifications were performed using ImageJ software. Each band intensity for phospho- and total-proteins were first normalized to actin and then phospho-proteins were normalized to total proteins. Values for siLkb1 condition were indexed to siCont.

MitoTracker staining

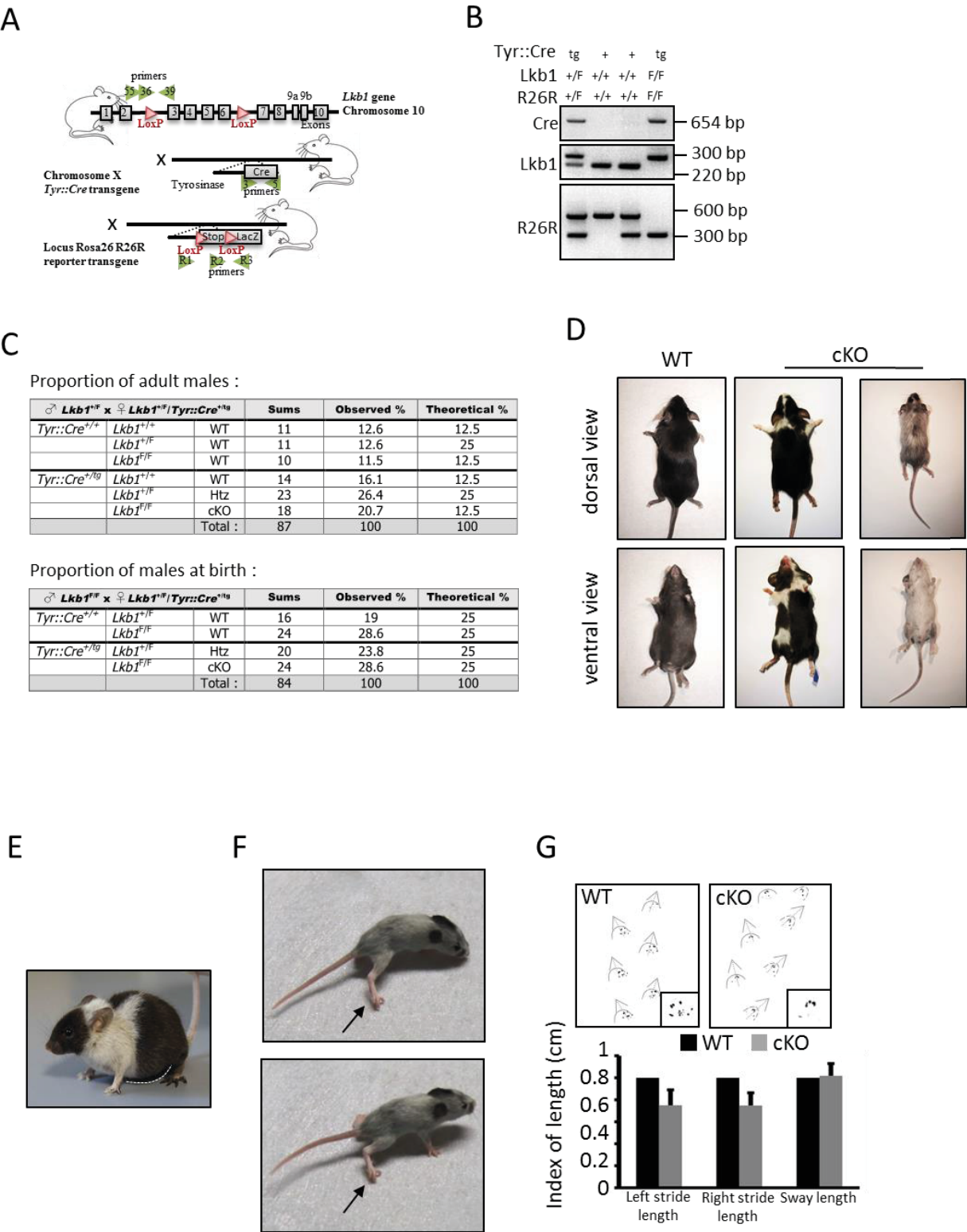
After the first cycle of siRNA transfection against *Lkb1*, 2×10^4 JoMa1.3 cells/ml were seeded on

coverslips coated with Fibronectine (10µg/µL, 1h at 37°C) and Poly-L-Lysine (10µg/µL, 1h at 37°C) and re-transfected as previously described. After 96h of the second cycle of transfection, cells were harvested and stained with 200 nM MitoTracker Red CMX-ROS (Invitrogen) or with MitoTracker Green (Invitrogen) for 30 min at 37°C in DMEM medium. For mitochondrial mass quantification, cells were directly analyzed by FACS (Accuri-C6, BD-Biosciences). To assess the mitochondrial network morphology, JoMa1.3 cells were rinsed 3 times in PBS. Cells were fixed in 4% paraformaldehyde and analyzed by biphoton confocal microscopy (LSM510, Zeiss).

RNA extraction and quantitative Real-Time PCR (RT-qPCR)

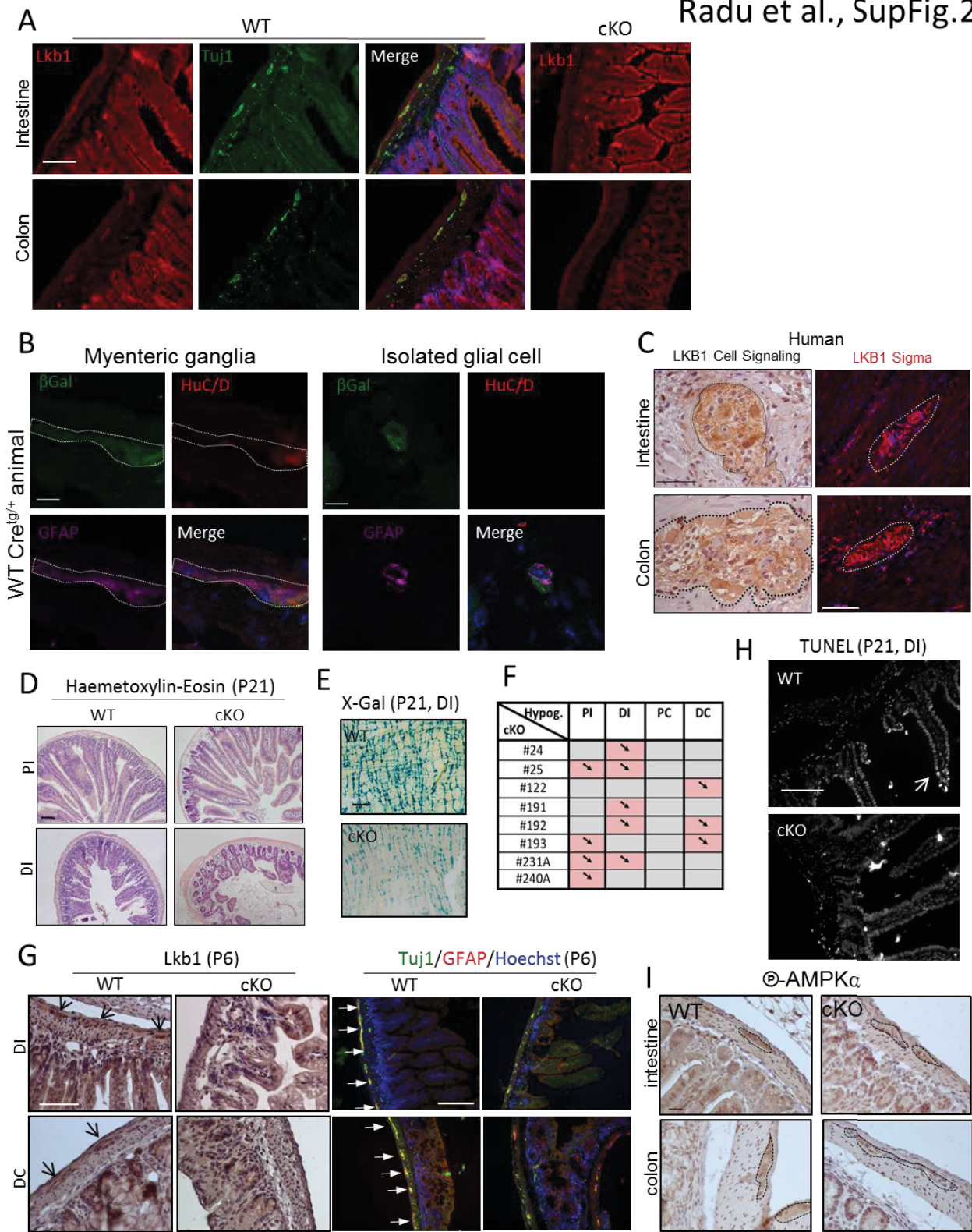
RNAs were extracted from about 10⁷ JoMa1.3 cells per condition using the Nucleospin miRNA Kit (Macherey-Nagel) according to the manufacturer's protocol and was quantified using a Nanodrop 1000.

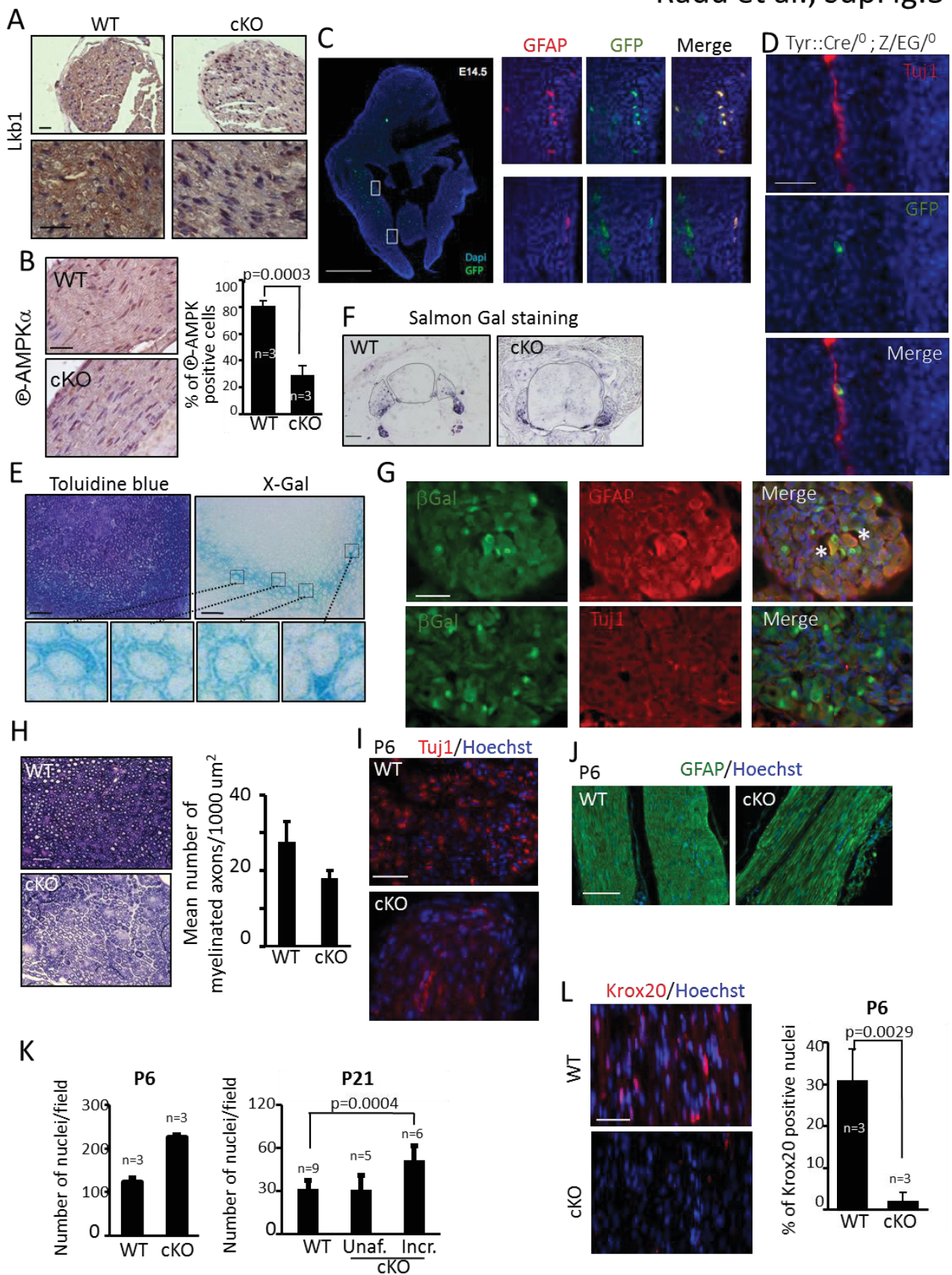
A total of 1µg was reverse transcribed using the i-Script gDNA Clear cDNA Synthesis (Biorad). For primer pairs giving no Ct before 30 cycles (*SOX10*, *p75^{NTR}*, *GFAP* and *S100B*), a pre-amplification step was performed using the SsoAdvanced Preamp Supermix (Biorad) according to the protocol. Relative quantitative PCRs were performed using Sso Advanced Universal SYBR Green Supermix (Biorad) with 2µl of cDNAs diluted 1/5 (in triplicates) and run on the CFX96 Touch Real-Time PCR Detection System (Biorad). Negative controls were performed in the same conditions without the transcriptase reverse. The housekeeping genes *AUP1* and *RELA* were used as controls. For each gene, expression levels were normalized to *AUP1* housekeeping genes using the Delta Ct method. For each point, results were expressed as a ratio (progenitor/glia or siLkb1/siCont.) of the means of DeltaDeltaCt values +/- standard deviation using data from 4 or 5 independent RT-qPCR experiments.

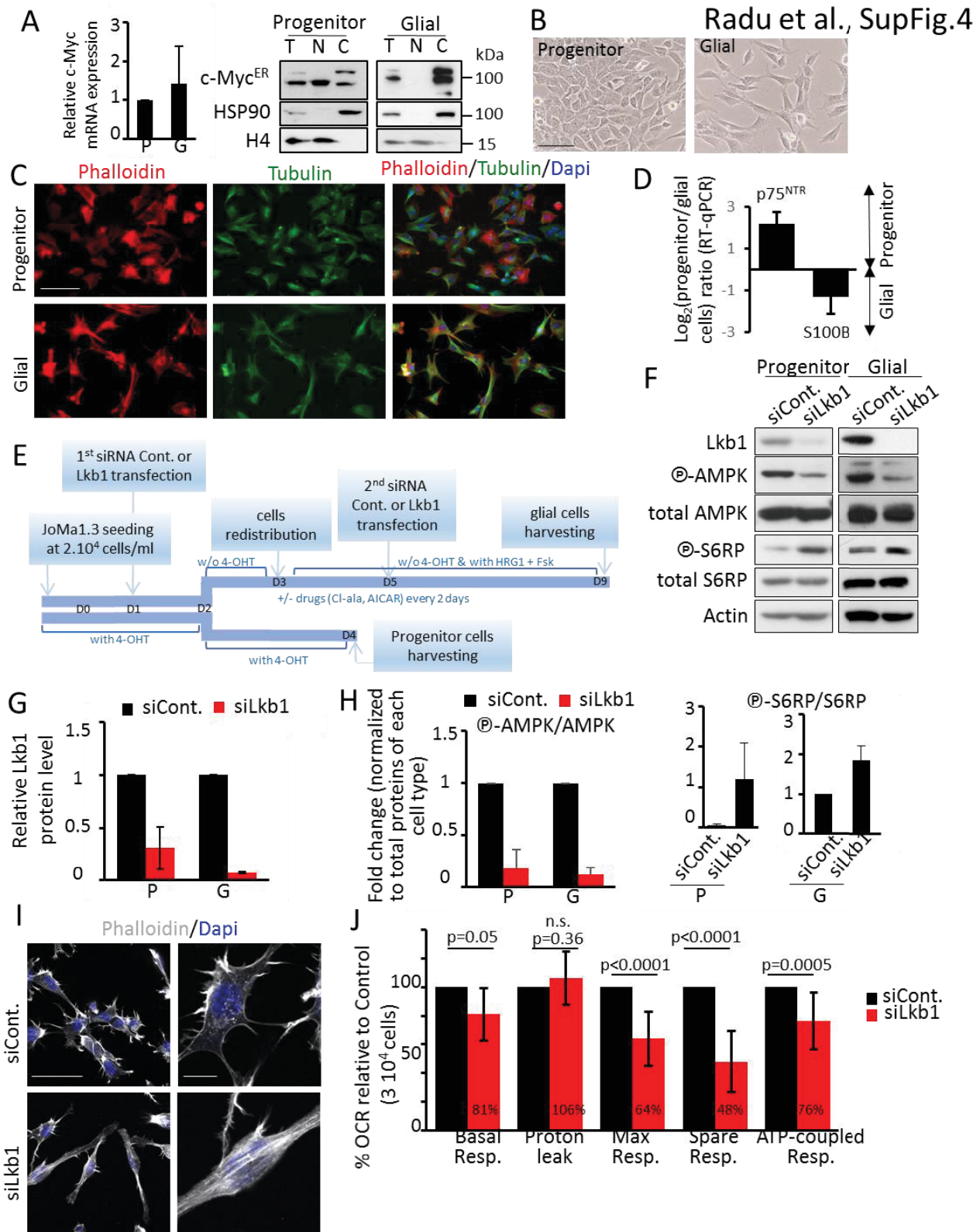


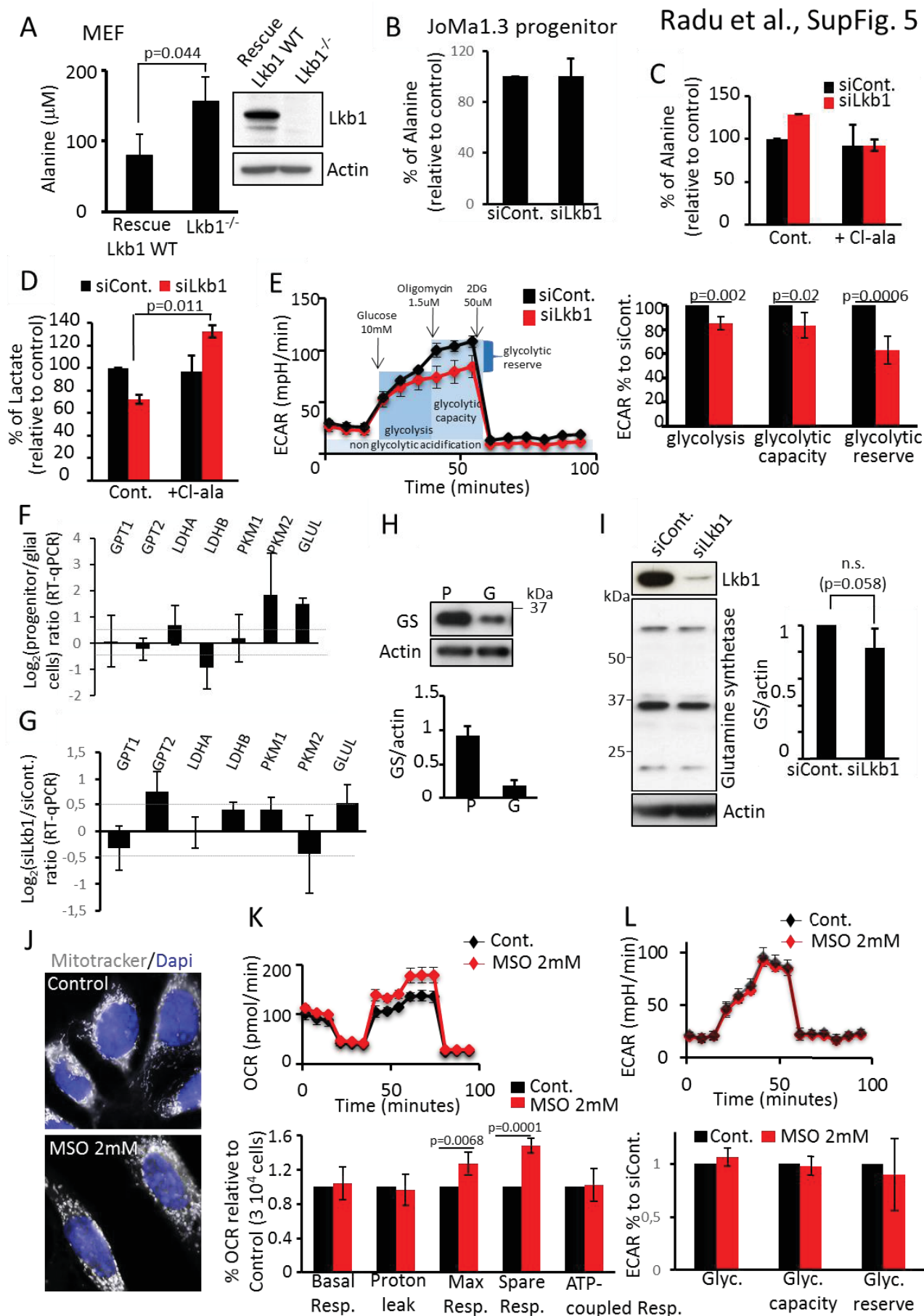
PROJECT 2. LKB1 METABOLIC & SIGNALING REGULATION IN NCC

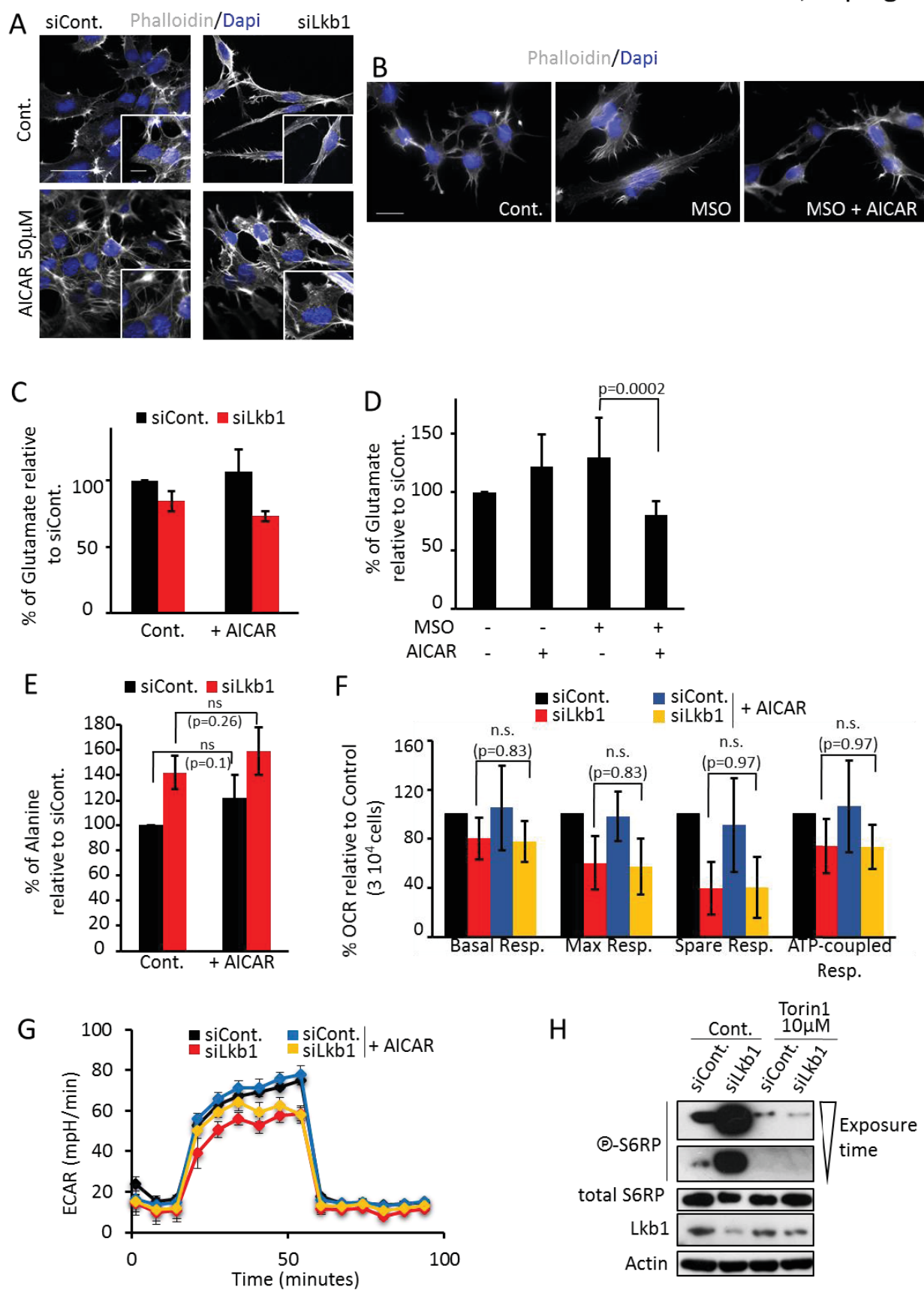
Radu et al., SupFig.2











1.3 Conclusions

During this second project which represents my main PhD project, I identified that *Lkb1* is crucial for the specification and maintenance of NCC-derivatives in the peripheral nervous system. Our work unveils a critical function of *Lkb1* in Schwann cell lineage as well as in the post-natal maintenance of myenteric and submucosal plexi of the enteric nervous system.

Several articles have already underlined the role of *Lkb1* in Schwann cell maturation and differentiation (Beirowski et al., 2014; Pooya et al., 2014; Shen et al., 2014). In these studies *Lkb1* was inactivated specifically in Schwann cells by using:

- myelin protein zero (P0)::Cre driver expressed at E14.5 in immature Schwann cells (Beirowski et al., 2014; Feltri et al., 1999) (Figure 1).
- or by using 2'3'-cyclic nucleotide 3'-phosphodiesterase (Cnp)::Cre driver. Cnp is expressed at E12.5 in neural crest cells and in central nervous system, in oligodendrocytes (Chandross et al., 1999; Genoud et al., 2002; Shen et al., 2014).

In a later stage, Cnp is expressed in myelin-forming Schwann cells (Figure 1) (Pooya S et al., 2014). Cnp::Cre expression is higher in the later stage and *Lkb1* role, in the literature, was associated only to this myelinating stage (Pooya S et al., 2014; Shen et al., 2014).

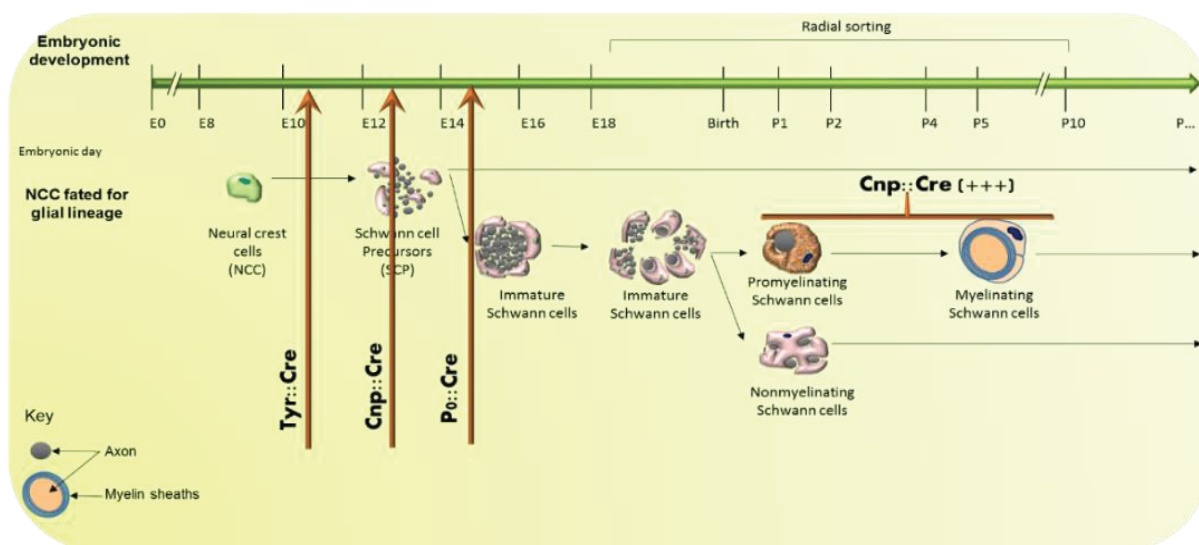


Figure 1. Cre drivers used for *Lkb1* conditional depletion in NCC or Schwann cell lineage

However, both existing models are not appropriated to study *Lkb1* functions in NCC lineage because P0 is expressed after NCC specification and Cnp is expressed also in central nervous system. Thereby, in our study, by using Tyrosinase (Tyr)::Cre driver we inactivated *Lkb1* specifically in NCC before their commitment to melanocytic, enteric or Schwann lineages (Figure 1), making it a good model to study NCC lineage.

Furthermore, by using this model and a NCC line able to be differentiated *in vitro* in glial cells, I uncovered a link between pyruvate-alanine cycling, the mTOR pathway and glial differentiation. *Lkb1* controls glial commitment by regulating the non-essential amino acids

levels (alanine, glutamate) through the mTOR pathway. These results are in line with the literature. Beirowski et al. have shown that mTORC1 activation blocked Schwann cell maturation. This phenotype is restored by Rapamycin, an mTORC1 inhibitor (Beirowski et al., 2017). The value-added contribution of our study to the existing literature is the original mechanism by which *Lkb1* regulates mTOR activation through alanine-pyruvate transamination. Moreover, in our study we highlighted that mTOR is not only important for Schwann cell maturation, but also earlier during NCC specification.

Several researchers have shown that AICAR reverts metabolic syndromes in murine models like insulin-resistant diabetic (*ob/ob*) mice (Song et al., 2002), obese (*fa/fa*) Zucker rats (Bergeron et al., 2001; Buhl et al., 2001) and insulin-resistant high-fat fed rats (Iglesias et al., 2002). In our study we have shown that AICAR rescued glial differentiation of *Lkb1*-deficient NCC and treatment of *Lkb1*-deficient mice with AICAR prevented the peripheral nerve and enteric nervous system phenotypes.

Even if AICAR has promising effects in murine models, it is not used in treatment of human pathologies like type 2 diabetes or other metabolic diseases because of its short half-life and poor bioavailability which compels to use high doses causing side effects of liver hypertrophy and lactic acidosis (Coughlan et al., 2014; Winder, 2008). Therefore it will be interesting to explore if other treatments like inhibitors of transaminases or diet alimentation are also able to prevent *Lkb1*-dependent NCC defects.

The phenotypes of the two mouse models with conditional inactivation of *Lkb1* specifically in NCC, presented in Projects 1 and 2 (“early” and “late” models respectively) recapitulate many clinical features of human NCC disorders called neurocristopathies (see Introduction, Chapter II.3). This suggests that defects of *Lkb1* signaling could be involved in a wider range of human pathologies than only the Peutz-Jeghers syndrome as described so far.

Furthermore, some ribosomopathies (pathologies due to defective ribosome biogenesis, also described in Introduction, Chapter II.3) harbors similar NCC defects as neurocristopathies. Several of these pathologies involve aberrant p53 activation and the pathological phenotype of several mouse models of neurocristopathies and ribosomopathies can be rescued by p53 inactivation (Introduction, Chapter III.B.4). Therefore, in the continuity of these results I analyzed the levels and activity of p53 in our NCC cell model and studied the *Lkb1*/p53 crosstalk in NCC development.

2. LKB1 regulates NCC differentiation by limiting p53 signaling and controlling lysosomal activity.

Article Nb3: Radu *et al.* in preparation

2.1 Scientific context and results summary

p53 is a transcription factor known as the guardian of the genome. Unrestrained signaling of p53 has been described in both human neural crest disorders and mouse models of neurocristopathies and ribosomopathies (see Introduction Chapter II.3). The transcription factor p53 is activated partly by phosphorylation on serine 15 in response to cellular stress such as accumulation of reactive oxygen species (ROS) and DNA damage. Activated p53 then modulates cellular adaptation to stress by acting on cell cycle, autophagy and metabolism and, depending on the stress level, on prooxidant or antioxidant actors. Along this line, ROS limitation, p53 genetic loss or p53 inhibition with the chemical inhibitor pifithrin- α prevented neural crest defects in several genetic mouse models (Hayano *et al.*, 2015; Jones *et al.*, 2008; McGowan *et al.*, 2008; Noack Watt *et al.*, 2016; Pani *et al.*, 2002a; Sakai *et al.*, 2016; Van Nostrand *et al.*, 2017; Watkins-Chow *et al.*, 2013); Introduction, Chapter III.B.4). Altogether, these data support the important contribution of oxidative stress and p53 signaling to neural crest formation and open new therapeutic strategies to counteract neural crest defects (Danilova and Gazda, 2015a; Van Nostrand and Attardi, 2014).

By using the NCC line and *in vitro* glial differentiation as in the previous study, I have shown that *Lkb1* loss triggers increased p53 phosphorylation on serine 15 during NCC-derived glial differentiation. This hyperphosphorylation in *Lkb1*-silenced NCC is promoted by oxidative DNA damage induced by increased ROS production. Treatment of NCC with the antioxidant N-acetyl cysteine, prevented ROS accumulation, DNA damage and p53 phosphorylation. p53 hyperphosphorylation was validated *in vivo* on sciatic nerve sections of *Lkb1* knockout animals from the “late” inactivation model (Tyr::Cre driver). Moreover, during this study I underlined a link between *Lkb1* signaling and lysosomal homeostasis. mTOR and LKB1/AMPK signaling are activated at the lysosome surface by the same protein complexes and their activation is highly dependent on amino acid levels (Introduction, Chapter IV.2). Interestingly, I demonstrated that *Lkb1* loss during glial differentiation leads to aberrant lysosomal topology and massive accumulation of autofluorescent granules with characteristic spectral emission. The granules, known as lipofuscin granules correspond to defective lysosomes which are filled with unsorted oxidized proteins, lipids and metal ions and they accumulate with aging in cells of various tissues. Increase of oxidative damage of DNA and accumulation of oxidized proteins and lipids represent a typical feature of premature aging resulting from imbalanced prooxidant and antioxidant activities. This recent study thus provides new insights into NCC development and expand our understanding of the role of LKB1 on oxidative stress regulation, partly via its crosstalk with p53 signaling and lysosomal homeostasis in neural crest disorders.

2.2 Results

Lkb1 prevents oxidative stress-induced p53 and controls lysosomal homeostasis during glial commitment of neural crest cells

Anca G. Radu¹, Sakina Torch¹, Anthony Lucas¹, Marie Mével¹, Renaud Blervaque¹, Karin Pernet-Gallay², Mylène Pezet³, Florence Fauvelle⁴, Laura Attardi⁵, Marc Billaud⁶, Pierre Hainaut¹, Chantal Thibert^{1*}

Tumor Molecular Pathology and Biomarkers, Univ. Grenoble Alpes, CNRS, Inserm, CHU Grenoble Alpes IAB, 38000 Grenoble, France

INSERM U836, F-38700 Grenoble, France; Univ. Grenoble Alpes, GIN, F-38700 Grenoble, France

Core facility on Optical microscopy, Univ. Grenoble Alpes, CNRS, Inserm, CHU Grenoble Alpes IAB, 38000 Grenoble, France

Grenoble MRI Facility IRMAGE, INSERM/CEA U817 Univ Grenoble Alpes, Grenoble Neurosciences Institut Grenoble, F-38700, France; Armed Forces Biomedical Research Institute

Stanford University, CA, USA

Clinical and experimental model of lymphomagenesis, Univ Lyon, Université Claude Bernard Lyon1, INSERM 1052, CNRS 5286, Centre Léon Bérard, Centre de recherche en cancérologie de Lyon, France.

* corresponding author: to whom correspondence should be sent: chantal.thibert@univ-grenoble-alpes.fr

Abstract

Neural crest cells constitute an embryonic subpopulation of highly invasive multipotent cells giving rise to many derivatives in several organs. These cells are particularly sensitive to oxidative stress and p53 signaling levels. We recently uncovered that the tumor suppressor and master kinase LKB1 contributes through pleiotropic roles to neural crest cells formation. In particular, we highlighted that LKB1-metabolic regulations are essential for neural crest cells-derived glial differentiation. In the present study, we explored if oxidative stress and p53 signaling contribute to LKB1-dependent control of neural crest cells fate. We reported, using a neural crest stem cell line, that Lkb1 limits oxidative DNA damage during glial differentiation. Mechanistic analyses showed that oxidative DNA damages upon *Lkb1* knockdown trigger p53 hyper-phosphorylation both *in vitro* and *in vivo*. Concomitant to aberrant p53 signaling, *Lkb1* loss triggers increased autophagy and defective lysosomal homeostasis leading to accumulation of oxidized lipids and proteins as well as metals. Strikingly, AICAR treatment, which rescues glial differentiation upon *Lkb1* loss, prevented p53 hyper-phosphorylation. Collectively, these results provide the first evidence that LKB1 limits oxidative DNA damages in neural crest cells, therefore preventing activation of the p53 signaling and extend our mechanistic understanding of the essential metabolic controls exerted by LKB1 during neural crest formation.

Key words: neural crest cells; glial differentiation; LKB1/AMPK; oxidative DNA damages, p53 signaling, lysosomal homeostasis

Introduction

The neural crest is composed of highly invasive multipotent cells called neural crest cells (NCC), that delaminate from the dorsal part of the neural tube and migrate along stereotypical paths. Once they reach

their target organs, they give rise to a broad range of derivatives such as osteocytes and chondrocytes of the craniofacial skeleton, pigment cells, enteric neurons and glial cells and sensory neurons and Schwann cells of the peripheral nerves (Le Douarin and Kalcheim, 1999). In human, defects in NCC formation lead to a wide group of disorders called neurocristopathies or ribosomopathies when genetic mutations affect ribosomal functions.

Cranial NCC naturally produce high levels of endogenous oxidative stress (Sakai et al., 2016). Furthermore, NCC are very sensitive to exogenous oxidative stress. Alcohol exposure in fetal alcohol disorders or high glucose levels in case of maternal diabetes are examples of causative agents leading to accumulation of reactive oxygen species (ROS) in NCC (Chen et al., 2013a, 2013b; Morgan et al., 2008; Sakai and Trainor, 2016; Wei and Loeken, 2014).

Additionally, aberrant signaling of the tumor suppressor and transcription factor p53 was observed in several genetic models targeting NCC formation (Danilova et al., 2010; Jones et al., 2008; Noack Watt et al., 2016; Pani et al., 2002b) as well as in patients with neural crest defects (Van Nostrand and Attardi, 2014). Half-life stabilization of p53 protein by blocking its degradation by Mdm2 triggers typical neural crest defects (Rinon et al., 2011; Van Nostrand et al., 2014b). Genetic loss or chemical inhibition of p53 prevented neural crest defects in several genetic models (Hayano et al., 2015; Jones et al., 2008; Noack Watt et al., 2016; Pani et al., 2002b; Van Nostrand et al., 2014b). It was shown recently that p53 activation is the result of increased oxidative stress and subsequent DNA damages (Sakai et al., 2016). Altogether, these data support the essential contribution of oxidative stress and aberrant p53 signaling to defects in crest formation (Danilova and Gazda, 2015b; Van Nostrand and Attardi, 2014).

We recently discovered the tumor suppressor and serine/threonine kinase LKB1 (encoded by the *STK11* gene) as a major actor of NCC formation. We described that LKB1 is required for vertebrate head

formation through the control of delamination, migration, survival and differentiation of cephalic NCC (Creuzet et al., 2016). We also highlighted that LKB1 is essential for the maintenance of the enteric nervous system as well as for glial commitment of the Schwann cell lineage (Radu et al., submitted). Our mechanistic analyses uncovered that LKB1 is required for glial commitment through the control of pyruvate-alanine cycling upstream of mTOR limitation. Interestingly, AICAR, an AMP precursor, prevented neural crest defects due to *Lkb1* loss *in vivo* (Radu et al., submitted).

LKB1 acts through the activation of 14 AMPK-related kinases that regulate cell polarization and energy metabolism during cell proliferation and differentiation among several cellular processes (Alessi et al., 2006b; Hezel and Bardeesy, 2008; Shackelford and Shaw, 2009; Shorning and Clarke, 2011). Regulation of energy metabolism by LKB1 occurs through the activation of the AMP-activated protein kinase (AMPK), a sensor that adapts energy supply to the nutrient demands of cells facing metabolic stress (Shackelford, 2013). LKB1 has been also shown to limit oxidative stress, thereby protecting the genome from oxidative damage (Xu et al., 2015). Furthermore, LKB1 preserves genome integrity and therefore protects cells from genotoxic stress through activation of the DNA repair BRCA1 pathway (Gupta et al., 2015).

To better understand if oxidative stress and p53 signaling contribute to LKB1-dependent control of NCC fate, we measured oxidative stress levels upon *Lkb1* knockdown during glial commitment of NCC. We report here, using a neural crest stem cell line, that *Lkb1* limits oxidative DNA damage during glial differentiation. Mechanistic analyses show that oxidative DNA damages upon *Lkb1* knockdown trigger p53 hyper-phosphorylation both *in vitro* and *in vivo*. Concomitant to aberrant p53 signaling, *Lkb1* loss triggers increased autophagy and defective lysosomal homeostasis leading to accumulation of oxidized lipids and proteins as well as metals. Strikingly, AICAR treatments, which rescue glial differentiation upon *Lkb1* loss, prevented p53 hyper-

phosphorylation. These results provide evidence that Lkb1 limits oxidative DNA damage of NCC progenitors and derivatives, therefore preventing activation of the p53 signaling.

Results

Lkb1 loss triggers oxidative DNA damages

Among metabolites previously identified by ¹H HRMAS RMN metabolomics profiling of sciatic nerves from wildtype or conditional NCC *Lkb1* knockout animals (Tyr::Cre;Lkb1^{F/F} mice; Radu et al., submitted), we observed that several antioxidant metabolites were upregulated upon *Lkb1* loss (Fig. 1A) as quantified for total creatine (Fig. 1B). This observation is suggestive of increased oxidative stress upon *Lkb1* inactivation as supported by data from the literature (Gupta et al., 2015; Xu et al., 2015). We therefore measured intracellular ROS levels *in vitro* using DCFDA, a fluorogenic dye that measures hydroxyl, peroxy and other ROS activity, in the JoMa1.3 mouse neural crest stem cell line that can either be maintained in a progenitor state or differentiated into glial cells among other NCC derivatives (Maurer et al., 2007). DCFDA fluorescence intensity was increased upon *Lkb1* knockdown in JoMa1.3 cells committed to glial lineage compare to control cells (Fig. 1C). This fluorescence indeed corresponds to increased ROS levels as it was completely abrogated by pre-treating the cells with the antioxidant N-Acetyl-Cystein (NAC) (Fig. 1D). Next, we assessed if *Lkb1* knockdown was also associated with oxidative DNA damage as a direct consequence of elevated ROS. Immunostaining of cells of γ -H2AX, a DNA damage marker, showed a clear increase in labelling (Fig. 1E). Pre-treatment of cells with the antioxidant NAC partially prevented the accumulation of DNA damage (Fig. 1F). Altogether, these data demonstrate that Lkb1 signaling protects cells committed to glial lineage from oxidative DNA damage.

Oxidative DNA damages upon Lkb1 loss cause p53 hyper-phosphorylation

Next, we explored if the increased oxidative stress observed upon *Lkb1* loss could trigger p53 signaling. We therefore explored p53 expression, stability and post-translational modifications upon *Lkb1* knockdown either in progenitors or glial derivatives NCC. Expression of *p53* gene was not modulated upon *Lkb1* knockdown as quantified by RT-qPCR on JoMa1.3 cells compared to control cells (Fig. 2A). Immunoblot analyses over several independent experiments did not show any reproducible p53 stabilization (Fig. 2B). However, they highlighted a 4-5 folds increase of p53 phosphorylated at Serine¹⁵ (Fig. 2B, images and graphs). Immunofluorescence staining confirmed the accumulation of phosphorylated p53 at Serine¹⁵ upon *Lkb1* knockdown either in progenitors or glial cells (Fig. 2C). Staining of phosphorylated p53 at serine¹⁵ on sciatic nerve sections upon conditional ablation of *Lkb1* in neural crest cells using the Tyr::Cre;Lkb1^{F/F} mice (Radu et al., submitted) confirmed *in vivo* the increased of p53 phosphorylation upon *Lkb1* loss (Fig. 2D). To assess if p53 induction was due to oxidative DNA damage during glial differentiation, we visualized phosphorylated p53 at serine¹⁵ in JoMa1.3 cells with or without NAC treatment. We observed that NAC effectively suppressed p53 hyper-phosphorylation (Fig. 2E).

Phosphorylation of p53 at serine¹⁵ has been associated with transcriptional activity of p53 (Khanna et al., 1998). We therefore evaluated p53 transcriptional activity upon *Lkb1* knockdown in JoMa1.3 cells by assessing the expression level of classical p53 target genes corresponding to several cell functions such as cell cycle, DNA repair, stem cell, maintenance or autophagy. None of them were upregulated upon *Lkb1* loss during glial commitment (Fig. 2F), suggesting that increase of p53 phosphorylated on serine¹⁵ was not associated with upregulation of the transcriptional activity of p53.

Together, these data thereby highlighted aberrant p53 signaling upon *Lkb1* loss as a consequence of increased oxidative stress.

Lkb1 sustains lysosomal proteolytic activity

p53 signaling is intimately related to autophagy flux (Kruiswijk et al., 2015). We therefore explored if hyper-phosphorylated p53 resulted in defective autophagy. *Lkb1* silencing in JoMa1.3 cells upon led to massive LC3-II accumulation and p62 degradation as assessed by western blot analyses (Fig. 3A). Increased autophagy was also detected *in vivo* by immunofluorescence staining of LC3 on sciatic nerves sections of *Lkb1* cKO animals compared to WT mice (Fig. 3B).

While performing immunofluorescence analysis of JoMa1.3 cells, we noticed upon *Lkb1* loss the presence of vesicles with a strong autofluorescence. Cells analyses without any labelling, confirmed the presence of autofluorescent vesicles with green brighter than blue or red fluorescence (Fig. 3C). Using confocal spectral microscopy, we better characterized the spectral properties of these autofluorescent inclusions and showed that control cells compare to cells with *Lkb1* knockdown exhibit very few of these structures (Fig 3D, pictures) and their spectral properties are distinct to those in cells with *Lkb1* knockdown (Fig. 3D, graph). Strikingly, electron microscopy analyses of JoMa1.3 glial cells highlighted strongly aberrant late endosomal/lysosomal compartment upon *Lkb1* knockdown whereas these structures were seen in control cells to a much lower extent and never as large as in the absence of *Lkb1* (Fig. 3E). These late endosomes/lysosomes upon *Lkb1* silencing appeared particularly charged in structures very dense to electron. Data collected from epifluorescence and confocal spectral microscopy as well as from electron microscopy strongly suggest that these autofluorescent inclusions correspond to lipofuscin granules known to accumulate in cells over time and use as markers of premature aging.

In vivo, we did not detect strong accumulation of such autofluorescent inclusions neither in dissociated nerves fibers nor in nerve sections upon *Lkb1* loss. However, while analyzing electron microscopy data performed on sciatic nerve sections of *Lkb1* cKO

animals, we observed that myelinating Schwann cells upon *Lkb1* loss harbored aberrant lysosomal structures corresponding to polymorphic late endosomes (Fig. 3F).

Off note, we observed that although phosphorylated p53 was localized in the nucleus of some cells, in others it localized at specific perinuclear structures that correspond to autofluorescent inclusions (Fig. 3G).

AICAR rescues glial differentiation by preventing p53 activation and lysosomal defects

In our previous study, we demonstrated that AICAR, an AMP precursor, was able to rescue glial differentiation *in vitro* upon *Lkb1* silencing and prevented *in vivo* the neural crest defects due to *Lkb1* inactivation (Radu et al., submitted). Surprisingly, when analyzing immunofluorescence staining of JoMa1.3 cells with the glial marker S100, we noticed a disappearance of the perinuclear inclusions upon AICAR treatment (Fig. 4A). Western blot analyses upon AICAR treatment showed that AICAR limited p53 phosphorylation at Serine¹⁵ (Fig. 4B). Immunofluorescence staining in JoMa1.3 cells confirmed that AICAR prevented phospho-p53 accumulation (Fig. 4C). Together, these data suggest that AICAR treatment prevented p53 activation and rescued lysosomal homeostasis.

Discussion

Neural crest cells are very sensitive to oxidative stress accumulated upon genetic mutations disturbing endogenous signaling or upon exposure to environmental factors such as alcohol or high glucose levels. Along this line, our work reveals that LKB1 controls metabolic pathways essential to limit the production of reactive oxygen species (ROS), and consequently DNA damages and p53 signaling, during NCC differentiation.

Our study also uncovers a major regulation exerted by the LKB1/AMPK pathway on lysosomal homeostasis. Indeed, we observed massive

defective lysosomal activity upon *Lkb1* loss either *in vivo* in myelinating Schwann cells of sciatic nerves or *in vitro* either in progenitors or in cells committed to the glial lineage. Under conditions of metabolic stress, LKB1/AMPK are activated by protein complexes (a vATPase and the Ragulator complex) localized at the lysosomal surface. These proteins are the same that activates mTOR signaling when the cells are in high nutrients conditions. Therefore, lysosomal membrane surface assembles and coordinates the activities of the antagonistic kinase hubs mTOR complex 1 and AMPK. Our previous work has shown the important link between LKB1/AMPK and mTOR signaling during metabolic modulations during differentiation (Radu et al., submitted). Both mTOR and AMPK control lysosomal homeostasis. mTOR activity triggers lysosomal tubulation, a dynamic process that requires lysosome moving along microtubules (Hipolito et al., 2018). Indeed, mTOR stimulates the level of Arl8b GTPase on lysosomes which boosts the motor protein kinesin-1 activity and therefore lysosome extension. AMPK inhibits both mTORC1/2 and the transcription factor TFEB, a master regulator of a transcriptional program of cellular adaptation to stress (Hipolito et al., 2018; Martina and Puertollano, 2017). Collectively, our data uncovering the crucial involvement of LKB1/AMPK in NCC formation also highlighted how this signaling impacts cytoskeleton dynamic. Indeed, LKB1 contributes to cranial NCC formation through a sequential activation of the AMPK/Rho/ROCK1 pathway to control phospho-MRLC and actin dynamic (Creuzet et al., 2016). We also described that metabolic deregulations of amino acid levels and impaired glial differentiation are associated with massive actin and tubulin cytoskeleton reorganization upon *Lkb1* loss (Radu et al., submitted). Moreover, LKB1 through its downstream kinase NUA1, immobilizes mitochondria along microtubules, an essential process during terminal axon branching in neurons (Courchet et al., 2013).

Our observations, collectively with massive data from the literature, suggest that impaired LKB1/AMPK

activity triggers a metabolic energy imbalance with a drop cellular ATP pool. Along this line, we identified that the AMP precursor AICAR is able to rescue glial differentiation (Radu et al., submitted). In this study, we also observed that AICAR limits oxidative DNA damages and subsequent p53 hyperphosphorylation, as well as rescue lysosomal function. One hypothesis to explain this striking result is that AICAR refurnishes the ATP pool of the cell. Indeed, AICAR is an IMP analog and therefore an AMP and then ATP precursor through several enzymatic reactions belonging to the late steps of the pentose phosphate pathway. Therefore, AICAR treatment of cells could refurnish the ATP pool, which in turn could contribute to various cellular processes required to adjust cell homeostasis upon LKB1 loss. One example among several concerns kinesin-1 activity since to direct lysosome motility on microtubules, this motor protein requires ATP. Altogether, emerging knowledge highlights that lysosomes remodeling is essential for cell adaptation in response to various stresses. Exploring the molecular mechanisms linking amino acid levels, LKB1/mTOR pathways and lysosomes motility on cell cytoskeleton is therefore of critical interest.

Neurocristopathies represent a large group of human diseases due to defects in neural crest formation. These pathologies associate several clinical phenotypes such as craniofacial abnormalities, hearing loss, megacolon (as a result of enteric ganglia agenesis), cardiac or pigmentation defects (Mayor and Theveneau, 2013)(Mayor and Theveneau, 2013). Similar abnormal development of the neural crest also occurs in diseases with deficient ribosome biogenesis called ribosomopathies, besides defects in blood cells formation leading in particular to anemia (Danilova and Gazda, 2015b). Many genetic factors are associated with the etiology of these pathologies. However, these diseases often present a phenotypic variability that is independent of the genotype and which could be the results of environmental factors leading to oxidative stress. Multiple reconstructive surgeries improve the condition of patients with craniofacial malformations

whereas removal of the aganglionic segment is the current treatment for megacolon. Nonetheless, surgery is rarely fully corrective and efforts have been made recently to explore preventive therapeutic approaches. Limiting oxidative stress in particular gave very promising results (Sakai et al., 2016). Therefore, future exploration of LKB1-controlled oxidative DNA damages during neural crest formation will be an essential part of a more general approach to identify molecular events limiting neural crest defects upon oxidative stress and which will be of crucial importance in developing potential preventing therapies.

Methods

Animals and genotyping

Generation and genotyping of the *Tyr::Cre;Lkb1^{FF};R26R* mice to conditionally inactivate *Lkb1* in neural crest-derived tissues have been reported previously (Radu et al., submitted). Since the *Tyr::Cre* transgene is located on the chromosome X, the study was restricted to male animals. All animal experimental procedures were conducted according to the standard operating procedures of the lab animal facility and were approved by the Animal Ethics Committee of Grenoble (Permit number 261_ IAB-U823-CT-01).

Neural crest cell culture conditions, siRNA transfection and metabolic drug treatments

Mouse immortalized neural crest cells (JoMa1.3) were cultured as described previously (Radu et al., submitted). Commitment of these cells into the glial lineage was achieved by adding Heregulin (50 ng/mL; Peprotech,120-02) and Forskolin 5 μ M (Sigma) to the JoMa1.3 culture medium during 6 days.

Short interfering RNAs (siRNA) against the mouse *Lkb1* gene and the Non-targeting control siRNA were purchased from Dharmacon (ON-TARGET plus mouse Stk11 SMART pool and ON-TARGET plus Non-targeting Pool, Dharmacon). siRNAs were transfected (11 nM) into JoMa1.3 cells by using JetPrime (Ozyme) according the manufacturer's

protocol. For non-differentiated JoMa1.3, experiments were realized 72h post-transfection. For differentiated JoMa1.3, two cycles of 96h of *Lkb1* knockdown were performed, as described previously (Radu et al., submitted).

During the 6 days of cell differentiation and the second cycle of *Lkb1* inactivation, cells were incubated at 37°C in NCC medium changed every two days from D4 to D9 with or without 50 μ M AICAR (a metabolic regulator and AMPK agonist).

Histology, Immunohistochemistry and immunofluorescence staining

Sciatic nerves samples were dehydrated, embedded in paraffin and sectioned by Anipath (Lyon, France). For immunohistochemistry, sections were deparaffinized and rehydrated, rinsed in PBS and boiled for 20 minutes at 95°C in a decloaking chamber (Biocare Medical) in 10 mM Sodium citrate antigen retrieval buffer (pH 6). Sections were then treated with 1% H₂O₂ for 20 minutes. After 1 hour incubation in a blocking buffer (PBS-3% BSA-10% Goat preimmune serum for polyclonal antibodies or ABC MOM kit from Vector laboratories for monoclonal antibodies according to the supplier's protocol), sections were incubated overnight at 4°C with the primary antibody (see Table 3 for dilutions and antibodies references). Secondary antibodies used for immunohistochemistry were anti Mouse- and anti Rabbit-Biotin conjugated (Vector laboratories). DAB peroxidase substrate kit was used for detection of the antibodies (Vectors laboratories). Sections were then counterstained with Harris Hematoxylin (Sigma-Aldrich), dehydrated and mounted in Merckoglas (Merck).

For immunofluorescence, sections and cells cultivated on glass coverslips were treated with standard protocols using primary antibodies as described in Table 3. Secondary antibodies used were from Jackson ImmunoResearch (Donkey anti-Mouse Alexa-488, Donkey anti-Mouse Cy3, Donkey anti-Rabbit Alexa-488, Donkey anti-Rabbit Cy3, Donkey anti-Rabbit Cy2 and Goat anti-Chicken A488). For tissue sections, nuclei were stained with

Hoechst 33342 (10 μ g/ml, Invitrogen). For JoMa1.3 cells, nuclei were stained with Dapi. Sections and cells were mounted in mowiol. Analyses and acquisitions were performed using a Zeiss AxioImager Z1 microscope equipped with an AxioCam MRm camera, a Zeiss AxioImager M2 microscope, equipped with a Hamamatsu Orca R2 camera or for confocal microscopy a Zeiss AxioObserver Z1 multiparameter microscope LSM710 NLO – LIVE7 – Confocor3.

Confocal spectral microscopy

Spectral imaging was performed using a Zeiss LSM710 spectral confocal (Carl Zeiss, Jena, Germany) with 2-photon excitation at 840 nm on stain-free samples. Lambda stack acquisition was collected from 421 to 721 nm in a spectral resolution of 977 nm (QUASAR-PMT with 32 channels). Emission spectra were measured in *Lkb1*-knockdown cells for 39 inclusions from 4 different fields and for 6 inclusions in control cells from 5 different fields in ZEN 2010 software (Carl Zeiss, Jena, Germany). Fluorescence intensity was measured. Fluorescence spectra represent mean fluorescence normalized to the value of the emission bandwidth with the highest intensity.

Cell sorting and ROS quantification with DCF-DA probe

Control or *Lkb1* knockdown JoMa1.3 cells were differentiated into glial cells and treated daily with various concentrations of N-acetyl cysteine (NAC 10, 12 and 15 μ M). One hour prior to the end of the treatment, 50 μ M of 2',7'-dichlorofluorescein diacetate (DCFDA) was added to the medium and incubated for 30 minutes at 37°C. The cells were then washed with PBS and kept in culture media (with 10% SVF and without red phenol) for 30 minutes at 37°C. Cells were harvested, washed, and analyzed by flow cytometry with the red laser channel (FL-3) using a C6 BD-Accuri analyzer.

Western blot analysis.

Western blot analysis was performed as described previously (Radu et al., submitted). Antibodies and

blotting conditions used for this study are listed in Table 1. Quantifications were performed using ImageJ software. Each band intensity for phospho- and total-proteins were first normalized to actin and then phospho-proteins were normalized to total proteins. Values for *siLkb1* condition were indexed to *siCont*.

RNA extraction and quantitative Real-Time PCR (RT-qPCR)

RNAs from glial committed cells transfected with non-targeting or *Lkb1*-targeting siRNA were extracted, reverse transcribed and relative quantitative PCRs were performed as previously described (Radu et al., submitted). Negative controls were performed in the same conditions without the transcriptase reverse. The housekeeping genes *AUP1* and *RELA* were used as controls. For each gene, expression levels were normalized to *AUP1* housekeeping genes using the Delta Ct method. For each point, results were expressed as a ratio (progenitor/glial or *siLkb1*/*siCont*.) of the means of DeltaDeltaCt values +/- standard deviation using data from 4 or 5 independent RT-qPCR experiments.

Electron microscopy

Electron microscopy analyses were performed on sciatic nerve sections of Tyr::Cre;*Lkb1*;R26R mice and JoMa1.3 cells using the same protocol as described previously (Radu et al., submitted).

Graphical representations and Statistical analyses

All cell culture experiments were realized at least by three independent experiments and for one experiment, each condition was performed in triplicate. *In vivo* analyses were conducted with at least three animals per condition. The exact number of experiments is indicated in the figures or in the legends. Values are given as mean with standard deviation. Normality of the data was checked with the F-Test. The unpaired Student's *t*-test was used to generate p-values for selected pairwise comparisons and *p* < 0.05 was considered significant.

Acknowledgments

We thank P. Vernet from the animal facility of the Institute for Advanced Biosciences and A. Piras and C. Colomb from the animal facility PHTA of Grenoble. A. Bertrand, from the electron microscopy facility of the Neuroscience Institute of Grenoble performed semi-thin sections, staining and electronic microscopy experiments and analyses supervised by KPG. We thank N. Gadot and the ANIPATH facility, University Lyon1 Laennec, for tissue sections. We thank the photonic microscopy-cell imaging facility "MicroCell" from the Institute for Advanced Biosciences. The confocal microscopy tool was partly funded by the Association for Research on Cancer, French Ministry "Enseignement Supérieur et Recherche" and the Rhone-Alpes region (CPER 2007-2013). Most of this work was funded by "la Ligue régionale contre le cancer" (comité de l'Isère) and « l'Association pour la Recherche contre le Cancer ».

Bibliography

Alessi DR, Sakamoto K, Bayascas JR. 2006. LKB1-dependent signaling pathways. *Annu Rev Biochem* 75: 137–163.

Chen X, Liu J, Chen S. 2013a. Over-expression of Nrf2 diminishes ethanol-induced oxidative stress and apoptosis in neural crest cells by inducing an antioxidant response. *Reprod Toxicol Elmsford N* 42: 102–109.

Chen Y, Fan J, Zhang Z, Wang G, Cheng X, Chuai M, Lee KKH, Yang X. 2013b. The negative influence of high-glucose ambience on neurogenesis in developing quail embryos. *PLoS One* 8: e66646.

Courchet J, Lewis TL, Lee S, Courchet V, Liou D-Y, Aizawa S, Polleux F. 2013. Terminal axon branching is regulated by the LKB1-NUAK1 kinase pathway via presynaptic mitochondrial capture. *Cell* 153: 1510–1525.

Creuzet SE*, Viallet JP*, Ghawitlan M, Torch S, Thélu J, Alrajeh M, Radu AG, Bouvard D, Costagliola F, Borgne ML, et al. 2016. LKB1 signaling in cephalic neural crest cells is essential for vertebrate head development. *Dev Biol* 418: 283–296. * contribute equally to this work.

Danilova N, Gazda HT. 2015. Ribosomopathies: how a common root can cause a tree of pathologies. *Dis Model Mech* 8: 1013–1026.

Danilova N, Kumagai A, Lin J. 2010. p53 upregulation is a frequent response to deficiency of cell-essential genes. *PLoS One* 5: e15938.

Gupta R, Liu AY, Glazer PM, Wajapeyee N. 2015. LKB1 preserves genome integrity by stimulating BRCA1 expression. *Nucleic Acids Res* 43: 259–271.

Hayano S, Komatsu Y, Pan H, Mishina Y. 2015. Augmented BMP signaling in the neural crest inhibits nasal cartilage morphogenesis by inducing p53-mediated apoptosis. *Dev Camb Engl* 142: 1357–1367.

Hezel AF, Bardeesy N. 2008. LKB1; linking cell structure and tumor suppression. *Oncogene* 27: 6908–6919.

Hipolito VEB, Ospina-Escobar E, Botelho RJ. 2018. Lysosome remodelling and adaptation during phagocyte activation. *Cell Microbiol*.

Jones NC, Lynn ML, Gaudenz K, Sakai D, Aoto K, Rey J-P, Glynn EF, Ellington L, Du C, Dixon J, et al. 2008. Prevention of the neurocristopathy Treacher Collins syndrome through inhibition of p53 function. *Nat Med* 14: 125–133.

Khanna KK, Keating KE, Kozlov S, Scott S, Gatei M, Hobson K, Taya Y, Gabrielli B, Chan D, Lees-Miller SP, et al. 1998. ATM associates with and phosphorylates p53: mapping the region of interaction. *Nat Genet* 20: 398–400.

Kruiswijk F, Labuschagne CF, Voudsen KH. 2015. p53 in survival, death and metabolic health: a lifeguard with a licence to kill. *Nat Rev Mol Cell Biol* 16: 393–405.

Le Douarin N, Kalcheim C. 1999. *The neural crest*. 2nd ed. Cambridge University Press, Cambridge, UK; New York, NY, USA.

Martina JA, Puertollano R. 2017. TFEB and TFE3: The art of multi-tasking under stress conditions. *Transcription* 8: 48–54.

Maurer J, Fuchs S, Jäger R, Kurz B, Sommer L, Schorle H. 2007. Establishment and controlled differentiation of neural crest stem cell lines using conditional transgenesis. *Differ Res Biol Divers* 75: 580–591.

Mayor R, Thevenneau E. 2013. The neural crest. *Dev Camb Engl* 140: 2247–2251.

Morgan SC, Relaix F, Sandell LL, Loeken MR. 2008. Oxidative stress during diabetic pregnancy disrupts cardiac neural crest migration and causes outflow tract defects. *Birt Defects Res A Clin Mol Teratol* 82: 453–463.

Noack Watt KE, Achilleos A, Neben CL, Merrill AE, Trainor PA. 2016. The Roles of RNA Polymerase I and III Subunits Polr1c and Polr1d in Craniofacial Development and in Zebrafish Models of Treacher Collins Syndrome. *PLoS Genet* 12: e1006187.

Pani L, Horal M, Loeken MR. 2002. Rescue of neural tube defects in Pax-3-deficient embryos by p53 loss of function: implications for Pax-3- dependent development and tumorigenesis. *Genes Dev* 16: 676–680.

Radu AG*, Torch S*, Fauvelle F, Pernet-Gallay K, Blervaque R, Lucas A, Delmas V, Schlattner U, Tricaud N, Lafenechère L, Hainaut P, Tricaud N, Pingault V, Bondurand N, Bardeesy N, Larue L, Thibert C[§] and Billaud M.[§] LKB1 controls glial differentiation of multipotent neural crest cells through pyruvate-alanine transamination. Submitted.

*Contribute equally to this work; [§]co-senior and co-corresponding authors.

Rinon A, Molchadsky A, Nathan E, Yovel G, Rotter V, Sarig R, Tzahor E. 2011. p53 coordinates cranial neural crest cell growth and epithelial-mesenchymal transition/delamination processes. *Dev Camb Engl* 138: 1827–1838.

Sakai D, Dixon J, Achilleos A, Dixon M, Trainor PA. 2016. Prevention of Treacher Collins syndrome craniofacial anomalies in mouse models via maternal antioxidant supplementation. *Nat Commun* 7: 10328.

Sakai D, Trainor PA. 2016. Face off against ROS: Tcof1/Treacle safeguards neuroepithelial cells and progenitor neural crest cells from oxidative stress during craniofacial development. *Dev Growth Differ* 58: 577–585.

Shackelford DB. 2013. Unravelling the connection between metabolism and tumorigenesis through studies of the liver kinase B1 tumour suppressor. *J Carcinog* 12: 16.

Shackelford DB, Shaw RJ. 2009. The LKB1-AMPK pathway: metabolism and growth control in tumour suppression. *Nat Rev Cancer* 9: 563–575.

Shorning BY, Clarke AR. 2011. LKB1 loss of function studied in vivo. *FEBS Lett* 585: 958–966.

Van Nostrand JL, Attardi LD. 2014. Guilty as CHARGED: p53's expanding role in disease. *Cell Cycle Georget Tex* 13: 3798–3807.

Van Nostrand JL, Brady CA, Jung H, Fuentes DR, Kozak MM, Johnson TM, Lin C-Y, Lin C-J, Swiderski DL, Vogel H, et al. 2014. Inappropriate p53 activation during development induces features of CHARGE syndrome. *Nature* 514: 228–232.

Wei D, Loeken MR. 2014. Increased DNA methyltransferase 3b (Dnmt3b)-mediated CpG island methylation stimulated by oxidative stress inhibits expression of a gene required for neural tube and neural crest development in diabetic pregnancy. *Diabetes* 63: 3512–3522.

Xu H-G, Zhai Y-X, Chen J, Lu Y, Wang J-W, Quan C-S, Zhao R-X, Xiao X, He Q, Werle KD, et al. 2015. LKB1 reduces ROS-mediated cell damage via activation of p38. *Oncogene* 34: 3848–3859.

Figure legends

Figure 1. *Lkb1* loss during glial differentiation induces ROS and DNA damages.

(A) Loadings of the predictive component of the multivariate statistical model built with spectral

buckets of WT and cKO mouse ¹H HRMAS NMR spectra for identification of up (positive) and down (negative) regulated metabolites in cKO mice (data from Radu et al., submitted). The loading plots are colored according to variable importance to the projection. Assignments of some antioxidant metabolites are indicated illustrating their up-regulation upon *Lkb1* loss. WT n=16, cKO n=13 mice. (B) Mean relative amplitude of total creatine peaks in each mouse group, relative to TSP 0 ppm. (C) Representative FACS[®] profile for DCFDA oxidation in control cells (siCont.) and *Lkb1* knockdown cells (siLkb1). Profile of cells without incubation with the probe is also shown (light blue curve). (D) Same as (C) following antioxidant NAC treatment during the time course of glial differentiation of JoMa1.3 cells. (E) □H2AX DNA damage staining with or without NAC treatment. Quantification is shown on the right (n=3). (F) Immunostaining of DNA damages using □H2AX marker.

Figure 2. Oxidative DNA damage upon *Lkb1* loss triggers p53 hyper-phosphorylation.

(A) *p53* mRNA level are not change upon *Lkb1* knockdown during glial differentiation of JoMa1.3 cells. (B) Representative images of western blot showing accumulation of phospho-p53^{Ser15} in progenitors (left) and glial (right) JoMa1.3 cells. Quantification of 3 independent experiments is shown (graphs in right). (C) Immunofluorescence staining showing the increase number of positive cells for phospho-p53^{Ser15}. Quantifications are shown below (n=3). (D) Immunofluorescence staining for phospho-p53^{Ser15} on sciatic nerve sections of wildtype animals (WT) or upon inactivation of *Lkb1* (cKO). (E) Representative images of immunofluorescence staining for phospho-p53^{Serine15} upon NAC treatment of glial cells. Quantification is shown below. (F). RT-qPCR showing expression of *p53* gene in glial JoMa1.3 cells upon *Lkb1* silencing (siLkb1) compare to control cells (siCont.) (n=4).

Figure 3. *Lkb1* sustains lysosomal activity.

(A) Western blot analysis showing accumulation of LC3-II staining upon *Lkb1* knockdown associated

with p62 decrease. (B) Increased LC3 immunofluorescence staining in sciatic nerve sections upon *Lkb1* loss. (C) Epifluorescence microscopy showing autofluorescent inclusions in glial JoMa1.3 cells upon *Lkb1* knockdown mainly in the green channel. (D) Confocal spectral microscopy confirmed the large spectrum of autofluorescence with a pic for green wavelength compare to spectra of the rare inclusions found in control cells (bottom graph). (E) representative electron microscopy images of glial JoMa1.3 cells upon *Lkb1* knockdown (siLkb1) showing the accumulation of aberrant late endosomal/lysosomal compartment (arrows) compare to control cells (siCont., arrow). Images below correspond to zoom on late endosomal/lysosomal structures. m: mitochondria. (F) Electron microscopy images of sciatic nerve sections of mice with *Lkb1* inactivation (*Tyr::Cre Lkb1^{F/F}* mice) showing the increase of polymorphic endosomes in Schwann cells upon *Lkb1* loss (arrows). my.s.: myelin sheet; The percentage of myelinating Schwann cells harboring these structures is shown (bottom right). Of note, the endo-

lysosomal structures in myelinating Schwann cells of wildtype animals were never as large and filled of electron-dense material than those observed in Schwann cells of *Lkb1* cKO animals. (G) Immunofluorescence staining for phospho-p53^{Ser15} illustrating the localization of phospho-p53 to cytoplasmic inclusions (Arrows).

Figure 4: AICAR treatment limits p53 hyperphosphorylation and defective lysosomes upon *Lkb1* loss.

(A) S100 immunofluorescence of glial JoMa1.3 cells upon AICAR treatment showing the disappearance of the inclusions. (B) Representative western blot images illustrating the ability of AICAR to prevent phospho-p53^{Ser15} accumulation upon *Lkb1* knockdown. (C) Immunofluorescence staining for phospho-p53^{Ser15} in control or *Lkb1*-silenced glial JoMa1.3 cells illustrating the decrease of phospho-p53 positive cells upon AICAR treatment.

PROJECT 2. LKB1 METABOLIC & SIGNALING REGULATION IN NCC

qPCR	Primer sequences	
<i>AUP1</i>	mAUP1-F:	5'-tgcgctccgtgtacaacagc-3'
	mAUP1-R:	5'-tttgtcgcgttcattgtgtct-3'
<i>RELA</i>	mRELA-F:	5'-cgggatggctactatgagg-3'
	mRELA-R:	5'-ctccagggtctcgcttctt-3'
<i>p53</i>	mp53-F:	5'-CCGCGCCATGGCCATCTACA-3'
	mp53-R:	5'-GGGGAGGAGCCAGGCCATCA-3'
<i>p21</i>	mp21-F:	5'-CACAGCTCAGTGGACTGGAA-3'
	mp21-R:	5'-CACAGCTCAGTGGACTGGAA-3'
<i>Gadd45a</i>	mGadd45a-F:	5'-GCAGAGCAGAAGACCGAAAG-3'
	mGadd45a-R:	5'-GTAATGGTGGCTGACTCC-3'
<i>Btg2</i>	mBtg2-F:	5'-GCGAGCAGAGACTCAAGGT-3'
	mBtg2-R:	5'-CCAGTGGTGTGTTGTAATGATCG-3'
<i>Trp53inp1</i>	mTrp53inp1-F:	5'-TAAGACTCACGGGCACAGAA-3'
	mTrp53inp1-R:	5'-CAAGTGCTGCCACACAGC-3'
<i>Ddb2</i>	mDdb22-F:	5'-CAGAACAATGAGATTCCGGTTT-3'
	mDdb2-R:	5'-AGGTTGTGCCGTGAATGC-3'
<i>Notch1</i>	mNotch1-F:	5'-CCTCACCTGGTGCAGACC-3'
	mNotch1-R:	5'-GTTCTGAGGCTGGAGCTGTAA-3'
<i>Cptc1</i>	mCptc1-F:	5'-GGGAACATGGCTGAGGCACAC-3'
	mCptc1-R:	5'-GCGCAGGGCACAGAGGTAAA-3'
<i>Aldh4</i>	mAldh4-F:	5'-GGGCCTCCATTCCATACTCT-3'
	mAldh4-R:	5'-GCTCTCCCTGGCTACCACT-3'
<i>Tigar</i>	mTigar-F:	5'-GGAGGAGAGACAGTTGAGCAG-3'
	mTigar-R:	5'-TGCCAAAGAGCTTTCCAAAC-3'
<i>Sens1</i>	mSens1-F:	5'-TGTCCCAACGTTTCGTGTC-3'
	mSens1-R:	5'-TGGATAGAGACGATTCACCAGA-3'
<i>Sens2</i>	mSens2-F:	5'-CAGCGCTTTCATTCCAGTG-3'
	mSens2-R:	5'-CCGGGTGTAGACCCATCA-3'
<i>Ulk1</i>	mUlk1-F:	5'-AAGGGAAGTGCCAGTGAGG-3'
	mUlk1-R:	5'-CCTTCAAGTACAGAACCAGTTGC-3'
<i>Ulk2</i>	mUlk2-F:	5'-TTGGAACTTGGCCATCAAT-3'
	mUlk2-R:	5'-TGCATGACAGCTTCCAAGAG-3'

Table 1- Primers used for genotyping and qPCR.

Technic	Primary antibody	Producing specie	Dilution	References
IF	LKB1	Rabbit, polyclonal	1/100	Sigma
	Tuj1	Mouse, monoclonal	1/1000	Covance
	S100	Rabbit, Polyclonal	1/1000	Dako
	phospho-p53 (Ser 15)	Rabbit, monoclonal	1/1000	Cell Signaling
	LC3	Mouse, monoclonal	1/100	Novus Biological
	γH2AX	Rabbit, monoclonal	1/100	Abcam
WB	LKB1 Ley37DG6	Mouse, monoclonal	1/1000	Santa Cruz
	HSP90 (AC88)	Mouse, monoclonal	1/2000	Stressgen
	Actin	Mouse, monoclonal	1/1000	Sigma
	phospho-p53 (Ser 15)	Rabbit, monoclonal	1/1000	Cell Signaling
	Total p53 CM5	Rabbit, polyclonal	1/1000	Leica
	LC3	Mouse, monoclonal	1/1000	Novus Biological
	P62	Mouse, monoclonal	1/1000	Abnova

Table 2- Antibodies used throughout the study.

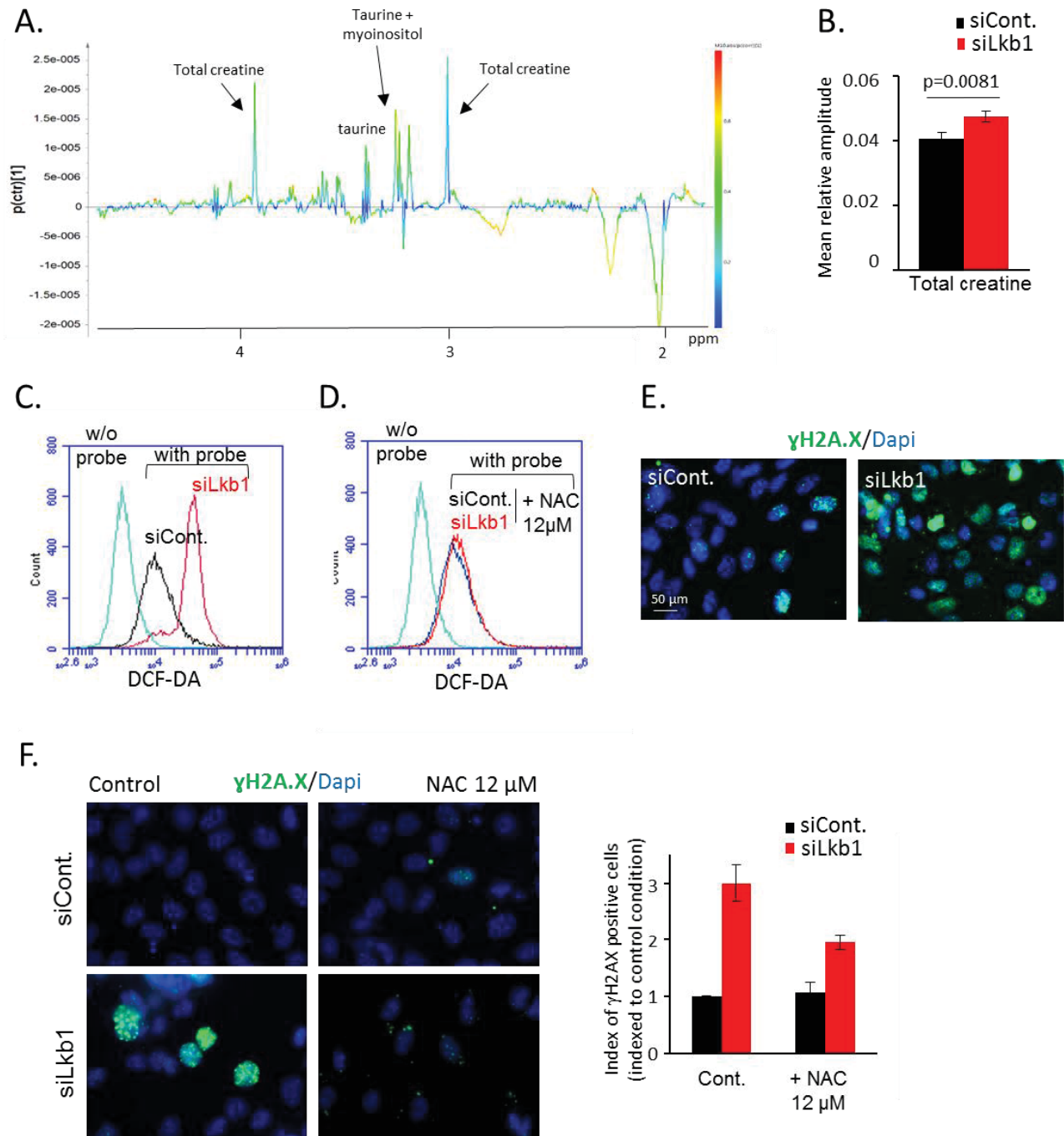


Figure 1 : *Lkb1* loss during glial differentiation triggers oxidative DNA damages

PROJECT 2. LKB1 METABOLIC & SIGNALING REGULATION IN NCC

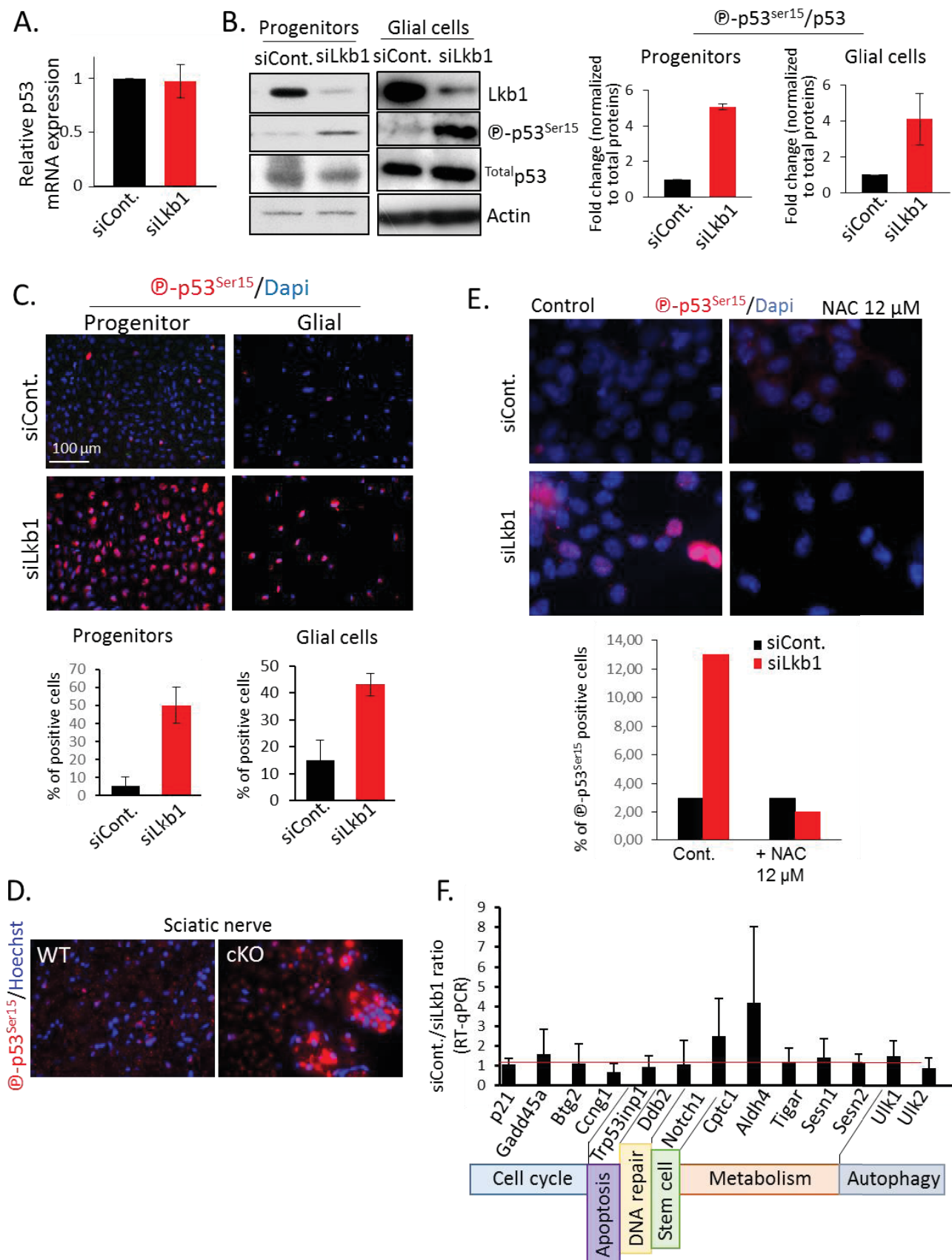


Figure 2: Oxidative DNA damages trigger p53 hyperphosphorylation both *in vitro* and *in vivo*

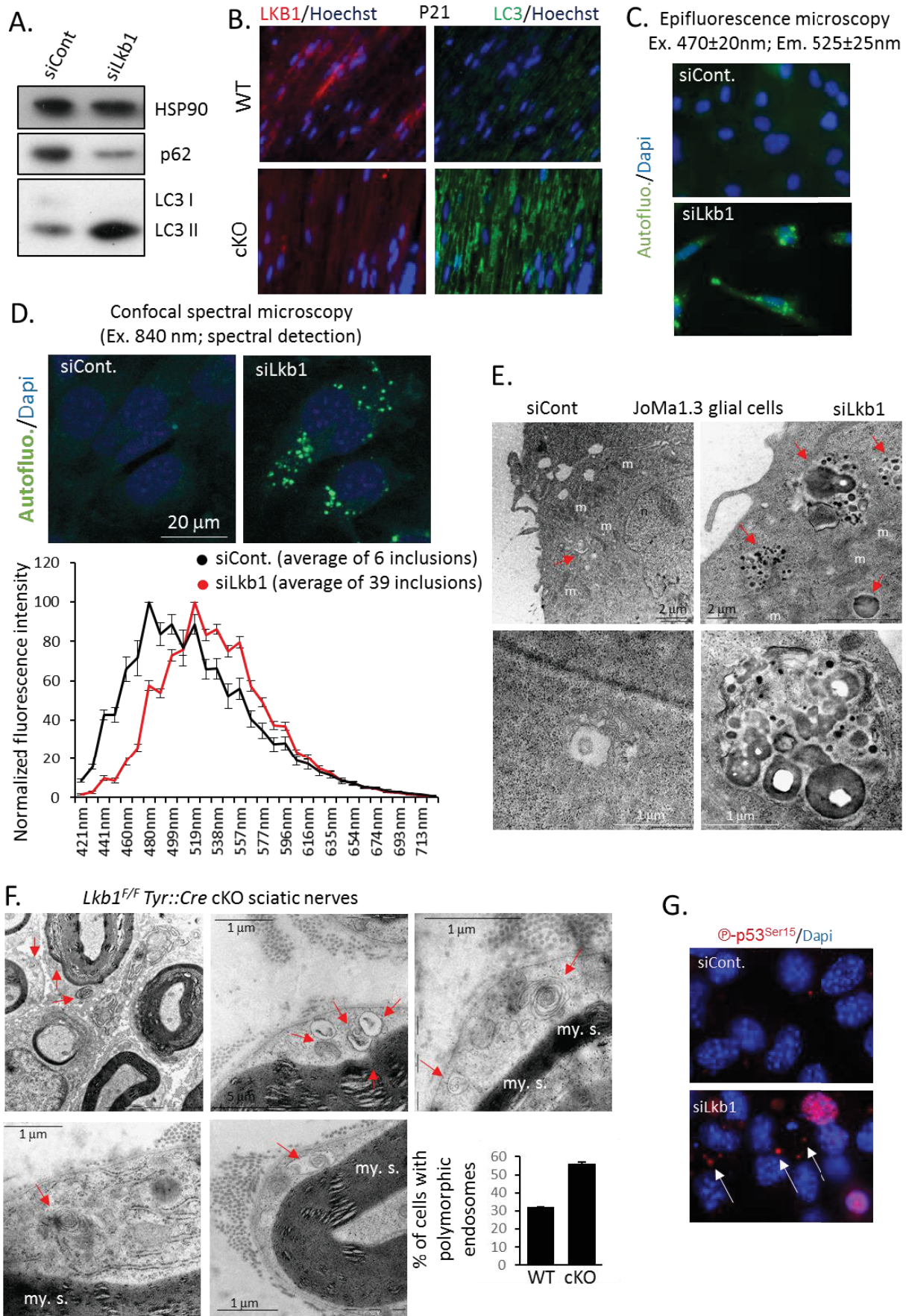


Figure 3: *Lkb1* loss triggers autophagy and defective lysosomal homeostasis

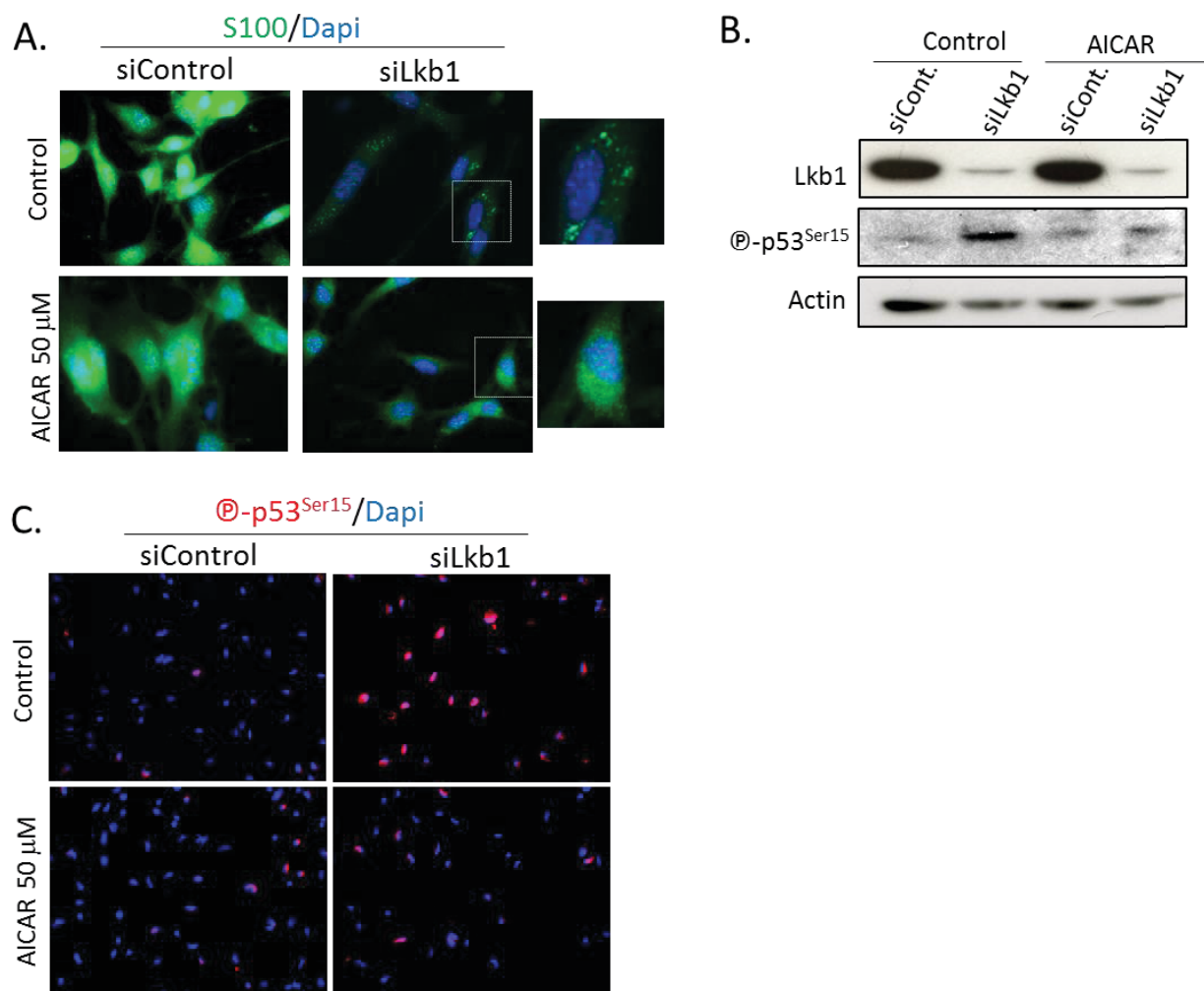


Figure 4: AICAR rescues glial differentiation impaired upon *Lkb1* loss through lysosomal and p53 regulation

2.3 Conclusions and perspectives

The present study underlined the existence of a crosstalk between Lkb1 and p53 signaling in NCC and pointed out that this crosstalk is crucial for NCC-derivatives development. Indeed, we observed that during glial differentiation, Lkb1 limits p53 activation through the control of ROS production and subsequently DNA damages. The results obtained are in line with previously published data identifying that p53 is activated by oxidative DNA damage (see Introduction Chapter III.B.1.2) and that Lkb1 protects the genome from ROS-induced oxidation by regulating antioxidant gene products (see Introduction Chapter III.A.3.1.3).

Increased p53 signaling has been described in biopsies of patients with neurocristopathies and *p53* loss in neurocristopathy mouse models rescues the pathological phenotype. To complete this study, it will be interesting to analyze if combined loss of Lkb1

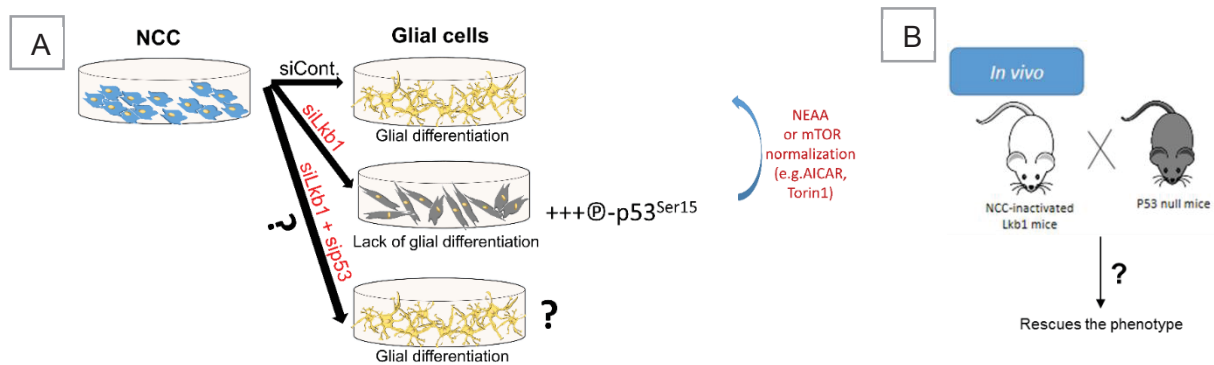


Figure 5. Lkb1/p53 crosstalk to control cell fate

and p53 rescues *in vivo* and *in vitro* impaired NCC differentiation and maintenance. For *in vitro* analyzes, the lab will perform a double knockdown of both *Lkb1* and *p53* in NCC and evaluate if it rescues glial differentiation (Figure 5A). For *in vivo* analyzes, Anthony Lucas has undertaken crossing of “early” NCC-inactivated *Lkb1* mice (Ht-PA::Cre, *Lkb1*^{F/FI}) with heterozygous or homozygous p53 loss mice (Figure 5B). Phenotypic characterization of these mice will be performed on tissues previously described to exhibit defects upon *Lkb1* loss: formation of the head, enteric nervous system, sciatic nerve and melanocytes.

Furthermore I uncovered that *Lkb1* loss promotes accumulation of lysosomes charged with lipofuscin granules which are characteristic features of premature aging in degenerative diseases (see Introduction Chapter IV 3.2). I observed that AICAR, in absence of *Lkb1*, limited the formation of lipofuscin granules. The lab will therefore pursue the characterization of lysosomal activity linked with deregulation of *Lkb1*/AMPK signaling during glial differentiation, and assess if *Lkb1* loss triggers senescence and premature aging that can be prevented by AICAR. Characterizing AICAR as a preventing drug of metabolic defects and premature aging will open a broad range of new therapeutic perspectives.

AICAR also normalized the phosphorylation of p53 on serine15 accumulated in absence of *Lkb1*. Phosphorylated p53 on serine15 is not only associated with its nuclear functions but also with its localization to the lysosomal membrane through lysosome-localized adaptor protein (LAPF) interaction (see Introduction Chapter IV.2.3). Thus, it is possible that upon *Lkb1* loss, phosphorylated p53 translocates to lysosomal membrane. To test this hypothesis, the lab could isolate lysosomes from *Lkb1* knockdown NCC and analyze by western blot the presence of p53 as well as the interaction between p53 and LAPF. In a second time, depending on the results obtained, they could analyze the role of p53 at lysosomal surface by studying mTOR activation and lipofuscin granules formation.

III. Project 3 Energy metabolic regulations of Lkb1 signaling in other polarized cells.

Epithelia are polarized cells that form barriers crucial for tissue homeostasis (Marchiando et al., 2010). The primary characteristic of epithelial barrier formation is the inter-cellular tight junction present along plasma membrane (Marchiando et al., 2010). This is particularly true in testes, where Sertoli cells, which are epithelial somatic cells of the seminiferous tubules, are forming the blood-testis barrier through tight, adherent and gap junctions (Mruk and Cheng, 2015). This structure supports the maturation of germ cells and prevents their recognition by immune cells (Jiang et al., 2014). Perturbation of these junctions represents both the effect and the cause of human diseases. For example, patients with Peutz-Jeghers syndrome have modifications of tight junctions in the blood-testis barrier (Bertoldo et al., 2015). Disruption of blood-testis barrier cause immunological or other damages to meiotic and postmeiotic germ cells and consequently promotes alteration of sperm production and male infertility (Jiang et al., 2014).

Interestingly, Sertoli cells provide the adequate ionic and metabolic environment (export of alanine and lactate) essential for germ cells maturation. Thus, the metabolic communication between Sertoli cells-germ cells relies on a very similar process that the one for glial-neuronal cells described in Introduction (Chapter I.3.2).

Like Sertoli cells, intestinal epithelial cells are forming a barrier, but only through tight junctions, which is crucial for tissue homeostasis. It controls microbial interactions and contributes to nutrient and water transport (Peterson and Artis, 2014). Intestinal epithelial cells metabolism is also important for a cellular dialogue with their neighboring cells (see Introduction, Chapter I.3.2).

LKB1 is required for both Sertoli cells and intestinal epithelial cells polarity to control the establishment of blood-testis barrier (Tanwar et al., 2012) and intestinal barrier respectively (Partanen et al., 2013). Several studies identified a link between energy metabolism and polarity (Ghosh, 2017; see Introduction Chapter III.A.3.2). For instance, AMPK stabilizes tight junctions and regulates cell polarity and intestinal epithelial barrier (Aznar et al., 2016) and malfunctions of this barrier have been associated with metabolic disorders (Bauer and Duca, 2016; McCreight et al., 2016; Wu et al., 2017). Therefore, targeting AMPK-dependent stress polarity pathway has been proposed as a therapeutic strategy to control the gut barrier and consequently to correct metabolic disorders (Ghosh, 2017).

However, the exact molecular mechanisms by which LKB1 regulates energy metabolism in Sertoli and intestinal epithelial cells have been less explored.

Thus, we first analyzed LKB1 functions in Sertoli polarity and cell metabolism as well as its role in cellular communication between Sertoli cells and the neighboring cells.

Secondly, in collaboration with R. Almeida lab (IPATIMUP, Porto, Portugal), I studied the energy metabolic regulations exerted by MEX-3A, a putative downstream effector in LKB1 signaling, in Caco2 (Colorectal adenocarcinoma) cells which are intestinal epithelial cells characterized by polarity and tight junctions formation at postconfluency.

1. Lkb1-metabolic regulations in Sertoli cells are essential for testis homeostasis and germ cells maturation.

Article in preparation, Torch S.*, Radu AG.*, Lucas A., Fauvelle F.,
Hainaut P., Billaud M. and Thibert C, *equally contributing authors

1.1 Scientific context and results summary

LKB1 role in Sertoli cells has been already described: *Lkb1* inactivation in Sertoli cells was performed by expressing Cre recombinase under the promoter of the receptor of Anti Mullerian Hormone (AMH) Receptor (Tanwar et al., 2012). This inactivation leads to Sertoli cell polarity loss, perturbation of blood-testis barrier as well as suppression of AMPK and activation of mTOR signaling. However metabolic defects were not explored in this study.

To explore LKB1 metabolic regulations in Sertoli cells, our team generated a mouse model of conditional ablation of *Lkb1* specifically in these cells. To do so, *Lkb1* Flox mice were crossed with mice expressing the recombinase Cre under the promoter of AMH, generated by F. Guillou and P. Crepieux, INRA, Rennes (Lécureuil et al., 2002). Using the AMH::Cre model, the team confirmed the crucial role of *Lkb1* in fertility since mutant male mice were sterile with no mature germ cells neither in testis nor epididymis. Seminiferous tubules were totally disorganized in the absence of *Lkb1*. Sertoli cell polarity was impaired and the hemato-testicular barrier was absent. The team also observed increased proliferation of myoid and Leydig cells.

During my PhD I contributed to the phenotypic characterization of these mutant mice. I have shown that *Lkb1* loss triggers a mislocalization of immature germ cells.

Further, the team explored whole testis metabolism and observed an aberrant up-regulation of the nutrient-sensing mTOR pathway as well as lipids and carbohydrate accumulation within and around seminiferous tubules in the absence of *Lkb1*. Furthermore, HRMAS RMN metabolomics analyses of testes revealed profound metabolic deregulations upon *Lkb1* loss with increased levels of several metabolites such as alanine and glutamine.

To better characterize the capacity of *Lkb1* to regulate Sertoli cell metabolism and to analyze the underlying molecular mechanism, I used a Sertoli cell line (TM4 cells). First, I

confirmed that *Lkb1* loss promotes an increase of mTOR pathway and a decrease of AMPK phosphorylation. Second, I demonstrated that glycolysis was not affected in the absence of *Lkb1* whereas oxidative phosphorylation (OXPHOS) was clearly augmented, thus leading to an increase of energy production. Finally, I have shown that *Lkb1* controls phagocytosis, one of the most characterized Sertoli cell function.

Altogether, these findings highlight a novel function of LKB1 as a crucial metabolic regulator in Sertoli cells, necessary to control their functions and whole testis development.

1.2 Results

1.2.1 *Lkb1* inactivation in Sertoli cells influences germ cell

localization and maturation.

As a reminder, Sertoli cells are located in the seminiferous tubules from their basal part to their lumen, being in contact with germ cells (Figure 1A, left panel). Germ cells undergo progressive maturation from the basal part of the tubule, where they are called spermatogonia, to the lumen, where they are differentiated into spermatozoa. Mouse spermatogenesis starts with mitotic proliferation of type A and type B spermatogonia. Type B spermatogonia are forming spermatocytes through symmetric divisions. This step represents the beginning of a meiotic phase. Spermatocytes I are diploid cells which undergo meiosis and generate two haploid spermatocytes II that have 50% of the number of chromosomes. Spermatocytes II enter also in meiosis and produce haploid round spermatids which mature into spermatozoa (Laiho et al., 2013). The first wave of maturation of spermatogonia into round spermatids starts a few days after birth, takes approximately 35 days and is synchronized (Oakberg, 1957; Tanaka and Baba, 2005). Spermatocytes appear at 9 days after birth (P9) and spermatid appear at P20 (Bellvé et al., 1977). The seminiferous tubules are surrounded by myoid cells while Leydig cells are localized in interstitial spaces adjacent to seminiferous tubules (Fig.1A).

The team has recently demonstrated that *Lkb1* in Sertoli cells is crucial for fertility since male mice which are not expressing *Lkb1* specifically in Sertoli cells were sterile. Macroscopic observations of testis revealed that cKO mice exhibited increased testis weight at 3 weeks after birth (P21) called macro-orchidism followed by a progressive regression of the testicular volume and a marked micro-orchidism at 3 months after birth (P90). In order to better characterize the macro-orchidism, I quantified the surface of seminiferous tubules of wild type and *Lkb1* conditional knockout mice at P21, on testis cross-sections. Thus, I have shown that the increased testicular weight is associated to an increase of the seminiferous tubules area (Fig.1B).

The team underlined that *Lkb1* in Sertoli cells limits neighboring cells proliferation and preserves tissue homeostasis of the testis. Indeed, in the absence of *Lkb1* in Sertoli cell, they observed an aberrant hyper-proliferation of myoid and Leydig cells which correlates with the

macro-orchy. The team also observed an absence of spermatozoid in seminiferous tubules or epididymis of mutant mice at 90 days after birth (P90). However, the role of *Lkb1* in Sertoli cell on germ cell proliferation and differentiation remained to be clarified.

To address this question I first analyzed the number of germ cells in seminiferous tubules in the presence or absence of *Lkb1* and uncovered that *Lkb1* loss did not affected the total number of germ cells per mm² (Fig.1C). However, considering that the surface of seminiferous tubules is increased, the total number of germ cells also increased. This result suggests that *Lkb1* expressed in Sertoli cells regulates germ cell proliferation.

Second, I performed immunolabelling of VASA, a cytoplasmic protein specifically expressed in germ cells from spermatogonia to round spermatids stages, with its highest expression being at the early spermatocyte stage. In spermatogonia, the accumulation of VASA protein is much lower and depends on the stage of differentiation. It has been suggested that weak VASA staining corresponds to type A spermatogonia (undifferentiated state with self-renewal capacity) also called germ stem cells, while intermediate staining corresponds to type B spermatogonia (differentiated into spermatocyte) (Castrillon et al., 2000; Toyooka et al., 2000). As the first wave of germ cell maturation in the testis is synchronized, the most mature germ cells at P21 are spermatocytes (Bellvé et al., 1977; Laiho et al., 2013). As observed in Fig.1D, I have shown that in the absence of *Lkb1* there is the same number of cells with low VASA staining (at the basal membrane) compared to control and therefore, same number of spermatogonia. In our experiments, VASA immunostaining did not allow us to distinguish between spermatogonia type A (Ad and Ap) or Type B (Figure 1.A right panel).

Further, in order to better characterize the germ cell differentiation, I performed immunostaining for synaptonemal complex protein 3 (SCP3), a specific marker of meiotic germ cells (spermatocytes I and II). At P21 there was no significant difference between the numbers of SCP3 positive cells in wild type or *Lkb1* conditional knock out murine testes (Fig.1E). Instead, SCP3 positive cells localization in seminiferous tubules was aberrant upon *Lkb1* loss. In normal conditions, SCP3 positive cells are more at the basal membrane than in absence of *Lkb1* (Fig.1E). Mislocalization of SCP3 positive cells upon *Lkb1* loss was even more pronounced at P90 (Fig.1F). In normal conditions, spermatocytes are organized in one cell layer near the basal part of the tubules whereas spermatozoa (which have a smaller nucleus) are localized in the tubule's lumen. Instead, in *Lkb1* conditional knockout murine testes, the germ cell distribution is disorganized, with many spermatocytes in the tubule's lumen and no spermatozoa (Fig.1F).

Interestingly, the number of spermatocytes was not affected at P21 upon *Lkb1* loss. However, *Lkb1* absence triggered their mislocalization in the seminiferous tubule. This suggest that impaired maturation of germ cells into spermatozoa may be a consequence of spermatocytes mislocalization which probably is due to the disruption of blood-testis barrier integrity.

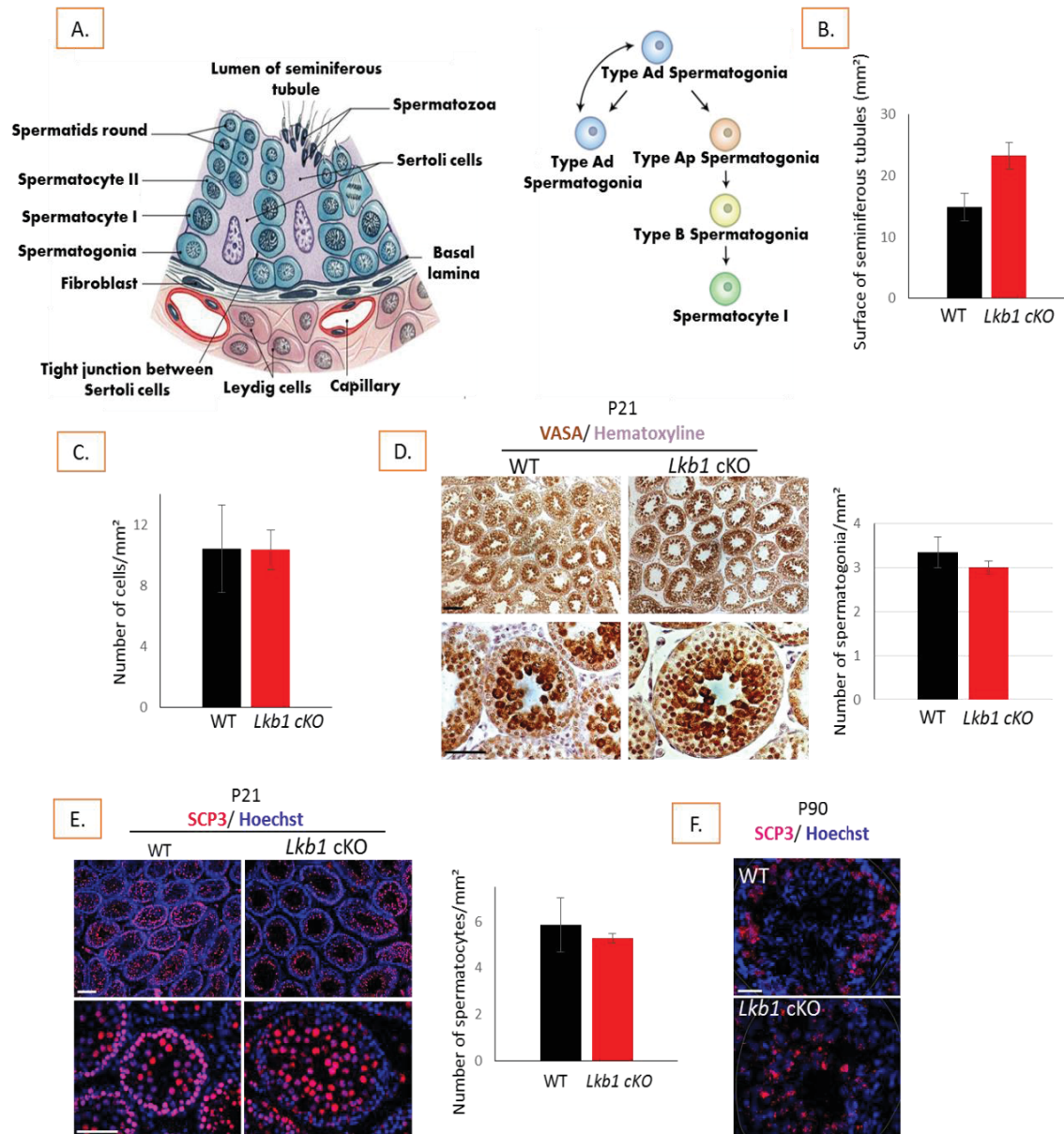


Figure.1 Sertoli cells-LKB1 regulates germ cells proliferation, localization and maturation.

A. Left panel: Schematic representation of seminiferous tubules organization. **Right panel:** Schematic representation of different types of spermatogonia. Spermatogonia Ad (dark) are germ stem cells, Spermatogonia Ap (pale) and B undergo a symmetric division. **B.** Quantification of seminiferous tubules area from 4 WT and 4 LKB1 cKO at P21. **C.** Quantification of germ cells on transversal sections of testes of 3 WT and 3 LKB1 cKO at P21. **D.** Transverse section of WT and LKB1 cKO testis at P21 subjected to immunohistochemistry (IHC) with VASA antibody. VASA is a marker of germ cells from spermatogonia to round spermatids. Scale bars: 100 μ m the top panels and 50 μ m bottom panels. Quantification of spermatogonia (right panel) were performed on only 2 WT and 2 LKB1 cKO mice and 8 seminiferous tubules/animal were used for counting. **E and F.** SCP3 immunofluorescence on transverse section of WT and LKB1 cKO testes at **E**, P21 and **F** P90. SCP3 is a marker of spermatocytes I and II. This experiments were done on 3 WT and 3 LKB1 cKO animals.

Thus, these results suggest that Lkb1 expressed in Sertoli cells regulates germ cell proliferation, localization and consequently is involved in their differentiation.

1.2.2 Lkb1 inactivation compromises Sertoli cells metabolism.

Previous data of the team have established that the absence of *Lkb1* in Sertoli cells rewires testis metabolism. First, the team showed on transverse sections of testes from wild type and *Lkb1* conditional knockout mice that Lkb1 controls AMPK/mTOR pathway known to be essential for metabolic regulation. Second, they observed that *Lkb1* loss affects lipid and glucid metabolism. Finally, they characterized the metabolome of testes. For that purpose, they performed high-resolution magic angle spinning (HRMAS) proton NMR spectroscopy on testes at P21 and P90 (with F. Fauvelle, GIN, Grenoble, France). Most discriminant changes in metabolite levels between WT and *Lkb1* conditional knockout testes concerned alanine, glutamine, lactate, succinate and glucose, all being increased.

In order to better understand the mechanisms underlying Lkb1-dependent metabolic regulation, I used a murine Sertoli cell line. By using this cell line, I confirmed that absence of *Lkb1* in Sertoli cells led to decreased AMPK activity associated with up-regulation of the mTOR pathway (Fig.2 A). I also assessed the energy metabolism of Lkb1-deficient Sertoli cells with the Seahorse metabolic analyzer. I uncovered that the basal glycolysis, glycolytic capacity and the glycolytic reserve, based on extracellular acidification rate measurement, were not affected by *Lkb1* knockdown (Fig.2B). However, oxygen consumption during basal and maximal respiration was strongly increased (Fig.2C). In addition, ATP production was significantly increased (Fig.2C).

To evaluate how polarity and metabolism impact Sertoli functionality, I also analyzed Lkb1 role during phagocytosis, a well characterized Sertoli cell function. Preliminary results have shown that absence of Lkb1 triggered a decrease in phagocytosis (Fig.2D). Further, our team will confirm this result and will analyze other Sertoli cell functions such as cell polarity through the establishment of cell-cell junctions and the role of metabolism in the control of these functions.

Taken together, these data demonstrate that Lkb1 has critical functions in the control of energy metabolism of Sertoli cells and tissue homeostasis and a publication is in preparation.

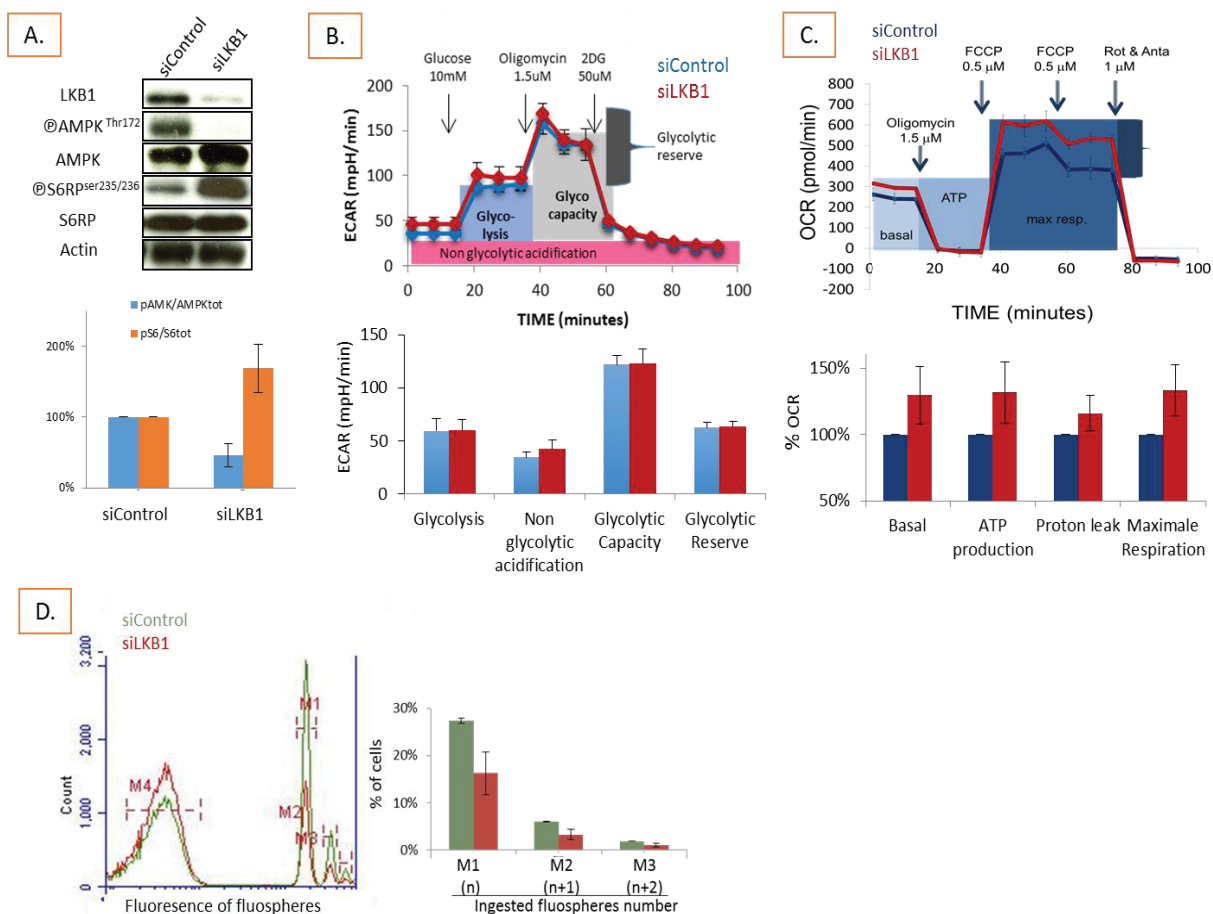


Figure 2: Lkb1 is a novel metabolic regulator of Sertoli cells and controls their phagocytic function.

A. Western blot to validate *Lkb1* knockdown at the protein level. Phosphorylation of AMPK and S6RP (as an indicator of mTOR activity) are also shown compare to total protein level. Actin was used as a loading control. The right panel is showing the percentage of phospho-AMPK to total AMPK protein (experiments realized 2 times ($n=2$)) or phospho-S6RP to total S6RP protein ($n=2$) relative to siControl. **B.** Representative curves showing changes in medium acidification (ECAR, top) obtained by Seahorse analyzer and quantification of ECAR (bottom) ($n=3$). **C.** Representative curves showing change in oxygen consumption (OCR, top) analyzed by Seahorse and quantification of % OCR relative to siControl ($n=3$). **D.** siCont and siLKB1 TM4 cells were incubated 2h with fluospheres, then harvested, washed and analyzed by flow cytometry. Phagocytotic cells can be detected by fluorescence spectroscopy at 645nm. M4 represents the cells considered non phagocytotic, M1 represents the cells which ingested n fluospheres, M2 ingested $n+1$ fluospheres and M3 ingested $n+2$ fluospheres. Quantification of the % of phagocytotic cells is presented in the right panel.

1.3 Conclusions

Sertoli cells is an interesting model of polarized cells sharing functional metabolic similarities with NCC-derived glial cells. Indeed, these cells sustain proliferation, survival and maturation of their neighboring cells, either neurons in case of glial cells or germ, myoid and Leydig cells in case of Sertoli cells. Glial and Sertoli cells both regulate adjacent cell fate through paracrine factors such as amino acids (alanine) or other metabolites (lactate, pyruvate). Therefore, the lab was interested in exploring metabolic regulations exerted by LKB1 in Sertoli cells and I participated to this analysis during my PhD.

I emphasized that *Lkb1* regulates global tissue architecture, germ cell maturation, neighboring cell proliferation and Sertoli cell metabolism. All these data suggest that *Lkb1* is a new regulator of the metabolic dialog between Sertoli cells and germ cells, responsible for spermatozoa formation.

However, it is not clear if *Lkb1* expressed in Sertoli cells regulates germ cell differentiation directly or if it is a consequence of blood-testis barrier loss. I have shown that in absence of *Lkb1* there is the same amount of spermatogonia type B and spermatocytes compared to control. Instead, nothing is known about *Lkb1* role in spermatogonia type A, the germ stem cells. Therefore, further studies with the germ stem cell marker, PLZF (Filipponi et al., 2007; Phillips et al., 2010), need to be done in order to better characterize the role of *Lkb1* in germ stem cell functions such as self-renewal capacity and differentiation.

Interestingly, similarly to our previous study on neural crest derivatives of the peripheral nervous system, *Lkb1* loss in testis triggers an increase in non-essential amino acids such as alanine and glutamine. Altogether, these projects regarding the role of *Lkb1* in neural crest cells and Sertoli cells allowed us to uncover that *Lkb1* signaling exerts a crucial control of energy metabolism via non-essential amino acids levels during cell differentiation and maintenance and that this process is mainly conserved across tissues.

1.4 Materials and methods

Animals

Floxed *Lkb1* mice were obtain from RA. DePinho (Boston, USA). For the generation of Sertoli cells specific *Lkb1* null mice, conditional *Lkb1* floxed mice were bred with AMH-Cre mice (Lecureuil et al., 2002). Homozygous floxed *Lkb1* animals expressing Cre recombinase were considered as Sertoli specific knockout mice. Mice were maintained under standard housing conditions and maintained on a mixed genetic background.

Cell line and cell culture

The mouse TM4 Sertoli cells was obtained from American Tissue Culture Collection. Cells were cultured in 37C with DMEM: F12 supplemented with 15mM N-(2-hydroxyethyl)

piperazine-N-2 ethanesulfonic acid (HEPES) buffer, 2.5% horse serum and 1% penicillin-streptomycin.

Short interfering RNAs (siRNA) against the mouse Lkb1 gene and the Non-targeting control siRNA were purchased from Dharmacon (ON-TARGET plus mouse Stk11 SMART pool and ON-TARGET plus Non-targeting Pool, Dharmacon). siRNAs were transfected (11 nM) into TM4 cells by using JetPrime (Ozyme) according to the manufacturer's protocol. Experiments were realized 72h post-transfection.

Histology, Immunohistochemistry and immunofluorescence staining

P21 and P90 mice testes were collected, rinsed in cold PBS, and then fixed in 4 % PFA overnight at 4°C. Tissue samples were dehydrated, embedded in paraffin and sectioned into 5 µm-thick transverse sections.

For immunohistochemistry, sections were deparafinized and rehydrated, rinsed in PBS and boiled for 20 minutes at 95°C in a decloacking chamber (Biocare Medical) in 10 mM Sodium citrate antigen retrieval buffer (pH 6). Sections were then treated with 1% H₂O₂ for 20 minutes. After 1 hour incubation in a blocking buffer (PBS-3% BSA-10% Goat preimmune serum for polyclonal antibodies), sections were incubated overnight at 4°C with VASA antibody (Abcam, ab13840) at 1/200. ImmPRESS anti-Rabbit-HRP conjugated secondary antibody was used to amplify the staining, according to the supplier's protocol (Clinisciences). DAB peroxidase substrate kit was used for detection of the antibodies (Vectors laboratories) for 2 minutes. Sections were then counterstained with Hematoxylin (Sigma-Aldrich) diluted at 1/10 for 2 minutes, dehydrated and mounted in Merckoglas (Merck).

For Immunofluorescence, P21 paraffin testes sections were treated with standard protocols using 10mM EDTA antigen retrieval buffer (pH9) and SCP3 antibody (Abcam, ab15092) at 1/500 overnight. P90 frozen testes sections were incubated with PBS-BSA 0.3%-Triton100X 0.5% for 10 min and after were incubated for 1h with PBS-BSA 3%-GPI 10% and with the same SCP3 antibody at the same concentration as above, overnight. Secondary antibody used was from Jackson ImmunoResearch, a Donkey anti-Rabbit Cy3 (1/1000). Nuclei were stained with Hoechst 33342 (10 µg/ml, Invitrogen).

Western blot analysis

Western blot analysis was performed as described previously (Radu et al., submitted). Briefly, 20g of protein extracts were separated in SDS-10% polyacrylamide gels and transferred to PVDF Immobilon-P membranes (Millipore). After blocking, membranes were incubated overnight with different antibodies as described Table1 in blocking solution at 4°C and with horseradish peroxidase-conjugated anti-rabbit or anti-mouse immunoglobulin G (Biorad) for 1 h at room temperature. ImageJ software was used to quantify the intensity of phospho-AMPK, phospho-S6Rp, AMPK, S6Rp and β-actin bands. Each intensity measurement for phospho-

PROJECT 3. LKB1 METABOLIC CONTROL IN POLARIZED CELLS

AMPK and phospho-S6 was divided by the corresponding total AMPK and S6. The resulted values, were then divided by the corresponding standardized β -actin measurement, and the numbers are normalized to the control.

Antibodies	Species	Dilutions	References
Lkb1	Mouse	1/1000	Santa Cruz Ley37DG6
@AMPK^{Thr172}	Rabbit	1/1000	Cell Signaling
AMPKα1/2 (H-300)	Rabbit	1/1000	Santa Cruz Biotechnologie
@S6RP^{235/236}	Rabbit	1/1000	Cell Signaling
S6RP (5G10)	Rabbit	1/1000	Cell Signaling
Actin	Mouse	1/5000	MAB1501 Millipore

Table1. Primary antibodies used for western blot analysis

Seahorse analysis

The extracellular acidification rate (ECAR) and oxygen consumption rate (OCR) were analyzed by using the Seahorse XF96-Analyzer (Seahorse Bioscience). 1.5×10^4 TM4 cells were seeded in 96-well Seahorse plates in normal cell culture medium 16 h before assay. Seahorse analyzes were done as previously described (Project 2.1; Radu et al, submitted).

Treatments	OCR	ECAR
Glucose	-	10mM
Oligomycin	1.5 μ M	1.5 μ M
FCCP	2 x 0.5 μ M	-
Rotenon and Antimycin A	1 μ M	-
2DG	-	50 μ M

Table2. Treatments injected by Seahorse analyzer for OCR and ECAR measurements.

Briefly, the media was replaced with Seahorse assay media specific for OCR or ECAR measurements and equilibrated in non-CO₂ incubator for 1 hr. Basal OCR and ECAR were measured for 3 min every 10 min for 3 points, followed by sequential injection of different drogues (Table2). OCR and ECAR were

normalized by cell density. For both respiration and glycolysis, quantifications were performed by calculating for each category the mean and standard deviation from the values obtained from four independent experiments.

Phagocytosis

To assay the phagocytosis activity, TM4 cells were plated at 2×10^4 cells/well, in a 6 well plate and 24h after, the cells were transfected with siRNA targeting *Lkb1* (siLKB1) or Non-targeting control siRNA (siControl) for 72h. After the 72h, the cells were incubated with F8816 Fluospheres Carboxylate-Modified Microspheres, 1 μ m, crimson fluorescent (625/645) at a ratio of 40 beads per cell. The incubation lasted 2h at 37°C. Once the incubation is completed, the cells are washed with PBS 3 or 4 times, gently trypsinized, centrifuged 4 min at 1200 rpm and resuspended in 500 μ l PBS. Analysis of phagocytic cells was performed using the flow cytometer C6 BD-Accui.

2. Characterization of MEX-3A-associated metabolic profile

Collaboration with R. Almeida and B. Pereira (Institute of Molecular Pathology and Immunology of the University of Porto, IPATIMUP, Portugal)

2.1 Scientific context and results summary

Several years ago, MEX3, an RNA-binding protein, has been characterized as a novel downstream target of Lkb1 important for *Caenorhabditis elegans* embryogenesis (Draper et al., 1996; Huang et al., 2002). The nematode LKB1 homologue, Par4, negatively regulates MEX3 activity in the posterior part of the early embryo and thus controls the formation of the anterior-posterior embryo axis (Huang and Hunter, 2015). M. Billaud lab then identified and characterized the 4 mammal MEX3 proteins called MEX3A to MEX3D (Buchet-Poyau et al., 2007). However, MEX3 functions and contribution to LKB1 signaling in mammals are still largely unknown.

Our team and others identified that members of MEX3 family are involved in fertility by controlling Sertoli cell polarity (Le Borgne et al., 2014) or in energy metabolism balance (Jiao et al., 2012a, 2012b). To further explore the coordinated regulation between cell polarity and metabolism, we developed a collaboration with Almeida R. lab. They have shown that MEX3A is involved in intestinal differentiation, polarization and stemness associated with gastrointestinal carcinogenesis (Pereira et al., 2013). However, the exact mechanism by which MEX3A controls these biological functions is not known. Therefore, the aim of R. Almeida lab was to better define MEX3A involvement in regulation of cellular differentiation, metabolism and polarity in gastrointestinal tract during homeostasis and carcinogenesis. Furthermore, R. Almeida lab showed a novel putative role for mammalian MEX3A on the regulation of the Lkb1-AMPK-mTOR signaling pathway.

Thus, in the continuity of my previous studies and in collaboration with R. Almeida lab, I characterized the metabolic status in another polarized cell type that is the colorectal adenocarcinoma (Caco2) cell line. At pre-confluency these cells are in an immature state while at confluency they exhibit spontaneous differentiated characteristics and they form a polarized epithelial monolayer characterized by brushborder microvilli and tight junctions. Thus, these cells, as Sertoli cells, are essential for the establishment of protective barriers through tight junctions formation. Pereira and its colleagues have shown that MEX3A overexpression in Caco2 cells alters the maintenance of these junctions (Pereira et al, 2013).

2.2 Results

During this collaborative metabolic study, I used Caco2 MOCK and MEX3A stably transfected cell lines. I have shown that upon MEX3A overexpression in pre-confluent cells, the oxygen consumption during basal and maximal respiration and thereby the ATP production are decreased (Fig.1A) while the glycolytic capacity is increased (Fig.1B). These results were further confirmed by Almeida R. team since they observed by RT-qPCR that several metabolic genes which regulate OXPHOS are down-regulated upon MEX3A overexpression (data not shown).

As presented above, Caco2 cells differentiate with time of culture. Thus, I also analyzed the energy metabolism of Caco2 cells in post-confluent conditions defined as cells cultured 12 days after reaching confluence. As presented in Fig.1C (top), post-confluent MOCK cells undergo higher OXPHOS than pre-confluent cells. Instead, glycolysis is not increased although we observed some increase of glycolytic capacity and reserve in post confluence MOCK cells. (Fig.1C, bottom).

In post-confluent condition, upon MEX3A overexpression, both mitochondrial respiration (Fig.1D) and glycolysis (Fig.1E) are impaired and limitation of cell respiration associated with MEX3A overexpression is stronger in post-confluence than in pre-confluence (Fig.1F).

2.3 Conclusions

It is known from the literature that pluripotent cells or stem cells exhibit a stronger dependence on glycolytic metabolism rather than OXPHOS while differentiated cells switch their energy metabolism to OXPHOS, producing more energy (see Introduction, Chapter I.2). In this line, I have shown in control Caco2 cells that post-confluence conditions, in which the cells are less proliferative and more differentiated, trigger an increase of cell respiration in comparison with pre-confluent cells.

I also observed that respiration is impaired upon MEX3A overexpression in pre-confluent conditions and that the glycolytic reserve is strongly increased. Therefore, these results support R. Almeida lab hypotheses that MEX3A regulates energy metabolism to control cellular differentiation.

In post-confluency, MEX3A overexpression promotes a decrease of both OXPHOS and glycolysis. Thus, suggesting they might use other metabolic pathways to fuel cellular processes. Maybe the pentose phosphate pathway is activated or glutamine or fatty acid catabolism are used to produce ATP. Therefore, further studies need to be done in order to better characterize the energy metabolism of MEX3A overexpressed cells in post-confluency.

Hence, this study brings new insights regarding the connection between energetic stress and cell polarity. Moreover, both metabolic results presented in this study and MEX3A

effects observed by Almeida R team on cellular differentiation, strongly suggest that MEX3A controls intestinal cell fate by regulating the energy metabolism and this control may involve the LKB1-AMPK-mTOR pathway. Further explorations are currently ongoing by Almeida R lab and a paper is in preparation.

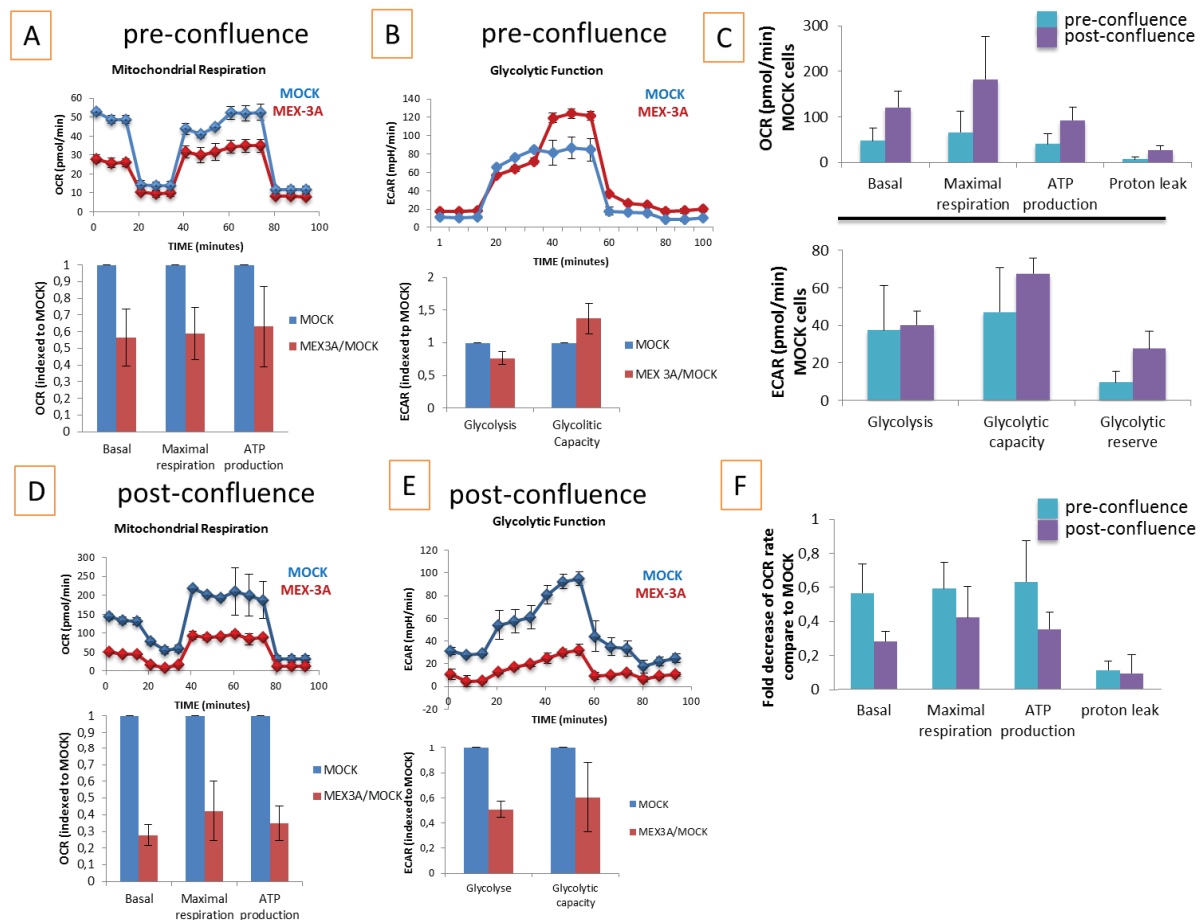


Figure1: MEX-3A a novel metabolic regulator involved in cell fate control. Caco2 cells overexpressing MEX-3A or Caco2 control cells (MOCK) were cultured for 3 days (pre-confluence) or 18 days (post-confluence) and analyzed by Seahorse. **A.** (pre-confluence) & **D.**(post-confluence). Representative curves showing change in oxygen consumption (OCR) analyzed by Seahorse (top) and quantification of % OCR relative to the control (MOCK)(Bottom). **B.** (pre-confluence) & **E.** (post-confluence). Representative curves showing changes in medium acidification (ECAR) obtained by Seahorse analyzer and quantification of ECAR (bottom). **C.** Comparison between the MOCK cells in pre and post-confluence conditions regarding OCR (top) and ECAR (bottom) quantifications. **F.** Quantification of MEX-3A regulation of OCR relative to MOCK in pre and post confluence conditions. All the experiments were performed three times. with three replicates in each experiment.

2.4 Materials and methods

Cell line and cell culture

The CaCo2 (heterogeneous human epithelial colorectal adenocarcinoma) cells transfected with MEX3A or MOCK were sent by Almeida R. lab. For these transfections they used pCMV-MEX3A expression vector together with a pCMV-Tag3B empty vector (Agilent Technologies) (Peirera et al., 2013).

Cells were cultured in 37C with DMEM (Ref. 41966-029, ThermoFisher Scientific) supplemented with 10% FBS and 1% penicillin-streptomycin. These are stable clones and G418 has been included in the medium at a concentration of 300ug/m. The medium was replaced every two days.

Seahorse analysis

Cells were plated at 1×10^5 cells per well of a 6-well plate. The metabolic measurements by Seahorse were done with cells in pre-confluency conditions, 3 days after plating (pre-confluency) or 12 days after reaching confluence (post-confluency). To do so, 3×10^4 cells (pre-confluency) or 2.5×10^5 cells (post-confluency) were seeded in 96-well Seahorse plate coated with fibronectin, in normal cell culture medium 30 minutes before assay. The plate was centrifuged at 200g for 1min (no centrifugal braking). After 30 minutes, the medium was replaced with Seahorse assay medium specific for OCR or ECAR measurements and equilibrated in non-CO₂ incubator for 1 hr. Seahorse analyzer uses a cartridge with 96 optical fluorescent O₂ and pH sensors to measure OCR (pmol/min) and ECAR (mPh/min). Basal OCR and ECAR were measured for 3 min every 10 min for 3 points, followed by sequential injection of different drogues presented in the previous project (see Tabel2 of Project3 1.2). Each treatment was measured for 3 min every 10 min for 3 points. OCR and ECAR were normalized by cell density. For both respiration and glycolysis, quantifications were performed by calculating for each category the mean and standard deviation from the values obtained from 3 independent experiments.

Conclusions

During my PhD I highlighted the role of LKB1 as an energy metabolic regulator in several polarized cells such as neural crest cells (NCC) and Sertoli cells. I also uncovered that MEX-3A, an LKB1 potential downstream target, is a metabolic regulator of colorectal adenocarcinoma cells, another polarized cell type. (Figure 1).

The first project revealed that Lkb1 regulates vertebrate head formation by controlling cranial NCC delamination, migration, polarity and survival through actin dynamic. Lkb1 in cranial NCC activates AMPK pathway which positively regulates ROCK kinase and consequently the actin molecular motor Myosin II. In the second part of this first project we uncovered the acetyl transferase GCN5 as a novel modulator of Lkb1 signaling during embryonic development and NCC formation. We showed that GCN5 controls LKB1 acetylation on K48 and suggested that this post translational modification may represent a crucial regulator of vertebrate head development.

The second project, emphasized the role of Lkb1 in truncal, vagal and sacral NCC differentiation and maintenance (Figure 1). We demonstrated that Lkb1 is essential for intestinal motricity, peripheral nerve formation and coat pigmentation through the control of NCC lineage. In particular, Lkb1 regulates neural crest specification into Schwann cells as well as the maintenance of neural crest derivatives involved in enteric nervous system such as satellite glial cells and enteric neurons. Our results pointed out a novel function of Lkb1 as a metabolic regulator of non-essential amino acids, like alanine and glutamate, during NCC specification. Our data brought complementary insights about how Lkb1 metabolic function impacts lysosomal activity, NCC fate and aging. We also uncovered a specific crosstalk between Lkb1 and p53 crucial for NCC ontogeny. Further, it will be of particular interest to analyze the contribution of p53 to NCC defects and to explore the link between GCN5 and p53.

The third project of my PhD was focused on a better characterization of Lkb1 signaling capacities to regulate energy metabolism in other polarized cells such as Sertoli cells and intestinal cells. We highlighted that Lkb1 expressed in Sertoli cells controls male fertility by regulating Sertoli cell polarity, hematotesticular blood barrier, myoid and Leydig cell proliferation, germ cell localization and maturation. Furthermore, our data described how LKB1 influences the energy metabolism of Sertoli cells potentially by limiting amino-acid levels such as alanine and glutamine (Figure 1). Finally, I showed that Mex-3A, a potential downstream target of Lkb1, controls the energy metabolism of intestinal cells and consequently their differentiation. (Result. Project 3.2) (Figure 1).

Altogether, these data obtained during my PhD projects delineated that LKB1 signaling is a key regulator of both cell polarity and energy metabolism during cell fate and could exert a coordinated connection between these two cellular processes.

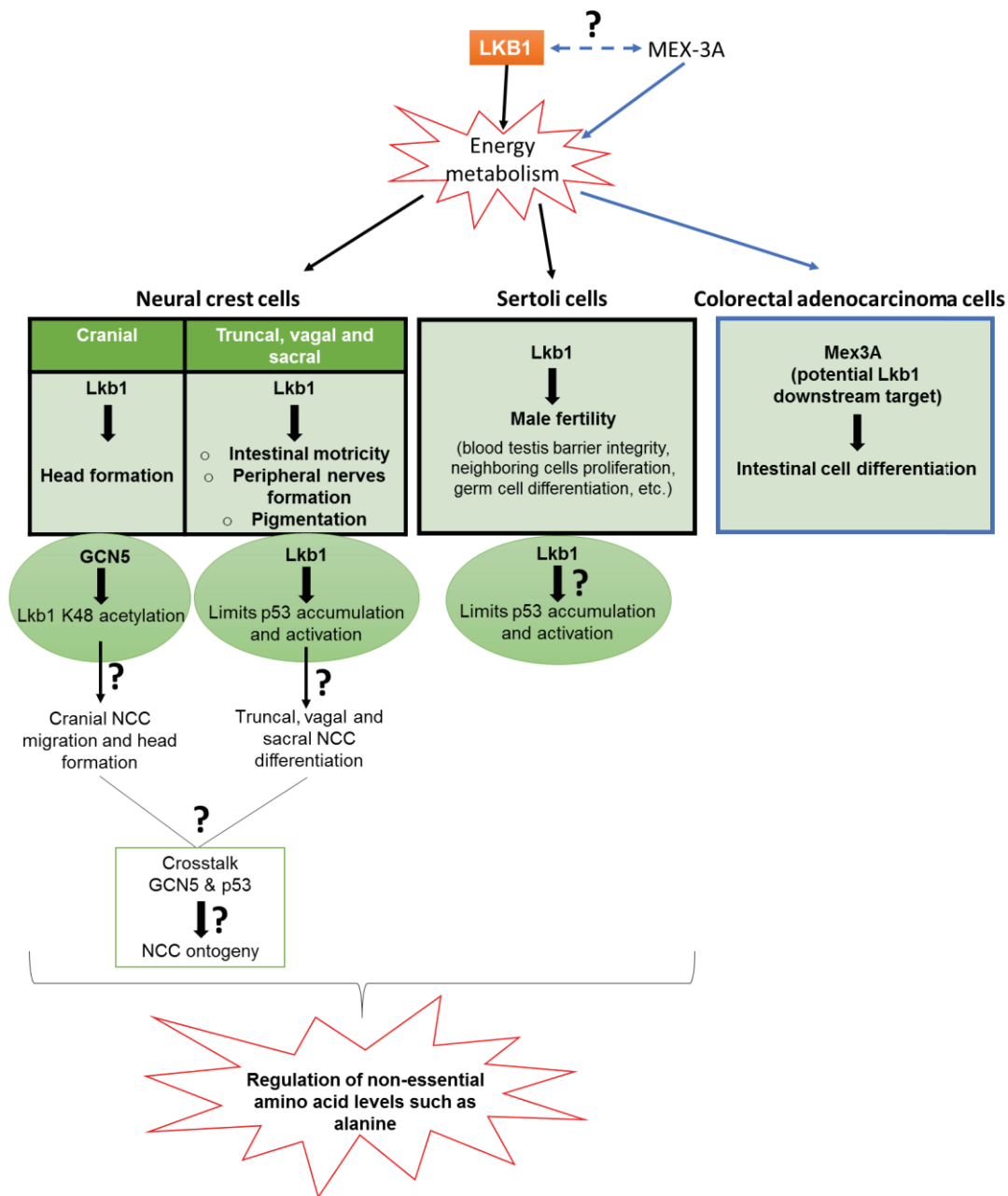


Figure 1. Schematic representation of my PhD projects

*General discussions &
Prospects*

I. LKB1 contributions to neural crest cells and underlying mechanisms.

1. LKB1 in neural crest cells lineage

As presented in the introduction chapters, neural crest cells (NCC) are embryonic multipotent cells that delaminate from neural tube and undergo polarized migration following stereotypical routes. NCC localization along the anterior-posterior axis of neural tube defines several NCC subpopulations that differentiate into many cell types (Introduction Chapter II.2). Our findings showed that *Lkb1* is essential for NCC lineage and governs several aspects of cranial, truncal, vagal and/or sacral NCC formation.

In particular, we identified that *Lkb1* regulates cranial NCC delamination and migration through AMPK/ROCK pathway and actin dynamics. Cranial NCC have the particularity to delaminate from the neural tube all at the same time (Theveneau and Mayor, 2011). Thus they start their migration as multilayered cell group, in opposition to other NCC like trunk NCC that delaminate progressively from neural tube and migrate as a single chainlike group (Theveneau and Mayor, 2011). Therefore, it will be interesting to analyze if *Lkb1* controls also the polarized migration of other NCC subpopulations like trunk NCC and if this regulation requires the AMPK/ROCK pathway.

Next, in order to better characterize the role of *Lkb1* during NCC lineage, Anthony Lucas, a 1st year PhD student working with Chantal Thibert, is currently completing the phenotypic characterization of the mice with “early” *Lkb1* inactivation in NCC used so far only to study the head formation. To begin, phenotypic characterization will be performed on enteric nervous system. Preliminary data of the team have shown that *Lkb1* loss in this model led to an aganglionosis in the distal colon, a phenotype reminiscent to human Hirschsprung disease. Moreover, *Lkb1* loss triggered a hypoganglionosis in the intestine. Indeed, the number of enteric neurons and satellite glial cells were reduced in absence of *Lkb1*. However, NCC migration alongside the gut during embryonic development of the enteric nervous system was not affected. Further, A. Lucas will confirm these results and, by using primary cultures of enteric neurospheres, *ex vivo*, will analyze the proliferation, survival, differentiation and metabolism of enteric NCC and their derivatives. Next, he will characterize the NCC specification into Schwann cells and the NCC-derived melanoblasts in the skin. Finally, he will evaluate the impact of *Lkb1* loss on the formation of other organs containing NCC-derivatives such as heart and thyroid. Providing an overall phenotyping of NCSC-derived tissues upon *Lkb1*-deficiency will reinforce our understanding of the importance of LKB1 signaling in NCSC and its potential contribution to human neural crest disorders.

Furthermore, in the continuity of our two first projects, the team will analyze by the technics described in the result chapters, if LKB1 acetylation at lysine 48 by GCN5 contributes to NCC development (see Results, Project I.2.3) and if p53 signaling also participates to the neurocristopathy phenotype due to *Lkb1* inactivation.

p53 accumulation blocks cranial NCC proliferation and impairs NCC delamination from the neural tube as well as their migration (Rinon et al., 2011; Van Nostrand et al., 2014b). Thus, p53 levels during early development are essential for vertebrate face formation. Our first project provided evidence suggesting that GCN5, the upstream regulator of LKB1, may also be a regulator of cranial NCC migration and head development. From the literature, we know that deletion of GCN5 in mice led to early embryonic lethality and inactivation of both GCN5 and p53 partially rescued the phenotype: embryos lived longer although they still die at mid gestation (Bu et al., 2007). This strongly suggest that p53 is accumulated also in absence of GCN5 and could affect early embryonic development in this model. Hence, we could study this hypothesis *in vitro* by inactivating GCN5 in NCC and analyze LKB1 acetylation on lysine 48, p53 accumulation, NCC differentiation and migration. If the differentiation and/or migration are impaired and p53 is accumulated and activated, we could double knockdown *GCN5* and *p53* to see if it rescues the phenotype. Further, we could analyze if this role of GCN5 as a p53 regulator is linked to its capacity to acetylate LKB1 on lysine 48. If *in vitro* results are promising, *in vivo* experiments could be performed on chick embryos in collaboration with Sylvie Dufour (Institut H. Mondor pour la Recherche Biomédicale, Créteil, France).

In conclusion, these studies will (i) reveal if the role of LKB1 in cell migration is conserved in other NCC subpopulations than the cephalic ones, (ii) underline the role of *Lkb1* during NCC lineage and (iii) uncover if there is a crosstalk between GCN5 and p53 important for NCC development.

2. LKB1 & Neurocristopathies

LKB1, a modulator gene in human neurocristopathies?

The complex phenotype developed by the genetically engineered mice that we generated to inactivate *Lkb1* in NCC recapitulates the symptoms of human neurocristopathies and suggests that LKB1 could contribute to the etiology of these disorders.

As a brief reminder, neurocristopathies are human diseases due to NCC defects at various developmental stages such as their formation, delamination, migration, differentiation and survival (Introduction, Chapter I.3.1). Neurocristopathies include a broad group of diseases and syndromes like colon aganglionosis, craniofacial malformations (cleft lip/palate, sensorineural deafness, smelling defects), heart malformations, skin/hair pigmentation defects and for some patients, demyelination. Although neurocristopathies have a high medical and

societal impact, the main treatment is surgery but is often variable and rarely entirely corrective. In some cases, the surgery is not even possible. Moreover, our understanding regarding the molecular and genetic networks responsible for these pathologies is still very preliminary.

In order to test if *LKB1* is a modulator gene in these pathologies, in collaboration with scientists working in this field, we could sequence the genes coding proteins of the LKB1 holoenzyme (LKB1, MO25, STRAD α and β) in patients with neurocristopathies to search for mutations.

Analyses of LKB1 holoenzyme in neurocristopathies are strongly relevant given that bi-allelic deletions of exons 9 to 13 of the *STRAD α* gene are responsible for the human syndrome Polyhydramnios Megalencephaly Symptomatic Epilepsy (PMSE). This syndrome is a developmental disorder characterized by craniofacial abnormalities, infantile-onset epilepsy and neurocognitive delay (Puffenberger et al., 2007). The PMSE-causing mutation in humans represents a loss-of-function mutation that destabilizes STRAD α and prevents it from activating LKB1 (Orlova et al., 2010; Zeqiraj et al., 2009). Therefore, PMSE patients have an increased mTOR pathway. Interestingly treatment of 5 PMSE patients with Sirolimus, the mTORC1 inhibitor rapamycin, limited seizures frequency (Parker et al., 2013).

The most interesting neurocristopathy to seek for mutations of genes of LKB1 signaling is the Peripheral demyelinating neuropathy, Central dysmyelination, Waardenburg syndrome, and Hirschsprung disease (PCWH), a subgroup of Waardenburg-Shah syndrome (WS4). Indeed, the complex phenotypes developed by our mouse models (coat depigmentation, peripheral neuropathy and demyelination, intestinal pseudo-obstruction and distal colon aganglionosis) are very evocative of the symptom of PCWH patients. All PCWH patients harbor Sox10 mutations which are associated with about half of WS4 cases and 15% of Waardenburg Syndrome II cases (Pingault et al., 2010). Sox10 mutations often occur at the heterozygous state and can be germline or de novo mutations. High phenotypic variability with an incomplete penetrance of each symptoms has been observed in the few familial cases described yet. So far, the causes of this phenotypic discrepancy, especially between WS2, WS4 and PCWH patients is not clear although the nature of the mutations (truncating or missense mutations) has been proposed to explain phenotype variability (Chaoui et al., 2011, 2015). Furthermore, modulator genes could contribute to NCC defects along with Sox10 mutations. Such genetic interactions have been already described between Sox10 and the transcription factor Zeb2, the receptor/ligand EDNRB/EDN3 or Integrin β 1 (Stanchina et al., 2010; Watanabe et al., 2013, 2017). It will thus be of interest to study the involvement of Lkb1 signaling in PCWH. However, WS4 and PCWH are very rare genetic disorders and less than 30 cases of PCWH have been reported in the literature. The identification and validation of mutations would then be difficult and hardly statistical due to low number of patients.

Is LKB1 involved in NCC defects associated with lysosomal storage disorders?

Lysosomes have recently been proposed as signaling hubs: they integrate and relay external and nutritional information thus controlling proteolysis and cell senescence to prevent premature aging (Carmona-Gutierrez et al., 2016). As specified in results, project II.2, the team will further explore how the signaling pathways Lkb1 and p53 controls lysosomal proteolysis to limit lipofuscin formation, senescence and premature aging in NCC.

Lysosomes control intracellular Ca^{2+} levels and defects in Ca^{2+} uptake are responsible for several lysosomal storage disorders (Lloyd-Evans, 2016; Lloyd-Evans et al., 2008; Styrt et al., 1988). As calcium regulates NCC migration (see Introduction, Chapter IV.3.1), defects of lysosomal Ca^{2+} uptake may also lead to neurocristopathies. In 2003, Hanson et al. showed that several lysosomal storage disorders are associated with dermal melanocytosis, a pathology due to perturbed migration of melanocytes from neural crest to the developing epidermis (Hanson et al., 2003). This pathology is part of the criteria for a subgroup of neurocristopathies named Phakomatosis pigmentovascularis (Hanson et al., 2003). Moreover, it has been reported in 2015 the case of a 3 years old child which developed symptoms of both Hirschsprung's disease, a neurocristopathy described in chapter II.3.1, and cystinosis, a lysosomal storage disorder characterized by body accumulation of the amino acid cysteine (Mittal et al., 2015). Finally, as presented in the introduction (Chapter II.3), many ribosomopathies with NCC defects are associated with acute myeloid leukemia (AML). Part of AML patients have accumulation of misfolded proteins (Schardt et al., 2009) and lysosomal defects (Sukhai et al., 2013) probably caused by increased iron levels which subsequently enhance the sensitivity to oxidative stress and lysosomal alkalization. Interestingly, treatments decreasing oxidative stress such as iron chelators, vitamin E and glutathione treatments, delay lipofuscin production and accumulation in murine models (Brunk and Terman, 2002; Skoczyńska et al., 2017). These treatments are also efficient for neurocristopathies like the Treacher Collins Syndrome (Trainor et al., 2009; Sakai and Trainor, 2016; Sakai et al., 2016). However, for the moment, very little is known about the molecular links between neurocristopathies and lysosomal defects.

Apolipoprotein D (ApoD), which is a glial derived lipid binding protein produced by astrocytes and Schwann cells (García-Mateo et al., 2014), is also accumulated in neurodegenerative diseases, aging brain and peripheral nervous system injury (Dassati et al., 2014; García-Mateo et al., 2014; Martínez et al., 2013; Sanchez et al., 2015). ApoD has been proposed as a marker of lysosomes that are the most vulnerable to oxidative stress (Ganforina et al., 2010; Pascua-Maestro et al., 2017). Therefore, we could study if there is an accumulation of ApoD in our mouse models and if this accumulation depends on alanine

aminotransferase (ALAT) activity and alanine-pyruvate cycling. Further it will be interesting to analyze ApoD in patients with neurocristopathies.

Such data would expand our understanding of the role of LKB1 on oxidative stress regulation, partly via its crosstalk with p53 signaling, lysosomal homeostasis and premature aging in neural crest disorders.



Overall, our projects will provide relevant information on the pathological underpinning of neural crest diseases as well as on mechanisms linking metabolism and cell fate such as differentiation but also premature aging. However, it remains difficult to transpose these knowledges in patients with neurocristopathies. Therefore, it will be interesting to analyze the role of Lkb1 in other human pathologies related to NCC-derivatives defects like mesenchymal stem cells-derived-Schwann cell precursors defects.

3. Regulation of Schwann Cell Precursors by LKB1?

Schwann Cell Precursors (SCP) derive from cranial, truncal and vagal NCC. They conserve the multipotency and high plasticity of NCC, being therefore able to generate several cell types during both embryogenesis and adulthood such as Schwann cells, neurons and melanocytes (Introduction, Chapter II.2.3). SCP multipotency has been discovered many years ago (Sherman et al., 1993) by *in vitro* studies. However, only very recently it has been clearly shown by *in vivo* analyses that SCP also differentiate into melanocytes, enteric neurons or bone marrow mesenchymal stem cells (see Introduction, Chapter II.2.3). Our results strongly suggest that Lkb1 signaling is essential for SCP maintenance.

While studying Cre expression in the “late” model of *Lkb1* inactivation (using the Tyr::Cre driver) we identified that some cells in the bone marrow also expressed the recombinase Cre (see Results, Project II.1 submitted article Sup.Fig.3 F). These cells most probably are SCP-derivatives and Lkb1 may thus be also inactivated in SCP-derived mesenchymal stem cells. It could be interesting to further validate this hypothesis and evaluate if this is also the case in the “early” model of *Lkb1* inactivation in NCC. Of note, AMPK controls the proliferation of mesenchymal stem cells (de Meester et al., 2014) and contributes to tight junctions formation in these cells (Rowart et al., 2017). Studying *Lkb1* inactivation in mesenchymal stem cells and the consequences for the homeostasis of the hematopoietic niche as well as the establishment and maintenance of hematopoietic stem cells and derivatives would then be of great interest. Bone marrow and blood composition analyses could be easily performed on the 2 mice models generated by the lab.

A biobank of mesenchymal stem cells has been collected at the hospital of Grenoble by S. Park (IAB, EFS, UGA, CHU, Grenoble) from patients with myelodysplasia, some of them due to the 5q deletion responsible of a ribosomopathy (see chapter II.3). Control samples were collected from sternal puncture during cardiac surgeries. Assessing the status of LKB1/AMPK/mTOR signaling in this collection of cells could be a first step in the exploration of LKB1 defective signaling in NCC and SCP in human disorders. As the genetic screening for proteins of the LKB1 holoenzyme is difficult in neurocristopathies due to the low number of patients, we could undergo genetic analyses in mesenchymal stem cells of patients with myelodysplasia.

SCP have an important potential for clinical use and for developing new therapeutic approaches, due to their multipotency and the fact that they persist in adult nerves. However, we still do not know so far how energy metabolism regulates SCP fate. Therefore, this study about the role of LKB1 in mesenchymal stem cells could also represent an important step for a better characterization of the underlying molecular mechanisms.

II. LKB1 contributions to intercellular communication and tissue homeostasis

Our work highlighted that LKB1 is essential to maintain whole tissue homeostasis. Indeed, *Lkb1* conditional inactivation:

- in Schwann cells promoted neurodegeneration (Results, Project II.1).
- in Sertoli cells perturbed germ cell maturation and Leydig and myoid cells proliferation (Results.Project III.1).
- in enteric nervous system affected differentiation and/or maintenance of intestinal epithelial cells and potentially smooth muscle cells (data not shown).

The enteric glial cells are important for gastrointestinal motricity and to control the epithelial barrier integrity (Neunlist et al., 2014). They help maintaining the intestinal barrier by forming a cellular and molecular bridge between enteric nerves, immune cells as well as enteroendocrine cells within the intestinal epithelium (Sharkey, 2015).

Preliminary observations during our studies, showed that *Lkb1* inactivation in enteric neurons and satellite glial cells promoted a lack of Paneth cells in the intestinal epithelium as well as defects in stromal tissue such as loss of adherence between cells (data not shown). In order to better characterize this role of *Lkb1* the team initiated a collaboration with R. Almeida lab. Immunostaining for various markers of intestinal or smooth muscle differentiation will confirm if *Lkb1* absence in enteric nervous system affects cell differentiation and survival. Hence, this project will contribute to understand the interaction between enteric nervous

system and adjacent cells and analyze a novel function of Lkb1 as regulator of this cell-cell communication.

Cell to cell communication is an ancient process through which one cell is capable of modulating the behavior of another via the secretion of signal molecules.

In our studies, one explanation could be that Lkb1 loss leads to deregulated intercellular communication due to defective metabolites. This metabolic communication may be controlled by Lkb1-dependent regulation of transaminases, also known as aminotransferases.

III. Metabolic regulations exerted by LKB1

As a brief reminder aminotransferases are enzymes able to transfer nitrogenous groups between an amino acid and an α -keto acid. They belong to class EC. 2.6.1 and so far, there are 101 transaminases described on ExPASy database (Bioinformatics Resource Portable).

Our studies revealed that Lkb1 controls NCC specification into glial cells by repressing a non-essential amino acid biosynthetic program coupled to pyruvate-alanine transamination (Results, Project II.1). Our data thus led us to hypothesize that Lkb1 limits alanine-aminotransferase (ALAT) activity whereas it favors glutamate synthetase (GS) activity. ALAT catalyzes alanine production by transferring an amino group from L-glutamate to pyruvate in order to form L-alanine and α -ketoglutarate (this reaction is reversible).

Lkb1 expressed in Sertoli cells controls germ cell maturation also by regulating non-essential amino acid levels (Results, Project III.1).

One of the most affected amino acid in both studies (NCC and Sertoli cells) was alanine which was up-regulated. Thus, this role of Lkb1 as a new metabolic regulator of pyruvate-alanine cycling seems conserved across cell types sharing similar metabolic functions.

1. Feedback loops between aminotransferases and the mTOR pathway.

Coloff and its coworkers have shown that aminotransferases are important regulators of the proliferation - quiescence balance (see Introduction, Chapter I-3.3 and Figure7). They observed that mTOR pathway regulates positively mRNA expression of aminotransferases such as PhosphoSerine AminoTransferase1 (PSAT1), Aspartate AminoTransferase1 (AAT1 or GOT1) and Alanine AminoTransferase2 (ALAT2 or GPT2) (Table1). However, mTOR inhibition with TORIN1, a drug which inhibits both mTORC1 and mTORC2 complexes, reduced only PSAT1 and ALAT2 protein expression and decreased only alanine levels (Coloff et al., 2016).

In my studies, I have shown that both ALAT and mTOR inhibition are able to restore glial differentiation in absence of Lkb1 (see Results, Project II.1). However, it is the alanine

production which regulates mTOR pathway because ALAT inhibition, and therefore, alanine down-regulation, partially normalized (decreased) the mTOR pathway. This result correlates with the literature since it is known that mTOR is activated at lysosomal surface in an amino acid dependent manner (see Introduction, Chapter IV.2.1). So far, most research has been focused on leucine and glutamine/glutamate amino acids whereas the control of mTOR activity by alanine has received less attention, although alanine was shown a long time ago to be involved in proteolysis (lysosomal activity) regulation (Caro et al., 1989; Leverve et al., 1987). Our study showed for the first time that alanine also regulates mTOR and that Lkb1 controls this mTOR amino acid-dependent regulation. Thus, our results in association with Coloff et al. results suggest that there is a feedback loop: aminotransferases as well as amino acid levels regulate mTOR activity and activated mTOR controls aminotransferases and amino acids expression. To analyze if there is a feedback loop in our system, we could treat *Lkb1* knockdown cells with mTOR inhibitor (TORIN1) and measure amino acid levels (alanine, glutamate) as well as ALAT and GS activity (in our system ALAT mRNA or protein expression is not affected).

2. How LKB1 signaling regulates aminotransferases activity?

Until last year, nothing was known about LKB1 and aminotransferases. Recently, the molecular links between LKB1 and these enzymes started to be a topic of high interest and several studies underlined this link (Table 1):

- N. Bardeesy lab has shown that LKB1 downregulates PSAT1 expression and activity leading to serine metabolism inhibition (Table1). Serine metabolism fuel the methionine salvage pathway that produces the methyl donor S-adenosyl methionine (SAM) (Figure 1). Thus, LKB1 deficiency increased serine metabolism and consequently DNA methylation which regulates gene expression. This role of LKB1 was detected in pancreatic cancer cells and is essential for its tumor suppressor activity (Kottakis et al., 2016).

- Another aminotransferase linked to LKB1 signaling is Glutamine:Fructose-6-phosphate AmidoTransferase 1 (GFAT1). It has been shown that AMPK, the LKB1 downstream substrate, inhibits GFAT1 activity by its phosphorylation on serine 243 (Table1) (Scott and Oakhill, 2017; Zibrova et al., 2017). GFAT1 is a negative regulator of angiogenesis and it has been shown to be linked to diabetic state (Cooksey et al., 1999; Hebert et al., 1996). GFAT1 activation promotes an increase in O-linked- β -N-glucosamine acetylation (O-GlcNAcylation) of proteins which is a hallmark of vascular complications of type 2 diabetes (Ma

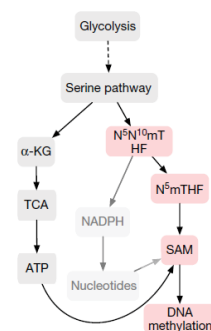


Figure 1. Serine glycine one carbon network promotes DNA methylation in absence of Lkb1. (Kottakis et al., 2017)

and Hart, 2013; Srinivasan et al., 2007). Therefore, the AMPK-GFAT1 crosstalk regulates vascular dysfunction associated with metabolic disorders (Zibrova et al., 2017)

- Recently C. Perret team (Paris, Institut Cochin) has shown that hepatocellular Lkb1 negatively regulates Alanine Glyoxylate AminoTransferase (AGXT) expression at the transcriptional level (Table1) (data not published yet). AGXT is highly expressed in liver and has a double function: it detoxifies glyoxylate and is involved in gluconeogenesis from serine (Ichiyama, 2011). C. Perret team demonstrated that Lkb1 regulates hepatic gluconeogenesis

Aminotransferases regulated by LKB1/AMPK /mTOR	Regulators	Regulations	Expression	Functions of these regulations	References
PhosphoSerine AminoTransferase (PSAT1)	Lkb1	Downregulation of protein expression and activity	Pancreatic cancer cells	Tumor suppressor activity, limits proliferation and tumor growth	Kotakis et al., 2017 (Nature)
PSAT1	mTORC1	Upregulation of their mRNA levels and protein levels	Breast cancer cells	Tumor suppressor activity, limits proliferation	Coloff et al., 2016 (Cell Metab)
Alanine AminoTransferase (ALAT2/GPT2)					
Aspartate AminoTransferase (AAT1/GOT1)					
Glutamine:Fructose-6-phosphate AminoTransferase1 (GFAT1)	AMPK	Decrease GFAT1 activity by its phosphorylation at Ser243	Endothelial cells	Pro-angiogenesis	Zibrova et al., 2017 (Biochemical journal)
AGXT1	Lkb1	Downregulates mRNA and protein levels	Hepatocytes	Limits gluconeogenesis	C.Perret, not yet published
ALAT ?	Lkb1?	Its not affecting mRNA or protein expression Decrease ALAT activity?	- NCC derived-glial cell, - Embryonic fibroblastes, - Sertoli cells ?	NCC differentiation Male fertility?	Radu et al., submitted Torch et al., in preparation

Table1: Aminotransferases regulated by LKB1/AMPK/mTOR

by downregulating AGXT aminotransferase expression and therefore limiting the availability of amino acids such as alanine, glutamine and serine as gluconeogenic precursors (Charawi S et al., data not published yet).

- In addition to these studies, I have shown that Lkb1 regulates ALAT although the underlying mechanisms are still unknown (Table1). I observed that neither the expression nor the protein stability of ALAT and other metabolic enzymes were drastically impaired upon *Lkb1* loss. Measurement of ALAT activity in control cells or *Lkb1* knockdown cells are necessary to further confirm our first results.

Our data suggest that post-translational modifications could regulate the enzymatic activities. As LKB1 is a master kinase acting through downstream kinases such as AMPK, the lab will thus explore if the phosphorylation status of ALAT enzyme is modified upon *Lkb1* loss. In particular, ALAT1 phosphorylation has been observed in large scale mammal

phosphoproteome analyses (Zhou et al., 2013; Bian et al., 2014). The sequence surrounding the phosphorylated site threonine 22 in ALAT partially matches the AMPK phosphorylation motif recently described (Schaffer et al., 2015). We will thus further investigate in NCC-derived glial cells if ALAT activity is controlled by its phosphorylation status through AMPK kinases. We will assess the phosphorylation by blotting immunoprecipitated ALAT with a mix of monoclonal antibodies that specifically recognizes phosphorylated serine/threonine in AMPK motifs (LXRXX(pS/pT); Cell Signaling Technology). If we identify that the potential sites in ALAT are indeed phosphorylated by AMPK, we will generate non-phosphorylatable mutants and assess the impact on their enzymatic activities.

Collectively, these data will complete the very recent literature regarding the link between LKB1 signaling pathway and aminotransferases and will provide evidence that LKB1 is a key regulator of cell behavior through the control of ALAT and alanine biosynthesis.

IV. Wider implication for LKB1 in human metabolic diseases and cancers?

So far, mutations of *LKB1* are associated only with tumor formation: germline mutations are responsible for the human Peutz-Jeghers syndrome whereas somatic mutations are associated with sporadic tumors (Introduction, Chapter III.A.5). Owing to all the cellular processes regulated by LKB1 signaling, we could expect a broader implication of LKB1 in human diseases.

Our results suggested that aberrant LKB1 metabolic signaling underlines the etiology of various human pathologies such as neurocristopathies potentially associated with lysosomal storage disorders; metabolic syndromes, peripheral neuropathies as well as cancers.

1. Is LKB1 involved in neurocristopathies associated with metabolic syndromes?

Nowadays, little is known about the involvement of metabolism defects to neurocristopathies occurrence. There is so far only one article suggesting that some metabolic syndromes such as Pyruvate Deshydrogenase deficiency and Oxidative phosphorylation deficiency can be associated with neurocristopathies since these metabolic diseases are associated with similar facial abnormalities (Table 2) (Berio A., 2011).

The link between oxidative phosphorylation and transaminases activity is still not very clear. During our study, we surprisingly observed that the aminotransferase ALAT activity and the production of non-essential amino acids such as alanine, are crucial for NCC differentiation independently of oxidative phosphorylation (Results, Project II.1). Indeed, glial differentiation

was restored whereas oxidative phosphorylation was still strongly impaired. These data underline the importance of transaminases and amino acid levels for cell fate.

In the last 10 years, several epidemiologic studies have shown that elevated levels of ALAT and aspartate aminotransferase (AST) in blood, known as biomarkers for liver diseases (Kew, 2000), can also be serum biomarkers for metabolic syndromes like type 2 diabetes even in the absence of hepatocellular damages (Bonora and Targher, 2012; Goessling, 2012; Goessling et al., 2008; Sookoian and Pirola, 2012). Thus, we could measure if there is an increase in serum alanine levels and ALAT activity in our mouse models reminiscent of neurocristopathies. However, we have to be precautious because it may be difficult to observe any increase of ALAT in blood upon specific *Lkb1* inactivation only in some cell types (Schwann cells, enteric neurons, satellite glial cells, melanocytes, cranial NCC, etc.) which are not known to have a high ALAT activity.

We could also analyze ALAT activity in plasma of patients with neurocristopathies and study if this enzyme could be a biomarker of neurocristopathies associated with metabolic syndromes. These studies would complete the analyses proposed in paragraph I.1 regarding the screening of genes coding for proteins of the LKB1 holoenzyme in patients with neurocristopathies.

2. Does LKB1 contribute to regulate peripheral neuropathies through the control of alanine levels?

As already described, *Lkb1* inactivation in neural crest cells promoted a peripheral neuropathy among other phenotypes (Results, Project 2.1).

Increased alanine levels have been associated with peripheral neuropathies such as hereditary sensory and autonomic neuropathy type 1 (HSAN1) (OMIM 162400). This disorder is characterized by sensory loss and lower limbs paralysis due to defective neurons with smaller mean axon diameter of myelinated and nonmyelinated fibers and abnormal Schwann cells (Garofalo et al., 2011). However, this pathology is not caused by ALAT defects but rather by serine palmitoyltransferase (SPT) missense mutations (Garofalo et al., 2011; Othman et al., 2012). Serine palmitoyltransferase catalyzes the formation of sphinganine, a precursor of sphingolipids (cell membrane lipids), from L-serine and palmitoyl-CoA (Figure 2A). This enzyme, in specific conditions, is able to use also other substrates such as L-alanine (Figure 3A). In presence of L-alanine it forms deoxysphinganine which is not degraded by the canonical sphingolipid degradation pathway and is neurotoxic (Figure 2B). Garofalo and his colleagues have shown that 10% of L-alanine enriched diet increases deoxysphinganine levels in plasma, sciatic nerves and liver and promoted a severe peripheral neuropathy in mice (Garofalo et al., 2011). The levels of deoxysphinganine were measured by chromatography-mass spectrometry (LC-MS), as described by Eckardstein team (Penno et al., 2010). L-serine

enriched diet rescued the phenotype (Garofalo et al., 2011). This suggests that there is a balance between alanine and serine, their levels being associated to neurotoxic product formation and peripheral neuropathy development. Therefore, alanine accumulation observed in sciatic nerves of *Lkb1* conditional knockout mice (Results, Project II.1) may correlate with an increase in deoxysphingolipids which aggravates the peripheral neuropathy. In order to test this hypothesis, we could analyze the levels of deoxysphingolipids first *in vitro*, in NCC-derived glial cells knockdown for *Lkb1* and second in plasma and sciatic nerves of *Lkb1* conditional knockout mice, by lipid extraction, sequential acid and basic hydrolysis and chromatography-mass spectrometry (method described in Penno et al., 2010). If an increase in deoxysphingolipids is observed, the lab could further test if L-serine enriched diet rescues the peripheral neuropathy.

Clinically, HSAN1 is very similar to diabetic peripheral neuropathy. Recently, elevated plasma levels of deoxysphingolipids have been identified as a novel biomarker for diabetes and correlate with distal sensorimotor polyneuropathy (Dohrn et al., 2015; Hammad et al.,

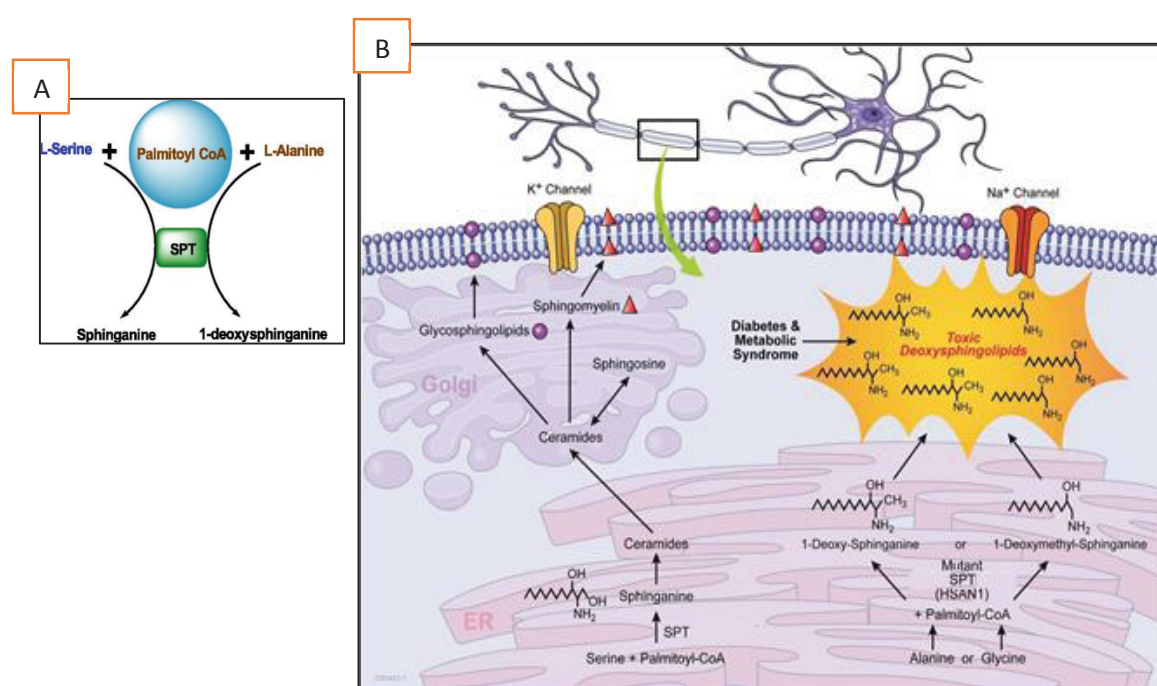


Figure 2: Serine and alanine regulate the generation of bioactive sphingolipids and toxic deoxy-sphingolipids. **A.** Formation of bioactive sphinganine and toxic deoxy-sphinganine (modified from Kowlurum A, 2014). **B.** Sphingolipid de novo synthesis is catalyzed by the SPT enzyme through the condensation of palmitoyl-CoA and L-serine to form sphinganine in the endoplasmic reticulum (ER). In HSAN1, mutant SPT prefer alanine or glycine instead of serine and form deoxy- or deoxymethyl-sphingolipids, which can no longer be metabolized to complex sphingolipids or degraded by the canonical degradation pathway, thus leading to toxic accumulation (Klein, 2015).

2017; Mwinyi et al., 2017; Othman et al., 2015a). Decreasing plasma deoxysphingolipids, by oral L-serine supplementation, improves neuropathy in diabetic rats (Othman et al., 2015b).

Altogether, these data suggest that increased alanine levels are responsible for deoxysphingolipids formation and accumulation which are neurotoxic and affect Schwann cells and lead to peripheral neuropathy. The project proposed here will bring evidence about the molecular mechanisms by which Lkb1-dependent metabolic control of non-essential amino acids impacts deoxysphingolipids formation and peripheral neuropathy regulation.

3. How metabolic regulations exerted by LKB1 contribute to its tumor suppressor activity?

As already described, during my PhD I studied the metabolic regulation exerted by Lkb1 using both *in vivo* and *in vitro* approaches as well as the crosstalk between Lkb1 and p53 signaling pathways. So far, we focused on exploring Lkb1 contribution to developmental steps and how defects in Lkb1 signaling could be part of developmental diseases. Transposition of these findings observed during development to cancer cells is crucial especially regarding recent data from the literature highlighting (i) the important role of lactate and glutamine in the metabolism of tumor cells and (ii) the role of transaminases in cancer cell proliferation (see Introduction, Chapter I.3.3).

(i) Pyruvate has different fates: it can be transformed into lactate by lactate dehydrogenase (LDH), into alanine by ALAT or it can enter into the mitochondria to fuel TCA cycle. Our results unveil a key role played by Lkb1 in limiting pyruvate-alanine cycling in both NCC and Sertoli cells. However, there are some tissue specificity since we observed that *Lkb1* loss in Sertoli cells, by contrast to NCC, promotes lactate accumulation and oxidative phosphorylation augmentation. These increases of both alanine and lactate are also observed in cancer cells. In tumors, the concentration of lactate is 80 times higher than in normal situations, reaching 40 mM. Many clinical studies highlighted that lactate accumulation is a marker of poor prognosis in cancers (Romero-Garcia et al., 2016). Recently it has been shown that cancer cells prefer to use lactate instead of glucose for oxidative phosphorylation (Harjes, 2017; Faubert et al., 2017; Hensley et al., 2016; Hui et al., 2017). Thus, it will be interesting to study if LKB1 controls lactate turnover in cancer cells. In support to this idea AMPK has been shown recently to control LDH activity and metabolic homeostasis in muscle stem self-renewal (Theret et al., 2017).

Rapid proliferation and survival of some cancer cells is dependent on high glutamine uptake from exogenous supply (Cluntun et al., 2017). By contrast, other tumor cells exhibit upregulated glutamine synthesis (Cluntun et al., 2017). Tissue origin of cancer cells is one possible explanation of this metabolic heterogeneity between tumors. Very recently, it was shown that *Lkb1* loss confers glutamine dependency during kidney development and was

associated with kidney polycystic disease (Flowers et al., 2018). We also observed during testis development that *Lkb1* deficiency is associated with glutamine accumulation along with alanine increase.

Exploring how LKB1 regulates both lactate and glutamine by measuring their levels, uptake and biosynthesis in lung cancer cells is therefore very important.

(ii) As previously presented, N. Bardeesy lab showed that LKB1 regulates pancreatic cancer cell growth by downregulating PSAT1 expression and activity leading to serine metabolism inhibition and DNA methylation loss (Table 1) (Kottakis et al., 2016). Coloff and his colleagues analyzed aminotransferases mRNA expression in breast cancer using The Cancer Genome Atlas (TCGA) breast cancer RNA-sequencing dataset. They identified that PSAT1, ASAT1 and ALAT2 expression positively correlated with highly proliferative breast tumors. Further, by using the TCGA reverse-phase protein array (RPPA) database, they underlined a correlation between the expression of previously detected aminotransferases and mTOR activity (Coloff et al., 2016). These data coupled with our own observation that LKB1 negatively regulates ALAT which controls mTOR pathway during embryonic development, prompts us to investigate if this function of LKB1 is also part of its tumor suppressor activity.

LKB1 mutants associated with tumors are often truncating mutations leading to *LKB1* loss. *LKB1* mutations strongly potentiate tumor progression due to KRas^{G12D} oncogenic mutations. Molecular profiling performed by combining genetic and histological studies of an international lung tumors biobank collected in part at Grenoble by E. Brambilla lab, revealed that *LKB1* and *KRas* mutations and consequent mTOR upregulation are associated with 30% of lung adenocarcinomas (Cancer Genome Atlas Research Network, 2014). However, patients harboring triple mutations in *KRas*, *LKB1* and *p53* are very rare although *p53* is also very frequently mutated in lung adenocarcinomas. This observation supports the idea that *LKB1* loss in a context of *KRas* mutation could modify *p53* signaling endogenously present in tumor cells. Moreover, *LKB1* has been shown to promote metabolic flexibility in lung cancer cells upon energy stress (Parker et al., 2017).

The lab is thus interested in further exploring LKB1 metabolic regulations and LKB1-*p53* crosstalk in lung cancer cells. To these purposes, the lab developed lung cancer cells that express KRas^{G12D} oncogenic mutant and are null for *LKB1* and *p53* (collaboration C Thibert with L Attardi and M. Winslow, Stanford, CA, USA). Several cell lines of lung tumors from patients are also available to the lab. Therefore, Marie Mevel, a second year Master student under the supervision of Chantal Thibert, will study metabolic regulations by LKB1 in lung cancer cells. The cell models described above will allow to study lung cancer cells null for *LKB1* with rescued LKB1 expression (either wildtype or mutants) along with or without *p53* using retroviral infections to re-express *p53* wild type. With this model, the group will also study the role of LKB1 acetylated at K48 in lung cancer cells and its link to *p53*.

Finally, M. Billaud lab identified a potential antitumoral drug, named L6, by a screen on *LKB1* null cells compared to *LKB1* wildtype cells. This drug belongs to the family of biguanides, such as Metformin, widely used in type 2 diabetes treatment and known to control energy metabolism of the cells. Using Metformin for several years to limit diabetes, an antitumoral role was suspected and more than hundred clinical trial are currently ongoing. M. Billaud lab observed that the biguanide L6 acts with much lower doses than Metformin and could have a mode of action on energy metabolism different than the one of Metformin. Therefore, the lab will analyze if L6 treatment of lung cancer cells target deregulated metabolic pathways due to *LKB1* loss such as amino acid levels and transaminases activity. Exploring antitumoral properties of L6 on lung cancer progression *in vivo* will be explored using chick models of cancer cells grafts, either on the chorioallantoic membrane (InOvation startup, Grenoble) or in the proper tumoral microenvironment (OncoFactory startup, Lyon) as well as in mice (Optimal, IAB, Grenoble).



Altogether, these projects open new perspectives of translational research based on the use of aminotransferase inhibitors, AICAR or compounds such as biguanides acting on metabolic pathways that might be effective in certain forms of neuropathies, metabolic syndromes and in *LKB1*-deficient tumor cells. In this context, the research conducted by the lab will bring new insights for future therapeutic applications.

Bibliography

- Acloque, H., Adams, M.S., Fishwick, K., Bronner-Fraser, M., and Nieto, M.A. (2009). Epithelial-mesenchymal transitions: the importance of changing cell state in development and disease. *J. Clin. Invest.* 119, 1438–1449.
- Adameyko, I., and Lallemand, F. (2010). Glial versus melanocyte cell fate choice: Schwann cell precursors as a cellular origin of melanocytes. *Cell. Mol. Life Sci. CMLS* 67, 3037–3055.
- Adameyko, I., Lallemand, F., Aquino, J.B., Pereira, J.A., Topilko, P., Müller, T., Fritz, N., Beljajeva, A., Mochii, M., Liste, I., et al. (2009). Schwann cell precursors from nerve innervation are a cellular origin of melanocytes in skin. *Cell* 139, 366–379.
- Adameyko, I., Lallemand, F., Furlan, A., Zinin, N., Aranda, S., Kitambi, S.S., Blanchart, A., Favaro, R., Nicolis, S., Lübke, M., et al. (2012). Sox2 and Mitf cross-regulatory interactions consolidate progenitor and melanocyte lineages in the cranial neural crest. *Dev. Camb. Engl.* 139, 397–410.
- Alessi, D.R., Sakamoto, K., and Bayascas, J.R. (2006a). LKB1-dependent signaling pathways. *Annu. Rev. Biochem.* 75, 137–163.
- Alessi, D.R., Sakamoto, K., and Bayascas, J.R. (2006b). LKB1-dependent signaling pathways. *Annu. Rev. Biochem.* 75, 137–163.
- Alford, R.L., and Sutton, V.R. (2011). *Medical Genetics in the Clinical Practice of ORL* (Karger Medical and Scientific Publishers).
- Almog, N., and Rotter, V. (1997). Involvement of p53 in cell differentiation and development. *Biochim. Biophys. Acta* 1333, F1-27.
- Ames, B.N., Shigenaga, M.K., and Hagen, T.M. (1993). Oxidants, antioxidants, and the degenerative diseases of aging. *Proc. Natl. Acad. Sci. U. S. A.* 90, 7915–7922.
- Amiel, J., and Lyonnet, S. (2001). Hirschsprung disease, associated syndromes, and genetics: a review. *J. Med. Genet.* 38, 729–739.
- Anderson, R.B., Newgreen, D.F., and Young, H.M. (2013). *Neural Crest and the Development of the Enteric Nervous System* (Landes Bioscience).
- Andrews, D.A., Yang, L., and Low, P.S. (2002). Phorbol ester stimulates a protein kinase C-mediated agatoxin-TK-sensitive calcium permeability pathway in human red blood cells. *Blood* 100, 3392–3399.
- Aramaki, M., Udaka, T., Kosaki, R., Makita, Y., Okamoto, N., Yoshihashi, H., Oki, H., Nanao, K., Moriyama, N., Oku, S., et al. (2006). Phenotypic spectrum of CHARGE syndrome with CHD7 mutations. *J. Pediatr.* 148, 410–414.
- Arias, S. (1971). Genetic heterogeneity in the Waardenburg syndrome. *Birth Defects Orig. Artic. Ser.* 07, 87–101.
- Armstrong, G.T., Stovall, M., and Robison, L.L. (2010). Long-term effects of radiation exposure among adult survivors of childhood cancer: results from the childhood cancer survivor study. *Radiat. Res.* 174, 840–850.

- Armstrong, J.F., Kaufman, M.H., Harrison, D.J., and Clarke, A.R. (1995). High-frequency developmental abnormalities in p53-deficient mice. *Curr. Biol. CB* 5, 931–936.
- Avruch, J., Long, X., Lin, Y., Ortiz-Vega, S., Rapley, J., Papageorgiou, A., Oshiro, N., and Kikkawa, U. (2009a). Activation of mTORC1 in two steps: Rheb-GTP activation of catalytic function and increased binding of substrates to raptor. *Biochem. Soc. Trans.* 37, 223–226.
- Avruch, J., Long, X., Ortiz-Vega, S., Rapley, J., Papageorgiou, A., and Dai, N. (2009b). Amino acid regulation of TOR complex 1. *Am. J. Physiol. Endocrinol. Metab.* 296, E592–602.
- Baas, A.F., Smit, L., and Clevers, H. (2004a). LKB1 tumor suppressor protein: PARTaker in cell polarity. *Trends Cell Biol.* 14, 312–319.
- Baas, A.F., Kuipers, J., van der Wel, N.N., Batlle, E., Koerten, H.K., Peters, P.J., and Clevers, H.C. (2004b). Complete polarization of single intestinal epithelial cells upon activation of LKB1 by STRAD. *Cell* 116, 457–466.
- Baehrecke, E.H. (2005). Autophagy: dual roles in life and death? *Nat. Rev. Mol. Cell Biol.* 6, 505–510.
- Baggiolini, A., Varum, S., Mateos, J.M., Bettosini, D., John, N., Bonalli, M., Ziegler, U., Dimou, L., Clevers, H., Furrer, R., et al. (2015). Premigratory and migratory neural crest cells are multipotent in vivo. *Cell Stem Cell* 16, 314–322.
- Balaburski, G.M., Hontz, R.D., and Murphy, M.E. (2010). p53 and ARF: unexpected players in autophagy. *Trends Cell Biol.* 20, 363–369.
- Balakrishnan, A., Stykel, M.G., Touahri, Y., Stratton, J.A., Biernaskie, J., and Schuurmans, C. (2016). Temporal Analysis of Gene Expression in the Murine Schwann Cell Lineage and the Acutely Injured Postnatal Nerve. *PLOS ONE* 11, e0153256.
- Bálint, É., and Vousden, K.H. (2001). Activation and activities of the p53 tumour suppressor protein. *Br. J. Cancer* 85, 1813–1823.
- Ballabio, A., and Gieselmann, V. (2009). Lysosomal disorders: from storage to cellular damage. *Biochim. Biophys. Acta* 1793, 684–696.
- BANNO, K., KISU, I., YANOKURA, M., MASUDA, K., UEKI, A., KOBAYASHI, Y., HIRASAWA, A., and AOKI, D. (2013). Hereditary gynecological tumors associated with Peutz-Jeghers syndrome (Review). *Oncol. Lett.* 6, 1184–1188.
- Bardeesy, N., Sinha, M., Hezel, A.F., Signoretti, S., Hathaway, N.A., Sharpless, N.E., Loda, M., Carrasco, D.R., and DePinho, R.A. (2002). Loss of the Lkb1 tumour suppressor provokes intestinal polyposis but resistance to transformation. *Nature* 419, 162–167.
- Barnes, A.P., Lilley, B.N., Pan, Y.A., Plummer, L.J., Powell, A.W., Raines, A.N., Sanes, J.R., and Polleux, F. (2007). LKB1 and SAD kinases define a pathway required for the polarization of cortical neurons. *Cell* 129, 549–563.
- Bar-Peled, L., Schweitzer, L.D., Zoncu, R., and Sabatini, D.M. (2012). An expanded Ragulator is a GEF for the Rag GTPases that signal amino acid levels to mTORC1. *Cell* 150, 1196–1208.
- Barriga, E.H., Franze, K., Charras, G., and Mayor, R. (2018). Tissue stiffening coordinates morphogenesis by triggering collective cell migration *in vivo*. *Nature*.

- Bauer, P.V., and Duca, F.A. (2016). Targeting the gastrointestinal tract to treat type 2 diabetes. *J. Endocrinol.* **230**, R95–R113.
- Bays, J.L., Campbell, H.K., Heidema, C., Sebbagh, M., and DeMali, K.A. (2017). Linking E-cadherin mechanotransduction to cell metabolism through force mediated activation of AMPK. *Nat. Cell Biol.* **19**, 724–731.
- Beirowski, B., Babetto, E., Golden, J.P., Chen, Y.-J., Yang, K., Gross, R.W., Patti, G.J., and Milbrandt, J. (2014). Metabolic regulator LKB1 plays a crucial role in Schwann cell-mediated axon maintenance. *Nat. Neurosci.* **17**, 1351–1361.
- Beirowski, B., Wong, K.M., Babetto, E., and Milbrandt, J. (2017). mTORC1 promotes proliferation of immature Schwann cells and myelin growth of differentiated Schwann cells. *Proc. Natl. Acad. Sci.* **114**, E4261–E4270.
- Bekri, A., Billaud, M., and Thélu, J. (2014). Analysis of NUA1 and NUA2 expression during early chick development reveals specific patterns in the developing head. *Int. J. Dev. Biol.* **58**, 379–384.
- Bellvé, A.R., Cavicchia, J.C., Millette, C.F., O’Brien, D.A., Bhatnagar, Y.M., and Dym, M. (1977). Spermatogenic cells of the prepuberal mouse. Isolation and morphological characterization. *J. Cell Biol.* **74**, 68–85.
- Benavides, S.H., Monserrat, A.J., Fariña, S., and Porta, E.A. (2002). Sequential histochemical studies of neuronal lipofuscin in human cerebral cortex from the first to the ninth decade of life. *Arch. Gerontol. Geriatr.* **34**, 219–231.
- Bensaad, K., Tsuruta, A., Selak, M.A., Vidal, M.N.C., Nakano, K., Bartrons, R., Gottlieb, E., and Vousden, K.H. (2006). TIGAR, a p53-inducible regulator of glycolysis and apoptosis. *Cell* **126**, 107–120.
- Bensaad, K., Cheung, E.C., and Vousden, K.H. (2009). Modulation of intracellular ROS levels by TIGAR controls autophagy. *EMBO J.* **28**, 3015–3026.
- Bergeron, R., Ren, J.M., Cadman, K.S., Moore, I.K., Perret, P., Pypaert, M., Young, L.H., Semenkovich, C.F., and Shulman, G.I. (2001). Chronic activation of AMP kinase results in NRF-1 activation and mitochondrial biogenesis. *Am. J. Physiol. Endocrinol. Metab.* **281**, E1340–1346.
- Berkers, C.R., Maddocks, O.D.K., Cheung, E.C., Mor, I., and Vousden, K.H. (2013). Metabolic regulation by p53 family members. *Cell Metab.* **18**, 617–633.
- Bertoldo, M.J., Faure, M., Dupont, J., and Froment, P. (2015). AMPK: a master energy regulator for gonadal function. *Front. Neurosci.* **9**.
- Bhatt, S., Diaz, R., and Trainor, P.A. (2013). Signals and Switches in Mammalian Neural Crest Cell Differentiation. *Cold Spring Harb. Perspect. Biol.* **5**.
- Biswas, S.K. (2015). Metabolic Reprogramming of Immune Cells in Cancer Progression. *Immunity* **43**, 435–449.
- Bitto, A., Lerner, C.A., Nacarelli, T., Crowe, E., Torres, C., and Sell, C. (2014). p62/SQSTM1 at the interface of aging, autophagy, and disease. *Age* **36**.
- Blake, J.A., and Ziman, M.R. (2014). Pax genes: regulators of lineage specification and progenitor cell maintenance. *Dev. Camb. Engl.* **141**, 737–751.

- Bode, A.M., and Dong, Z. (2004). Post-translational modification of p53 in tumorigenesis. *Nat. Rev. Cancer* 4, 793–805.
- Bondurand, N., Natarajan, D., Thapar, N., Atkins, C., and Pachnis, V. (2003). Neuron and glia generating progenitors of the mammalian enteric nervous system isolated from foetal and postnatal gut cultures. *Development* 130, 6387–6400.
- Bondurand, N., Natarajan, D., Barlow, A., Thapar, N., and Pachnis, V. (2006). Maintenance of mammalian enteric nervous system progenitors by SOX10 and endothelin 3 signalling. *Development* 133, 2075–2086.
- Bonora, E., and Targher, G. (2012). Increased risk of cardiovascular disease and chronic kidney disease in NAFLD. *Nat. Rev. Gastroenterol. Hepatol.* 9, 372–381.
- Borchers, A., David, R., and Wedlich, D. (2001). Xenopus cadherin-11 restrains cranial neural crest migration and influences neural crest specification. *Dev. Camb. Engl.* 128, 3049–3060.
- Boudeau, J., Sapkota, G., and Alessi, D.R. (2003a). LKB1, a protein kinase regulating cell proliferation and polarity. *FEBS Lett.* 546, 159–165.
- Boudeau, J., Baas, A.F., Deak, M., Morrice, N.A., Kieloch, A., Schutkowski, M., Prescott, A.R., Clevers, H.C., and Alessi, D.R. (2003b). MO25alpha/beta interact with STRADalpha/beta enhancing their ability to bind, activate and localize LKB1 in the cytoplasm. *EMBO J.* 22, 5102–5114.
- Boullerne, A.I., Skias, D., Hartman, E.M., Testai, F.D., Kalinin, S., Polak, P.E., and Feinstein, D.L. (2015). A single-nucleotide polymorphism in serine-threonine kinase 11, the gene encoding liver kinase B1, is a risk factor for multiple sclerosis. *ASN Neuro* 7.
- Bracha, A.L., Ramanathan, A., Huang, S., Ingber, D.E., and Schreiber, S.L. (2010). Carbon metabolism-mediated myogenic differentiation. *Nat. Chem. Biol.* 6, 202–204.
- Brady, C.A., and Attardi, L.D. (2010). p53 at a glance. *J. Cell Sci.* 123, 2527–2532.
- Bragado, P., Armesilla, A., Silva, A., and Porras, A. (2007). Apoptosis by cisplatin requires p53 mediated p38alpha MAPK activation through ROS generation. *Apoptosis Int. J. Program. Cell Death* 12, 1733–1742.
- Broders-Bondon, F., Paul-Gilloteaux, P., Carlier, C., Radice, G.L., and Dufour, S. (2012). N-cadherin and β 1-integrins cooperate during the development of the enteric nervous system. *Dev. Biol.* 364, 178–191.
- Broders-Bondon, F., Paul-Gilloteaux, P., Gazquez, E., Heysch, J., Piel, M., Mayor, R., Lambris, J.D., and Dufour, S. (2016). Control of the collective migration of enteric neural crest cells by the Complement anaphylatoxin C3a and N-cadherin. *Dev. Biol.* 414, 85–99.
- Bronner, M.E., and Le Douarin, N.M. (2012). Development and evolution of the neural crest: an overview. *Dev. Biol.* 366, 2–9.
- Brooks, C.L., and Gu, W. (2006). p53 ubiquitination: Mdm2 and beyond. *Mol. Cell* 21, 307–315.
- Brown, C.J., Lain, S., Verma, C.S., Fersht, A.R., and Lane, D.P. (2009). Awakening guardian angels: drugging the p53 pathway. *Nat. Rev. Cancer* 9, 862–873.
- Brownell, J.E., and Allis, C.D. (1995). An activity gel assay detects a single, catalytically active histone acetyltransferase subunit in Tetrahymena macronuclei. *Proc. Natl. Acad. Sci. U. S. A.* 92, 6364–6368.

- Brunk, U.T., and Terman, A. (2002). The mitochondrial-lysosomal axis theory of aging: accumulation of damaged mitochondria as a result of imperfect autophagocytosis. *Eur. J. Biochem.* 269, 1996–2002.
- Bu, P., Evrard, Y.A., Lozano, G., and Dent, S.Y.R. (2007a). Loss of Gcn5 acetyltransferase activity leads to neural tube closure defects and exencephaly in mouse embryos. *Mol. Cell. Biol.* 27, 3405–3416.
- Buchet-Poyau, K., Courchet, J., Le Hir, H., Séraphin, B., Scoazec, J.-Y., Duret, L., Domon-Dell, C., Freund, J.-N., and Billaud, M. (2007). Identification and characterization of human Mex-3 proteins, a novel family of evolutionarily conserved RNA-binding proteins differentially localized to processing bodies. *Nucleic Acids Res.* 35, 1289–1300.
- Budanov, A.V., and Karin, M. (2008a). p53 target genes sestrin1 and sestrin2 connect genotoxic stress and mTOR signaling. *Cell* 134, 451–460.
- Budanov, A.V., and Karin, M. (2008b). The p53-regulated Sestrin gene products inhibit mTOR signaling. *Cell* 134, 451–460.
- Budanov, A.V., Lee, J.H., and Karin, M. (2010). Stressin' Sestrins take an aging fight. *EMBO Mol. Med.* 2, 388–400.
- Buhl, E.S., Jessen, N., Schmitz, O., Pedersen, S.B., Pedersen, O., Holman, G.D., and Lund, S. (2001). Chronic treatment with 5-aminoimidazole-4-carboxamide-1-beta-D-ribofuranoside increases insulin-stimulated glucose uptake and GLUT4 translocation in rat skeletal muscles in a fiber type-specific manner. *Diabetes* 50, 12–17.
- Bungard, D., Fuerth, B.J., Zeng, P.-Y., Faubert, B., Maas, N.L., Viollet, B., Carling, D., Thompson, C.B., Jones, R.G., and Berger, S.L. (2010). Signaling kinase AMPK activates stress-promoted transcription via histone H2B phosphorylation. *Science* 329, 1201–1205.
- Burns, A.J., and Le Douarin, N.M. (1998). The sacral neural crest contributes neurons and glia to the post-umbilical gut: spatiotemporal analysis of the development of the enteric nervous system. *Dev. Camb. Engl.* 125, 4335–4347.
- Burns, A.J., Champeval, D., and Le Douarin, N.M. (2000). Sacral neural crest cells colonise aganglionic hindgut in vivo but fail to compensate for lack of enteric ganglia. *Dev. Biol.* 219, 30–43.
- Bursac, S., Brdovcak, M.C., Donati, G., and Volarevic, S. (2014). Activation of the tumor suppressor p53 upon impairment of ribosome biogenesis. *Biochim. Biophys. Acta BBA - Mol. Basis Dis.* 1842, 817–830.
- Butler Tjaden, N.E., and Trainor, P.A. (2013). The developmental etiology and pathogenesis of Hirschsprung disease. *Transl. Res. J. Lab. Clin. Med.* 162, 1–15.
- Calamaras, T.D., Lee, C., Lan, F., Ido, Y., Siwik, D.A., and Colucci, W.S. (2012). Post-translational modification of serine/threonine kinase LKB1 via Adduction of the Reactive Lipid Species 4-Hydroxy-trans-2-nonenal (HNE) at lysine residue 97 directly inhibits kinase activity. *J. Biol. Chem.* 287, 42400–42406.
- Cancer Genome Atlas Research Network (2014). Comprehensive molecular profiling of lung adenocarcinoma. *Nature* 511, 543–550.
- Cantó, C., and Auwerx, J. (2009). PGC-1alpha, SIRT1 and AMPK, an energy sensing network that controls energy expenditure. *Curr. Opin. Lipidol.* 20, 98–105.

- Carlson, C.A., and Kim, K.H. (1973). Regulation of hepatic acetyl coenzyme A carboxylase by phosphorylation and dephosphorylation. *J. Biol. Chem.* **248**, 378–380.
- Carmona-Fontaine, C., Thevenneau, E., Tzekou, A., Tada, M., Woods, M., Page, K.M., Parsons, M., Lambris, J.D., and Mayor, R. (2011). Complement fragment C3a controls mutual cell attraction during collective cell migration. *Dev. Cell* **21**, 1026–1037.
- Carmona-Gutierrez, D., Hughes, A.L., Madeo, F., and Ruckenstein, C. (2016). The crucial impact of lysosomes in aging and longevity. *Ageing Res. Rev.* **32**, 2–12.
- Caro, L.H., Plomp, P.J., Leverve, X.M., and Meijer, A.J. (1989). A combination of intracellular leucine with either glutamate or aspartate inhibits autophagic proteolysis in isolated rat hepatocytes. *Eur. J. Biochem.* **181**, 717–720.
- Carré, C., Szymczak, D., Pidoux, J., and Antoniewski, C. (2005). The histone H3 acetylase dGcn5 is a key player in *Drosophila melanogaster* metamorphosis. *Mol. Cell. Biol.* **25**, 8228–8238.
- Carroll, B., and Dunlop, E.A. (2017). The lysosome: a crucial hub for AMPK and mTORC1 signalling. *Biochem. J.* **474**, 1453–1466.
- Carroll, B., Korolchuk, V.I., and Sarkar, S. (2015). Amino acids and autophagy: cross-talk and co-operation to control cellular homeostasis. *Amino Acids* **47**, 2065–2088.
- Castrillon, D.H., Quade, B.J., Wang, T.Y., Quigley, C., and Crum, C.P. (2000). The human VASA gene is specifically expressed in the germ cell lineage. *Proc. Natl. Acad. Sci. U. S. A.* **97**, 9585–9590.
- Chance, B., Sies, H., and Boveris, A. (1979). Hydroperoxide metabolism in mammalian organs. *Physiol. Rev.* **59**, 527–605.
- Chandel, N.S., Jasper, H., Ho, T.T., and Passequé, E. (2016). Metabolic regulation of stem cell function in tissue homeostasis and organismal ageing. *Nat. Cell Biol.* **18**, 823–832.
- Chandross, K.J., Cohen, R.I., Paras, P., Gravel, M., Braun, P.E., and Hudson, L.D. (1999). Identification and Characterization of Early Glial Progenitors Using a Transgenic Selection Strategy. *J. Neurosci.* **19**, 759–774.
- Chang, T.-Y., Chang, C.C.Y., Ohgami, N., and Yamauchi, Y. (2006). Cholesterol sensing, trafficking, and esterification. *Annu. Rev. Cell Dev. Biol.* **22**, 129–157.
- Chaoui, A., Watanabe, Y., Touraine, R., Baral, V., Goossens, M., Pingault, V., and Bondurand, N. (2011). Identification and functional analysis of SOX10 missense mutations in different subtypes of Waardenburg syndrome. *Hum. Mutat.* **32**, 1436–1449.
- Chaoui, A., Kavo, A., Baral, V., Watanabe, Y., Lecerf, L., Colley, A., Mendoza-Londono, R., Pingault, V., and Bondurand, N. (2015). Subnuclear re-localization of SOX10 and p54NRB correlates with a unique neurological phenotype associated with SOX10 missense mutations. *Hum. Mol. Genet.* **24**, 4933–4947.
- Chavez-Reyes, A., Parant, J.M., Amelse, L.L., de Oca Luna, R.M., Korsmeyer, S.J., and Lozano, G. (2003). Switching mechanisms of cell death in mdm2- and mdm4-null mice by deletion of p53 downstream targets. *Cancer Res.* **63**, 8664–8669.
- Chehab, N.H., Malikzay, A., Appel, M., and Halazonetis, T.D. (2000). Chk2/hCds1 functions as a DNA damage checkpoint in G1 by stabilizing p53. *Genes Dev.* **14**, 278–288.

- Chen, C.-S. (2002). Phorbol ester induces elevated oxidative activity and alkalization in a subset of lysosomes. *BMC Cell Biol.* 3, 21.
- Chen, J., Marechal, V., and Levine, A.J. (1993). Mapping of the p53 and mdm-2 interaction domains. *Mol. Cell. Biol.* 13, 4107–4114.
- Chen, X., Liu, J., and Chen, S. (2013a). Over-expression of Nrf2 diminishes ethanol-induced oxidative stress and apoptosis in neural crest cells by inducing an antioxidant response. *Reprod. Toxicol. Elmsford N* 42, 102–109.
- Chen, Y., Fan, J., Zhang, Z., Wang, G., Cheng, X., Chuai, M., Lee, K.K.H., and Yang, X. (2013b). The negative influence of high-glucose ambience on neurogenesis in developing quail embryos. *PloS One* 8, e66646.
- Cheung, E.C., Ludwig, R.L., and Vousden, K.H. (2012). Mitochondrial localization of TIGAR under hypoxia stimulates HK2 and lowers ROS and cell death. *Proc. Natl. Acad. Sci. U. S. A.* 109, 20491–20496.
- Chiacchiera, F., and Simone, C. (2010). The AMPK-FoxO3A axis as a target for cancer treatment. *Cell Cycle Georget. Tex* 9, 1091–1096.
- Chukov, S., Kurash, J.K., Wilson, J.R., Xiao, B., Justin, N., Ivanov, G.S., McKinney, K., Tempst, P., Prives, C., Gamblin, S.J., et al. (2004). Regulation of p53 activity through lysine methylation. *Nature* 432, 353–360.
- Chung, S., Dzeja, P.P., Faustino, R.S., Perez-Terzic, C., Behfar, A., and Terzic, A. (2007). Mitochondrial oxidative metabolism is required for the cardiac differentiation of stem cells. *Nat. Clin. Pract. Cardiovasc. Med.* 4, S60–S67.
- Cichorek, M., Wachulska, M., Stasiewicz, A., and Tyminińska, A. (2013). Skin melanocytes: biology and development. *Adv. Dermatol. Allergol. Dermatol. Alergol.* 30, 30–41.
- Clarke, J.T.R., and Iwanochko, R.M. (2005). Enzyme replacement therapy of Fabry disease. *Mol. Neurobiol.* 32, 43–50.
- Cluntun, A.A., Lukey, M.J., Cerione, R.A., and Locasale, J.W. (2017). Glutamine Metabolism in Cancer: Understanding the Heterogeneity. *Trends Cancer* 3, 169–180.
- Coffey, E.E., Beckel, J.M., Laties, A.M., and Mitchell, C.H. (2014). Lysosomal alkalization and dysfunction in human fibroblasts with the Alzheimer’s disease-linked presenilin 1 A246E mutation can be reversed with cAMP. *Neuroscience* 263, 111–124.
- Collado, M., and Serrano, M. (2010). Senescence in tumours: evidence from mice and humans. *Nat. Rev. Cancer* 10, 51–57.
- Coloff, J.L., Murphy, J.P., Braun, C.R., Harris, I.S., Shelton, L.M., Kami, K., Gygi, S.P., Selfors, L.M., and Brugge, J.S. (2016). Differential Glutamate Metabolism in Proliferating and Quiescent Mammary Epithelial Cells. *Cell Metab.* 23, 867–880.
- Conde, E., Suarez-Gauthier, A., García-García, E., Lopez-Rios, F., Lopez-Encuentra, A., García-Lujan, R., Morente, M., Sanchez-Verde, L., and Sanchez-Cespedes, M. (2007). Specific pattern of LKB1 and phospho-acetyl-CoA carboxylase protein immunostaining in human normal tissues and lung carcinomas. *Hum. Pathol.* 38, 1351–1360.

- Consoli, A., Nurjhan, N., Reilly, J.J., Bier, D.M., and Gerich, J.E. (1990). Contribution of liver and skeletal muscle to alanine and lactate metabolism in humans. *Am. J. Physiol.* 259, E677-684.
- Cooksey, R.C., Hebert, L.F., Zhu, J.H., Wofford, P., Garvey, W.T., and McClain, D.A. (1999). Mechanism of hexosamine-induced insulin resistance in transgenic mice overexpressing glutamine:fructose-6-phosphate amidotransferase: decreased glucose transporter GLUT4 translocation and reversal by treatment with thiazolidinedione. *Endocrinology* 140, 1151–1157.
- Cooper, G.M. (2000). *The Cell* (Sinauer Associates).
- Cornel, E.B., Smits, G.A., Oosterhof, G.O., Karthaus, H.F., Deburyn, F.M., Schalken, J.A., and Heerschap, A. (1993). Characterization of human prostate cancer, benign prostatic hyperplasia and normal prostate by in vitro ¹H and ³¹P magnetic resonance spectroscopy. *J. Urol.* 150, 2019–2024.
- Corton, J.M., Gillespie, J.G., Hawley, S.A., and Hardie, D.G. (1995). 5-aminoimidazole-4-carboxamide ribonucleoside. A specific method for activating AMP-activated protein kinase in intact cells? *Eur. J. Biochem.* 229, 558–565.
- Coughlan, K.A., Valentine, R.J., Ruderman, N.B., and Saha, A.K. (2014). AMPK activation: a therapeutic target for type 2 diabetes? *Diabetes Metab. Syndr. Obes. Targets Ther.* 7, 241–253.
- Courchet, J., Lewis, T.L., Lee, S., Courchet, V., Liou, D.-Y., Aizawa, S., and Polleux, F. (2013). Terminal axon branching is regulated by the LKB1-NUAK1 kinase pathway via presynaptic mitochondrial capture. *Cell* 153, 1510–1525.
- Creuzet, S., Couly, G., and Le Douarin, N.M. (2005). Patterning the neural crest derivatives during development of the vertebrate head: insights from avian studies. *J. Anat.* 207, 447–459.
- Creuzet, S.E., Viallet, J.P., Ghawitani, M., Torch, S., Thélou, J., Alrajeh, M., Radu, A.G., Bouvard, D., Costagliola, F., Borgne, M.L., et al. (2016). LKB1 signaling in cephalic neural crest cells is essential for vertebrate head development. *Dev. Biol.* 418, 283–296.
- Crichton, D., Wilkinson, S., O’Prey, J., Syed, N., Smith, P., Harrison, P.R., Gasco, M., Garrone, O., Crook, T., and Ryan, K.M. (2006). DRAM, a p53-induced modulator of autophagy, is critical for apoptosis. *Cell* 126, 121–134.
- Crute, B.E., Seefeld, K., Gamble, J., Kemp, B.E., and Witters, L.A. (1998). Functional domains of the alpha1 catalytic subunit of the AMP-activated protein kinase. *J. Biol. Chem.* 273, 35347–35354.
- Dady, A., and Duband, J.-L. (2017). Cadherin interplay during neural crest segregation from the non-neural ectoderm and neural tube in the early chick embryo. *Dev. Dyn. Off. Publ. Am. Assoc. Anat.* 246, 550–565.
- Dahmani, R., Just, P.-A., Delay, A., Canal, F., Finzi, L., Prip-Buus, C., Lambert, M., Sujobert, P., Buchet-Poyau, K., Miller, E., et al. (2015). A novel LKB1 isoform enhances AMPK metabolic activity and displays oncogenic properties. *Oncogene* 34, 2337–2346.
- Danilova, N., and Gazda, H.T. (2015). Ribosomopathies: how a common root can cause a tree of pathologies. *Dis. Model. Mech.* 8, 1013–1026.
- Danilova, N., Kumagai, A., and Lin, J. (2010). p53 upregulation is a frequent response to deficiency of cell-essential genes. *PLoS One* 5, e15938.
- Dassati, S., Waldner, A., and Schweigreiter, R. (2014). Apolipoprotein D takes center stage in the stress response of the aging and degenerative brain. *Neurobiol. Aging* 35, 1632–1642.

- Daujat, S., Neel, H., and Piette, J. (2001). MDM2: life without p53. *Trends Genet.* *TIG* 17, 459–464.
- Davies, S.P., Carling, D., Munday, M.R., and Hardie, D.G. (1992). Diurnal rhythm of phosphorylation of rat liver acetyl-CoA carboxylase by the AMP-activated protein kinase, demonstrated using freeze-clamping. Effects of high fat diets. *Eur. J. Biochem.* *203*, 615–623.
- el-Deiry, W.S., Kern, S.E., Pietenpol, J.A., Kinzler, K.W., and Vogelstein, B. (1992). Definition of a consensus binding site for p53. *Nat. Genet.* *1*, 45–49.
- Delmas, V., Martinozzi, S., Bourgeois, Y., Holzenberger, M., and Larue, L. (2003). Cre-mediated recombination in the skin melanocyte lineage. *Genes. N. Y. N* 2000 *36*, 73–80.
- Demers-Lamarche, J., Guillebaud, G., Tlili, M., Todkar, K., Bélanger, N., Grondin, M., Nguyen, A.P., Michel, J., and Germain, M. (2016). Loss of Mitochondrial Function Impairs Lysosomes. *J. Biol. Chem.* *291*, 10263–10276.
- Demetriades, C., Doumpas, N., and Teleman, A.A. (2014). Regulation of TORC1 in Response to Amino Acid Starvation via Lysosomal Recruitment of TSC2. *Cell* *156*, 786–799.
- Denison, F.C., Hiscock, N.J., Carling, D., and Woods, A. (2009). Characterization of an Alternative Splice Variant of LKB1. *J. Biol. Chem.* *284*, 67–76.
- Divangahi, M., Balghi, H., Danialou, G., Comtois, A.S., Demoule, A., Ernest, S., Haston, C., Robert, R., Hanrahan, J.W., Radzioch, D., et al. (2009a). Lack of CFTR in skeletal muscle predisposes to muscle wasting and diaphragm muscle pump failure in cystic fibrosis mice. *PLoS Genet.* *5*, e1000586.
- Divangahi, M., Chen, M., Gan, H., DeJardins, D., Hickman, T.T., Lee, D.M., Fortune, S., Behar, S.M., and Remold, H.G. (2009b). Mycobacterium tuberculosis evades macrophage defenses by inhibiting plasma membrane repair. *Nat. Immunol.* *10*, 899–906.
- Dixon, J., Jones, N.C., Sandell, L.L., Jayasinghe, S.M., Crane, J., Rey, J.-P., Dixon, M.J., and Trainor, P.A. (2006). Tcof1/Treacle is required for neural crest cell formation and proliferation deficiencies that cause craniofacial abnormalities. *Proc. Natl. Acad. Sci. U. S. A.* *103*, 13403–13408.
- Dohrn, N., Le, V.Q., Petersen, A., Skovbo, P., Pedersen, I.S., Ernst, A., Krarup, H., and Petersen, M.B. (2015). ECEL1 mutation causes fetal arthrogryposis multiplex congenita. *Am. J. Med. Genet. A.* *167A*, 731–743.
- Dominy, J.E., Lee, Y., Jedrychowski, M.P., Chim, H., Jurczak, M.J., Camporez, J.P., Ruan, H.-B., Feldman, J., Pierce, K., Mostoslavsky, R., et al. (2012). The deacetylase Sirt6 activates the acetyltransferase GCN5 and suppresses hepatic gluconeogenesis. *Mol. Cell* *48*, 900–913.
- Donehower, L.A., Harvey, M., Slagle, B.L., McArthur, M.J., Montgomery, C.A., Butel, J.S., and Bradley, A. (1992). Mice deficient for p53 are developmentally normal but susceptible to spontaneous tumours. *Nature* *356*, 215–221.
- Donoghue, P.C.J., Graham, A., and Kelsh, R.N. (2008). The origin and evolution of the neural crest. *BioEssays News Rev. Mol. Cell. Dev. Biol.* *30*, 530–541.
- Dornan, D., Wertz, I., Shimizu, H., Arnott, D., Frantz, G.D., Dowd, P., O'Rourke, K., Koeppen, H., and Dixit, V.M. (2004). The ubiquitin ligase COP1 is a critical negative regulator of p53. *Nature* *429*, 86–92.
- Le Douarin, N.L., and Kalcheim, C. (1999). *The Neural Crest* (Cambridge University Press).

- Le Douarin, N.M, Creuzet, S., Couly, G., and Dupin, E. (2004). Neural crest cell plasticity and its limits. *Development* 131, 4637–4650.
- Drakos, E., Atsaves, V., Li, J., Leventaki, V., Andreeff, M., Medeiros, L.J., and Rassidakis, G.Z. (2009). Stabilization and activation of p53 downregulates mTOR signaling through AMPK in mantle cell lymphoma. *Leukemia* 23, 784–790.
- Draper, B.W., Mello, C.C., Bowerman, B., Hardin, J., and Priess, J.R. (1996). MEX-3 is a KH domain protein that regulates blastomere identity in early *C. elegans* embryos. *Cell* 87, 205–216.
- Du, W., Jiang, P., Li, N., Mei, Y., Wang, X., Wen, L., Yang, X., and Wu, M. (2009). Suppression of p53 activity by Siva1. *Cell Death Differ.* 16, 1493–1504.
- Duband, J.L., Monier, F., Delannet, M., and Newgreen, D. (1995). Epithelium-mesenchyme transition during neural crest development. *Acta Anat. (Basel)* 154, 63–78.
- Duband, J.-L., Dady, A., and Fleury, V. (2015). Resolving time and space constraints during neural crest formation and delamination. *Curr. Top. Dev. Biol.* 111, 27–67.
- Dupin, E., and Le Douarin, N.M. (2014). The neural crest, A multifaceted structure of the vertebrates. *Birth Defects Res. Part C Embryo Today Rev.* 102, 187–209.
- Dupin, E., and Sommer, L. (2012). Neural crest progenitors and stem cells: From early development to adulthood. *Dev. Biol.* 366, 83–95.
- Durán, R.V., Oppliger, W., Robitaille, A.M., Heiserich, L., Skendaj, R., Gottlieb, E., and Hall, M.N. (2012). Glutaminolysis activates Rag-mTORC1 signaling. *Mol. Cell* 47, 349–358.
- de Duve, C. (2005). The lysosome turns fifty. *Nat. Cell Biol.* 7, 847–849.
- de Duve, C., Pressman, B.C., Gianetto, R., Wattiaux, R., and Appelmans, F. (1955). Tissue fractionation studies. 6. Intracellular distribution patterns of enzymes in rat-liver tissue. *Biochem. J.* 60, 604–617.
- Dyachuk, V., Furlan, A., Shahidi, M.K., Giovenco, M., Kaukua, N., Konstantinidou, C., Pachnis, V., Memic, F., Marklund, U., Müller, T., et al. (2014). Neurodevelopment. Parasympathetic neurons originate from nerve-associated peripheral glial progenitors. *Science* 345, 82–87.
- Eberharter, A., and Becker, P.B. (2004). ATP-dependent nucleosome remodelling: factors and functions. *J. Cell Sci.* 117, 3707–3711.
- Egan, D.F., Shackelford, D.B., Mihaylova, M.M., Gelino, S., Kohnz, R.A., Mair, W., Vasquez, D.S., Joshi, A., Gwinn, D.M., Taylor, R., et al. (2011). Phosphorylation of ULK1 (hATG1) by AMP-activated protein kinase connects energy sensing to mitophagy. *Science* 331, 456–461.
- El-Deiry, W.S. (2016). p21(WAF1) Mediates Cell-Cycle Inhibition, Relevant to Cancer Suppression and Therapy. *Cancer Res.* 76, 5189–5191.
- Espinosa-Medina, I., Outin, E., Picard, C.A., Chettouh, Z., Dymecki, S., Consalez, G.G., Coppola, E., and Brunet, J.-F. (2014). Neurodevelopment. Parasympathetic ganglia derive from Schwann cell precursors. *Science* 345, 87–90.
- Espinosa-Medina, I., Jevans, B., Boismoreau, F., Chettouh, Z., Enomoto, H., Müller, T., Birchmeier, C., Burns, A.J., and Brunet, J.-F. (2017). Dual origin of enteric neurons in vagal Schwann cell precursors and the sympathetic neural crest. *Proc. Natl. Acad. Sci.* 114, 11980–11985.

- Etchevers, H.C., Amiel, J., and Lyonnet, S. (2006). Molecular bases of human neurocristopathies. *Adv. Exp. Med. Biol.* 589, 213–234.
- Fabbro, M., and Henderson, B.R. (2003). Regulation of tumor suppressors by nuclear-cytoplasmic shuttling. *Exp. Cell Res.* 282, 59–69.
- Faubert, B., Li, K.Y., Cai, L., Hensley, C.T., Kim, J., Zacharias, L.G., Yang, C., Do, Q.N., Doucette, S., Burguete, D., et al. (2017). Lactate Metabolism in Human Lung Tumors. *Cell* 171, 358-371.e9.
- Fawal, M.-A., Brandt, M., and Djouder, N. (2015). MCRS1 binds and couples Rheb to amino acid-dependent mTORC1 activation. *Dev. Cell* 33, 67–81.
- Felig, P. (1973). The glucose-alanine cycle. *Metabolism.* 22, 179–207.
- Felig, P., Pozefsky, T., Marliss, E., and Cahill, G.F. (1970). Alanine: key role in gluconeogenesis. *Science* 167, 1003–1004.
- Feltri, M.L., Poitelon, Y., and Previtali, S.C. (2016). How Schwann Cells Sort Axons: New Concepts. *Neurosci. Rev. J. Bringing Neurobiol. Neurol. Psychiatry* 22, 252–265.
- Feng, Z., Zhang, H., Levine, A.J., and Jin, S. (2005). The coordinate regulation of the p53 and mTOR pathways in cells. *Proc. Natl. Acad. Sci. U. S. A.* 102, 8204–8209.
- Feng, Z., Hu, W., de Stanchina, E., Teresky, A.K., Jin, S., Lowe, S., and Levine, A.J. (2007). The regulation of AMPK beta1, TSC2, and PTEN expression by p53: stress, cell and tissue specificity, and the role of these gene products in modulating the IGF-1-AKT-mTOR pathways. *Cancer Res.* 67, 3043–3053.
- Figueiredo, A.L., Maczkowiak, F., Borday, C., Pla, P., Sittewelle, M., Pegoraro, C., and Monsoro-Burq, A.H. (2017). PFKFB4 control of AKT signaling is essential for premigratory and migratory neural crest formation. *Development* 144, 4183–4194.
- Filipponi, D., Hobbs, R.M., Ottolenghi, S., Rossi, P., Jannini, E.A., Pandolfi, P.P., and Dolci, S. (2007). Repression of kit expression by Plzf in germ cells. *Mol. Cell. Biol.* 27, 6770–6781.
- Fisslthaler, B., and Fleming, I. (2009). Activation and signaling by the AMP-activated protein kinase in endothelial cells. *Circ. Res.* 105, 114–127.
- Flowers, E.M., Sudderth, J., Zacharias, L., Mernaugh, G., Zent, R., DeBerardinis, R.J., and Carroll, T.J. (2018). Lkb1 deficiency confers glutamine dependency in polycystic kidney disease. *Nat. Commun.* 9, 814.
- Fogarty, S., and Hardie, D.G. (2010). Development of protein kinase activators: AMPK as a target in metabolic disorders and cancer. *Biochim. Biophys. Acta* 1804, 581–591.
- Folkerth, R.D. (1999). Abnormalities of developing white matter in lysosomal storage diseases. *J. Neuropathol. Exp. Neurol.* 58, 887–902.
- Force, T., Krause, D.S., and Van Etten, R.A. (2007). Molecular mechanisms of cardiotoxicity of tyrosine kinase inhibition. *Nat. Rev. Cancer* 7, 332–344.
- Forcet, C., Etienne-Manneville, S., Gaude, H., Fournier, L., Debilly, S., Salmi, M., Baas, A., Olschwang, S., Clevers, H., and Billaud, M. (2005). Functional analysis of Peutz-Jeghers mutations reveals that the LKB1 C-terminal region exerts a crucial role in regulating both the AMPK pathway and the cell polarity. *Hum. Mol. Genet.* 14, 1283–1292.

- Foretz, M., Hébrard, S., Leclerc, J., Zarrinpashneh, E., Soty, M., Mithieux, G., Sakamoto, K., Andreelli, F., and Viollet, B. (2010). Metformin inhibits hepatic gluconeogenesis in mice independently of the LKB1/AMPK pathway via a decrease in hepatic energy state. *J. Clin. Invest.* *120*, 2355–2369.
- Fu, D., Wakabayashi, Y., Lippincott-Schwartz, J., and Arias, I.M. (2011). Bile acid stimulates hepatocyte polarization through a cAMP-Epac-MEK-LKB1-AMPK pathway. *Proc. Natl. Acad. Sci. U. S. A.* *108*, 1403–1408.
- Furlan, A., Dyachuk, V., Kastriti, M.E., Calvo-Enrique, L., Abdo, H., Hadjab, S., Chontorotzea, T., Akkuratova, N., Usoskin, D., Kamenev, D., et al. (2017). Multipotent peripheral glial cells generate neuroendocrine cells of the adrenal medulla. *Science* *357*.
- Furness, J.B., and Stebbing, M.J. (2018). The first brain: Species comparisons and evolutionary implications for the enteric and central nervous systems. *Neurogastroenterol. Motil. Off. J. Eur. Gastrointest. Motil. Soc.* *30*.
- Furness, J.B., Callaghan, B.P., Rivera, L.R., and Cho, H.-J. (2014). The enteric nervous system and gastrointestinal innervation: integrated local and central control. *Adv. Exp. Med. Biol.* *817*, 39–71.
- Gambino, V., De Michele, G., Venezia, O., Migliaccio, P., Dall'Olio, V., Bernard, L., Minardi, S.P., Fazio, M.A.D., Bartoli, D., Servillo, G., et al. (2013). Oxidative stress activates a specific p53 transcriptional response that regulates cellular senescence and aging. *Aging Cell* *12*, 435–445.
- Gan, R.-Y., and Li, H.-B. (2014). Recent Progress on Liver Kinase B1 (LKB1): Expression, Regulation, Downstream Signaling and Cancer Suppressive Function. *Int. J. Mol. Sci.* *15*, 16698–16718.
- Gan, B., Hu, J., Jiang, S., Liu, Y., Sahin, E., Zhuang, L., Fletcher-Sananikone, E., Colla, S., Wang, Y.A., Chin, L., et al. (2010). Lkb1 regulates quiescence and metabolic homeostasis of haematopoietic stem cells. *Nature* *468*, 701–704.
- Ganforina, M.D., Do Carmo, S., Martínez, E., Tolivia, J., Navarro, A., Rassart, E., and Sanchez, D. (2010). ApoD, a glia-derived apolipoprotein, is required for peripheral nerve functional integrity and a timely response to injury. *Glia* *58*, 1320–1334.
- García-Mateo, N., Ganforina, M.D., Montero, O., Gijón, M.A., Murphy, R.C., and Sanchez, D. (2014). Schwann cell-derived Apolipoprotein D controls the dynamics of post-injury myelin recognition and degradation. *Front. Cell. Neurosci.* *8*, 374.
- Gargiulo, P.Á., and Mesones-Arroyo, H.L. (2017). *Psychiatry and Neuroscience Update - Vol. II: A Translational Approach* (Springer).
- Garofalo, K., Penno, A., Schmidt, B.P., Lee, H.-J., Frosch, M.P., von Eckardstein, A., Brown, R.H., Hornemann, T., and Eichler, F.S. (2011). Oral l-serine supplementation reduces production of neurotoxic deoxysphingolipids in mice and humans with hereditary sensory autonomic neuropathy type 1. *J. Clin. Invest.* *121*, 4735–4745.
- Gaude, H., Aznar, N., Delay, A., Bres, A., Buchet-Poyau, K., Caillat, C., Vigouroux, A., Rogon, C., Woods, A., Vanacker, J.-M., et al. (2012). Molecular chaperone complexes with antagonizing activities regulate stability and activity of the tumor suppressor LKB1. *Oncogene* *31*, 1582–1591.
- Gazquez, E., Watanabe, Y., Broders-Bondon, F., Paul-Gilloteaux, P., Heysch, J., Baral, V., Bondurand, N., and Dufour, S. (2016). Endothelin-3 stimulates cell adhesion and cooperates with β 1-integrins during enteric nervous system ontogenesis. Endothelin-3 stimulates cell adhesion and cooperates with β 1-integrins during enteric nervous system ontogenesis. *Sci. Rep. Sci. Rep.* *6*, 37877–37877.

- Genoud, S., Lappe-Siefke, C., Goebbels, S., Radtke, F., Aguet, M., Scherer, S.S., Suter, U., Nave, K.-A., and Mantei, N. (2002). Notch1 control of oligodendrocyte differentiation in the spinal cord. *J. Cell Biol.* 158, 709–718.
- Georgakopoulou, E., Tsimaratou, K., Evangelou, K., Fernandez, M.-P., Zoumpourlis, V., Trougakos, I., Kletsas, D., Bartek, J., Serrano, M., and Gorgoulis, V. (2012). Specific lipofuscin staining as a novel biomarker to detect replicative and stress-induced senescence. A method applicable in cryo-preserved and archival tissues. *Aging* 5, 37–50.
- Ghosh, P. (2017). The stress polarity pathway: AMPK ‘GIV’-es protection against metabolic insults. *Aging* 9, 303–314.
- Gilbert, S.F. (2000). The Neural Crest.
- Gilkes, D.M., Chen, L., and Chen, J. (2006). MDMX regulation of p53 response to ribosomal stress. *EMBO J.* 25, 5614–5625.
- Goessling, W. (2012). Hepatic stellate cells and cirrhosis: fishing for cures. *Hepatol. Baltim. Md* 56, 1596–1598.
- Goessling, W., Massaro, J.M., Vasan, R.S., D’Agostino, R.B., Ellison, R.C., and Fox, C.S. (2008). Aminotransferase Levels and 20-year Risk of Metabolic Syndrome, Diabetes, and Cardiovascular Disease. *Gastroenterology* 135, 1935-1944.e1.
- Goo, M.S., Sancho, L., Slepak, N., Boassa, D., Deerinck, T.J., Ellisman, M.H., Bloodgood, B.L., and Patrick, G.N. (2017). Activity-dependent trafficking of lysosomes in dendrites and dendritic spines. *J Cell Biol jcb.201704068*.
- Gorrini, C., Harris, I.S., and Mak, T.W. (2013). Modulation of oxidative stress as an anticancer strategy. *Nat. Rev. Drug Discov.* 12, 931–947.
- Green, D.R., and Kroemer, G. (2009). Cytoplasmic functions of the tumour suppressor p53. *Nature* 458, 1127–1130.
- Greiner-Tollersrud, O.K., and Berg, T. (2013). Lysosomal Storage Disorders (Landes Bioscience).
- Grossman, S.R., Deato, M.E., Brignone, C., Chan, H.M., Kung, A.L., Tagami, H., Nakatani, Y., and Livingston, D.M. (2003). Polyubiquitination of p53 by a ubiquitin ligase activity of p300. *Science* 300, 342–344.
- Gu, W., and Roeder, R.G. (1997). Activation of p53 sequence-specific DNA binding by acetylation of the p53 C-terminal domain. *Cell* 90, 595–606.
- Gu, J., Kawai, H., Nie, L., Kitao, H., Wiederschain, D., Jochemsen, A.G., Parant, J., Lozano, G., and Yuan, Z.-M. (2002). Mutual dependence of MDM2 and MDMX in their functional inactivation of p53. *J. Biol. Chem.* 277, 19251–19254.
- Guertin, D.A., and Sabatini, D.M. (2007). Defining the role of mTOR in cancer. *Cancer Cell* 12, 9–22.
- Guha, S., Coffey, E.E., Lu, W., Lim, J.C., Beckel, J.M., Laties, A.M., Boesze-Battaglia, K., and Mitchell, C.H. (2014). Approaches for detecting lysosomal alkalization and impaired degradation in fresh and cultured RPE cells: evidence for a role in retinal degenerations. *Exp. Eye Res.* 126, 68–76.

- Guigas, B., Taleux, N., Foretz, M., Demaille, D., Andreelli, F., Viollet, B., and Hue, L. (2007). AMP-activated protein kinase-independent inhibition of hepatic mitochondrial oxidative phosphorylation by AICA riboside. *Biochem. J.* *404*, 499–507.
- Gupta, R., Liu, A.Y., Glazer, P.M., and Wajapeyee, N. (2015). LKB1 preserves genome integrity by stimulating BRCA1 expression. *Nucleic Acids Res.* *43*, 259–271.
- Gurumurthy, S., Xie, S.Z., Alagesan, B., Kim, J., Yusuf, R.Z., Saez, B., Tzatsos, A., Oszolak, F., Milos, P., Ferrari, F., et al. (2010). The Lkb1 metabolic sensor maintains haematopoietic stem cell survival. *Nature* *468*, 659–663.
- Gwinn, D.M., Shackelford, D.B., Egan, D.F., Mihaylova, M.M., Mery, A., Vasquez, D.S., Turk, B.E., and Shaw, R.J. (2008). AMPK phosphorylation of raptor mediates a metabolic checkpoint. *Mol. Cell* *30*, 214–226.
- Hainaut, P., and Hollstein, M. (2000). p53 and human cancer: the first ten thousand mutations. *Adv. Cancer Res.* *77*, 81–137.
- Hall, B.K. (2008). The neural crest and neural crest cells: discovery and significance for theories of embryonic organization. *J. Biosci.* *33*, 781–793.
- Hammad, S.M., Baker, N.L., El Abiad, J.M., Spassieva, S.D., Pierce, J.S., Rembiesa, B., Bielawski, J., Lopes-Virella, M.F., Klein, R.L., and Investigators, D.G. of (2017). Increased Plasma Levels of Select Deoxy-ceramide and Ceramide Species are Associated with Increased Odds of Diabetic Neuropathy in Type 1 Diabetes: A Pilot Study. *Neuromolecular Med.* *19*, 46–56.
- Hanahan, D., and Weinberg, R.A. (2011). Hallmarks of Cancer: The Next Generation. *Cell* *144*, 646–674.
- Hanson, M., Lupski, J.R., Hicks, J., and Metry, D. (2003). Association of dermal melanocytosis with lysosomal storage disease: clinical features and hypotheses regarding pathogenesis. *Arch. Dermatol.* *139*, 916–920.
- Hardie, D.G., and Alessi, D.R. (2013). LKB1 and AMPK and the cancer-metabolism link - ten years after. *BMC Biol.* *11*, 36.
- Hardie, D.G., Ross, F.A., and Hawley, S.A. (2012). AMPK: a nutrient and energy sensor that maintains energy homeostasis. *Nat. Rev. Mol. Cell Biol.* *13*, 251–262.
- Harjes, U. (2017). Metabolism: More lactate, please. *Nature Reviews Cancer*.
- Harper, J.W., Adami, G.R., Wei, N., Keyomarsi, K., and Elledge, S.J. (1993). The p21 Cdk-interacting protein Cip1 is a potent inhibitor of G1 cyclin-dependent kinases. *Cell* *75*, 805–816.
- Harris, J., Robert, E., and Källén, B. (1997). Epidemiology of choanal atresia with special reference to the CHARGE association. *Pediatrics* *99*, 363–367.
- Haupt, Y., Maya, R., Kazaz, A., and Oren, M. (1997). Mdm2 promotes the rapid degradation of p53. *Nature* *387*, 296–299.
- Hawley, S.A., Boudeau, J., Reid, J.L., Mustard, K.J., Udd, L., Mäkelä, T.P., Alessi, D.R., and Hardie, D.G. (2003). Complexes between the LKB1 tumor suppressor, STRAD alpha/beta and MO25 alpha/beta are upstream kinases in the AMP-activated protein kinase cascade. *J. Biol.* *2*, 28.

- Hawley, S.A., Pan, D.A., Mustard, K.J., Ross, L., Bain, J., Edelman, A.M., Frenguelli, B.G., and Hardie, D.G. (2005). Calmodulin-dependent protein kinase kinase-beta is an alternative upstream kinase for AMP-activated protein kinase. *Cell Metab.* 2, 9–19.
- Hayano, S., Komatsu, Y., Pan, H., and Mishina, Y. (2015). Augmented BMP signaling in the neural crest inhibits nasal cartilage morphogenesis by inducing p53-mediated apoptosis. *Development* 142, 1357–1367.
- Heanue, T.A., and Pachnis, V. (2007). Enteric nervous system development and Hirschsprung's disease: advances in genetic and stem cell studies. *Nat. Rev. Neurosci.* 8, 466–479.
- Hebert, L.F., Daniels, M.C., Zhou, J., Crook, E.D., Turner, R.L., Simmons, S.T., Neidigh, J.L., Zhu, J.S., Baron, A.D., and McClain, D.A. (1996). Overexpression of glutamine:fructose-6-phosphate amidotransferase in transgenic mice leads to insulin resistance. *J. Clin. Invest.* 98, 930–936.
- Heidenreich, D.J., Reedy, M.V., and Brauer, P.R. (2008). Homocysteine enhances cardiac neural crest cell attachment in vitro by increasing intracellular calcium levels. *Dev. Dyn.* 237, 2117–2128.
- Hemminki, A., Markie, D., Tomlinson, I., Avizienyte, E., Roth, S., Loukola, A., Bignell, G., Warren, W., Aminoff, M., Höglund, P., et al. (1998). A serine/threonine kinase gene defective in Peutz-Jeghers syndrome. *Nature* 391, 184–187.
- Henin, N., Vincent, M.F., and Van den Berghe, G. (1996). Stimulation of rat liver AMP-activated protein kinase by AMP analogues. *Biochim. Biophys. Acta* 1290, 197–203.
- Hensley, C.T., Faubert, B., Yuan, Q., Lev-Cohain, N., Jin, E., Kim, J., Jiang, L., Ko, B., Skelton, R., Loudat, L., et al. (2016). Metabolic heterogeneity in human lung tumors. *Cell* 164, 681–694.
- Hezel, A.F., and Bardeesy, N. (2008). LKB1; linking cell structure and tumor suppression. *Oncogene* 27, 6908–6919.
- Hezel, A.F., Gurumurthy, S., Granot, Z., Swisa, A., Chu, G.C., Bailey, G., Dor, Y., Bardeesy, N., and Depinho, R.A. (2008). Pancreatic LKB1 deletion leads to acinar polarity defects and cystic neoplasms. *Mol. Cell. Biol.* 28, 2414–2425.
- Higashitsuji, H., Higashitsuji, H., Itoh, K., Sakurai, T., Nagao, T., Sumitomo, Y., Sumitomo, H., Masuda, T., Dawson, S., Shimada, Y., et al. (2005). The oncoprotein gankyrin binds to MDM2/HDM2, enhancing ubiquitylation and degradation of p53. *Cancer Cell* 8, 75–87.
- Hipolito, V.E.B., Ospina-Escobar, E., and Botelho, R.J. (2018). Lysosome remodelling and adaptation during phagocyte activation. *Cell. Microbiol.*
- Hla, T., and Dannenberg, A.J. (2012). Sphingolipid signaling in metabolic disorders. *Cell Metab.* 16, 420–434.
- Höhn, A., Jung, T., Grimm, S., and Grune, T. (2010). Lipofuscin-bound iron is a major intracellular source of oxidants: role in senescent cells. *Free Radic. Biol. Med.* 48, 1100–1108.
- Hollstein, M., and Hainaut, P. (2010). Massively regulated genes: the example of TP53. *J. Pathol.* 220, 164–173.
- Holz, M.K., Ballif, B.A., Gygi, S.P., and Blenis, J. (2005). mTOR and S6K1 mediate assembly of the translation preinitiation complex through dynamic protein interchange and ordered phosphorylation events. *Cell* 123, 569–580.

- Hou, X., Xu, S., Maitland-Toolan, K.A., Sato, K., Jiang, B., Ido, Y., Lan, F., Walsh, K., Wierzbicki, M., Verbeuren, T.J., et al. (2008). SIRT1 regulates hepatocyte lipid metabolism through activating AMP-activated protein kinase. *J. Biol. Chem.* 283, 20015–20026.
- Hou, X., Liu, J.-E., Liu, W., Liu, C.-Y., Liu, Z.-Y., and Sun, Z.-Y. (2011). A new role of NUAK1: directly phosphorylating p53 and regulating cell proliferation. *Oncogene* 30, 2933–2942.
- Houde, V.P., Ritorto, M.S., Gourlay, R., Varghese, J., Davies, P., Shpiro, N., Sakamoto, K., and Alessi, D.R. (2014). Investigation of LKB1 Ser431 phosphorylation and Cys433 farnesylation using mouse knockin analysis reveals an unexpected role of prenylation in regulating AMPK activity. *Biochem. J.* 458, 41–56.
- Howell, J.J., Hellberg, K., Turner, M., Talbott, G., Kolar, M.J., Ross, D.S., Hoxhaj, G., Saghatelian, A., Shaw, R.J., and Manning, B.D. (2017). Metformin Inhibits Hepatic mTORC1 Signaling via Dose-Dependent Mechanisms Involving AMPK and the TSC Complex. *Cell Metab.* 25, 463–471.
- Hu, W., Zhang, C., Wu, R., Sun, Y., Levine, A., and Feng, Z. (2010). Glutaminase 2, a novel p53 target gene regulating energy metabolism and antioxidant function. *Proc. Natl. Acad. Sci. U. S. A.* 107, 7455–7460.
- Huang, N.N., and Hunter, C.P. (2015). The RNA binding protein MEX-3 retains asymmetric activity in the early *Caenorhabditis elegans* embryo in the absence of asymmetric protein localization. *Gene* 554, 160–173.
- Huang, N.N., Mootz, D.E., Walhout, A.J.M., Vidal, M., and Hunter, C.P. (2002). MEX-3 interacting proteins link cell polarity to asymmetric gene expression in *Caenorhabditis elegans*. *Dev. Camb. Engl.* 129, 747–759.
- Hubert, V., Peschel, A., Langer, B., Gröger, M., Rees, A., and Kain, R. (2016). LAMP-2 is required for incorporating syntaxin-17 into autophagosomes and for their fusion with lysosomes. *Biol. Open* 5, 1516–1529.
- Hui, S., Ghergurovich, J.M., Morscher, R.J., Jang, C., Teng, X., Lu, W., Esparza, L.A., Reya, T., Le Zhan, Yanxiang Guo, J., et al. (2017). Glucose feeds the TCA cycle via circulating lactate. *Nature* 551, 115–118.
- Hurov, J., and Piwnica-Worms, H. (2007). The Par-1/MARK family of protein kinases: from polarity to metabolism. *Cell Cycle Georget. Tex* 6, 1966–1969.
- Ibsen, K.H., and Marles, S.W. (1976). Inhibition of chicken pyruvate kinases by amino acids. *Biochemistry (Mosc.)* 15, 1073–1079.
- Ichiyama, A. (2011). Studies on a unique organelle localization of a liver enzyme, serine:pyruvate (or alanine:glyoxylate) aminotransferase. *Proc. Jpn. Acad. Ser. B Phys. Biol. Sci.* 87, 274–286.
- Idone, V., Tam, C., Goss, J.W., Toomre, D., Pypaert, M., and Andrews, N.W. (2008). Repair of injured plasma membrane by rapid Ca²⁺-dependent endocytosis. *J. Cell Biol.* 180, 905–914.
- Iglesias, M.A., Ye, J.-M., Frangioudakis, G., Saha, A.K., Tomas, E., Ruderman, N.B., Cooney, G.J., and Kraegen, E.W. (2002). AICAR administration causes an apparent enhancement of muscle and liver insulin action in insulin-resistant high-fat-fed rats. *Diabetes* 51, 2886–2894.
- Inoki, K., Zhu, T., and Guan, K.-L. (2003). TSC2 mediates cellular energy response to control cell growth and survival. *Cell* 115, 577–590.

- Inoue, K., Khajavi, M., Ohyama, T., Hirabayashi, S., Wilson, J., Reggin, J.D., Mancias, P., Butler, I.J., Wilkinson, M.F., Wegner, M., et al. (2004). Molecular mechanism for distinct neurological phenotypes conveyed by allelic truncating mutations. *Nat. Genet.* 36, 361–369.
- Isern, J., García-García, A., Martín, A.M., Arranz, L., Martín-Pérez, D., Torroja, C., Sánchez-Cabo, F., and Méndez-Ferrer, S. (2014). The neural crest is a source of mesenchymal stem cells with specialized hematopoietic stem cell niche function. *ELife* 3.
- Issekutz, K.A., Graham, J.M., Prasad, C., Smith, I.M., and Blake, K.D. (2005). An epidemiological analysis of CHARGE syndrome: preliminary results from a Canadian study. *Am. J. Med. Genet. A.* 133A, 309–317.
- Ito, K., and Suda, T. (2014). Metabolic requirements for the maintenance of self-renewing stem cells. *Nat. Rev. Mol. Cell Biol.* 15, 243–256.
- Ito, A., Kawaguchi, Y., Lai, C.-H., Kovacs, J.J., Higashimoto, Y., Appella, E., and Yao, T.-P. (2002). MDM2–HDAC1-mediated deacetylation of p53 is required for its degradation. *EMBO J.* 21, 6236–6245.
- Jacinto, E., Loewith, R., Schmidt, A., Lin, S., Ruegg, M.A., Hall, A., and Hall, M.N. (2004). Mammalian TOR complex 2 controls the actin cytoskeleton and is rapamycin insensitive. *Nat. Cell Biol.* 6, 1122–1128.
- Jäger, S., Handschin, C., St-Pierre, J., and Spiegelman, B.M. (2007). AMP-activated protein kinase (AMPK) action in skeletal muscle via direct phosphorylation of PGC-1 α . *Proc. Natl. Acad. Sci. U. S. A.* 104, 12017–12022.
- Jain, A.K., and Barton, M.C. (2010). Making sense of ubiquitin ligases that regulate p53. *Cancer Biol. Ther.* 10, 665–672.
- Jang, S.Y., Shin, Y.K., Park, S.Y., Park, J.Y., Lee, H.J., Yoo, Y.H., Kim, J.K., and Park, H.T. (2016). Autophagic myelin destruction by Schwann cells during Wallerian degeneration and segmental demyelination. *Glia* 64, 730–742.
- Jansen, M., Ten Klooster, J.P., Offerhaus, G.J., and Clevers, H. (2009). LKB1 and AMPK family signaling: the intimate link between cell polarity and energy metabolism. *Physiol. Rev.* 89, 777–798.
- Jeninga, E.H., Schoonjans, K., and Auwerx, J. (2010). Reversible acetylation of PGC-1: Connecting energy sensors and effectors to guarantee metabolic flexibility. *Oncogene* 29.
- Jenne, D.E., Reimann, H., Nezu, J., Friedel, W., Loff, S., Jeschke, R., Müller, O., Back, W., and Zimmer, M. (1998). Peutz-Jeghers syndrome is caused by mutations in a novel serine threonine kinase. *Nat. Genet.* 18, 38–43.
- Jeppesen, J., Maarbjerg, S.J., Jordy, A.B., Fritzen, A.M., Pehmøller, C., Sylow, L., Serup, A.K., Jessen, N., Thorsen, K., Prats, C., et al. (2013). LKB1 Regulates Lipid Oxidation During Exercise Independently of AMPK. *Diabetes* 62, 1490–1499.
- Jessen, K.R., and Mirsky, R. (2005). The origin and development of glial cells in peripheral nerves. *Nat. Rev. Neurosci.* 6, 671–682.
- Jessen, K.R., Mirsky, R., and Lloyd, A.C. (2015a). Schwann Cells: Development and Role in Nerve Repair. *Cold Spring Harb. Perspect. Biol.* 7, a020487.

- Jessen, K.R., Mirsky, R., and Arthur-Farraj, P. (2015b). The Role of Cell Plasticity in Tissue Repair: Adaptive Cellular Reprogramming. *Dev. Cell* 34, 613–620.
- Ji, H., Ramsey, M.R., Hayes, D.N., Fan, C., McNamara, K., Kozlowski, P., Torrice, C., Wu, M.C., Shimamura, T., Perera, S.A., et al. (2007). LKB1 modulates lung cancer differentiation and metastasis. *Nature* 448, 807–810.
- Jiang, X.-H., Bukhari, I., Zheng, W., Yin, S., Wang, Z., Cooke, H.J., and Shi, Q.-H. (2014). Blood-testis barrier and spermatogenesis: lessons from genetically-modified mice. *Asian J. Androl.* 16, 572–580.
- Jiao, Y., George, S.K., Zhao, Q., Hulver, M.W., Hutson, S.M., Bishop, C.E., and Lu, B. (2012a). Mex3c mutation reduces adiposity and increases energy expenditure. *Mol. Cell. Biol.* 32, 4350–4362.
- Jiao, Y., Bishop, C.E., and Lu, B. (2012b). Mex3c regulates insulin-like growth factor 1 (IGF1) expression and promotes postnatal growth. *Mol. Biol. Cell* 23, 1404–1413.
- Jishage, K., Nezu, J., Kawase, Y., Iwata, T., Watanabe, M., Miyoshi, A., Ose, A., Habu, K., Kake, T., Kamada, N., et al. (2002). Role of Lkb1, the causative gene of Peutz-Jegher's syndrome, in embryogenesis and polyposis. *Proc. Natl. Acad. Sci. U. S. A.* 99, 8903–8908.
- Joerger, A.C., and Fersht, A.R. (2010). The Tumor Suppressor p53: From Structures to Drug Discovery. *Cold Spring Harb. Perspect. Biol.* 2.
- Johnston, A.P.W., Naska, S., Jones, K., Jinno, H., Kaplan, D.R., and Miller, F.D. (2013). Sox2-mediated regulation of adult neural crest precursors and skin repair. *Stem Cell Rep.* 1, 38–45.
- Johnston, A.P.W., Yuzwa, S.A., Carr, M.J., Mahmud, N., Storer, M.A., Krause, M.P., Jones, K., Paul, S., Kaplan, D.R., and Miller, F.D. (2016). Dedifferentiated Schwann Cell Precursors Secreting Paracrine Factors Are Required for Regeneration of the Mammalian Digit Tip. *Cell Stem Cell* 19, 433–448.
- Jolly, R.D., Douglas, B.V., Davey, P.M., and Roiri, J.E. (1995). Lipofuscin in bovine muscle and brain: a model for studying age pigment. *Gerontology* 41 Suppl 2, 283–295.
- Jones, N.C., Lynn, M.L., Gaudenz, K., Sakai, D., Aoto, K., Rey, J.-P., Glynn, E.F., Ellington, L., Du, C., Dixon, J., et al. (2008). Prevention of the neurocristopathy Treacher Collins syndrome through inhibition of p53 function. *Nat. Med.* 14, 125–133.
- Jones, S.N., Roe, A.E., Donehower, L.A., and Bradley, A. (1995). Rescue of embryonic lethality in Mdm2-deficient mice by absence of p53. *Nature* 378, 206–208.
- Joseph, N.M., Mukoyama, Y.-S., Mosher, J.T., Jaegle, M., Crone, S.A., Dormand, E.-L., Lee, K.-F., Meijer, D., Anderson, D.J., and Morrison, S.J. (2004). Neural crest stem cells undergo multilineage differentiation in developing peripheral nerves to generate endoneurial fibroblasts in addition to Schwann cells. *Dev. Camb. Engl.* 131, 5599–5612.
- Jung, T., Bader, N., and Grune, T. (2007). Lipofuscin: formation, distribution, and metabolic consequences. *Ann. N. Y. Acad. Sci.* 1119, 97–111.
- Kane, D.A. (2014). Lactate oxidation at the mitochondria: a lactate-malate-aspartate shuttle at work. *Front. Neurosci.* 8.
- Kapur, R.P. (1999). Early death of neural crest cells is responsible for total enteric aganglionosis in Sox10(Dom)/Sox10(Dom) mouse embryos. *Pediatr. Dev. Pathol. Off. J. Soc. Pediatr. Pathol. Paediatr. Pathol. Soc.* 2, 559–569.

- Kaucka, M., Ivashkin, E., Gyllborg, D., Zikmund, T., Tesarova, M., Kaiser, J., Xie, M., Petersen, J., Pachnis, V., Nicolis, S.K., et al. (2016). Analysis of neural crest-derived clones reveals novel aspects of facial development. *Sci. Adv.* 2, e1600060.
- Kaukua, N., Shahidi, M.K., Konstantinidou, C., Dyachuk, V., Kaucka, M., Furlan, A., An, Z., Wang, L., Hultman, I., Ährlund-Richter, L., et al. (2014). Glial origin of mesenchymal stem cells in a tooth model system. *Nature* 513, 551–554.
- Kawai, H., Wiederschain, D., Kitao, H., Stuart, J., Tsai, K.K.C., and Yuan, Z.-M. (2003). DNA damage-induced MDMX degradation is mediated by MDM2. *J. Biol. Chem.* 278, 45946–45953.
- Kawauchi, K., Araki, K., Tobiume, K., and Tanaka, N. (2008). p53 regulates glucose metabolism through an IKK-NF-kappaB pathway and inhibits cell transformation. *Nat. Cell Biol.* 10, 611–618.
- Kemphues, K.J., Priess, J.R., Morton, D.G., and Cheng, N.S. (1988). Identification of genes required for cytoplasmic localization in early *C. elegans* embryos. *Cell* 52, 311–320.
- Kenzelmann Broz, D., and Attardi, L.D. (2010). In vivo analysis of p53 tumor suppressor function using genetically engineered mouse models. *Carcinogenesis* 31, 1311–1318.
- Kew, M.C. (2000). Serum aminotransferase concentration as evidence of hepatocellular damage. *Lancet Lond. Engl.* 355, 591–592.
- Khanna, K.K., Keating, K.E., Kozlov, S., Scott, S., Gatei, M., Hobson, K., Taya, Y., Gabrielli, B., Chan, D., Lees-Miller, S.P., et al. (1998). ATM associates with and phosphorylates p53: mapping the region of interaction. *Nat. Genet.* 20, 398–400.
- Kilberg, M.S., Terada, N., and Shan, J. (2016). Influence of Amino Acid Metabolism on Embryonic Stem Cell Function and Differentiation. *Adv. Nutr. Bethesda Md* 7, 780S–9S.
- Kim, A., and Cunningham, K.W. (2015). A LAPF/phafin1-like protein regulates TORC1 and lysosomal membrane permeabilization in response to endoplasmic reticulum membrane stress. *Mol. Biol. Cell* 26, 4631–4645.
- Kim, I., and Lemasters, J.J. (2011). Mitochondrial degradation by autophagy (mitophagy) in GFP-LC3 transgenic hepatocytes during nutrient deprivation. *Am. J. Physiol. Cell Physiol.* 300, C308–317.
- Kim, J.E., and Chen, J. (2004). Regulation of peroxisome proliferator-activated receptor-gamma activity by mammalian target of rapamycin and amino acids in adipogenesis. *Diabetes* 53, 2748–2756.
- Kim, H.-R., Roe, J.-S., Lee, J.-E., Cho, E.-J., and Youn, H.-D. (2013a). p53 regulates glucose metabolism by miR-34a. *Biochem. Biophys. Res. Commun.* 437, 225–231.
- Kim, S.G., Buel, G.R., and Blenis, J. (2013b). Nutrient Regulation of the mTOR Complex 1 Signaling Pathway. *Mol. Cells* 35, 463–473.
- Kimura, S.H., Ikawa, M., Ito, A., Okabe, M., and Nojima, H. (2001). Cyclin G1 is involved in G2/M arrest in response to DNA damage and in growth control after damage recovery. *Oncogene* 20, 3290–3300.
- Kitamura, N., Nakamura, Y., Miyamoto, Y., Miyamoto, T., Kabu, K., Yoshida, M., Futamura, M., Ichinose, S., and Arakawa, H. (2011). Mieap, a p53-inducible protein, controls mitochondrial quality by repairing or eliminating unhealthy mitochondria. *PLoS One* 6, e16060.

- Knight, R.D., and Schilling, T.F. (2013). Cranial Neural Crest and Development of the Head Skeleton (Landes Bioscience).
- Kojima, Y., Miyoshi, H., Clevers, H.C., Oshima, M., Aoki, M., and Taketo, M.M. (2007). Suppression of tubulin polymerization by the LKB1-microtubule-associated protein/microtubule affinity-regulating kinase signaling. *J. Biol. Chem.* 282, 23532–23540.
- Kong, F., Wang, M., Huang, X., Yue, Q., Wei, X., Dou, X., Peng, X., Jia, Y., Zheng, K., Wu, T., et al. (2017). Differential regulation of spermatogenic process by Lkb1 isoforms in mouse testis. *Cell Death Dis.* 8, e3121.
- Kononenko, N.L. (2017). Lysosomes convene to keep the synapse clean. *J Cell Biol jcb.* 201707070.
- Koppenol, W.H., Bounds, P.L., and Dang, C.V. (2011). Otto Warburg's contributions to current concepts of cancer metabolism. *Nat. Rev. Cancer* 11, 325–337.
- Kottakis, F., Nicolay, B.N., Roumane, A., Karnik, R., Gu, H., Nagle, J.M., Boukhali, M., Hayward, M.C., Li, Y.Y., Chen, T., et al. (2016). LKB1 loss links serine metabolism to DNA methylation and tumorigenesis. *Nature* 539, 390–395.
- Kruiswijk, F., Labuschagne, C.F., and Vousden, K.H. (2015). p53 in survival, death and metabolic health: a lifeguard with a licence to kill. *Nat. Rev. Mol. Cell Biol.* 16, 393–405.
- Kubbutat, M.H., Jones, S.N., and Vousden, K.H. (1997). Regulation of p53 stability by Mdm2. *Nature* 387, 299–303.
- Kulesa, P.M., Bailey, C.M., Kasemeier-Kulesa, J.C., and McLennan, R. (2010). Cranial Neural Crest Migration: New Rules for an Old Road. *Dev. Biol.* 344, 543–554.
- Kuma, A., Hatano, M., Matsui, M., Yamamoto, A., Nakaya, H., Yoshimori, T., Ohsumi, Y., Tokuhiisa, T., and Mizushima, N. (2004). The role of autophagy during the early neonatal starvation period. *Nature* 432, 1032–1036.
- Kuntz, A. (1910). The development of the sympathetic nervous system in birds. *J. Comp. Neurol. Psychol.* 20, 283–308.
- Kurihara, Y., Kurihara, H., Suzuki, H., Kodama, T., Maemura, K., Nagai, R., Oda, H., Kuwaki, T., Cao, W.H., and Kamada, N. (1994). Elevated blood pressure and craniofacial abnormalities in mice deficient in endothelin-1. *Nature* 368, 703–710.
- Kurz, E.U., and Lees-Miller, S.P. (2004). DNA damage-induced activation of ATM and ATM-dependent signaling pathways. *DNA Repair* 3, 889–900.
- Kurz, T., Terman, A., Gustafsson, B., and Brunk, U.T. (2008). Lysosomes in iron metabolism, ageing and apoptosis. *Histochem. Cell Biol.* 129, 389–406.
- Lai, D., Chen, Y., Wang, F., Jiang, L., and Wei, C. (2012). LKB1 controls the pluripotent state of human embryonic stem cells. *Cell. Reprogramming* 14, 164–170.
- Laiho, A., Kotaja, N., Gyenesi, A., and Sironen, A. (2013). Transcriptome profiling of the murine testis during the first wave of spermatogenesis. *PloS One* 8, e61558.
- Lake, A.N., and Bedford, M.T. (2007). Protein methylation and DNA repair. *Mutat. Res.* 618, 91–101.
- Lake, J.I., and Heuckeroth, R.O. (2013). Enteric nervous system development: migration, differentiation, and disease. *Am. J. Physiol. Gastrointest. Liver Physiol.* 305, G1-24.

- Lalani, S.R., Safiullah, A.M., Fernbach, S.D., Harutyunyan, K.G., Thaller, C., Peterson, L.E., McPherson, J.D., Gibbs, R.A., White, L.D., Hefner, M., et al. (2006). Spectrum of CHD7 Mutations in 110 Individuals with CHARGE Syndrome and Genotype-Phenotype Correlation. *Am. J. Hum. Genet.* **78**, 303–314.
- Lan, F., Cacicedo, J.M., Ruderman, N., and Ido, Y. (2008). SIRT1 modulation of the acetylation status, cytosolic localization, and activity of LKB1. Possible role in AMP-activated protein kinase activation. *J. Biol. Chem.* **283**, 27628–27635.
- Lanoue, K.F., Meijer, A.J., and Brouwer, A. (1974). Evidence for electrogenic aspartate transport in rat liver mitochondria. *Arch. Biochem. Biophys.* **161**, 544–550.
- Laplane, M., and Sabatini, D.M. (2012). mTOR signaling in growth control and disease. *Cell* **149**, 274–293.
- Le Borgne, M., Chartier, N., Buchet-Poyau, K., Destaing, O., Faurobert, E., Thibert, C., Rouault, J.-P., Courchet, J., Nègre, D., Bouvard, D., et al. (2014). The RNA-binding protein Mex3b regulates the spatial organization of the Rap1 pathway. *Dev. Camb. Engl.* **141**, 2096–2107.
- Le Douarin, N., and Kalcheim, C. (1999). *The neural crest* (Cambridge, UK ; New York, NY, USA: Cambridge University Press).
- Le Douarin, N.M., and Teillet, M.A. (1973). The migration of neural crest cells to the wall of the digestive tract in avian embryo. *J. Embryol. Exp. Morphol.* **30**, 31–48.
- Lebedeva, M.A., Eaton, J.S., and Shadel, G.S. (2009). Loss of p53 causes mitochondrial DNA depletion and altered mitochondrial reactive oxygen species homeostasis. *Biochim. Biophys. Acta* **1787**, 328–334.
- Lecerf, L., Kavo, A., Ruiz-Ferrer, M., Baral, V., Watanabe, Y., Chaoui, A., Pingault, V., Borrego, S., and Bondurand, N. (2014). An impairment of long distance SOX10 regulatory elements underlies isolated Hirschsprung disease. *Hum. Mutat.* **35**, 303–307.
- Lécureuil, C., Fontaine, I., Crepieux, P., and Guillou, F. (2002). Sertoli and granulosa cell-specific Cre recombinase activity in transgenic mice. *Genes. N. Y. N* **2000** **33**, 114–118.
- Lee, A.F., Ho, D.K., Zanassi, P., Walsh, G.S., Kaplan, D.R., and Miller, F.D. (2004). Evidence that DeltaNp73 promotes neuronal survival by p53-dependent and p53-independent mechanisms. *J. Neurosci. Off. J. Soc. Neurosci.* **24**, 9174–9184.
- Lee, J.H., Koh, H., Kim, M., Kim, Y., Lee, S.Y., Karess, R.E., Lee, S.-H., Shong, M., Kim, J.-M., Kim, J., et al. (2007). Energy-dependent regulation of cell structure by AMP-activated protein kinase. *Nature* **447**, 1017–1020.
- Leese, H.J. (2012). Metabolism of the preimplantation embryo: 40 years on. *Reprod. Camb. Engl.* **143**, 417–427.
- Leese, H.J. (2015). History of oocyte and embryo metabolism. *Reprod. Fertil. Dev.* **27**, 567–571.
- Leng, R.P., Lin, Y., Ma, W., Wu, H., Lemmers, B., Chung, S., Parant, J.M., Lozano, G., Hakem, R., and Benchimol, S. (2003). Pirh2, a p53-induced ubiquitin-protein ligase, promotes p53 degradation. *Cell* **112**, 779–791.
- Lengner, C.J., Steinman, H.A., Gagnon, J., Smith, T.W., Henderson, J.E., Kream, B.E., Stein, G.S., Lian, J.B., and Jones, S.N. (2006). Osteoblast differentiation and skeletal development are regulated by Mdm2-p53 signaling. *J. Cell Biol.* **172**, 909–921.

- Lerin, C., Rodgers, J.T., Kalume, D.E., Kim, S., Pandey, A., and Puigserver, P. (2006). GCN5 acetyltransferase complex controls glucose metabolism through transcriptional repression of PGC-1 α . *Cell Metab.* **3**, 429–438.
- Leverve, X.M., Caro, L.H., Plomp, P.J., and Meijer, A.J. (1987). Control of proteolysis in perfused rat hepatocytes. *FEBS Lett.* **219**, 455–458.
- Levine, A.J., and Oren, M. (2009). The first 30 years of p53: growing ever more complex. *Nat. Rev. Cancer* **9**, 749–758.
- Levine, B., and Abrams, J. (2008). p53: The Janus of autophagy? *Nat. Cell Biol.* **10**, 637–639.
- Li, D., Ropert, N., Koulakoff, A., Giaume, C., and Oheim, M. (2008). Lysosomes Are the Major Vesicular Compartment Undergoing Ca²⁺-Regulated Exocytosis from Cortical Astrocytes. *J. Neurosci.* **28**, 7648–7658.
- Li, M., Brooks, C.L., Wu-Baer, F., Chen, D., Baer, R., and Gu, W. (2003). Mono- versus polyubiquitination: differential control of p53 fate by Mdm2. *Science* **302**, 1972–1975.
- Li, N., Zheng, Y., Chen, W., Wang, C., Liu, X., He, W., Xu, H., and Cao, X. (2007). Adaptor Protein LAPF Recruits Phosphorylated p53 to Lysosomes and Triggers Lysosomal Destabilization in Apoptosis. *Cancer Res.* **67**, 11176–11185.
- Lin, J., Handschin, C., and Spiegelman, B.M. (2005). Metabolic control through the PGC-1 family of transcription coactivators. *Cell Metab.* **1**, 361–370.
- Lindor, N.M., and Greene, M.H. (1998). The concise handbook of family cancer syndromes. Mayo Familial Cancer Program. *J. Natl. Cancer Inst.* **90**, 1039–1071.
- Liu, W., Monahan, K.B., Pfefferle, A.D., Shimamura, T., Sorrentino, J., Chan, K.T., Roadcap, D.W., Ollila, D.W., Thomas, N.E., Castrillon, D.H., et al. (2012). LKB1/STK11 Inactivation Leads to Expansion of a Prometastatic Tumor Subpopulation in Melanoma. *Cancer Cell* **21**, 751–764.
- Llorente, P., Marco, R., and Sols, A. (1970). Regulation of Liver Pyruvate Kinase and the Phosphoenolpyruvate Crossroads. *Eur. J. Biochem.* **13**, 45–54.
- Lloyd-Evans, E. (2016). On the move, lysosomal CAX drives Ca²⁺ transport and motility. *J Cell Biol* **212**, 755–757.
- Lloyd-Evans, E., Morgan, A.J., He, X., Smith, D.A., Elliot-Smith, E., Sillence, D.J., Churchill, G.C., Schuchman, E.H., Galione, A., and Platt, F.M. (2008). Niemann-Pick disease type C1 is a sphingosine storage disease that causes deregulation of lysosomal calcium. *Nat. Med.* **14**, 1247–1255.
- Locasale, J.W. (2013). Serine, glycine and one-carbon units: cancer metabolism in full circle. *Nat. Rev. Cancer* **13**, 572–583.
- Locasale, J.W., and Cantley, L.C. (2011). Metabolic flux and the regulation of mammalian cell growth. *Cell Metab.* **14**, 443–451.
- Londesborough, A., Vaahtomeri, K., Tiainen, M., Katajisto, P., Ekman, N., Vallenius, T., and Mäkelä, T.P. (2008). LKB1 in endothelial cells is required for angiogenesis and TGF β -mediated vascular smooth muscle cell recruitment. *Dev. Camb. Engl.* **135**, 2331–2338.

- Longnus, S.L., Wambolt, R.B., Parsons, H.L., Brownsey, R.W., and Allard, M.F. (2003). 5-Aminoimidazole-4-carboxamide 1-beta -D-ribofuranoside (AICAR) stimulates myocardial glycogenolysis by allosteric mechanisms. *Am. J. Physiol. Regul. Integr. Comp. Physiol.* *284*, R936-944.
- Lorincz, A.B., and Kuttner, R.E. (1965). Response of malignancy to phenylalanine restriction. A preliminary report on a new concept of managing malignant disease. *Nebr. State Med. J.* *50*, 609–617.
- Lorincz, A.B., Kuttner, R.E., and Brandt, M.B. (1969). Tumor response to phenylalanine-tyrosine-limited diets. *J. Am. Diet. Assoc.* *54*, 198–205.
- Loughery, J., and Meek, D. (2013). Switching on p53: an essential role for protein phosphorylation? *BioDiscovery BioDiscovery* *8*.
- Lozano, G. (2010). Mouse Models of p53 Functions. *Cold Spring Harb. Perspect. Biol.* *2*.
- Lu, M., Zhou, L., Stanley, W.C., Cabrera, M.E., Saidel, G.M., and Yu, X. (2008). Role of the Malate-Aspartate Shuttle on the Metabolic Response to Myocardial Ischemia. *J. Theor. Biol.* *254*, 466–475.
- Lum, J.J., Bauer, D.E., Kong, M., Harris, M.H., Li, C., Lindsten, T., and Thompson, C.B. (2005). Growth factor regulation of autophagy and cell survival in the absence of apoptosis. *Cell* *120*, 237–248.
- Lumb, R., Buckberry, S., Secker, G., Lawrence, D., and Schwarz, Q. (2017). Transcriptome profiling reveals expression signatures of cranial neural crest cells arising from different axial levels. *BMC Dev. Biol.* *17*, 5.
- Lumsden, A., Sprawson, N., and Graham, A. (1991). Segmental origin and migration of neural crest cells in the hindbrain region of the chick embryo. *Development* *113*, 1281–1291.
- Luukko, K., Ylikorkala, A., Tiainen, M., and Mäkelä, T.P. (1999). Expression of LKB1 and PTEN tumor suppressor genes during mouse embryonic development. *Mech. Dev.* *83*, 187–190.
- Ma, J., and Hart, G.W. (2013). Protein O-GlcNAcylation in diabetes and diabetic complications. *Expert Rev. Proteomics* *10*, 365–380.
- Maddocks, O.D.K., and Vousden, K.H. (2011). Metabolic regulation by p53. *J. Mol. Med. Berl. Ger.* *89*, 237–245.
- Magistretti, P.J., and Allaman, I. (2015). A cellular perspective on brain energy metabolism and functional imaging. *Neuron* *86*, 883–901.
- Mahmoudi, A., Rami, M., Khattala, K., Elmadi, A., Afifi, M.A., and Youssef, B. (2013). Shah-Waardenburg Syndrome. *Pan Afr. Med. J.* *14*.
- Maier, B., Gluba, W., Bernier, B., Turner, T., Mohammad, K., Guise, T., Sutherland, A., Thorner, M., and Scrabble, H. (2004). Modulation of mammalian life span by the short isoform of p53. *Genes Dev.* *18*, 306–319.
- Marchenko, N.D., and Moll, U.M. (2007). The role of ubiquitination in the direct mitochondrial death program of p53. *Cell Cycle Georget. Tex* *6*, 1718–1723.
- Marchenko, N.D., Hanel, W., Li, D., Becker, K., Reich, N., and Moll, U.M. (2010). Stress-mediated nuclear stabilization of p53 is regulated by ubiquitination and importin-alpha3 binding. *Cell Death Differ.* *17*, 255–267.

- Marchiando, A.M., Graham, W.V., and Turner, J.R. (2010). Epithelial barriers in homeostasis and disease. *Annu. Rev. Pathol.* 5, 119–144.
- Martina, J.A., and Puertollano, R. (2017). TFEB and TFE3: The art of multi-tasking under stress conditions. *Transcription* 8, 48–54.
- Martínez, E., Navarro, A., Ordóñez, C., Del Valle, E., and Tolivia, J. (2013). Oxidative stress induces apolipoprotein D overexpression in hippocampus during aging and Alzheimer's disease. *J. Alzheimers Dis. JAD* 36, 129–144.
- Marzabadi, M.R., Sohal, R.S., and Brunk, U.T. (1991). Mechanisms of lipofuscinogenesis: effect of the inhibition of lysosomal proteinases and lipases under varying concentrations of ambient oxygen in cultured rat neonatal myocardial cells. *APMIS Acta Pathol. Microbiol. Immunol. Scand.* 99, 416–426.
- Mathupala, S.P., Heese, C., and Pedersen, P.L. (1997). Glucose catabolism in cancer cells. The type II hexokinase promoter contains functionally active response elements for the tumor suppressor p53. *J. Biol. Chem.* 272, 22776–22780.
- Matoba, S., Kang, J.-G., Patino, W.D., Wragg, A., Boehm, M., Gavrilova, O., Hurley, P.J., Bunz, F., and Hwang, P.M. (2006). p53 regulates mitochondrial respiration. *Science* 312, 1650–1653.
- Maurer, J., Fuchs, S., Jäger, R., Kurz, B., Sommer, L., and Schorle, H. (2007). Establishment and controlled differentiation of neural crest stem cell lines using conditional transgenesis. *Differ. Res. Biol. Divers.* 75, 580–591.
- Mayor, R., and Theveneau, E. (2013). The neural crest. *Dev. Camb. Engl.* 140, 2247–2251.
- McCommis, K.S., Chen, Z., Fu, X., McDonald, W.G., Colca, J.R., Kletzien, R.F., Burgess, S.C., and Finck, B.N. (2015). Loss of Mitochondrial Pyruvate Carrier 2 in Liver Leads to Defects in Gluconeogenesis and Compensation via Pyruvate-Alanine Cycling. *Cell Metab.* 22, 682–694.
- McCreight, L.J., Bailey, C.J., and Pearson, E.R. (2016). Metformin and the gastrointestinal tract. *Diabetologia* 59, 426–435.
- McDonald-McGinn, D.M., and Sullivan, K.E. (2011). Chromosome 22q11.2 deletion syndrome (DiGeorge syndrome/velocardiofacial syndrome). *Medicine (Baltimore)* 90, 1–18.
- McGarrity, T.J., Kulin, H.E., and Zaino, R.J. (2000). Peutz-Jeghers syndrome. *Am. J. Gastroenterol.* 95, 596–604.
- McGowan, K.A., Li, J.Z., Park, C.Y., Beaudry, V., Tabor, H.K., Sabnis, A.J., Zhang, W., Fuchs, H., de Angelis, M.H., Myers, R.M., et al. (2008). Ribosomal mutations cause p53-mediated dark skin and pleiotropic effects. *Nat. Genet.* 40, 963–970.
- McKeown, S.J., Mohsenipour, M., Bergner, A.J., Young, H.M., and Stamp, L.A. (2017). Exposure to GDNF Enhances the Ability of Enteric Neural Progenitors to Generate an Enteric Nervous System. *Stem Cell Rep.* 8, 476–488.
- McNeill, A., Magalhaes, J., Shen, C., Chau, K.-Y., Hughes, D., Mehta, A., Foltynie, T., Cooper, J.M., Abramov, A.Y., Gegg, M., et al. (2014). Amboxol improves lysosomal biochemistry in glucocerebrosidase mutation-linked Parkinson disease cells. *Brain J. Neurol.* 137, 1481–1495.
- de Meester, C., Timmermans, A.D., Balteau, M., Ginion, A., Roelants, V., Noppe, G., Porporato, P.E., Sonveaux, P., Viollet, B., Sakamoto, K., et al. (2014). Role of AMP-activated protein kinase in regulating hypoxic survival and proliferation of mesenchymal stem cells. *Cardiovasc. Res.* 101, 20–29.

- Mehenni, H., Gehrig, C., Nezu, J., Oku, A., Shimane, M., Rossier, C., Guex, N., Blouin, J.L., Scott, H.S., and Antonarakis, S.E. (1998). Loss of LKB1 kinase activity in Peutz-Jeghers syndrome, and evidence for allelic and locus heterogeneity. *Am. J. Hum. Genet.* 63, 1641–1650.
- Meijer, A.J. (2003). Amino acids as regulators and components of nonproteinogenic pathways. *J. Nutr.* 133, 2057S-2062S.
- Meijer, A.J., and Van Dam, K. (1974). The metabolic significance of anion transport in mitochondria. *Biochim. Biophys. Acta* 346, 213–244.
- Melchionda, M., Pittman, J.K., Mayor, R., and Patel, S. (2016). $\text{Ca}^{2+}/\text{H}^{+}$ exchange by acidic organelles regulates cell migration in vivo. *J. Cell Biol.* 212, 803–813.
- Merrill, G.F., Kurth, E.J., Hardie, D.G., and Winder, W.W. (1997). AICA riboside increases AMP-activated protein kinase, fatty acid oxidation, and glucose uptake in rat muscle. *Am. J. Physiol.* 273, E1107-1112.
- Metallo, C.M., and Vander Heiden, M.G. (2013). Understanding metabolic regulation and its influence on cell physiology. *Mol. Cell* 49, 388–398.
- Migliorini, D., Lazzerini Denchi, E., Danovi, D., Jochemsen, A., Capillo, M., Gobbi, A., Helin, K., Pelicci, P.G., and Marine, J.-C. (2002). Mdm4 (Mdmx) regulates p53-induced growth arrest and neuronal cell death during early embryonic mouse development. *Mol. Cell. Biol.* 22, 5527–5538.
- Mikanagi, K. (2012). Purine and Pyrimidine Metabolism in Man VI: Part A: Clinical and Molecular Biology (Springer Science & Business Media).
- Mills, A.A., Zheng, B., Wang, X.J., Vogel, H., Roop, D.R., and Bradley, A. (1999). p63 is a p53 homologue required for limb and epidermal morphogenesis. *Nature* 398, 708–713.
- Minoux, M., and Rijli, F.M. (2010). Molecular mechanisms of cranial neural crest cell migration and patterning in craniofacial development. *Dev. Camb. Engl.* 137, 2605–2621.
- Minsky, N., and Oren, M. (2004). The RING Domain of Mdm2 Mediates Histone Ubiquitylation and Transcriptional Repression. *Mol. Cell* 16, 631–639.
- Miranda, L., Carpentier, S., Platek, A., Hussain, N., Gueuning, M.-A., Vertommen, D., Ozkan, Y., Sid, B., Hue, L., Courtoy, P.J., et al. (2010). AMP-activated protein kinase induces actin cytoskeleton reorganization in epithelial cells. *Biochem. Biophys. Res. Commun.* 396, 656–661.
- Mittal, D., Bagga, A., Tandon, R., Sharma, M.C., and Bhatnagar, V. (2015). Hirschsprung's disease with infantile nephropathic cystinosis. *J. Indian Assoc. Pediatr. Surg.* 20, 153–154.
- Miyoshi, H., Nakau, M., Ishikawa, T., Seldin, M.F., Oshima, M., and Taketo, M.M. (2002). Gastrointestinal hamartomatous polyposis in Lkb1 heterozygous knockout mice. *Cancer Res.* 62, 2261–2266.
- Mizushima, N., and Levine, B. (2010). Autophagy in mammalian development and differentiation. *Nat. Cell Biol.* 12, 823–830.
- Molchadsky, A., Shats, I., Goldfinger, N., Pevsner-Fischer, M., Olson, M., Rinon, A., Tzahor, E., Lozano, G., Zipori, D., Sarig, R., et al. (2008). p53 Plays a Role in Mesenchymal Differentiation Programs, in a Cell Fate Dependent Manner. *PLOS ONE* 3, e3707.

- Momand, J., Zambetti, G.P., Olson, D.C., George, D., and Levine, A.J. (1992). The mdm-2 oncogene product forms a complex with the p53 protein and inhibits p53-mediated transactivation. *Cell* 69, 1237–1245.
- Momcilovic, M., Hong, S.-P., and Carlson, M. (2006). Mammalian TAK1 activates Snf1 protein kinase in yeast and phosphorylates AMP-activated protein kinase in vitro. *J. Biol. Chem.* 281, 25336–25343.
- Montes de Oca Luna, R., Wagner, D.S., and Lozano, G. (1995). Rescue of early embryonic lethality in mdm2-deficient mice by deletion of p53. *Nature* 378, 203–206.
- Morgan, S.E., and Kastan, M.B. (1997). p53 and ATM: cell cycle, cell death, and cancer. *Adv. Cancer Res.* 71, 1–25.
- Morgan, S.C., Relaix, F., Sandell, L.L., and Loeken, M.R. (2008). Oxidative stress during diabetic pregnancy disrupts cardiac neural crest migration and causes outflow tract defects. *Birt. Defects Res. A. Clin. Mol. Teratol.* 82, 453–463.
- Morozov, V.E., Falzon, M., Anderson, C.W., and Kuff, E.L. (1994). DNA-dependent protein kinase is activated by nicks and larger single-stranded gaps. *J. Biol. Chem.* 269, 16684–16688.
- Morselli, E., Tasdemir, E., Maiuri, M.C., Galluzzi, L., Kepp, O., Criollo, A., Vicencio, J.M., Soussi, T., and Kroemer, G. (2008). Mutant p53 protein localized in the cytoplasm inhibits autophagy. *Cell Cycle Georget. Tex* 7, 3056–3061.
- Mruk, D.D., and Cheng, C.Y. (2015). The Mammalian Blood-Testis Barrier: Its Biology and Regulation. *Endocr. Rev.* 36, 564–591.
- Mwinyi, J., Boström, A., Fehrer, I., Othman, A., Waeber, G., Marti-Soler, H., Vollenweider, P., Marques-Vidal, P., Schiöth, H.B., Eckardstein, A. von, et al. (2017). Plasma 1-deoxysphingolipids are early predictors of incident type 2 diabetes mellitus. *PLOS ONE* 12, e0175776.
- Nag, S., Qin, J., Srivenugopal, K.S., Wang, M., and Zhang, R. (2013). The MDM2-p53 pathway revisited. *J. Biomed. Res.* 27, 254–271.
- Nakada, D., Saunders, T.L., and Morrison, S.J. (2010). Lkb1 regulates cell cycle and energy metabolism in haematopoietic stem cells. *Nature* 468, 653–658.
- Nakano, A., and Takashima, S. (2012). LKB1 and AMP-activated protein kinase: regulators of cell polarity. *Genes Cells Devoted Mol. Cell. Mech.* 17, 737–747.
- Narla, A., and Ebert, B.L. (2010). Ribosomopathies: human disorders of ribosome dysfunction. *Blood* 115, 3196–3205.
- Narlikar, G.J., Fan, H.-Y., and Kingston, R.E. (2002). Cooperation between complexes that regulate chromatin structure and transcription. *Cell* 108, 475–487.
- Nemajerova, A., Palacios, G., Nowak, N.J., Matsui, S.-I., and Petrenko, O. (2009). Targeted deletion of p73 in mice reveals its role in T cell development and lymphomagenesis. *PloS One* 4, e7784.
- Nemajerova, A., Kramer, D., Siller, S.S., Herr, C., Shomroni, O., Pena, T., Gallinas Suazo, C., Glaser, K., Wildung, M., Steffen, H., et al. (2016). TAp73 is a central transcriptional regulator of airway multiciliogenesis. *Genes Dev.* 30, 1300–1312.

- Neunlist, M., Rolli-Derkinderen, M., Latorre, R., Van Landeghem, L., Coron, E., Derkinderen, P., and De Giorgio, R. (2014). Enteric glial cells: recent developments and future directions. *Gastroenterology* 147, 1230–1237.
- Nicastro, R., Sardu, A., Panchaud, N., and De Virgilio, C. (2017). The Architecture of the Rag GTPase Signaling Network. *Biomolecules* 7, 48.
- van Niel, G., Wubbolts, R., Ten Broeke, T., Buschow, S.I., Ossendorp, F.A., Melief, C.J., Raposo, G., van Balkom, B.W., and Stoorvogel, W. (2006). Dendritic cells regulate exposure of MHC class II at their plasma membrane by oligoubiquitination. *Immunity* 25, 885–894.
- Nilsson, E., Ghassemifar, R., and Brunk, U.T. (1997). Lysosomal heterogeneity between and within cells with respect to resistance against oxidative stress. *Histochem. J.* 29, 857–865.
- Nissen, R.M., Yan, J., Amsterdam, A., Hopkins, N., and Burgess, S.M. (2003). Zebrafish foxi one modulates cellular responses to Fgf signaling required for the integrity of ear and jaw patterning. *Dev. Camb. Engl.* 130, 2543–2554.
- Noack Watt, K.E., Achilleos, A., Neben, C.L., Merrill, A.E., and Trainor, P.A. (2016). The Roles of RNA Polymerase I and III Subunits Polr1c and Polr1d in Craniofacial Development and in Zebrafish Models of Treacher Collins Syndrome. *PLoS Genet.* 12.
- Nony, P., Gaude, H., Rossel, M., Fournier, L., Rouault, J.-P., and Billaud, M. (2003). Stability of the Peutz–Jeghers syndrome kinase LKB1 requires its binding to the molecular chaperones Hsp90/Cdc37. *Oncogene* 22, 9165–9175.
- Oakberg, E.F. (1957). Gamma-ray sensitivity of spermatogonia of the mouse. *J. Exp. Zool.* 134, 343–356.
- Ochocki, J.D., and Simon, M.C. (2013). Nutrient-sensing pathways and metabolic regulation in stem cells. *J. Cell Biol.* 203, 23–33.
- Okamoto, K., and Beach, D. (1994). Cyclin G is a transcriptional target of the p53 tumor suppressor protein. *EMBO J.* 13, 4816–4822.
- Okuda, A., Uranishi, K., and Suzuki, A. (2017). Discovery of a new role for the p53 family in the onset of mesendodermal differentiation of embryonic stem cells. *Stem Cell Investig.* 4.
- Oliveira, P.F., and Alves, M.G. (2015). *Sertoli Cell Metabolism and Spermatogenesis* (Springer International Publishing).
- Olivier, M., Hollstein, M., and Hainaut, P. (2010). TP53 mutations in human cancers: origins, consequences, and clinical use. *Cold Spring Harb. Perspect. Biol.* 2, a001008.
- Ollila, S., and Mäkelä, T.P. (2011). The tumor suppressor kinase LKB1: lessons from mouse models. *J. Mol. Cell Biol.* 3, 330–340.
- O’Neill, H.M., Maarbjerg, S.J., Crane, J.D., Jeppesen, J., Jørgensen, S.B., Schertzer, J.D., Shyroka, O., Kiens, B., van Denderen, B.J., Tarnopolsky, M.A., et al. (2011). AMP-activated protein kinase (AMPK) beta1beta2 muscle null mice reveal an essential role for AMPK in maintaining mitochondrial content and glucose uptake during exercise. *Proc. Natl. Acad. Sci. U. S. A.* 108, 16092–16097.
- Onyenwoke, R.U., and Brenman, J.E. (2015). Lysosomal Storage Diseases-Regulating Neurodegeneration. *J. Exp. Neurosci.* 9s2, JEN.S25475.

- Orlova, K.A., Parker, W.E., Heuer, G.G., Tsai, V., Yoon, J., Baybis, M., Fenning, R.S., Strauss, K., and Crino, P.B. (2010). STRAD α deficiency results in aberrant mTORC1 signaling during corticogenesis in humans and mice. *J. Clin. Invest.* 120, 1591–1602.
- Othman, A., Rütli, M.F., Ernst, D., Saely, C.H., Rein, P., Drexel, H., Porretta-Serapiglia, C., Lauria, G., Bianchi, R., von Eckardstein, A., et al. (2012). Plasma deoxysphingolipids: a novel class of biomarkers for the metabolic syndrome? *Diabetologia* 55, 421–431.
- Othman, A., Saely, C.H., Muendlein, A., Vonbank, A., Drexel, H., von Eckardstein, A., and Hornemann, T. (2015a). Plasma 1-deoxysphingolipids are predictive biomarkers for type 2 diabetes mellitus. *BMJ Open Diabetes Res. Care* 3.
- Othman, A., Bianchi, R., Alecu, I., Wei, Y., Porretta-Serapiglia, C., Lombardi, R., Chiorazzi, A., Meregalli, C., Oggioni, N., Cavaletti, G., et al. (2015b). Lowering Plasma 1-Deoxysphingolipids Improves Neuropathy in Diabetic Rats. *Diabetes* 64, 1035–1045.
- Owen, D.J., Ornaghi, P., Yang, J.C., Lowe, N., Evans, P.R., Ballario, P., Neuhaus, D., Filetici, P., and Travers, A.A. (2000). The structural basis for the recognition of acetylated histone H4 by the bromodomain of histone acetyltransferase gcn5p. *EMBO J.* 19, 6141–6149.
- Pan, Y., and Chen, J. (2003). MDM2 promotes ubiquitination and degradation of MDMX. *Mol. Cell. Biol.* 23, 5113–5121.
- Pani, L., Horal, M., and Loeken, M.R. (2002). Rescue of neural tube defects in Pax-3-deficient embryos by p53 loss of function: implications for Pax-3- dependent development and tumorigenesis. *Genes Dev.* 16, 676–680.
- Panieri, E., and Santoro, M.M. (2016). ROS homeostasis and metabolism: a dangerous liason in cancer cells. *Cell Death Dis.* 7, e2253.
- Pappas, K., Xu, J., Zairis, S., Resnick-Silverman, L., Abate, F., Steinbach, N., Ozturk, S., Saal, L.H., Su, T., Cheung, P., et al. (2017). p53 Maintains Baseline Expression of Multiple Tumor Suppressor Genes. *Mol. Cancer Res. MCR* 15, 1051–1062.
- Parant, J., Chavez-Reyes, A., Little, N.A., Yan, W., Reinke, V., Jochemsen, A.G., and Lozano, G. (2001). Rescue of embryonic lethality in Mdm4-null mice by loss of Trp53 suggests a nonoverlapping pathway with MDM2 to regulate p53. *Nat. Genet.* 29, 92–95.
- Parisi, M.A. (1993). Hirschsprung Disease Overview. In *GeneReviews®*, M.P. Adam, H.H. Ardinger, R.A. Pagon, S.E. Wallace, L.J. Bean, K. Stephens, and A. Amemiya, eds. (Seattle (WA): University of Washington, Seattle), p.
- Parker, S.J., Svensson, R.U., Divakaruni, A.S., Lefebvre, A.E., Murphy, A.N., Shaw, R.J., and Metallo, C.M. (2017). LKB1 promotes metabolic flexibility in response to energy stress. *Metab. Eng.* 43, 208–217.
- Parker, W.E., Orlova, K.A., Parker, W.H., Birnbaum, J.F., Krymskaya, V.P., Goncharov, D.A., Baybis, M., Helfferich, J., Okochi, K., Strauss, K.A., et al. (2013). Rapamycin Prevents Seizures After Depletion of STRADA in a Rare Neurodevelopmental Disorder. *Sci. Transl. Med.* 5, 182ra53.
- Partanen, J.I., Tervonen, T.A., and Klefström, J. (2013). Breaking the epithelial polarity barrier in cancer: the strange case of LKB1/PAR-4. *Philos. Trans. R. Soc. B Biol. Sci.* 368.

- Pascua-Maestro, R., Diez-Hermano, S., Lillo, C., Ganfornina, M.D., and Sanchez, D. (2017). Protecting cells by protecting their vulnerable lysosomes: Identification of a new mechanism for preserving lysosomal functional integrity upon oxidative stress. *PLoS Genet.* *13*, e1006603.
- Patel, S., and Cai, X. (2015). Evolution of acidic Ca^{2+} stores and their resident Ca^{2+} -permeable channels. *Cell Calcium* *57*, 222–230.
- Patel, K., Foretz, M., Marion, A., Campbell, D.G., Gurlay, R., Boudaba, N., Tournier, E., Titchenell, P., Pegg, M., Deak, M., et al. (2014). The LKB1-salt-inducible kinase pathway functions as a key gluconeogenic suppressor in the liver. *Nat. Commun.* *5*, 4535.
- Pauli, S., Bajpai, R., and Borchers, A. (2017). CHARGEd with neural crest defects. *Am. J. Med. Genet. C Semin. Med. Genet.* *175*, 478–486.
- Penno, A., Reilly, M.M., Houlden, H., Laurá, M., Rentsch, K., Niederkofer, V., Stoeckli, E.T., Nicholson, G., Eichler, F., Brown, R.H., et al. (2010). Hereditary Sensory Neuropathy Type 1 Is Caused by the Accumulation of Two Neurotoxic Sphingolipids. *J. Biol. Chem.* *285*, 11178–11187.
- Pereira, B., Sousa, S., Barros, R., Carreto, L., Oliveira, P., Oliveira, C., Chartier, N.T., Plateroti, M., Rouault, J.-P., Freund, J.-N., et al. (2013). CDX2 regulation by the RNA-binding protein MEX3A: impact on intestinal differentiation and stemness. *Nucleic Acids Res.* *41*, 3986–3999.
- Persons, D.L., Yazlovitskaya, E.M., and Pelling, J.C. (2000). Effect of extracellular signal-regulated kinase on p53 accumulation in response to cisplatin. *J. Biol. Chem.* *275*, 35778–35785.
- Petersen, J., and Adameyko, I. (2017). Nerve-associated neural crest: peripheral glial cells generate multiple fates in the body. *Curr. Opin. Genet. Dev.* *45*, 10–14.
- Peterson, L.W., and Artis, D. (2014). Intestinal epithelial cells: regulators of barrier function and immune homeostasis. *Nat. Rev. Immunol.* *14*, 141–153.
- Phillips, B.T., Gassei, K., and Orwig, K.E. (2010). Spermatogonial stem cell regulation and spermatogenesis. *Philos. Trans. R. Soc. Lond. B. Biol. Sci.* *365*, 1663–1678.
- Pingault, V., Ente, D., Dastot-Le Moal, F., Goossens, M., Marlin, S., and Bondurand, N. (2010). Review and update of mutations causing Waardenburg syndrome. *Hum. Mutat.* *31*, 391–406.
- Pivtoraiko, V.N., Stone, S.L., Roth, K.A., and Shacka, J.J. (2009). Oxidative Stress and Autophagy in the Regulation of Lysosome-Dependent Neuron Death. *Antioxid. Redox Signal.* *11*, 481–496.
- Pluquet, O., Qu, L.-K., Baltzis, D., and Koromilas, A.E. (2005). Endoplasmic reticulum stress accelerates p53 degradation by the cooperative actions of Hdm2 and glycogen synthase kinase 3 β . *Mol. Cell. Biol.* *25*, 9392–9405.
- Pomeranz, H.D., Rothman, T.P., and Gershon, M.D. (1991). Colonization of the post-umbilical bowel by cells derived from the sacral neural crest: direct tracing of cell migration using an intercalating probe and a replication-deficient retrovirus. *Dev. Camb. Engl.* *111*, 647–655.
- Pooya, S., Liu, X., Kumar, V.B.S., Anderson, J., Imai, F., Zhang, W., Ciraolo, G., Ratner, N., Setchell, K.D.R., Yoshida, Y., et al. (2014). The tumour suppressor LKB1 regulates myelination through mitochondrial metabolism. *Nat. Commun.* *5*, 4993.
- Porter, K., Nallathambi, J., Lin, Y., and Liton, P.B. (2013). Lysosomal basification and decreased autophagic flux in oxidatively stressed trabecular meshwork cells: implications for glaucoma pathogenesis. *Autophagy* *9*, 581–594.

- Powell, S.R., Wang, P., Divald, A., Teichberg, S., Haridas, V., McCloskey, T.W., Davies, K.J.A., and Katzeff, H. (2005). Aggregates of oxidized proteins (lipofuscin) induce apoptosis through proteasome inhibition and dysregulation of proapoptotic proteins. *Free Radic. Biol. Med.* 38, 1093–1101.
- Praitis, V., Simske, J., Kniss, S., Mandt, R., Imlay, L., Feddersen, C., Miller, M.B., Mushi, J., Liszewski, W., Weinstein, R., et al. (2013). The secretory pathway calcium ATPase PMR-1/SPCA1 has essential roles in cell migration during *Caenorhabditis elegans* embryonic development. *PLoS Genet.* 9, e1003506.
- Puffenberger, E.G., Strauss, K.A., Ramsey, K.E., Craig, D.W., Stephan, D.A., Robinson, D.L., Hendrickson, C.L., Gottlieb, S., Ramsay, D.A., Siu, V.M., et al. (2007). Polyhydramnios, megalencephaly and symptomatic epilepsy caused by a homozygous 7-kilobase deletion in LYK5. *Brain J. Neurol.* 130, 1929–1941.
- Qu, L., Huang, S., Baltzis, D., Rivas-Estilla, A.-M., Pluquet, O., Hatzoglou, M., Koumenis, C., Taya, Y., Yoshimura, A., and Koromilas, A.E. (2004). Endoplasmic reticulum stress induces p53 cytoplasmic localization and prevents p53-dependent apoptosis by a pathway involving glycogen synthase kinase-3 β . *Genes Dev.* 18, 261–277.
- Rama Rao, K.V., and Kielian, T. (2016). Astrocytes and lysosomal storage diseases. *Neuroscience* 323, 195–206.
- Rato, L., Alves, M.G., Socorro, S., Duarte, A.I., Cavaco, J.E., and Oliveira, P.F. (2012). Metabolic regulation is important for spermatogenesis. *Nat. Rev. Urol.* 9, 330–338.
- Reddy, A., Caler, E.V., and Andrews, N.W. (2001). Plasma membrane repair is mediated by Ca(2+)-regulated exocytosis of lysosomes. *Cell* 106, 157–169.
- van Riggelen, J., Yetil, A., and Felsher, D.W. (2010). MYC as a regulator of ribosome biogenesis and protein synthesis. *Nat. Rev. Cancer* 10, 301–309.
- Rinon, A., Molchadsky, A., Nathan, E., Yovel, G., Rotter, V., Sarig, R., and Tzahor, E. (2011a). p53 coordinates cranial neural crest cell growth and epithelial-mesenchymal transition/delamination processes. *Dev. Camb. Engl.* 138, 1827–1838.
- Rodier, F., and Campisi, J. (2011). Four faces of cellular senescence. *J. Cell Biol.* 192, 547–556.
- Rodnina, M.V., and Wintermeyer, W. (2009). Recent mechanistic insights into eukaryotic ribosomes. *Curr. Opin. Cell Biol.* 21, 435–443.
- Rodríguez-Colman, M.J., Schewe, M., Meerlo, M., Stigter, E., Gerrits, J., Pras-Raves, M., Sacchetti, A., Hornsveid, M., Oost, K.C., Snippert, H.J., et al. (2017). Interplay between metabolic identities in the intestinal crypt supports stem cell function. *Nature* 543, 424–427.
- Romero-Garcia, S., Moreno-Altamirano, M.M.B., Prado-Garcia, H., and Sánchez-García, F.J. (2016). Lactate Contribution to the Tumor Microenvironment: Mechanisms, Effects on Immune Cells and Therapeutic Relevance. *Front. Immunol.* 7.
- Ross, A.P., and Zarbalis, K.S. (2014). The emerging roles of ribosome biogenesis in craniofacial development. *Front. Physiol.* 5, 26.
- Rossi, D.J., Ylikorkala, A., Korsisaari, N., Salovaara, R., Luukko, K., Launonen, V., Henkemeyer, M., Ristimäki, A., Aaltonen, L.A., and Mäkelä, T.P. (2002). Induction of cyclooxygenase-2 in a mouse model of Peutz–Jeghers polyposis. *Proc. Natl. Acad. Sci.* 99, 12327–12332.

- Rowan, A., Churchman, M., Jefferey, R., Hanby, A., Poulson, R., and Tomlinson, I. (2000). In situ analysis of LKB1/STK11 mRNA expression in human normal tissues and tumours. *J. Pathol.* *192*, 203–206.
- Rowart, P., Erpicum, P., Krzesinski, J.-M., Sebbagh, M., and Jouret, F. (2017). Mesenchymal Stromal Cells Accelerate Epithelial Tight Junction Assembly via the AMP-Activated Protein Kinase Pathway, Independently of Liver Kinase B1. *Stem Cells Int.* *2017*.
- Ruderman, N.B., Carling, D., Prentki, M., and Cacicedo, J.M. (2013). AMPK, insulin resistance, and the metabolic syndrome. *J. Clin. Invest.* *123*, 2764–2772.
- Rufini, A., Tucci, P., Celardo, I., and Melino, G. (2013). Senescence and aging: the critical roles of p53. *Oncogene* *32*, 5129–5143.
- Ruiz-Lozano, P., Hixon, M.L., Wagner, M.W., Flores, A.I., Ikawa, S., Baldwin, A.S., Chien, K.R., and Gualberto, A. (1999). p53 is a transcriptional activator of the muscle-specific phosphoglycerate mutase gene and contributes in vivo to the control of its cardiac expression. *Cell Growth Differ. Mol. Biol. J. Am. Assoc. Cancer Res.* *10*, 295–306.
- Ryall, J.G., Cliff, T., Dalton, S., and Sartorelli, V. (2015). Metabolic Reprogramming of Stem Cell Epigenetics. *Cell Stem Cell* *17*, 651–662.
- Sabatini, D.M. (2017). Twenty-five years of mTOR: Uncovering the link from nutrients to growth. *Proc. Natl. Acad. Sci.* *114*, 11818–11825.
- Saftig, P., and Klumperman, J. (2009). Lysosome biogenesis and lysosomal membrane proteins: trafficking meets function. *Nat. Rev. Mol. Cell Biol.* *10*, 623–635.
- Sah, V.P., Attardi, L.D., Mulligan, G.J., Williams, B.O., Bronson, R.T., and Jacks, T. (1995). A subset of p53-deficient embryos exhibit exencephaly. *Nat. Genet.* *10*, 175–180.
- Saher, G., and Stumpf, S.K. (2015). Cholesterol in myelin biogenesis and hypomyelinating disorders. *Biochim. Biophys. Acta* *1851*, 1083–1094.
- Sahin, F., Maitra, A., Argani, P., Sato, N., Maehara, N., Montgomery, E., Goggins, M., Hruban, R.H., and Su, G.H. (2003). Loss of Stk11/Lkb1 expression in pancreatic and biliary neoplasms. *Mod. Pathol. Off. J. U. S. Can. Acad. Pathol. Inc* *16*, 686–691.
- Saito, Y., and Nakada, D. (2014). The role of the Lkb1/AMPK pathway in hematopoietic stem cells and Leukemia. *Crit. Rev. Oncog.* *19*, 383–397.
- Sakai, D., and Trainor, P.A. (2016). Face off against ROS: Tcof1/Treacle safeguards neuroepithelial cells and progenitor neural crest cells from oxidative stress during craniofacial development. *Dev. Growth Differ.* *58*, 577–585.
- Sakai, D., Dixon, J., Achilleos, A., Dixon, M., and Trainor, P.A. (2016). Prevention of Treacher Collins syndrome craniofacial anomalies in mouse models via maternal antioxidant supplementation. *Nat. Commun.* *7*, 10328.
- Sancak, Y., Bar-Peled, L., Zoncu, R., Markhard, A.L., Nada, S., and Sabatini, D.M. (2010). Ragulator-Rag complex targets mTORC1 to the lysosomal surface and is necessary for its activation by amino acids. *Cell* *141*, 290–303.

- Sanchez, D., Bajo-Grañeras, R., Del Caño-Espinel, M., Garcia-Centeno, R., Garcia-Mateo, N., Pascua-Maestro, R., and Ganfornina, M.D. (2015). Aging without Apolipoprotein D: Molecular and cellular modifications in the hippocampus and cortex. *Exp. Gerontol.* 67, 19–47.
- Sanchez-Cespedes, M. (2007). A role for LKB1 gene in human cancer beyond the Peutz-Jeghers syndrome. *Oncogene* 26, 7825–7832.
- Sanchez-Cespedes, M., Parrella, P., Esteller, M., Nomoto, S., Trink, B., Engles, J.M., Westra, W.H., Herman, J.G., and Sidransky, D. (2002). Inactivation of LKB1/STK11 is a common event in adenocarcinomas of the lung. *Cancer Res.* 62, 3659–3662.
- Sanlaville, D., Etchevers, H.C., Gonzales, M., Martinovic, J., Clément-Ziza, M., Delezoide, A.-L., Aubry, M.-C., Pelet, A., Chemouny, S., Cruaud, C., et al. (2006). Phenotypic spectrum of CHARGE syndrome in fetuses with CHD7 truncating mutations correlates with expression during human development. *J. Med. Genet.* 43, 211–217.
- Santagati, F., and Rijli, F.M. (2003). Cranial neural crest and the building of the vertebrate head. *Nat. Rev. Neurosci.* 4, 806–818.
- Sapkota, G.P., Boudeau, J., Deak, M., Kieloch, A., Morrice, N., and Alessi, D.R. (2002a). Identification and characterization of four novel phosphorylation sites (Ser31, Ser325, Thr336 and Thr366) on LKB1/STK11, the protein kinase mutated in Peutz-Jeghers cancer syndrome. *Biochem. J.* 362, 481–490.
- Sapkota, G.P., Deak, M., Kieloch, A., Morrice, N., Goodarzi, A.A., Smythe, C., Shiloh, Y., Lees-Miller, S.P., and Alessi, D.R. (2002b). Ionizing radiation induces ataxia telangiectasia mutated kinase (ATM)-mediated phosphorylation of LKB1/STK11 at Thr-366. *Biochem. J.* 368, 507–516.
- Sapkota, G.P., Boudeau, J., Deak, M., Kieloch, A., Morrice, N., and Alessi, D.R. (2002c). Identification and characterization of four novel phosphorylation sites (Ser31, Ser325, Thr336 and Thr366) on LKB1/STK11, the protein kinase mutated in Peutz-Jeghers cancer syndrome. *Biochem. J.* 362, 481–490.
- Sasselli, V., Pachnis, V., and Burns, A.J. (2012). The enteric nervous system. *Dev. Biol.* 366, 64–73.
- Sato, T., Nakashima, A., Guo, L., and Tamanoi, F. (2009). Specific activation of mTORC1 by Rheb G-protein in vitro involves enhanced recruitment of its substrate protein. *J. Biol. Chem.* 284, 12783–12791.
- Scarpa, E., and Mayor, R. (2016). Collective cell migration in development. *J. Cell Biol.* 212, 143–155.
- Schaffer, B.E., Levin, R.S., Hertz, N.T., Maures, T.J., Schoof, M.L., Hollstein, P.E., Benayoun, B.A., Banko, M.R., Shaw, R.J., Shokat, K.M., et al. (2015). Identification of AMPK Phosphorylation Sites Reveals a Network of Proteins Involved in Cell Invasion and Facilitates Large-Scale Substrate Prediction. *Cell Metab.* 22, 907–921.
- Schardt, J.A., Weber, D., Eyholzer, M., Mueller, B.U., and Pabst, T. (2009). Activation of the unfolded protein response is associated with favorable prognosis in acute myeloid leukemia. *Clin. Cancer Res. Off. J. Am. Assoc. Cancer Res.* 15, 3834–3841.
- Schilling, T.F., and Kimmel, C.B. (1994). Segment and cell type lineage restrictions during pharyngeal arch development in the zebrafish embryo. *Dev. Camb. Engl.* 120, 483–494.

Schultz, M.L., Tecedor, L., Chang, M., and Davidson, B.L. (2011). Clarifying lysosomal storage diseases. *Trends Neurosci.* 34, 401–410.

Schwann, T., and Schleyden, M.J. (1847). Microscopical researches into the accordance in the structure and growth of animals and plants (London: Printed for the Sydenham Society).

Schwartzenberg-Bar-Yoseph, F., Armoni, M., and Karnieli, E. (2004). The tumor suppressor p53 down-regulates glucose transporters GLUT1 and GLUT4 gene expression. *Cancer Res.* 64, 2627–2633.

Scott, J.W., and Oakhill, J.S. (2017). The sweet side of AMPK signaling: regulation of GFAT1. *Biochem. J.* 474, 1289–1292.

Sebbagh, M., Santoni, M.-J., Hall, B., Borg, J.-P., and Schwartz, M.A. (2009). Regulation of LKB1/STRAD localization and function by E-cadherin. *Curr. Biol. CB* 19, 37–42.

Shackelford, D.B. (2013). Unravelling the connection between metabolism and tumorigenesis through studies of the liver kinase B1 tumour suppressor. *J. Carcinog.* 12, 16.

Shackelford, D.B., and Shaw, R.J. (2009). The LKB1-AMPK pathway: metabolism and growth control in tumor suppression. *Nat. Rev. Cancer* 9, 563–575.

Sharkey, K.A. (2015). Emerging roles for enteric glia in gastrointestinal disorders. *J. Clin. Invest.* 125, 918–925.

Shaulsky, G., Ben-Ze'ev, A., and Rotter, V. (1990). Subcellular distribution of the p53 protein during the cell cycle of Balb/c 3T3 cells. *Oncogene* 5, 1707–1711.

Shaw, R.J. (2009a). LKB1 and AMP-activated protein kinase control of mTOR signalling and growth. *Acta Physiol. Oxf. Engl.* 196, 65–80.

Shaw, R.J. (2009b). Tumor Suppression by LKB1: SIK-ness Prevents Metastasis. *Sci. Signal.* 2, pe55–pe55.

Shaw, R.J., Kosmatka, M., Bardeesy, N., Hurley, R.L., Witters, L.A., DePinho, R.A., and Cantley, L.C. (2004). The tumor suppressor LKB1 kinase directly activates AMP-activated kinase and regulates apoptosis in response to energy stress. *Proc. Natl. Acad. Sci. U. S. A.* 101, 3329–3335.

Shaw, R.J., Lamia, K.A., Vasquez, D., Koo, S.-H., Bardeesy, N., DePinho, R.A., Montminy, M., and Cantley, L.C. (2005). The Kinase LKB1 Mediates Glucose Homeostasis in Liver and Therapeutic Effects of Metformin. *Science* 310, 1642–1646.

Shay, J.W., and Roninson, I.B. (2004). Hallmarks of senescence in carcinogenesis and cancer therapy. *Oncogene* 23, 2919–2933.

Shelly, M., Cancedda, L., Heilshorn, S., Sumbre, G., and Poo, M.-M. (2007). LKB1/STRAD promotes axon initiation during neuronal polarization. *Cell* 129, 565–577.

Shen, Y.-A.A., Chen, Y., Dao, D.Q., Mayoral, S.R., Wu, L., Meijer, D., Ullian, E.M., Chan, J.R., and Lu, Q.R. (2014). Phosphorylation of LKB1/Par-4 Establishes Schwann Cell Polarity to Initiate and Control Myelin Extent. *Nat. Commun.* 5, 4991.

Sheng, Y., Laister, R.C., Lemak, A., Wu, B., Tai, E., Duan, S., Lukin, J., Sunnerhagen, M., Srisailam, S., Karra, M., et al. (2008). Molecular basis of Pirh2-mediated p53 ubiquitylation. *Nat. Struct. Mol. Biol.* 15, 1334–1342.

- Sherman, L., Stocker, K.M., Morrison, R., and Ciment, G. (1993). Basic fibroblast growth factor (bFGF) acts intracellularly to cause the transdifferentiation of avian neural crest-derived Schwann cell precursors into melanocytes. *Dev. Camb. Engl.* 118, 1313–1326.
- Shimizu, S., Kanaseki, T., Mizushima, N., Mizuta, T., Arakawa-Kobayashi, S., Thompson, C.B., and Tsujimoto, Y. (2004). Role of Bcl-2 family proteins in a non-apoptotic programmed cell death dependent on autophagy genes. *Nat. Cell Biol.* 6, 1221–1228.
- Shin, J.-S., Ebersold, M., Pypaert, M., Delamarre, L., Hartley, A., and Mellman, I. (2006). Surface expression of MHC class II in dendritic cells is controlled by regulated ubiquitination. *Nature* 444, 115–118.
- Shorning, B.Y., and Clarke, A.R. (2011). LKB1 loss of function studied in vivo. *FEBS Lett.* 585, 958–966.
- Shorning, B.Y., Zabkiewicz, J., McCarthy, A., Pearson, H.B., Winton, D.J., Sansom, O.J., Ashworth, A., and Clarke, A.R. (2009). Lkb1 Deficiency Alters Goblet and Paneth Cell Differentiation in the Small Intestine. *PLOS ONE* 4, e4264.
- Shyh-Chang, N., Daley, G.Q., and Cantley, L.C. (2013). Stem cell metabolism in tissue development and aging. *Development* 140, 2535–2547.
- Sif, S. (2004). ATP-dependent nucleosome remodeling complexes: Enzymes tailored to deal with chromatin. *J. Cell. Biochem.* 91, 1087–1098.
- Simeonova, I., Jaber, S., Draskovic, I., Bardot, B., Fang, M., Bouarich-Bourimi, R., Lejour, V., Charbonnier, L., Soudais, C., Bourdon, J.-C., et al. (2013). Mutant mice lacking the p53 C-terminal domain model telomere syndromes. *Cell Rep.* 3, 2046–2058.
- Simões-Costa, M., and Bronner, M.E. (2015). Establishing neural crest identity: a gene regulatory recipe. *Dev. Camb. Engl.* 142, 242–257.
- Sitte, N., Huber, M., Grune, T., Ladhoff, A., Doecke, W.D., Von Zglinicki, T., and Davies, K.J. (2000). Proteasome inhibition by lipofuscin/ceroid during postmitotic aging of fibroblasts. *FASEB J. Off. Publ. Fed. Am. Soc. Exp. Biol.* 14, 1490–1498.
- Skába, R., Dvorská, S., Václavíková, E., Vlcek, P., Frantlová, M., and Bendlová, B. (2006). The risk of medullary thyroid carcinoma in patients with Hirschsprung's disease. *Pediatr. Surg. Int.* 22, 991–995.
- Skoczyńska, A., Budzisz, E., Trznadel-Grodzka, E., and Rotsztein, H. (2017). Melanin and lipofuscin as hallmarks of skin aging. *Adv. Dermatol. Allergol. Dermatol. Alergol.* 34, 97–103.
- Smith, E.R., Belote, J.M., Schiltz, R.L., Yang, X.J., Moore, P.A., Berger, S.L., Nakatani, Y., and Allis, C.D. (1998). Cloning of Drosophila GCN5: conserved features among metazoan GCN5 family members. *Nucleic Acids Res.* 26, 2948–2954.
- Song, X.M., Fiedler, M., Galuska, D., Ryder, J.W., Fernström, M., Chibalin, A.V., Wallberg-Henriksson, H., and Zierath, J.R. (2002). 5-Aminoimidazole-4-carboxamide ribonucleoside treatment improves glucose homeostasis in insulin-resistant diabetic (ob/ob) mice. *Diabetologia* 45, 56–65.
- Sookoian, S., and Pirola, C.J. (2012). Alanine and aspartate aminotransferase and glutamine-cycling pathway: Their roles in pathogenesis of metabolic syndrome. *World J. Gastroenterol. WJG* 18, 3775–3781.

- Sousa, C.M., Biancur, D.E., Wang, X., Halbrook, C.J., Sherman, M.H., Zhang, L., Kremer, D., Hwang, R.F., Witkiewicz, A.K., Ying, H., et al. (2016). Pancreatic stellate cells support tumour metabolism through autophagic alanine secretion. *Nature* 536, 479–483.
- Srinivasan, V., Sandhya, N., Sampathkumar, R., Farooq, S., Mohan, V., and Balasubramanyam, M. (2007). Glutamine fructose-6-phosphate amidotransferase (GFAT) gene expression and activity in patients with type 2 diabetes: inter-relationships with hyperglycaemia and oxidative stress. *Clin. Biochem.* 40, 952–957.
- Srivastava, R.A.K., Pinkosky, S.L., Filippov, S., Hanselman, J.C., Cramer, C.T., and Newton, R.S. (2012). AMP-activated protein kinase: an emerging drug target to regulate imbalances in lipid and carbohydrate metabolism to treat cardio-metabolic diseases. *J. Lipid Res.* 53, 2490–2514.
- Stad, R., Little, N.A., Xirodimas, D.P., Frenk, R., van der Eb, A.J., Lane, D.P., Saville, M.K., and Jochemsen, A.G. (2001). Mdmx stabilizes p53 and Mdm2 via two distinct mechanisms. *EMBO Rep.* 2, 1029–1034.
- Stambolsky, P., Weisz, L., Shats, I., Klein, Y., Goldfinger, N., Oren, M., and Rotter, V. (2006). Regulation of AIF expression by p53. *Cell Death Differ.* 13, 2140–2149.
- Stanchina, L., Baral, V., Robert, F., Pingault, V., Lemort, N., Pachnis, V., Goossens, M., and Bondurand, N. (2006). Interactions between Sox10, Edn3 and Ednrb during enteric nervous system and melanocyte development. *Dev. Biol.* 295, 232–249.
- Stanchina, L., Van de Putte, T., Goossens, M., Huylebroeck, D., and Bondurand, N. (2010). Genetic interaction between Sox10 and Zfhx1b during enteric nervous system development. *Dev. Biol.* 341, 416–428.
- Stein, L.R., and Imai, S. (2012). The dynamic regulation of NAD metabolism in mitochondria. *Trends Endocrinol. Metab. TEM* 23, 420–428.
- Stiewe, T. (2007). The p53 family in differentiation and tumorigenesis. *Nat. Rev. Cancer* 7, 165–168.
- Stommel, J.M., and Wahl, G.M. (2004). Accelerated MDM2 auto-degradation induced by DNA-damage kinases is required for p53 activation. *EMBO J.* 23, 1547–1556.
- Stommel, J.M., Marchenko, N.D., Jimenez, G.S., Moll, U.M., Hope, T.J., and Wahl, G.M. (1999). A leucine-rich nuclear export signal in the p53 tetramerization domain: regulation of subcellular localization and p53 activity by NES masking. *EMBO J.* 18, 1660–1672.
- Styrt, B., Pollack, C.R., and Klempner, M.S. (1988). An abnormal calcium uptake pump in Chediak-Higashi neutrophil lysosomes. *J. Leukoc. Biol.* 44, 130–135.
- Sui, G., Affar, E.B., Shi, Y., Brignone, C., Wall, N.R., Yin, P., Donohoe, M., Luke, M.P., Calvo, D., Grossman, S.R., et al. (2004). Yin Yang 1 is a negative regulator of p53. *Cell* 117, 859–872.
- Sukhai, M.A., Prabha, S., Hurren, R., Rutledge, A.C., Lee, A.Y., Srisanthadevan, S., Sun, H., Wang, X., Skrtic, M., Seneviratne, A., et al. (2013). Lysosomal disruption preferentially targets acute myeloid leukemia cells and progenitors. *J. Clin. Invest.* 123, 315–328.
- Sullivan, J.E., Carey, F., Carling, D., and Beri, R.K. (1994). Characterisation of 5'-AMP-activated protein kinase in human liver using specific peptide substrates and the effects of 5'-AMP analogues on enzyme activity. *Biochem. Biophys. Res. Commun.* 200, 1551–1556.

- Sumoza-Toledo, A., Lange, I., Cortado, H., Bhagat, H., Mori, Y., Fleig, A., Penner, R., and Partida-Sánchez, S. (2011). Dendritic cell maturation and chemotaxis is regulated by TRPM2-mediated lysosomal Ca²⁺ release. *FASEB J. Off. Publ. Fed. Am. Soc. Exp. Biol.* 25, 3529–3542.
- Sun, G., Reynolds, R., Leclerc, I., and Rutter, G.A. (2011). RIP2-mediated LKB1 deletion causes axon degeneration in the spinal cord and hind-limb paralysis. *Dis. Model. Mech.* 4, 193–202.
- Suzuki, S., Tanaka, T., Poyurovsky, M.V., Nagano, H., Mayama, T., Ohkubo, S., Lokshin, M., Hosokawa, H., Nakayama, T., Suzuki, Y., et al. (2010). Phosphate-activated glutaminase (GLS2), a p53-inducible regulator of glutamine metabolism and reactive oxygen species. *Proc. Natl. Acad. Sci. U. S. A.* 107, 7461–7466.
- Tamás, P., Hawley, S.A., Clarke, R.G., Mustard, K.J., Green, K., Hardie, D.G., and Cantrell, D.A. (2006). Regulation of the energy sensor AMP-activated protein kinase by antigen receptor and Ca²⁺ in T lymphocytes. *J. Exp. Med.* 203, 1665–1670.
- Tanaka, H., and Baba, T. (2005). Gene expression in spermiogenesis. *Cell. Mol. Life Sci. CMLS* 62, 344–354.
- Tanwar, P.S., Kaneko-Tarui, T., Zhang, L., and Teixeira, J.M. (2012). Altered LKB1/AMPK/TSC1/TSC2/mTOR signaling causes disruption of Sertoli cell polarity and spermatogenesis. *Hum. Mol. Genet.* 21, 4394–4405.
- Taraviras, S., Marcos-Gutierrez, C.V., Durbec, P., Jani, H., Grigoriou, M., Sukumaran, M., Wang, L.C., Hynes, M., Raisman, G., and Pachnis, V. (1999). Signalling by the RET receptor tyrosine kinase and its role in the development of the mammalian enteric nervous system. *Dev. Camb. Engl.* 126, 2785–2797.
- Tardito, S., Oudin, A., Ahmed, S.U., Fack, F., Keunen, O., Zheng, L., Miletic, H., Sakariassen, P.Ø., Weinstock, A., Wagner, A., et al. (2015). Glutamine synthetase activity fuels nucleotide biosynthesis and supports growth of glutamine-restricted glioblastoma. *Nat. Cell Biol.* 17, 1556–1568.
- Tasdemir, E., Maiuri, M.C., Galluzzi, L., Vitale, I., Djavaheri-Mergny, M., D’Amelio, M., Criollo, A., Morselli, E., Zhu, C., Harper, F., et al. (2008). Regulation of autophagy by cytoplasmic p53. *Nat. Cell Biol.* 10, 676–687.
- Tassabehji, M., Read, A.P., Newton, V.E., Harris, R., Balling, R., Gruss, P., and Strachan, T. (1992). Waardenburg’s syndrome patients have mutations in the human homologue of the Pax-3 paired box gene. *Nature* 355, 635–636.
- Terman, A., and Brunk, U.T. (1998). Lipofuscin: mechanisms of formation and increase with age. *APMIS Acta Pathol. Microbiol. Immunol. Scand.* 106, 265–276.
- Tessem, M.-B., Swanson, M.G., Keshari, K.R., Albers, M.J., Joun, D., Tabatabai, Z.L., Simko, J.P., Shinohara, K., Nelson, S.J., Vigneron, D.B., et al. (2008). Evaluation of Lactate and Alanine as Metabolic Biomarkers of Prostate Cancer Using 1H HR-MAS Spectroscopy of Biopsy Tissues. *Magn. Reson. Med. Off. J. Soc. Magn. Reson. Med. Soc. Magn. Reson. Med.* 60, 510–516.
- Theret, M., Gsaier, L., Schaffer, B., Juban, G., Ben Larbi, S., Weiss-Gayet, M., Bultot, L., Collodet, C., Foretz, M., Desplanches, D., et al. (2017). AMPK α 1-LDH pathway regulates muscle stem cell self-renewal by controlling metabolic homeostasis. *EMBO J.* 36, 1946–1962.
- Theveneau, E., and Mayor, R. (2011). Collective cell migration of the cephalic neural crest: The art of integrating information. *Genesis* 49, 164–176.

- Theveneau, E., and Mayor, R. (2012). Neural crest migration: interplay between chemorepellents, chemoattractants, contact inhibition, epithelial-mesenchymal transition, and collective cell migration. *Wiley Interdiscip. Rev. Dev. Biol.* *1*, 435–445.
- Theveneau, E., Steventon, B., Scarpa, E., Garcia, S., Trepas, X., Streit, A., and Mayor, R. (2013). Chase-and-run between adjacent cell populations promotes directional collective migration. *Nat. Cell Biol.* *15*, 763–772.
- Thibert, C., Perret, C., and Billaud, M. (2015). AMPK potentiation by LKB1 isoforms. *Oncotarget* *6*, 35139–35140.
- Tohma, H., Hepworth, A.R., Shavlakadze, T., Grounds, M.D., and Arthur, P.G. (2011). Quantification of ceroid and lipofuscin in skeletal muscle. *J. Histochem. Cytochem.* *59*, 769–779.
- Towler, M.C., Fogarty, S., Hawley, S.A., Pan, D.A., Martin, D.M.A., Morrice, N.A., McCarthy, A., Galardo, M.N., Meroni, S.B., Cigorruga, S.B., et al. (2008). A novel short splice variant of the tumour suppressor LKB1 is required for spermiogenesis. *Biochem. J.* *416*, 1–14.
- Toyama, E.Q., Herzig, S., Courchet, J., Lewis, T.L., Losón, O.C., Hellberg, K., Young, N.P., Chen, H., Polleux, F., Chan, D.C., et al. (2016). AMP-activated protein kinase mediates mitochondrial fission in response to energy stress. *Science* *351*, 275–281.
- Toyooka, Y., Tsunekawa, N., Takahashi, Y., Matsui, Y., Satoh, M., and Noce, T. (2000). Expression and intracellular localization of mouse Vasa-homologue protein during germ cell development. *Mech. Dev.* *93*, 139–149.
- Trainor, P.A. (2005). Specification of neural crest cell formation and migration in mouse embryos. *Semin. Cell Dev. Biol.* *16*, 683–693.
- Trainor, P. (2013). *Neural Crest Cells: Evolution, Development and Disease*. Academic Press.
- Trainor, P.A., Dixon, J., and Dixon, M.J. (2009). Treacher Collins syndrome: etiology, pathogenesis and prevention. *Eur. J. Hum. Genet. EJHG* *17*, 275–283.
- Trevisiol, A., and Nave, K.-A. (2015). Brain Energy Metabolism: Conserved Functions of Glycolytic Glial Cells. *Cell Metab.* *22*, 361–363.
- Tsukamoto, S., Hara, T., Yamamoto, A., Ohta, Y., Wada, A., Ishida, Y., Kito, S., Nishikawa, T., Minami, N., Sato, K., et al. (2013). Functional analysis of lysosomes during mouse preimplantation embryo development. *J. Reprod. Dev.* *59*, 33–39.
- Tsurubuchi, T., Ichi, S., Shim, K.-W., Norkett, W., Allender, E., Mania-Farnell, B., Tomita, T., McLone, D.G., Ginsberg, N., and Mayanil, C.S. (2013). Amniotic fluid and serum biomarkers from women with neural tube defect-affected pregnancies: a case study for myelomeningocele and anencephaly: clinical article. *J. Neurosurg. Pediatr.* *12*, 380–389.
- Tyner, S.D., Venkatachalam, S., Choi, J., Jones, S., Ghebranious, N., Igelmann, H., Lu, X., Soron, G., Cooper, B., Brayton, C., et al. (2002). p53 mutant mice that display early ageing-associated phenotypes. *Nature* *415*, 45–53.
- Uesaka, T., Nagashimada, M., and Enomoto, H. (2015). Neuronal Differentiation in Schwann Cell Lineage Underlies Postnatal Neurogenesis in the Enteric Nervous System. *J. Neurosci. Off. J. Soc. Neurosci.* *35*, 9879–9888.

- Um, S.H., Frigerio, F., Watanabe, M., Picard, F., Joaquin, M., Sticker, M., Fumagalli, S., Allegrini, P.R., Kozma, S.C., Auwerx, J., et al. (2004). Absence of S6K1 protects against age- and diet-induced obesity while enhancing insulin sensitivity. *Nature* 431, 200–205.
- Vaclavikova, E., Dvorakova, S., Skaba, R., Pos, L., Sykorova, V., Halkova, T., Vcelak, J., and Bendlova, B. (2014). RET Variants and Haplotype Analysis in a Cohort of Czech Patients with Hirschsprung Disease. *PLOS ONE* 9, e98957.
- Van Nostrand, J.L., and Attardi, L.D. (2014). Guilty as CHARGED: p53's expanding role in disease. *Cell Cycle Georget. Tex* 13, 3798–3807.
- Van Nostrand, J.L., Brady, C.A., Jung, H., Fuentes, D.R., Kozak, M.M., Johnson, T.M., Lin, C.-Y., Lin, C.-J., Swiderski, D.L., Vogel, H., et al. (2014). Inappropriate p53 Activation During Development Induces Features of CHARGE Syndrome. *Nature* 514, 228–232.
- Van Nostrand, J.L., Bowen, M.E., Vogel, H., Barna, M., and Attardi, L.D. (2017). The p53 family members have distinct roles during mammalian embryonic development. *Cell Death Differ.* 24, 575–579.
- Varum, S., Rodrigues, A.S., Moura, M.B., Momcilovic, O., Easley, C.A., Ramalho-Santos, J., Van Houten, B., and Schatten, G. (2011). Energy Metabolism in Human Pluripotent Stem Cells and Their Differentiated Counterparts. *PLoS ONE* 6.
- van Veelen, C.W., Staal, G.E., Verbiest, H., and Vlug, A.M. (1977). Alanine inhibition of pyruvate kinase in gliomas and meningiomas. A diagnostic tool in surgery for gliomas? *Lancet Lond. Engl.* 2, 384–385.
- Vincent, M.F., Marangos, P.J., Gruber, H.E., and Berghe, G. van den (1991). Inhibition by AICA Riboside of Gluconeogenesis in Isolated Rat Hepatocytes. *Diabetes* 40, 1259–1266.
- Viollet, B., Athea, Y., Mounier, R., Guigas, B., Zarrinpashneh, E., Horman, S., Lantier, L., Hebrard, S., Devin-Leclerc, J., Beauloye, C., et al. (2009). AMPK: Lessons from transgenic and knockout animals. *Front. Biosci. Landmark Ed.* 14, 19–44.
- Vissers, L.E.L.M., van Ravenswaaij, C.M.A., Admiraal, R., Hurst, J.A., de Vries, B.B.A., Janssen, I.M., van der Vliet, W.A., Huys, E.H.L.P.G., de Jong, P.J., Hamel, B.C.J., et al. (2004). Mutations in a new member of the chromodomain gene family cause CHARGE syndrome. *Nat. Genet.* 36, 955–957.
- Volikos, E., Robinson, J., Aittomäki, K., Mecklin, J.-P., Järvinen, H., Westerman, A.M., de Rooji, F.W.M., Vogel, T., Moeslein, G., Launonen, V., et al. (2006). LKB1 exonic and whole gene deletions are a common cause of Peutz-Jeghers syndrome. *J. Med. Genet.* 43, e18.
- Volkenhoff, A., Weiler, A., Letzel, M., Stehling, M., Klämbt, C., and Schirmeier, S. (2015). Glial Glycolysis Is Essential for Neuronal Survival in *Drosophila*. *Cell Metab.* 22, 437–447.
- Vousden, K.H., and Ryan, K.M. (2009). p53 and metabolism. *Nat. Rev. Cancer* 9, 691–700.
- Wade, M., Wang, Y.V., and Wahl, G.M. (2010). The p53 orchestra: Mdm2 and Mdmx set the tone. *Trends Cell Biol.* 20, 299–309.
- Wang, C., Ivanov, A., Chen, L., Fredericks, W.J., Seto, E., Rauscher, F.J., and Chen, J. (2005). MDM2 interaction with nuclear corepressor KAP1 contributes to p53 inactivation. *EMBO J.* 24, 3279–3290.

- Wang, C., Lee, J.-E., Lai, B., Macfarlan, T.S., Xu, S., Zhuang, L., Liu, C., Peng, W., and Ge, K. (2016). Enhancer priming by H3K4 methyltransferase MLL4 controls cell fate transition. *Proc. Natl. Acad. Sci.* *113*, 11871–11876.
- Wang, D.B., Kinoshita, C., Kinoshita, Y., and Morrison, R.S. (2014). p53 and mitochondrial function in neurons. *Biochim. Biophys. Acta* *1842*, 1186–1197.
- Wang, J., Alexander, P., Wu, L., Hammer, R., Cleaver, O., and McKnight, S.L. (2009). Dependence of Mouse Embryonic Stem Cells on Threonine Catabolism. *Science* *325*, 435–439.
- Wang, Q., Zou, Y., Nowotschin, S., Kim, S.Y., Li, Q.V., Soh, C.-L., Su, J., Zhang, C., Shu, W., Xi, Q., et al. (2017). The p53 Family Coordinates Wnt and Nodal Inputs in Mesendodermal Differentiation of Embryonic Stem Cells. *Cell Stem Cell* *20*, 70–86.
- Wang, X., Kua, H.-Y., Hu, Y., Guo, K., Zeng, Q., Wu, Q., Ng, H.-H., Karsenty, G., de Crombrughe, B., Yeh, J., et al. (2006). p53 functions as a negative regulator of osteoblastogenesis, osteoblast-dependent osteoclastogenesis, and bone remodeling. *J. Cell Biol.* *172*, 115–125.
- Wang, Z.J., Churchman, M., Avizienyte, E., McKeown, C., Davies, S., Evans, D.G., Ferguson, A., Ellis, I., Xu, W.H., Yan, Z.Y., et al. (1999). Germline mutations of the LKB1 (STK11) gene in Peutz-Jeghers patients. *J. Med. Genet.* *36*, 365–368.
- Warburg, O. (1956). On the Origin of Cancer Cells. *Science* *123*, 309–314.
- Ward, P.S., and Thompson, C.B. (2012). Metabolic reprogramming: a cancer hallmark even warburg did not anticipate. *Cancer Cell* *21*, 297–308.
- Watanabe, Y., Broders-Bondon, F., Baral, V., Paul-Gilloteaux, P., Pingault, V., Dufour, S., and Bondurand, N. (2013). Sox10 and Itgb1 interaction in enteric neural crest cell migration. *Dev. Biol.* *379*, 92–106.
- Watanabe, Y., Stanchina, L., Lecerf, L., Gacem, N., Conidi, A., Baral, V., Pingault, V., Huylebroeck, D., and Bondurand, N. (2017). Differentiation of Mouse Enteric Nervous System Progenitor Cells Is Controlled by Endothelin 3 and Requires Regulation of Ednrb by SOX10 and ZEB2. *Gastroenterology* *152*, 1139-1150.e4.
- Watkins-Chow, D.E., Cooke, J., Pidsley, R., Edwards, A., Slotkin, R., Leeds, K.E., Mullen, R., Baxter, L.L., Campbell, T.G., Salzer, M.C., et al. (2013). Mutation of the Diamond-Blackfan Anemia Gene Rps7 in Mouse Results in Morphological and Neuroanatomical Phenotypes. *PLOS Genet.* *9*, e1003094.
- Watts, J.L., Morton, D.G., Bestman, J., and Kemphues, K.J. (2000). The *C. elegans* par-4 gene encodes a putative serine-threonine kinase required for establishing embryonic asymmetry. *Dev. Camb. Engl.* *127*, 1467–1475.
- Wei, D., and Loeken, M.R. (2014). Increased DNA methyltransferase 3b (Dnmt3b)-mediated CpG island methylation stimulated by oxidative stress inhibits expression of a gene required for neural tube and neural crest development in diabetic pregnancy. *Diabetes* *63*, 3512–3522.
- Wellen, K.E., and Thompson, C.B. (2012). A two-way street: reciprocal regulation of metabolism and signalling. *Nat. Rev. Mol. Cell Biol.* *13*, 270–276.
- Winder, W.W. (2008). Can Patients with Type 2 Diabetes Be Treated with AMPK-Activators? *Diabetologia* *51*, 1761–1764.

- Winder, W.W., Holmes, B.F., Rubink, D.S., Jensen, E.B., Chen, M., and Holloszy, J.O. (2000). Activation of AMP-activated protein kinase increases mitochondrial enzymes in skeletal muscle. *J. Appl. Physiol.* Bethesda Md 1985 88, 2219–2226.
- Wingo, S.N., Gallardo, T.D., Akbay, E.A., Liang, M.-C., Contreras, C.M., Boren, T., Shimamura, T., Miller, D.S., Sharpless, N.E., Bardeesy, N., et al. (2009). Somatic LKB1 mutations promote cervical cancer progression. *PLoS One* 4, e5137.
- Woodhoo, A., and Sommer, L. (2008). Development of the Schwann cell lineage: from the neural crest to the myelinated nerve. *Glia* 56, 1481–1490.
- Woods, A., Johnstone, S.R., Dickerson, K., Leiper, F.C., Fryer, L.G.D., Neumann, D., Schlattner, U., Wallimann, T., Carlson, M., and Carling, D. (2003). LKB1 is the upstream kinase in the AMP-activated protein kinase cascade. *Curr. Biol.* CB 13, 2004–2008.
- Wu, T., Horowitz, M., and Rayner, C.K. (2017). New insights into the anti-diabetic actions of metformin: from the liver to the gut. *Expert Rev. Gastroenterol. Hepatol.* 11, 157–166.
- Wullschlegel, S., Loewith, R., and Hall, M.N. (2006). TOR signaling in growth and metabolism. *Cell* 124, 471–484.
- Xiao, B., Heath, R., Saiu, P., Leiper, F.C., Leone, P., Jing, C., Walker, P.A., Haire, L., Eccleston, J.F., Davis, C.T., et al. (2007). Structural basis for AMP binding to mammalian AMP-activated protein kinase. *Nature* 449, 496–500.
- Xie, Z., Dong, Y., Scholz, R., Neumann, D., and Zou, M.-H. (2008). Phosphorylation of LKB1 at Serine 428 by Protein Kinase C- ζ Is Required for Metformin-Enhanced Activation of the AMP-Activated Protein Kinase in Endothelial Cells. *Circulation* 117, 952–962.
- Xu, H.-G., Zhai, Y.-X., Chen, J., Lu, Y., Wang, J.-W., Quan, C.-S., Zhao, R.-X., Xiao, X., He, Q., Werle, K.D., et al. (2015). LKB1 reduces ROS-mediated cell damage via activation of p38. *Oncogene* 34, 3848–3859.
- Xu, W., Edmondson, D.G., Evrard, Y.A., Wakamiya, M., Behringer, R.R., and Roth, S.Y. (2000). Loss of Gcn5l2 leads to increased apoptosis and mesodermal defects during mouse development. *Nat. Genet.* 26, 229–232.
- Yang, A., Schweitzer, R., Sun, D., Kaghad, M., Walker, N., Bronson, R.T., Tabin, C., Sharpe, A., Caput, D., Crum, C., et al. (1999). p63 is essential for regenerative proliferation in limb, craniofacial and epithelial development. *Nature* 398, 714–718.
- Yang, A., Walker, N., Bronson, R., Kaghad, M., Oosterwegel, M., Bonnin, J., Vagner, C., Bonnet, H., Dikkes, P., Sharpe, A., et al. (2000). p73-deficient mice have neurological, pheromonal and inflammatory defects but lack spontaneous tumours. *Nature* 404, 99–103.
- Yang, Z.J.P., Broz, D.K., Noderer, W.L., Ferreira, J.P., Overton, K.W., Spencer, S.L., Meyer, T., Tapscott, S.J., Attardi, L.D., and Wang, C.L. (2015). p53 suppresses muscle differentiation at the myogenin step in response to genotoxic stress. *Cell Death Differ.* 22, 560–573.
- Ylikorkala, A., Rossi, D.J., Korsisaari, N., Luukko, K., Alitalo, K., Henkemeyer, M., and Mäkelä, T.P. (2001). Vascular abnormalities and deregulation of VEGF in Lkb1-deficient mice. *Science* 293, 1323–1326.

- Yu, L., Alva, A., Su, H., Dutt, P., Freundt, E., Welsh, S., Baehrecke, E.H., and Lenardo, M.J. (2004). Regulation of an ATG7-beclin 1 program of autophagic cell death by caspase-8. *Science* 304, 1500–1502.
- Zaman, A., Capper, R., and Baddoo, W. (2015). Waardenburg syndrome: more common than you think! *Clin. Otolaryngol. Off. J. ENT-UK Off. J. Neth. Soc. Oto-Rhino-Laryngol. Cervico-Facial Surg.* 40, 44–48.
- Zambetti, G.P., Horwitz, E.M., and Schipani, E. (2006). Skeletons in the p53 tumor suppressor closet: genetic evidence that p53 blocks bone differentiation and development. *J. Cell Biol.* 172, 795–797.
- Zang, Y., Yu, L.-F., Pang, T., Fang, L.-P., Feng, X., Wen, T.-Q., Nan, F.-J., Feng, L.-Y., and Li, J. (2008). AICAR induces astroglial differentiation of neural stem cells via activating the JAK/STAT3 pathway independently of AMP-activated protein kinase. *J. Biol. Chem.* 283, 6201–6208.
- Zauberman, A., Flusberg, D., Haupt, Y., Barak, Y., and Oren, M. (1995). A functional p53-responsive intronic promoter is contained within the human mdm2 gene. *Nucleic Acids Res.* 23, 2584–2592.
- Zeng, P.-Y., and Berger, S.L. (2006). LKB1 is recruited to the p21/WAF1 promoter by p53 to mediate transcriptional activation. *Cancer Res.* 66, 10701–10708.
- Zeng, X., and Kinsella, T.J. (2007). A novel role for DNA mismatch repair and the autophagic processing of chemotherapy drugs in human tumor cells. *Autophagy* 3, 368–370.
- Zentner, G.E., Hurd, E.A., Schnetz, M.P., Handoko, L., Wang, C., Wang, Z., Wei, C., Tesar, P.J., Hatzoglou, M., Martin, D.M., et al. (2010). CHD7 functions in the nucleolus as a positive regulator of ribosomal RNA biogenesis. *Hum. Mol. Genet.* 19, 3491–3501.
- Zeqiraj, E., Filippi, B.M., Goldie, S., Navratilova, I., Boudeau, J., Deak, M., Alessi, D.R., and van Aalten, D.M.F. (2009). ATP and MO25 α Regulate the Conformational State of the STRAD α Pseudokinase and Activation of the LKB1 Tumour Suppressor. *PLoS Biol.* 7.
- Zhang, Y., and Xiong, Y. (2001a). A p53 amino-terminal nuclear export signal inhibited by DNA damage-induced phosphorylation. *Science* 292, 1910–1915.
- Zhang, Y., and Xiong, Y. (2001b). Control of p53 ubiquitination and nuclear export by MDM2 and ARF. *Cell Growth Differ. Mol. Biol. J. Am. Assoc. Cancer Res.* 12, 175–186.
- Zhang, C., Lin, M., Wu, R., Wang, X., Yang, B., Levine, A.J., Hu, W., and Feng, Z. (2011). Parkin, a p53 target gene, mediates the role of p53 in glucose metabolism and the Warburg effect. *Proc. Natl. Acad. Sci. U. S. A.* 108, 16259–16264.
- Zhang, C., Liu, J., Liang, Y., Wu, R., Zhao, Y., Hong, X., Lin, M., Yu, H., Liu, L., Levine, A.J., et al. (2013a). Tumour-associated mutant p53 drives the Warburg effect. *Nat. Commun.* 4, 2935.
- Zhang, C.-S., Jiang, B., Li, M., Zhu, M., Peng, Y., Zhang, Y.-L., Wu, Y.-Q., Li, T.Y., Liang, Y., Lu, Z., et al. (2014). The lysosomal v-ATPase-Ragulator complex is a common activator for AMPK and mTORC1, acting as a switch between catabolism and anabolism. *Cell Metab.* 20, 526–540.
- Zhang, C.-S., Li, M., Ma, T., Zong, Y., Cui, J., Feng, J.-W., Wu, Y.-Q., Lin, S.-Y., and Lin, S.-C. (2016). Metformin Activates AMPK through the Lysosomal Pathway. *Cell Metab.* 24, 521–522.

- Zhang, C.-S., Li, M., Zong, Y., and Lin, S.-C. (2018). Determining AMPK Activation via the Lysosomal v-ATPase-Ragulator-AXIN/LKB1 Axis. *Methods Mol. Biol. Clifton NJ* 1732, 393–411.
- Zhang, Y.-L., Guo, H., Zhang, C.-S., Lin, S.-Y., Yin, Z., Peng, Y., Luo, H., Shi, Y., Lian, G., Zhang, C., et al. (2013b). AMP as a low-energy charge signal autonomously initiates assembly of AXIN-AMPK-LKB1 complex for AMPK activation. *Cell Metab.* 18, 546–555.
- Zhang, Z., Chen, G., Zhou, W., Song, A., Xu, T., Luo, Q., Wang, W., Gu, X., and Duan, S. (2007). Regulated ATP release from astrocytes through lysosome exocytosis. *Nat. Cell Biol.* 9, 945–953.
- Zhao, R.-X., and Xu, Z.-X. (2014). Targeting the LKB1 tumor suppressor. *Curr. Drug Targets* 15, 32–52.
- Zhao, L., Samuels, T., Winckler, S., Korgaonkar, C., Tompkins, V., Horne, M.C., and Quelle, D.E. (2003). Cyclin G1 Has Growth Inhibitory Activity Linked to the ARF-Mdm2-p53 and pRb Tumor Suppressor Pathways1 1 DEQ from the American Cancer Society (RSG-98-254-04-MGO) and NIH (RO1 CA90367), and by a grant from the NIH to MCH (RO1 GM56900). *Mol. Cancer Res.* 1, 195–206.
- Zhao, Y., Hu, X., Liu, Y., Dong, S., Wen, Z., He, W., Zhang, S., Huang, Q., and Shi, M. (2017). ROS signaling under metabolic stress: cross-talk between AMPK and AKT pathway. *Mol. Cancer* 16.
- Zibrova, D., Vandermoere, F., Göransson, O., Pegg, M., Mariño, K.V., Knierim, A., Spengler, K., Weigert, C., Viollet, B., Morrice, N.A., et al. (2017). GFAT1 phosphorylation by AMPK promotes VEGF-induced angiogenesis. *Biochem. J.* 474, 983–1001.
- Ziegler, A., von Kienlin, M., Décorps, M., and Rémy, C. (2001). High glycolytic activity in rat glioma demonstrated in vivo by correlation peak 1H magnetic resonance imaging. *Cancer Res.* 61, 5595–5600.
- Zurkirchen, L., and Sommer, L. (2017). Quo vadis: tracing the fate of neural crest cells. *Curr. Opin. Neurobiol.* 47, 16–23.
- Zuzarte-Luis, V., Berciano, M.T., Lafarga, M., and Hurlé, J.M. (2006). Caspase redundancy and release of mitochondrial apoptotic factors characterize interdigital apoptosis. *Apoptosis Int. J. Program. Cell Death* 11, 701–715.

Abstract

The tumor suppressor LKB1 codes for a serine/threonine kinase. It acts as a key regulator of cell polarity and energy metabolism partly through the activation of the AMP-activated protein kinase (AMPK), a sensor that adapts energy supply to the nutrient demands of cells facing situations of metabolic stress. To achieve metabolic adaptations, AMPK phosphorylates numerous substrates which inhibit anabolic processes while activating catabolic reactions. In particular, AMPK inhibits the mammalian target of rapamycin (mTOR).

During my PhD, based on genetically engineered mouse models, I uncovered that Lkb1 signaling is essential for neural crest cells (NCC) formation. NCC are multipotent cells that originate from the neural tube and give rise to various derivatives including bones and cartilage of the face, pigmented cells in the skin and glial and neural cells in peripheral nerves and the enteric nervous system. I demonstrated that Lkb1 is essential for vertebrate head formation and for the differentiation and maintenance of NCC-derivatives in the peripheral nervous system. I also emphasized that LKB1 is acetylated on lysine 48 by the acetyltransferase GCN5 and that this acetylation could regulate cranial NCC ontogeny and head formation. Furthermore, I discovered that Lkb1 controls NCC-derived glial differentiation through metabolic regulations involving amino acid biosynthesis coupled to pyruvate-alanine cycling upstream of mTOR signaling.

Phenotypes due to *Lkb1* loss in NCC recapitulate clinical features of human disorders called neurocristopathies and therefore suggest that aberrant Lkb1 metabolic signaling underlies the etiology of these pathologies. Abnormal activation of the tumor suppressor p53 has been described in some NCC disorders and *p53* inactivation in neurocristopathy mouse models rescues the pathological phenotype. By using a NCC line that can be cultivated as progenitors or differentiated in glial cells *in vitro*, I demonstrated that Lkb1 expression in NCC-derivatives controls p53 activation by limiting oxidative DNA damage and prevents the formation of lysosomes filled with oxidized proteins and lipids called lipofuscin granules. Interestingly, activation of mTOR and LKB1/AMPK pathways is governed by amino acid sensors and takes place at the lysosome surface. Lysosomes have been proposed as a signaling hub controlling proteolysis and aging. Thus Lkb1 and p53 signaling could converge especially through lysosome homeostasis thereby potentially impacting cellular aging.

Strikingly, Sertoli cells, that are epithelial somatic cells, located in seminiferous tubules in testes, and which govern germ cells maturation and whole testis homeostasis, share similar metabolic functions with glial cells. For example, they secrete lactate and alanine to fuel mitochondria of neighboring cells (germ cells or neurons respectively) to control their survival and maturation. During my PhD, we highlighted that Lkb1 is essential for testis homeostasis and spermatogenesis by regulating Sertoli cell polarity and, as observed in glial cells, energy metabolism through pyruvate-alanine cycling. These data suggest that this particular Lkb1 metabolic regulation is conserved in tissues with similar function.

Taken together, these studies reveal the underlying molecular mechanisms that coordinately regulate energy metabolism and cell fate. They provide new insights into NCC development and expand our understanding of the role of LKB1 as an energy metabolic regulator. Finally, my PhD projects uncover the existence of a crosstalk between Lkb1 and p53 and underline its importance in NCC disorders.

Résumé

Le suppresseur de tumeur et sérine/thréonine kinase LKB1 est un régulateur clé de la polarité cellulaire et du métabolisme énergétique en partie grâce à l'activation de sa kinase substrat AMPK. Cette protéine est un senseur métabolique pour adapter les apports énergétiques aux besoins nutritionnels des cellules confrontées à un stress. Pour cela, AMPK phosphoryle divers substrats qui activent les réactions cataboliques et inhibent les processus anaboliques dont la kinase mTOR.

Au cours de ma thèse, via l'utilisation de modèles murins d'inactivation conditionnelle, j'ai découvert que Lkb1 est crucial pour la formation des cellules de crête neurale (CCN). Ces cellules multipotentes, originaires du tube neural, donnent naissance à divers dérivés, comme les cellules des os et cartilage de la face, les cellules pigmentées de la peau et les cellules gliales et neurales des nerfs périphériques et du système nerveux entérique. J'ai démontré que Lkb1 est essentiel pour la formation de la tête des vertébrés et pour la différenciation et le maintien des dérivés des CCN dans le système nerveux périphérique. J'ai également mis en évidence l'acétylation de LKB1 sur la lysine 48 par l'acétyltransférase GCN5 et son rôle dans l'ontogenèse des CCN céphaliques et la formation de la tête. De plus, j'ai découvert que Lkb1 contrôle la différenciation des cellules gliales en réprimant un programme de biosynthèse d'acides aminés couplé à la transamination du pyruvate en alanine, en amont de la voie de signalisation mTOR.

Les phénotypes dus à la perte de Lkb1 dans les CCN récapitulent les caractéristiques cliniques de maladies humaines appelées neurocristopathies. L'activation anormale du suppresseur de tumeur p53 est également associée à certaines neurocristopathies et l'ablation de p53 sauve le phénotype pathologique. Ainsi, j'ai montré que Lkb1 dans les cellules gliales contrôle p53 en limitant les dommages à l'ADN. Lkb1 est aussi essentiel pour maintenir l'homéostasie lysosomale et le recyclage des protéines et ainsi empêcher la formation de granules nommés lipofuscine, chargés en protéines et lipides oxydés. De façon intéressante, les voies mTOR et LKB1/AMPK sont activées à la surface des lysosomes de façon dépendante des niveaux d'acides aminés. Des données récentes de la littérature suggèrent que les lysosomes constitueraient une plateforme de signalisation pour contrôler la protéolyse et le devenir cellulaire. Ainsi, nos données proposent que les signalisations Lkb1 et p53 pourraient réguler l'homéostasie lysosomale et en conséquence le vieillissement cellulaire.

De façon intéressante, les cellules de Sertoli, des cellules somatiques épithéliales, localisées dans les tubes séminifères des testicules, et qui régissent la maturation des cellules germinales et l'homéostasie testiculaire, partagent des fonctions métaboliques similaires avec les cellules gliales. En effet, ces cellules sécrètent le lactate et l'alanine qui alimentent les mitochondries des cellules voisines (cellules germinales ou neurones respectivement) contrôlant ainsi leur survie et leur maturation. Au cours de ma thèse, nous avons observé que Lkb1 est requis pour l'homéostasie testiculaire et la spermatogenèse en régulant la polarité des cellules de Sertoli et leur métabolisme énergétique par le cycle pyruvate-alanine. Ces résultats suggèrent une conservation des régulations métaboliques par Lkb1 dans divers tissus.

Dans leur ensemble, mes travaux de thèse ont apporté une meilleure connaissance des mécanismes sous-jacents des régulations métaboliques lors du devenir cellulaire. Ces résultats fournissent de nouvelles perspectives sur le développement des CCN et élargissent notre compréhension du contrôle métabolique exercé par LKB1. Enfin, mes projets de doctorat ont mis en évidence l'existence d'une communication entre la voie de signalisation Lkb1 et p53 et suggèrent l'importance de cette communication dans les pathologies humaines dues à des défauts des CCN.